PB85-161891

Symposium on the Transfer and Utilization of Particulate Control Technology (4th)
Volume 1. Fabric Filtration

Denver Research Inst., CO

Prepared for

Environmental Protection Agency
Research Triangle Park, NC

Nov 84

U.S. Department of Commerce
National Technical Information Service
NTIS

United States
Environmental Protection
Agency

Industrial Environmental Research
Laboratory
Research Triangle Park NC 27711

EPA-600/9-84-025a
November 1984

Research and Development

PB85-161891

EPA

Fourth Symposium on the Transfer and Utilization of Particulate Control Technology:

Volume I. Fabric Filtration

REPRODUCED BY
NATIONAL TECHNICAL
INFORMATION SERVICE
U.S. DEPARTMENT OF COMMERCE
SPRINGFIELD, VA. 22161

TECHNICAL REPORT DATA
(Please read Instructions on the reverse before completing)

1. REPORT NO. EPA/600/9-84/025a

2.

3. RECIPIENT'S ACCESSION NO. PB85-161891/AS

4. TITLE AND SUBTITLE Fourth Symposium on the Transfer and Utilization of Particulate Control Technology; Volume I. Fabric Filtration

5. REPORT DATE November 1984

6. PERFORMING ORGANIZATION CODE

7. AUTHOR(S) F.P. Venditti, J.A. Armstrong, and M.D. Durham (Compilers)

8. PERFORMING ORGANIZATION REPORT NO.

9. PERFORMING ORGANIZATION NAME AND ADDRESS
Denver Research Institute
P.O. Box 10127
Denver, Colorado 80210

10. PROGRAM ELEMENT NO.

11. CONTRACT/GRANT NO. Cooperative Agreement CR809301

12. SPONSORING AGENCY NAME AND ADDRESS
Air and Energy Engineering Research Laboratory
Office of Research and Development
U.S. Environmental Protection Agency
Research Triangle Park, NC 27711

13. TYPE OF REPORT AND PERIOD COVERED Proceedings; 1/82-10/84

14. SPONSORING AGENCY CODE EPA/600/13

15. SUPPLEMENTARY NOTES IERL-RTP project officer is Dale L. Harmon, Mail Drop 61, 919/541-2429.

16. ABSTRACT

The papers in the three volumes (of which this is one) were presented at the Fourth Symposium on the Transfer and Utilization of Particulate Control Technology in Houston, TX, October 11-14, 1982. Volume I relates to fabric filtration; Volume II, to electrostatic precipitation; and Volume III, to mechanical collectors, coal characteristics, inhalable particulates, and advanced energy and novel control devices. The symposium brought together researchers, manufacturers, users, government representatives, educators, and students to discuss new technology. It provided an effective way to transfer this technology out of the laboratory and into the user's hands. The various technologies were discussed from the perspectives of economics, new technical advances in science and engineering, and applications. Several papers dealt with combinations of devices and technologies, leading to a concept of using a systems (rather than a device) approach to particulate control. Other topic areas were high temperature/high pressure applications, fugitive emissions, measurement techniques, and cost analysis.

17. KEY WORDS AND DOCUMENT ANALYSIS

a. DESCRIPTORS		b. IDENTIFIERS/OPEN ENDED TERMS	c. COSATI Field/Group	
Pollution	Fabrics	Pollution Control	13B	11E
Particles	Electrostatics	Stationary Sources	14G	20C
Electrostatic Precipitators	Measurement	Particulate Control		14B
Scrubbers	Cost Analysis	Fabric Filters	13I	14A
Filters	Processing	Fugitive Emissions	07A	13H
	Leakage			

18. DISTRIBUTION STATEMENT Release to Public

19. SECURITY CLASS *(This Report)* Unclassified

20. SECURITY CLASS *(This page)* Unclassified

21. NO. OF PAGES 572

22. PRICE

EPA Form 2220-1 (9-73)

EPA-600/9-84-025a
November 1984

FOURTH SYMPOSIUM ON THE TRANSFER AND UTILIZATION OF PARTICULATE CONTROL TECHNOLOGY:
VOLUME I. FABRIC FILTRATION

Compiled by:

F. P. Venditti, J. A. Armstrong, and Michael D. Durham

Denver Research Institute
P. O. Box 10127
Denver, Colorado 80210

Grant Number: CR 809301

Project Officer

Dale L. Harmon
Office of Environmental Engineering and Technology
Industrial Environmental Research Laboratory
Research Triangle Park, North Carolina 27711

INDUSTRIAL ENVIRONMENTAL RESEARCH LABORATORY
OFFICE OF RESEARCH AND DEVELOPMENT
U. S. ENVIRONMENTAL PROTECTION AGENCY
RESEARCH TRIANGLE PARK, NORTH CAROLINA 27711

DISCLAIMER

This document has been reviewed in accordance with U.S. Environmental Protection Agency policy and approved for publication. Mention of trade names or commercial products does not constitute endorsement or recommendation for use.

ABSTRACT

The papers in these three volumes of Proceedings were presented at the Fourth Symposium on the Transfer and Utilization of Paticulate Control Technology held in Houston, Texas during 11 October through 14 October 1982, sponsored by the Particulate Technology Branch of the Industrial Environmental Research Laboratory of the Environmental Protection Agency and coordinated by the Denver Research Institute of the University of Denver.

The purpose of the symposium was to bring together researchers, manufacturers, users, government agencies, educators and students to discuss new technology and to provide an effective means for the transfer of this technology out of the laboratories and into the hands of the users.

The three major categories of control technologies - electrostatic precipitators, scrubbers, and fabric filters - were the major concern of the symposium. These technologies were discussed from the perspectives of economics; new technical advancements in science and engineering; and applications. Several papers dealt with combinations of devices and technologies, leading to a concept of using a systems approach to particulate control rather than device control. Additional topic areas included novel control devices, high temperature/high pressure applications, fugitive emissions, measurement techniques, and economics and cost analysis.

Each volume of these proceedings contains a set of related session topics to provide easy access to a unified technology area.

Since the spirit and style of the panel discussion are not reproducible in print, the initial remarks presented by the panelists have been included in the volume to which their input to the panel pertained, in the interest of providing unified technological organization.

CONTENTS

Page

VOLUME I - CONTENTS v
VOLUME II - CONTENTS viii
VOLUME III - CONTENTS xii

Section A - Fabric Filters: Fundamentals

THEORY OF THE TEMPORAL DEVELOPMENT OF PRESSURE DROP ACROSS A FABRIC FILTER DURING CAKE INITIATION 1
E.A. Samuel

PULSE JET FILTRATION THEORY - A STATE-OF-THE-ART ASSESSMENT. . . 22
R. Dennis, L.S. Hovis

LABORATORY TECHNIQUES FOR DEVELOPING PULSE JET COLLECTORS. . . . 37
R.R. Banks, J.T. Foster

OFF-LINE PULSE-JET CLEANING SYSTEM 48
T.C. Sunter

Section B - Fabric Filters: Measurement Techniques

FIELD EVALUATION OF THE DRAG OF INDIVIDUAL FILTER BAGS 62
W.T. Grubb, R.R. Banks

A DUAL-DETECTOR BETA-PARTICLE BACKSCATTER GAUGE FOR MEASURING DUST CAKE THICKNESS ON OPERATING BAG FILTER AND ESP UNITS. . . . 77
R.P. Gardner, R.P. Donovan, L.S. Hovis

MIT FLEX ENDURANCE TESTS AT ELEVATED TEMPERATURE 91
J.T. Foster, W.T. Grubb

THE ONE-POINT IN-SITU CALIBRATION METHOD FOR USING A BETA-PARTICLE BACKSCATTER GAUGE FOR CONTINUOUSLY MEASURING DUST CAKE THICKNESS ON OPERATING BAG FILTER AND ESP UNITS 107
R.P. Gardner, R.P. Donovan, L.S. Hovis

Section C - Fabric Filters: Coal Fired Boilers

PULSE-JET FABRIC FILTER EXPERIENCE USING NON-GLASS MEDIA AT AIR TO CLOTH RATIOS OF 5 TO 1 ON A PULVERIZED COAL FIRED BOILER 121
G. Pearson, D.D. Capps

START-UP AND OPERATION OF A FABRIC FILTER CONTROLLING PARTICULATE EMISSIONS FROM A 250 MW PULVERIZED COAL-FIRED BOILER 132
C.B. Barranger, N. Spence, J. Saibini

Preceding page blank

PERFORMANCE OF A 10 MW FABRIC FILTER PILOT PLANT AND COMPARISON TO FULL-SCALE UNITS 148
W.B. Smith, K.M. Cushing, R.C. Carr

THE DESIGN, INSTALLATION, AND INITIAL OPERATION OF THE W.H. SAMMIS PLANT, UNIT 3 FABRIC FILTER 164
D.R. Ross, J.R. Howard, R.M. Golightley

RESULTS FROM THE FABRIC FILTER EVALUATION PROGRAM AT COYOTE UNIT #1 179
H.J. Peters, A.A. Reisinger, W.T. Grubb, M. Lewis

BAGHOUSE PERFORMANCE AND ASH CHARACTERIZATION AT THE ARAPAHOE POWER STATION 192
R.S. Dahlin, D.R. Sears, G.P. Green

AN EVALUATION OF FULL-SCALE FABRIC FILTERS ON UTILITY BOILERS. 210
J.W. Richardson, J.D. McKenna, J.C. Mycock

STATUS OF SPS INVESTIGATION OF HARRINGTON STATION UNIT 2 FABRIC FILTER SYSTEM 226
R. Chambers, D. Harmon

UPDATE OF SPS PILOT BAGHOUSE OPERATION 239
R. Chambers, S. Kunka, D. Harmon

THE USE OF SONIC AIR HORNS AS AN ASSIST TO REVERSE AIR CLEANING OF A FABRIC FILTER DUST COLLECTOR 255
A. Menard, R.M. Richards

Section D - Fabric Filters: Electrostatic Enhancement

ELECTROSTATIC STIMULATION OF REVERSE-AIR-CLEANED FABRIC FILTERS 287
D.A. Furlong, G.P. Greiner, D.W. VanOsdell, L.S. Hovis

ELECTRICAL STIMULATION OF FABRIC FILTRATION: ENHANCEMENT BY PARTICLE PRECHARGING 303
G.E.R. Lamb, R. Jones, W. Lee

ESFF AS A FIELD EFFECT 316
L.S. Hovis, G.H. Ramsey, R.P. Donovan

ELECTRICAL ENHANCEMENT OF FABRIC FILTRATION: PRECHARGING VS. BAG ELECTRODES 327
R.P. Donovan, L.S. Hovis, G.H. Ramsey

PERMEABILITY OF DUST CAKES COLLECTED UNDER THE INFLUENCE OF AN ELECTRIC FIELD 342
D.W. VanOsdell, R.P. Donovan, D.A. Furlong, L.S. Hovis

Section E - Fabric Filters: Practical Considerations

HIGH VELOCITY FABRIC FILTRATION FOR INDUSTRIAL COAL-FIRED BOILERS 357
G.P. Greiner, S. Delaney, L.S. Hovis

OPTIMIZING THE LOCATION OF ANTI-COLLAPSE RINGS IN FABRIC BAGS 382
J. Musgrove

PULSE JET ON-LINE CLEANING FILTER FOR FLY ASH 420
W.G. Wellan

TOP INLET VERSUS BOTTOM INLET BAGHOUSE DESIGN 431
R.M. Jensen

UPGRADE OF FLY ASH COLLECTION CAPABILITY AT THE CROMBY STATION 446
T.J. Ingram, R.J. Biese, R.O. Jacob

HIGH SULFUR FUEL, FABRIC FILTER STARTUP EXPERIENCE 460
P. Hanson, L. Adair, R.N. Roop, R.B. Moyer

FUNDAMENTAL STRATEGIES FOR CLEANING REVERSE AIR BAGHOUSES. . . . 482
M. Ketchuck, M.A. Walsh, O.F. Fortune,
M.L. Miller, M. Whittlesey,

Section F - Dry Scrubbers

DESIGN CONSIDERATIONS FOR BAGHOUSE - DRY SO_2 SCRUBBER SYSTEMS 494
O.F. Fortune, R.L. Miller

RESULTS OF BAGHOUSE AND FABRIC TESTING AT RIVERSIDE 506
H.W. Spencer III, Y.J. Chen, M.T. Quach

REACTIVITY OF FLY ASHES IN A SPRAY DRYER/FABRIC FILTER FGD PILOT PLANT 521
W.T. Davis, R.E. Pudelek, G.D. Reed

Section G - Plenary Session

FABRIC FILTRATION - AS IT WAS, HAS BEEN, IS NOW AND SHALL BE 536
E.R. Frederick

AUTHOR INDEX 551

VOLUME II

ELECTROSTATIC PRECIPITATION

Section A - Industrial Applications

MODELING OF WET BOTTOM AGITATOR SYSTEMS FOR ELECTROSTATIC PRECIPITATORS ON RECOVERY BOILERS 1
M.A. Sandell, R.R. Crynack

DESIGN AND PERFORMANCE OF ELECTROSTATIC PRECIPITATORS UTILIZING A NEW RIGID DISCHARGE ELECTRODE DESIGN 17
G.R. Gawreluk, R.L. Bump

DEVELOPMENT AND EVALUATION OF NEW PRECIPITATOR EMITTER ELECTRODE 35
R.L. Adams, P. Gelfand,

INDUSTRIAL APPLICATIONS OF TWO STAGE TUBULAR ELECTROSTATIC PRECIPITATORS 51
H. Surati, M.R. Beltran

Section B - Advanced Technology

PILOT DEMONSTRATION TWO-STAGE ESP TEST RESULTS 65
P. Vann Bush, D.H. Pontius

EVALUATION OF PRECHARGERS FOR TWO-STAGE ELECTROSTATIC PRECIPITATORS 84
G. Rinard, D. Rugg, M. Durham

INITIAL EXPERIMENTS WITH AN ELECTRON BEAM PRECIPITATOR TEST SYSTEM 96
W.C. Finney, R.H. Davis, J.S. Clements, E.C. Trexler, J.S. Halow, O. Tokunaga

EXPERIMENTS WITH WIDE DUCTS IN ELECTROSTATIC PRECIPITATORS . . . 111
E. Weber

A RECONCILIATION: WIDE VERSUS NARROW SPACED COLLECTING PLATES FOR PRECIPITATORS 126
D.G. Puttick

PULSE CORONA AS ION SOURCE AND ITS BEHAVIORS IN MONOPOLAR CURRENT EMISSION 139
S. Masuda, Y. Shishikui

VOLUME II CONTENTS (Cont.)

Section C - Fundamentals

A NEW CORRECTION METHOD OF MIGRATION VELOCITY IN DEUTSCH EFFICIENCY EQUATION FOR CONVERSION OF ELECTROSTATIC PRECIPITATOR SIZING FROM A PILOT-SCALE TO FULL-SCALE 154
F. Isahaya

DISTORTION OF PULSE VOLTAGE WAVE FORM ON CORONA WIRES DUE TO CORONA DISCHARGE 169
S. Masuda, H. Nakatani

ELECTROSTATIC PRECIPITATOR ANALYSIS AND SYNTHESIS 184
T. Chiang, T.W. Lugar

COMPUTER MODEL USE FOR PRECIPITATOR SIZING 194
G.W. Driggers, A.A. Arstikaitis, L.A. Hawkins

IMPROVEMENTS IN THE EPA/SRI ESP PERFORMANCE MODEL 204
M.G. Faulkner, R.B.Mosley, J.R. McDonald, L.E. Sparks

NUMERICAL SIMULATION OF THE EFFECTS OF VELOCITY FLUCTUATIONS ON THE ELECTROSTATIC PRECIPITATOR PERFORMANCE 218
E.A. Samuel

CORONA - INDUCED TURBULENCE 230
M. Mitchner, G.L. Leonard, S.A. Self

VELOCITY AND TURBULENCE FIELDS IN NEGATIVE CORONA WIRE-PLATE PRECIPITATOR 243
H.P. Thomsen, P.S. Larsen, E.M. Christensen, J.V. Christiansen

THE EFFECT OF TURBULENCE ON ELECTROSTATIC PRECIPITATOR PERFORMANCE 261
D.E. Stock

FACTORS LEADING TO ELECTRICAL BREAKDOWN OF RESISTIVE DUST LAYERS AND SUSTAINED BACK CORONA 271
P.A. Lawless, L.E. Sparks

ELECTRICAL BREAKDOWN OF PARTICULATE LAYERS 288
G.B. Moslehi, S.A. Self

ELECTROMECHANICS OF PARTICULATE LAYERS 306
G.B. Moslehi, S.A. Self

LATERAL PROPAGATION OF BACK CORONA IN TWIN-ELECTRODE TYPE PRECIPITATORS 322
S. Masuda, T. Itagaki

FIRST MEASUREMENTS OF AEROSOL PARTICLE CHARGING BY FREE ELECTRONS 337
J.L. DuBard, M.G. Faulkner, L.E. Sparks

VOLUME II CONTENTS (Cont.)

Section D - Operation & Maintenance

GAS FLOW DISTRIBUTION MODEL TESTING 349
D.R. Cook, J.M. Ebrey, D. Novogoratz

AIR FLOW MODEL STUDIES 369
L.H. Bradley

COLLECTING ELECTRODE RAPPING DESIGNED FOR HIGH EFFICIENCY ELECTRIC UTILITY BOILER ELECTROSTATIC PRECIPITATORS 384
A. Russell-Jones, A.P. Baylis

ELECTROSTATIC PRECIPITATOR AND FABRIC FILTER OPERATING AND MAINTENANCE EXPERIENCE 401
P.R. Goldbrunner, W. Piulle

Section E - Conditioning

ECONOMICAL FLY ASH COLLECTION BY FLUE GAS CONDITIONING 416
E.L. Coe, Jr.

EXPERIENCES AT DETROIT EDISON COMPANY WITH DECLINING PERFORMANCE OF SULFUR TRIOXIDE FLUE GAS CONDITIONING EQUIPMENT 430
L.A. Kasik, W.A. Rugenstein, J.L. Gibbs

ESP CONDITIONING WITH AMMONIA AT THE MONROE POWER PLANT OF DETROIT EDISON COMPANY 444
E.B. Dismukes, J.P. Gooch, G.H. Marchant, Jr.

FLY ASH CHEMISTRY INDICES FOR RESISTIVITY AND EFFECTS ON ELECTROSTATIC PRECIPITATOR DESIGN AND PERFORMANCE 459
H.J. Hall

Section F - Control Systems

A NEW ENERGIZATION METHOD FOR ELECTROSTATIC PRECIPITATORS MITSUBISHI INTERMITTENT ENERGIZATION SYSTEM 474
T. Ando, N. Tachibana, Y. Matsumoto

SOME MEASURED CHARACTERISTICS OF AN ELECTROSTATIC PRECIPITATOR OBTAINED USING A MICROCOMPUTER CONTROLLER 489
M.J. Duffy, T.S. Ng, Z. Herceg, K.L. McLean

ELECTROSTATIC PRECIPITATOR ENERGIZATION AND CONTROL SYSTEMS . . 499
K.M. Bradburn, K. Darby

APPLYING MODULAR MICROCOMPUTER CONTROL ELEMENTS IN A PRECIPITATOR CONTROL SYSTEM 521
I.M. Wexler

Section G - Plenary Session

THE CURRENT STATUS, FUTURE DIRECTIONS, AND ECONOMIC CONDITIONS IN THE APPLICATION OF ESP'S 534
S. Oglesby

AUTHOR INDEX 539

VOLUME III

ECONOMICS, MECHANICAL COLLECTORS, COAL CHARACTERISTICS, INHALABLE PARTICULATES, ADVANCED ENERGY AND NOVEL DEVICES

Keynote Address

PARTICULATE CONTROL TECHNOLOGY AND WHERE IT IS GOING xv
K.E. Yeager

Section A - Economic Comparisons

A COMPARISON OF A BAGHOUSE VS. ESP'S WITH AND WITHOUT GAS CONDITIONING FOR LOW SULFUR COAL APPLICATIONS 1
W.H. Cole

APPLICATION OF THE BUBBLE CONCEPT TO FUEL BURNING SOURCES AT A NAVAL INDUSTRIAL COMPLEX 12
C.S Thompson

Section B - Mechanical Collectors

CYCLONE PERFORMANCE: A COMPARISON OF THEORY WITH EXPERIMENTS 26
J.A. Dirgo, D. Leith

HIGH FLOW CYCLONE DEVELOPMENT 41
W.B. Giles

CYCLONE SCALING EXPERIMENTS 53
W.B. Giles

TEST METHODS AND EVALUATION OF MIST ELIMINATOR CARRYOVER 66
V. Boscak, A. Demian

Section C - Coal Characterization

FILTRATION CHARACTERISTICS OF FLY ASHES FROM VARIOUS COAL PRODUCING REGIONS 81
J.A. Dirgo, M.A. Grant, R. Dennis, L.S. Hovis

FLY ASH FROM TEXAS LIGNITE AND WESTERN SUBBITUMINOUS COAL: A COMPARATIVE CHARACTERIZATION 97
D.R. Sears, S.A. Benson, D.P. McCollor, S.J. Miller

USE OF FUEL DATABANKS FOR THE EFFECTIVE DESIGN OF STEAM GENERATORS AND AQC EQUIPMENT 114
N.W. Frisch, T.P. Dorchak

VOLUME III CONTENTS (Cont.)

Section D - Inhalable Particulate Matter

DEVELOPMENT OF INHALABLE PARTICULATE (IP) EMISSION FACTORS . . . 131
D.L. Harmon

INHALABLE PARTICULATE MATTER RESEARCH COMPLETED BY GCA/TECHNOLOGY DIVISION 141
S. Gronberg

RESULTS OF TESTING FOR INHALABLE PARTICULATE MATTER AT MIDWEST RESEARCH INSTITUTE 154
K. Wilcox, F. Bergman, J. Kinsey, T. Cuscino

INHALABLE PARTICULATE EMISSION FACTORS TEST PROGRAMS 166
J.W. Davison,

CHARACTERIZATION OF PARTICULATE EMISSION FACTORS FOR INDUSTRIAL PAVED AND UNPAVED ROADS 183
C. Cowherd, Jr., J.P. Reider, P.J. Englehart

CONDENSIBLE EMISSIONS MEASUREMENTS IN THE INHALABLE PARTICULATE PROGRAM 198
A.D. Williamson, J.D. McCain

Section E - Advanced Energy Applications

GAS CLEANING AND ENERGY RECOVERY FOR PRESSURIZED FLUIDIZED BED COMBUSTION 211
A. Brinkmann, P.M. Kutemeyer

DEMONSTRATION OF THE FEASIBILITY OF A MAGNETIC STABILIZED BED FOR THE REMOVAL OF PARTICULATE AND ALKALI 226
L.P. Golan, J.L. Goodwin, E.S. Matulevicius

TEST RESULTS OF A HIGH TEMPERATURE, HIGH PRESSURE ELECTROSTATIC PRECIPITATOR 241
D. Rugg, G. Rinard, J. Armstrong, T. Yamamoto, M. Durham

COAL-ASH DEPOSITION IN A HIGH TEMPERATURE CYCLONE 256
K.C. Tsao, A. Rehmat, D.M. Mason

DUST FILTRATION USING CERAMIC FIBER FILTER MEDIA — A STATE-OF-THE-ART SUMMARY — 271
R. Chang, J. Sawyer, W. Kuby, M. Shackleton, O.J. Tassicker, S. Drenker

HIGH TEMPERATURE AND PRESSURE PARTICULATE FILTERS FOR FLUID BED COMBUSTION 282
D.F. Ciliberti, T.E. Lippert, O.J. Tassicker, S. Drenker

VOLUME III CONTENTS (Cont.)

MOVING BED-CERAMIC FILTER FOR HIGH EFFICIENCY PARTICULATE AND ALKALI VAPOR REMOVAL AT HIGH TEMPERATURE AND PRESSURE . . . 300
D. Stelman, A.L. Kohl, C.A. Trilling

TESTING AND VERIFICATION OF GRANULAR BED FILTERS FOR REMOVAL OF PARTICULATES AND ALKALIS 318
T.E. Lippert, D.F. Ciliberti, R. O'Rourke

BAGHOUSE OPERATION IN GEORGETOWN UNIVERSITY COAL-FIRED, FLUIDIZED-BED BOILER PLANT, WASHINGTON, D.C. 335
V. Buck, D. Suhre

Section F - Novel Devices

PARTICLE CAPTURE MECHANISMS ON SINGLE FIBERS IN THE PRESENCE OF ELECTROSTATIC FIELDS 347
M.A. Ranade, F.L. Chen, D.S. Ensor, L.S. Hovis

PILOT DEMONSTRATION OF PARTICULATE REMOVAL USING A CHARGED FILTER BED 362
P.H. Sorenson

PILOT DEMONSTRATION OF MAGNETIC FILTRATION WITH CONTINUOUS MEDIA REGENERATION 370
C.E. Ball, D.W. Coy

Section G - Plenary Session

NOVEL PARTICULATE CONTROL TECHNOLOGY 386
S. Masuda

AUTHOR INDEX 406

THEORY OF THE TEMPORAL DEVELOPMENT OF PRESSURE DROP ACROSS A FABRIC FILTER DURING CAKE INITIATION

by: Eric A. Samuel
General Electric Environmental Services, Inc.
Lebanon, Pennsylvania 17042

ABSTRACT

The time variation of the pressure drop across a fabric filter characteristic of cake initiation in a new fabric as well as in a seasoned fabric is derived on the basis of the Carman-Kozeny hypothesis, which is well known for its prediction of the linear growth of pressure drop with time characteristic of cake filtration. The non-linear growth of pressure drop during cake initiation in a new fabric is associated with the filling of the voids within the fabric prior to cake establishment. The non-linear growth of pressure drop during cake initiation in a seasoned fabric is associated with non-uniform dust loading on the fabric. The non-uniform loading may either be an initial condition following cleaning, or be induced by inertial or external forces. Experimental evidence in support of the theory is presented.

INTRODUCTION

The time development of the pressure drop across a fabric filter, through which a constant flow is maintained, is usually discussed in terms of two separate processes: (1) cake initiation, and (2) cake establishment. The time variation of the pressure drop across the filter is in general non-linear during cake initiation, but is invariably linear after cake establishment, when the dust concentration in the gas is constant. The linear time variation of the filter pressure drop after cake establishment is consistent with Darcy's law(1), which expresses the proportionality of the filter pressure drop to the average superficial flow velocity, v, across the filter (air-to-cloth ratio) and the areal dust loading, W:

$$\Delta P = K_2 W v \tag{1}$$

The proportionality constant, K_2, is called the coefficient of specific resistance. There are two well known theories by which the coefficient of specific resistance of a filter cake may be calculated purely from knowledge of the size distribution of the particles comprising the filter cake, and the filter cake porosity. The two models are: (1) the Carman-Kozeny model, and (2) the Happel model. Each model is based on a different notion as to the origin of the flow resistance of the filter cake. The Carman-Kozeny model(2) is based on regarding the filter cake as an assembly of capillaries. In contrast, the Happel model(3) is based on regarding the filter cake as an assembly of independent spherical cells, each cell containing a single dust particle surrounded by a fluid-filled envelope.

The Carman-Kozeny and Happel models are widely used to characterize filter cakes across which the pressure drop increases linearly with time (filtration after filter cake establishment). There are currently no theories which deal with the non-linear time variation of the filter pressure drop characteristic of cake initiation. The present paper seeks to fill this need by proposing a theory, based on the Carman-Kozeny hypothesis, for predicting the shape of the filter pressure drop vs. time curve during cake initiation, including the transition to the linear regime characteristic of cake filtration. The time evolution of the filter pressure drop for a new fabric will be discussed separately from that for a seasoned fabric. The central idea relating to the development of the pressure drop across a new filter is the filling of the pores and voids within the fabric as a necessary precursor to the establishment of a filter cake. Non-uniform loading, either as an initial condition following cleaning or as a result of weaving flaws in the fabric; or induced by the action of inertial or external forces continously or discontinously present during filtration, is the central idea which will be seen to be consistent with anomalous time development of the filter pressure drop in seasoned fabrics. Three different, experimentally observed causes of non-uniform dust loadings on seasoned fabrics will be discussed: (1) non-uniform dust loading as an initial condition arising from non-uniform cleaning of the filter cake, (2) pinhole formation on weaving flaws in the fabric, and (3) influence on inertial forces or external forces (such as a corona field). The theoretical predictions of the filter pressure drop vs. time curves will be compared with corresponding experimental curves to demonstrate areas of agreement with experiment, and also to point out areas in which refinements to the proposed theory could be made.

The objective guiding the present investigation into understanding the shape of the filter pressure drop vs. time curve is in providing a fundamental theoretical basis for improving experimental characterizations of fabric filtration. The following benefits are expected to accrue from such a theory:
(1) Characterization of fabrics using flow measurements in addition to the presently used methods based on weave characteristics, fabric strength tests, and physical properties.
(2) Characterization of fabric-particle combinations with respect to pressure drop and cleanability using flow measurements.
(3) Evaluation of fabric finishes and fabric coatings based on flow measurements in the laboratory without recourse to extensive pilot testing.
(4) Using filter pressure drop vs. time curve as a diagnostic tool to detect abnormal operating conditions in fabric filter operation.
(5) Characterizing anomalous effects in fabric filtration, such as the effect of electric fields.

Better criteria for fabric selection, better understanding of fabric filter operation and better evaluation of schemes for fabric filter enhancements are the ultimate goals of the present work.

THEORY

NEW FABRIC

Introduction

The area of applicability of the conventional Carman-Kozeny model to only cake filtration may be extended to include cake initiation also by considering the filling up of the pores within the fabric as a necessary condition for the establishment of a filter cake. In the Carman-Kozeny model, the filtering medium is regarded as an assembly of identical capillaries of diameter, d_c, and length, L_c, such that: (1) the total internal surface area of the capillaries is equal to the total surface area of the particles comprising the filter medium, and (2) the total internal volume of the capillaries is equal to the volume of the voids in the filter medium. The flow rate through the capillaries is governed by the Hagen-Poisuelle law(4). When considering cake initiation within the Carman-Kozeny model, the surface area of the fabrics is added to the particulate surface area. Taking the instant when flow is first initiated through the new fabric as time t = 0, cake initiation will proceed up to a characteristic time, τ_f, which is the time required to entirely fill up the pores within the fabric. The filtration taking place after time $t = \tau_f$ may be characterized as cake filtration. The theory for the time development of the filter pressure drop during cake initiation is as follows.

Cake Initiation ($t \leq \tau_f$)

Assuming that there are n(t) Carman-Kozeny capillaries, each of effective length, L_c, and diameter, d_c, in an area, A, of the fabric characterized by a porosity, ε_f, and a thickness, L_f, formed by N(t) particles of known size distribution uniformly dispersed throughout the voids within the fabric, the Carman-Kozeny hypothesis may be expressed by the following equations:

$$n \pi d_c L_c = A A_f + N \pi \overline{d^2} \quad \text{(surface area relationship)} \qquad (2)$$

$$n (\pi/4) d_c^2 L_c = A L_f \varepsilon \quad \text{(volume relationship)} \qquad (3)$$

$$A L_f (1 - \varepsilon) = A V_f + N (\pi/6) \overline{d^3} \quad \text{(porosity definition)} \qquad (4)$$

$$A L_f (1 - \varepsilon_f) = A V_f \quad \text{(porosity definition)} \qquad (5)$$

$$A \eta_f u c \tau_f = A \rho_p L_f \varepsilon_f (1 - \varepsilon_p) \quad (\tau_f \text{ definition}) \qquad (6)$$

$$A \eta_f u c t = N \rho_p (\pi/6) \overline{d^3}$$ (mass conservation) (7)

$$Q/n = [\pi d_c^4 / (128 \mu L_c)] \Delta P$$ (Hagen-Poisuelle equation for one capillary) (8)

$$L_c = k L_f$$ (correction for capillary length due to tortous path through capillaries) (9)

$$Q = A u$$ (air-to-cloth ratio definition) (10)

In the above equations, Q is the total gas flow rate through area A of the fabric, u the air-to-cloth ratio, ΔP the pressure drop across the fabric filter, η_f the average collection efficiency of the fabric during cake initiation, ρ_p the true particulate density, and ε_p the porosity of the particulate packing within the fabric voids at time $t = \tau_f$ (at the end of the cake initiation period). The parameters, A_f and V_f, are measurable characteristics of the new fabric representing the fiber surface area and fiber volume per unit cloth area. The effective capillary length, L_c, will be expected to be larger than the fabric thickness, L_f, because of the winding path a gas molecule may take through the filter. If F(z) dz is the probability of finding particles whose diameters lie between z and z+dz in the particle distribution, the average diameters used in Equations (2), (4), and (7) are defined as follows:

$$\overline{d^q} = \int F(z) z^q dz / \int F(z) dz \tag{11}$$

The averages, $\overline{d^2}$ and $\overline{d^3}$ are sometimes written as d_s^2 and d_v^3 where d_s and d_v are called the surface diameter and volume diameter respectively. The diameter, $\overline{d^3}/\overline{d^2}$, is sometimes written as d_{sv} and called the surface to volume diameter.

Equations (2) to (10) may be solved for n, N, d_c, ε and ΔP. The solutions are:

$$N = 6 A \eta_f u c t / (\pi \rho_p \overline{d^3}) \tag{12}$$

$$= [6 A L_f / (\pi \overline{d^3})] (\varepsilon_f - \varepsilon) \tag{13}$$

$$n = 4 A \varepsilon / (\pi d_c^2 k) \tag{14}$$

$$d_c = 4 L_f \varepsilon / [(6/d_{sv}) (\varepsilon_f - \varepsilon) + (A_f/L_f)] \tag{15}$$

$$\Delta P = 32\, k^2\, \mu\, L_f\, u \,/\, (d_c^2\, \varepsilon) \tag{16}$$

$$\varepsilon = \varepsilon_f - \eta_f\, u\, c\, t \,/\, (\rho_p\, L_f) \tag{17}$$

$$= \varepsilon_f\, [\, 1 - (1 - \varepsilon_p)\, t/\tau_f\,] \tag{18}$$

$$\tau_f = \rho_p\, L_f\, \varepsilon_f\, (1 - \varepsilon_p) \,/\, (\eta_f\, u\, c) \tag{19}$$

Equation (18) shows that the effective porosity, ε, decreases linearly with time up to time $t = \tau_f$. Equation (16) coupled with Equations (18) and (19) yield the filter pressure drop as a function of time during cake initiation. The present model for cake initiation also shows the effective capillary diameter, d_c, and the effective number of capillaries, n, are also functions of time. The important feature in the model presented above is the relevance of the fabric characteristics, A_f and L_f, to the time development of the filter pressure drop during cake initiation. The fabric thickness, L_f, may be measured with the aid of a micrometer screw gauge. Equations (15) and (16) applied for the case of a new fabric without dust particles, suggest one method of obtaining the fiber area per unit fabric area (A_f). In the limit $\varepsilon \to \varepsilon_f$, the above two Equations give:

$$\Delta P = S_f\, u \tag{20}$$

$$S_f = 2\, k^2\, \mu\, A_f^2 \,/\, (\varepsilon_f^3\, L_f) \tag{21}$$

Equation (20) indicates a linear relationship between the pressure drop across a new fabric (without dust particles) and the air-to-cloth ratio. The proportionality constant, S_f, is usually called the fabric drag. A linear relationship between ΔP and u is also observed for a new fabric, for small u, as predicted by Equation (20). The parameter, A_f, could be obtained from the slope, S_f, of the ΔP vs. u graph, through Equation (21), provided ε_f and k are known. The porosity, ε_f, may be obtained from knowledge of the fabric thickness, L_f, the mass per unit area of the fabric, m_f, and the density, ρ_f, of the material comprising the fabric fibers, through the relationship:

$$m_f = \varepsilon_f\, L_f\, (1 - \varepsilon_f) \tag{22}$$

The correction factor, k, has been found to be in the range $\sqrt{3}/2$ to $\sqrt{5}/2$ for cake filtration(5). The correction factor, k, applicable to fabrics in the absence of dust particles has not been investigated. Because of the relatively open pore structure of fabrics in comparison with that of a filter cake which is formed from particles having large surface area, the correction factor, k, for a new fabric is likely to be closer to unity. The uncertainty in obtaining A_f from the filter drag, S_f, is directly related to the uncertainty with which k is known. Measurement of the surface area of a fabric by gas adsorption, usin the B.E.T. Equation, is an alternative method of obtaining A_f (6).

Cake Filtration ($t > \tau_f$)

The Carman-Kozeny hypothesis corresponding to cake filtration including the effect of the fabric, the pores within which are filled with dust particles during the earlier cake initiation period, may be expressed by the following equations:

$$n \pi d_c L_c = A A_f + N \pi \overline{d^2} \quad \text{(surface area relationship)} \qquad (23)$$

$$n (\pi d_c^2/4) L_c = A L_f \varepsilon_f \varepsilon_p + A (L - L_f) \varepsilon'_p \qquad (24)$$
(volume relationship)

$$A L (1 - \varepsilon) = A L_f (1 - \varepsilon_f) + A L_f \varepsilon_f (1 - \varepsilon_p) + A (L - L_f)(1 - \varepsilon'_p) \qquad (25)$$
(overall porosity definition)

$$A \eta_c u c t / \rho_p = N (\pi/6) \overline{d^3} \quad \text{(mass conservation)} \qquad (26)$$

$$A (L - L_f)(1 - \varepsilon'_p) = u c (t - \tau_f) / \rho_p \qquad (27)$$
(cake porosity definition)

$$L_c = k L \quad \text{(correction for capillary length)} \qquad (28)$$

In Equations (23) to (28), $(L - L_f)$ is the thickness of the filter cake, of porosity, ε'_p, growing on the fabric substrate, the pores within which have been filled with particles to a porosity, ε_p, during cake initiation. The porosities, ε_p and ε'_p, are not necessarily equal. The solutions to Equations (23) to (28) for the filter pressure drop, ΔP, and the Carman-Kozeny capillary characteristics, n, N, and d_c, are of identical form to those corresponding to cake initiation summarized in Equations (12) to (16). The overall porosity, ε, is given for the case of cake filtration by:

$$\varepsilon = \varepsilon'_p - \frac{\varepsilon'_p - \varepsilon_f \varepsilon_p}{1 + \dfrac{u c (t - \tau_f)}{\rho_p L_f (1 - \varepsilon'_p)}} \qquad (29)$$

with the characteristic time for cake initiation, τ_f, given by Equation (19). The effective porosity, ε, as given by Equation (29), also varies with time, as in the case of cake initiation, starting with the value $\varepsilon = \varepsilon_f \varepsilon_p$ at time $t = \tau_f$ and assymptotically approaching the value $\varepsilon = \varepsilon_p'$ for large times $t >> \tau_f$. The parameter, η_c, in Equation (26) represents the average collection efficiency (by mass) of the filter during cake filtration. In general, η_c is higher than η_f. The pressure drop, ΔP, for cake filtration is:

$$\Delta P = 32\ k^2\ \mu\ L\ u\ /\ (d_c^2\ \varepsilon) \qquad (30)$$

with the capillary diameter, d_c, given by Equation (15). The porosity applicable in Equation (30) is given by Equation (29).

The coefficient of specific resistance, K_2^{CK}, as predicted by the Carman-Kozeny model may be obtained by recasting Equation (30) in a form consistent with Darcy's law, and recognizing that the areal dust loading is given by:

$$W = L\ \rho_p\ (1 - \varepsilon) \qquad (31)$$

The desired result is:

$$K_2^{CK} = 32\ k^2\ \mu\ /\ [\ \varepsilon\ (1 - \varepsilon)\ d_c^2\ ] \qquad (32)$$

In the limit of $t >> \tau_f$, the Carman-Kozeny specific resistance approaches the constant value:

$$K_2^{CK} = 4\ k^2\ (1 - \varepsilon_p')\ /\ (\tau_p\ \varepsilon_p'^3) \qquad (33)$$

where τ_p is the average particle relaxation time, given by,

$$\tau_p = d_{sv}^2\ \rho_p\ /\ (18\ \mu) \qquad (34)$$

Equation (33) represents the conventional Craman-Kozeny result widely used in studies of cake filtration.

SEASONED FABRIC

Non-Uniform Cleaning

The salient features of the filter pressure drop vs. time characteristic of a seasoned fabric may be obtained by considering a simple distribution for the initial non-uniform areal loading resulting from the filter cleaning operation. The filter is regarded as being seasoned in the sense that the pores within the fabric are assumed to be saturated with particles, so that its operation may be described by cake filtration theory. Filter cleaning is assumed to result in two distinct areas, each area characterized by a constant areal loading. The above assumption is broadly consistent with experimental observations using reverse air cleaning in an abnormally operating fabric filter, which leaves patches of relatively clean fabric (lower areal loading, W_1) on a filter cake (having the higher loading, W_2). The simple non-uniform initial loading described above is illustrated in Figure 2(a). When constant volume flow through the cleaned filter is resumed, the initial velocity through the relatively cleaner patches will be higher than the average air-to-cloth ratio. Because of the above fact, the initial rate of increase of the filter pressure drop will be higher than that when the fabric loading is uniform over the entire fabric (in which case the flow velocity over the entire cake is the air-to-cloth ratio). As filtration continues, the rate of increase of the filter pressure drop assymptotically approaches the value characteristic of uniform areal loading over the whole fabric. The time development of the filter pressure drop across a seasoned fabric with a two-segment areal loading as an initial condition may be described by the following equations (see Figure 2(a)):

$$\Delta P = K_2 \; v_1(t) \; [\; W_1 + c \int_0^t v_1(t') \; dt' \;] \tag{35}$$

$$\Delta P = K_2 \; v_2(t) \; [\; W_2 + c \int_0^t v_2(t') \; dt' \;] \tag{36}$$

$$A_1 \; v_1(t) + A_2 \; v_2(t) = (A_1 + A_2) \; u \tag{37}$$

Equations (35) and (36) are expressions of Darcy's law for cake filtration through areas A_1 and A_2 respectively. Equation (37) expresses the constancy of the total flow rate through the filter at all times. These Equations do not appear to be amenable to an exact analytical solution. An approximate analytical solution to the above Equations may be obtained using perturbation theory, as follows:

$$\begin{aligned} \Delta P = {} & K_2 \; F_1 \; [\; W_1 + c \; u \; t - c \; \alpha_1 \; \tau_c \; (1 - e^{-t/\tau_c}) \;] \; (u - \alpha_1 \; e^{-t/\tau_c}) \; + \\ & K_2 \; F_2 \; [\; W_2 + c \; u \; t - c \; \alpha_2 \; \tau_c \; (1 - e^{-t/\tau_c}) \;] \; (u - \alpha_2 \; e^{-t/\tau_c}) \end{aligned} \tag{38}$$

where

$$F_1 = A_1 \; / \; (A_1 + A_2) \tag{39}$$

$$F_2 = A_2 \; / \; (A_1 + A_2) = 1 - F_1 \tag{40}$$

$$\alpha_1 = u - v_1(0) = (W_1 - W_2) \; F_2 \; u \; / (F_1 \; W_2 + F_2 \; W_1) \tag{41}$$

$$\alpha_2 = (F_1/F_2) \; \alpha_1 = (W_1 - W_2) \; F_1 \; u \; / \; (F_1 \; W_2 + F_2 \; W_1) \tag{42}$$

$$\tau_c = (W_1 - W_2) / [c (\alpha_1 + \alpha_2)]$$

$$= (F_1 W_2 + F_2 W_1) / (c u) \tag{43}$$

The time dependent velocities through the areas A_1 and A_2 are given by:

$$v_1(t) = \frac{1}{2} \{ (u - \alpha_1 e^{-t/\tau_c}) + \frac{\Delta P}{K_2 [W_1 + c u t - c \alpha_1 \tau_c (1 - e^{-t/\tau_c})]} \} \tag{44}$$

$$v_2(t) = \frac{1}{2} \{ (u - \alpha_2 e^{-t/\tau_c}) + \frac{\Delta P}{K_2 [W_2 + c u t - c \alpha_2 \tau_c (1 - e^{-t/\tau_c})]} \} \tag{45}$$

As will be seen below, the approximate analytical solutions to the time development of cake filtration initiated from a non-uniform loading, as summarized in Equations (38) to (45), compare reasonably well with the exact solution, which may be obtained by using numerical techniques. The time constant, τ_c, can be interpreted as being a characteristic time for the transition of the ΔP vs. t development from its initially high rate of increase to the linear rate of increase corresponding to uniform areal loading over the entire filter. The Equations (43) give a simple relationship for estimating this characteristic time from the initial areal loading distribution, the air-to-cloth ratio and the concentration.

Cake Filtration in the Presence of Pinholes

Experiments on cake filtration have indicated the presence of pinholes in the filter cakes formed on fabrics with weaving flaws. The pinholes were always centered around the weaving flaws; not every weaving flaw, however, had an accompanying pinhole. Pinhole formation appears to be also characterized by sudden jumps in the filter pressure drop. These pressure drop spurts may by due to the dynamics of pinhole rearrangement during filtration, and to pinhole filling in low velocity regions. Figure 2(b) shows a simplified representation of a filter cake containing pinholes. If the filter cake is assumed to comprise m identical pinholes, each of diameter, d_m, and if K_2 is the coefficient of specific resistance corresponding to those areas (A_1) of the filter cake containing no pinholes, the Equations governing the ΔP vs. t development are as follows:

$$\Delta P = K_2 (\eta_p c v_1 t) v_1 \tag{46}$$

$$\Delta P = K_p v_2 \tag{47}$$

with $$K_p = 32 \mu (c v_1 t) / [d_m^2 \rho_p (1 - \varepsilon)] \tag{48}$$

$$A_1\ v_1 + A_2\ v_2 = (A_1 + A_2)\ u \tag{49}$$

with $$A_2 = m\ (\pi\ d_m^2)/4 \tag{50}$$

As in previous discussions, Equation (46) is an expression of Darcy's law for filtration through area A_1. Equations (47) and (48) assume that the flow rate through the pinholes is governed by the Hagen-Poisuelle law(4). Equations (49) and (50) indicate incompressible flow at a constant flow rate through the filter. In these Equations, η_p is the collection efficiency of the filter cake having no pinholes (area A_1), ε the porosity of this filter cake, and ρ_p the true density of the particulate matter comprising the filter cake in area A_1. Since the length of the capillary corresponding to a pinhole is assumed to be the same as the thickness of the filter cake in area A_1, the velocities v_1 and v_2 through area A_1 and through the pinholes will be independent of time. The solutions to Equations (46) to (50) are:

$$\Delta P = \frac{K_2'}{[\ F_1 + (K_2'/K_p)\ F_2\ ]^2} \tag{51}$$

$$v_1 = u\ /\ [\ F_1 + (K_2'/K_p)\ F_2\ ] \tag{52}$$

$$v_2 = (K_2'/K_p)\ v_1 \tag{53}$$

$$= u\ /\ [\ (K_p/K_2')\ F_1 + F_2\ ] \tag{54}$$

with $$K_2' = \eta_p\ K_2 \tag{55}$$

$$F_1 = A_1\ /\ (A_1 + A_2) \tag{56}$$

$$F_2 = 1 - F_2 = A_2\ /\ (A_1 + A_2) \tag{57}$$

Equation (51) shows that the pressure drop acro-s a filter cake in the presence of pinholes will increase linearly with time, under the present assumptions. The slope of the ΔP vs. t line, however, will be different from the value, $K_2'\ u^2\ c$, expected in the absence of pinholes. The slope will be lower than the value in the absence of pinholes when $K_p < K_2'$, as is invariably the case.

Filtration in the Presence of Inertial Forces

A simple representation of a filter cake formed in the presence of inertial forces acting on the particles is shown in Figure 2(c). In this representation, the filter cake is composed of two discrete areas with different coefficients of specific resistance. The difference in the mean size of the particles comprising the two discrete areas is attributable to inertial forces in the presence of which larger particles are diverted from the flow streamlines. If f_1 and f_2 are the mass fractions of particles collected in areas A_1 and A_2 resulting in coefficients of specific resistance, K_{21} and K_{22}, and flow velocities, v_1 and v_2 for the two discrete areas, the Equations governing the time development of the filter pressure drop are:

$$\Delta P = K_{21}\ (c_1\ v_1\ t)\ v_1 \tag{58}$$

$$\Delta P = K_{22}\ (c_2\ v_2\ t)\ v_2 \tag{59}$$

$$A_1\ v_1 + A_2\ v_2 = (A_1 + A_2)\ u \tag{60}$$

or

$$F_1\ v_1 + F_2\ v_2 = u \tag{61}$$

with F_1 anf F_2 as defined in earlier discussions. In the above Equations, the concentrations, c_1 and c_2, in the gas streams entering the areas A_1 and A_2 are related to the concentration, c, of all particles entering the entire filter, by:

$$c_1\ A_1\ v_1 = c\ f_1\ u \tag{62}$$

$$c_2\ A_2\ v_2 = c\ f_2\ u \tag{63}$$

Equations (58) to (63) may be solved for the pressure drop, ΔP, and the velocities, v_1 and v_2, as:

$$\Delta P = [f_1\ f_2\ K_{21}\ K_{22}\ /\ (F_1^2\ f_2\ K_{22} + F_2^2\ f_1\ K_{21})\ ]\ u^2\ t \tag{64}$$

$$v_1 = [F_1\ f_2\ K_{22}\ /\ (F_1^2\ f_2\ K_{22} + F_2^2\ f_1\ K_{21})\ ]\ u \tag{65}$$

and similarly for v_2. The term between brackets in Equation (64) is the effective coefficient of specific resistance for the whole filter, which is seen to depend on A_1, A_2, f_1, f_2, K_{21} and K_{22}. It is informative to rewrite

Equation (64) in terms of the loadings, W_1 and W_2, on the areas A_1 and A_2, as:

$$\Delta P = K_{21}\ W_1\ u\ /\ [\ F_1 + F_2\ (K_{21}\ W_1)/(K_{22}\ W_2)\ ] \tag{66}$$

with

$$W_1 = (f_1\ c\ u\ t)\ /\ A_1 \tag{67}$$

$$W_2 = (f_2\ c\ u\ t)\ /\ A_2 \tag{68}$$

Equation (66) shows that the filter pressure drop will be larger than the value, K_1W_1u, corresponding to the entire filter being characterized by a coefficient of specific resistance equal to K_{21} and an areal loading W_1, if $K_{22}W_2 > K_{21}W_1$, i.e., if the filter drag for area A_2 is greater than for area A_1. The areal loadings W_1 and W_2 are equal if $f_1/A_1 = f_2/A_2$. For the above case, the filter pressure drop will be larger than $K_{21}W_1u$ if $K_{22} > K_{21}$. The Carman-Kozeny model for cake filtration shows that the coefficient of specific resistance, is in general, inversely proportional to d_{sv}^2, where d_{sv} is the surface-to-volume diameter of the particle distribution comprising the filter cake (see Equations (33) and (34)). Because of the above relationship, the filter pressure drop in the presence of inertial forces could be significantly different from that in the absence of inertial forces, in which case the entire filter cake can be characterized by a single coefficient of specific resistance.

Filtration in the Presence of External Forces

The theory in this section will be confined to those cases in which the velocity of the particles in the presence of the external forces is much greater than the flow velocity. In this case, the dust particles will be diverted away from the flow streamlines along the same paths. The profile of dust deposition, $\xi(x,t)$, at time t, x being the lateral distance along the filter cake with respect to the flow direction (see Figure 2(d)), normalized by the total mass of dust in the filter cake, will under the above assumption be independent of time. i.e.,

$$\xi(x,t)\ /\ (c\ u\ t) = \psi(x) \tag{69}$$

The influence of an externally induced non-uniform distribution on the filter pressure drop has also been discussed elsewhere(7). The Equations governing the time variation of the filter pressure drop for a filter of unit dimensions (unit filter area) are:

$$\Delta P = K_2\ \psi(x)\ c\ u\ t\ v(x) \tag{70}$$

$$\int_0^1 v(x)\ dx = u \tag{71}$$

with the equation defining the normalization of the function describing the dust deposition profile:

$$\int_{0}^{1} \Psi(x)\ dx = 1 \tag{72}$$

Solving Equations (70), (71), and (72) yields the expressions for the filter pressure drop and the velocity across a non-uniform filter cake formed in the presence of external forces, as:

$$\Delta P = K_2 \left\{ c\ u\ t \Big/ \left[\int_{0}^{1} dx/\Psi(x) \right] \right\} u \tag{73}$$

$$v(x) = \left[u/\Psi(x) \right] \left[1\Big/ \int_{0}^{1} dx/\Psi(x) \right] \tag{74}$$

The case of $\Psi(x) = 1$ yields the equations characteristic of uniform dust deposition discussed earlier. Because of the normalization condition imposed by Equation (72), $\Psi(x) \leq 1$, for every x. In this case, $\int dx/\Psi(x) \geq 1$, the equality applying to the case of uniform dust deposition, for which case the pressure drop is the greatest. The pressure drop in the case of non-uniform dust deposition is always lower than that for the case of uniform deposition, for the same areal loading of dust and the same coefficient of specific resistance.

EXPERIMENTAL RESULTS AND COMPARISON WITH THEORY

NEW FABRIC

Figure 3(a) shows the observed time development of the filter pressure drop for a new woven glass fabric. The measurement was carried out in a bench-scale apparatus comprising a flow straightening section, an expansion nozzle, a filter holder and an automatic flow controller. A maximum cloth area of 0.33 ft^2 could be attached to the filter holder in the above setup. The sigmoidal shape of the experimental ΔP vs. t curve indicates the presence of the two transitions associated with cake initiation and cake establishment. Figure 3(b) is the theoretically predicted ΔP vs. t curve obtained from Equations (16) and (30). Experimentally measured values for the parameters u, c, L_f, ε_f, ρ_p, and d_{sv} were used in generating the curve shown in Figure 3(b). The air-to-cloth ratio, u, was obtained using a calibrated orifice. The dust concentration was measured by weighing the dust collected in the filter over a known filtration time at constant u. The cloth thickness was measured with the aid of a micrometer screw gauge. The clean fabric porosity, ε_f, was measured with the aid of Equation(22). The surface to volume diameter, d_{sv}, was obtained from a measurement of the particle size distribution of a filter cake sample performed with the aid of a "Micromeritics Sedigraph" instrument which is based on the sedimentation technique. The parameters, A_f, ε_p, and ε'_p were systematically adjusted until reasonable agreement with the experimental curve of Figure 3(a) was obtained. The theoretical curve of

Figure 3(b) also displays two transitions. The first transition, in which the rate of increase of the filter pressure drop progressively increases up to a maximum value, is characteristic of cake initiation. The pres within the fabric are progressively filled during this stage. Figure (4) indicates the linear decrease of the effective porosity theoretically predicted for this stage. After reaching a minimum value corresponding to complete filling of the fabric pores, the effective porosity increses with time during the period of cake establishment. As filtration progresses in this stage the effective porosity assymptotically approaches the value characteristic of only the filter cake formed on the fabric substrate. Both the experimental and theoretical ΔP vs. t curves show a linear rate of increase of the filter pressure drop when sufficiently long time has elapsed since cake establishment. This linear rate is characteristic of cake filtration. The largest area of disagreement between experiment and theory occurs in the time range over which the transition between cake establishment and cake filtration takes place. The sharp transition theoretically predicted for this case is based on cake initiation ending sharply at time $t = \tau_f$ and cake establishment commencing immediately thereafter. Experimentally, this transition is seen to be much smoother than theoretically predicted. Simultaneous deposition of the dust within the fabric pores and on the fabric surface is an effect not included in the theory which will lead to a smoother transition.

SEASONED FABRIC

Non-Uniform Cleaning

Figure 5 compares the approximate solution to the time development of the pressure drop across a filter with non-uniform initial loadings, as given by Equation (38), with the exact numerical solution for Equations (35), (36), and (37). Figure 6 is a comparison between the approximate and exact solutions to the time development of the superficial velocity through the filter areas with relatively high and relatively low dust loadings. The error between the approximate and exact solutions for the pressure drop time development, which is the largest in the neighborhood of the knee which is characteristic of the transition between cake initiation and cake establishment, is seen to increase with decreasing fraction, A_1, of the relatively clean area following cleaning. For fractions, $A_1 < 0.5$, the agreement between the approximate and exact solutions to both pressure drop and velocity time development appears to be reasonably good.

The shapes of experimental ΔP vs. t curves are similar to those of the theoretical curves shown in Figure 5. However, a detailed comparison of experimantal data with theory appears to require more than a two-segment model treated in this paper. Experiments currently in progress attempt to obtain data relevant to comparison with a multi-sement model. Results of this comparison may be reported at a future date.

Filtration in the Presence of Pinholes

Measurements have been carried out in bench-scale and pilot-scale apparatus with fly ash having a log-normal size distribution characterized by a mean diameter and a standard deviation. These experiments appear to indicate an increasing density of pinholes (number of pinholes per unit area) with incraesing air-to-cloth ratio. The highest specific coefficient resistance characteristic of a given fly ash is obtained with closely woven fabric on which the filter cake showed no pinhole formation. Every pinhole has been found to be associated with a flaw in the fabric weave. However, not every fabric weave flaw is associated with a pinhole. The rate of change of filter pressure drop in the presence of pinholes is linear, as in the case of no pinhole formation, but with an anomalously low slope of $\Delta P/\Delta t$. This lower slope is due to the diversion of an appreciable amount of the filter flow through the pinholes. Slight fluctuations observed in the ΔP vs. t curve may be due to the dynamic process of pinhole movement across the fabric and of pinhole filling in the low velocity regions.

Filtration in the Presence of External Forces

Experimental results on fabric filter pressure drop in the presence of external forces have been reported elsewhere(7). The observed ΔP reduction in the presence of electric fields has compared favorably with the theory presented in this paper, which is based on an externally induced non-uniform dust deposition pattern. The central phenomenon which reduces the filter pressure drop of a non-uniform cake relative to that of a uniform cake (both having the same total mass of dust) is the diversion of a large part of the flow through the filter areas with the lower dust thickness while the external force diverts the particle deposition away from the flow streamlines.

CONCLUSION

The central theme throughout this paper has been the effect of non-uniform dust deposition patterns on the fabric filter pressure drop. Different phenomena are shown to result in different dust deposition patterns. Most observed physical phenomena observed in fabric filtration have been shown to be amenable to simple physical description. It is hoped that this paper will initiate experimental and theoretical investigations which will improve the models presented herein, and eventually improve our understanding of fabric filtration.

ACKNOWLEDGEMENT

Thanks are due to Tom Bechtel for his encouragement of the work presented herein.

REFERENCES

1. Billings, C. E. and Wilder, J. Handbook of Fabric Filter Technology. PB-200-648. National Technical Information Service, 1970.

2. Carman, P. C. Flow of Gases Through Porous Media. Academic Press, New York, 1956.

3. Happel, J. Viscous Flow in Multi-Particle Systems: Slow Motion of Fluids Relative to Beds of Spherical Particles. A. I. Ch. E. Journal. 4: 197 - 201, 1958.

4. Rudnick, S. N. and First, M. W. Specific Resistance (K_2) of Filter Dust Cakes: Comaprison of Theory and Experiments. In: Proceedings of the Third Symposium on Fabric Filters for Particulate Collection. EPA-600/7-78-087. U. S. Environmental Protection Agency, 1978. p 251 - 288.

5. Dalla Valle, J. M. Micromeritics, The Technology of Fine Particles. Pitman, New York, 1948.

6. Brunauer, S. Physical Adsorption. Princeton University Press, Princeton, New Jersey, 1943.

7. Chiang, T. K., Samuel, E. A. and Wolpert, K. E. Theoretical Aspects of Pressure Drop Reduction in a Fabric Filter with Charged Particles. In: Proceedings of the Third Symposium on the Transfer and Utilization of Particulate Control Technology, Volume III. Particulate Control Devices. EPA-600/9-82-005c. U. S. Environmental Protection Agency, Research Triangle Park, N. C. 27711, July 1982. p 250 - 260.

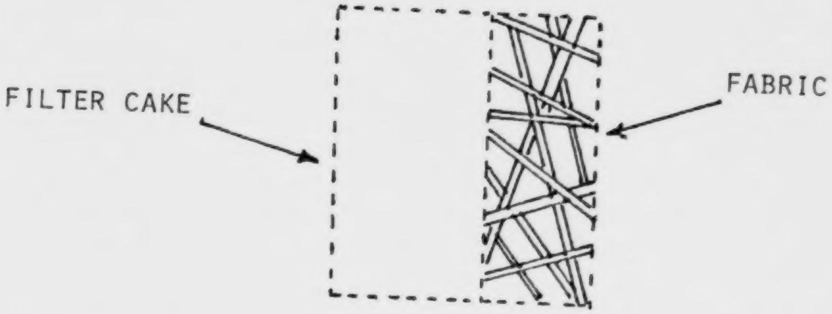

Figure 1. Representation of a fabric substrate. In the present work, the filling up of the voids within the fabric substrate is referred to as cake initiation. Complete filling of the substrate voids, referred to as cake establishment, is assumed to be a necessary precursor to cake filtration, which is characterized by a linear increase with time of the filter pressure drop.

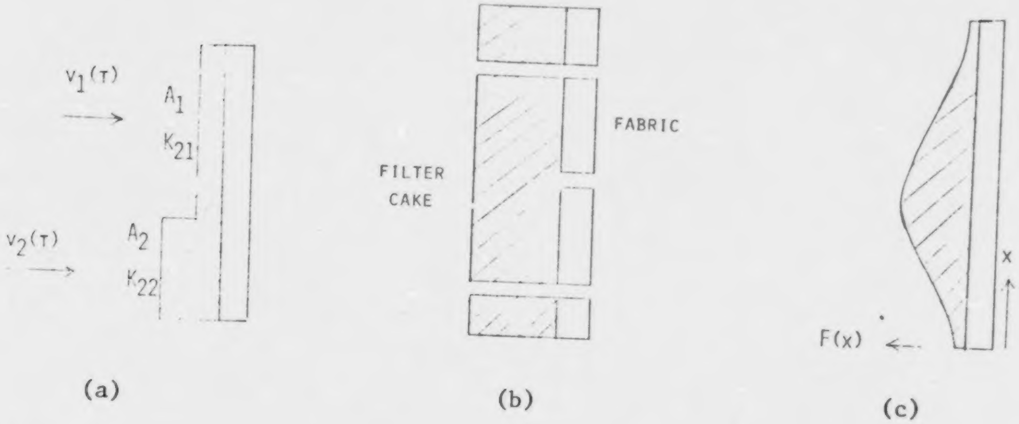

Figure 2. Non-uniform dust loadings on seasoned fabrics arising from different physical conditions: (a) improperly cleaned filter resulting in areas of low dust loading and areas of high dust loading, (b) filter with pinholes formed on fabric weave flaws, (c) filter with externally induced non-uniform dust deposition pattern; the external force draws the particles away from the flow streamlines and llows the flow to pass through the filter areas with relatively low dust loadings.

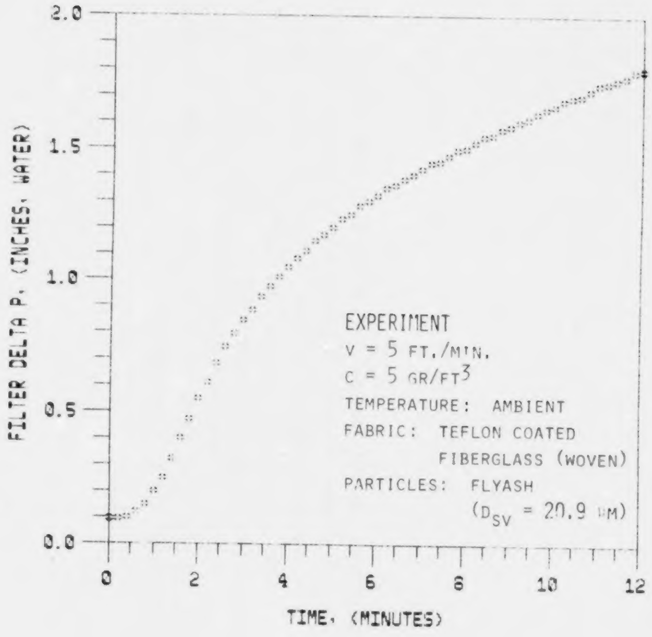

Figure 3(a). Experimental ΔP vs. t curve obtained at ambient temperature in a bench-scale patchwork filter apparatus.

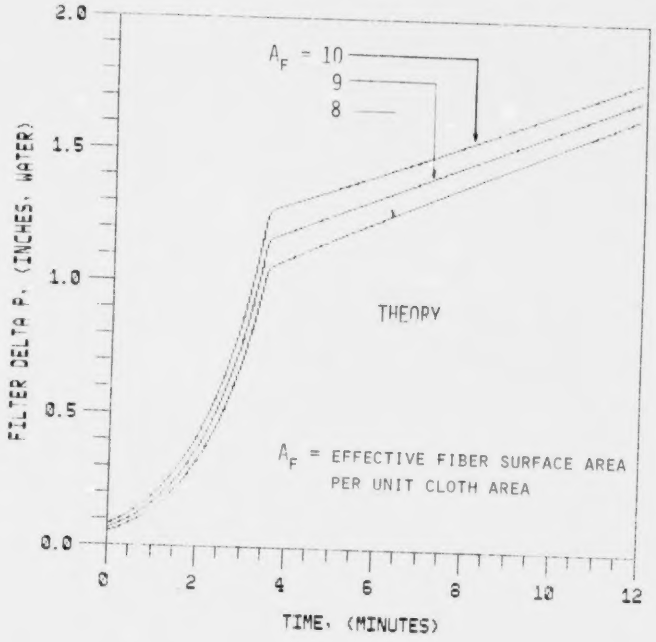

Figure 3(b). Theoretical P vs. t curve based on Equations (29) and (30) corresponding to the experimental conditions of Figure 3(a).

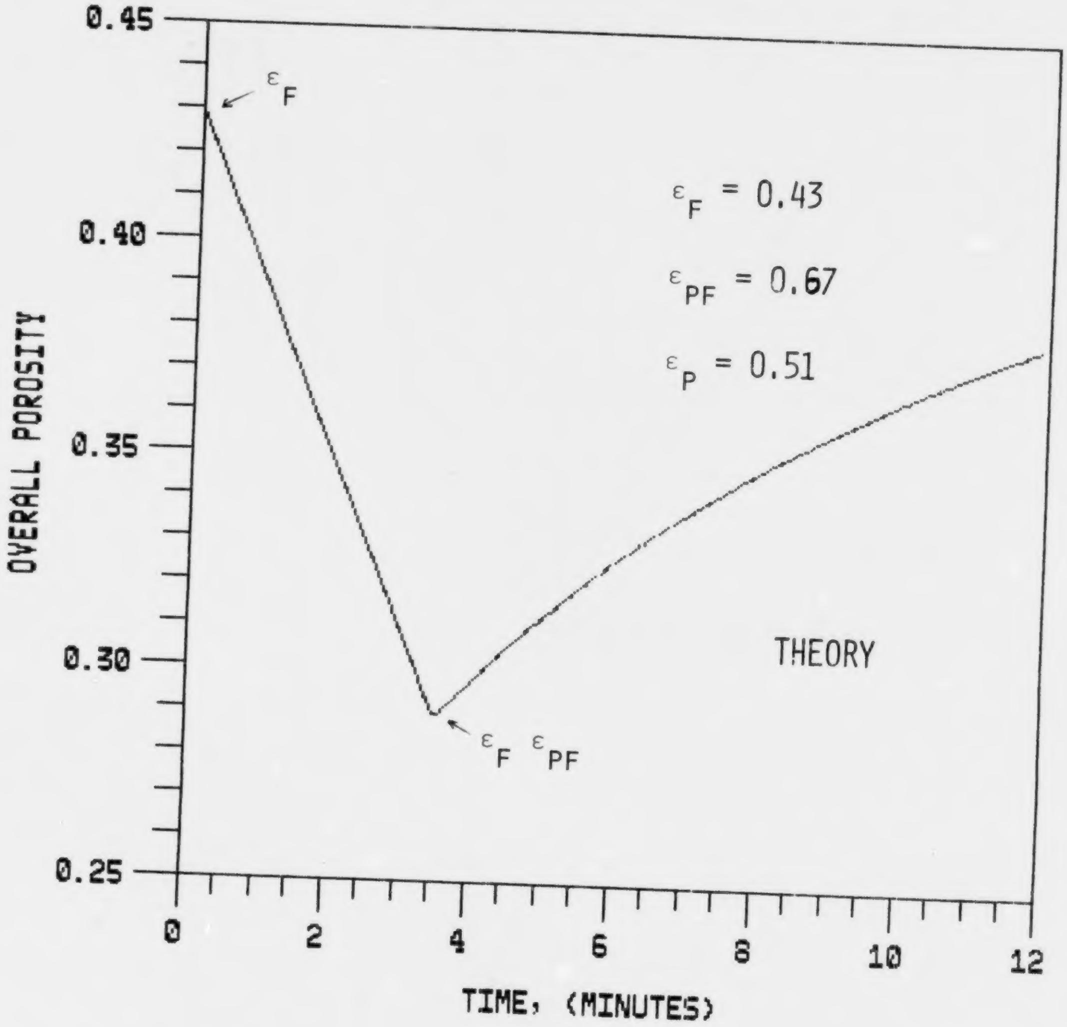

Figure 4. Theoretical prediction of the effective porosity during cake initiation, cake establishment, and cake filtration, based on Equation (29). The minimum porosity is reached at the instant when all the pores within the fabric are filled up (cake establishment). After this time the porosity increases and assymptotically approaches the porosity of the filter cake.

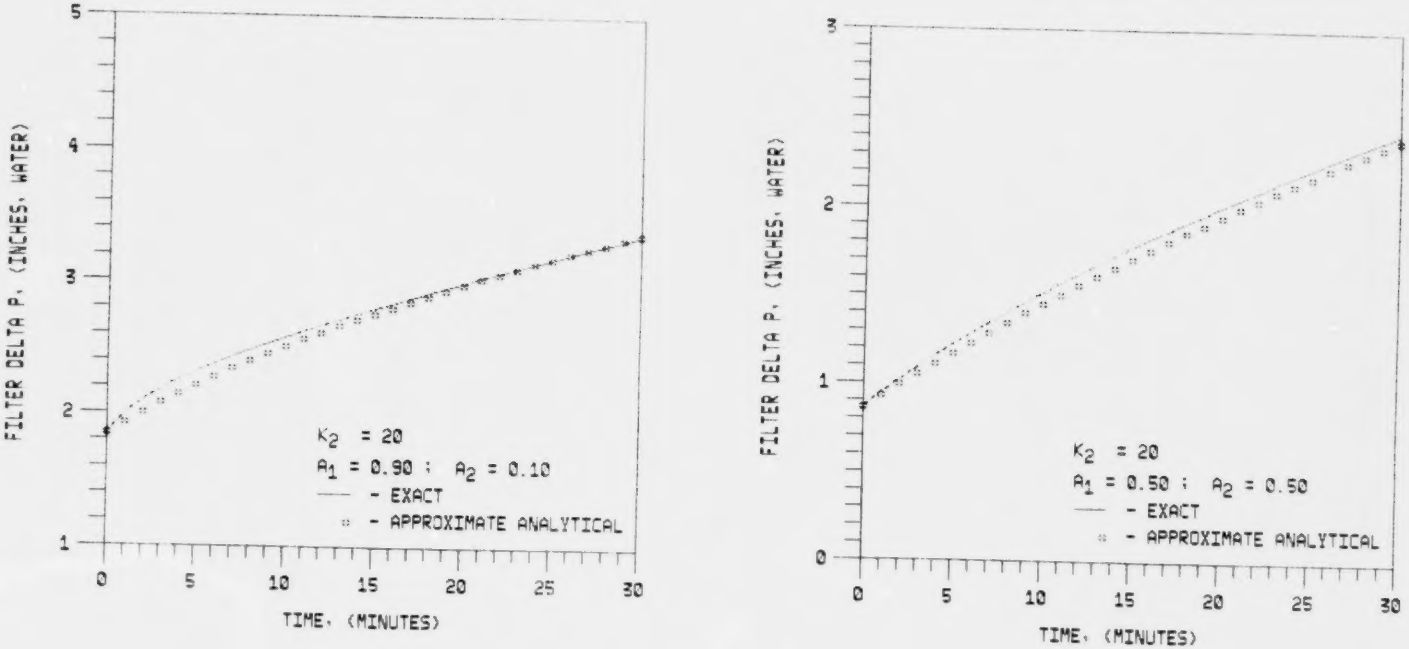

Figure 5. Comparison of the exact(numerical) and approximate analytical (Equations (38) to (43)) solutions to the time development of the filter pressure drop across a seasoned filter with a non-uniform initial dust loading arising from improper cleaning. In this example the following parameters were assumed: air-to-cloth ratio = 2.0 ft/min; inlet loading = 3.0 gr/acf; dust loading on relatively clean area (A_2) = 0.013 lb/ft^2; dust loading on relatively dirty area (A_1) = 0.064 lb/ft^2; τ = 21 min. The units of the coefficient of specific resistance, K_2, are: inches water/(ft/min)/(lb/ft^2).

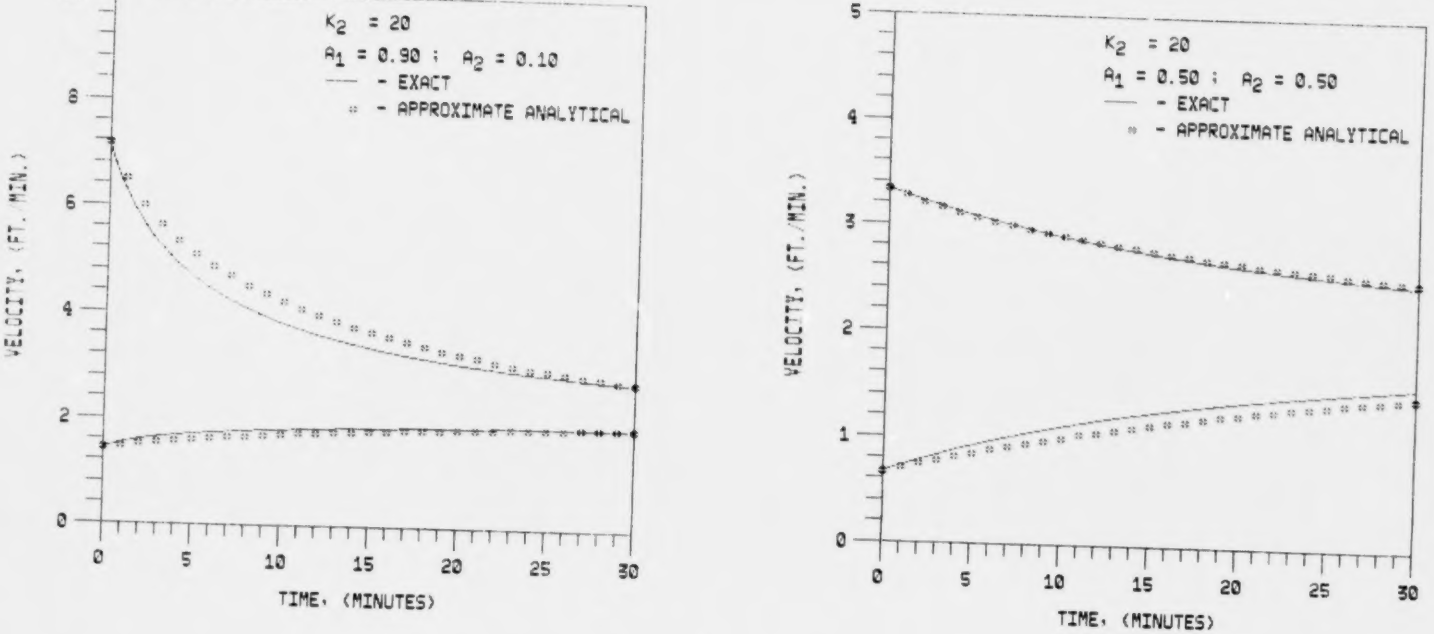

Figure 6. Comparison of the exact (numerical) and approximate analytical (Equations (43) and (44)) solutions to the time development of the filter velocities across the seasoned filter having the pressure drop time development shown in Figure 5.

PULSE JET FILTRATION THEORY - A STATE-OF-THE-ART ASSESSMENT

by: Richard Dennis
GCA/Technology Division
213 Burlington Road
Bedford, MA 01730

Louis S. Hovis
Industrial Environmental Research Laboratory
U.S. Environmental Protection Agency
Research Triangle Park, NC 27711

ABSTRACT

The relevant literature on pulse jet filter theory and applications was assessed to develop coherent guidelines for designing predictive filter models. Observations of several foreign and U.S. researchers not previously subjected to rigorous comparisons showed that there is a considerable unanimity in technical perspectives when data and theories are viewed from a common baseline. Common misconceptions are clarified such as (a) the "air bubble" that descends through the bag during pulsing, (b) dust removal by air flushing rather than mechanical projection from a rapidly decelerating fabric, or (c) failure to recognize that only a small (1-5 percent) fraction of dust dislodged by pulse action actually reaches the hopper. Data from several sources suggest that not only the compressed air pressure, but also the rate of pressure rise within a bag and the fabric mobility determine dust removal effectiveness. Unique pairings of pressure intensity and dust dislodgeability (as defined by dust/fabric adhesive properties) appear essential for complete removal of surface dust layers. When air jets are correctly placed for specified pulse jet parameters, the surface dust layer should be completely dislodged. Various investigators also suggest that the residual dust (i.e., the irreversibly embedded dust) is relatively constant for fixed dust/fabric combinations.

This paper has been reviewed in accordance with the U.S. Environmental Protection Agency's peer and administrative review policies and approved for presentation and publication.

INTRODUCTION

The pulse jet cleaning concept introduced commercially during the late 1950's (1,2,3) sees extensive application, particularly where stability in gas flow rates, space economy, and a capability to handle high dust loadings (up to 25 g/m^3) are sought. Despite many successful installations, relatively few investigators have attempted to describe the cleaning process from a theoretical perspective. Furthermore, the high costs associated with sophisticated instrumentation, along with complex interactions among key variables contributing to the cleaning process have restricted most functions for predicting collector performance to semi-empirical equations. Their proper application usually requires one set of actual performance data for the dust/fabric combination of interest with all relevant design and operating parameters clearly specified. The above constraint applies to available models for predicting performance of both single and multi-bag units. Optimum application of pulse jet units has been hampered by certain common misconceptions that still prevail despite the fact that the experimental findings of several investigators should have long since dispelled them.

For example, a precursor cleaning technique, "Reverse-Jet Cleaning," developed by Hersey and introduced during the early 1950's, (2,4) relied on a high velocity, 1830 to 2440 m/min (6000 to 8000 ft/min) air jet directed against the clean air (outside) surface of a bag to remove the dust cake. Dust dislodgement by this process is correctly attributed to a combination of aerodynamic forces and fabric flexing at the point of jet impact, the latter effect causing cake fracture and severance of adhesive bonds. What has been ignored by some individuals, however, is the fact that air velocities produced during pulse jet cleaning are at least 100 times smaller than those encountered with the Hersey collectors. Hence, dust removal by air drag alone is relatively unimportant with pulse jet devices (3,5,6).

The persistence of false impressions is partly attributable to a failure to publish relevant experimental data in readily accessible journals, as well as to the sparsity of overview documents in which the studies and concepts of various investigators are compared and evaluated. A primary objective of this paper is to review various independent studies to determine which concepts relate best to pulse jet collector performance with specific emphasis on the pulse jet cleaning process. Although most field and/or performance tests have concentrated on application problems rather than the theoretical aspects of pulse jet systems, their appraisal has proven helpful in evaluating current filtration and cleaning theories.

COMMON MISUNDERSTANDINGS OF PULSE JET COLLECTOR OPERATION

PROPOSED BUBBLE CLEANING CONCEPT

Pulse jet cleaning is still described in some documents, accompanied by imaginative illustrations, as the rapid passage of an air bubble through the bag. During its descent, localized fabric distension is supposed to loosen the dust layer while the transient reverse flow completes the dust dislodgement from the upstream filtering surface. Although there is some truth in the above concept, it overlooks the fact that typical pulse durations of at least 0.06 sec far exceed the time for the shock wave to travel to the bottom of conventional felt bags, roughly 0.0036 and 0.01 sec, respectively, for 1.22 m and 3.05 m (4 ft and 10 ft) long bags (3,5,7). In reality, while the pressure front is advancing, the continued arrival of pulse air, at successively increasing rates until the solenoid valve is fully open, maintains the inflating pressure behind the front. Because pulse air entry continues well after the bottom of the bag is fully pressurized, the concept of an advancing bubble is not consistent with the mechanics of the process which can be inferred analytically and has been confirmed by actual measurements (3,5).

Observed Pressure Changes During Pulsing

If, for analytical purposes, it is assumed that none of the pulse air injected into a bag escapes over the time span required for the solenoid valve to open fully (0.01 sec), the time frame for pressure changes at the top and bottom of a 1.22 m (4 ft) bag following pulse initiation can be represented by Figure 1. Variations in bag pressure with distance from the top of the bag and time following pulse initiation are shown in Figure 2. Note that the axial, top to bottom, pressure gradient diminishes when the "full-open" pressure front has reached the bottom of the bag 0.0136 sec after valve activation. Simultaneous clean-side pressure profiles determined at two locations for a 1.83 m (6 ft) long felt bag, Figure 3, display the characteristic time lag indicated in Figure 1 over the 0.01 sec valve opening period (3). Pressure/time traces for Figures 3 and 4, however, also reveal that once the valve is fully open, the pressure decreases rapidly to a lower and nearly constant level where it remains until the solenoid valve begins to close. Figure 4 depicts more sophisticated pressure measurements on a 1.22 m x 11.4 cm bag under typical filtration conditions (5). The abrupt pressure reduction is attributed to the sudden dislodgement of the surface dust layer that facilitates venting of pulse air in the reverse flow direction. The fact that pressure gradients remain nearly constant (except for the valve opening and closing intervals) also suggests that negligible dust removal takes place once the valve is fully opened (5). It has also been observed that pulse durations as long as 30 sec produced no discernible differences in dust removal and/or operating pressure loss across the baghouse (5).

Postulated Bag Deformation During Pulsing

In the preceding discussion, the physical response of the bag to pressure imbalance was not considered except for the erroneous bubble concept. In the following paragraphs, the temporal and spatial aspects of bag deformation are examined for what are considered to be the bounding conditions for bag motion. Let us first assume that the fabric is infinitely flexible such that any part of the bag will be displaced almost immediately when subjected to a pressure differential. The extent of the displacement or inflation depends on how tightly the bag is fitted to the supporting cage; i.e., the degree of slack available. Additionally, the greater the combined areal density of the bag and its dust loading, the slower will be its response to a pressure change. Hence, very rapid inflation is associated not only with high flexibility but also a low system mass, as will be discussed later. When the fabric response is nearly instantaneous, the bag contours at selected times after pulse initiation should appear as if they had been generated by thrusting a frustum of an inverted cone into the bag at sonic velocity, Figure 5. The maximum diameter for the hypothetical cone will be approximately the same as that for the fully inflated bag. Maximum lateral displacement at the top of the bag occurs when the valve is fully open (after 0.01 sec). Because of the sonic lag, however, maximum displacement will be seen 0.0136 sec later at the bottom of the bag. The purported bubble effect, Figure 5a, is shown for reference.

Predicted Bag Response to Pulse Pressure

Under actual filtration conditions, inherent fabric stiffness plus the inertia of the combined dust/fabric mass will cause an appreciable lag in bag response to internal pressurization. The initial radial motion imparted to the dust-laden fabric, as described in earlier studies (5,8), consists of a rapid shift or "flip flop" from the normal deflated (filtering) position to its inflated state where the fabric no longer presses against its supporting cage. The approximate lateral (radial) movement can be estimated by:

$$\rho \frac{d^2 r}{dt^2} + \frac{r}{G} = \Delta p \qquad (1)$$

where ρ is the combined dust/fabric mass per unit area, G the flexing parameter, r the radial or lateral displacement, and Δp the pressure acting on the fabric. By equating the restoring force, r/G, that opposes fabric flexure to the opposing acceleration force

$$\rho \frac{d^2 r}{dt^2} \text{ or } \rho \bar{a},$$

and by treating the lateral displacement or "flip flop" as a simple harmonic motion; i.e.,

$$\bar{a} = 4\pi^2 f^2 r = 4\pi^2 r/t^2 \qquad (2)$$

the characteristic oscillation period, τ, for a fabric element, may be estimated as $2\pi\sqrt{G\rho}$. Therefore, the time required for the fabric to attain its maximum velocity from a dead start becomes $\tau/4$ or roughly $1.6\sqrt{\rho G}$. When $\tau/4$ is less than or equal to the time required for the pulse to reach its maximum pressure differential (∿0.01 sec), the fabric tends to move with the pulse. Conversely, if $\tau/4$ is much greater than the pulse rise time, a sluggish response should be anticipated with poor cleaning characteristics until the pulse is lengthened. Based on prior determinations of G for wool and Dacron felts (5), $\tau/4$ is expected to range from 0.005 to 0.01 sec, thus suggesting a minimal delay in bag inflation for many commercial applications. This paper briefly reviews the roles of the flexing parameter, G, gross fabric areal density, ρ, and fabric tensile properties as they apply to fabric cleaning intensity.

PROPOSED "DEPTH" FILTRATION CONCEPT

Cake Versus Depth Filtration

There are many misconceptions and divergent opinions as to how pulse jet collectors operate. For example, felt filtration is sometimes incorrectly described as "depth" filtration, implying that the fabric functions as a deep-bed filter in which high bed porosity allows the interstitial fibers to play a commanding role in particle capture. Although base line efficiencies for most felts exceed those for conventional woven fabrics, 90 and 40 percent, respectively, with atmospheric dust (5), it is the surface dust layer and not the felt substrate that is mainly responsible for the high efficiency collection. Except for brief periods, about 0.1 sec, when flow direction is reversed by the pulse action, fabric surface loadings fall in the same range, 400 to 1000 g/m^2 (5,6,8), seen for mechanically shaken or reverse-air-cleaned woven fabrics. Therefore, aside from a transient recovery period, primary dust capture should be attributed to sieving by the surface dust layer, whose presence has been well defined photographically (5,9,10).

Some descriptions of pulse jet cleaning also suggest that the maximum surface loading is equal to the amount of dust deposited on the felt during the nominal 1 to 2 minute filtration cycle. If this were so, fabric loadings, W, immediately before cleaning would be expected to range from 2 to 70 g/m^2 rather than the 400 to 800 g/m^2 actually determined by experimental measurement (5,9,11,12,13). Furthermore, since steady state operation demands equal dust arrival and removal rates, the only dust remaining on the fabric immediately after pulsing must be that imbedded within the felt. Were this the actual case, there would be some justification for the "depth" filtration concept.

Pressure Loss Considerations

The classical relationship for expressing total pressure loss, P, across a dust-laden fabric, i.e.,

$$P = P_R + P_D = P_R + K_2VW \qquad (3)$$

is often incorrectly applied to pulse jet filter systems. In fact, Equation (3) should only be used when total pressure loss can be divided into two distinct components: P_R, the pressure loss across the fabric per se with or without its residual dust holding, W_R, and P_D, the pressure loss across the surface dust layer. P_D depends upon the specific resistance coefficient for the dust, K_2; the filtration velocity, V; and the areal density, W, for the dust cake. Based upon average values noted for P_R, $\sim$0.1 kPa, the surface dust loadings of 2 to 70 g/m^2 cited earlier could never be expected to produce the much higher pressure losses observed during typical pulse jet filtration, Figure 6. As discussed later, this problem arises because Equation (3) fails to account for the actual surface loadings of 400 to 800 g/m^2 that contribute significantly to total system pressure loss.

UNIQUE FEATURES OF PULSE JET OPERATION

DISLODGEMENT FORCES AND CAKE SEPARATION

Most investigators agree that the impulse imparted to a fabric, by mechanical shaking or high pressure air pulse, plays a major role in fabric cleaning. Additionally, the degree of cleaning has been related to the quantity of dust on or within the fabric (6-8). Regardless of fabric type, the dust separating force, F_s, has been defined as the product of the local fabric loading, W, and the maximum deceleration of the supporting fabric beneath it; i.e., $F_s = W a_{max}$. Typical a_{max} values have been indicated as 1 g for simple bag collapse systems and 3 to 5 g for mechanically shaken bags (7). In the case of pulse jet collectors, however, the combined dust/fabric mass may experience decelerations in the 250 g range, which afford the potential for 100 percent dislodgement of the dust cake as compared to 10 to 50 percent for reverse flow and mechanically cleaned devices (5,8,9,12).

Irrespective of cleaning method, dust removal can occur only when F_s exceeds the local adhesive force, F_A, whose magnitude is established by (a) the unique interfacial bonding properties for a specific dust/fabric combination and (b), any pre-pulse mechanical disturbance of the dust layer. Additionally, past studies have shown that dust separation occurs principally at the interface between the dust cake and the fabric where the adhesive bonds are considerably weaker than those within the dust cake (5,8,9).

PROJECTED DISTRIBUTION FOR ADHESIVE FORCES

When a completely cleaned or new fabric is first placed in service, the dust cake and the adhesive forces are expected to be uniformly distributed, barring significant particle fractionation. On the other hand, instantaneous values for separating forces can vary from point to point depending on the method of cleaning and type of fabric support. The first dust to be dislodged is that from areas where local adhesive forces have been exceeded. The fact that only 10 percent removal takes place does not preclude near uniformity for initial adhesion levels because adhesive forces for the uncleaned regions need only exceed the separating forces by a small amount. The "uniformity" concept becomes even more tenable based on the observation that repetitive collapsing, shaking, or pulsing always removes additional dust. Such secondary dislodgement may be attributed to partial severance of adhesive bonds during the first cleaning that decreases adhesion levels over much of the uncleaned surface. After many successive filtration and cleaning cycles, cake adhesion values are expected to envelop a fairly broad force spectrum such as that shown in Figure 7 for a fly ash/cotton fabric system. If it is assumed that the napped cotton surface provides about as many contact points as those for a Dacron felt and hence approximately the same adhesive properties, extrapolation of the Figure 7 adhesion/force curve suggests that separating forces must exceed 200 N/m^2 to obtain complete dust cake separation with a single pulse.

The computation of F_s values for pulse jet systems, as indicated below, shows that separating forces well in excess of those essential for complete cake dislodgement, roughly 1000 to 2000 N/m^2, are attainable.

FABRIC DECELERATION AND SEPARATING FORCES

Maximum Projected Dust Dislodgement

Maximum fabric deceleration, a_{max}, which is imparted to the overlying dust layer, W, determines the separating force exerted at the dust/fabric interface when further bag inflation is constrained by bag tensile properties. Dennis and Wilder have calculated a_{max} from the relationship (5,8),

$$a_{max} = \frac{G}{\sqrt{\rho M_e}} \cdot d\,(\Delta p)/dt \qquad (4)$$

Increasing values for the flexibility parameter, G, and the rate of bag pressure increase, $d(\Delta p)/dt$, will increase bag deceleration. Conversely, an increase in gross bag weight, ρ, and stretch properties as defined by the elongation parameter, M_e, will produce the opposite effect. Additional data for the terms appearing in Equation (4) are summarized in Table 1. It is emphasized that bag deceleration rates of 125 to 250 g's (which should be easily obtainable in routine field applications), coupled with typical fabric dust loadings of 400 to 800 g/m^2 will generate unit separating forces of 500 to 2000 Pa. Thus, if the surface fiber dispersion for Dacron felts can be approximated by that for a sateen weave cotton (as visual inspection seems to indicate) the force levels should suffice to dislodge completely the surface dust layer.

TABLE 1. FABRIC AND PRESSURE PARAMETERS FOR ESTIMATING MAXIMUM DECELERATION OF A LIGHTWEIGHT, MODERATELY STIFF DACRON FELT

Parameter	Typical values[a] (cgs units)	Definition
G	5.51×10^{-5} cm^2 - s^2/g	Radial displacement per unit pressure
M_e	2.04×10^{-6} cm^2 - s^2/g	Elongation per unit pressure
ρ	1.26×10^{-1} g/cm^2	Combined dust/fabric areal density
$d(\Delta p)/dt$	2.49×10^{6} g/cm - s^3	Rate of pressure increase
a_{max}	2.71×10^{5} cm/s^2 (276 g)	Maximum dust (or fabric) deceleration

[a] Nominal values for tests described in Figure 6.

Conditions Preventing Complete Surface Cleaning

It is recognized that complete dislodgement of the dust cake may not always be attainable. For example, if the time required to establish a sufficiently heavy dust layer for removal by a fixed set of pulse jet parameters exceeds that for a normal 8-hour shift, complete dust removal and, hence, steady state operation may not be obtained. Additionally, improper jet placement may result in secondary air entrainment from the "dirty" side of the bag that can actually increase dust deposition on the upper end of the bag during the pulse interval. In the absence of cleaning, a fraction of the upper fabric surface is lost just as effectively as if the bag were actually shortened. Finally, any dust subject to hydration or other chemical reactions may undergo a cementing action that reduces cake porosity and greatly increases its adherence to the fabric. This problem is accentuated when a filter remains idle in atmospheres where moisture condensation, extraneous reactants, and high temperatures prevail.

RECYCLED DUST LOADING, W_c

The transient character of the flow interruption during pulse jet cleaning, about 0.1 sec, permits a small fraction of the dislodged dust to reach the hopper. In contrast, practically all dust removed during cleaning processes where compartment flows are interrupted for 0.5 to 2 minutes settles to the hopper or is swept into the inlet ducts of adjoining on-line compartments. It has been estimated that 1 to 5 percent of the dust actually dislodged reaches the hopper (5,6,8) and that the remainder is immediately redeposited on the pulsed and/or adjacent bags (5,8). Because the dislodged dust consists principally of large, 50 to 100 μm agglomerates (5), the coarseness restricts redeposition to the surface region, and its specific resistance coefficient has been estimated as 5 to 7 times lower than that for a freshly deposited fly ash (8). Low K_2 values for the redeposited or "cycling" layer, W_c, may be inferred from the fact that at steady state operation an average cycling layer of 600 g/m^2 contributes less than 0.6 kPa to the total pressure loss whereas an overlying, freshly deposited layer of only 60 g/m^2 causes a 0.4 kPa increase, Figure 6 (5,8). The precise manner in which W_c contributes to total pressure loss is discussed later.

The term re-entrainment has been used inadvisedly to describe the recycling layer, W_c, as well as referring to hopper dust swept into the air stream when overfilling takes place. Although the latter condition should definitely be eliminated, the true W_c layer plays an important role in the filtration process by providing a barrier that minimizes dust penetration through the relatively inefficient, cleaned fabric. Additionally, it reduces variability in air flow that often cannot be tolerated with many ventilation and process applications. Thus, when adopting off-line cleaning as a means of reducing operating pressure loss, one must also accept the performance penalties of higher emissions and flow variability. The preferred method to enhance performance is to select cleaning parameters that enable complete surface dust dislodgement.

ESTABLISHMENT OF STEADY-STATE FILTRATION

Transition From Conditioning to Steady-State Phase

When pulse jet filtration is initiated either with unused or uniformly cleaned fabrics, the pressure loss increases in accordance with the rate of dust arrival, the filtration velocity, and the K_2 value for the freshly deposited dust. In Figure 8, which simulates the real pressure/time relationshps graphed in Figure 6, successive filtering and cleaning cycles are shown for the first 4 minutes and final 3 minutes of the 60-minute operating period required to reach constant operating pressure (or steady-state filtration). The pressure/time trace for the 60th minute corresponds roughly to the D-690 curve of Figure 6 except for the time scale compression.

At the end of 1 minute, the first pulse dislodges a very small fraction of the initial deposit such that the average (transient) pressure loss arising from unequal flows through the just-cleaned and uncleaned surfaces, respectively, is that designated by the triangles. The almost immediate redeposition, however, of most of the dislodged dust, elevates the pressure to a much higher level depicted by the x symbols while arrival of fresh dust over the 1-minute filtering period raises the overall filter resistance to an even higher level as shown by the circles. With repetition of filtration-cleaning cycles, the pressure loss before cleaning will reach its maximum value when maximum surface dust removal is attained. In some cases, surface dust removal may not be complete either because of poor nozzle placement or adhesion problems caused by moisture condensation or chemically reactive dusts. After 60 minutes, the transient pressure loss just before redeposition of the cycling load (designated by triangles) must decrease to the base level depicting pressure loss for the uniformly cleaned fabric. Because the interim quantities of dust returned to the fabric must also increase during the conditioning phase, the pressure loss values immediately following redeposition of the cycling load, W_c, also increase until steady-state operation is attained. In Figure 8, the "X" values indicate the pressure that would be obtained if the curves of Figure 6 were extrapolated linearly to zero time. The latter value has been described as the "effective" bag pressure loss, $(Pe)_{\Delta W}$, at the resumption of a filtration cycle in which the newly arriving dust is characterized by the term, ΔW. Its use in predictive modeling (Equation 6) has been discussed by Dennis and Klemm (7).

Fundamental Pressure Loss Relationships

In the absence of a recycling layer, W_c, Equation (3) affords a good estimate of total pressure loss based on the respective contributions of the cleaned fabric, P_R, with its residual dust holding and the freshly deposited dust layer, $K_2 V \Delta W$. It has been pointed out, however, that the above approach must be modified to account for the very significant contribution of the cycling layer (7,8); i.e.,

$$P = P_R + (K_2)_c V W_c + K_2 V \Delta W \qquad (5)$$

The additional right-hand term depicts the pressure loss across the redeposited or cycling layer in terms of its unique and much lower K_2 value (because of its agglomerate structure) and the filtration velocity, V. Owing to problems in measuring $(K_2)_c$ and W_c, Equation (5) has been reduced to a simpler form for modeling purposes (7,8),

$$P = (P_E)_{\Delta W} + K_2 V \Delta W \tag{6}$$

where $(P_E)_{\Delta W}$ can be evaluated for a broad range of design, flow, and pulse cleaning parameters. On the premise that there does exist a unique W_c layer that can be described as discussed in the following paragraph and, furthermore, that complete dislodgement of this layer is possible under optimum cleaning conditions, Equation (6) and its derivatives become important modeling tools (7,8).

STEADY-STATE OPERATING CONDITIONS

Fabric Dust Loadings Versus Dust Concentration and Filtration Velocity

The basic criterion for 100 percent dust cake removal is that the separating force, F_S, exceed the maximum adhesive force, F_A, the latter uniquely determined by the dust/fabric combination of interest. Therefore, once the pulse characteristics that determine fabric deceleration are fixed, there is a minimum and unique fabric loading, W_c, required for 100 percent cleaning. Variations in inlet dust concentration, C_i, and filtration velocity, V_i, have a negligible impact on W_c as suggested by the loading data shown in Table 2 (5,7). Bakke's tests, Figure 9, also reflect the independence of fabric loading on inlet concentration (14). For example, with operating pressure loss fixed at 875 Pa, filtration velocities leveled off at nearly constant values irrespective of the broad range in inlet concentrations, 0 to 22 g/m^3. Since pressure loss and velocity were constant, it can be inferred that the cycling loading, W_c, must also have been constant. Ellenbecker and Leith have also reported that steady-state or "cycled" dust holdings were essentially independent of filtration velocity over the range 3 to 7.5 m/min (11). Additionally, for comparable operating conditions, their tests revealed not only fabric loadings similar to those reported by Dennis and Wilder (5), 425 and 406 g/m^3, respectively, but also relatively uniform dust deposition over nearly the full length of the bags.

TABLE 2. EFFECT OF PULSE PRESSURE, INLET CONCENTRATION, AND FILTRATION VELOCITY ON STEADY-STATE (W_c) FABRIC LOADING (5)

Pulse[a] pressure kPa (psig)	Fabric dust loading, g/m^2	
	C = 2.0 g/m^3 V = 2.6 m/min	C = 22.7 g/m^3 V = 1.89 m/min
276 (40)	405	503
483 (70)	366	423

[a] Pulse duration = 0.06 sec.; pulse interval = 1 min.

Dust Removal Versus Pulse Jet Pressure

Although we believe that nearly 100 percent dislodgement of the surface dust layer should occur, except for the special circumstances cited earlier in this paper, Ellenbecker and Leith have expressed reservations that 100 percent cleaning takes place or that the major cleaning process results mainly from a surface layer release and not some interstitial reorientation of the dust/fiber structure (6,11). Iinoya and Mori, however, describe tests on a three bag collector, Figure 10, where pulse pressures ranging from 200 to 700 kPa (29 to 102 psig) resulted in up to 75 percent removal of the total dust holding, 600 g/m^2, before pulsing (12). Because no further removal was noted beyond 550 kPa, we have assumed that surface removal was essentially complete and that the remaining 150 g/m^2 constituted the interstitial and difficult-to-dislodge residual loading, W_R. Although W_R values for relatively new felts and woven fabrics may be as low as 36 g/m^2, it is anticipated that gradual plugging after extended service may lead to values in excess of 200 g/m^2 (7).

Past and current GCA tests (7,10) also suggest, based on a combination of photographic evidence and fabric weighings before and after pulsing, that 100 percent removal is attainable under the proper operating conditions, Figure 4 and Table 3. For example, the curvilinear extrapolation of the pressure/time traces, Figure 4, indicates approximate residual pressure losses of 0.1 to 0.2 kPa just before re-deposition of the W_c fraction of the dislodged dust. The latter values are consistent with P_R levels displayed by used felts with no surface dust loading.

TABLE 3. FRACTIONAL SURFACE CLEANING OF USED DACRON FELT VERSUS PULSE PRESSURE--LABORATORY PANEL TESTS

Pulse pressure N/m^2 (psig)	Surface dust loading, g/m^2		Surface fraction cleaned
	Before pulse	After pulse	
183 (20)	467	100	0.79
276 (40)	467	25	0.95

Optimum Performance Criteria

As indicated in previous studies (5,7,8), attainment of optimum operating conditions, which includes 100 percent dislodgement of the surface dust layer, depends upon several pulse-related factors; i.e., pulse pressure and volume relative to bag size, solenoid valve opening time, location of jet relative to bag exit, pulse frequency, and minimum pulse duration.

The effectiveness of the cleaning action also depends on fabric mobility as defined by its flexibility, tensile properties, and inertia, while service life is determined by resistance to corrosion, abrasion, and thermal stresses.

Choice of certain design or operating parameters, such as top versus bottom inlet, air-to-cloth ratio, and (most importantly) conditioning processes plays a key role in obtaining optimum system performance. For example, fabric life can be extended and its residual pressure loss kept at a minimum by avoiding overcleaning and by initiating no pulse action until pressure loss limitations demand it.

REFERENCES

1. Reinauer, T. V. "No Moving Parts Inside Hot Dust Collector," Chemical Engineering 64:188, August 1957.

2. Billings, C. E., and J. E. Wilder. Handbook of Fabric Filter Technology, Volume I, Fabric Filter Systems Study. U.S. Environmental Protection Agency, Control Systems Laboratory, Research Triangle Park, North Carolina. EPA-APTD 0690 (NTIS No. PB-200-648). December 1970.

3. Dennis, R., and L. Silverman. "Fabric Filter Cleaning by Intermittent Reverse Air Pulse," ASHRAEJ 4(3):43, March 1962.

4. Hersey, H. J. Jr. "New Developments in Reverse Jet Filters," AIHA Quarterly 14:3, 1953.

5. Dennis, R., and J. E. Wilder. Fabric Filter Cleaning Studies. U.S. Environmental Protection Agency, Control Systems Laboratory, Research Triangle Park, North Carolina. EPA-650/2-75-009 (NTIS No. PB-240-372/3T1). January 1975.

6. Ellenbecker, M. J., and Leith, D. "Dust Removal from Non-Woven Fabrics--Cleaning Methods Need to be Improved," Filtration and Separation 18:315, 1981.

7. Dennis, R., and H. A. Klemm. "Modeling Concepts for Pulse Jet Filtration," JAPCA 30:38, 1980.

8. Dennis, R., J. E. Wilder, and D. L. Harmon. "Predicting Pressure Loss for Pulse Jet Filters," JAPCA 31:987, 1981.

9. Chudleigh, P. W. "Fabric Filter Performance: Effect of and Cleaning Efficiency," Filtration and Separation 19:388, 1982.

10. Development and Evaluation of Improved Fine Particulate Filter System. EPA Contract 68-02-3151 Mod No. 2, March 1980 to July 1983, GCA/Technology Division, Bedford, MA 01730. Report in Preparation.

11. Ellenbecker, M. J., and D. H. Leith, "Dust Deposit Profiles in a High Velocity Pulse-Jet Filter," JAPCA 29:1236, 1979.

12. Iinoya, K., and Y. Mori. "Fundamental Experiments of Fabric Filters." In Symposium on the Transfer and Utilization of Particulate Control Technology, Volume 2. Fabric Filters and Current Trends in Control Equipment, EPA-600/7-79-044b (NTIS No. PB-295-227). February 1979.

13. Lefkowitz, L. R. "Evaluation of Felted Glass Media under Simulated Pulse Jet Operating Conditions." In Symposium on the Transfer and Utilization of Particulate Control Technology, Volume 2. Fabric Filters and Current Trends in Control Equipment, EPA-600/7-79-044b (NTIS No. PB-295-227). February 1979.

14. Bakke, E. "Optimizing Filtration Parameters," JAPCA 24:1150, 1974.

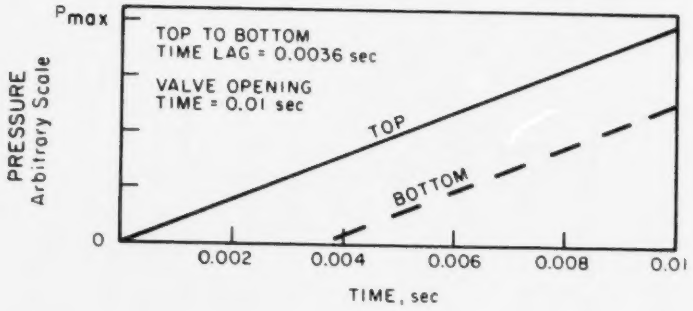

Figure 1. Presure gradient vs. location and time after pulse initiation for 1.22 m (4 ft) Dacron felt bag.

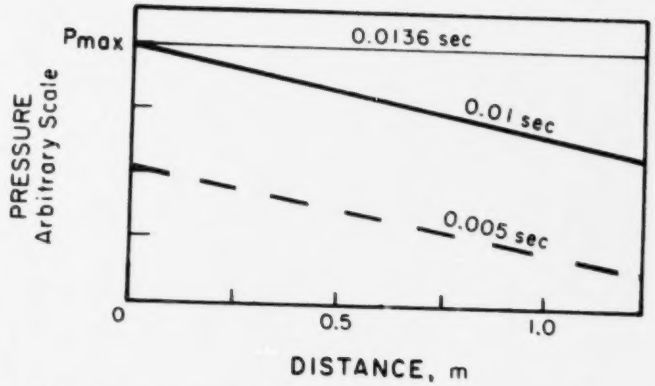

Figure 2. Pressure gradient along 1.22 m (4 ft) bag vs. solenoid valve open time.

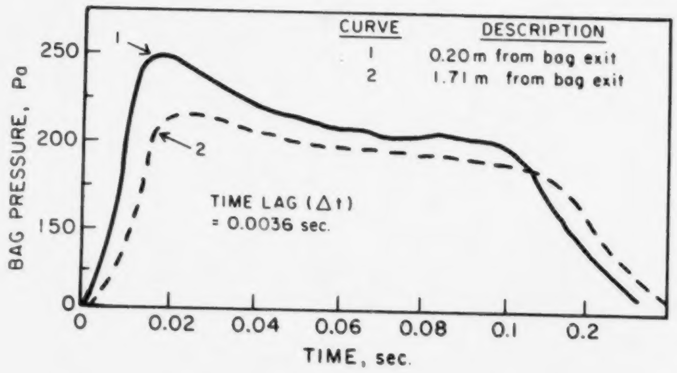

Figure 3. Concurrent pressure/time traces, 1.83 m (nominal 6 ft) Dacron felt bag 621 kPa (90 psig) pulse, 0.1 sec duration.

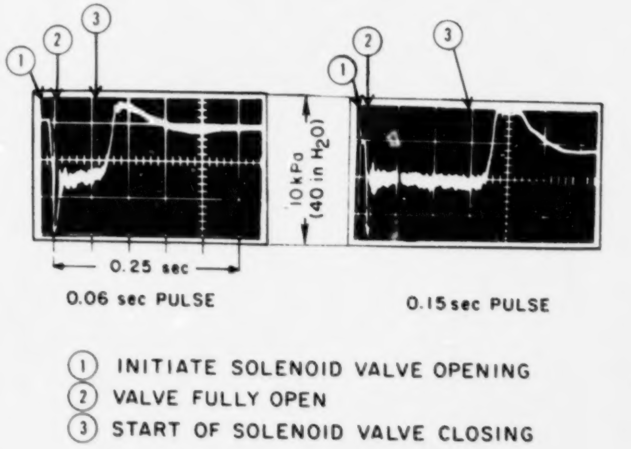

Figure 4. Pressure/time traces for 483 kPa (70 psig) pulses for 1.22 m x 11.4 cm (4 ft x 4-1/2 in) Dacron felt bag.

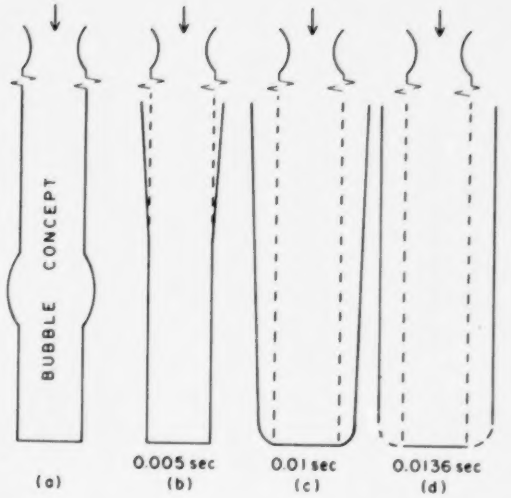
BUBBLE CONCEPT
(a)
0.005 sec
(b)
0.01 sec
(c)
0.0136 sec
(d)

Figure 5. Bag profiles vs. time after pulse initiation for a 1.22 m (4 ft) long bag. Bubble concept (a) vs. theory (b)(c)(d).

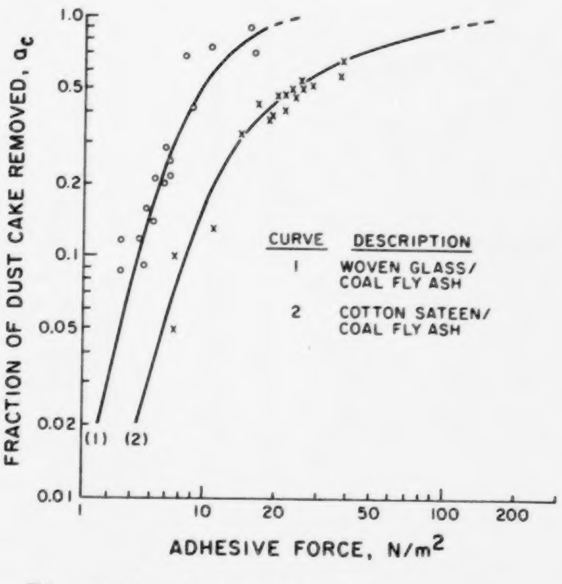

Figure 7. Fractional dust removal vs. estimated adhesive force.

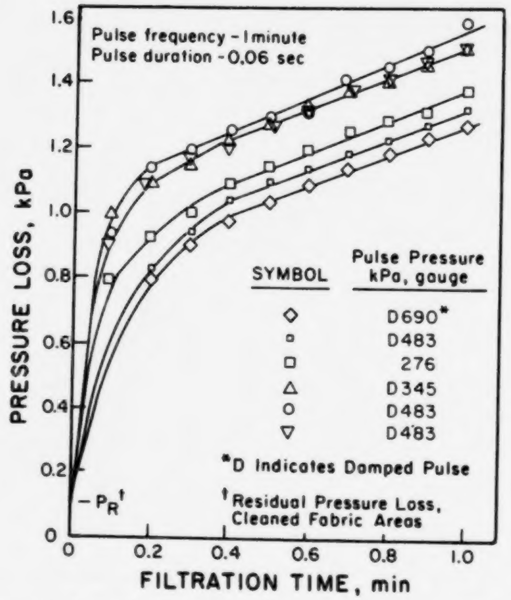

Figure 6. Resistance characteristics for fly ash and Dacron felt at C_i = 27.6 g/m³ and V = 2.6 m/min.

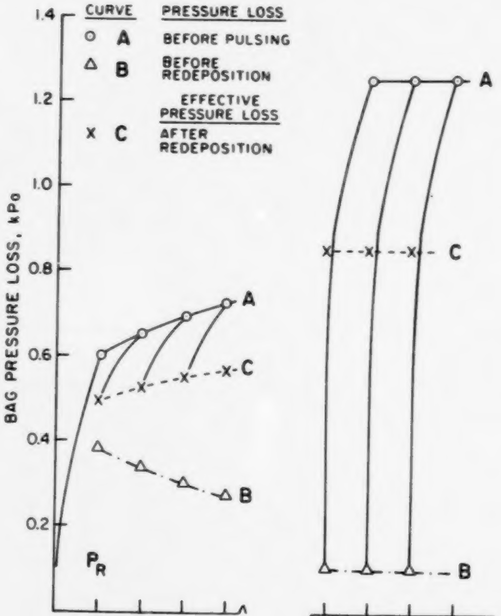

Figure 8. Characteristic pressures before and after steady-state filtration is achieved.

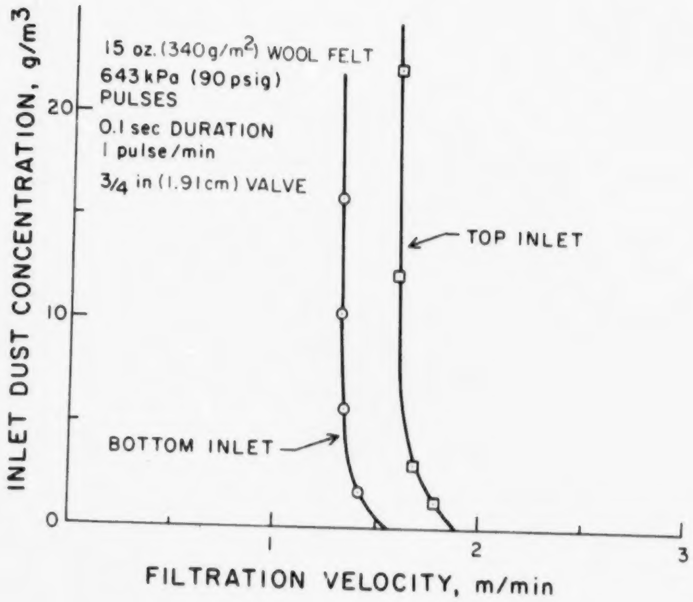

Figure 9. Talc filtration velocity vs inlet concentration at constant pressure loss. Source: Reference 14.

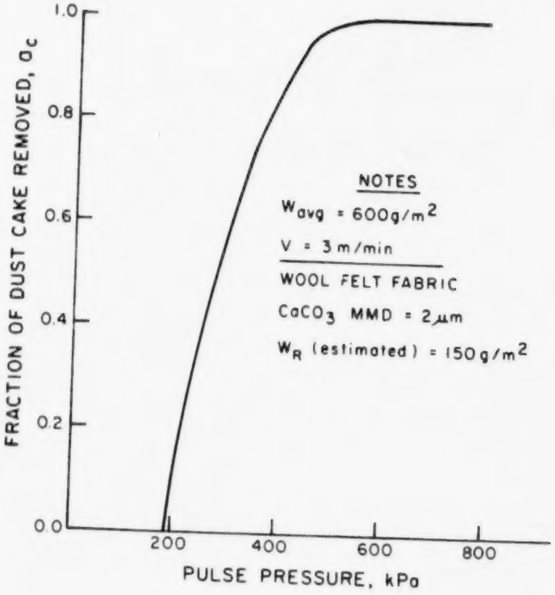

Figure 10. Fractional dust removal vs. pulse jet pressure at constant W. Source; Reference 12.

LABORATORY TECHNIQUES FOR DEVELOPING PULSE JET COLLECTORS

Robert R. Banks and John T. Foster
Wheelabrator-Frye Inc.
Air Pollution Control Division
Technical Center
5100 Casteel Drive
Coraopolis, Pennsylvania 15108

ABSTRACT

A major factor in the performance of a pulse jet collector is its effectiveness in using compressed air. The manifold configuration, venturi design and other factors determine this effectiveness. To expedite the study of these factors over a wide range, two sets of apparatus were built.

The first, the impact force tester, measures the momentum of the air pulse from each hole in a manifold and the pressure along the manifold. The momentum of the jets can be equalized by varying the hole size along the manifold.

The second test rig measures the characteristic of the ejector or jet pump formed by the air jet and venturi so that the geometry of this part of the system can be optimized. Jet pump curves were found to predict relative performance as measured in a laboratory pilot collector. Testing by these methods takes only a fraction of the time required using a pilot collector. Data from tests leading to an optimum pulse jet cleaning system design will be shown.

INTRODUCTION

At Wheelabrator-Frye pulse jet collectors have been developed through several generations of designs. The first collectors were small and performance requirements not demanding. Changes in design could be based on observation and modifications to commercial collectors. As development continued, each improvement in performance or economy became more difficult to achieve. To reduce the cost and time required to generate improved designs, laboratory techniques were developed for generating preliminary performance information.

The main areas of technical study have been the more effective utilization of air in the pulse cleaning system, the flow and distribution of air and dust on the dirty side of the collector, and improvements in filter media. This paper confines itself to the cleaning system.

DEVELOPMENT TECHNIQUES

In the early stages of development, laboratory work consisted mainly of making pressure measurements on the header and in the manifold. Because of the speed of these transient phenomena, a light writing oscillograph was used to record pressures measured by means of pressure transducers. The data was principally used to study air consumption per pulse and valve timing compared with electrical signals.

THREE BAG COLLECTOR

At this stage changes in the design of a pulse jet collector were studied by trying the changes on a full-size operating unit. Consideration was given to building a laboratory collector using three full-size manifolds, as it was felt that it is necessary to use a full-size manifold in order to get the proper cleaning pulse for test work and that the minimum number of rows that would not result in overloading the bags not being cleaned would be three. At this point, it was suggested that it was unnecessary to use a bag at every hole in the manifold but rather, use one hole per manifold for cleaning and discharge the air from the other holes into the atmosphere. In this way, the bags would be cleaned by the pulse exactly as in a full-scale collector, but the amount of air and dust to be handled would be much more appropriate for laboratory studies.

A small collector was built following this principle using three bags in triangular arrangement inside a circular shell. The shell is made in sections so that its length can be adjusted for use with different size bags. The clean air plenum is flanged at the cell plate level so that spacers can be inserted to permit changing the distance between the manifold and venturi for test purposes. The air header is the same size that would be used on a full-size collector so that the pressure at the dump valve follows the same pattern as in a full-size collector. This collector is shown in Figure 1.

The equipment is designed so that the manifold or blow pipe can be slid through the clean air plenum permitting any hole in it to be centered over the bags. This was done because measurements of pressure along the manifold showed a rise in pressure as the velocity dropped from air being bled off. Rough calculations using Bernouilli's theorem give figures fairly close to the measured values. Tests were carried out that showed better cleaning performance at the end of the manifold remote from the dump valve. Most developmental testing was done using the jet closest to the dump valve so that the results would be conservative.

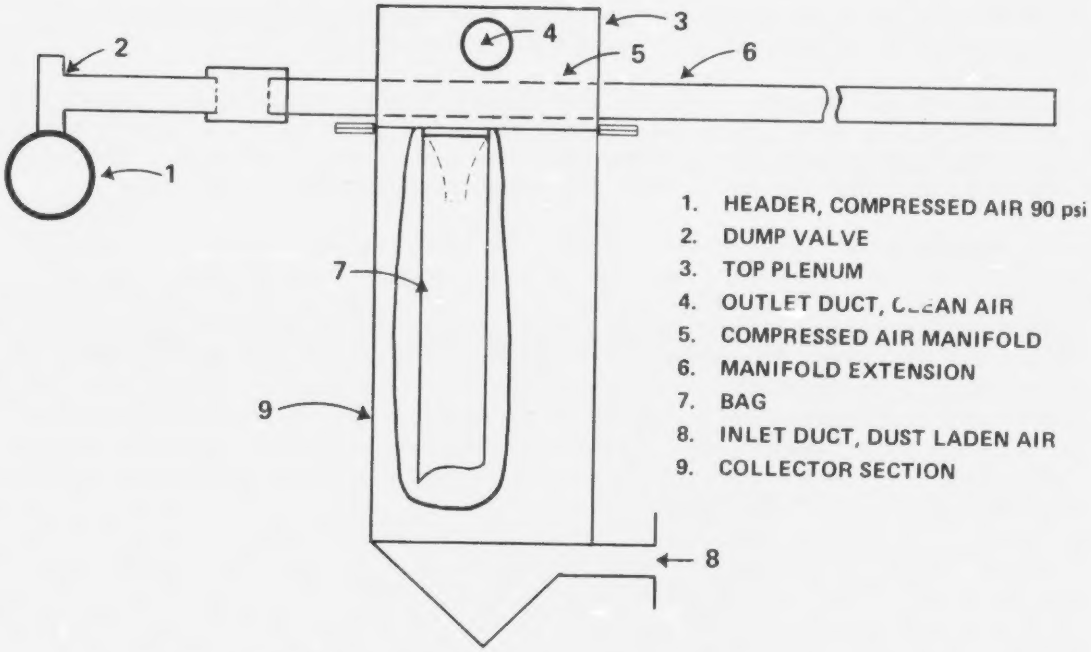
2
4
3
5
6
1
7
9
8
1. HEADER, COMPRESSED AIR 90 psi
2. DUMP VALVE
3. TOP PLENUM
4. OUTLET DUCT, CLEAN AIR
5. COMPRESSED AIR MANIFOLD
6. MANIFOLD EXTENSION
7. BAG
8. INLET DUCT, DUST LADEN AIR
9. COLLECTOR SECTION

FIGURE 1. THREE BAG PULSE-JET COLLECTOR

In carrying out a test on this unit it is operated at a fixed air-to-cloth ratio until stable operation is reached and then the ratio is raised and the procedure repeated until the pressure drop on the collector does not stabilize but continues to rise.

Tests on this type of equipment led to the adoption of the double diaphram dump valve, a new venturi, optimization of manifold to venturi spacing and other features embodied in our present design of pulse jet collectors.

Ideas based on observations made in the course of the development work described suggested ways in which further improvements could be made in the performance of the cleaning system. A program was planned to follow up on these ideas to improve the pulse jet cleaning system and develop a new generation of pulse jet collectors. One area of prime interest was the manifold design.

PULSE FORCE MEASUREMENT

As described earlier, the manifold of uniform section and with uniform size orifices gives progessively more cleaning force along its length. In order to compensate for the increase in the pressure as the velocity decreases along the length of the manifold or blow pipe, two options are available; 1) taper the pipe so that the velocity remains constant, or 2) use larger orifices where the pressure is lower. It was felt that using graduated hole sizes along the length of the manifold would be less costly than producing a tapered or stepped manifold.

Use of the laboratory three bag pulse-jet collector would obviously be impractical for developing the optimum drilling pattern for a variable hole size manifold because of the time required for a test. The pulse force equipment was devised to do this job expeditiously and economically.

In the pulse jet cleaning system the jet acts in combination with the venturi or the open end of the bag as a jet pump to entrain air from the outlet plenum to get a large volume; low pressure pulse that actually performs the cleaning. Since the jet pump is a momentum transfer device, a means for measuring the momentum of the jets could be used as a measure of the cleaning power available at each orifice. The simplest means for measuring the momentum of a stream is to measure the force generated when it impacts on a fixed plate. In most of the cases studied the velocity is sonic and the increased momentum of the jet is due to the increased density of the air at the higher pressure.

A device was set up as shown in Figure 2.

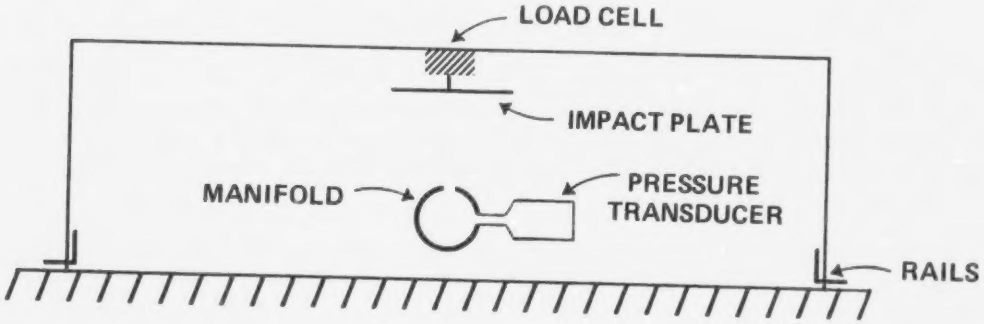

FIGURE 2. PULSE FORCE EQUIPMENT

It consists of circular plate four inches in diameter mounted on a load cell and positioned opposite a hole in the manifold. The output of the load cell is recorded on the light writing oscillograph after going through a signal conditioner. The support for the force transducer is mounted so that it can be slid along rails and clamped in position over each of the manifold holes in turn. A full-size header and standard dump valve are used to feed the manifold. In all of the test work reported in this paper, the header size was held constant and the initial header pressure was 90 psig. In addition to measurements of pulse force, measurements of pressure along the manifold are made using a pressure transducer.

Using this technique, curves as shown in Figure 3 were developed. The pulse force for a manifold with uniform hole size (U) varied from 5.4 lbf at the nearest the valve to 8.0 lbf at the 15th hole. By progressively reaming the holes the pattern called "A" was developed. In these drilling patterns, the number of different hole sizes was limited to make fabrication on a production basis simpler.

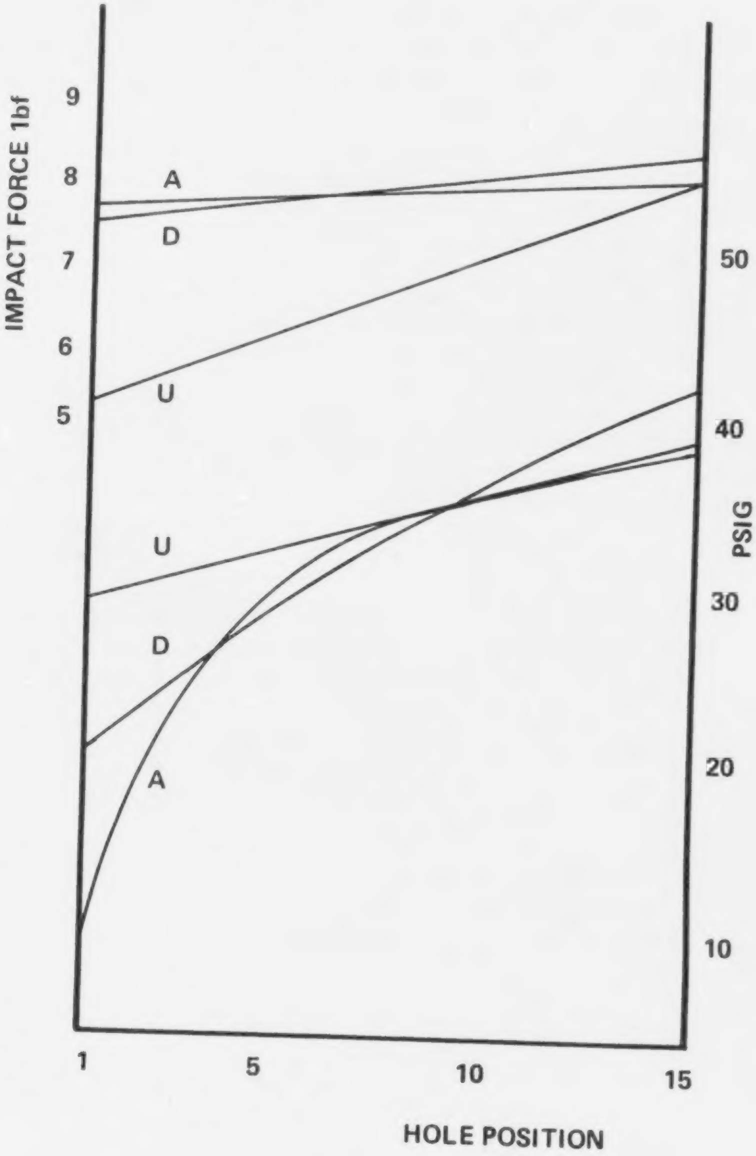

FIGURE 3. PULSE FORCE AND MANIFOLD PRESSURE VS. HOLE POSITION

When evaluated, the first holes in the "A" drilling did not give the expected performance. It was reasoned that the cause of this was that the pressure in the manifold at the first few holes was too low to give the critical pressure ratio. The flow from these holes was thus below sonic velocity while the remainder of the holes were operating at sonic velocity. In order to correct this, several other drillings were tested and the pattern referred to as "D" was selected. The impact force measurements with drilling "D" are not quite as uniform as is the case for drilling "A" but the overall performance is slightly better. Peak pressure at the first hole for the "D" drilling is 37 psia so that the pressure ratio is about 2.5 versus 1.9 for the "A" drilling. The critical pressure ratio for air is about 2.

JET PUMP CURVE APPARATUS

The next area of the cleaning system to be studied was the jet pump itself. In this part of the program, we wanted to measure the flow and pressure developed by the jet pump comprising the jet of air from the manifold and the venturi or similar device at the open end of the bag. The first course considered was to measure all of these factors dynamically. While the results from such a system would be the most realistic, it was felt that the cost of setting up the equipment and the time to develop the technique for making that type of measurement would be excessive. As an alternative, it was decided to study the jet pump characteristics under steady state conditions. It was felt that this approach would be acceptable, since the final test would be an operating collector in any case. Figure 4 shows the equipment set up for these measurements.

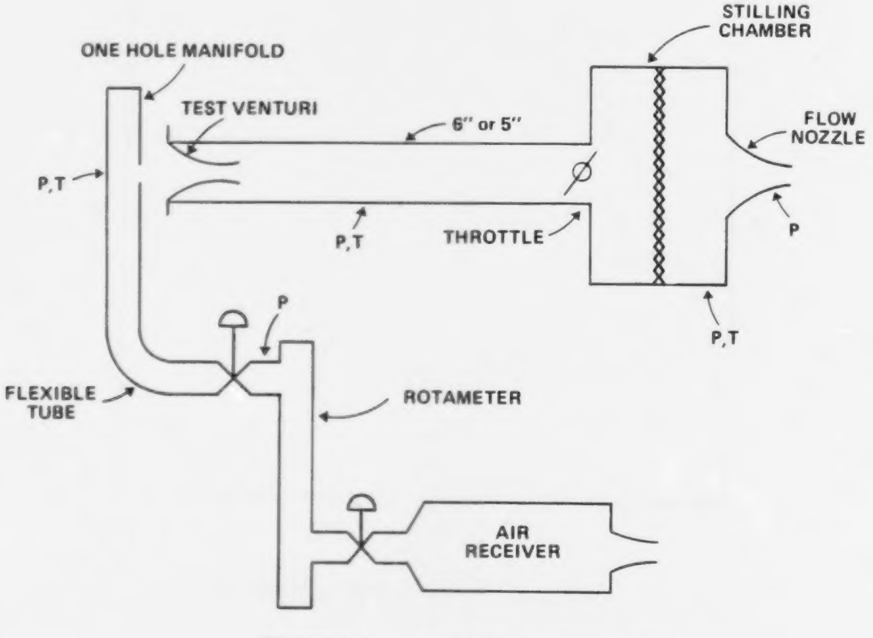

FIGURE 4. JET PUMP EQUIPMENT

The air compressors and receivers used have sufficient capacity to provide a flow in excess of 130 cfm for the tests. This flow was calculated by dividing the volume of air discharged by a dump valve in a single pulse by the length of time of the pulse, and by the number of holes in the manifold. For the tests, a manifold with a single hole to the size being studied is used. The pressure and temperature in this manifold are measured and its position relative to the rest of the equipment is readily adjusted. The flow to this manifold is adjusted by means of two valves, one is used to adjust the flow, and the other is used to provide the 90 psi back-pressure required by the calibration of the rotameter used to measure the flow of compressed air.

The air jet from the manifold is directed into the end of either a five inch or six inch diameter steel tube representing the bag that would be cleaned in an operating collector. Venturis or similar devices can be mounted at the end of this tube. Pressure in the tube is measured at pressure taps about halfway down its length. At the far end of the tube, there is a butterfly valve that is used to provide variable back pressure in determining the jet pump characteristic. Beyond the butterfly valve, the air enters a stilling chamber prior to exiting through a standard ASME flow nozzle used to measure the combined flow of the compressed air and induced air. The back half of the equipment is essentially the same equipment that is used for measuring the characteristics of a fan, and is designed in accordance with the standards of the AMCA and ASHRAE.

In carrying out a test, the air flow to the one hole manifold is regulated so that the pressure in the manifold is the same as that found in an operating manifold on the pulse force equipment. The compressed air flow for that condition is measured and that flow rate is used for all subsequent tests on that orifice size. To determine the characteristic of the jet pump, the butterfly valve is locked in various positions and the pressure and flow are measured. The data from these measurements are plotted to give a curve as shown in Figures 5 - 8.

Figure 5 shows the effect on the jet pump characteristic of the differences in pulse force shown in Figure 3 for the uniform hole size manifold (Drilling U). The performance for the conditions at the first hole are appreciably lower than for the last hole which produces about 25% higher flow.

By using the variable hole manifold (Drilling D), as shown in Figure 6 the performance at the conditions of the first and last holes are quite close and, in fact, the first hole shows slightly more power. The performance of the jet from the last hole is also increased slightly.

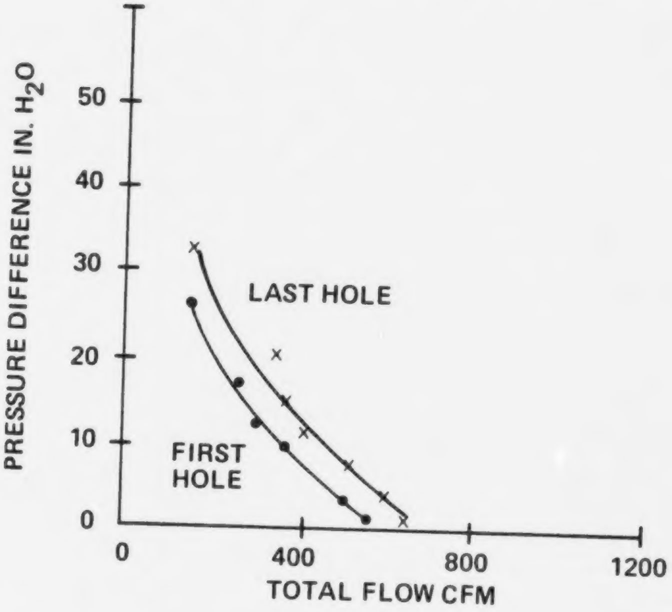

FIGURE 5. JET PUMP CURVE - VENTURI T DRILLING U

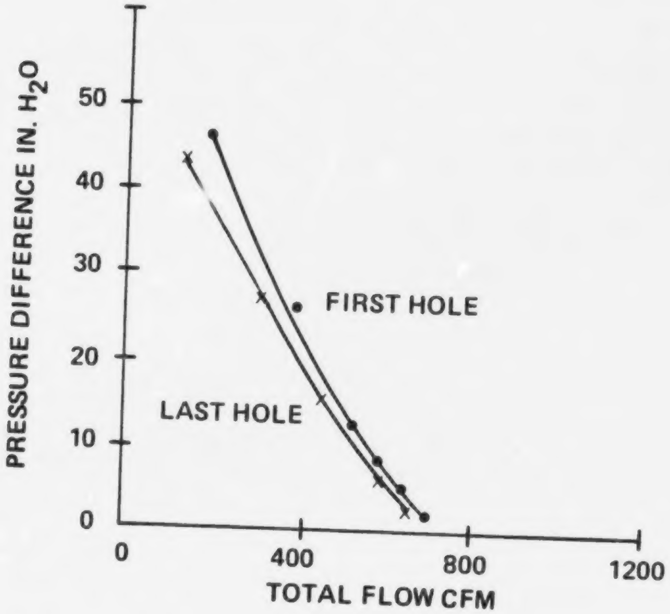

FIGURE 6. JET PUMP CURVE - VENTURI T DRILLING D

Figure 7 shows more clearly the difference in performance between manifold with uniform holes and variable sized holes. These curves are for the first holes in the two manifolds using the same venturi and show almost 50% improvement in performance by using the variable hole manifold.

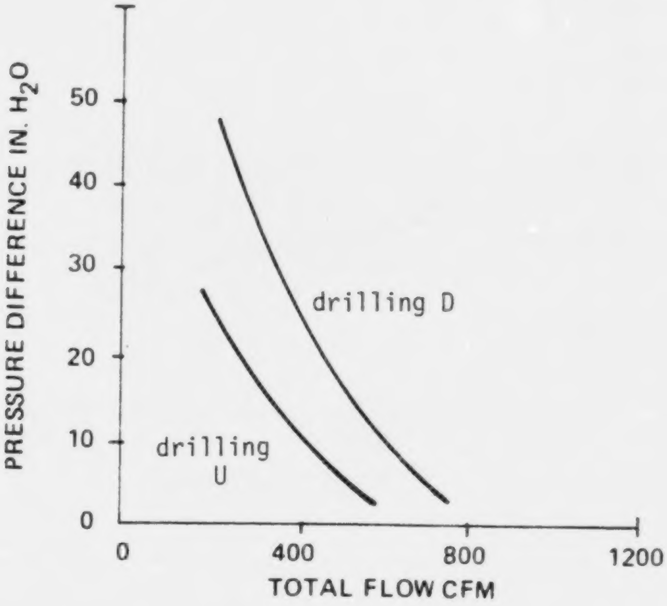

FIGURE 7. JET PUMP CURVE - VENTURI T HOLE 1

VENTURI DEVELOPMENT

The next component of the pulse cleaning system to be studied was the venturi. Various designs of venturis were tested using the jet pump equipment. In these tests the distance from the manifold to venturi was varied and the optimum determined. If too close a spacing is used with some short venturis the jet tends to blow through without touching the walls and poor performance results.

Figure 8 shows the performance of three of the venturis tested. Venturi T is a fairly conventional design and shows a high maximum pressure that falls off rapidly as the total flow volume increase. Venturi O is of increased throat size and shows a low maximum pressure but it will handle a larger air flow. By trying several intermediate designs Venturi F was developed to give an intermediate maximum pressure with an air flow even better than the O design.

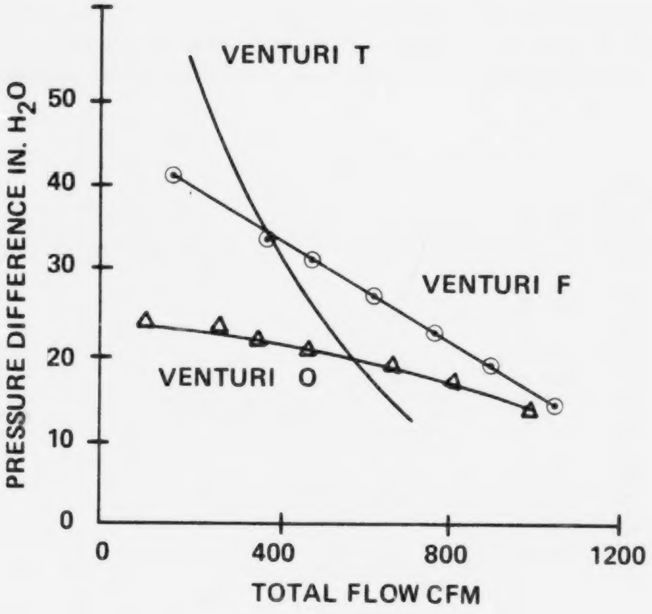

FIGURE 8. JET PUMP CURVE - DRILLING D HOLE 1

EVALUATION

The performance of these venturis was evaluated in the three bag pulse jet collector. Table 1 shows the air-to-cloth ratio that could be attained using the three venturis whose characteristics are illustrated in Figure 8.

TABLE 1 AIR-TO-CLOTH RATIO VS. VENTURI DESIGN

Venturi	Air-To-Cloth Ratio
T	7.0
O	8.0
F	10.0

If the results shown in Table 1 are compared with the curves in Figure 8, it appears that the jet pump in a collector must be operating in the high flow-low pressure section of the characteristic. In the flow range above 600 cfm the sequence of performance in the jet pump equipment is the same as in the three bag collector. It would thus appear that high induced flow is more important than high peak pressure in cleaning pulse-jet bags.

SUMMARY

Several pieces of equipment have been built to expedite the development of pulse-jet cleaning systems.

By use of these systems, an improved pulse-jet cleaning system has been developed and preliminary evaluation performed in the three bag collector.

The final test -- field evaluation -- is in progress.

The work described in this paper was not funded by the U. S. Environmental Protection Agency and therefore the contents do not necessarily reflect the views of the Agency and no official endorsement should be inferred.

OFF-LINE PULSE-JET CLEANING SYSTEM

BY: Thomas C. Sunter
C-E Air Preheater
Div. of Combustion Engineering, Inc.
Wellsville, New York 14895

ABSTRACT

The paper discusses off-line pulse-jet cleaning systems by formulating a set of simplified mathematical equations to describe the cleaning process. A computer model is developed from the equations and manipulated to simulate both time-based and differential pressure-based control of the pulse-jet system.

Practical application of this information is discussed as it affects system control, bag life, energy consumption and system operation.

INTRODUCTION

Off-line cleaning of a multi-module pulse-jet dust collection system offers advantages over the conventional on-line cleaning system utilized with felted fabrics. In terms of bag life and total cleaning energy, it is the preferred method for those systems employing woven glass fabric bags.

This paper discussed off-line cleaning under three main headings:

1. A simplified mathematical formulation of the cleaning process which lends itself to computerized simulation.
2. Manipulation of this model under both time-based and differential pressure-based cleaning control systems.
3. Discussion of the practical application of this information as it affects system control, bag life, energy consumption and general system operation.

MATHEMATICAL FORMULATION

ASSUMPTIONS

The following simplifying assumptions were used in the formulation of the equation sets which describe the cleaning cycle:

1. Filter drag for the fabric and dust cake is linear with respect to total dust deposition and within any particular model iteration, independent of filtration velocity. K_2, the dust permeability is measured in grains/sq. ft/ins. H_2O/fpm and measures the slope of the drag-dust load line.
2. The value of filter drag occurring immediately after the cleaning of a module is constant and independent of the drag just before cleaning.
3. The component of system pressure drop not related to the filter fabric and dust cake; i.e. all duct, venturi and inlet/outlet losses obey a strictly square law relationship between pressure loss and volume and are identical for each module.
4. Isolation of a compartment for cleaning and subsequent de-isolation for return to the on-line condition each occur instantaneously.
5. The system volumetric flow rate is constant.
6. The pressure drop contribution of the fabric and dust cake is linear with respect to filter drag where filtration velocity is the constant of proportionality.

It should be emphasized that the assumptions inherent in the formulation will produce results which differ from measured values in an operating system. This study is less concerned with predicting field values than it is with study of the effects on system operation of changes in the system parameters and control variables.

FORMULATION

The formulation covers a system of N modules, each containing A sq. ft. of fabric with a total fixed system volume of Q ACFM. Three sets of equations are used to describe system behavior as follows:

Gross Condition

$$P_t = (D_n{}^t) \times (\nu_n{}^t)_G + \left[\frac{(\nu_n{}^t)_G}{R_o}\right]^2 \qquad (1)$$

For all N values of n

$$\sum_{n=N}^{n=1} (\nu_n{}^t)_G = \frac{Q}{A} \qquad (2)$$

Where P_t = System pressure drop - ins. H_2O at time t.

$D_n{}^t$ = Drag of nth module at time t.

$(\nu_n{}^t)_G$ = Filtration velocity. FPM gross condition for nth module at time t.

R_o = Gross filter ratio for which all air losses equal 1 ins. H_2O.

Net Condition

$$P_t = (D_n{}^t) \times (\nu_n{}^t)_N + \left[\frac{(\nu_n{}^t)_N}{R_o}\right]^2 \qquad (3)$$

For all n values escept $n = n_c$

$$\sum_{n=N}^{n=1} (\nu_n{}^t)_N = \frac{Q}{A} \qquad (4)$$

Except $n = n_c$

Where $(\nu_n{}^t)_N$ = Filtration velocity FPM net condition for nth module at time t.

Drag Calculation

$$D_n^{t+t_o} = D_n^{t} + (\nu_n^{t})_{G/N}\ t_o g/K_2 \qquad (5)$$

Where g = Dust load grains per acf.

K_2 = Dust permeability grains/sq. ft./ins. H_2O/fpm.

t_o = Time increment minutes for incremental drag calculation.

Equation (5) simplifies drag calculations by avoiding a set of differential equations. The degree of accuracy required can be attained by adjusting the value of t_o.

System behavior is essentially described by stringing together a series of the basic sequence ABCD shown in Figure 1.

This shows the cleaning cycle for one module only and can be described as follows in Table 1:

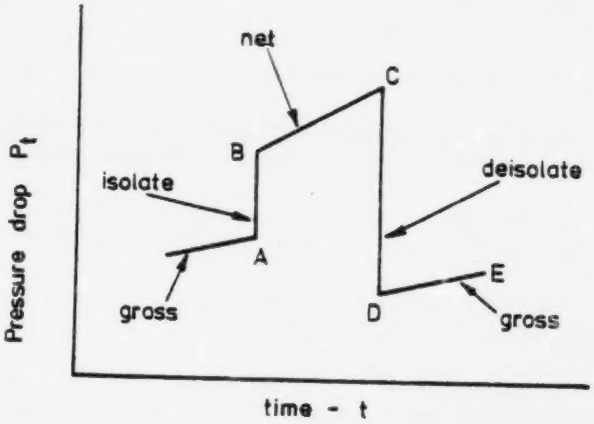

Figure 1. Cleaning cycle for one module.

TABLE 1. CALCULATIONS FOR THE BASIC CLEANING CYCLE

Point	Mode	Calculation
A	Gross condition before insolation	Equations (1) & (2)
B	Net condition after isolation	Equations (3) & (4)
BC	Net condition during isolation	Equations (3) & (4) & (5)
C	Net condition before deisolation	Equations (3) & (4) & (5)
D	Gross condition after deisolation	Equations (1) & (2)

Separate computer programs where developed from the formulations discussed above for off-line cleaning under time based and differential pressure based cleaning system control.

Programs were arranged to provide output for up to 100 complete cleaning cycles.

Output included values of P_t, D_n^t, $(\nu_n^t)_G$ and $(\nu_n^t)_N$ for all modules and all cycles so that the basic system pressure-time graph could be drawn for any particular cleaning cycle number.

Values of (ν_n^t), both gross and net, were included in the output as they provide information on the flow distribution among the modules at any time.

MANIPULATION

TIME-BASED CLEANING

Figure 2 and Tables 2 and 3 show the input and output for the first 3 cleaning cycles of a four module system with time-based cleaning.

Both the graphical and mathematical output show that system stability is near completion after one cycle and complete after three cleaning cycles.

Under stable conditions during the third cycle, gross ratios vary from 2.1 to 4.1 fpm and net values from 3.2 to 4.8 fpm.

During the first cycle, gross ratios vary from 1.1 to 6.3 fpm and net values from 1.7 to 7.0 fpm.

Comparison of the drag values for all modules at t = 5 minutes shows that if there were no air losses ($R_o = \infty$), the flow distribution would be more skewed with module no. 1 passing 73% of the total system flow.

It is the contribution of the air losses; i.e., the $(\nu_n^t)^2$ term in equations (1) and (3), which tends to even out the flow maldistribution occuring in the system due to the different drag values for each module.

TABLE 2. INPUT DATA FOR THE TIME BASED CLEANING CYCLE

```
 VAR.
_NAME__________________________________________________________________

  N      NUMBER OF MODULES
__A______MODULE_FILTER AREA_(SQ.FT.)_________________________________4
  Q      SYSTEM VOLUMN (ACFM)_____________________________________2000.
  XK2    DUST PERMEABILITY (GRNS/SQ.FT./INSH2O/FPM)              24000.
__G______DUST_LOAD (GRAINS/ACF)__                                  350.
  P0     SYSTEM DIFFL. PRESS @ T=0 (INS.WG)______________________  2.0
  T1     MODULE ISOLATION TIME (MINS.)                           5.0000
__T2_____MODULE_DWELL TIME_(MINS.)__                                5.0
  T0     TIME INCREMENT FOR DRAG CALCS. (MINS.)___________________  2.0
  R0     GROSS F.R. FOR UNITY AIR LOSSES (FPM)                      .10
_D0______POST_CLEANING MODULE_DRAG VALUE_(INSH2O/FPM)               4.5
  XT     NO. CLEANING CYCLES (TOTAL)_____________________________.200000
  X1     OUTPUT REQD FOR CLEANING CYCLE NO.                        10.0
_PLOW____LOW_PRESS DIFFL. SETTING_(INS._WG)                          1.
_                         ______________________________________   0.0
```

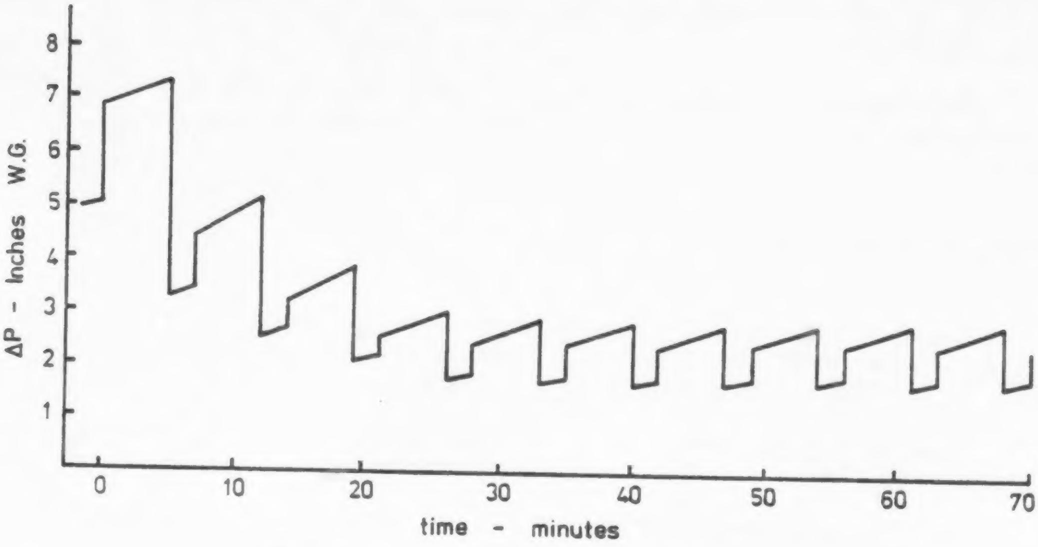

Figure 2. Time based cleaning.

TABLE 3. COMPUTER PRINT-OUT FOR FIGURE 2

```
        CYC PRES   PRES      MOD  I          MOD  2        MOD  3        MOD  4
TIME    NO. GROSS  NET    DR  VG  VN    DR   VG  VN   DR   VG  VN   DR   VG  VN
  0.00   1  5.00  6.86   151  30   0   151   30  39  151   30  39  151   30  39
  5.00   1  3.25  7.32    20  63   0   163   18  40  163   18  40  163   18  40
  7.00   1  3.46  4.38    27  60  70   165   19   0  165   19  24  165   19  24
 12.00   1  2.51  5.12    46  38  65    20   53   0  172   13  27  172   13  27
 14.00   1  2.69  3.20    50  38  44    26   51  58  174   14   0  174   14  17
 19.00   1  2.06  3.83    63  26  44    42   34  55   20   47   0  179   11  20
 21.00   1  2.21  2.53    66  27  30    46   34  38   25   45  50  181   11   0
 26.00   1  1.75  3.02    75  20  32    57   25  39   39   31  47   20   42   0
 28.00   2  1.87  2.42    78  21   0    60   25  31   42   31  38   24   41  49
 33.00   2  1.70  2.90    20  41   0    69   21  33   54   25  39   38   31  46
 35.00   2  1.82  2.38    24  40  48    72   21   0   57   25  32   42   31  38
 40.00   2  1.68  2.85    38  31  46    20   41   0   66   21  34   53   25  39
 42.00   2  1.80  2.36    41  31  38    24   40  48   69   22   0   56   26  32
 47.00   2  1.57  2.84    53  25  39    38   31  46   20   41   0   65   21  34
 49.00   2  1.79  2.36    55  26  32    41   31  38   24   40  48   68   22   0
 54.00   2  1.67  2.84    65  21  34    52   25  39   38   31  46   20   41   0
 56.00   3  1.79  2.36    68  22   0    55   26  32   41   31  38   24   40  48
 61.00   3  1.67  2.84    20  41   0    65   21  34   52   25  39   38   31  46
 63.00   3  1.79  2.36    24  40  48    68   22   0   55   26  32   41   31  38
 68.00   3  1.67  2.84    38  31  46    20   41   0   65   21  34   52   25  39
 70.00   3  1.79  2.36    41  31  38    24   40  48   68   22   0   55   26  32
 75.00   3  1.67  2.84    52  25  39    38   31  46   20   41   0   65   21  34
 77.00   3  1.79  2.36    55  26  32    41   31  38   24   40  48   68   22   0
 82.00   3  1.67  2.83    65  21  34    52   25  39   38   31  46   20   41   0
 84.00   4  1.79  2.36    68  22   0    55   26  32   41   31  38   24   40  48
```

It is readily apparent that the variation in system inserted pressure drop is most marked at the beginning of the first cleaning cycle (i.e. 4.07 ins. wg in the first ABCD loop) and reduces rapidly as the overall system drag diminishes.

The cleaning frequency is of course determined by the control system setting and in this case, for any particular module, is once every 28 minutes.

PRESSURE-BASED CLEANING

Figure 3 shows the differential pressure-time plot for the same (4) module system under pressure-based cleaning with set points of 3 and 5 ins. wg. for the low and high levels respectively.

Gross ratios vary from 1.3 to 6.3 fpm during the first cycle, but stay in the range 1.4 to 6.1 fpm after stabilization.

The inserted system differential pressure varies over the range of 2.3-6.9 ins wg. in the stable condition.

The cleaning frequency is determined by the system operating parameters particularly the rate of pressure rise in the gross condition. In this case cleaning frequency for any particular module is once every 101 minutes.

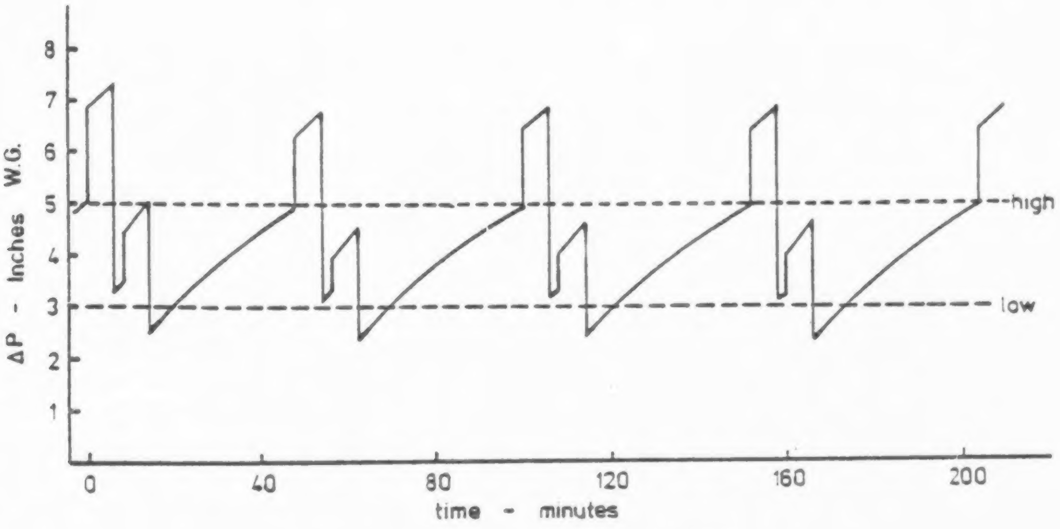

Figure 3. Pressure based cleaning.

PRACTICAL APPLICATION

COMPARISON OF TIME AND PRESSURE BASED CLEANING

The essential advantage of a differential pressure based cleaning system is that it cleans on demand; i.e., provided that the system runs below the high set point, no cleaning occurs and all modules are on line. Another and more effective way of stating this advantage is in terms of the automatic accommodation of a system under ΔP cleaning to load changes, both up and down. Such is not the case with time based cleaning. In the event of load reduction, either the control system must be adjusted to a longer cleaning cycle or the system will overclean down a lower system differential pressure.

OPTIMIZATION OF THE CLEANING CYCLE

In discussing possible modifications to cleaning cycle control systems with a view to optimization, a number of requirements, some conflicting, must be considered.

Pulse Pressure Versus Pulse Frequency

There is adequate experimental evidence to conclude that generally speaking, the amount of dust removed from the bags of an off-line module will increase both with increase in pulse pressure and with the number of pulses to which the bags are subjected. It can also be speculated that:

-There is some pulse pressure below which little bag cleaning, if any occurs.

-The dust removal rate is highest for the first of a number of pulses and diminishes with successive pulsing.

What is not readily apparent is precisely what effect variations in pulse pressure and frequency have on bag life; e.g., what are the comparative equivalent effects on bag life of 1 pulse @ 100 psig versus 2 pulses each at 50 psig?

Our uninformed opinion in the example quoted is that frequency contributes more than pressure to shorter bag life, thus the latter is worse than the former.

Provision Of A Safety Factor

In the specification and selection of a pulse-jet system to control a particular process, the Application Engineer may frequently be faced with a lack of complete process definition on some or all of the following items:

-The process is new, therefore no dust sample is available.

-The process is different so that the dust load and particle size analysis of the dust are approximate.

-The system design volume is imprecise.

-The exact nature and duration of upset conditions are speculative.

-The gap between normal and design volume is very large.

These conditions are frequently met today in applying fabric filtration systems to fluid bed boilers.

Lack of definition for any of the process variables enumerated above suggest that the wise approach is the incorporation of some safety factor into the pulse-jet system design.

Since provision of too large a safety factor is economic suicide, another approach is a control system design which lends itself to system operation beyond the norm, but retains the optimizing capability at all system conditions.

System Versus Module Control

System control under differential pressure-based cleaning usually involves module cleaning in response to the total system differential presure; i.e., flange-to-flange pressure drop through the baghouse.

While this control method monitors and controls the most important system variable; i.e., flange-to-flange pressure drop, it falls short of highlighting and controlling conditions in the individual system modules. Thus, for example, control by this method will not immediately identify a module which, for some reason, is not being cleaned. Failure to do so will eventually lead to unacceptable system operation and bag life.

It should be noted here that comparison of the tube-sheet differential pressure after module cleaning with some pre-set value is not a good indication of cleaning performance, since the differential pressure value associated with good cleaning will vary with the condition of all the other modules in the system at that time.

Unattended Operation

There is a predilection among industrial users to run pollution control systems unattended or monitored periodically. Alarms and/or enunciators may be incorporated to signal a problem to a manned station, but unattended operation must necessarily place greater demands on the control system.

OFF-LINE CLEANING SYSTEM SIZING

Sizing of a pulse-jet off-line cleaning system for a particular application involves the following series of steps:

- Determination of the overall allowable inserted system pressure drop.

- Breakdown of this pressure drop into its (3) constituent parts:

    - Pressure required to satisfy the gas only system losses (with no particulate).
    - Pressure required to overcome the residual filter drag of the cleaned fabric.
    - Pressure required to support the cleaning cycle as the dust load on each module varies throughout the cycle.

- Maximization of this latter component of total differential pressure by component sizing and fabric selection.

- Filter ratio selection to provide:

    - Adequate bag life.
    - Acceptable cleaning cycle frequency.
    - Differential pressure within the allowable limits.

- Control system and instrumentation specification to provide:

    - Allowance for upset conditions
    - Accommodation to load changes.
    - Possible selection errors.

CONTROL SYSTEM DESIGN - ΔP CONTROL

The two basic control methods; i.e., time- and pressure-based cleaning, have already been compared. While pressure-based cleaning does have the built in capability of automatic accommodation to load changes, it suffers from one inherent disadvantage; namely, that the system reverts to time-based cleaning if the low differential pressure set point cannot be satisfied by the pre-set cleaning cycle. Several other features should be noted:

1. If system conditions vary sufficiently that not only the low ΔP setting cannot be satisfied, but also the high ΔP setting cannot be maintained then the system approaches instability which is normally signaled by an alarm on a high-high ΔP setting. At this point, system recovery may be irreversible; i.e., the bags are already plugged and will not clean down.

2. The setting of the low ΔP value is arbitrary in two ways:

    - It is different from the high ΔP setting; i.e., it automatically imposes a wider variation in system ΔP than for time-based cleaning, where effectively the high and low ΔP values are equal.

    - It automatically provides for a finite period in the gross condition between cleaning cycles, which is required to accommodate upset conditions.

3. Module isolation times would normally be selected so that under normal load conditions at least 50 - 75% of the modules would require cleaning to satify the low ΔP setting.

   Note: The remaining 50 - 25 % uncleaned modules supply a safety factor for high load or upset conditions.

   However, at partial loads, the low ΔP might well be satisfied by cleaning only one module, which would impose a severe asymmetric flow distribution through the total system.

CONTROL SYSTEM DESIGN - ALTERNATIVES

In situations where a pulse-jet off-line cleaning system is operated at normal design conditions under ΔP control and it is found that the low ΔP setting is never satisfied, several corrective options are possible, both manual and automatic.

Manual readjustment of the low ΔP set point to a higher value will correct the problem as illustrated in figures 4 and 5. Figure 6 also shows an alternative manual adjustment where the module dwell and isolate times have been reduced so that the module cleaning frequency is increased.

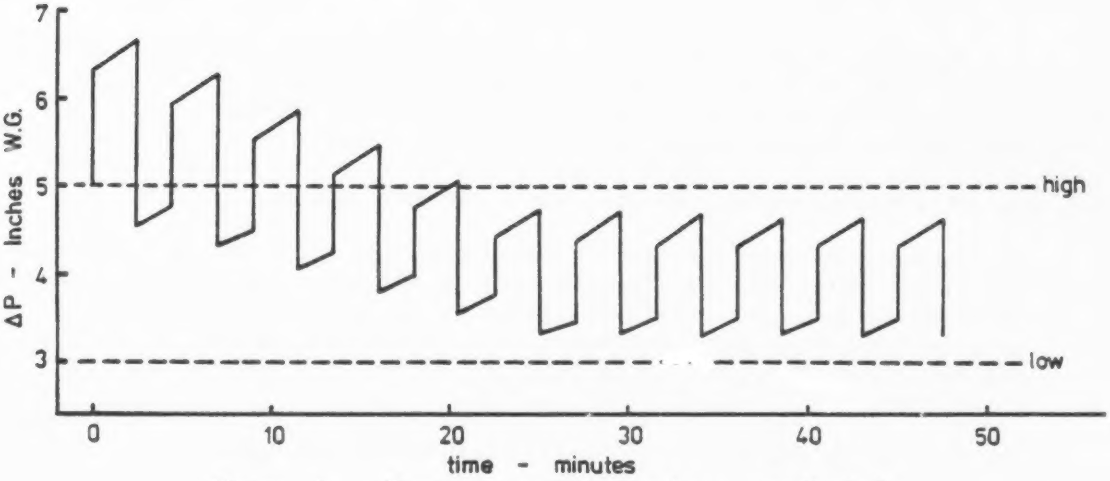

Figure 4. Pressure based cleaning - unadjusted.

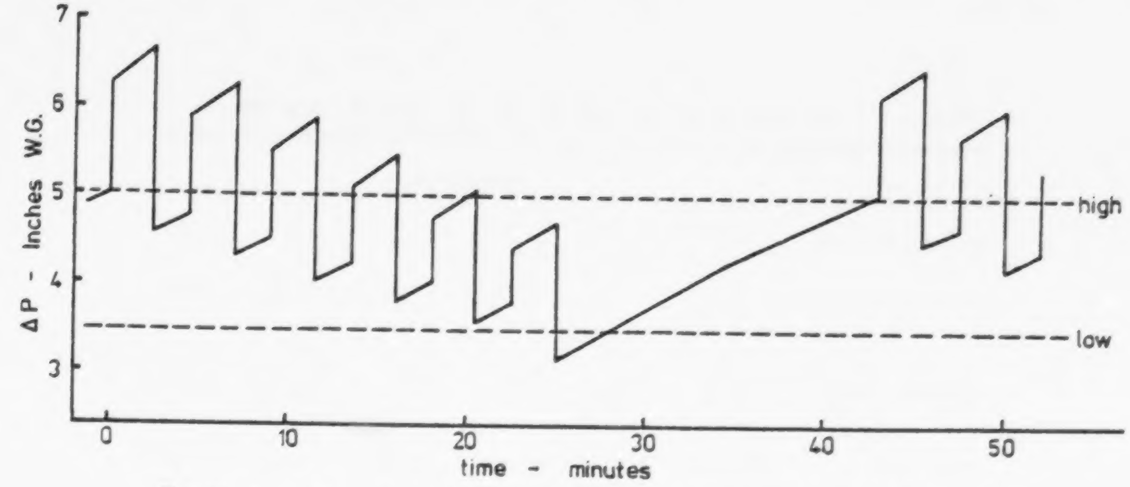

Figure 5. Pressure based cleaning - pressure adjusted.

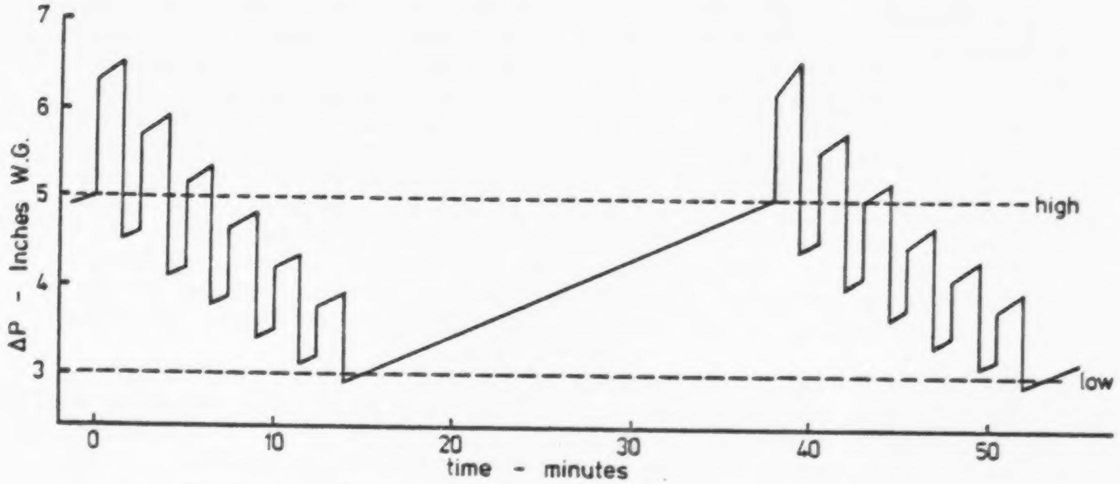

Figure 6. Pressure based cleaning - time adjusted

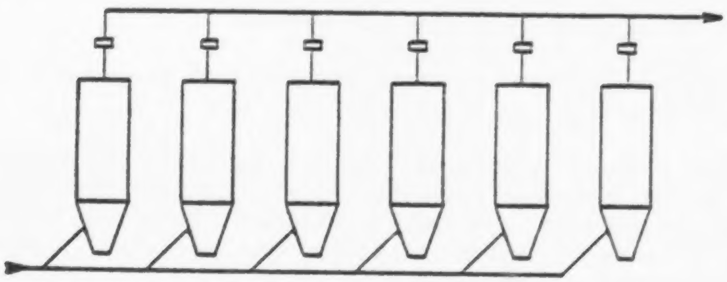

Figure 7. 5 module system with on-line trim.

Table 4. On-line trim sequence for 6 module system.

mode	sequence					
pure off-line	1	2	3	4	5	6
first trim	1/2T	2/3T	3/4T	4/5T	5/6T	6/1T
second trim	1/2-3	2/3-4T	3/4-5T	4/5-6T	5/6-1T	6/1-2T
third trim	1/2-3-4T	2/3-4-5T	3/4-5-6T	4/5-6-1T	5/6-1-2T	6/1-2-3T

A novel way in which this problem can be corrected automatically has been designated "on-line trim" and is illustrated in figure 7 and Table 4. The system essentially superimposes on-line cleaning of selected modules on the normal off-line cleaning sequence. Thus if under normal off-line cleaning with ΔP control, the low ΔP value is not satisfied at the end of the first cleaning cycle (all modules), the first trim step in introduced; i.e., the off-line cleaning of any module during the second cycle occurs simultaneously with the on-line cleaning of the next module in the cleaning sequence. If the low ΔP setting is not satisfied at the end of the second cleaning cycle, then additional on-line trim is introduced where during off-line cleaning of a particular module, on-line cleaning of the next 2, 3 or 4 modules in the cleaning sequence is successively initiated.

The on-line trim is not intended as a cleaning process equivalent to off-line cleaning, but rather as a suppressor of filter cake formation during the trim period so that the system reacts in terms of ΔP as if the number of modules in the system is reduced by one for each trim increment.

As a practical matter, it is desirable to invoke the trim condition at a higher pulse pressure than is used for off-line cleaning. This involves the provision of two separate compressed air systems, either of which can supply the pulse valve reservoirs on demand.

Such a system is presently at the installation stage on a large fluid bed boiler application.

One further comment is apropos. Normal operation of an off-line pulse-jet system under differential pressure cleaning control involves two ΔP settings, namely a high and low value. It should be noted, however, that from the point of view of system stability, the low value is superfluous; i.e., if at the end of a system cleaning cycle the ΔP is no higher than it was at the start of the cycle, then the system is stable.

BAG LIFE

Bag life in an off-line pulse-jet system is dependent on many factors, not the least of which is the frequency and pressure level of the bag pulsing system.

The fact that there is some correlation among bag life, pulse pressure and pulse frequency can scarcely be in doubt, but its exact nature is unknown to this author. The advent of the microprocessor may prove helpful in this regard as it can provide a vast increase in control system operating flexibility and data accummulation.

CONCLUSIONS

It is hoped that this paper provides some additional insight to the mechanics of multi-module pulse-jet off-line cleaning systems.

The author believes that the control system, with automatic response to changes in operating condtions, is the heart of such a system. Additional work is required to throw light on the effect on bag life and system efficiency of variations in pulsing pressure and frequency of the cleaning system.

The work described in this paper was not funded by the U.S. Environmental Protection Agency and therefore the contents do not necessarily reflect the views of the Agency and no official endorsement should be inferred.

FIELD EVALUATION OF THE DRAG OF INDIVIDUAL FILTER BAGS

W. T. Grubb and R. R. Banks
Wheelabrator-Frye Inc.
Air Pollution Control Division
Technical Center
5100 Casteel Drive
Coraopolis, Pennsylvania 15108

ABSTRACT

Evaluation of the performance of filtration fabrics has heretofore necessitated a full compartment test, as only general observations could be made using a few test bags.

Compact, inexpensive, readily portable equipment was developed to measure the filter drag of a single bag by blowing a metered flow of ambient air through the bag and measuring the pressure drop. The test apparatus is set up in the baghouse compartment to minimize disturbance to the bag and its dust cake.

Test results show reproducibility and statistically significant differences among bags made of different cloths and at different sites. Evaluation of the performance of various filter fabrics on the basis of a limited number of trial bags is possible. Selected data will be presented reflecting experience with tests on fiberglass and synthetic bags in five large utility collectors.

INTRODUCTION

In evaluating the performance of fabric filter media in a baghouse filter, one of the primary considerations is the pressure drop across the operating filter media. This pressure drop is a function of the filter drag of the fabric/dust cake system, the superficial velocity of the gas passing through the fabric, and the viscosity of the gas. (1) In a constant temperature situation the gas viscosity does not vary, and the following relationship exists:

$$S = \frac{\Delta P}{V}$$

where: S = Filter Drag (in H_2O-min/ft)

ΔP = Pressure drop across the filter media (in H_2O)

V = Superficial velocity (ft/min)

and $$V = \frac{Q}{A}$$

where: Q = Total gas flow through the filter (ft^3/min)

A = Effective cloth area (ft^2)

The filter drag varies during the filtration/cleaning cycle with the amount of dust cake deposition on the filter. Filter drag just after cleaning is referred to as "residual drag" and just prior to cleaning as "terminal drag." The drag of the filter at any given time during the filtration cycle is the sum of the residual drag, S_R, and the drag of the dust deposited on the fabric during filtration subsequent to the cleaning cycle. In a given baghouse filtration situation, if only one compartment of the baghouse is considered, the factors which affect the drag of the filtered dust layer should be the same for each individual bag within the compartment, assuming uniform flow distribution within that compartment. These factors include dust properties such as specific surface, particle size and density, inlet dust concentration, time since cleaning and filtering velocity. (2) If the filter drag variance with time remains constant, then the residual drag of the "cleaned" fabric would be the factor governing the overall filter drag and pressure drop.

The residual drag of a filter is determined by the properties of the media used, the characteristics of the dust, the interaction of fabric and dust in the formation of the residual cake and the effectiveness of the cleaning method employed. Again considering one compartment of a single baghouse and assuming uniform flow distribution, the dust characteristics and cleaning method should not vary from bag to bag, and if the identical fabric is used for all bags, the residual drag should be the same for all bags.

The determination of actual operating filter drag in a baghouse is a difficult proposition. This is especially true in a multicompartmented, periodically cleaned baghouse where velocity changes occur due to changes in available filter area resulting from compartment isolation during the cleaning cycle. The resultant changes in ΔP due to increased air-to-cloth ratio and increased drag due to dust deposition may cause the fan output to vary, and if reverse-flow cleaning is used, the flow will be increased by the reverse-gas volume. All of these factors combine to make it extremely difficult to obtain simultaneous readings for flow and pressure drop (exclusive of inlet and outlet losses) on individual compartments. To complicate the matter, few commercial baghouses are instrumented to obtain such data. (1)

The comparative evaluation of the filter drag of various fabric filter media in an operating unit requires that, as nearly as possible, the test fabrics be subjected to the same process variables and equipment operation. Testing of a full unit of fabric is not economically feasible, nor is it possible to control process variables during the course of consecutive full-unit tests conducted during different time periods. Single compartment tests have their deficiencies due to flow and dust load variations among compartments and due to the above-stated difficulties in measuring flow and ΔP. The evaluation of a small quantity of test bags within a single compartment by subjective, physical examination or by permeability testing of bags removed from service has been a common practice. Determination of the relative quantity of residual dust cake either by feel or by weighing is not indicative of the cleanability of the filter bags because there is no way of determining the relative flow through the different bags. For example, a fabric with zero permeability would accumulate no residual cake because no dust-laden air would pass through it. Permeability tests of used bags are of limited value because the dust cake is disturbed during bag removal and shipment.

In order to facilitate the evaluation of a limited quantity of test filter bags, Wheelabrator-Frye has developed a method for field testing the filter drag of individual bags in an isolated baghouse compartment, thus minimizing disturbance of the bag and its dust cake.

DESCRIPTION OF TEST EQUIPMENT

The "single bag filter drag" test apparatus consists of a centrifugal blower, 10 5/8 inch wheel diameter, powered by a one horsepower electric motor. The blower intake is equipped with a blast gate allowing the air flow to be controlled. The blower outlet is connected by an adapter to a four-foot length of five-inch diameter flexible hose, which is attached to a two-section metal pipe, five feet long and five inches in diameter. An orifice plate is mounted between the flanged ends of the pipe sections, and felt gaskets are utilized to prevent air leakage. Pressure taps are located one diameter (5") upstream and one-half diameter (2.5") downstream of the orifice, and an inclined manometer is used to measure the ΔP across the orifice during the the test. An orifice calibration curve (ΔP_o vs. Flow) as shown in Figure 1, is prepared by comparison to a standard elliptical flow nozzle.

The outlet end of the metal pipe is inserted into a metal box, one-foot square with three sloping sides, which serves as the inlet into the test bag. The top of the box is equipped with a flange which allows the mounting of a flanged thimble of the type used for bottom attachment of the bags being tested. The inlet box is also equipped with a pressure tap allowing the measurement of static pressure across the test bag, using a vertical manometer. A schematic of this test apparatus is shown in Figure 2, and photographs are shown in Figures 3 and 4. The test apparatus can be easily disassembled for shipment and is readily portable, by two persons, while fully assembled.

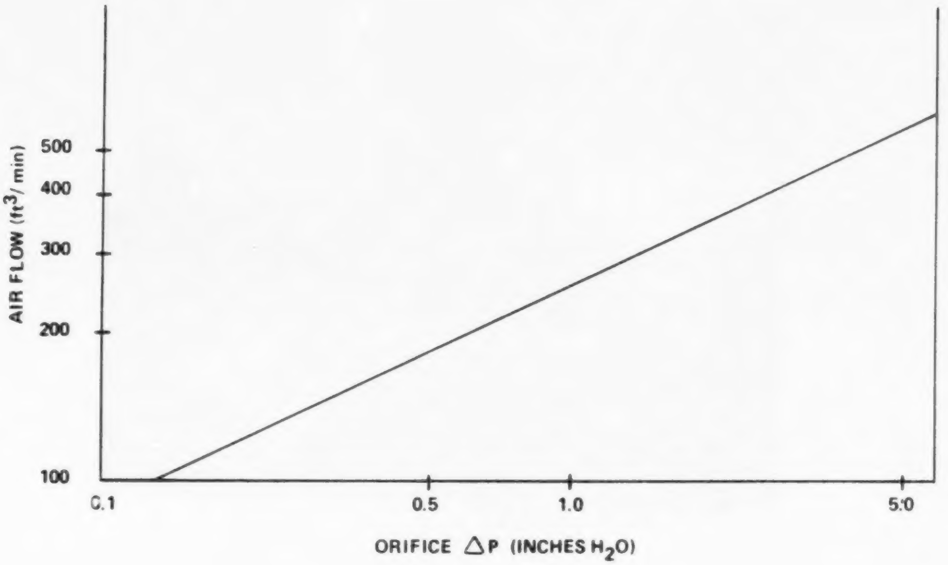

FIGURE 1. CALIBRATION CURVE FOR 3.75 INCH ORIFICE

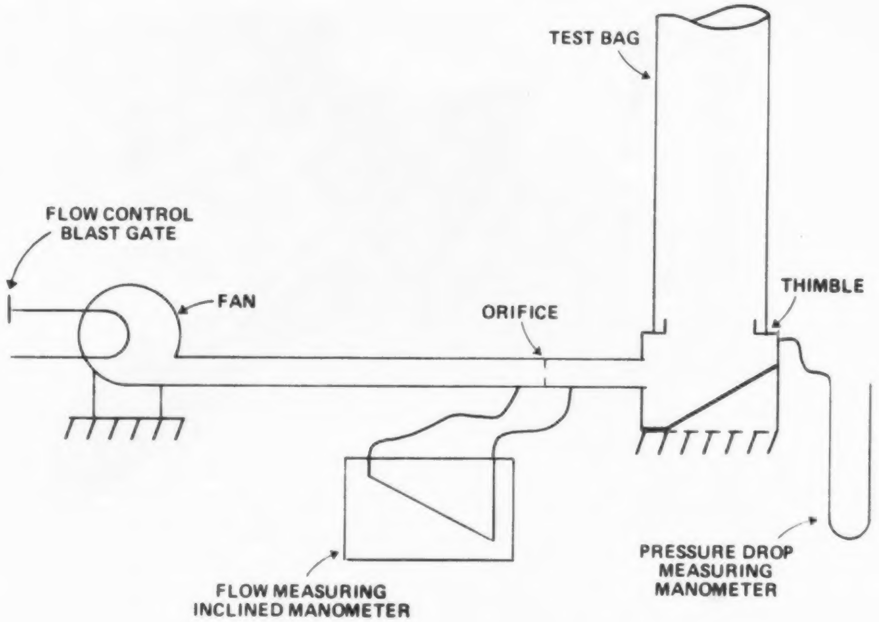
TEST BAG
FLOW CONTROL
BLAST GATE
FAN
ORIFICE
THIMBLE
FLOW MEASURING
INCLINED MANOMETER
PRESSURE DROP
MEASURING
MANOMETER

FIGURE 2. "SINGLE BAG FILTER DRAG" TEST APPARATUS

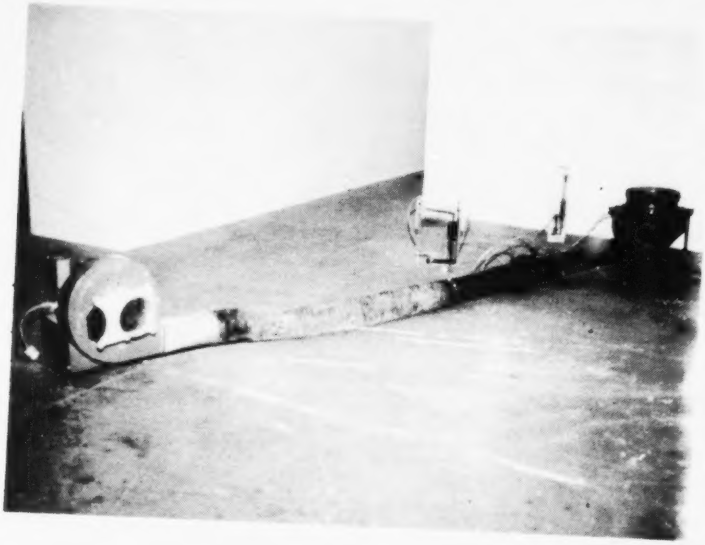

FIGURE 3. "SINGLE BAG FILTER DRAG" TEST APPARATUS: FULL LENGTH VIEW

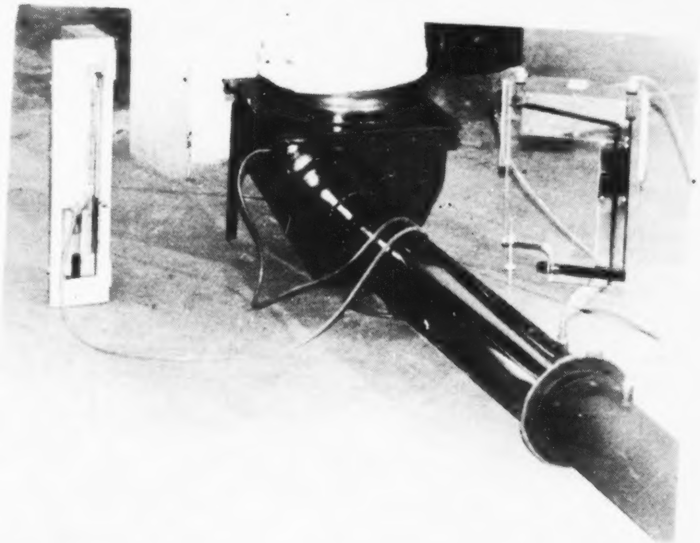

FIGURE 4. "SINGLE BAG FILTER DRAG" TEST APPARATUS:
INLET CHAMBER, THIMBLE, ORIFICE PLATE, AND MANOMETER ARRANGEMENT

DESCRIPTION OF TEST METHOD

The "single bag filter drag" test equipment is assembled and set up in the aisle of the isolated compartment in which bags are to be tested. The inlet box/test thimble is located adjacent to the test bag. The bag is detensioned at the upper suspension level and relaxed slightly to allow the bag bottom to be disconnected from its thimble. The bag cap is removed from its suspension hook, and the bag is manually suspended by any suitable means. The bag is lowered slightly to allow the bottom to be attached to the test thimble, then it is raised to remove any slack. In this configuration, the bag is at a slight angle from the vertical in order to avoid contact with the upper suspension level walkway.

The blower motor is started, and the desired air flow is obtained by utilizing the sliding blast gate to control the orifice ΔP. Tests are usually run at two or more air flows, including the normal operating flow and the maximum flow obtainable by the test blower. When a stable flow condition is reached, manometer readings are taken for both the orifice ΔP and the bag ΔP.

The test bag is then removed from the test thimble, weighed with a 100-lb. spring scale, reconnected to its thimble, and reset to its proper operating tension.

Orifice ΔP readings are converted to air flow (ft^3/min) using the orifice calibration curve. Filter velocity (air-to-cloth ratio) is calculated by dividing the flow by the effective filter area (ft^2), $V = \frac{Q}{A}$. Filter drag (S) is calculated for each bag ΔP reading (ΔP_B) as $S = \frac{\Delta P_B}{V}$. Units of filter drag are inches H_2O-min/ft. Dust loading is determined by subtracting the weight of a new bag and cap from the test bag weight.

TEST RESULTS

During the past two years, eleven (11) series of single bag filter drag tests have been performed on six (6) different coal-fired utility boiler baghouses. These test programs have been divided between the following two approaches:

1. Evaluation of different types of test bags installed in a single compartment.
2. Evaluation of selected bags from full compartment tests.

Results of six series of tests at three different sites are discussed herein.

PP & L HOLTWOOD STATION - BAGHOUSE B

Pennsylvania Power and Light's Holtwood Station had experienced an operating pressure drop which was somewhat higher than expected in their Baghouse B during its initial six months of operation. Sonic horns were installed to augment the reverse flow cleaning system, resulting in significant reduction in system pressure drop. There was however some concern about the fabric used for the original equipment bags, and PP & L initiated a bag test program in May 1981. (3) Six different types of finished glass fabric were used by four different bag suppliers to fabricate twenty-four test bags (three to seven of each type). These bags were installed in Compartment 32, rows C and D. Bags of each type were uniformly distributed from front to rear of the compartment to minimize any positional differences in flow. The sonic horns were rendered inoperable in order to duplicate the design reverse flow cleaning mode in the test compartment. PP & L contracted the services of Wheelabrator-Frye to perform filter drag tests on the individual test bags and on originally installed bags used as controls. Three series of tests were performed: after two months, six months and fifteen months of test bag operation.

Four different glass fabric constructions were evaluated, but only the three variations of 10 oz/yd^2 fabric will be considered herein. These three fabrics have many common properties, differing only in yarn construction, as given in Table 1.

TABLE 1. FABRIC SPECIFICATIONS: PP & L HOLTWOOD BAGHOUSE B TEST BAGS

Fiber:	Glass (ECDE)
Weight:	10 oz/yd^2 (nominal)
Count (Warp x Fill):	54 x 30
Weave:	3 x 1 Twill
Permeability:	35-55 ft^3/min/ft^2 @ 0.5" H_2O

Fabric Code	Yarn Construction	
	Warp	Fill
A	75 1/0	37 1/0 texturized
B	75 1/0	50 1/0 texturized 150 1/0 filament
C	150 1/2	150 1/4 texturized

Four different finish variations were also evaluated. Fabrics A and B were finished with Teflon B (10% loading) applied to greige (not heat-cleaned) fabric. Fabric C was also finished with 10% Teflon B, but was heat-cleaned prior to finishing. Fabric B was also obtained with two different commercially available "acid resistant" finishes, both of which are applied to heat-cleaned fabric.

Significant differences were observed in filter drag of the various bag types as shown in Table 2.

TABLE 2. SINGLE BAG FILTER DRAG DATA FOR VARIOUS 10 OZ/YD^2 GLASS FABRICS: PP & L HOLTWOOD STATION BAGHOUSE B

Fabric Construction	Finish Type	Filter Drag After Indicated Length of Service (In. H_2O-min/ft)		
		Two Months	Six Months	Fifteen Months
A	Teflon B[•]	0.98[+]	1.15[+]	0.95[+]
A	Teflon B[•]	0.74	1.19	0.98
B	Teflon B[•]	0.82	1.07	0.86
C	Teflon B	0.70	0.83	0.64
B	Acid Resistant-1	0.79	0.93	0.67
B	Acid Resistant-2	0.70	0.93	0.74

[•] These finishes were applied to greige (not heat-cleaned) fabric. All others were applied to heat-cleaned fabric.

[+] Originally installed bags, in service for seven months longer than the test bags, tested as controls.

The original equipment bag fabric, type A, was observed to have the highest filter drag. This is probably the result of the "singles" texturized filling yarn construction and application of the finish over greige fabric, both of which may have resulted in increased penetration of particulate into the filling yarn fiber bundle. Fabric B, with the more conventional plied/reinforced filling yarn construction, has a significantly lower drag than fabric A, but substantially higher drag than the three fabrics which had been heat-cleaned prior to finishing. Direct comparisons between fabric constructions B and C could not be made because they were finished differently.

Note the variation in filter drag data among the three test programs conducted at different times. This variation is due to the length of service of the test bags, cleaning cycle variations, boiler operating conditions during the period prior to testing and the procedure used to shut down the boiler or isolate the compartment prior to testing. In spite of these variable conditions, the filter drag values of the different fabrics relative to each other remained virtually the same for the two tests conducted after the bags had achieved a stable residual dust cake. The residual dust loading of the various fabrics was determined during the filter drag testing and is given in Table 3.

TABLE 3. RESIDUAL DUST LOADING ON TEST BAGS PP & L HOLTWOOD BAGHOUSE B

Fabric Construction	Finish Type	Residual Dust Loading (Lbs.) After Indicated Length of Service		
		Two Months	Six Months	Fifteen Months
A	Teflon B	59*	60*	64*
A	Teflon B	26	57	55
B	Teflon B	24	55	56
C	Teflon B	22	54	44
B	Acid Resistant-1	23	54	42
B	Acid Resistant-2	22	52	48

* Originally installed bags, in service for seven months longer than the test bags, and tested as controls.

It is evident that the test bags had not achieved a stable operating condition after two months service. It is also evident that variations in residual dust mass alone do not account for the substantial difference in filter drag among the test fabrics.

PP & L BRUNNER ISLAND

Pennsylvania Power and Light also experienced high operating pressure drop during the initial year of operation in their Brunner Island Station Unit #1 baghouse. This twenty-four compartment baghouse has a design air-to cloth ratio of 2.13:1 (net) and utilizes reverse flow cleaning for its 11.5 inch diameter by 35 foot 4 inch long bags. (4) A bag test program, similar to the one at Holtwood, was initiated in December 1981. Forty-four (44) test bags, fabricated from eight different fabric/finish combinations, by five different bag suppliers, were installed in compartment 3B of the baghouse. Bags of each type were uniformly distributed between the two aisles and from front to rear of the compartment to minimize positional differences in flow. Filter drag tests were performed by Wheelabrator-Frye on the individual test bags and control bags after two and one-half months and after eight and one-half months operation.

Four different glass fabric constructions were utilized, but for purposes of this paper only the three variations of 10 oz/yd^2 glass fabrics will be discussed. As in the Holtwood test, these fabrics are similar, differing only in yarn construction. Variations B and C were again evaluated, along with the original equipment bag fabric, variation D, as described in Table 4.

TABLE 4. FABRIC SPECIFICATIONS: PP & L BRUNNER ISLAND UNIT #1 TEST BAGS

Fiber:	Glass (ECDE)
Weight:	10 oz/yd^2 (nominal)
Count (Warp x Fill):	54 x 30
Weave:	3 x 1 Twill
Permeability:	35-55 ft^3/min/ft^2 @ 0.5" H_2O

	Yarn Construction	
Fabric Code	Warp	Fill
B	75 1/0	50 1/0 Texturized 150 1/0 Filament
C	150 1/2	150 1/4 Texturized
D	150 1/2	75 1/2 Texturized

Five different finish variations were utilized. Fabric D, the original equipment bag fabric was finished with Teflon B (10%) over greige goods. All other finishes were applied to heat-cleaned fabric. Fabrics B and C were treated with Teflon B (10%) finish applied by the same finishing company, and in addition fabric C with Teflon B finish was obtained from a different finisher. Fabric B was also obtained with two different "acid resistant" finishes. Another variable, introduced for evaluation purposes, was the positioning of the smooth filament warp face on the inside filtration surface of the bags made from fabric B with acid resistant finish #3. The results of filter drag tests on the Brunner Island bags are given in Table 5.

The most significant result obtained in the Brunner Island testing was that the bags utilizing the smooth warp face as the filtering surface exhibited a twenty to forty percent lower filter drag than any of the other test bags. These bags also retained 65-75% less dust load than any of the other test bags. Fabric variation C appeared to result in somewhat lower filter drag than fabric B, however additional analysis of recently obtained data and additional testing will be necessary to validate this conclusion.

TABLE 5. SINGLE BAG FILTER DRAG DATA FOR VARIOUS 10 OZ/YD^2 GLASS FABRICS PP & L BRUNNER ISLAND UNIT #1 BAGHOUSE

Fabric Construction	Finish Type	Filter Drag (In H_2O-Min/Ft^2) After Indicated Length of Service	
		2 ½ Months	8 ½ Months
D	Teflon B[•]	2.38[+]	1.47[+]
D	Teflon B[•]	1.52	1.34
C	Teflon B[*]	1.37	1.20
C	Teflon B[§]	1.23	1.04
B	Teflon B[§]	1.54	1.25
B	Acid Resistant 2	1.57	1.24
B[#]	Acid Resistant 3	1.05	0.85

[•] This finish was applied over greige fabric. All others were applied over heat-cleaned fabric.

[+] Originally installed bags, in service for fourteen (14) months longer than the test bags, tested as controls.

[*] Supplier I

[§] Supplier II

[#] Bags utilized with warp face as the filtering surface. All others utilized the texturized filling face.

Filter drag values obtained during the second phase of Brunner Island testing were substantially lower than those obtained during the first phase, in spite of greatly increased residual dust loading in the bags (Table 6). A possible explanation for this phenomenon is that the initial testing was performed in the compartment shortly after it was isolated during normal baghouse operation, but the second phase of testing was performed during a boiler outage with the baghouse cold.

TABLE 6. RESIDUAL DUST LOADING ON TEST BAGS
PP & L BRUNNER ISLAND UNIT #1

Fabric Construction	Finish Type	Residual Dust Loading (Lbs.) After Indicated Length of Service	
		2 ½ Months	8 ½ Months
D	Teflon B[•]	76[+]	>85[+]
D	Teflon B[•]	30	>75
C	Teflon B[*]	24	55
C	Teflon B[§]	19	60
B	Teflon B[§]	29	69
B	Acid Resistant 2	29	58
B[#]	Acid Resistant 3	7	20

[•] This finish was applied over greige fabric. All others were applied over heat-cleaned fabric.

[+] Data on original bags, in service for fourteen (14) months prior to the installation of test bags.

[*] Supplier I

[§] Supplier II

[#] Bags utilized with warp face as the filtering surface. All others utilized the texturized filling face.

SOUTHWESTERN PUBLIC SERVICE COMPANY

Filter drag testing was performed on bags at the Southwestern Public Service Company's Harrington Station. Bags were tested in five (5) compartments of the Unit 2 baghouse and three (3) compartments of the Unit 3 baghouse. These Wheelabrator-Frye baghouses collect fly ash from two identical boilers burning the same western sub-bituminous coal. The baghouses utilize deflate/shake cleaning, and are essentially identical except for the net air-to-cloth ratio which is 3.4:1 in Unit 2 and 3.0:1 in Unit 3 at full load. (5)

The purpose of these tests, in addition to the evaluation of various fabric types, was to determine if there were any positional flow variations within a single compartment or among the various compartments, which might have an effect on the filter drag as measured on individual bags. Each compartment contained bags of a single fabric/finish type. In general, controlled comparison of the filter drag of various bags installed in different compartments of the same baghouse is difficult due to positional flow variation among compartments. The selection of adjacent test compartments which contain bags having the same length of service will minimize any potential flow variation. Care must also be taken to isolate the test compartments at the same temporal position in their filtration/cleaning cycle, preferably immediately after cleaning.

No significant differences in filter drag or bag weight were observed within any of the test compartments which might indicate flow variation as a function of bag position (Table 7). Eight (8) bags were randomly selected and tested along the two outer aisles of the compartment. The center aisle, was avoided due to suspected disturbance of the bags caused by air currents entering the isolated compartment door.

TABLE 7. SOUTHWESTERN PUBLIC SERVICE COMPANY HARRINGTON STATION: SINGLE BAG FILTER DRAG DATA

Unit #	Compartment #	Filter Drag (In H_2O-Min/Ft) Mean	Filter Drag (In H_2O-Min/Ft) Std. Deviation	Bag Weight (Lbs.) Mean	Bag Weight (Lbs.) Std. Deviation
2	4	1.38	0.07	30	2.0
2	6	1.30	0.10	28	1.3
2	16	1.38	0.09	30	0.68
2	22	1.08	0.14	28	1.3
2	26	1.31	0.12	16	0.66
3	2	1.35	0.17	35	1.6
3	19	1.42	0.09	25	0.64
3	27	1.26	0.13	24	1.5

A comparison was made between compartments 19 and 27 on the east side of Unit 3, both of which contained bags of the same fabric type which were installed at the same time. The filter drag in compartment 19, the seventh compartment from the inlet, was significantly higher at 1.42 inches H_2O-min/ft than the filter drag in compartment 27, the third compartment from the inlet, which was 1.26 inches H_2O-min/ft. This data coincides with observations at Harrington Station and many other baghouse installations that compartmental ΔP increases with increasing distance from the flue gas inlet.

PULSE-JET SINGLE BAG DRAG TEST

Wheelabrator-Frye has recently designed and built a unit for testing filter drag of individual pulse-jet type bags. The test apparatus and method is based on the principles previously discussed in this paper. A large number of bags can be tested very rapidly with this method compared to the inside-collecting bag test method. It is anticipated that this method will be as useful for evaluating pulse-jet equipment design features as for evaluating various filter media. Initial field testing has been performed, and the results of this and other tests will be the subject of future technical papers.

SUMMARY AND CONCLUSIONS

A method for field testing of the filter drag of individual bags has been developed, and used extensively to gather data in utility coal-fired boiler baghouses. This method has proved to be valuable in evaluating various bag fabric types while requiring that only a small number of test bags of each type be installed in a single compartment. Meaningful evaluation requires good experimental design, multiple tests conducted over a period of time, and careful data analysis. It should be stressed that this type of evaluation may be valid only for the particular operating conditions existing within the baghouse tested, and generalizations concerning the optimum filtration fabric for any specific coal-fired boiler should not be made solely on the basis of data obtained by this test method in other collectors.

The work described in this paper was not funded by the U.S. Environmental Protection Agency and therefore the contents do not necessarily reflect the views of the Agency and no official endorsement should be inferred.

ACKNOWLEDGEMENTS

The authors wish to acknowledge the support and assistance of Noel Wagner, Senior Project Engineer, Pennsylvania Power and Light Company, in the conduct of the field test program. The authors also acknowledge Greg Lear and Harry Smith of Pennsylvania Power and Light and Richard Chambers and Jerry Hermsmeyer of Southwestern Public Service for their cooperation in the field test program.

REFERENCES

1. "Air Pollution Manual, Part II, Control Equipment", American Industrial Hygiene Association, Detroit, Michigan, 1968.

2. Billings, C. E. and Wilder, J., "Handbook of Fabric Filter Technology, Vol. I, Fabric Filter Systems Study", National Technical Information Service, PB-200 648, Springfield, Virginia, 1970.

3. "Discussion: Report on Operating Experience with Fabric Filter Bags", Proceedings: First Conference on Fabric Filter Technology for Coal-Fired Power Plants, Denver, Colorado, July 15-17, 1981, EPRI CS-2238 Contract WS 81-206.

4. Murray, R. W. and Lear, G. L. "Design, Start-up and Initial Operation of the Brunner Island - Unit 1 Bag Filter." Fifth International Fabric Alternatives Forum Proceedings, Scottsdale, Arizona, January 1981.

5. Chambers R., Ladd, K. and Kunka, S., "Fabric Wear Studies at Harrington Station," Third Symposium on the Transfer and Utilization of Particulate Control Technology, Vol. I, EPA-600/9-82-005a, July 1982.

A DUAL-DETECTOR BETA-PARTICLE BACKSCATTER GAUGE FOR MEASURING DUST CAKE THICKNESS ON OPERATING BAG FILTER AND ESP UNITS

By: Robin P. Gardner
Center for Engineering Applications of Radioisotopes
P.O. Box 5636
North Carolina State University
Raleigh, North Carolina 27650

R.P. Donovan
Process and Chemical Engineering Division
Research Triangle Institute
P.O. Box 12194
Research Triangle Park, North Carolina 27709

L.S. Hovis
Utilities and Industrial Processes Division
Industrial Environmental Research Laboratory
U.S. Environmental Protection Agency
Research Triangle Park, North Carolina 27711

ABSTRACT

To avoid the use of moving mechanical parts in the hostile environment of dust collection that is necessary with the dual-beam beta-particle backscatter gauge, an alternative measurement principle has been sought that still allows the measurement of dust cake density thickness independent of distance from the device. It is found that the use of a dual-detector system, in which each detector detects the response of a different part of the backscattered beta-particle spectra from a single radioisotope source, can be used to accomplish this.

The system investigated here consists of a Sr-90 source and two thin end-window GM counters, one covered with a simple paper filter with density thickness of 0.050 g/cm^2. The two responses obtained differ significantly with dust cake density thickness so that models of each response can be solved simultaneously for two experimental responses to give dust cake density thickness independent of distance from the device. Laboratory results on a prototype device using paper samples of known density thickness to simulate dust cake density thickness yield standard errors of 0.0278 and 0.0151 g/cm^2 for bag filter and ESP unit configurations, respectively. The range of distances

and simulated dust cake density thickness investigated were 3.4 to 7.4 cm and 0 to 0.2133 g/cm^2, respectively.

This paper has been reviewed in accordance with the U.S. Environmental Protection Agency's peer and administrative review policies and approved for presentation and publication.

INTRODUCTION

To avoid the use of moving mechanical parts in the hostile dust collection environment that is necessary when using the dual-beam beta-particle backscatter gauge for measuring dust cake density thickness on operating bag filters independent of the distance to the device (1), the alternative approach of using the intensities of two ranges of beta-particle energies is investigated here. This approach requires a detection system capable of beta-particle spectrometry. Preliminary feasibility investigations were carried out with a CaF_2 (Eu) scintillation detector coupled to a photomultiplier tube and high voltage supply, and connected to a multichannel analyzer through a preamplifier and amplifier.

The backscattered beta particles from a Sr-90 source with maximum energies of 2.26 MeV were detected with this system for simulated dust cake samples. It became evident from considering the spectra so obtained that a number of other possible approaches existed for the measurement of dust cake density thickness independent of the distance to the device when beta-particle backscatter spectroscopy is employed. It was found that the beta-particle backscatter spectra are unique for each dust cake density thickness and distance. Therefore, probably the most general approach consists of storing backscattered beta-particle spectra for the range of dust cake density thicknesses and distances from the analyzer system. Then the dust cake density thickness and distance for a spectrum obtained for a particular sample at a particular distance can be obtained by a double interpolation procedure. Or one might accomplish the same thing by first developing a model to predict the backscattered spectrum as a function of the dust cake density thickness and distance from the analyzer and then use a nonlinear search to minimize differences between model and experimental spectra to find these parameters. The sensitivity and accuracy of these methods will depend upon how much the backscattered spectra vary with dust cake density thickness and distance from the device.

A number of other simpler methods might also be possible and more practical. These include a range of empirical and mathematical model methods. The original idea of using the intensities of two energy ranges could be extended to the use of the intensities of multiple energy ranges. Another approach is based on reasoning that the shape of these backscattered spectra may be reasonably insensitive to the distance to the dust cake. In this case, simple measures of the spectrum shape might be correlated directly to the dust cake density thickness. Or one might consider any alternate method for measuring distance from the device to the sample (such as the use of an ultrasonic method) used with a single beta-particle backscatter gauge (2).

In the present paper a very simple and practical method for accomplishing the desired measurement is investigated. The method chosen is called the dual-detector beta-particle backscatter gauge and is based on using two thin end-window GM counters with a single radioisotope beta-particle source. One of the GM counters is used with a simple paper filter placed over the thin end window so that the lower energy range of the backscattered beta particles will be adsorbed in, or deflected by, the filter and not be detected. This simple, rugged, inexpensive system provided the two necessary responses to different energy ranges of the backscattered beta particles.

THE PROTOTYPE DEVICE

A prototype dual-detector backscatter beta-particle gauge has been constructed that consists of two thin end-window GM counters and a shielded Sr-90 radioisotope source as shown in Figure 1. The GM counters were made by the Amperex Company and have mica end windows with density thicknesses of 0.0014 g/cm^2. The Sr-90 source has a nominal intensity of 0.1 mCi. It is encapsulated in a welded aluminum cylinder with a diameter of 0.3 cm and a length of 2.2 cm. The source itself is in the shape of a circular disc and is placed at one end of the aluminum-encapsulation cylinder with a covering of only about 0.005 cm. One of the GM counters is used with a paper filter with density thickness in the range of 0.0077 to 0.050 g/cm^2 placed over the end window.

GAUGE CALIBRATION MODELS

BAG FILTER AND DUST CAKE

In the case of a bag filter with accumulation of dust cake on the inside, the model for a single beta-particle backscatter gauge mounted outside the bag filter can be taken as (3):

$$R = Bf(d)[1-\exp(-vy)] + Cf(d)\exp(-v'y)[1-\exp(-ux)] + N \qquad (1)$$

where R is the gauge response in counts per second (c/s); B, C, N, u, v, and v' are model parameters to be determined by a least-squares analysis of calibration data; f(d) represents the effect of sample distance d (in cm) on the backscatter response; y is the bag density thickness in g/cm^2; and x is the dust cake density thickness in g/cm^2. The parameters B and C are the saturation responses in c/s for infinitely thick samples of the bag filter and dust cake (by itself), respectively. The parameter N is the background counting rate in c/s when neither bag filter nor dust cake is present; v and u are the backscatter coefficients for the bag filter and dust cake in cm^2/g, respectively; and v' is the attenuation coefficient of the backscattered beta particles through the filter bag in cm^2/g.

ESP COLLECTOR PLATE AND DUST CAKE

In the case of an ESP collector plate with accumulation of dust cake on the same side as the gauge, the model for a single beta-particle backscatter gauge can be taken as:

$$R = Cf(d)[1-\exp(-ux)] + Pf(d)\exp(-u'x)[1-\exp(-wz)] + N \qquad (2)$$

where the parameters are the same as in Equation 1; P, w, and u' are the model parameters to be determined by a least-squares analysis of calibration data; and z is the density thickness of the collector plate in g/cm^2. The parameters P and w are the saturation response and backscatter coefficient for the collector plate in c/s and cm^2/g, respectively. The parameter u' is the attenuation coefficient for the backscattered beta particles through the dust cake in cm^2/g. In the present case, when an infinitely thick collector plate is of interest, Equation 2 becomes:

$$R = Cf(d)[1-\exp(-ux)] + Pf(d)\exp(-u'x) + N \qquad (3)$$

GEIGER-MUELLER TUBE DETECTOR DEAD TIME

It was found that for the Geiger-Mueller (GM) tube detector and the source used in the beta-particle backscatter gauge, a considerable counting loss due to detector dead time was often encountered. To correct for this, the model for observed (R) and true (R') counting rates, in terms of the detector dead time (r) for a paralyzable detector (3), was used. This model is:

$$R = R'\exp(-rR') \qquad (4)$$

The two-source method (2) utilizing the exact model of Equation 4 was used to obtain the detector dead time (r). This method consisted of obtaining the counting rates of the background, Source 1 plus background, Sources 1 and 2 plus background, and Source 2 plus background, in that order. Then the appropriate model of Equation 4 was used, and iterations on trial values of r were made until all the experimental and calculated values of the counting rates agreed to within a specified amount.

For example, for the counting rates described of 1.10, 1094.00, 2046.00, and 1309.00 c/s, respectively, the detector dead time is found to be 114.6 μsec. The average dead time found for several determinations for the GM tube used here was 115.0 μsec.

LABORATORY RESULTS

BAG FILTER APPLICATION

The prototype gauge was used to obtain results for various paper thicknesses on top of a piece of bag filter (density thickness of 0.0375 g/cm^2) at various distances to simulate bag filter dust cake samples. Results were obtained for a number of detector filter thicknesses in the range from 0.0077 to 0.050 g/cm^2 on one of the detectors while the other detector was used without a filter. When the bag filter density thickness is constant, as in the present case, Equation 1 can be reduced to:

$$R = B'f(d) + C'f(d)[1-\exp(-ux)] + N \tag{5}$$

where B' and C' are $B[1-\exp(-vy)]$ and $C\exp(-v'y)$, respectively. The form of f(d) was found to be adequately represented by:

$$f(d) = \exp(-ad) \tag{6}$$

where the parameter a in cm^{-1} is found by a least-squares analysis of data. However, it was found that the value of a was not equal in both places that it appears when Equation 6 is substituted in Equation 5. In this case Equation 5 must be taken as:

$$R = B'\exp(-ad) + C'\exp(-a'd)[1-\exp(-ux)] + N \tag{7}$$

While a rigorous complete optimization has not been completed, the results obtained so far indicate that the detector filter thickness of 0.050 g/cm^2 is the most promising. Results for this case are given in Table 1 and plotted in Figures 2 and 3.

Note that one may use the derived response obtained by subtracting the filtered GM tube response from the unfiltered GM tube response as well as the two direct responses. From these three possible responses there are three possible combinations of the two required responses. The optimum two responses for a particular case depend upon the detector filter thickness being used. However, in most cases the two optimum responses are the filtered GM tube response and the unfiltered minus the filtered GM tube response, since this combination gives the two responses that represent the extremes in backscattered beta-particle source energies. This was the case for the 0.050 g/cm^2 filter. The choice of the optimum two responses is also affected by the fact that the derived response is somewhat correlated to each of the two direct responses, while the two direct responses are completely uncorrelated.

The model parameters obtained by a least-squares analysis of the data were: $u = 15.593$, $a' = 0.29432$, $a = 0.31036$, $C' = 98.477$, $B' = 244.880$, and $N = 13.77$ for R1; and $u = 11.059$, $a' = 0.20905$, $a = 0.36427$, $C' = 35.207$, $B' = 62.746$, and $N = 11.66$ for R2. The reduced χ^2 values, assuming that the standard deviations were 0.01 R, were 2.98 and 5.08, respectively. When only dust cake density thicknesses less than 0.11 g/cm^2 are considered, the measurement standard deviation of the dust cake density thickness is reduced to 0.0178 g/cm^2. When the exact known distances are used in Equation 7 with experimental values of R2 and the model parameters for this case, the standard deviation of the measured values of the dust cake density thickness is reduced to only 0.0134 g/cm^2 for all cases and 0.0036 g/cm^2 for only those samples with dust cake density thickness less than 0.11 g/cm^2.

ESP APPLICATION

The prototype gauge was also used to obtain results for various paper thicknesses at various distances on a 0.16 cm thick stainless steel plate to simulate the dust cake and collector plate samples in an operating ESP unit. The same range of distances (3.4 to 7.4 cm) and simulated dust cake density thicknesses (0 to 0.2133 g/cm^2) were investigated as with the bag filter case.

The optimum gauge detector filter again appears to be that of 0.050 g/cm^2, and the two optimum responses are again the filtered response and the unfiltered minus the filtered response. The results are given in Table 2 and shown plotted in Figures 4 and 5.

The appropriate model in this case (when there is an infinitely thick stainless steel plate) is given by Equation 3 using the exponential form for f(d) that appears in Equation 3. However, it is also found that the same value can be used for u' and u in Equation 3. With these changes the model for the ESP application becomes:

$$R = C\exp(-ad)[1-\exp(-ux)] + P\exp(-a'd)\exp(-ux) + N \tag{8}$$

The model parameters obtained by a least-squares analysis of the data were: u = 16.853, a = 0.29881, a' = 0.25512, C = 210.370, P = 750.847, and N = 13.84 for R1; and u = 11.516, a = 0.22239, a' = 0.22056, C = 22.005, P = 480.422, and N = 11.16 for R2. The reduced χ^2 values, assuming that the standard deviations were 0.01 R, were 2.24 and 2.02, respectively. When only dust cake density thicknesses larger than 0.050 g/cm^2 are considered, the measurement standard deviation of the dust cake density thickness is reduced to 0.00585 g/cm^2. When the exact known distances are used in Equation 8 with the experimental values of R2 and the model parameters for this case, the standard deviation of the measured values of the dust cake density thickness is reduced to only 0.00255 g/cm^2 for all cases and 0.00262 g/cm^2 for only those samples with dust cake density thickness larger than 0.050 g/cm^2.

ERROR ANALYSIS

In addition to determining the standard deviations for the measurement of dust cake density thickness by comparing the measured to the known values, the measurement errors are also obtained by a random number method. The method consists of first randomly choosing the dual-detector responses according to Gaussian distributions of specified standard deviation. Then 10 or more sets of these randomly chosen responses are used to determine measured values of the dust cake density thickness. Finally, the various measured values obtained by this method are used in the general estimator to obtain the measured value of the standard deviation or error of the dust cake density thickness measurement for the particular distance and dust cake density thickness of interest. This has been done for the range of distances and dust cake density thicknesses previously used, and the results are given in Table 3 for Gaussian distributed dual-detector responses with standard deviations of 1 percent.

Examination of the results in Table 3 indicates that the standard deviations or errors calculated by the random number method appear to be consistent with the actual errors given in Tables 1 and 2. The random number errors are approximately two-thirds of the values actually obtained, indicating that a 1 percent error in the dual-detector responses is a fairly representative estimate.

Note that the predicted error increases with increasing dust cake density thickness and is almost independent of distance for the bag filter case. The predicted error decreases with increasing dust cake density thickness for the smallest distance (3.4 cm) for the ESP case, but then exhibits a minimum at 0.16 g/cm^2 for the 4.9 cm distance and at 0.11 g/cm^2 for the 7.4 cm distance.

DISCUSSION AND CONCLUSIONS

From the results it is clear that the dual-detector beta-particle backscatter gauge described and demonstrated here should prove very useful for the measurement of dust cake density thickness in bag filter and ESP units in those cases where the distance to the device is unknown and variable. While the accuracy attainable is not as good as that for the single gauge (2), it is significantly better than that for the previously reported dual-beam gauge (1). For the bag filter case the standard deviation for the dust cake density thickness is 0.0680 g/cm^2 for the dual-beam gauge (1), 0.0196 g/cm^2 for the single gauge used at a known distance (2), and 0.0278 g/cm^2 for the present dual-detector gauge. For the ESP case the standard deviation for the dust cake density thickness is 0.00496 g/cm^2 for the single gauge used at a known distance (2) and 0.0151 g/cm^2 for the present dual-detector gauge.

The accuracy obtained with the present dual-detector gauge is intermediate between that for the single gauge used at a known distance and that for the previously reported dual-beam gauge. There are several compensating advantages for the present dual-detector gauge over the previously reported dual-beam gauge. First of all, there are no moving parts in the dual-detector gauge to become fouled in the harsh environment of the bag filter or ESP units. Secondly, there is only one radioisotope source required, which means that there are no problems of matching source intensities or making more than one correction for decay.

It is likely that better accuracy can be obtained for a dual-gauge device of some other design. For example, one might use an appropriate ultrasonic device to make an accurate separate measurement of the distance of the bag filter or collector plate from the device and then use a simple single beta-particle backscatter gauge to measure dust cake density thickness. The limiting accuracy attainable with any dual-gauge device of this type is 0.0134 g/cm^2 and 0.00255 g/cm^2 for the bag filter and ESP units, respectively. These values are obtained with the Sr-90 source beta-particle backscatter gauge when the distance to the device is known exactly and a 0.050 g/cm^2 filter is used over the GM detector end window.

REFERENCES

1. Gardner, R.P., Donovan, R.P., and Hovis, L.S. A dual-beam backscatter beta-particle gauge for measuring the dust cake thickness on operating bag filters independent of position. In: Third Symposium on the Transfer and Utilization of Particulate Control Technology: Volume III. Particulate Control Devices, EPA-600/9-82-005c (NTIS PB 83-149609), July 1982, pages 128-139.

2. Gardner, R.P., Donovan, R.P., and Hovis, L.S. The one-point in-situ calibration method for using a beta-particle backscatter gauge for continuously measuring dust cake thickness on operating bag filter and ESP units. In these Proceedings.

3. Gardner, R.P. and Ely, Jr., R.L. Radioisotope Measurement Applications in Engineering. Reinhold Publishing Corporation, New York, 1967.

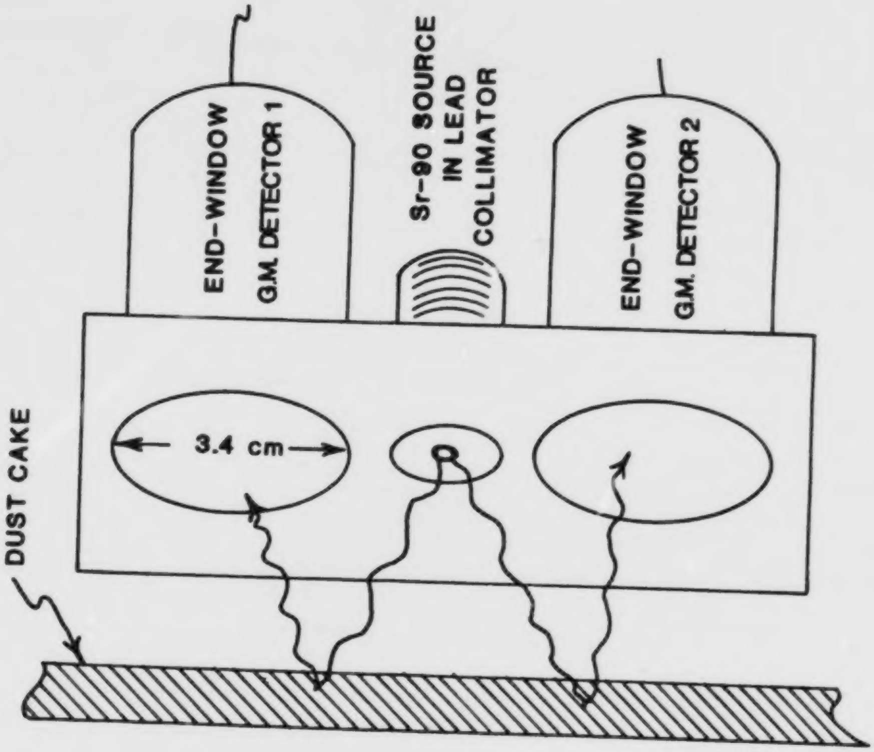
DUST CAKE
3.4 cm
END-WINDOW G.M. DETECTOR 1
Sr-90 SOURCE IN LEAD COLLIMATOR
END-WINDOW G.M. DETECTOR 2

Figure 1. Schematic drawing of the prototype dual-detector beta-particle backscatter gauge.

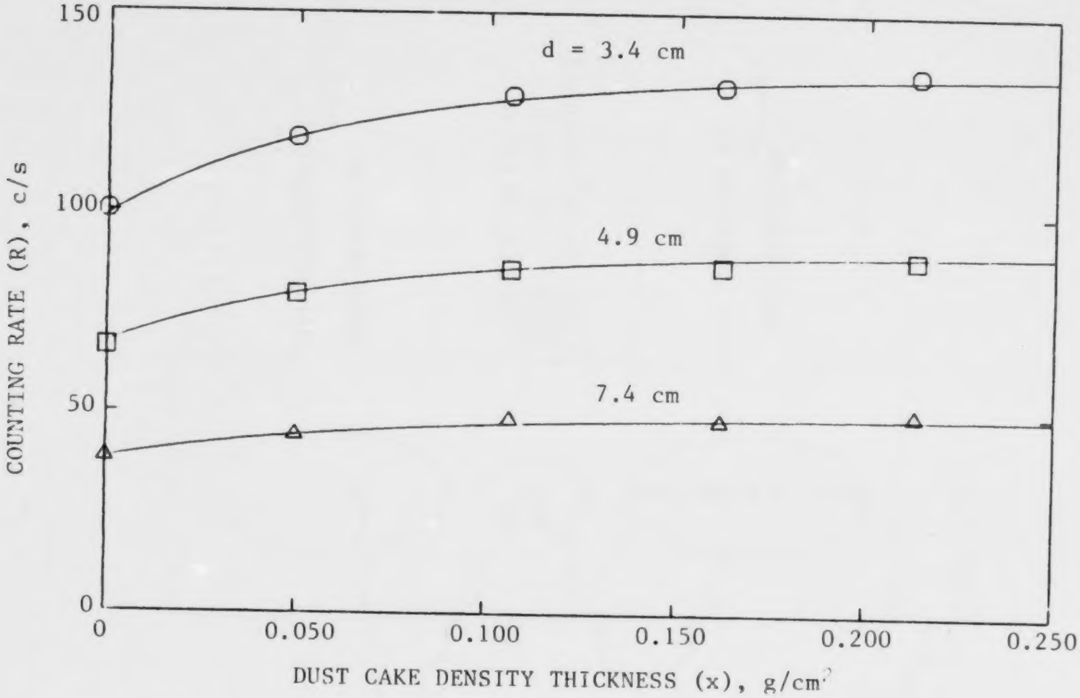

Figure 2. Simulated bag filter experimental and model results for Gauge 1.

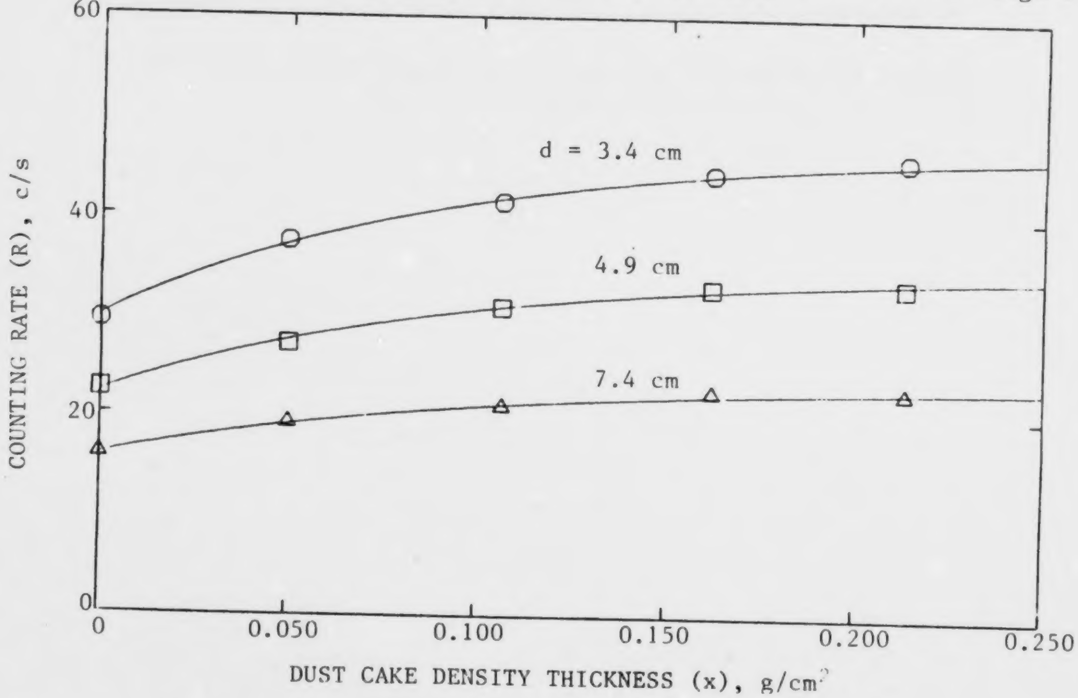

Figure 3. Simulated bag filter experimental and model results for Gauge 2.

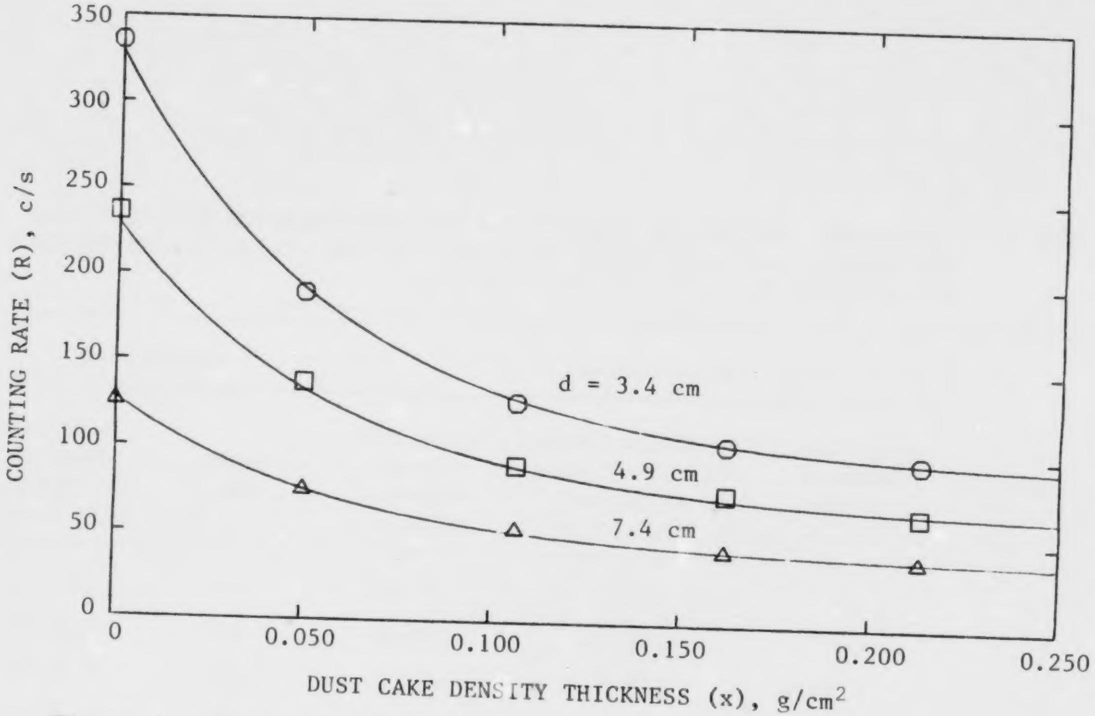

Figure 4. Simulated ESP experimental and model results for Gauge 1.

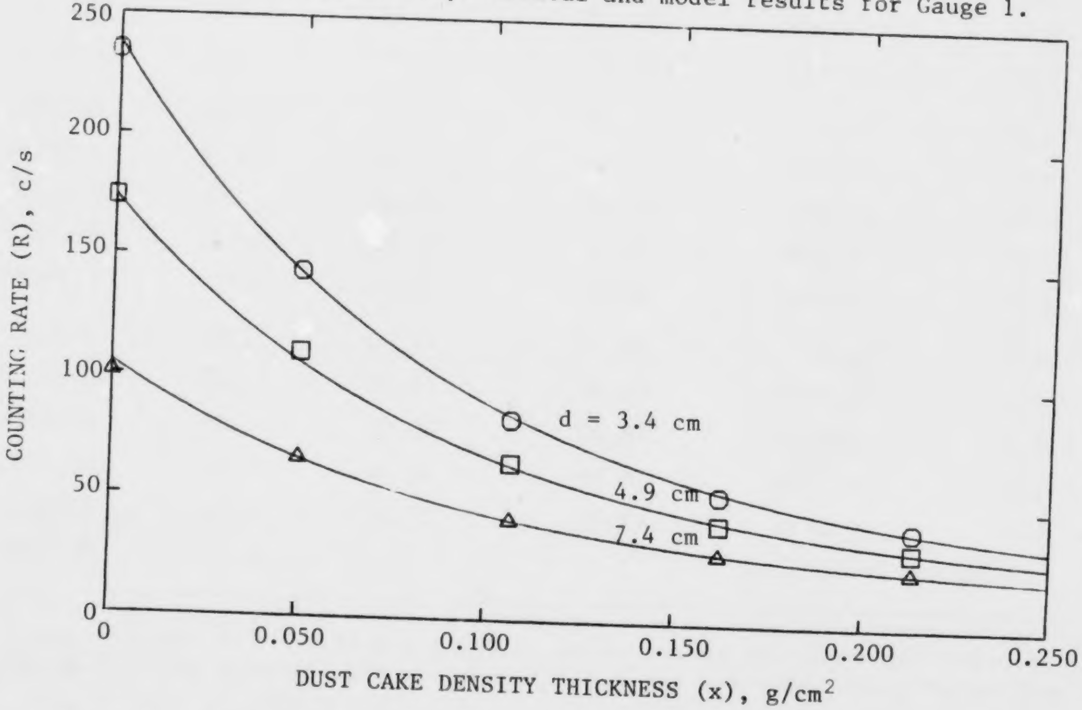

Figure 5. Simulated ESP experimental and model results for Gauge 2.

TABLE 1. LABORATORY CALIBRATION RESULTS FOR THE DUAL-DETECTOR BETA-PARTICLE BACKSCATTER GAUGE RESPONSES FOR SIMULATED BAG FILTER OPERATION WHEN ONE DETECTOR HAS A FILTER OF 0.050 g/cm^2

Experimental				Calculated	
Sample Distance (d), cm	Dust Cake Density Thickness (x), g/cm^2	Unfiltered Minus Filtered Gauge Response[a] (R1), c/s	Filtered Gauge Response[b] (R2), c/s	Sample Distance (d), cm	Dust Cake Density Thickness (x), g/cm^2
∞	---	13.77	11.66	---	---
3.4	0.0	100.26	29.39	2.885	0.01787
3.4	0.0499	118.57	37.52	3.460	0.05784
3.4	0.1062	129.33	41.50	3.311	0.08929
3.4	0.1618	131.87	44.41	3.429	0.17667
3.4	0.2133	134.95	45.86	3.375	0.21948
4.9	0.0	66.37	22.47	5.136	0.00907
4.9	0.0499	79.66	27.16	4.838	0.04169
4.9	0.1062	85.94	30.92	4.914	0.10790
4.9	0.1618	86.94	32.98	5.028	0.22371
4.9	0.2133	88.88	33.25	4.927	0.19824
7.4	0.0	38.48	15.90	7.385	-0.00023
7.4	0.0499	44.40	19.22	7.448	0.05536
7.4	0.1062	48.40	20.93	7.229	0.08587
7.4	0.1618	48.19	22.45	7.494	0.21892
7.4	0.2133	49.77	22.50	7.306	0.16842
Standard Deviations				0.170	0.0278

---

[a] Corrected for dead-time losses using Equation 4 with r = 115 μsec for the unfiltered gauge responses and r = 223 μsec for the filtered gauge responses.

[b] Corrected for dead-time losses using Equation 4 with r = 223 μsec.

TABLE 2. LABORATORY CALIBRATION RESULTS FOR THE DUAL-DETECTOR BETA-PARTICLE BACKSCATTER GAUGE RESPONSES FOR SIMULATED ESP OPERATION WHEN ONE DETECTOR HAS A FILTER OF 0.050 g/cm^2

	Experimental			Calculated	
Sample Distance (d), cm	Dust Cake Density Thickness (x), g/cm^2	Unfiltered Minus Filtered Gauge Response[a] (R1), c/s	Filtered Gauge Response[b] (R2), c/s	Sample Distance (d), cm	Dust Cake Density Thickness (x), g/cm^2
∞	---	13.84	11.66	---	---
3.4	0.0	335.41	234.78	5.226	-0.03501
3.4	0.0499	190.58	144.02	3.723	0.04279
3.4	0.1062	128.37	83.60	3.404	0.10838
3.4	0.1618	105.23	53.75	3.376	0.16598
3.4	0.2133	96.47	40.72	3.421	0.20966
4.9	0.0	235.94	173.90	6.426	-0.03024
4.9	0.0499	138.61	110.32	5.017	0.04346
4.9	0.1062	91.58	65.46	4.871	0.10481
4.9	0.1618	76.66	41.79	4.608	0.17262
4.9	0.2133	66.05	32.15	4.986	0.20916
7.4	0.0	125.38	100.79	8.904	-0.02576
7.4	0.0499	75.72	66.08	7.588	0.04568
7.4	0.1062	54.00	41.77	7.023	0.11475
7.4	0.1618	42.68	28.88	7.377	0.16516
7.4	0.2133	38.86	23.22	7.494	0.20911
Standard Deviations				0.771	0.0151

---

[a] Corrected for dead-time losses using Equation 4 with r = 115 μsec for the unfiltered gauge responses and r = 223 μsec for the filtered gauge responses.

[b] Corrected for dead-time losses using Equation 4 with r = 223 μsec.

TABLE 3. RANDOM NUMBER ERROR ANALYSIS OF THE DUAL-DETECTOR BETA-PARTICLE BACKSCATTER GAUGE FOR BAG FILTER AND ESP DUST CAKE MEASUREMENTS WHEN ONE DETECTOR HAS A FILTER OF 0.050 g/cm^2

Experimental		Calculated			
		Bag Filter		ESP	
Sample Distance (d), cm	Dust Cake Density Thickness (x), g/cm^2	Sample Distance (d), cm	Dust Cake Density Thickness (x), g/cm^2	Sample Distance (d), cm	Dust Cake Density Thickness (x), g/cm^2
3.4	0.0	0.260	0.0105	2.31	0.0476
3.4	0.0499	0.120	0.00995	0.268	0.00593
3.4	0.1062	0.0762	0.0138	0.117	0.00366
3.4	0.1618	0.0641	0.0183	0.0674	0.00282
3.4	0.2133	0.0656	0.0498	0.0348	0.00265
4.9	0.0	0.0961	0.00359	1.53	0.0309
4.9	0.0499	0.133	0.0121	0.268	0.00660
4.9	0.1062	0.0754	0.0131	0.108	0.00340
4.9	0.1618	0.0674	0.0259	0.0647	0.00232
4.9	0.2133	0.0535	0.0495	0.0507	0.00296
7.4	0.0	0.127	0.00459	2.13	0.0421
7.4	0.0499	0.102	0.0114	0.296	0.00651
7.4	0.1062	0.0821	0.0131	0.0915	0.00258
7.4	0.1618	0.0514	0.0301	0.105	0.00362
7.4	0.2133	0.0382	0.0314	0.0543	0.00398
Averages		0.0941	0.0198	0.499	0.0112

MIT FLEX ENDURANCE TESTS AT ELEVATED TEMPERATURE

John T. Foster and W. Theron Grubb
Wheelabrator-Frye Inc.
Air Pollution Control Division
Technical Center
5100 Casteel Drive
Coraopolis, Pennsylvania 15108

ABSTRACT

The MIT flex endurance test, originally devised for paper, is used to evaluate the fatigue life of woven filtration fabrics. This test is used in predicting the relative life of fiberglass fabric filter bags and in the development of finishes. In the past, MIT flex data has been published only for tests conducted at ambient (room) temperature. Fiberglass filter bags, however, are used at operating temperatures up to 550°F. Since the physical properties of the finishes which protect the cloth change with temperature, MIT flex tests conducted at the operating temperature of the cloth should provide more meaningful data.

An MIT flex tester designed to meet the specifications of ASTM method D2176, and to operate at temperatures as high as 600°F, has been built and tested. A relationship between flex endurance and operating temperature for several commercially finished fiberglass fabrics is presented.

INTRODUCTION

During the cleaning cycle in the operation of a fabric filter the filter media is subjected to some form of flexing regardless of whether shaker, reverse air or pulse jet cleaning is used. It is this flexing during cleaning that is particularly deleterious to bag life in the form of fatigue failure.

Fiberglass cloth is most commonly used in boiler applications for its low cost and high temperature capabilities. However, while individual glass fibers have relatively high tensile strength, the abrasive effect of one glass fiber rubbing against another during flexing of the cloth causes failure after very few cycles. In order to reduce the self abrasive effects of fiberglass cloth, temperature resistant finishes with high lubricity are commonly applied to the cloth during manufacture.

The MIT flex endurance test, originally developed to evaluate the fatigue life of paper and plastics, is a widely used method for evaluating the effectiveness of the finishes used to protect fiberglass cloth from abrasion. Published MIT flex data exists for the commercially available finishes but only at ambient laboratory temperatures (1). Since fiberglass cloth filter bags are used at temperatures ranging from 300°F to 550°F, finishes that protect the cloth would be more meaningfully evaluated if done at baghouse operating temperatures.

Part of Wheelabrator-Frye's commitment to study bag life and the factors affecting bag life involved the construction of an MIT flex tester designed to operate at temperatures up to 600°F. The hot MIT flex tester was constructed to operate within the requirements of ASTM test method D2176 and duplicate the motion of the Tinius Olsen MIT flex tester. Tests were conducted between early and mid 1982 comparing the performance of the hot MIT flex tester operating at ambient laboratory temperature and the Tinius Olsen MIT flex tester operating at the same temperature. Once enough data had been collected to determine that the Wheelabrator-Frye hot MIT flex tester and the Tinius Olsen MIT flex tester produced the same results, a program to evaluate several finishes at elevated temperatures was initiated. Three commonly used finishes on the same fiberglass cloth substrate were compared at 300°F, 400°F and 500°F. A discussion of the construction of the hot MIT flex tester and the results of the fiberglass cloth finish comparison at elevated temperatures is contained herein.

DESIGN OF THE HOT MIT FLEX TESTER

The Wheelabrator-Frye hot MIT flex tester was designed to conform to the requirements for the test apparatus described by ASTM method D2176-69 paragraph 2.1.1 to 2.1.4. The motion requirements for the oscillating folding head described in the above ASTM designation includes rotary oscillating motion 135° ± 2° both to the right and left of the unfolded specimen as shown in Figure I. The required folding frequency is 175 ± 25 left and right cycles per minute.

Parameters of the oscillating motion not considered by ASTM D2176-69 are the description of displacement, velocity and acceleration through the folding cycle. The universally accepted Tinius Olsen MIT flex tester makes use of a Scotch yoke oscillating mechanism, like the one shown in Figure 2, to impart oscillating motion to the lower sample clamp through a rack and pinion drive.

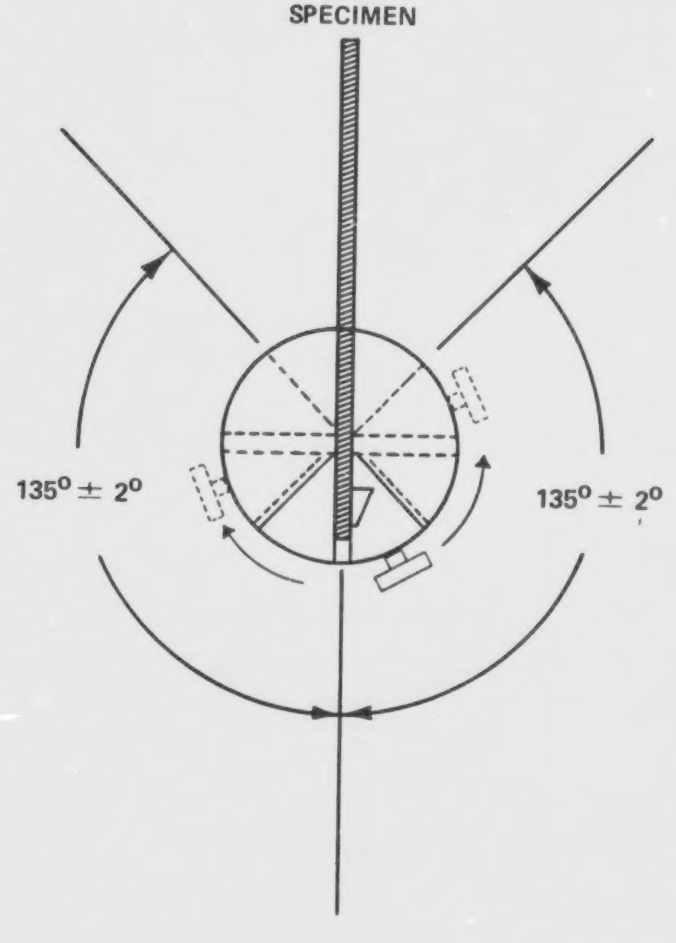
SPECIMEN
135° ± 2°
135° ± 2°

FIGURE 1. OSCILLATING LOWER HEAD

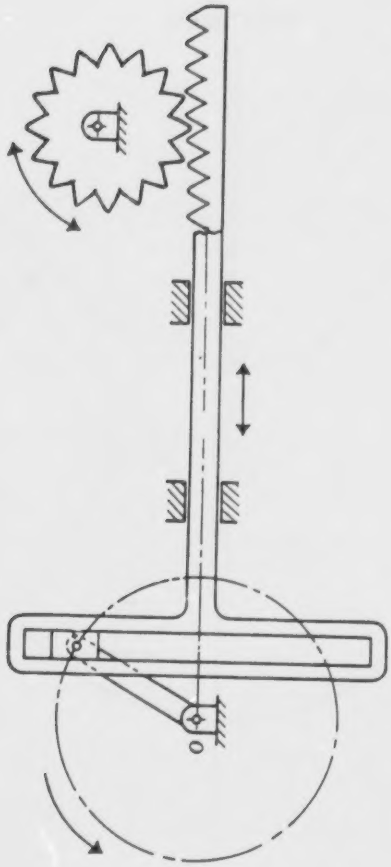

FIGURE 2. SCOTCH YOKE OSCILLATING MECHANISM WITH RACK AND PINION

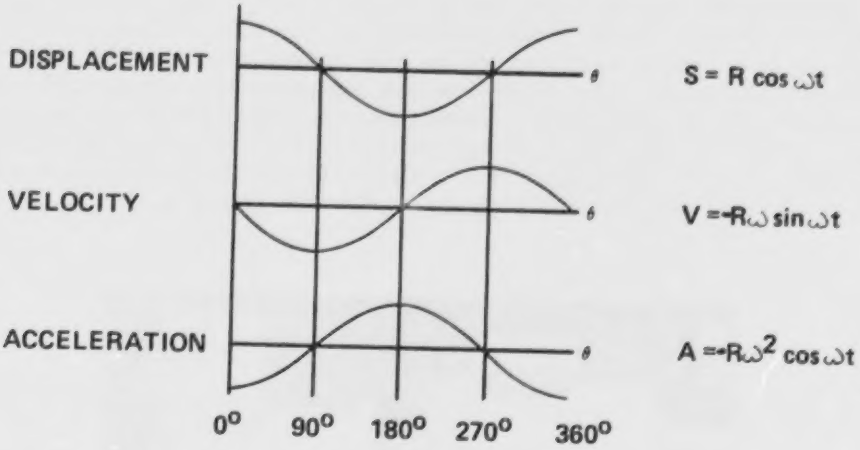

FIGURE 3. SIMPLE HARMONIC MOTION

A mechanism of this type produces simple harmonic motion as shown in Figure 3. In order to maintain comparable performance between the new hot MIT flex tester and the Tinius Olsen machine, an oscillating mechanism was designed to produce simple harmonic motion. Instead of machining the necessary parts to duplicate the Scotch yoke mechanism, the Ferguson right angle cam driven oscillating mechanism shown in Figure 4 was purchased.

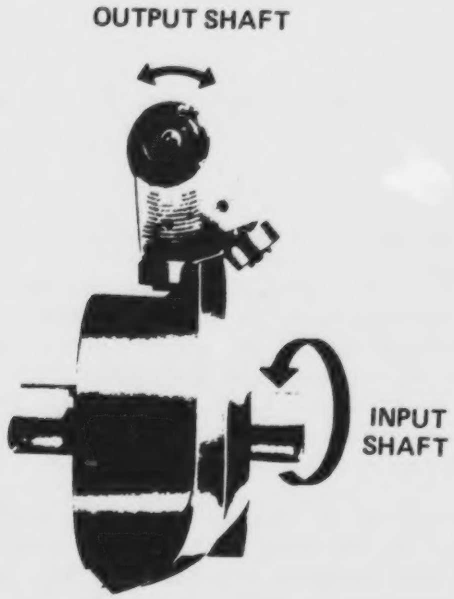

FIGURE 4. RIGHT ANGLE CAM DRIVEN OSCILLATING MECHANISM

This mechanism was selected for its low cost, durability and internal lubrication. Design limitations inherent in the right angle cam drive mechanism do not permit oscillation at the output shaft to be greater than 90° in each direction. The drive cam was custom cut by Ferguson according to Wheelabrator's specification, resulting in simple harmonic motion at the output shaft of the drive mechanism for a 67 1/2° left and 67 1/2° right rotation. Left and right 135° oscillation at the two output shafts used by the flex tester was achieved through 2:1 gearing.

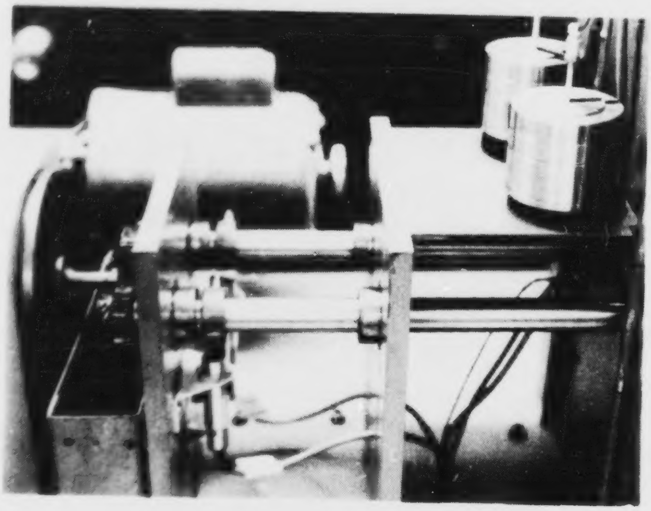

FIGURE 5. GENERAL LAYOUT OF HOT MIT FLEX TESTER

The photograph in Figure 5 shows the general layout of the drive and oscillating mechanisms. At 175 cycles/minute the Ferguson oscillating drive is rated at 760 in-lbs torque. Since the maximum torque required to flex a sample under maximum load is 4 in-lbs, the dual output shaft arrangement shown in the photograph was chosen to double the sample testing capacity of the machine. A magnetic proximity switch on each individual shaft is wired in series with a limit switch that is tripped when the sample breaks. This serves to separately register left and right sample flex cycle counts on two 6 digit electromechanical counters.

The photograph in Figure 6 shows the dual oscillating heads, limit switch housing, counters and oven controller. Upper and lower clamps, primary sheaves and dead weights are Tinius Olsen parts used in the design of the new machine. In addition to the aforementioned counter limit switches, a second pole on each of the two switches in the housing is wired in series to the motor switch to stop the oscillation once both samples have broken.

The oven is constructed of two layers of one inch thick Johns-Manville Marinite I separted by a 1" dead air space and rigid frame. Power to the oven is supplied by two 300 watt Chromalox strip heater elements and regulated by a Chromalox 3800 series analog controller using a J type thermocouple.

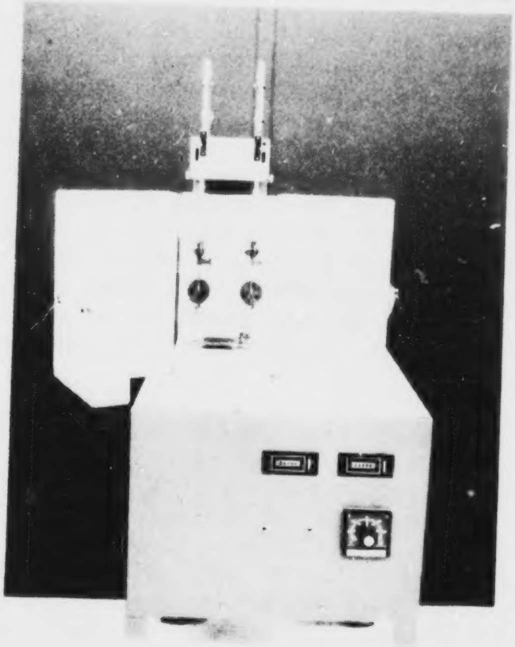

FIGURE 6. HOT MIT FLEX TESTER - FRONT VIEW

HOT MIT FLEX TESTING

In order to determine the variation in results between the Wheelabrator-Frye hot MIT flex tester and the Tinius Olsen flex tester, a series of flex tests were run using .03" lower clamps and a 14 oz/yd^2 fiberglass cloth. The tests were all conducted at ambient temperature with the oven doors of the hot flex tester held open. Each of the three .03" clamps was tested on the Tinius Olsen flex tester and in each of the two positions on the hot flex tester. Data from 100 sets of specimens (three per set) showed no variation between the Tinius Olsen machine and either left or right sides of the hot flex tester.

The Marinite I material used to fabricate the oven is hygroscopic in nature due to the sodium silicate binder that it contains. Initial warmup of the oven after setting several hours at ambient temperature was always accompanied by condensation on the adjacent metal surfaces of the machine. Trial tests conducted immediately after the oven was warmed up from ambient temperature consistently showed a lower number of cycles to failure than tests conducted on the same cloth after an eight hour oven preheat. The lower flex count is probably due to higher humidity associated with driving the excess moisture off of Marinite material during warmup. This assumption is consistent with other published data (2). All hot flex test data presented in this paper is for samples tested after a minimum eight hour preheat if the oven had been permitted to cool to ambient temperature.

Fiberglass cloth must be protected from the gripping surface of the upper and lower clamps during MIT flex testing. At ambient temperatures ordinary masking tape is sufficient for this purpose. However, at temperatures in the 300°F - 500°F range the masking tape deteriorates and the test specimen begins to slip from the clamp. After trials with several types of high temperature tape, DuPont Kapton polyimide tape was selected. The Kapton tape shows no change in properties over the range of test temperatures and has the ability to be impressed into the interstices of the weave of the specimen to prevent slipping. Kapton tape was used on all samples tested at elevated temperature.

EVALUATION OF THREE COMMON FIBERGLASS FINISHES

Three commonly used fiberglass cloth finishes were evaluated at 300°F, 400°F and 500°F using the hot MIT flex tester. In order to hold all parameters except the finish and temperature constant, the same substrate cloth, given below, was selected for all three finishes:

TABLE 1. SUBSTRATE CLOTH CONSTRUCTION

Warp	ECDE 37 1/0
Fill	ECDE 75 1/3 (2 texturized + 1 filament)
Weave	3 x 1 twill
Count	44 x 24 (warp x fill)

Samples with the selected finishes were obtained from the manufacturers and tested for compliance to that manufacturer's specifications with regard to permeability, weight and LOI.

TABLE 2. FINISHED FABRIC SPECIFICATIONS

Finish Type	A Silicone-Graphite-PTFE	B Acid Resistant	C PTFE
Weight (oz/yd^2)	[•]13.09/13.2 ± 5%	13.32/13.5±5%	14.00/14.2±5%
Permeability (CFM/Ft^2) -Avg. of warp and fill sides	58.4/50-65	43.2/35-50	45.0/35-50
LOI (%)	1.79/1.40[+]	4.19/3.80[+]	9.44/9.00[+]

[•] Tested/manufacturer's spec.

[+] Minimum

The effect of heat aging while flexing at elevated temperatures was eliminated by heat aging the samples at the intended test temperature for twenty-four hours in a stationary convection oven prior to testing. Specimens heat aged at 300°F, 400°F, 500°F and a set of virgin specimens were tested at ambient temperature on the Tinius Olsen flex tester. Another group of specimens heat aged at 300°F, 400°F and 500°F were tested at the corresponding elevated temperature in the hot MIT flex tester. Warp and fill directions of each sample were evaluated in this manner.

To minimize the effect of normal variations in the fabric, samples were prepared as shown in Figure 7. This method permits the comparison of one specimen heat aged at each temperature along the same warp or fill yarns.

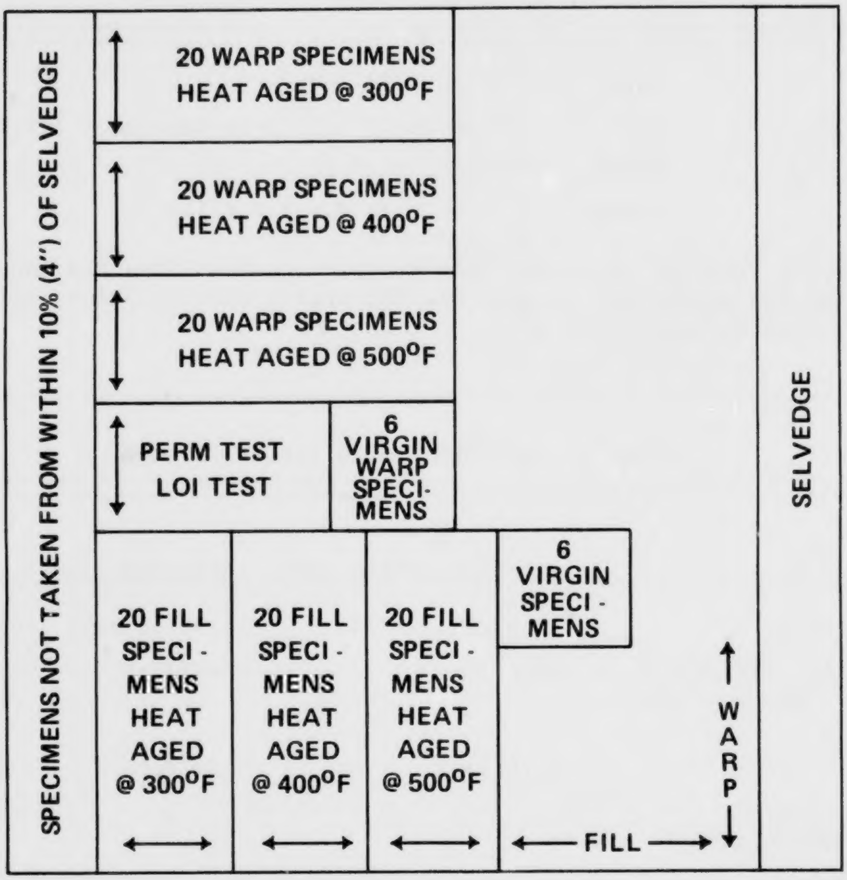
SPECIMENS NOT TAKEN FROM WITHIN 10% (4") OF SELVEDGE
20 WARP SPECIMENS HEAT AGED @ 300°F
20 WARP SPECIMENS HEAT AGED @ 400°F
20 WARP SPECIMENS HEAT AGED @ 500°F
PERM TEST LOI TEST
6 VIRGIN WARP SPECI-MENS
20 FILL SPECI-MENS HEAT AGED @ 300°F
20 FILL SPECI-MENS HEAT AGED @ 400°F
20 FILL SPECI-MENS HEAT AGED @ 500°F
6 VIRGIN SPECI-MENS
WARP
FILL
SELVEDGE

FIGURE 7. SAMPLE PREPARATION

Table III shows the results of ambient and elevated temperature testing. Each data point is the average of; 6 specimens for each virgin fabric test, 5 specimens for each of the ambient temperature tests on heat aged fabric, and 10 specimens for each of the elevated temperature tests on heat aged fabric. The value for a specimen was not used in the average if it was outside of the 95% level of certainty range for the group of specimens (3).

TABLE 3. HOT MIT FLEX TEST DATA

Finish	Virgin	Heat Aged @ 300°F		Heat Aged @ 400°F		Heat Aged @ 500°F	
	Specimens	Ambient	300°F	Ambient	400°F	Ambient	500°F
		(Cycles to Failure - Warp Direction)					
A	1900	1550	7780	2890	16900	4330	14900
B	4050	4800	32900	10100	42700	9620	28600
C	9800	44300	47100	21600	53100	8840	13300
		(Cycles to Failure - Fill Direction)					
A	444	323	464	457	453	580	510
B	1010	1190	2620	1810	2220	2000	1730
C	1170	3230	3810	1600	3250	492	567

The data from Table III has been compared graphically in Figures 8 a-f. In each figure the coordinate axis represents the heat aged temperature of the specimen. Comparison of the absolute values for flex testing a heat aged specimen at ambient temperature and its corresponding elevated temperature is not possible because the effect of the reduced relative humidity at elevated temperature on flex life is not presently known. However, a difference in the shape of the two curves would imply that the response of a given finish to elevated temperature testing is different from the measured effect of heat aging alone. The parallel curves in Figure 8 a and b show that no relative difference in the response of finish A is achieved by elevating the test temperature.

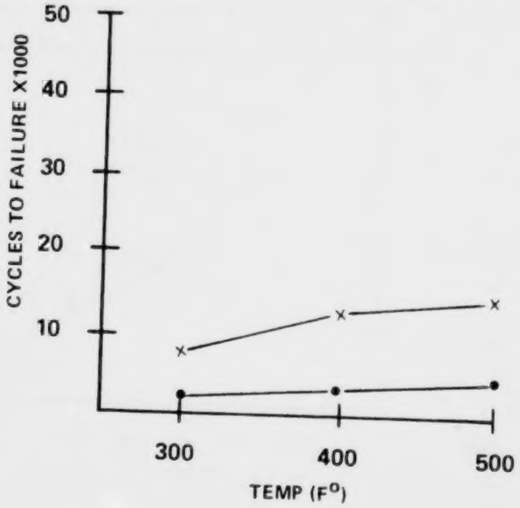

FIGURE 8 a.
FINISH A - WARP DIRECTION FLEX TESTS

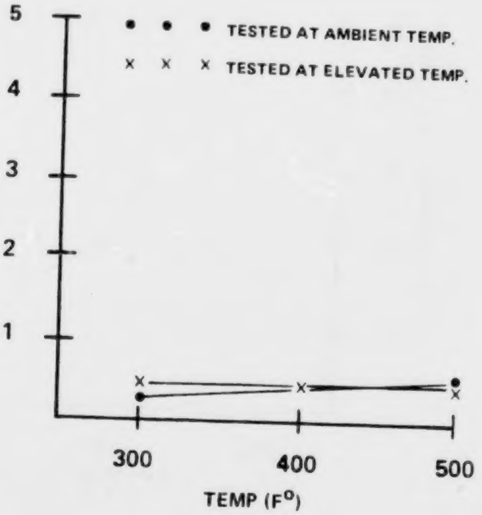

FIGURE 8 b.
FINISH A - FILL DIRECTION FLEX TESTS

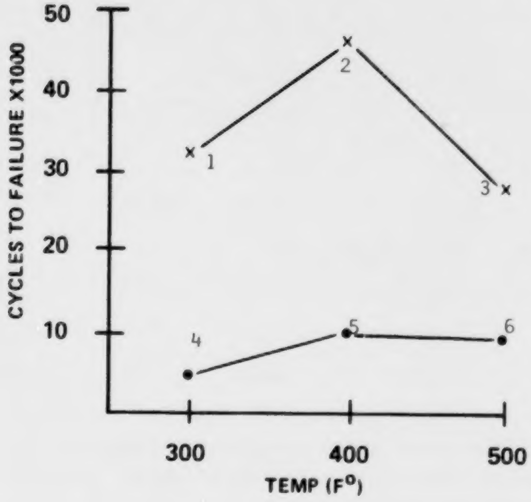

FIGURE 8 c.
FINISH B - WARP DIRECTION FLEX TESTS

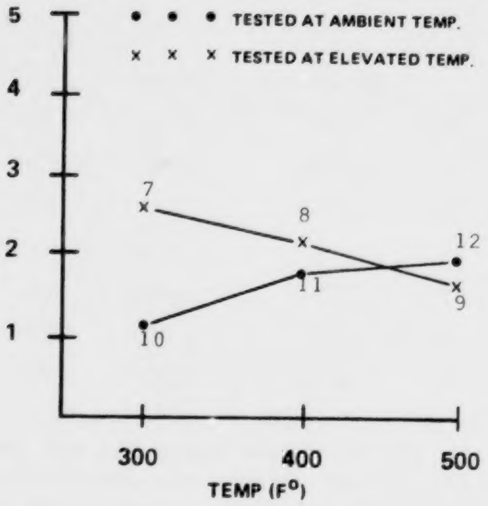

FIGURE 8 d.
FINISH B - FILL DIRECTION FLEX TESTS

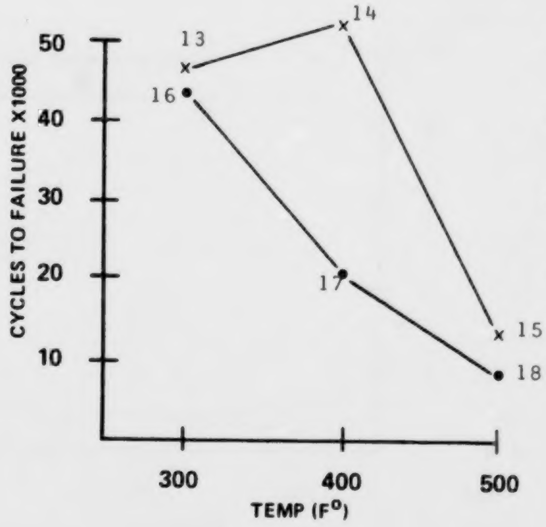

FIGURE 8 e.
FINISH C - WARP DIRECTION FLEX TESTS

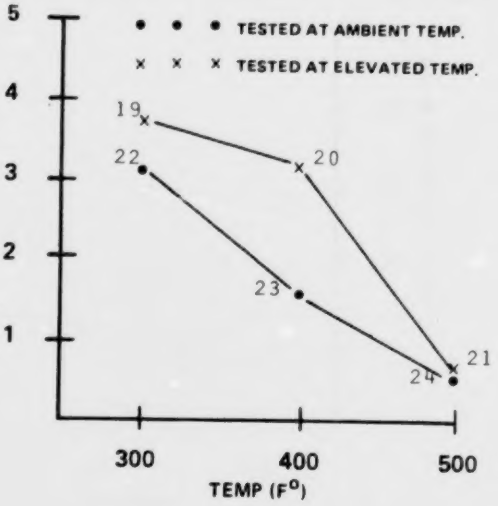

FIGURE 8 f.
FINISH C - FILL DIRECTION FLEX TESTS

The t test is used to determine whether the mean values of two sets of data belong to the same population (statistically the same value) or different population groups (are statistically different). The following set of equations was used to determine the t value between several sets of points in Figures 8 c through 8 f:

$$\hat{S}_W = \sqrt{\frac{(n_1-1)(\hat{S}_1^{\,2}) + (n_2-1)(\hat{S}_2^{\,2})}{n_1 + n_2 - 2}}$$

$$\hat{\sigma}_{\Delta\overline{X}} = S_W\sqrt{\frac{n_1 + n_2}{n_1\ n_2}}$$

$$t = \frac{\overline{x}_1 - \overline{x}_2}{\sigma\Delta X}$$

$\overline{x}_1$ = mean value of first data set
$\overline{x}_2$ = mean value of second data set
$\hat{S}_1$ = standard deviation for first data set
$\hat{S}_2$ = standard deviation for second data set
n_1 = number of points in first set
n_2 = number of points in second data set

t values between points were then compared to the t value for a 95% level of confidence that the two means are from different population groups. The results of the t test shows that for Figure 8 c-f:

Point $1 \neq 2$
$2 \neq 3$
$4 \neq 5$
$5 = 6$
$8 = 9 = 11 = 12$
$7 \neq 10$
$13 = 14 \neq 15$
$16 = 13 \neq 17 \neq 18$
$19 = 20 \neq 21$
$22 \neq 23 \neq 24$

The results of the above analysis show that the shapes of the elevated and ambient temperature test curves are statistically different from each other for finishes B and C. These nonparallel curves imply that the response of finishes B and C to elevated temperature testing is not due entirely to the effects of heat aging. Insufficient test data at elevated temperature precludes any further conclusions with regard to how the finishes compare to one another at elevated temperature.

The fill direction with finish B, Figure 8 d, shows a decrease in flex life with increasing temperature on the elevated test temperature curve compared to an increase in flex life with increasing temperature on the ambient test temperature curve.

One theory for this behavior is a loss of the finish's binding strength at elevated temperature permitting the glass filaments in the fill yarns, many of which are broken during the texturizing process, to pull apart rather than breaking cleanly. The photograph in Figure 9 shows heat aged fill direction specimens tested at elevated and ambient temperatures. The fill yarns of the specimen tested at elevated temperature appear to have pulled apart to a greater degree than the specimen tested at ambient temperature.

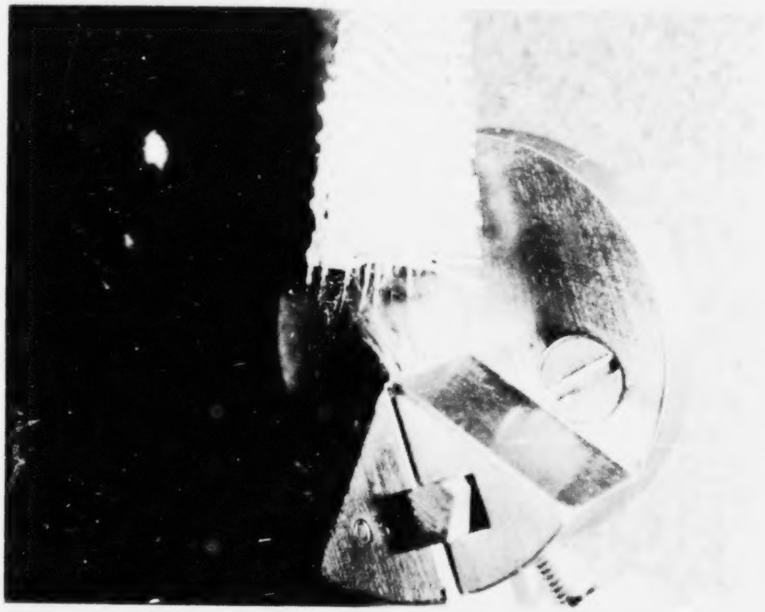

FIGURE 9 a. AMBIENT TEMPERATURE SPECIMEN

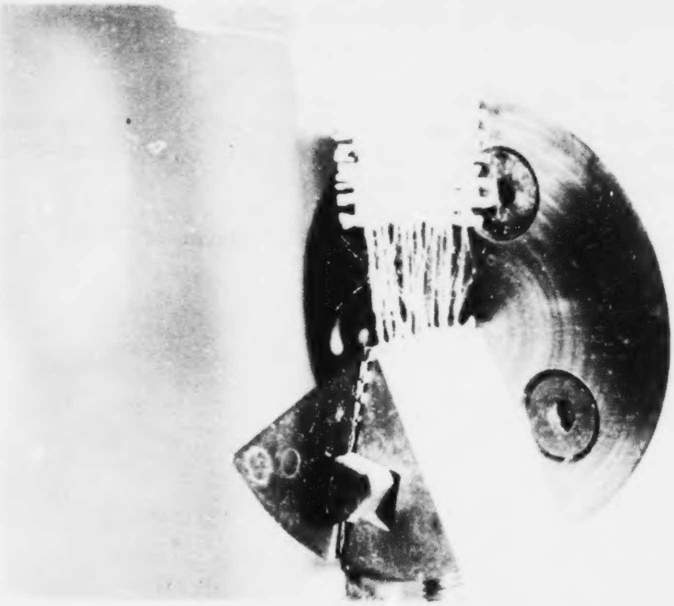

FIGURE 9 b. ELEVATED TEMPERATURE SPECIMEN

SUMMARY

The hot MIT flex tester successfully duplicates, at elevated temperature, the test described by ASTM D2176-69 and commonly performed by the Tinius Olsen MIT flex tester.

Heat aged fiberglass cloth with certain finishes responds differently to flex testing at elevated temperature compared to flex testing at ambient temperature. Some finishes exhibit a reduction in binding strength at elevated temperature as shown by the fill yarns pulling apart during testing in the fill direction.

The work described in this paper was not funded by the U.S. Environmental Protection Agency and therefore the contents do not necessarily reflect the views of the Agency and no official endorsement should be inferred.

REFERENCES

1. Knox, C.E., J. Murray, and J. Schoeck. Technology of Fiber Glass Filter Fabric Design. EPA Report EPA-600/7-79-044b Proceedings of Symposium on the Transfer and Utilization of Particulate Control Technology Vol. 2, 1979.

2. Boudreau, R.J., W. Hoffman and S.C. McCluskey. The Manufacture and Quality Assurance Testing of Fiberglass Filter Fabrics. Proceedings of the First Conference on Fabric Filter Technology for Coal-Fired Power Plants, Denver, Colorado, February 1982.

3. Chou, Y. Statistical Analysis 2nd Ed., Holt, Rinehart, Winston, 1969.

THE ONE-POINT IN-SITU CALIBRATION METHOD FOR USING A BETA-PARTICLE BACKSCATTER GAUGE FOR CONTINUOUSLY MEASURING DUST CAKE THICKNESS ON OPERATING BAG FILTER AND ESP UNITS

By: Robin P. Gardner
Center for Engineering Applications of Radioisotopes
P.O. Box 5636
North Carolina State University
Raleigh, North Carolina 27650

R.P. Donovan
Process and Chemical Engineering Division
Research Triangle Institute
P.O. Box 12194
Research Triangle Park, North Carolina 27709

L.S. Hovis
Utilities and Industrial Processes Division
Industrial Environmental Research Laboratory
U.S. Environmental Protection Agency
Research Triangle Park, North Carolina 27711

ABSTRACT

An an alternative to using the dual-beam beta-particle backscatter gauge to continuously measure dust cake thickness on operating bag filter or electrostatic precipitator (ESP) units independent of gauge distance from the dust, a one-point in-situ calibration method for using a simple beta-particle backscatter gauge is developed and demonstrated. The method consists of obtaining a response model for beta-particle backscatter in terms of dust cake density thickness (areal density), distance from the gauge, and either bag filter or collector plate density thickness. Then, assuming that the density thickness of the bag filter or the collector plate (on the ESP unit) without dust is either known or (for the ESP) larger than the saturation value for the beta-particle source being used, the initial gauge response before dust is present can be used to establish the gauge distance to the bag filter or collector plate.

This approach has been investigated in the laboratory with a system consisting of a Sr-90 beta-particle source and an end-window Geiger-Mueller (GM) tube detector. The ranges of distances and simulated dust cake density thicknesses investigated were 3.4 to 7.4 cm and 0 to 0.2133 g/cm^2, respectively.

The accuracies obtained were quite good. For the bag filter application, dust cake measurement accuracies of 0.015 g/cm^2 or better were obtained for all distances up to 7.4 cm and dust cake density thicknesses less than 0.05 g/cm^2. This assumes counting rate errors of 1 percent and an error in the measurement of the bag filter density thickness of 5 percent. For the ESP application the dust cake measurement accuracies for the equivalent error assumptions were even better, ranging from 0.0012 to 0.017 g/cm^2 for all distances and dust cake thicknesses investigated. This excellent accuracy for the ESP application is in part due to the basic sensitivity for this case (slope of the calibration curve) and in part because there is no error introduced by variations in the ESP collector plate thickness. The accuracies for both applications have been significantly improved by removing the rotating shield superstructure, greatly reducing the background response reported for the predecessor dual-beam gauge.

This paper has been reviewed in accordance with the U.S. Environmental Protection Agency's peer and administrative review policies and approved for presentation and publication.

INTRODUCTION

As an alternative to using the dual-beam beta-particle backscatter gauge to continuously measure dust cake thickness on an operating bag filter independent of gauge distance from the bag (1), and for the dust cake thickness on the collector plate of an electrostatic precipitator (ESP) unit, a one-point in-situ calibration method for using a simple beta-particle backscatter gauge is proposed and developed.

The basic idea is to develop a response model for a simple beta-particle backscatter gauge in terms of the dust cake and bag filter or collector plate density thickness and distance from the gauge. Then, assuming that the bag or collector plate density thickness is known, the initial gauge response with only air (no dust) entering the bag or the ESP unit can be used to establish the gauge distance from the bag or collector plate. Assuming that this distance remains constant throughout operation allows one to convert gauge responses during actual operation to sample density thickness. The assumption of fixed gauge-collector surface separation is very reasonable in the ESP application and has been shown to be surprisingly good for the bag filter as well (1). One can obviously extend this approach to a scanning gauge if the response as a function of vertical distance along the bag or collector plate is taken prior to the introduction of dust.

SINGLE GAUGE MODELS

BAG FILTER AND DUST CAKE

For a bag filter with accumulation of dust cake on the inside, the model for a single beta-particle backscatter gauge mounted outside the bag filter (the growing dust cake is on the side of the collector opposite to that of the gauge) can be taken as (2):

$$R = Bf(d)[1-\exp(-vy)] + Cf(d)\exp(-v'y)[1-\exp(-ux)] + N \qquad (1)$$

where R is the gauge response in counts per second (c/s); B, C, N, u, v, and v' are model parameters to be determined by a suitable least-squares analysis of calibration data; f(d) is the effect of sample distance d (in cm) on the backscatter response; y is the bag density thickness in g/cm^2; and x is the dust cake density thickness in g/cm^2. B and C are the saturation responses in c/s for infinitely thick samples of the bag filter and dust cake (by itself), respectively; N is the background counting rate in c/s when neither bag filter nor dust cake is present; u and v are the backscatter coefficients for the bag filter and dust cake in cm^2/g, respectively; and v' is the attenuation coefficient of the backscattered beta particles through the filter bag in cm^2/g. This equation predicts a response that increases with increasing x.

ESP COLLECTOR PLATE AND DUST CAKE

For an ESP collector plate with accumulation of dust cake on the same side as the gauge, the model for a single beta-particle backscatter gauge can be taken as:

$$R = Cf(d)[1-\exp(-ux)] + Pf(d)\exp(-u'x)[1-\exp(-wz)] + N \qquad (2)$$

where the parameters are the same as in Equation 1 with four additions: P, w, and u' are model parameters to be determined by a least-squares analysis of calibration data, and z is the density thickness of the collector plate in g/cm^2. P and w are the saturation response and backscatter coefficient for the collector plate in c/s and cm^2/g, respectively; and u' is the attenuation coefficient for the backscattered beta particles through the dust cake in cm^2/g. In this case, when an infinitely thick collector plate is of interest, Equation 2 becomes:

$$R = Cf(d)[1-\exp(-ux)] + Pf(d)\exp(-u'x) + N \qquad (3)$$

Both Equations 2 and 3 predict a response that decreases with increasing x, since P (the saturation response to the collector plate) is the dominant term where there is no dust cake and x is zero.

APPLICATION PROCEDURE

The procedure proposed for using this single-beam beta-particle backscatter gauge follows.

1. Calibrate the gauge in the laboratory using a representative piece of the filter bag or the collector plate with a known range of weights of additional material that is compositionally representative of the dust to be collected at various distances.

2. Take gauge responses with the gauge in each position of interest next to the operating bag filter or collector plate when dust-free air is being used, but operation is otherwise normal. Install the gauge on a traverse mechanism if desired.

3. Determine the distance to the gauge from the bag filter or collector plate at each position by using the gauge response with the known bag filter or collector plate density thickness.

4. Take gauge responses when the filter bag or ESP units are in normal operation with dust-laden air, and determine the dust cake density thickness from the calibration curve with the previously determined distance and known response to bag filter or collector plate density thickness.

GEIGER-MUELLER TUBE DETECTOR DEAD TIME

It was found that for the Geiger-Mueller (GM) tube detector and the source used in the beta-particle backscatter gauge, a considerable counting loss due to detector dead time was often encountered. To correct for this, the model for observed (R) and true counting rates (R') in terms of the detector dead time (r) for a paralyze detector (2) was used. This model is:

$$R = R'\exp(-rR') \qquad (4)$$

The two-source method (2) utilizing the exact model of Equation 4 was used to obtain the detector dead time (r). This method consisted of obtaining the counting rates of the background, Source 1 plus background, Sources 1 and 2 plus background, and Source 2 plus background, in that order. Then the appropriate model of Equation 4 was used, and iterations on trial values of r were made until all the experimental and calculated values of the counting rates agreed to within a specified amount.

For example, for the counting rates described of 1.10, 1094.00, 2046.00, and 1309.00 c/s, respectively, the detector dead time is found to be 114.6 μsec. The average dead time found for several determinations for the GM tube used here was 115.0 μsec.

RESULTS

BAG FILTER APPLICATION

The dual-beam beta-particle backscatter gauge previously used (1) was modified by removing the rotating shield and the superstructure necessary to mount it. An aluminum-encapsulated Sr-90 beta-particle source with nominal intensity of 0.1 mCi (3.7×10^{6} Bq) was used as the single source. The source was collimated by using a 0.3 cm diameter by 1.1 cm long hole in a lead shield. Experimental gauge responses were obtained with this device using a sample of an actual bag filter and various paper thicknesses at various distances to simulate bag filter and dust cake samples. The results are given in Table 1 and shown plotted in Figure 1. These results indicate a vast improvement in the signal-to-noise ratio for the single gauge as compared to the dual-beam beta-particle backscatter gauge for the bag filter application. (Note the background counting rate for the infinite sample distance. This is primarily the result of removing the superstructure necessary for mounting the rotating shield which provided a very large source of beta-particle backscatter.)

These results were obtained with the same (constant) bag filter density thickness so that the appropriate modification of Equation 1 is:

$$R = B'f(d) + C'f(d)[1-\exp(-ux)] + N \tag{5}$$

The form of f(d) was found to be:

$$f(d) = \exp(-ad) \tag{6}$$

Substituting Equation 6 into Equation 5 gives:

$$R = B'\exp(-ad) + C'\exp(-ad)[1-\exp(-ux)] + N \tag{7}$$

The values of the model parameters obtained by a least-squares analysis of the data were: B' of 285.308 c/s, C' of 155.714 c/s, a of 0.302 cm^{-1}, u of 14.209 cm^2/g, and N of 24.74 c/s. The values of R calculated from Equation 7 with the quoted model parameters and the known values of the density thickness x are given for comparison purposes in Table 1.

Equation 7, solved for the sample density thickness x, is:

$$x = -(1/u)\ln\{1-[R-B'\exp(-ad)-N]/[C'\exp(-ad)]\} \tag{8}$$

The values of x obtained from Equation 8 with the quoted model parameters and the experimental values of the gauge response R are also given in Table 1. Note that there are cases when the term inside the logarithm becomes negative and Equation 8 cannot be solved. This may occur when ordinary statistical counting rate fluctuations cause a value of R that is too large and is physically unrealistic. In this case it is recommended that one use a specified maximum value for x; 0.25 g/cm^2 is recommended here.

ESP APPLICATION

The gauge modified as previously described with the aluminum encapsulated Sr-90 source was used to obtain experimental results for various paper density thicknesses at various distances on a 0.16 cm thick stainless steel plate to simulate the dust cake and collector plate samples in an ESP unit. The results are given in Table 2 and shown plotted in Figure 2. These results also indicate an excellent signal-to-noise ratio for this application.

To provide additional information, gauge responses were taken for the paper samples both with and without the stainless steel collector plate, and both are given in Table 2. These data provided a basis for directly determining separate geometry factors and backscattering coefficients for the paper (simulating dust cake) and stainless steel collector plate. This revealed, somewhat surprisingly, that the geometry factors were different for the dust cake and stainless steel collector plate, but the scattering coefficients were identical; just the opposite of what was expected.

Due to these differences, Equation 3 is modified to provide an appropriate calibration relationship:

$$R = C\exp(-ad)[1-\exp(-ux)] + P\exp(-a'd)\exp(-ux) + N \tag{9}$$

The model parameter values for u, a, and N remain the same as for the bag filter application: 14.209 cm^2/g, 0.302 cm^{-1}, and 24.74 c/s, respectively. When these values are fixed and the value of a' is independently determined to be 0.245 cm^{-1}, a linear least-squares analysis of the data in Table 2 gives values for the remaining parameters: C = 258.390 c/s and P = 1257.714 c/s.

To obtain measured values of the dust cake density thickness, Equation 9 is solved explicitly for x. Note that if u were not equal to u' as in Equation 3, then a transcendental relationship would be obtained in solving for x. The relationship for x becomes:

$$x = -(1/u)\ln\{[C\exp(-ad)-R + N]/[C\exp(-a'd)-P\exp(-a'd)]\} \tag{10}$$

The values of x obtained from Equation 10 with the quoted model parameters and the experimental values of the gauge response R are also given in Table 2. As in the bag filter application, values of R can occur that yield negative values inside the logarithm so that Equation 10 cannot be solved. In this case this may occur when ordinary statistical counting rate fluctuations cause a value of R that is too small and is physically unrealistic. In this case it is recommended that one use a specified maximum value for x; 0.25 g/cm^2 is also recommended in this case.

ERROR ANALYSIS

The propagation of error in terms of the standard deviation of the measured dust cake density thickness s(x) is obtained in the usual way from the product of the slope of the calibration curve dx/dR and the standard deviation of the gauge response s(R):

$$s(x) = s(R)dx/dR \tag{11}$$

When two or more errors from uncorrelated independent measurements are propagated by addition or subtraction, the total standard deviation is:

$$s^2(R) = m^2(R) + n^2(R) + \ldots. \tag{12}$$

where m(R), n(R), ... are the individual standard deviations.

In this case the errors to be considered should include any error in the measurement of the distance from the gauge to the bag filter or collector plate and the usual error due to statistical counting rate fluctuations. The limiting error in the measurement of distance is also due to statistical counting rate fluctuations. In the bag filter application, any error caused by not knowing the density thickness of the bag filter should also be considered: this error is not pertinent for the ESP collector plate application since the collector plate has a density thickness that well exceeds the saturation thickness for steel for the Sr-90 beta particles and will yield the same backscatter intensity for any thickness larger than about 0.08 cm.

The standard deviation error in the distance measurement for the bag filter application is:

$$s^2(d) = (dd/dR)^2 s^2(R) + (dd/dy)^2 s^2(y) \tag{13}$$

where R in this case is given by Equation 1 with f(d) given by Equation 6 and a value of x of zero (since the measurement of the distance d is made when no dust cake is present). The s(R) and s(y) are the standard deviation errors in the measurement of R and the bag density thickness, respectively. R becomes:

$$R = B\exp(-ad)[1-\exp(-vy)] + N \tag{14}$$

The derivative terms of Equation 13 are obtained by differentiation of Equation 14:

$$dd/dR = \exp(ad)/\{aB[1-\exp(-vy)]\} \tag{15}$$

$$dd/dy = (v/a)\exp(-vy)/[1-\exp(-vy)] \tag{16}$$

As a rule-of-thumb (2), the standard deviation error for the counting rate can be taken as:

$$s(R) = R/100 \tag{17}$$

This assumes that the error due to statistical counting rate fluctuations can be held to less than 1 percent, and that other errors such as electronic instabilities that are proportional to the counting rate are controlling.

The error in the measurement of the bag filter density thickness is less certain. For the present it is assumed to be 5 percent of the true value:

$$s(y) = y/20 \tag{18}$$

The standard deviation error in the dust cake density thickness for the bag filter application consists of contributions from another measurement of R and the uncertainty in the distance measurement:

$$s^2(x) = (dx/dR)^2 s^2(R) + (dx/dd)^2 s^2(d) \tag{19}$$

Here R must include the term containing the dust cake density thickness, so it is given by Equation 7. The derivative terms of Equation 19 are obtained by differentiation of Equations 7 and 8, respectively:

$$dx/dR = \exp(ad)\exp(ux)/uC' \tag{20}$$

$$dx/dd = (a/u)\exp(ad)(R-N)/[C'+B'-(R-N)\exp(ad)] \tag{21}$$

The value of s(d) is obtained from Equation 13 using Equations 14 through 18. The value of s(R) is again taken as Equation 17, but this time with the value of R taken from Equation 7.

The standard deviation errors s(d) and s(x) using these relationships have been calculated for all the distances and simulated dust cake density thicknesses used in obtaining the calibration results given in Table 1. The values of s(d) are independent of dust cake density thickness and are found to be 0.132, 0.133, and 0.139 g/cm^2 for the distances 3.4, 4.9, and 7.4 cm, respectively. The values of s(x) are given in Table 3.

The error in the distance measurement for the collector plate in the ESP application is due only to counting rate fluctuations. If it is assumed as before that this error can be held to within a standard deviation of 1 percent of the counting rate when no dust cake is present and that the error in the actual measurement is 1 percent of the counting rate with dust, then the measurement error is:

$$s^2(x) = (dx/dR')^2 s^2(R') + (dx/dR)^2 s^2(R) \tag{22}$$

where R' and R are the counting rates when no dust is present and when dust is present, respectively. The derivative terms of this relationship are obtained by differentiation of Equation 9 when x is either zero or has some value:

$$dx/dR' = 1/[uP\exp(-a'd)\exp(-ux)] \tag{23}$$

$$dx/dR = 1/[uC\exp(-ad)\exp(-ux)-uP\ \exp(-a'd)\exp(-ux)] \tag{24}$$

The values of the standard deviation are:

$$s(R') = R'/100 \tag{25}$$

$$s(R) = R/100 \tag{26}$$

The standard deviation errors s(x) using these relationships have been calculated for all the distances and simulated dust cake density thicknesses used in obtaining the results given in Table 2. The values are given in Table 3.

DISCUSSION AND CONCLUSIONS

The analysis of the previous section and the resulting predicted measurement standard deviations in Table 3 indicate that the dust cake measurement for the bag filter application is improved over that for the dual-beam gauge previously reported (1). This is primarily due to the large background reduction which resulted from removal of the superstructure necessary for the rotating shield. While the advantage of having a measurement independent of distance from the bag is lost, better accuracy is obtained with the present method and one does not have the problem of the extensive maintenance necessary for the dual-beam backscatter gauge. For systems in which bag distance must be continuously determined, the single-beam, dual-detector technique described elsewhere in these proceedings by Gardner, Donovan, and Hovis (3) is preferable.

Gauge-collector plate distances in an ESP unit do not vary, so the technique is better suited for this application. And indeed, the results obtained for the ESP application are even more encouraging. The fact that the 0.16 cm stainless steel collector plate represents a saturation thickness for Sr-90 beta particles means that no error is introduced by normal variations in the thickness of this plate. In addition the slope of the gauge response with dust cake density thickness is excellent over an extended range. The resulting measurement standard deviations are excellent for a wide range of dust cake density thicknesses and collector plate distances from the gauge. The GM tube detector is quite rugged and should easily withstand the conditions within an operating ESP unit.

Note that the beta-particle backscatter response to paper is not the same as to that of dust cake, since the effective or average atomic number of the dust is higher than that of paper. This means that the actual sensitivity to dust cake will be somewhat higher for the bag filter application and somewhat lower than for the ESP application predicted here.

REFERENCES

1. Gardner, R.P., Donovan, R.P., and Hovis, L.S. A dual-beam backscatter beta-particle gauge for measuring the dust cake thickness on operating bag filters independent of position. In: Third Symposium on the Transfer and Utilization of Particulate Control Technology: Volume III. Particulate Control Devices, EPA-600/9-82-005c (NTIS PB 83-149609), July 1982, pages 128-139.

2. Gardner, R.P. and Ely, Jr., R.L. Radioisotope Measurement Applications in Engineering. Reinhold Publishing Corporation, New York, 1967.

3. Gardner, R.P., Donovan, R.P., and Hovis, L.S. A dual-detector beta-particle backscatter gauge for measuring dust cake thickness on operating bag filter and ESP units. In these Proceedings.

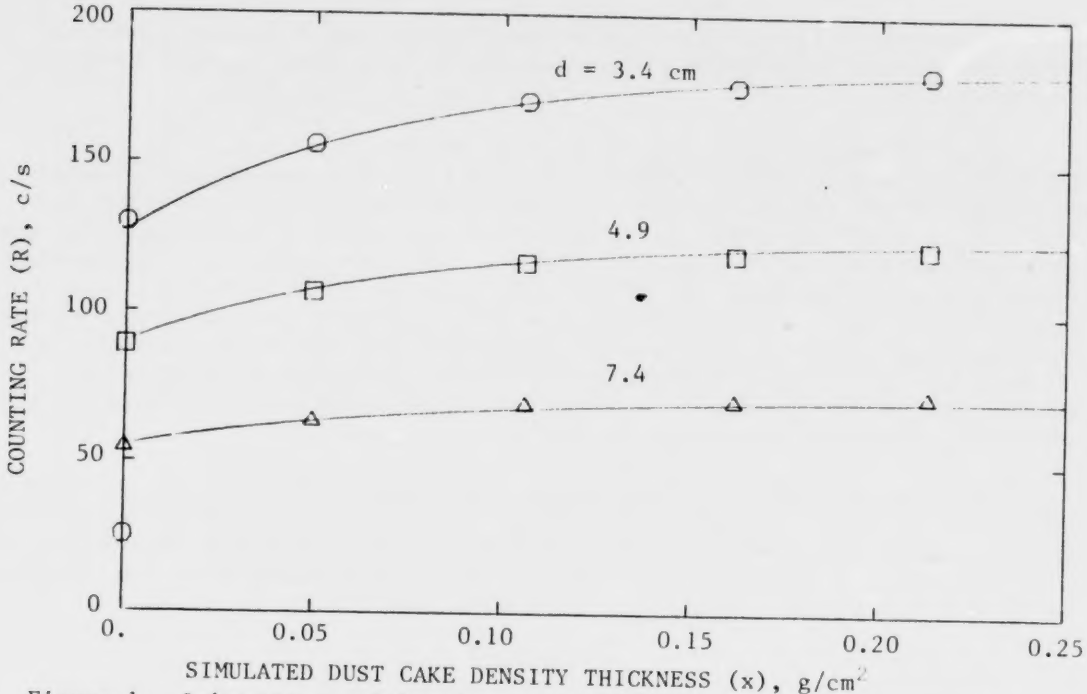

Figure 1. Laboratory calibration results for the single beta-particle backscatter gauge response to paper samples on a bag filter to simulate bag filter operation.

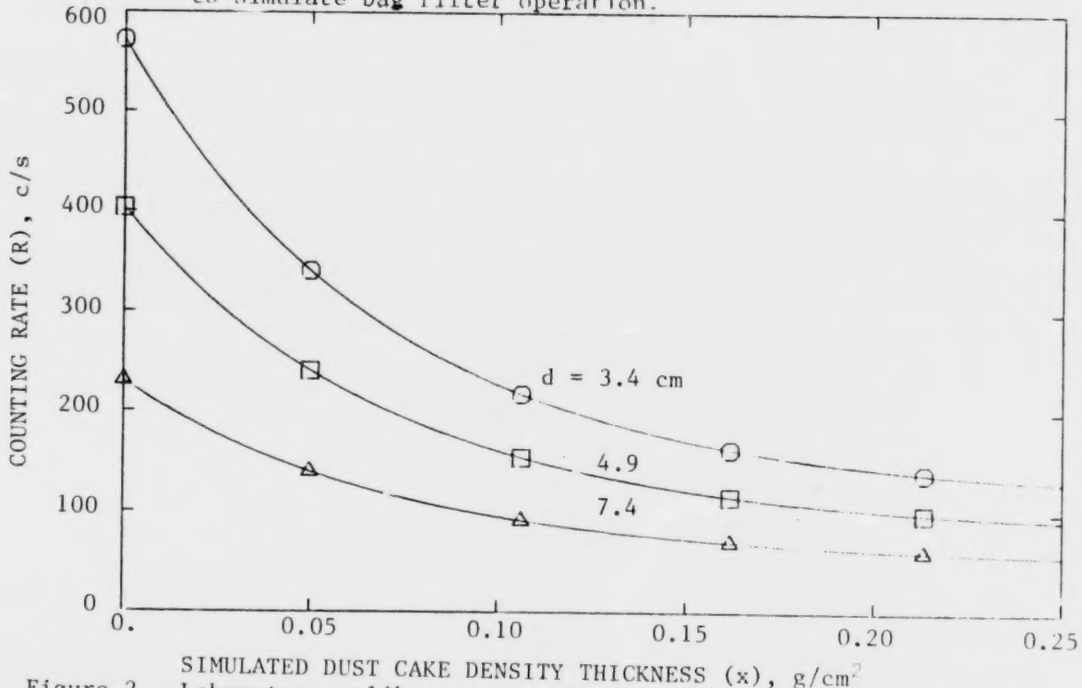

Figure 2. Laboratory calibration results for the single beta-particle backscatter gauge response to paper samples on a 0.16-cm thick stainless steel sheet to simulate ESP unit operation.

TABLE 1. LABORATORY CALIBRATION RESULTS FOR THE SINGLE BETA-PARTICLE BACKSCATTER GAUGE RESPONSE USING A BAG FILTER AND PAPER SAMPLES TO SIMULATE BAG FILTER OPERATION

	Experimental		Calculated	
Sample Distance (d), cm	Dust Cake (Paper) Density Thickness (x), g/cm^2	Gauge Response[a] (R), c/s	Gauge Response (R), c/s	Dust Cake (Paper) Density Thickness (x), g/cm^2
infinite	0.0	25.43	25.42	0.00261
3.4	0.0	129.65	126.92	0.00353
3.4	0.0499	156.09	155.24	0.05210
3.4	0.1062	170.83	170.36	0.10895
3.4	0.1618	176.28	177.09	0.15226
3.4	0.2133	180.81	180.00	0.23859
4.9	0.0	88.84	89.70	-0.00168
4.9	0.0499	106.82	107.70	0.04643
4.9	0.1062	116.86	117.31	0.10227
4.9	0.1618	119.92	121.59	0.13468
4.9	0.2133	122.13	123.44	0.17333
7.4	0.0	54.38	55.27	-0.00366
7.4	0.0499	63.62	63.73	0.04895
7.4	0.1062	69.33	68.25	0.13068
7.4	0.1618	70.64	70.26	0.17994
7.4	0.2133	72.27	71.13	0.25000[b]
	Standard Deviation			0.0196

---

[a] Corrected for dead-time losses by using Equation 4 with r = 115 μsec.

[b] The maximum value allowed and used when the term inside the logarithm in Equation 8 is negative, as at present.

TABLE 2. LABORATORY CALIBRATION RESULTS FOR THE SINGLE BETA-PARTICLE BACKSCATTER GAUGE RESPONSE TO PAPER SAMPLES ON A 0.16-CM THICK STAINLESS STEEL SHEET TO SIMULATE ESP UNIT OPERATION

	Experimental		Calculated	
Sample Distance (d), cm	Dust Cake (Paper) Density Thickness (x), g/cm^2	Gauge Response[a] (R), c/s	Gauge Response (R), c/s	Dust Cake (Paper) Density Thickness (x), g/cm^2
3.4	0.0	570.19(25.08)	571.52	0.00021
3.4	0.0499	326.60(82.78)	340.82	0.05453
3.4	0.1062	211.97(106.3)	217.73	0.11036
3.4	0.1618	158.98(118.2)	162.87	0.16808
3.4	0.2133	137.19(123.3)	139.21	0.22011
4.9	0.0	409.84(25.48)	403.37	-0.00141
4.9	0.0499	241.52(59.93)	240.95	0.04964
4.9	0.1062	157.04(75.81)	154.29	0.10351
4.9	0.1618	118.45(84.17)	115.66	0.15594
4.9	0.2133	98.20(87.59)	99.01	0.21709
7.4	0.0	226.17(24.45)	229.95	0.00152
7.4	0.0499	143.80(39.83)	139.77	0.04673
7.4	0.1062	95.77(50.93)	91.66	0.09919
7.4	0.1618	71.56(51.92)	70.21	0.15666
7.4	0.2133	62.08(54.34)	60.96	0.20468
	Standard Deviation			0.00496

---

[a] Corrected for dead-time losses by using Equation 4 with r = 115 µsec. The values in parentheses are for dust cake (paper) without the stainless steel collector plate.

TABLE 3. PREDICTED MEASUREMENT STANDARD DEVIATIONS FOR THE BAG FILTER AND ESP APPLICATIONS

Sample Distance (d), cm	Dust Cake Density Thickness (x), g/cm^2	Bag Filter Standard Deviation [s(x)], g/cm^2	ESP Standard Deviation [s(x)], g/cm^2
3.4	0.0	0.0054	0.00115
3.4	0.0499	0.0139	0.00184
3.4	0.1062	0.0345	0.00366
3.4	0.1618	0.0795	0.00775
3.4	0.2133	0.1683	0.01588
4.9	0.00	0.0055	0.00116
4.9	0.0499	0.0142	0.00187
4.9	0.1062	0.0351	0.00372
4.9	0.1618	0.0808	0.00789
4.9	0.2133	0.1712	0.01617
7.4	0.00	0.0059	0.00120
7.4	0.0499	0.0151	0.00196
7.4	0.1062	0.0372	0.00393
7.4	0.1618	0.0856	0.00833
7.4	0.2133	0.1812	0.01708
	Averages	0.0622	0.00624

PULSE-JET FABRIC FILTER EXPERIENCE USING NON-GLASS MEDIAS AT AIR TO CLOTH RATIOS OF 5 TO 1 ON A PULVERIZED COAL FIRED BOILER

By: G. L. Pearson
D. D. Capps
Adolph Coors Company
Golden, Colorado 80401

ABSTRACT

A 12-module baghouse system using the Carter-Day high temperature module has been in service since November 1979 controlling emissions from the 450,000 lb/hr Boiler No. 5 unit. Bags were made of felted "Ryton" and cleaning is accomplished via a low pressure-moderate volume, pulse-jet technique.

Experience to date with this baghouse system will be presented. Data on pressure drop, cleaning cycles, cleaning frequency, bag life experience and particulate emissions will be reviewed. Results of on-line evaluation of felted PBI bags will also be presented.

Prepared for Presentation at the Fourth Symposium on the Transfer and Utilization of Particulate Control Technology Sponsored by the U.S. Environmental Protection Agency and held in

Houston, Texas
October 11-15, 1982

Preceding page blank

INTRODUCTION

Energy availability considerations and cost projections motivated Coors to proceed with their second coal fired boiler (Unit No. 5) in late 1976. This unit was scheduled for start-up and went into service in November 1979. In the installation of this coal fired boiler, it was important to the Company that not only permit requirements were met, but that emissions were minimized to the lowest levels possible with current technology. However, both space and capital dollars were at a premium to accomplish these objectives. After study and careful consideration, a pulse-jet type modular system, offered by Carter-Day of Minneapolis, was selected to control particulate emissions. This modular system was ordered in April 1978 and went into service with the boiler in November 1979. It has operated successfully for the last 34 months.

BOILER DESCRIPTION

The boiler is a Combustion Engineering pulverized coal VU-40 type unit rated at 450,000 lb/hr of steam at 825 PSIG and 850°F. Coal is pulverized with three Raymond RB-613 bowl mills. A large fin tube boiler feedwater economizer is utilized to cool the flue gas to within the temperature range of 300°F to 360°F depending upon boiler load. The boiler was designed for, and operates with, a 3 to 1 turn-down capability.

BAGHOUSE MODULE DESCRIPTION

The basic configuration of the Carter-Day Model 376 RF10 high temperature unit is illustrated in Figure 1. Each circular unit has 376 oval pattern bags, 10 feet long for a filter area of 4800 square feet per module. (The 12-module system has 4512 bags and a filter area of 57,600 square feet.) Bags are installed over and supported by carbon steel 9-gauge wire frame cages. Flyash cake is accumulated on the outside of the bags and the filtered flue gas leaves at the top of the units and goes to the induced draft fan and stack. Bags are installed or removed through the top clam shell doors at the top of the units.

Bags are made of 22-ounce per square yard "Daytex" felted fabric. This fabric is essentially felted and needled "Ryton" fibers on a "Gortex" scrim. "Ryton" is the trademark name which Phillips Petroleum has given to Polyphenylene Sulfide. This material has both excellent acid resistance and temperature resistant characteristics up to 370°F.

Cleaning of the filter cake from the outside of the bags is accomplished by opening of the diaphragm valve at the top of the unit and discharging the 7.5 PSIG reservoir tank into the inside of the bags directly under the nozzles on the distribution manifold. Each reservoir tank is charged to 7.5 PSIG by a Miehle-Dexter Model Number 46-4006 positive displacement blower. Since each module has its own blower, tank, valve, etc., the reliability of the overall system is quite good. Tripping of the diaphragm valve is signaled by a pressure switch mounted on the reservoir tank. The distribution manifold is turned at one rotation per minute during cleaning via a small 1/2 HP motor and gear box to the side of the diaphragm valve. When in the cleaning mode, the diaphragm valve pulses approximately every 3.7 seconds.

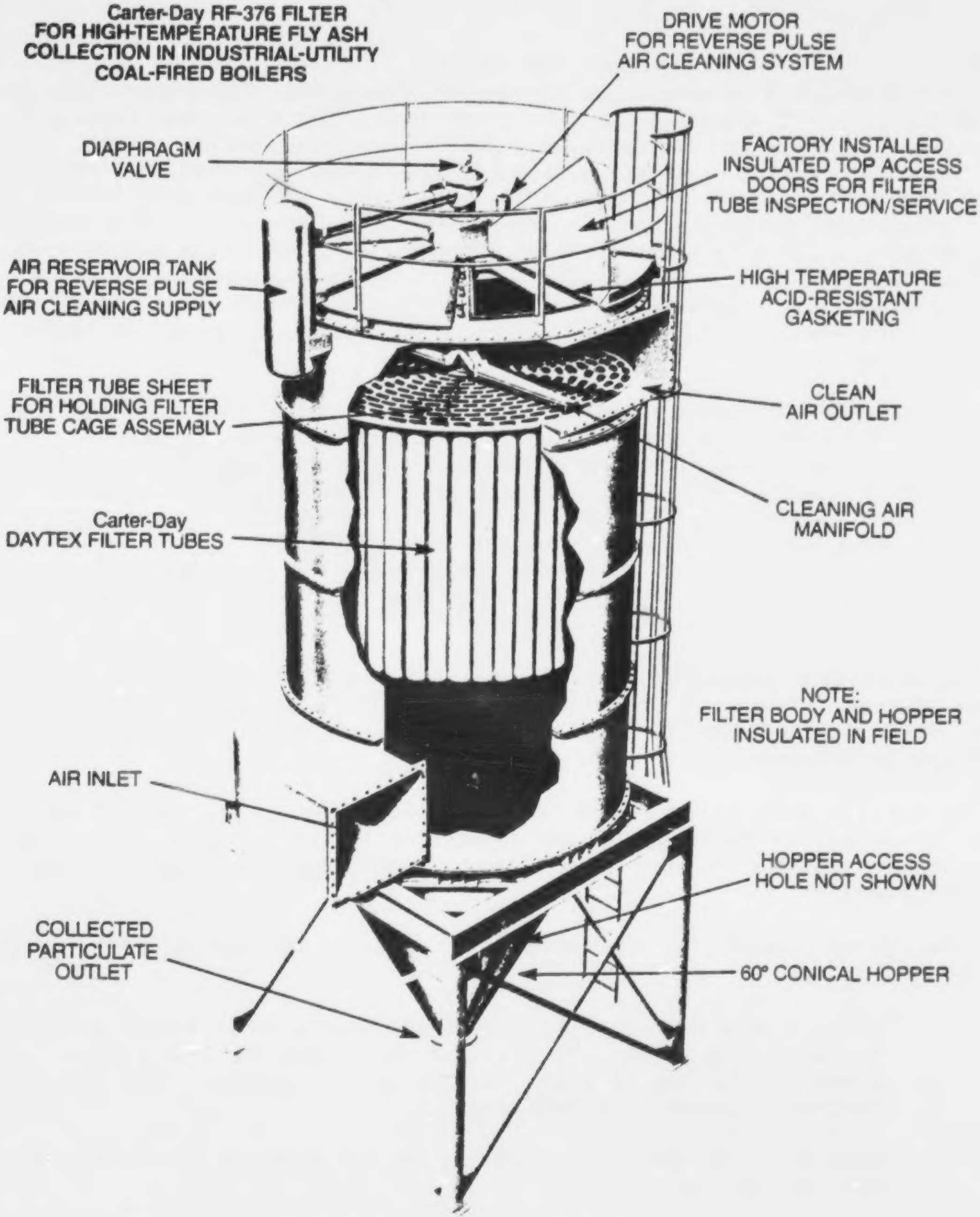
Carter-Day RF-376 FILTER
FOR HIGH-TEMPERATURE FLY ASH
COLLECTION IN INDUSTRIAL-UTILITY
COAL-FIRED BOILERS
DRIVE MOTOR
FOR REVERSE PULSE
AIR CLEANING SYSTEM
DIAPHRAGM
VALVE
FACTORY INSTALLED
INSULATED TOP ACCESS
DOORS FOR FILTER
TUBE INSPECTION/SERVICE
AIR RESERVOIR TANK
FOR REVERSE PULSE
AIR CLEANING SUPPLY
HIGH TEMPERATURE
ACID-RESISTANT
GASKETING
FILTER TUBE SHEET
FOR HOLDING FILTER
TUBE CAGE ASSEMBLY
CLEAN
AIR OUTLET
CLEANING AIR
MANIFOLD
Carter-Day
DAYTEX FILTER TUBES
NOTE:
FILTER BODY AND HOPPER
INSULATED IN FIELD
AIR INLET
HOPPER ACCESS
HOLE NOT SHOWN
COLLECTED
PARTICULATE
OUTLET
60° CONICAL HOPPER

FIGURE 1 MODULE GENERAL CONFIGURATION

BAGHOUSE INSTALLATION AND AUXILIARIES

To insure a good, economical and easy to operate and maintain system, considerable thought and engineering went into the installation. Figure 2 and 3 show the basic module installation configuration. The inlet and outlet plenums were designed to balance the distribution to each module and keep the ductwork free of ash drifts. In order to minimize troublesome and expensive expansion joints, all modules and some flue ducts are supported by hanging rods which allow adequate movement due to thermal expansion. The entire 12-module system has only 10 expansion joints. Each module has a minimum leakage type outlet damper, which can be operated remotely from the control room to either take a module off-line or to accomplish off-line cleaning. When this damper is closed, a small valve at the top of the unit opens, automatically letting air in to purge that particular module and prevent acid corrosion. Each module is equipped with a manually operated inlet damper for use when that module is in a maintenance mode. There are two 60-inch diameter bypass poppet type valves in the system which are used during start-up and oil firing of the boiler. These bypass valves are operated from the control room and can open against 40 inches W.G. pressure.

The conical ash hoppers are insulated with 10 inches of MT-8 mineral wool insulation and electric blanket heaters are used on the bottom 3'-6" portion of the cone to insure that the flyash will stay dry and convey easily. The main portion of the module and all flue ducts are insulated with 4 inches of MT-8 mineral wool insulation. The modules and flue ducts were metal lagged with "Reynolds Rainlock Rib" diamond embossed aluminum 0.0165 inches thick. The conical hoppers, and other difficult areas, were lagged with flat diamond embossed aluminum 0.025 inches thick. High ash level alarms are installed in each hopper.

An enclosure was built for the facility so that maintenance would be easier during bad weather conditions and to satisfy aesthetic considerations since it is located near the main entrance-visitors area of the plant. This enclosure is illustrated in Figures 2 and 3.

An opacity meter (Lear Siegler RM-41) is installed in the 13-foot diameter stack downstream of the baghouse and induced draft fan. Readout of opacity in the control room is located so as to be easily visible from the baghouse operator panel.

The operator panel for the baghouse, located in the control room, has the following features:

1. Pressure drop across the baghouse (inlet plenum to outlet plenum) is displayed on a meter. The operator can select the high pressure that he wants cleaning to start at and the low pressure where he wants cleaning to cease on this meter.
2. Temperature of the flue gas going to the baghouse is displayed on a meter on the control panel.
3. Conditions of either high baghouse pressure drop or high temperature are alarmed via red lights and buzzers.

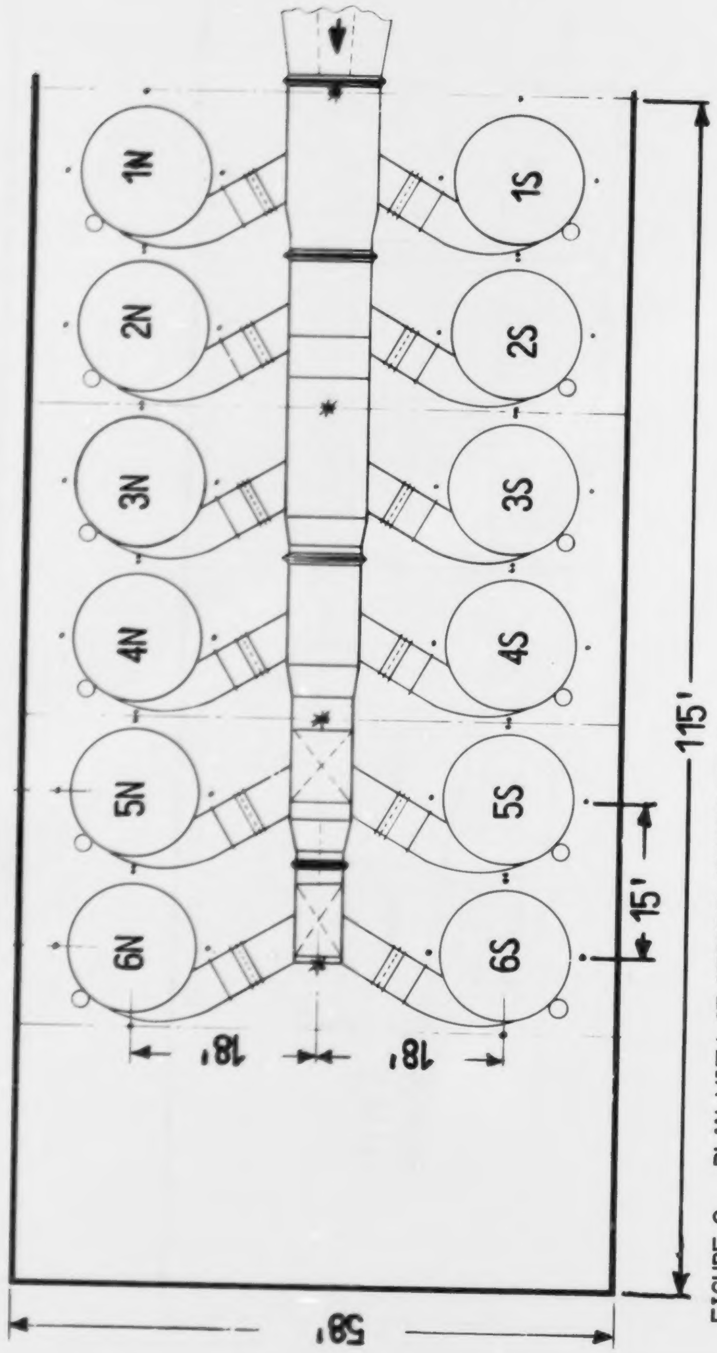
1N
2N
3N
4N
5N
6N
1S
2S
3S
4S
5S
6S
18'
18'
15'
115'
58'

FIGURE 2 PLAN VIEW OF MODULE ARRANGEMENT ILLUSTRATING INLET PLENUM

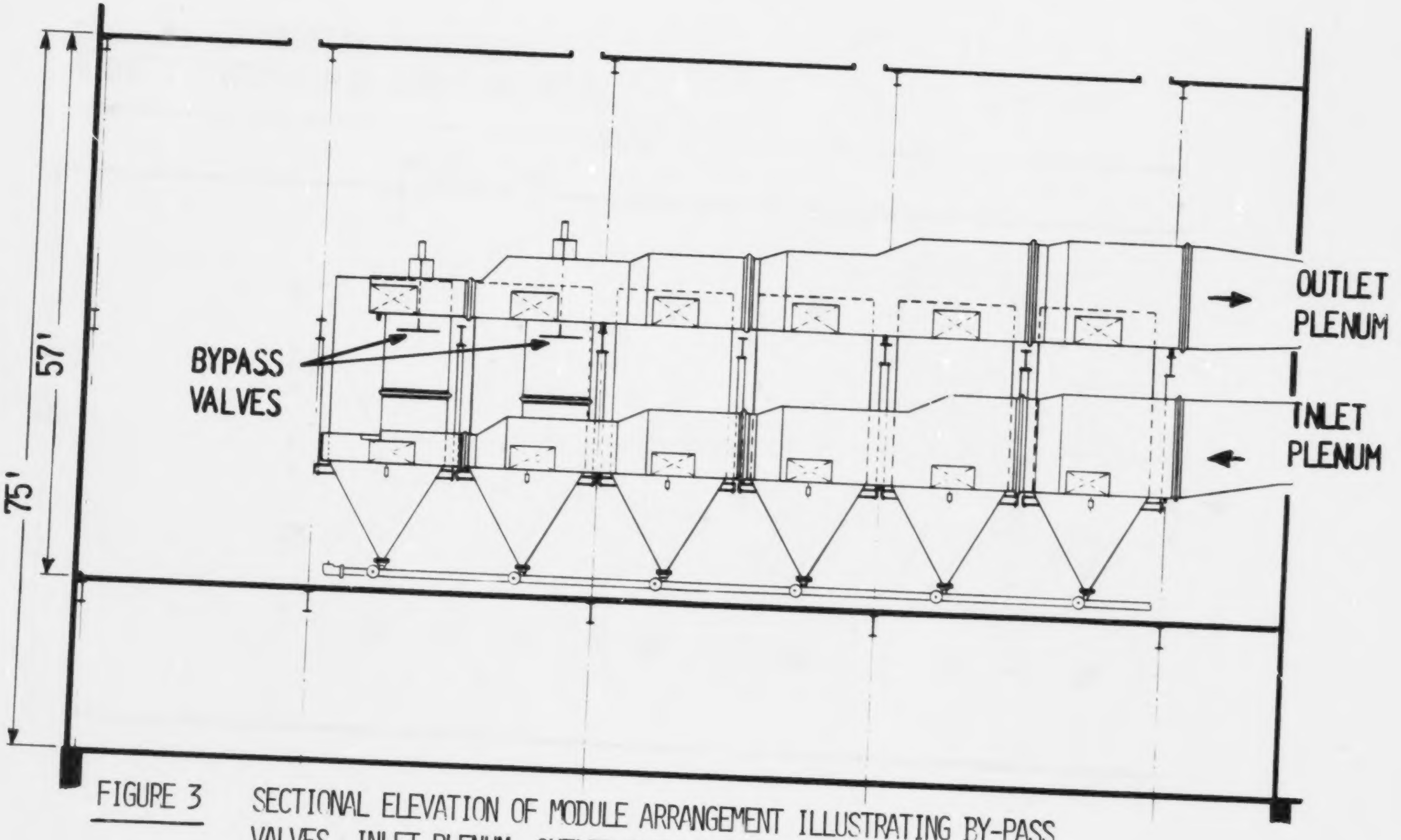
BYPASS VALVES
OUTLET PLENUM
INLET PLENUM
57'
75'

FIGURE 3 SECTIONAL ELEVATION OF MODULE ARRANGEMENT ILLUSTRATING BY-PASS VALVES, INLET PLENUM, OUTLET PLENUM, MODULE SUPPORT RODS, AND CONFIGURATION OF BUILDING ENCLOSURE.

4. The module outlet dampers can be either closed or opened from this panel to isolate a module or accomplish off-line cleaning. Damper position is indicated by status lights.

5. Bypass valves can be opened or closed from this panel. Status lights indicate their location at all times.

6. The status of which modules are in the clean mode is indicated on this panel to the operator via blower motor running status lights.

BAG CLEANING CYCLE LOGIC

The system has been operated since initial start-up with a pressure drop (inlet plenum to outlet plenum) initiated cleaning cycle. Typically, cleaning is initiated when the pressure across the baghouse builds up to 5 in. W.G. and continues through the cycle until the pressure drop is reduced to typically 3 in. W.G. The entire baghouse is then in the passive no-clean mode until the pressure builds back up to the higher set point of 5 in. W.G. When in the clean mode, four modules at a time are cleaned for a duration of five minutes (the other eight modules are in the passive no-clean mode). The group of four modules cleaned is sequentially stepped by the software of the PLC (programmable logic computer unit from Allen Bradley-Series 1774) so that all modules experience an equal amount of cleaning. All automatic cleaning to date has been on-line type cleaning. Some manually initiated off-line cleaning has been utilized infrequently during periods when above average amounts of flyash are being filtered, such as M.C.R. operation of the boiler with simultaneous sootblowing.

This method of cleaning has been very successful in maintaining the pressure drop within the desired 3 in. to 5 in. range and at the same time enhancing bag life, blower life, and saving energy. Any one bag is pulsed relatively infrequently.

Tests have been performed on this unit which demonstrate that off-line cleaning is both more effective and will clean the bags at system air to cloth ratios of roughly between five and six. Optimum off-line clean times for each module appear to be in the range of two to three minutes. However, there are no immediate plans to automate this unit to off-line cleaning.

EMISSION TESTS

Emission tests were performed at the stack of this unit on April 17 and April 18, 1980 as part of the Compliance Tests required on the permit for this coal fired boiler. The results of the EPA Method No. 5 particulate tests are shown in Figure 4. The average of the three tests via F Factor method is 0.023 pounds per million BTU particulate (roughly 1/4 of the permit requirements). Since this ratio is energy rate dependent, data is also presented with respect to the energy base of steam rate out and coal consumed.

The coal burned during the compliance tests had a heating value of 10,700 BTU/lb, a moisture content of 13.64%, an ash content of 5.89%, and a sulfur content of 0.53%, all on an as-received basis. This coal comes from Routt County, Colorado.

COMPLIANCE TESTS ON BOILER NO. 5
ADOLPH COORS COMPANY
(DATA PER EPA METHOD NO. 5)

	TEST #1 4-17-80 1200-1355	TEST #2 4-18-80 0902-1047	TEST #3 4-18-80 1240-1424	AVG. OF 3 TESTS
PARTICULATE EMISSION RATE (BASED ON F FACTOR)	0.019 $\frac{\text{LB}}{10^{6}\text{BTU}}$	0.031 $\frac{\text{LB}}{10^{6}\text{BTU}}$	0.018 $\frac{\text{LB}}{10^{6}\text{BTU}}$	.023 $\frac{\text{LB}}{10^{6}\text{BTU}}$
PARTICULATE EMISSION RATE (BASED ON STEAM RATE)	0.018 $\frac{\text{LB}}{10^{6}\text{BTU}}$	0.029 $\frac{\text{LB}}{10^{6}\text{BTU}}$	0.016 $\frac{\text{LB}}{10^{6}\text{BTU}}$	.021 $\frac{\text{LB}}{10^{6}\text{BTU}}$
PARTICULATE EMISSION RATE (BASED ON COAL RATE)	0.019 $\frac{\text{LB}}{10^{6}\text{BTU}}$	0.021 $\frac{\text{LB}}{10^{6}\text{BTU}}$	0.016 $\frac{\text{LB}}{10^{6}\text{BTU}}$	.019 $\frac{\text{LB}}{10^{6}\text{BTU}}$
BOILER STEAM OUTPUT	405,000 $\frac{\text{LB}}{\text{HR}}$	420,000 $\frac{\text{LB}}{\text{HR}}$	420,000 $\frac{\text{LB}}{\text{HR}}$	
ACTUAL VOLUME OF FLUE GAS THRU FILTER	276,000 ACFM	293,000 ACFM	288,000 ACFM	
AIR TO CLOTH RATIO	4.79	5.08	5.00	

FIGURE 4 EMISSION TEST RESULTS

Emission data beyond the compliance test has not been obtained. However, the plume has been essentially non-visible to a human observer during the last 34 months of operation.

Formal certification of the on-line stack monitors for this boiler was declared August 1, 1982.

"PBI" BAG TESTING

To evaluate the very promising potential of "PBI" (polybenzimidazole), a product of Celanese Corporation, 376 felted (22 to 26 ounce) bags made of this material were installed in Module 5-S (see Figure 2) on December 18, 1981. These bags went into service and performed very well. As of July 1982, they were holding up very well and showed no fabric deterioration as a result of either temperature or SO_2 in the boiler flue gas. Experience to date indicates that "PBI" is at least as good a filter media as "RYTON," although elaborate testing to date has not been accomplished.

SUMMARY OF OVERALL EXPERIENCE

The initial start-up of this system went quickly, easily and without any problems. Subsystems (blowers, plenum turning mechanisms, pulse valves, outlet dampers and all controls) were checked and operated several days prior to start-up. After the boiler was on-line with coal and operating properly, the baghouse was then put into service gradually over a period of approximately one hour. This system has been very easy to put into and take out of service.

During the 34 months of operation, this system has operated very well and up to expectations. The unit has required minimal maintenance and very little operator attention -- almost to the point where the operators take the baghouse for granted. The baghouse pressure drop has been maintained between 3 in. W.G. and 6 in. W.G. throughout the load range of the boiler (150,000 lb/hr to 450,000 lb/hr) even though a wide range of coals have been burned in the boiler. Colorado-Keenesburg coal with a heating value as low as 7,000 BTU/lb, a moisture content of 30% and an ash content of 12%, has been successfully handled in this system.

Through the first 32 months of operation, all felted "Ryton" bags maintained their integrity and there were no bag failures. Spot checking of bags at random in December 1981 and June 1982 indicated that considerable bag life remained. However, between August 1 and August 4, 1982, a very unfortunate incident occurred. The boiler had been shut down during the last part of July 1982 for annual inspection, maintenance of boiler components, and modification of the flame safety logic for the boiler. Light-off was attempted with Colorado-Keenesburg coal having a heating value of roughly 7000 BTU/lb and moisture content of 30% (a difficult coal to ignite). During attempts at light-off, the baghouse was on stream. Numerous attempts were made to develop a coal fire in the boiler without success during this period by the boiler operators. Apparently fine unburned pulverized coal was deposited in the baghouse during these attempts at light-off and then the inevitable finally happened -- sparks generated in the furnace ignited the coal on the surface of some of the bags in the baghouse. The intense heat from these localized fires on the surface of the bags destroyed the fabric in certain areas.

So far, it appears that a relatively small percentage of the 4512 bags in the system were damaged. As of September 24, 1982 (seven weeks after the incident), 256 bags had been found to have burned holes in them (246 were "Ryton" and 10 were "PBI"); 226 of these failed bags were identified and replaced within a week after the incident. Most burned bags have occurred in modules 1-S and 2-S (see Figure 2). Also, all burned holes have occurred in the lower three feet of the bags. It appears that most of the remaining 4256 bags (94%) were not significantly damaged during the incident.

It is very unlikely that a bag made of glass or "Teflon" would have faired any better than the bags made of "Ryton" and "PBI" because of the apparent intense heat. The lesson learned by this incident is that the boiler-baghouse system must be operated so that a fire cannot occur in the baghouse no matter what the bags are made of or how the baghouse is constructed. It is important that a baghouse be operated according to the following guidelines:

- Always bypass and isolate the baghouse during coal light-off conditions and other unstable firing conditions.
- Observe in the strictest sense the temperature limits of the fabric in the baghouse.
- Maintain O_2 levels at the lowest practical levels consistent with good combustion during all operating modes.

CONCLUSIONS

Based on the operating experience with this system and the testing which has been done, the following can be concluded:

- Felted "Ryton" is a practical and viable filter media for boiler stack gas flyash filtering applications.

- Felted "PBI" is a practical and viable filter media for boiler stack gas flyash filtering applications.

- The system discussed in this paper is operated successfully with on-line cleaning up to an air to cloth ratio of between 4.5 and 5 to 1.

- Operation at air to cloth ratios between 5 and 6 is practical with "Ryton" and "PBI" felted media in this PC fired boiler using the right off-line cleaning sequence. Operation at air to cloth ratios slightly higher than 6 has been demonstrated with the Boiler No. 3 spreader stoker fired unit which is another boiler-baghouse installation at the Golden, Colorado, facility.

- Proper design and selection of baghouse inlet dampers, outlet dampers, bypass dampers, and baghouse plenums is critical to good overall operation.

- Any boiler-baghouse system must be operated with such care that a fire condition is not allowed to occur in the baghouse. This requirement applies to glass, "Teflon" and "Nomex" bags, as well as "Ryton" and "PBI" bags.

START-UP AND OPERATION OF A FABRIC FILTER CONTROLLING PARTICULATE EMISSIONS FROM A 250 MW PULVERIZED COAL-FIRED BOILER

by: Charles B. Barranger
Flakt, Inc.
Knoxville, TN 37923

Norm Spence
Stone and Webster
Denver, CO

John Saibini
Sierra Pacific Power Co.
Reno, NE

ABSTRACT

Summarize and describe the design, construction, start-up and operation of the fabric filter baghouse controlling the particulate emissions from Boiler Unit No. 1 located at Sierra Pacific Power, North Valmy, Nevada. The basic design specification requirements will be described, i.e., fuel type, flue gas, fabric filter type, system arrangement and performance requirements. Actual pre-start checkout and system start-up procedure will be reviewed in detail. The fabric filter was put on-line in November of 1981. Resulting equipment operating conditions from start-up through date of the paper will be presented.

The work described in this paper was not funded by the U.S. Environmental Protection Agency and therefore the contents do not necessarily reflect the views of the agency and no official endorsement should be inferred.

DESIGN AND PERFORMANCE

INTRODUCTION

The North Valmy Electric Generating Station, jointly owned by Sierra Pacific Power Company and Idaho Power Company is located approximately 200 miles east of Reno, Nevada, just north of Interstate 80; Sierra Pacific manages operation of the station. The station consists of two 250 MW (nominally rated) coal-fired units. Unit No. 1 began commercial operation in the fall of 1981 and Unit No. 2 is under construction and scheduled for commercial operation in June, 1985. Both Sierra Pacific and Idaho Power share equally in the plant's cost and energy output, which provides electric power for customers in northern Nevada, northeastern California, and Idaho. Stone and Webster Engineering Corporation is the architect engineer and construction manager for the project.

UNIT DESIGN

The Unit No. 1 boiler is a Babcock and Wilcox balance draft furnace, natural circulation, drum type which produces 1,924,000 lbs/hr steam at 2600 psig/1000°F, with a single reheat exiting at 600 psig/1000°F. Separate primary and secondary air preheaters are provided of the Rothemuhle regenerative design.

Coal is the base fuel and is delivered to the Valmy site by unit train. No. 2 fuel oil is used for ignition. At the time of design/engineering for Unit No. 1, a single source of coal had not been determined. As a result, the unit was designed to accomodate full load operation firing any of nine alternate Western coals, including coals from mines in Utah, Colorado, Wyoming, New Mexico, and Montana.

These alternate coals yielded a significant impact on the design of the particulate collection equipment. Design of the equipment had to compensate for a 230% variation in grain loadings, 15% variation in flue gas volumes (velocities), and significant differences in flue gas composition and flyash constituent analyses.

Data pertaining to the nine alternate design coals is attached as Table 1. Unit No. 1 is presently firing the C-1 coal, which originates from Salina, Utah.

EVALUATION OF ALTERNATE PARTICULATE COLLECTION EQUIPMENT

In 1975, Sierra Pacific requested Stone and Webster to perform a study evaluating alternate particulate collection systems for Unit No. 1. The evaluation included a technical and economic assessment of alternate control systems including hot and cold-side electrostatic precipitators, and fabric filters. At the time, hot-side electrostatic precipitators appeared to be the predominate technology being applied for particulate control on new low sulfur western coal-fired units. However, the North Valmy design requirements of burning nine alternate coals presented problems to the precipitator suppliers. Significant variations in flue gas composition, coal ash chemistry and resistivity led to conservative precipitator designs which proved to be physically large with high initial capital and high annual operating costs.

As compared to the precipitator, the baghouse alternate presented advantages of independence from fuel and ash characteristics, and flue gas temperature; less dependence on gas distribution and velocity; and compartmentalized design allowed on-line maintenance for high availability to the boiler. In the overall evaluation, the baghouse was determined the most cost effective means of particulate control for North Valmy Unit No. 1.

BAGHOUSE DESIGN

General

In April, 1976 Stone and Webster issued design specifications for competitive bidding of the Unit No. 1 baghouse. In October, 1976 the Pollution Control Division of the Carborundum Company (now Flakt, Inc.) was awarded the contract to supply and erect the baghouse. Stone and Webster maintained responsibility for design of the baghouse support steel, interconnecting field wiring, and field insulation.

Baghouse Type

The baghouse is an all welded, gas tight, shop fabricated panel constructed unit, designed to operate under a pressure of ± 26" water gauge. An automatic reverse air system provides the necessary energy to clean the fiberglass filter bags. The baghouse is designed to meet a gross filter speed (air-to-cloth ratio) of 1.99 ft/min when firing the worst case coal and 2.42:1 ft/min (net) when firing the performance coal (See Table 2). Figure 1 shows the baghouse location in the flue gas train. It is located between the air heater outlets and the two induced draft fans.

Baghouse Arrangement (See Figure 2)

Arrangement of the baghouse is ten compartments total, five on either side of a common central plenum. Each compartment contains 648 filter bags making a total complex of 6,480 filter bags. Each filter bag is 12" in diameter by 32'-5" long. Filter bags are arranged such that the maintenance personnel need to reach by only two filter bags to reach the third (three bag reach). This three bag reach arrangement required the design of three lower and upper walkway systems inside each compartment. There are 36 rows of bags in the depth of each compartment and 18 bags in each row. Dimensionally large compartments resulted, i.e., 27'-9" wide by 45'-3" deep by 38'-0" tall compartments. It appears this size compartment is the largest baghouse compartment installed in the Utility Industry in the United States.

To compensate for thermal expansion in the baghouse, stub columns and low friction slide plates were designed to separate the non-expanding structural support structure from the baghouse. A centrally located point was fixed and the baghouse expands in all directions from this point at the slide plate level. This design considered air preheater failure and a resulting upset excursion gas temperature of 720°F.

Each baghouse compartment is equipped with a series of damper valves. All valves are vertical shaft poppet dampers and are operated by pneumatic air cylinders. Located at the clean gas side of each compartment there are three gas outlet valves, two reverse gas valves, and one compartment vent valve. At the gas inlet of each compartment there are two gas inlet valves.

The reverse gas, outlet gas, and inlet gas plenums are centrally located, run the length of the baghouse, and are built integrally within the baghouse. Two separate compartment vent manifolds run the length of the baghouse at the roof level. A 1/12 scale model study of all the baghouse compartments was completed and the results were incorporated into the compartment baffling system.

To facilitate the maintenance of the equipment, access walkways and platforms are located at the hopper discharge level, the inlet damper level, top and bottom section of the filter bags, and the baghouse roof. Access to these maintenance levels is via stairs.

Hoppers

Ten double pyramid hoppers, one per compartment, provide a minimum of 12 hour flyash storage at the maximum operating condition (16.1 tons per hour of flyash). Each hopper has been designed with two separate discharge points, so that the ten compartment baghouse requires 20 ash collection points. These hoppers have been extended to the center of the gas inlet plenum to promote self-cleaning. Should particulate fall out in the inlet plenum, it eventually is carried through the inlet damper opening and is deposited into the bottom of the ash hoppers. All hoppers are identical and have been designed with 55° valley angles.

Model Studies

To evaluate the aerodynamic design of the particulate control system a model study was performed at NELS, Inc. A plexiglass 1/12 scale model of all the ductwork and the baghouse was constructed. Parameters such as velocity and gas flow distribution, pressure losses, and particulate distributions were measured. Baffling, vaning, and design configurations were optimized and incorporated into the actual particulate control system designs. To further optimize the baghouse hopper design, a separate 1/6 scale model of a hopper, inlet damper system, and inlet plenum was built and tested.

Bag Filter Media and Construction

The filter bag material, Filter Media Division of Carborundum, Style No. 601B, is fiberglass coated with a Teflon "B" finish (see Table 2 for specifications). Each filter bag is constructed with seven unequally spaced anti-collapse rings, top cuff with retainer, and bottom cuff with cord. The bottom of the bag slips over an extended thimble in the tube sheet and is sealed with a quick release clamp. The top of the bag is fitted over a steel cap and held in place by the retainer band and lip on the cap. Bags are suspended from structural frames via a chain and spring, and held in place by clips inserted around the chain links.

Baghouse Controls and Instrumentation

The baghouse control panel was placed in the control house located adjacent to the baghouse. This panel includes a graphic display, annunciator, and instrumentation. Along with the graphic display, indication lights show open/closed positions of all compartment valves, on/off display of reverse air or vent fans, on/off display of hopper heaters, and indicates if high dust level exists in the hopper. Alarm and annunciation of reverse air fans, low and high gas temperature, low and high baghouse pressure drop, hopper heater failure, and high hopper dust level is installed. Pushbuttons are included to silence, test, and rest the annunciator. Also manual activation of the cleaning cycle and by-pass system is possible. Baghouse inlet and outlet gas temperatures and baghouse differential pressures are both monitored and continuously recorded.

The baghouse cleaning system is automatically activated by a signal from the differential pressure sensor. A stepping switch timer and dial adjustable timers have been included so that all cleaning cycle times can be varied and optimized to site specific conditions.

Supplementary Systems

There are three major baghouse supplementary systems. They are compartment ventilation, key interlock, and flue gas by-pass. All three are basic protective systems to protect either plant personnel or baghouse equipment. The compartment ventilation system will cool down the baghouse compartment as maintenance personnel work inside that compartment. Compartment key interlocks prevent access into the baghouse compartments before the damper valves isolate that compartment from the flue gas. Hopper key interlocks insure deactivation of the level detectors before personnel enter the hoppers. Flue gas by-pass system automatically protects the filter bags from high gas temperatures or high pressure transients.

BAGHOUSE OPERATION

Normal Filtering

Flyash laden gas from the boiler is drawn into the inlet manifold of the baghouse. The inlet manifold spans the length of the baghouse, and ducts the gases through inlet poppet valves into all the hoppers of the baghouse. These gases are directed upward into the filter bags of each compartment and particulate is deposited on the interior surface of the filter bags. Gases are filtered as they pass through the dust cake/bag material and are drawn upward through poppet valves into the common outlet plenum. Filtered gases exit the baghouse through the outlet ductwork, pass through the two Induced Draft Fans, and are discharged into the atmosphere through a common stack.

During this mode of operation only the compartment inlet and outlet poppet valves are in the open position (See Figure 3).

Automatic Fabric Cleaning

As particulate is filtered from the boiler flue gas, ash deposits gradually build up on the bag surface. These deposits or ash cake increase the fabric's resistance to flow, thus increasing the pressure loss across the bags. This ash cake must be periodically removed or the resistance to flow will increase the fabric's pressure to a level too high for the I.D. Fans to overcome. In the Valmy baghouse, cleaning these ash deposits is automatically accomplished. The filter bag cleaning system is automatically activated by the signal sent by the differential pressure indicator. (Sensors are located across the baghouse inlet and outlet duct.) The indicator is set to activate cleaning once the baghouse differential pressure is sensed at five inches water gauge (See Figure 7). Once the cleaning system is activated all bags in all compartments are sequentially cleaned one compartment at a time - compartment number one through compartment number ten. After the total baghouse is cleaned (approximately 30 minutes) and is operating somewhere below five inches water gauge, the differential pressure indicator is automatically reset and normal filtering resumes. At full boiler load and with one baghouse compartment down for maintenance, the normal filtering mode between baghouse cleanings continues for approximately 45 minutes. During the automatic baghouse cleaning mode, the only dampers which are opened and closed are the reverse air and compartment outlet dampers, the compartment vent damper remains closed and the compartment inlet dampers remain open (See Figure 4). Energy required to reverse gas clean these filter bags is via two 50% capacity centrifugal fan systems. These fans pull clean heated gases from the baghouse outlet duct and push the gas through the bags in a reverse direction. The particulate is dislodged from the bag surface and falls to the bottom of the hopper.

On-line Maintenance

The baghouse has been designed with a redundant maintenance compartment. This allows plant personnel access to the inside of any one compartment for inspection and/or maintenance without interrupting boiler load. To insure complete compartment isolation whenever access is desired, a key interlock lock system was installed. When the first key is turned and released from the key box in the control room, all compartment dampers automatically close in that specific compartment. When the last or sixth compartment door is locked open, the compartment vent damper opens and the vent fan is activated. Ambient cool air is drawn through all compartment doors and cools the interior of the compartment (See Figure 5). At full load only one compartment at any one time is allowed to be in the maintenance mode. To protect plant personnel from hot exposed steel partition walls, 7'-0" tall, expanded metal guards have been installed at the tube sheet and bag top levels inside each compartment.

Flue Gas By-Pass

The by-pass system provides the baghouse with a method to divert the flue gas around the filter bag compartments without interrupting boiler load. At the inlet to the baghouse, the outlet plenum is extended over the inlet duct to the baghouse (See Figure 6). In this section, nine vertical shaft poppet valves isolate the inlet duct from the baghouse outlet plenum. When the flue gas is to be by-passed around the filter bags, these by-pass poppet dampers open and all the other baghouse dampers are closed. At Valmy, the by-pass can be manually or automatically activated. Manual activation was used at start-up, and the automatic activation occurs whenever high differential pressure (above eight inches water gauge) or high baghouse inlet temperature (above 450°F) is sensed.

PERFORMANCE

The North Valmy Station was required to meet the emission level of 0.1 pounds per million BTU's fired and 20% opacity as specified in the Environmental Protection Agency, New Source Standards as adopted December 23, 1971. The baghouse was designed and guaranteed to perform below that emission level and opacity requirement. Further, the baghouse was designed to operate at a differential pressure loss of less than 6.5" of water and provide Sierra Pacific with a filter bag life of at least two years.

In January of 1982 performance tests were run in the discharge stack, and the unit was accepted and passed by the State of Nevada. Presently, the opacity in gas discharge stack is monitored and continuously recorded in the 2%-4% range. The baghouse differential pressure loss is also continuously monitored and recorded. Figure 7, an overlay traced from an actual strip recording shows the average operating pressure losses (between less than 5.0" and 6.5" water gauge). Since start-up some ten months ago, approximately eight filter bags have failed of the 6,480 bags installed.

BAGHOUSE CONSTRUCTION

SCHEDULE AND SEQUENCE OF ACTIVITIES

Date	Activity
5/79	Start Foundation Framework
1/80	Erect Support Steel
2/80	Start Baghouse Ground Assembly
3/80	Complete Support Steel
4/80	Erect Hoppers
5/80	Erect Grid Plates
6/80	Erect Vertical Walls and Plenums
8/80	Erect Roof
9/80	Erect Roof Dampers, Vent Duct, Reverse Gas Duct, etc.
10/80	Start Electrical Cable Tray Installation Perform Air Leak Test

Date	Activity
11/80	Start Field Insulation
2/81	Mechanical Erection Complete
4/81	Insulation Complete
5/81	Electrical Checkout
6/81	Tension Bags, Align Fans, Adjust Poppet Valves

Before erection, hoppers, vertical walls, roof, and baghouse internal trusses were ground assembled to their maximum to minimize the quantity of crane lifts required.

CONSTRUCTION PROBLEMS

Normal minor difficulties were encountered during erection, e.g., some misalignment problems with ducts and supports, knee brace interference, insulation interference with hopper reinforcing members, etc. One unexpected problem that did arise was after the filter bags were installed; it was found they were too long and proper tension could not be set. To cure this problem, Flakt had several fabric sewers from the Filter Media Division of the Carborundum Company come to the Valmy site to cut the bags to the proper length and resew bottom cuffs to the bags. This work was all performed inside each baghouse compartment with portable sewing machines as the bags hung from the top caps. In a span of approximately three weeks all the bags were properly resewn and properly tensioned.

BAGHOUSE START-UP

SCHEDULE AND SEQUENCE OF ACTIVITIES TO DATE

Date	Activity
6/81	Baghouse pre-start checkout
7/81	Boiler boil-out with number 2 oil
8/81	Baghouse ready for start-up
9/81	First coal-firing and turbine synchronization
11/81	Baghouse placed on line

PRE-START CHECKOUT

A visual inspection of the complete system was performed. Filter bag tension was checked and bags requiring retensioning were retensioned. Baghouse compartments, hoppers, and plenums were made clear of all tools and or debris. All mounting bolts were tightened, and all poppet valves were opened and closed and checked for proper sealing and operation. Reverse air and vent fans were checked for proper rotation and vibration. A thirty minute cleaning cycle was set at the timers in the control panel and a dry run of the clean cycle was run. Minor adjustments were made, and the baghouse was ready for start-up.

START-UP

At the time of the Baghouse Contract, it was envisioned that the bags would be precoated with lime or flyash prior to the baghouse compartments accepting flue gas. However, based on experience with other recent start-ups, Flakt recommended on-line coating of the bags upon achieving 100% coal-firing of the Unit.

The basic plan to start the baghouse was to run on by-pass until oil-firing (used for ignition) was discontinued and the boiler was on 100% coal-firing. On-line precoating of the filter media could then begin at a 50% load condition and be completed when the pressure rise across the fabric increased approximately 1.5" W.G.

During the Unit start-up period, the baghouse was set on by-pass. This period comprised of all initial oil-firing activities including boil-out, critical pipe steam blows, and initial turbine synchronization. Additionally, during the three to four week period following the initial coal-firing of the boiler, the baghouse could not be placed on-line because the Unit was load limited and prevented from operating without oil ignitor assistance. This inability to immediately achieve 100% coal-firing and greater than 50% load operation was caused by various minor start-up problems, e.g. primary air fan vibration due to imbalance, high silica levels in the boiler, etc.

Once 100% coal-firing and 125 MW (50% load) could be maintained with stability for an extended period, the baghouse by-pass was closed and flue gas was directed to the compartments and filter bags (November 4, 1981). Within three to four hours the bags were coated with ash and the stack cleared from a 100% opacity to a 4% to 8% opacity. The load was slowly increased to 255 MW and maintained. During the next several days, the stack opacity averaged approximately 6% and the baghouse system pressure drop ranged from three to six inches water gauge.

The basic problems experienced during the baghouse start-up were minor. The baghouse differential pressure sensor clogged and required cleaning; several bags came loose from the thimbles and had to be reinstalled.

Since start-up one year ago, the most major problem has been that expansion joints located on the discharge side of the baghouse reverse gas fans have developed leaks. These joints have been redesigned and were recently installed during a scheduled unit outage.

CONCLUSION

The design, installation, start-up, and performance of this baghouse has been a complete success. This, again, demonstrates that fabric filter baghouses are viable solutions to filtration problems resulting from burning low sulfur western coals when generating electric power.

TABLE 2. FILTER SPEEDS

Filter Speeds (FPM)*	Including Max. Reverse Gas Flow	Excluding Reverse Gas Flow
One compartment down for cleaning and one compartment down for maintenance	2.42	2.20
One compartment down for cleaning	2.15	1.96
All compartments on-line	N/A	1.76

*Based on flue gas flow rate for the boiler performance coal - 1,102,000 ACFM.

TABLE 3. FILTER MEDIA SPECIFICATIONS
STYLE NO. 601B

Material	Fiberglass
Finish	7% Teflon
Thread Count	54 X 30
Average Permeability	55
Average Weight (ounces per sq. yd.)	10.0
Construction	3 X 1 Twill
Yarn Type - Warp	150 1/2
Yarn Type - Fill	150 1/4 TEX
Mullen Burst (PSI)	450

TABLE 1. FUELS

	For Boiler Performance	Possible Fuels							
Coal Designation	C1	C2	C3	C4	C5	C6	C7	C8	C9
Heat Content (BTU/LB)	12,250	10,290	9,650	10,000	9,700	9,600	8,175	8,000	8,450
% Ash	7.5	8.1	6.0	10.0	10.8	11.5	5.8	11.0	9.0
% Sulfur	0.7	0.4	0.5	0.6	0.6	0.8	0.48	1.0	0.7
% Moisture	6.5	15.0	21.5	12.0	15.0	17.0	30.0	26.0	25.0
Flue Gas Flow Rate LB/HR X 10^3	2,841	2,889	2,921	2,974	2,883	2,864	3,133	2,830	3,098
ACFM X 10^3	1,102	1,126	1,145	1,160	1,126	1,117	1,246	1,109	1,227
Typical Part. Loading Grains/ACF	1.48	1.88	1.48	2.32	2.66	2.90	1.59	3.40	2.40

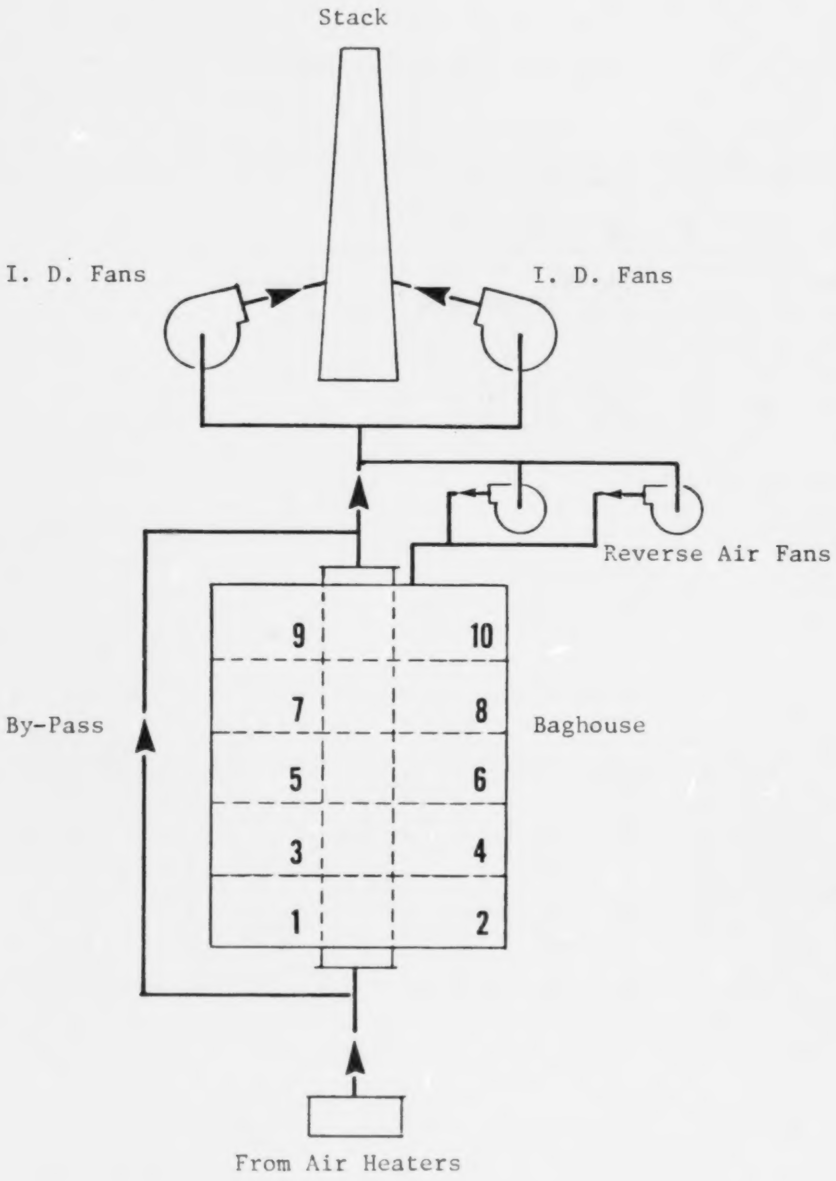
Stack
I. D. Fans
I. D. Fans
Reverse Air Fans
9
10
7
8
5
6
3
4
1
2
By-Pass
Baghouse
From Air Heaters

Figure 1. System Flow

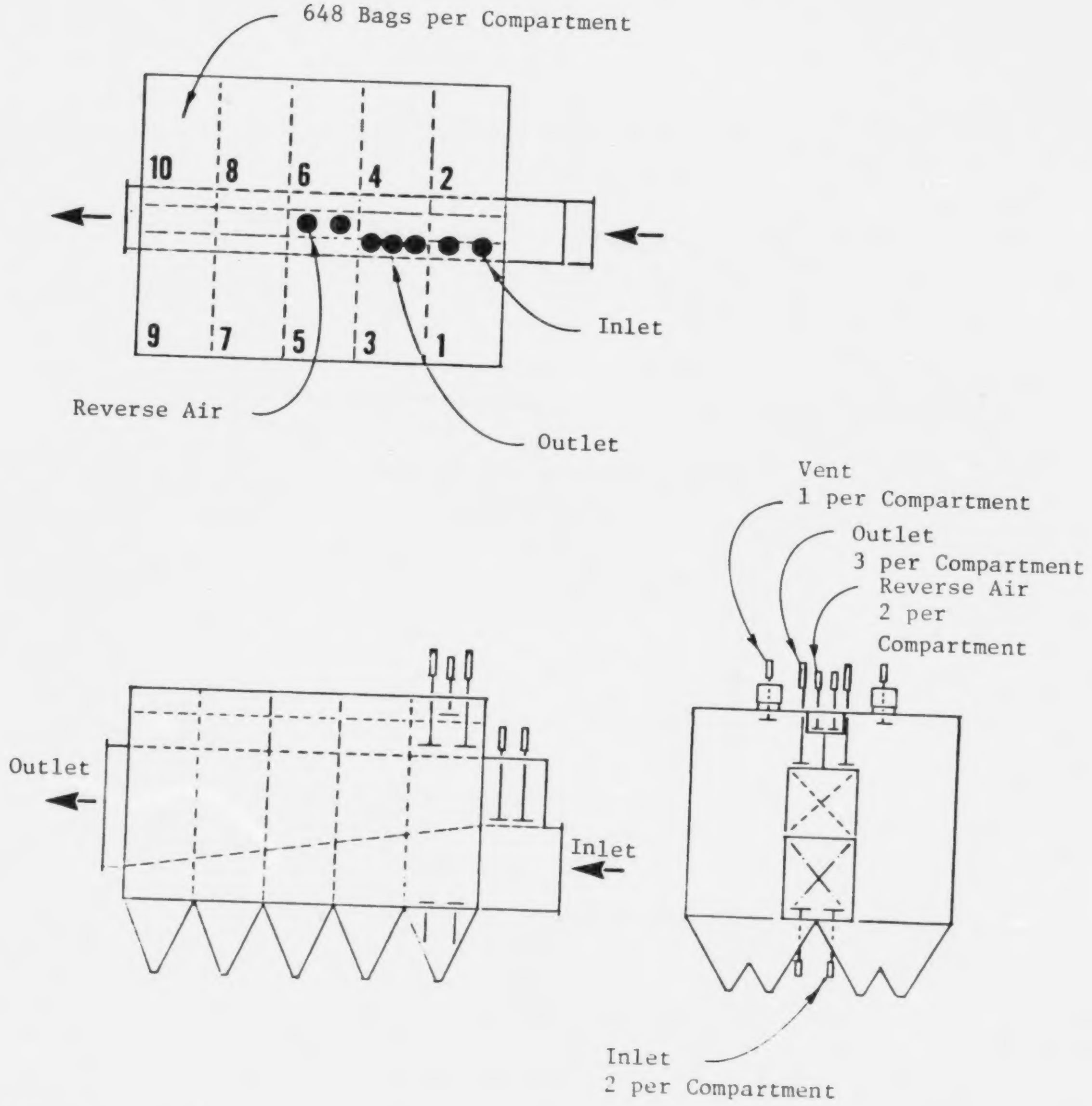
648 Bags per Compartment
10
8
6
4
2
9
7
5
3
1
Inlet
Reverse Air
Outlet
Vent
1 per Compartment
Outlet
3 per Compartment
Reverse Air
2 per
Compartment
Outlet
Inlet
Inlet
2 per Compartment

Figure 2. Baghouse Arrangement

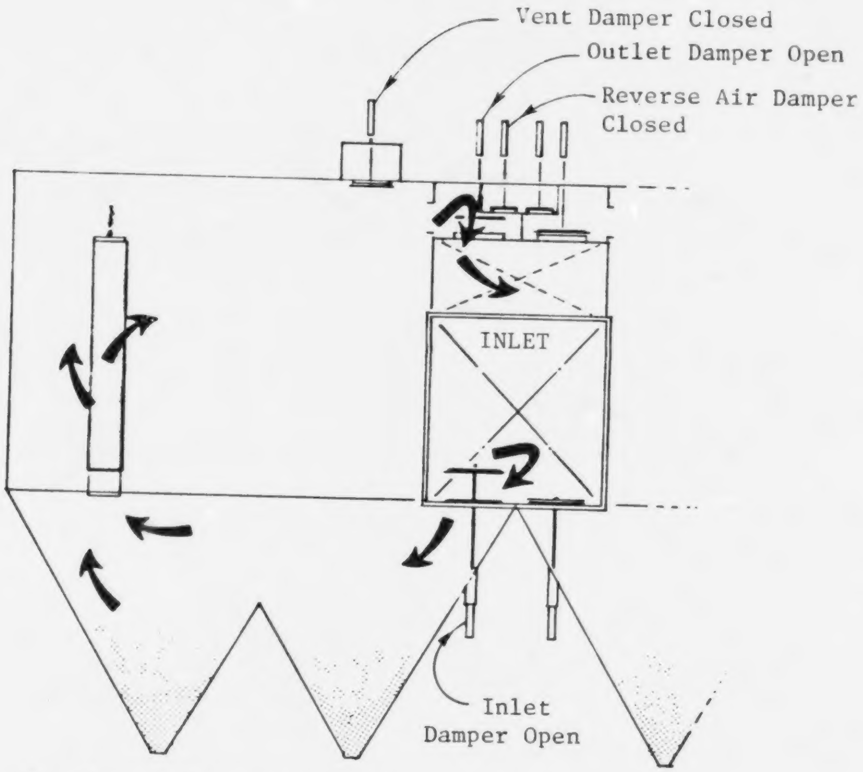
Vent Damper Closed
Outlet Damper Open
Reverse Air Damper Closed
INLET
Inlet Damper Open

Figure 3. Normal Filtering

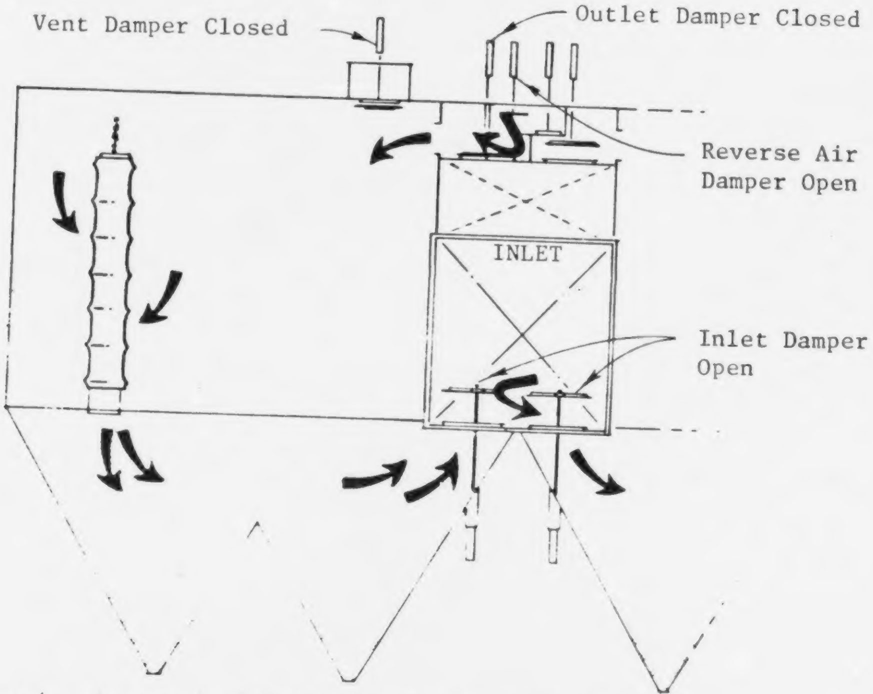
Vent Damper Closed
Outlet Damper Closed
Reverse Air Damper Open
INLET
Inlet Damper Open

Figure 4. Automatic Fabric Cleaning Reverse Air Flow

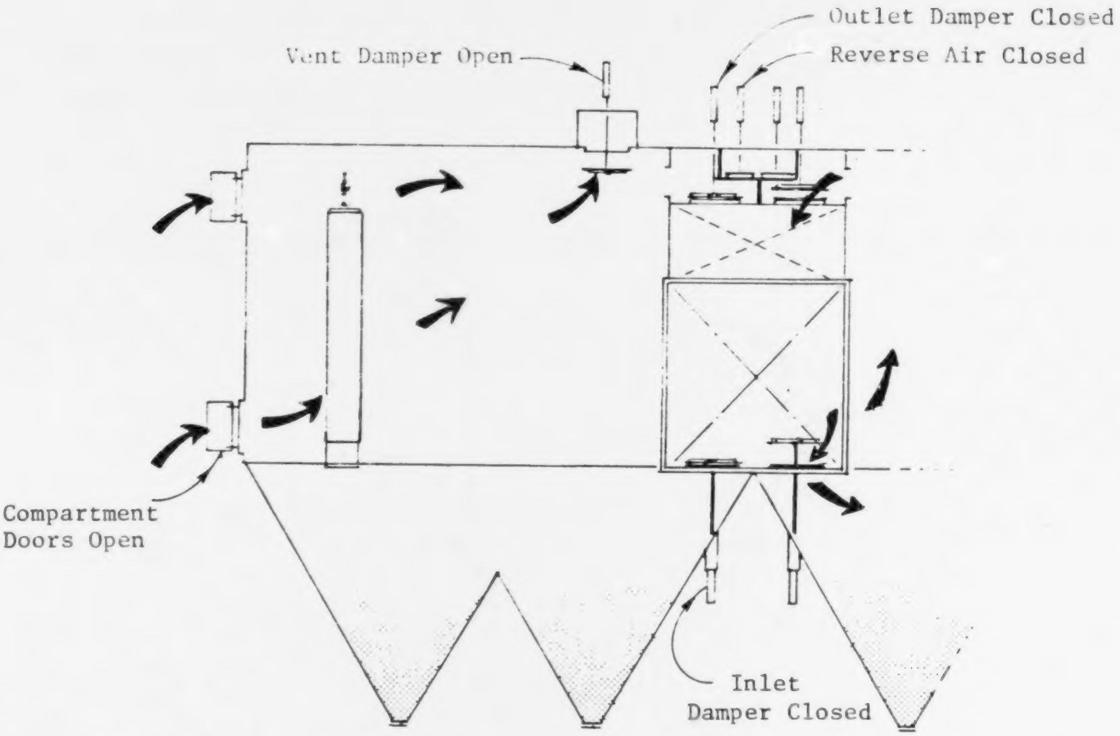
Outlet Damper Closed
Vent Damper Open
Reverse Air Closed
Compartment Doors Open
Inlet Damper Closed

Figure 5. On-Line Maintenance

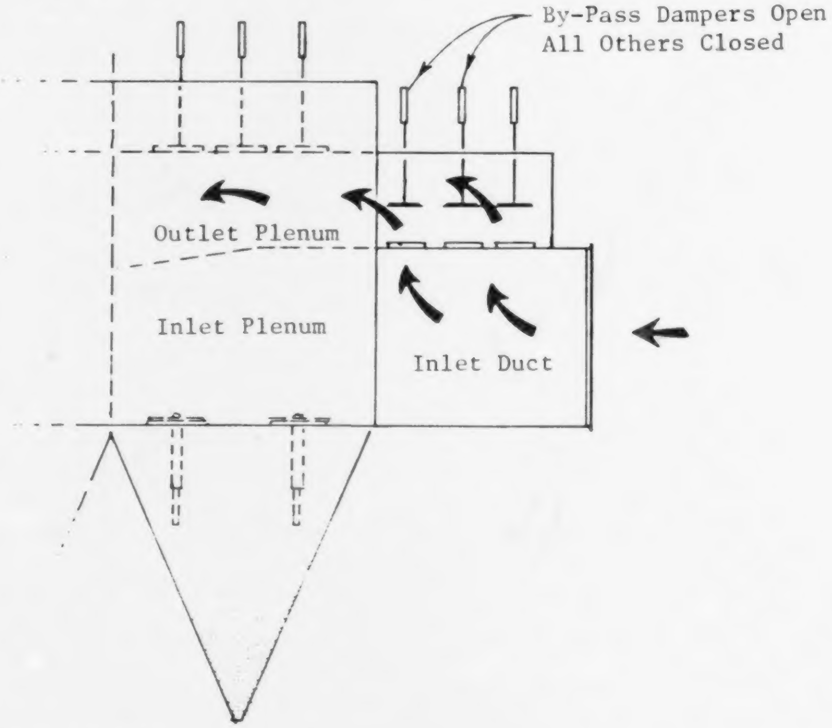
By-Pass Dampers Open
All Others Closed
Outlet Plenum
Inlet Plenum
Inlet Duct

Figure 6. Flue Gas By-Pass

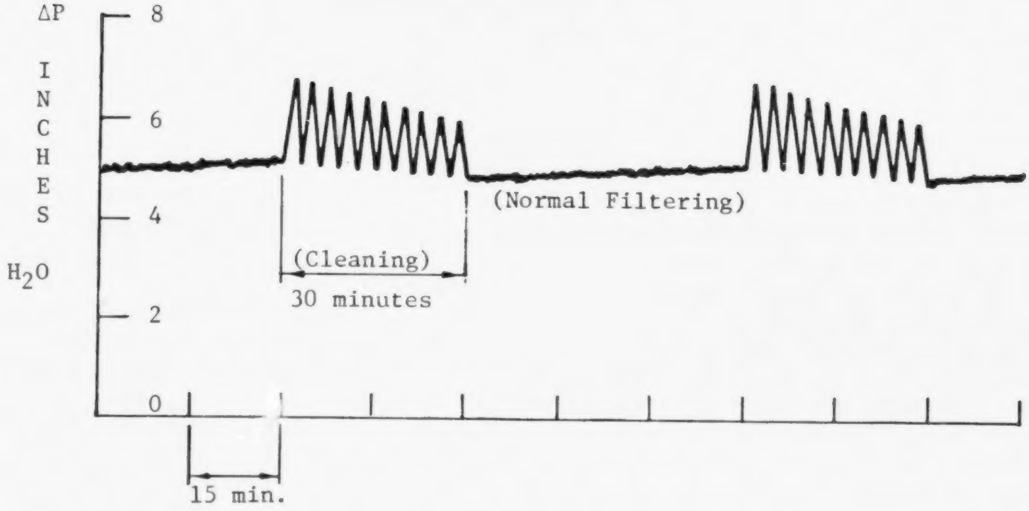

Figure 7. Typical ΔP Recordings During Cleaning
One Compartment Down for Cleaning and One Compartment Down for Maintenance.

PERFORMANCE OF A 10 MW FABRIC FILTER PILOT PLANT AND COMPARISON TO FULL-SCALE UNITS

by: Wallace B. Smith and Kenneth M. Cushing
Southern Research Institute
Birmingham, AL 35255

Robert C. Carr
Electric Power Research Institute
Palo Alto, CA 94303

ABSTRACT

This paper provides an update on EPRI's fabric filter research program currently being conducted by Southern Research Institute at the Arapahoe test facility in Denver, Colorado, and also several full-scale installations. Data are reported which suggest a quantitative relationship between tube-sheet pressure drop and air-to-cloth ratio for reverse-gas cleaned baghouses. Typical results show that average tube-sheet pressure drop increases from 4.5 to 8 in. H_2O (1.12 to 2.0 kPa) as the air-to-cloth ratio increases from 1.7 to 2.5 acfm/ft^2 (0.52 to 0.76 am /min). Large residual dust cakes of up to 1 lb/ft^2 (about 500 mg/cm^2) were measured in the bags after cleaning by reverse gas. Current tests indicate that approximately a 20 percent reduction in operating pressure drop could be achieved by increasing the reverse-gas velocity to 6 ft/min (3 cm/sec), although such a high value may be impractical for full-scale units. These results suggest that reverse-gas alone is only marginally effective as a method of cleaning bags in utility applications. Applying intense sonic energy (horns) during reverse-gas cleaning results in much better dust cake removal. Tests now underway indicate that this hybrid bag cleaning mode can reduce the operating pressure drop by more than a factor of two.

INTRODUCTION AND BACKGROUND

This paper contains information obtained during the period of July 1981 through August 1982 from the Electric Power Research Institute's fabric filter research program. The program includes an empirical analysis of the operation of a 10 megawatt pilot-scale baghouse, collecting data from several full-scale baghouses, and detailed laboratory analyses. The purpose of the program is to develop sufficient understanding of baghouse performance to allow the electric utilities to predict more accurately their performance before construction and to develop improved designs and operating procedures.

A description of the fabric filter pilot plant (FFPP) and results obtained between the startup in June 1980 and July 1981 have been published in earlier papers (1,2,3,4,5). The FFPP is a versatile, four compartment unit with a wide choice of operating modes. Each compartment can be operated independently. It is fully instrumented for controlling and monitoring its operation and conducting aerosol measurements.

The scope of the test program includes parametric investigations of operation with reverse gas and shake/deflate cleaning, and different fabrics. Since most utility installations are cleaned by reverse-gas, we have chosen to study that mode of operation first, although, some preliminary studies indicate that the deflate/shake mode of cleaning is very promising.

In the previous publications it was noted that the design of the FFPP provides a uniform distribution of gas flow and fly ash between the four compartments. It was found that several weeks were required for the system pressure drop (ΔP) to stabilize after a significant alteration in its operation for reverse-gas operation. Thus, the test periods are rather long for each parameter evaluated. In fact, it is not clear if the system ever truly stabilizes. It has been observed qualitatively, for example, that it is easier to make an adjustment in the FFPP operation (e.g. to reduce the magnitude of reverse gas) that degrades performance (ΔP) than the opposite (e.g. an increase in reverse gas, with a corresponding decrease in ΔP). This may indicate that reverse-gas cleaning is a marginal method and that the systems always tend to drift upwards toward a relatively high operating pressure. It was observed that heavy residual dust cakes, on the order of 0.5 lb/ft^2, accumulated on the bags in compartments cleaned by reverse gas. In some instances, the bags appeared to clean more effectively (decreased ΔP) after being left on line longer to accumulate heavier dust cakes. During a short period of operation in a deflate/shake mode, the bags appeared to clean much more thoroughly. Although several unplanned shutdowns have occurred and the compartments inadvertently cooled without being purged of flue gas, no irreversible "blinding" of bags has been observed. No bag failures have been experienced after more than 10,000 hours of operation (the bags are all Albany International "Tri-coat"). The collection efficiency for all particle sizes was greater than 99.9 per cent in all of the tests. Therefore, most of the tests have concentrated on a better understanding of factors controlling the operating pressure drop.

Further tests are described in this paper wherein the dependence of the operation upon the filtering air/cloth ratio (A/C), the cleaning or reverse gas air/cloth ratio (RA/C), and the physical and chemical nature of the dust cakes was investigated. Preliminary results from current tests of sonic cleaning are also described.

EXPERIMENTAL PROCEDURES

To understand the performance of a fabric filter system it is necessary to measure the physical and chemical properties of the aerosol and the operating characteristics of the system. The methods used to acquire these data at the FFPP have been described in the papers cited above. Similar techniques are also being used at the full-scale installations. Briefly, the data include: The baghouse design and mode of operation; the baghouse gas flow (magnitude and distribution); baghouse pressure losses and particle collection efficiency; gas temperature; chemical analyses of the ash and coal; particle sizes in the gas stream and bag dust cake; weight, permeability, and photographs of the dust cakes.

During the FFPP test program, compartments B, C, and D were operated in a reverse-gas or reverse-gas with sonic energy cleaning mode. Compartment A was operated in a deflate/shake cleaning mode during part of the tests and in a reverse-gas cleaning mode for others. In order to avoid confusion in interpreting the data, compartment C was operated throughout as a control with a filtering air/cloth ratio of 2.3 acfm/ft^2, dwell time (time between cleaning cycles) of 3 hours, and a reverse-gas air/cloth of 2.5 acfm/ft^2. The cleaning sequence in compartment C was: off line, 90 sec. null, 30 sec reverse gas, 60 sec. null, and back on line. The control data were used to observe and account for fluctuations in ΔP due to changes in the fuel and boiler load and long-term variations due to gradual changes in the dust cake. Operating parameters of the other compartments were varied as described in the next section. In order to take advantage of the FFPP's flexibility, the compartments were controlled and operated independently at constant gas flow. This method of operation facilitates interpretation of the data and is characterized by two distinct values of pressure drop; the pressure drop before cleaning the bags (ΔP_{BC}) and the pressure drop after cleaning the bags (ΔP_{AC}). It can be shown that the average pressure drop (ΔP_{ave}) calculated from ΔP_{BC} and ΔP_{AC} in a constant flow mode is within a few percent of the average pressure drop of a conventional multicompartment unit where the flow in each parallel compartment is balanced by the pressure drop.

All of the full-scale units tested had been on line long enough to be considered in a "stable" operating mode.

FABRIC FILTER PILOT PLANT

Perhaps the most important single parameter in the operation of a baghouse is the pressure drop during filtration. In the trade offs between capital cost, maintenance cost, and operating cost it is generally desirable to operate at the highest practical A/C ratio. A series of tests were performed to determine the dependence of the operating ΔP upon the filtering A/C and the dust loading on the surface of the bags. For these tests compartment C was operated as described above and again served as the control. Compartments B and D were operated at the same RA/C as compartment C, but the filtering A/Cs and dwell times were adjusted periodically to yield a range of data. The results of the A/C and dust loading tests are summarized in Figure 1.

The dust accumulation on the bags in each cycle is termed "Areal Loading/Cycle" and is calculated by assuming that all of the dust entering a compartment is evenly distributed on the bags. It was adjusted by extending the dwell time. The data sets taken at each value of A/C are shown in Figure 1 where ΔPave is plotted vs. areal loading/cycle. For each data set, ΔP_{BC} always had a positive slope (ΔP vs areal loading) and ΔP_{AC} always had a negative slope. However, the average (ΔP_{ave}), which most nearly represents conventional baghouse operation, shows only a weak dependence on areal loading, increasing for the higher values of A/C and decreasing for the lower values. From these data it is concluded that for typical utility operation, a benefit can be realized by extending the dwell time to keep more compartments in service on the average and reduce the stress of cleaning on the bags without any increase in ΔP.

Although reverse-gas cleaning is the most common mode for power plant baghouses, little information is available illustrating the relationship between bag cleaning effectiveness and the magnitude of the reverse gas. A series of tests were run on the FFPP to investigate this relationship. Compartment C was operated in the mode described above. Compartments B and D were operated in the same manner as C except that the dwell time in B was set at six hours. The magnitude or RA/C was set at 6, 4 and then 2 acfm/ft^2 during the tests for both B and D.

The results of the RA/C tests are illustrated in Figure 2. Compartments B and D were set first to a RA/C of 6 acfm/ft^2, operated for about 10 days, set to 4 acfm/ft^2 for about 10 days, and finally, set to 2 acfm/ft^2 for several days. ΔP_{AC} almost doubled as RA/C was decreased from 5 to 2 acfm/ft^2, while ΔP_{BC} changed very little. It does not appear that the operating pressure drop, ΔP_{ave}, is a strong function of RA/C; therefore increasing the reverse-gas flow is not recommended as a practical method of reducing the operating pressure drop of baghouses.

FULL SCALE UNITS

A data set describing the operation and performance of full-scale baghouses is being accumulated to supplement that taken at the FFPP. The following paragraphs contain a brief summary of data taken to characterize five full-scale units and additional data reported by others (6,7,8). Figure 3

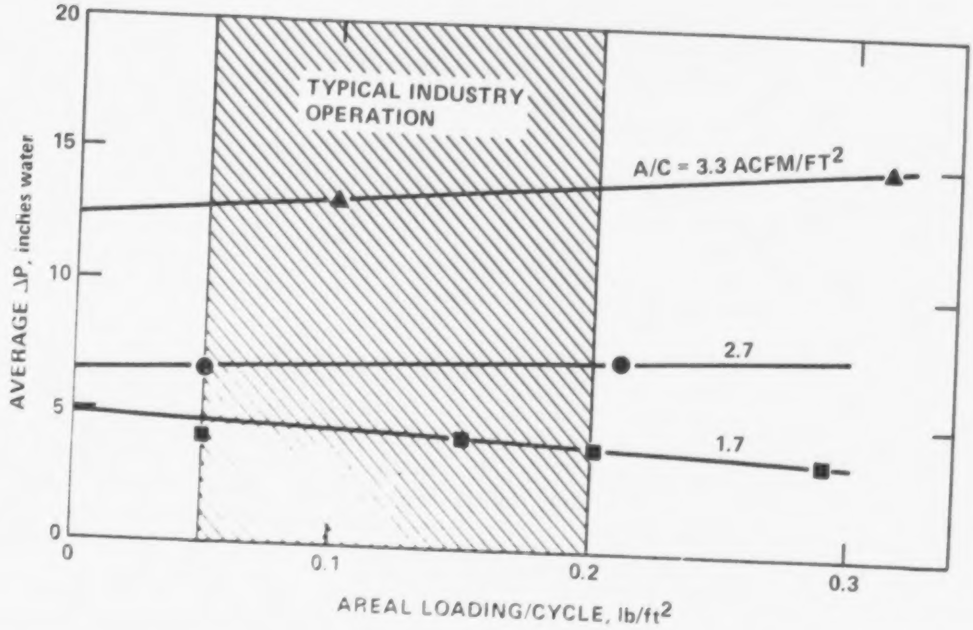

4517-255

Figure 1. FFPP tube sheet ΔP versus air/cloth ratio and dust load per unit area (areal loading) per filtering cycle.

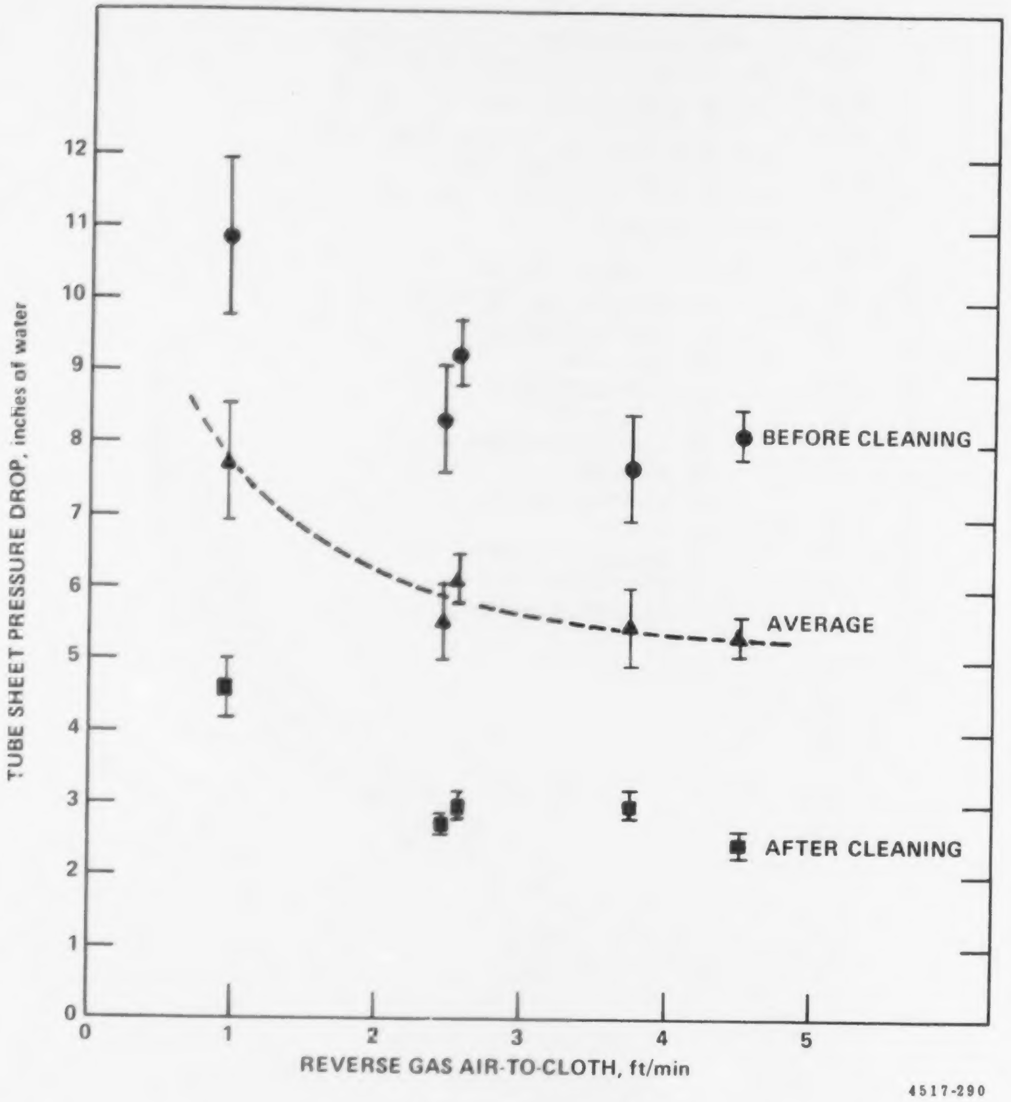

Figure 2. Tube sheet pressure drop versus reverse air-to-cloth.

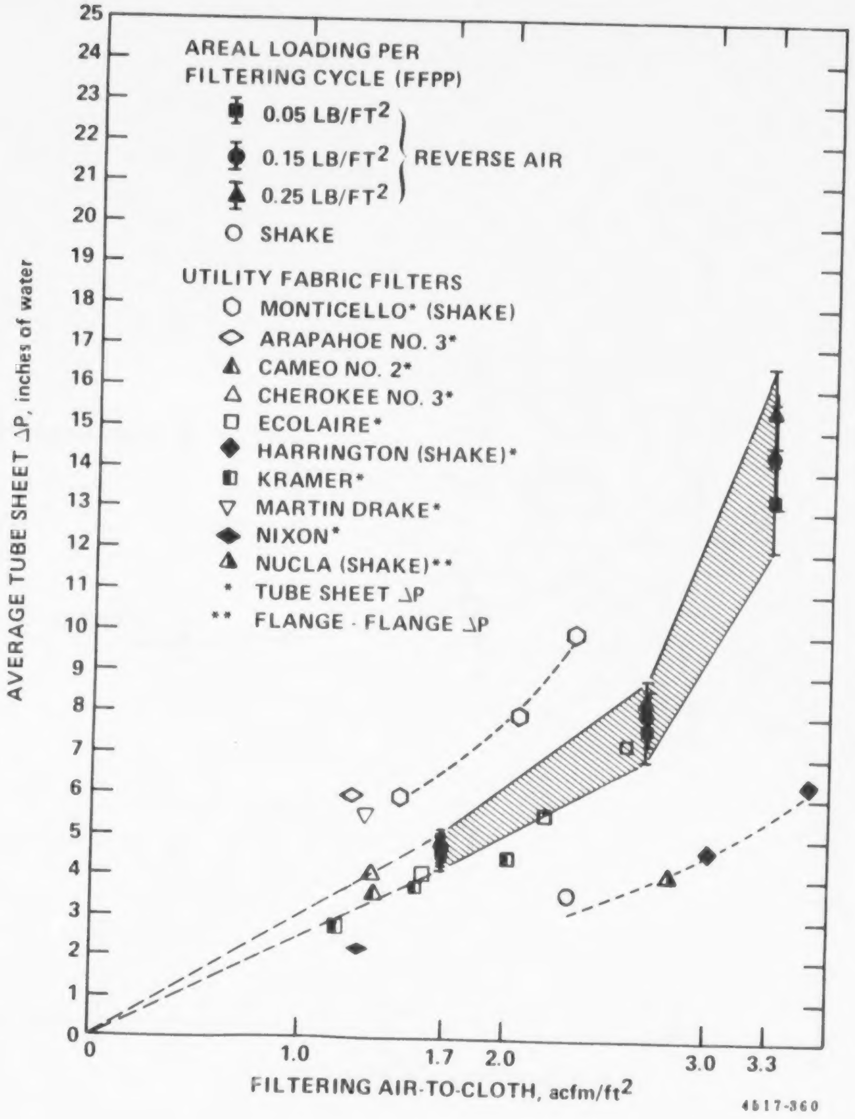

Figure 3. Average operating ΔP versus A/C for the FFPP and nine baghouses installed at coal fired plants.

is a summary of the average ΔP vs. air/cloth ratio for the reverse-gas compartments of the FFPP at three values of areal loading (from Figure 1), and five full scale reverse-gas units. Also, similar data are plotted for three shaker units and from the FFPP deflate/shake tests. Notice that it was possible to measure the actual tube sheet ΔP for some units, while at others only flange-flange data were available, which includes an unknown pressure drop across the ductwork. The data are generally similar for the reverse-gas units, all of which are located in Colorado and installed on boilers burning low-sulfur coal.

Good agreement is seen between data taken at the FFPP and the full-scale units. Notice the linear dependence of ΔP upon A/C below A/C = 3 acfm/ft^2, indicating the possibility of operating at higher A/C values than the traditional 2 acfm/ft^2 for savings in capital costs. The increased slope above A/C = 3 is not well understood, but appears to result from differences in permeability of dust cakes formed at different face velocities.

As expected the units cleaned by shake/deflate tend to operate at significantly lower pressure drops than the reverse-gas units, except at the Monticello station, which burns Texas lignite. This station has experienced continuous problems of high pressure drop and dust bleed through, and the interaction of its unusual ash with fabrics of different types is currently being studied.

DUST CAKE ANALYSIS

Samples were cut from the bags at each test site after the compartments were cleaned and shut down. Rather thick residual dust cakes were found in each instance. Figure 4 is a cross sectional photograph illustrating a typical example from a reverse-gas unit. The cake is rugged, with large nodular deposits, deep fissures, and a thinner deposit along the "fold line" where the bag flexed during reverse-gas cleaning. The actual weights of the dust cakes are summarized in Table 1. The weight of dust per unit area ranged from 0.4 to 0.6 lb/ft^2 for all of the installations investigated (40-60 lb/bag). Considering that this is the residual cake left after cleaning and that the calculated accumulation of dust during one hour of filtering is expected to be about 0.05 lb/ft^2, it is concluded that only about 10 per cent of the dust cake is removed by reverse-gas cleaning--probably the freshest part of the cake. Recall again that the data presented in Figure 4 and Table 1 are for bags that have been "cleaned" by reverse-gas. Thus, the residual dust cake is the one analyzed.

Studies were made of the bag swatches to determine how permeability of the dust cake, or alternately the drag (ΔP vs. A/C ratio) depended upon its physical properties. The swatches were placed in a large filter holder and their ΔP vs A/C characteristics measured. Dust was then removed from the swatches for further analysis. The distribution of particle sizes in the range of 4-80 μm was measured using a Coulter counter, and the results related to the measured drag.

Figure 5 is a summary of all the permeability data from 1 ft^2 samples taken from the top, middle, and bottom of bags at the five full-scale units

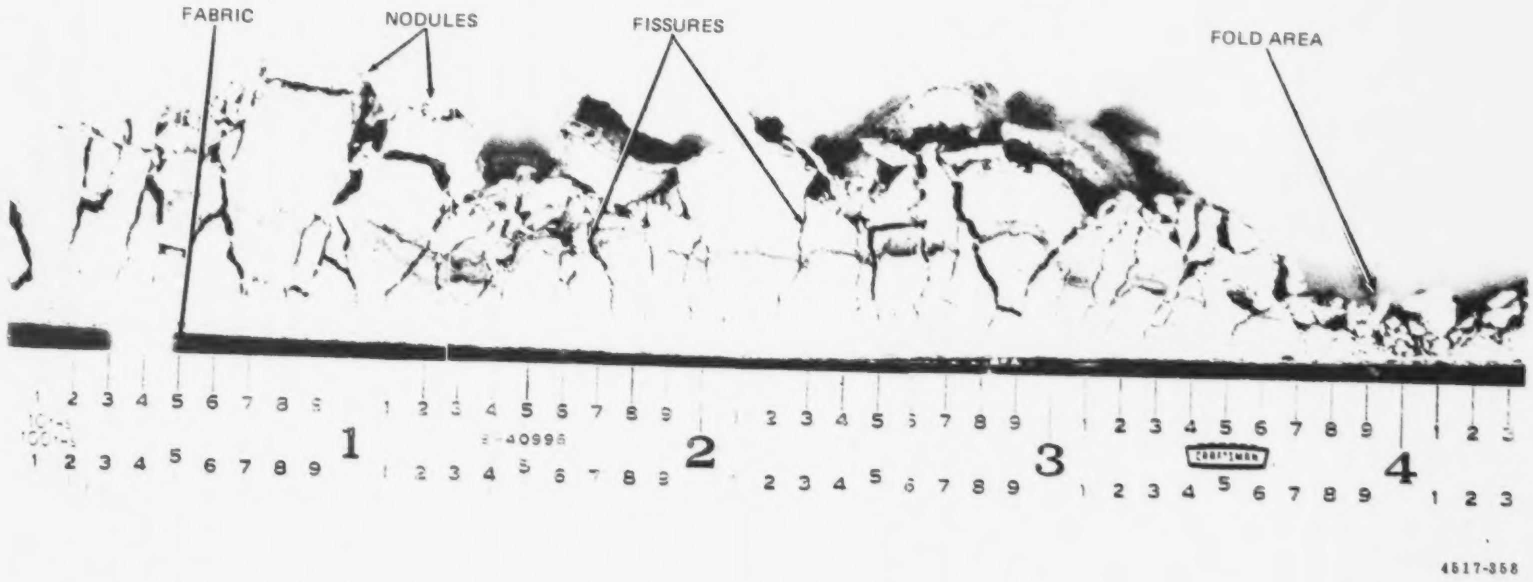
FABRIC
NODULES
FISSURES
FOLD AREA
1
2
3
4
4517-358

Figure 4. Cross sectional view of fiber glass bag and dust cake from a baghouse cleaned by reverse gas.

Table 1. Summary of the weights of dust cakes from several baghouse installations.

PLANT	BAG TYPE	SIZE OF BAGS (LxD)	AVERAGE RESIDUAL WEIGHT OF DUST CAKE (After Cleaning) LB/FT^2
MARTIN DRAKE	MENARDI SOUTHERN 601-T (9.5 oz/yd)	30.5′ x 12″	0.5
NIXON	MENARDI-SOUTHERN 601-T (9.5 oz/yd)	31.75′ x 12″	0.4
CHEROKEE (UNIT 3)	FIBERGLASS WITH ACID RESISTANT COAT (9.5 oz/yd)	33.8′ x 12″	0.4
CAMEO (UNIT 2)	MENARDI-SOUTHERN 601-T (9.5 oz/yd)	22.1′ x 8″	0.5
ARAPAHOE (UNIT 3)	MENARDI-SOUTHERN 601-T (9.5 oz/yd)	22.1′ x 8″	0.6
FFPP SHAKE (1/82)	ALBANY INTERNATIONAL Q53-S3016 TRICOAT TYPE 11T (NO RINGS) (9.2-9.6 oz/yd)	34′ x 11.5″	0.2
FFPP REV. AIR (1/81)	ALBANY INTERNATIONAL Q53-S3016 TRICOAT TYPE 12T (RINGS) (9.2-9.6 oz/yd)	34′ x 11.5″	0.2 (1/81) 0.6 (1/82)
ECOLAIRE PILOT PLANT	FABRIC FILTER CO. ACID-FLEX STYLE 504-1AF	24′ x 8″	0.15 (11/81) 1.0 (2/82)

4517-267

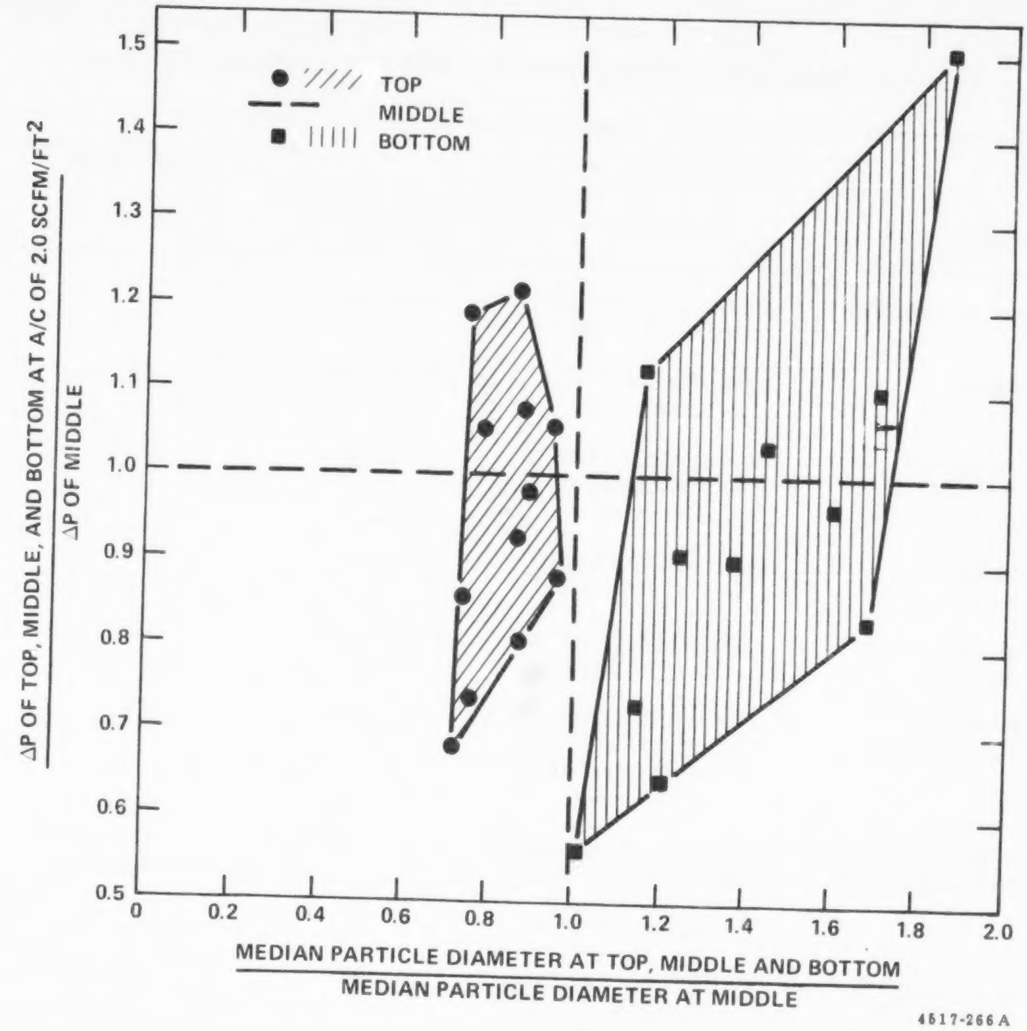

Figure 5. Relative size of particles and drag of dust cakes found at the top, middle, and bottom of bags from several baghouses.

and the FFPP. The data are normalized by dividing both the values of drag and median diameter measured at the top and bottom of the bags by the values obtained at the middle of the bags and dividing by the mass of dust per unit area. This method of normalization is intended to eliminate variations imposed by differences in the inlet particle size distribution at the different power plant installations and variations in thickness (weight) of the values.

From Figure 5 it can be seen that there is little correlation between the drag and the median diameters of the particles comprising the cakes. The Coulter analysis indicates that the particles near the top of the bags, however, were somewhat smaller than those from the middle and bottom. These data suggest that the drag is not determined by the thickness of the cake or particle size, but by the macroscopic structure; i.e., the cracks, voids, and fold lines.

Measurements of the ash chemistry, structure, and resistivity are being made in order to gain a better understanding of the factors that determine the drag, or pressure drop. Although the measured concentrations are small, the chemical analyses do show progressively higher concentrations of sulfate in (1) the hopper samples, (2) smooth cake samples, and (3) nodular cake samples, respectively. This is thought to confirm the conclusion that an equilibrium situation is reached wherein a relatively small amount of ash is deposited and removed during each filtering and cleaning cycle, while the heavy, residual cake remains relatively undisturbed. No cementitious structure has been found, however, in our microscopic analysis. Thus, there is no indication that the relatively higher sulfate concentration plays a significant role in the formation or tenacity of the dust cake nodules.

CURRENT FFPP TESTS

At the FFPP, research has been initiated to investigate the effectiveness of sonic energy enhancement on reverse gas cleaning. Two types of commercially available sonic energy sources (horns) are currently being evaluated. Cleaning sequences which are being tested range from simultaneous use of reverse gas and sonic energy to sonic energy alone. Early in 1983 testing will begin using a "generic" sonic energy source capable of operation at a continuum of fundamental frequencies and energy outputs. This will allow effective sonic energy density within a baghouse compartment (number of horns and location). The use of sonic energy to augment reverse air cleaning is dramatically illustrated in Figure 6. Here the sonic horn was activated for 10 seconds in the middle of a 30 second reverse gas period. The reverse gas air-to-cloth ratio was 2.5 ft/min. The pressure drop was reduced by more than one-half when the horn was used.

CONCLUSIONS

In the FFPP and the full-scale baghouses, heavy residual dust cakes are left on the bags after reverse-gas cleaning. Only about 10 per cent of the cake is removed during each cleaning cycle, yet the drag is reduced by approximately a factor of two. Accordingly, it is concluded that the

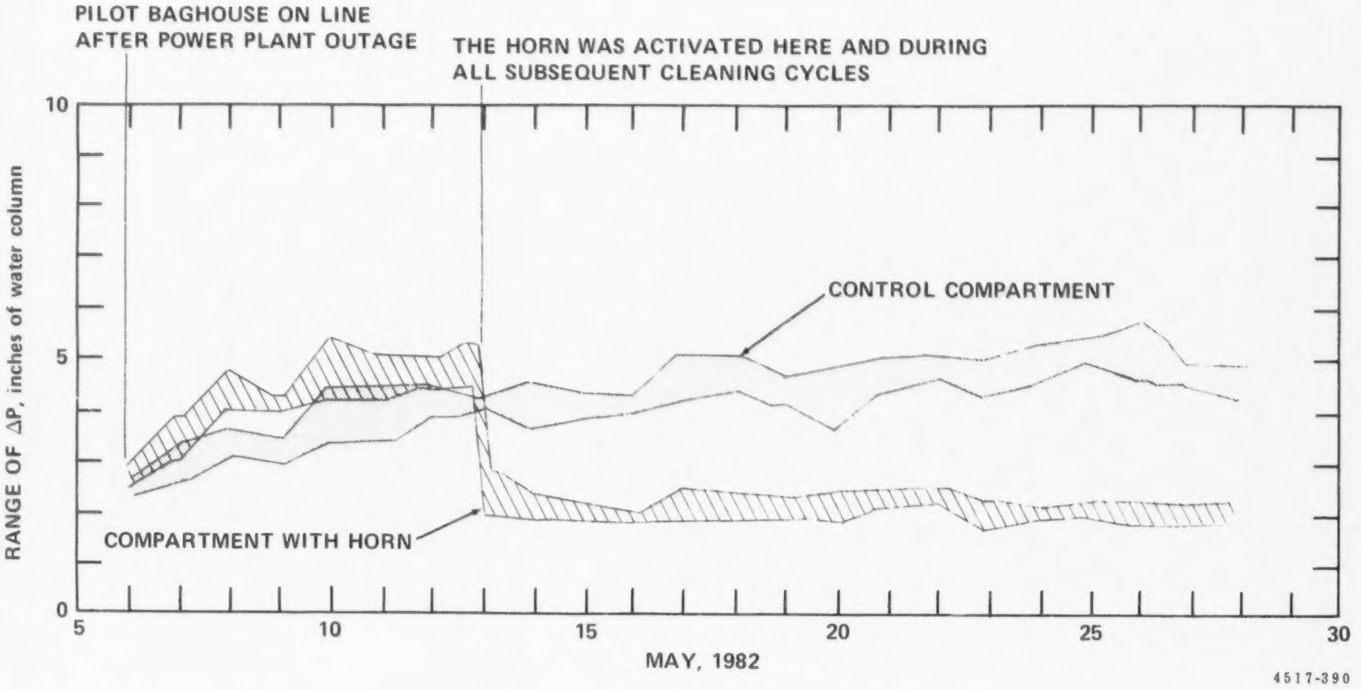

Figure 6. *Pressure drop/time history illustrating the effectiveness of sonic bag cleaning. Both compartments were operated at an A/C ratio of 1.2 ACFM/FT^2 and cleaned every 3 hours by reverse gas enhanced with sonic energy.*

pressure drop is determined as much by the structure of the cake as by the amount of dust present. For the sites evaluated, there was no particular correlation between the pressure drop and particle size or chemistry.

ΔP vs. air/cloth ratio appears to be a nearly linear function, with a sharp increase in slope near 3 acfm/ft^2. All of the reverse-gas units evaluated performed similarly, but at a higher pressure drop than has been reported for most shaker units. If a method could be found to remove the cake more effectively, it is expected that the operating pressure drop of reverse-gas baghouses could be lowered by a large fraction without a significant loss in collection efficiency.

The dependence of pressure drop on areal dust loading (time between cleaning) is complex. For higher values of air/cloth (>2.2 acfm/ft^2) the average pressure drop in the FFPP increased slightly as the dust loading on the bags (dwell time) increased. For lower values of air/cloth, the average pressure drop decreased as the dwell time increased.

After 10,000 hours of reverse-gas operation no bags have failed. The collection efficiency has consistently exceeded 99.9% after the first few days of operation. Several weeks are required for the system to stabilize for each test condition.

Over the range tested (RA/C of 2.0 to 6.0 acfm/ft^2), the effectiveness of bag cleaning was not a strong function of reverse-gas volume. Since a value of 6.0 acfm/ft^2 is very high for practical operation, reverse-gas cleaning appears to be a marginal method of removing dust cakes from fabric filters.

Preliminary indications are that a sonic aided reverse-gas cleaning is very effective in removing residual dust cakes. Future plans include detailed studies of that cleaning mode with the goal of determining the optimum distribution, intensity, frequency, and timing of the sonic energy. Extended tests of shake/deflate cleaning are also planned.

The emphasis in all these tests will be to achieve a reduction in pressure drop and baghouse size without sacrificing reliability or efficiency.

ACKNOWLEDGEMENTS

We would like to express our appreciation to the staff and management of the Public Service Company of Colorado and the Colorado Springs Department of Public Utilities for their cooperation and assistance in evaluating the fullscale baghouses. The data reported here were all taken by staff members of Southern Research Institute. The FFPP is operated by Kaiser Engineers under the direction of Lou Rettenmaier of EPRI. We would like to thank Richard Hooper of EPRI for his continuing support in acquiring and interpreting the data.

The work described in this paper was not funded by the U.S. Environmental Protection Agency and therefore the contents do not necessarily reflect the views of the Agency and no official endorsement should be inferred.

REFERENCES

1. Smith, W. B., R. C. Carr, K. M. Cushing, and G. B. Gilbert. Air load and startup tests of a 10 MW fabric filter pilot plant. Presented at the Fabric Filter Forum, Phoenix, Arizona, January 1981.

2. Smith, W. B., R. C. Carr, and K. M. Cushing. Characterization of a 10 MW fabric filter pilot plant. Presented at the Third Symposium on Transfer and Utilization of Particulate Control Technology. Sponsored by the U.S. EPA, Orlando, Florida, March 1981.

3. Carr, R. C., W. B. Smith, and K. M. Cushing. Characterization of a 10 MW fabric filter pilot plant. Paper 81-9.2. Presented at the Annual Meeting of the APCA, Philadelphia, Pennsylvania, June 1981.

4. Carr, R. C., W. B. Smith, and K. M. Cushing. Test results from operating fabric filters: full scale and Arapahoe 10MW pilot plant. Presented at the EPRI Conference on Fabric Filter Technology for Coal-Fired Power Plants, Denver, Colorado, July, 1981.

5. Smith, W. B., K. M. Cushing, and R. C. Carr. Measurement procedures and supporting research for fabric filters. Presented at the EPRI Conference on Fabric Filter Technology for Coal-Fired Power Plants, Denver, Colorado, July, 1981.

6. Ladd, K. L., R. L. Chambers, O. C. Plunk, and S. L. Kunka. Fabric filter system study second annual report. EPA-600/57-81-037, July, 1981.

7. Ensor, D. S., S. Cowen, A. Shendrikar, G. Markowski, G. Woffinden, R. Pearson, and R. Sheck. Kramer station fabric filter evaluation. EPRI Report No. CS-1669, January, 1981.

8. Ensor, D. S., R. G. Hooper, and R. W. Sheck. Determination of the fractional efficiency, opacity characteristics, engineering, and economic aspects of a fabric filter operating on a utility boiler, EPRI Report No. FP-297, November, 1976.

THE DESIGN, INSTALLATION, AND INITIAL OPERATION OF THE W. H. SAMMIS PLANT UNIT 3 FABRIC FILTER

by: Dennis R. Ross, P.E.
Generating Plant Staff Engineer
Ohio Edison Company
Akron, Ohio 44308

James R. Howard,
Plant Engineer
W. H. Sammis Plant
Ohio Edison Company
Stratton, Ohio 43961

R. Mark Golightley,
Plant Engineer
W. H. Sammis Plant
Ohio Edison Company
Stratton, Ohio 43961

ABSTRACT

This paper will discuss the design philosophy and preliminary operating experience of the first unit of four units to be retrofitted with fabric filters at the W. H. Sammis Plant. Each unit is 180 MW net. The unit was operational late August 1982.

The paper will identify design criteria initially specified, design enhancements during the course of the project, construction highlights, and preliminary operating experience. Results from the first months of operation will include pressure drop and opacity. In addition, start-up, shutdown, and maintenance procedures will be discussed.

INTRODUCTION

The W. H. Sammis Plant, located on the Ohio River north of Steubenville, Ohio, is the second largest of the Ohio Edison Company system coal-fired plants. Currently, the units burn coal mined locally as well as out-of-state coal. The first four units have a Net Demonstrated Capacity (NDC) of 180 MW each, with gas flows of approximately 755,000 ACFM each at 305°F. Unit 5 is 300 MW NDC with a gas flow of approximately 1,300,000 ACFM at 270°F. Units 6 & 7 are 600 MW NDC each, with gas flows of approximately 2,600,000 ACFM each at 270°F. Flue gas from Units 1 & 2 are combined into Chimney No. 1 and Units 3 & 4 are combined into Chimney No. 2. Each of these chimneys are 500' high. Units 5 & 6 share the No. 3 Chimney (850' high) while Unit 7 has its own 1,000' high chimney. All seven units have electrostatic precipitators which were originally installed with the boilers. Units 1-4 went into service during the period 1959-62, Unit 5-1967 and Units 6 & 7-1969 and 1971, respectively. The Company is currently engaged in a program to retrofit high efficiency particulate collection equipment on all seven units, as the existing precipitators can not achieve the level of collection required to satisfy the emission limits.

For the purpose of this discussion, primarily the equipment, fabric filters, which have been purchased for the Units 1-4 will be presented. Units 5-7 are being equipped with electrostatic precipitators.

BACKGROUND

All of the units were designed and equipped with the then current state-of-the art emission control features of electrostatic precipitators and tall stacks. The precipitators, for a variety of reasons, have never performed to the highest level expected of them. With development of particulate emission limitations as required by the Clean Air Act of 1970, it became apparent that further steps would be needed to meet the newly imposed regulations.

In 1972, Gilbert/Commonwealth, Ohio Edison's Architect/Engineer, was commissioned to perform detailed studies on all of the Ohio Edison Company plants to determine a compliance strategy to satisfy the limitations imposed by the new regulations. These studies were updated routinely, primarily because of changes in the proposed emission regulations and fuel availability. Most recently, in mid-1977, the U.S. EPA finalized SO_2 standards for Ohio.

The federal standards finalized in 1977 are site-specific and even stack-specific. Currently, the standards for the W. H. Sammis Plant are .1 lbs/MMBTU for particulate and 2.91 lbs/MMBTU for SO_2 from each chimney. Utilizing alternate equations to determine allowable SO_2 emissions permitted some variability to the emissions from individual chimneys. Needless to say, some interesting combinations were investigated by which compliance could be met. The ultimate goal was to establish a strategy to meet both particulate and SO_2 emission regulations through the selection of the proper combination of coals.

A predominant factor in the development and final selection of control strategies was the evaluation of site-specific requirements which also affected the economics. Probably the most important consideration was the space available for equipment installation.

The plant is located between railroad tracks and 500' high hills on the west and the Ohio River on the east. Between the plant and the Ohio River is Ohio Route 7, a four-lane highway. Available space for equipment between the plant and the highway was minimal at best.

Locating the control equipment on the plant roof and in the south yard were considered, but these locations, upon some detailed evaluation, were determined to be not feasible. Other ideas were explored, including the location of the equipment on a deck-like structure built over the highway. The more this concept was explored, the more feasible it appeared. Preliminary contact with the highway department was encouraging, and the concept was further developed.

The control strategy ultimately selected for particulate and SO_2 emission compliance was the use of low sulfur (less than 1%) for Units 1-4 and coal not to exceed 2.8% sulfur for Units 5-7 and the installation of new high efficiency particulate collection equipment on all seven units. This strategy was the least costly to satisfy the regulations. In accordance with this control strategy, it was determined that the particulate collectors had to have an efficiency of approximately 99.41% in order to meet the 0.1 lbs/MMBTU particulate emission regulation.

In January 1981, a Consent Order was signed with the U.S. EPA which established the compliance dates for meeting particulate emission limits, as shown in Table No. 1.

TABLE 1. W. H. SAMMIS PLANT COMPLIANCE SCHEDULE

Unit No.	Compliance Date
1	January 31, 1983
2	August 31, 1982
3	June 30, 1982
4	November 1, 1982
5	April 30, 1984
6	August 31, 1984
7	December 31, 1982

The Consent Order incorporated new particulate collection equipment installation on the seven boilers at the W. H. Sammis Plant and five boilers at three other plants and upgrading particulate collection equipment on eleven boilers at three plants. Non-compliance with particulate emission limitations at the W. H. Sammis Plant could cost Ohio Edison Company $7,500 per day per boiler. Interim deadlines established by the Consent Order which addressed primarily construction activities could also cost the Company $5,000 per boiler per day fines. (1)

The total effect of the Consent Order requires that Ohio Edison Company expend approximately $550 million to reduce particulate emissions. At the W. H. Sammis Plant alone, approximately $450 million will be expended.

CONSTRUCTION AND DESIGN HIGHLIGHTS

As stated previously, the site constraints posed a major problem from an engineering and construction standpoint. The deck concept became the only viable method of supporting equipment. The deck spans a four-lane highway between the plant and the Ohio River. It is 915 feet long and 140 feet wide and allows 20 feet of clearance above the highway. The foundation has 192 caisson piers approximately 6 feet in diameter that go to bedrock. Approximately 12,000 tons of structural steel, breeching, fabric filters and electrostatic precipitators, are supported by the deck. The deck construction cost approximately $27 million.(2) The deck is shown on Figure No. 1.

Access to the deck is limited, so construction is staged such that work activities progress from the plant toward the Ohio River and from the middle of the deck toward the ends of the deck. Material and subassemblies from a nearby marshalling yard were moved by barges to the deck as needed. Figure No. 2 shows construction activities on the deck.

Draft losses associated with the new fabric filters and the extensive ductwork necessitated new ID fans for the Units 1-4 boilers. Modified radial tip fans with two-speed PAM motors are being used. The PAM motors were selected to reduce low load power consumption, to allow easier fan start-up and to reduce the risk of boiler implosions.

Our design criteria for the fabric filters and the ductwork from the air heater outlet to the chimney is ±30 IWG. An economic evaluation was conducted relative to strengthening the boiler to meet the new design criteria for implosion protection. In lieu of boiler strengthening, it was decided to install additional draft controls. A Bailey Controls Network 90 implosion protection package was selected for the Units 1-4 boilers.

Throughout the course of the project, many types of models were utilized. Initially, our consultants developed a table-top scale model of the immediate plant vicinity. This was used internally to develop and present alternative equipment locations influenced by the site constraints. This model was subsequently used in discussions with various regulatory agencies in securing approvals for the deck and barge unloading facility construction, as well as negotiations relative to the Consent Order.

Construction of the deck had to be accomplished while maintaining highway traffic flow at all times. A model was constructed which incorporated scaled-equipment to aid in planning the deck construction.

Retrofit projects produce unique problems from a standpoint of engineering and construction. Site constraints, especially those imposed at the W. H. Sammis Plant, at times, make these problems even more burdensome. Existing facilities must be moved to accommodate new equipment and facilities must be altered and strengthened to accommodate the new design. Our consultants originally constructed a 3/8" scale model of the back portion of the plant from Units 4 through 7 to verify design layouts. All equipment, piping, steel and ducting was shown in detail. As the project progressed, this model became more of a design construction and planning tool than a design verification model. Interferences were quickly recognized and changes were made during the design stage.

With the addition of new ID fans and additional lengths of breeching, boiler control and implosion protection were of great concern. Our consultants mathematically modeled the gas side of the boiler and its controls. This model defined problem areas and analyzed the effectiveness of different control schemes.

As a standard design requirement, we require the precipitator vendors to flow model the precipitator and duct system to optimize flow distribution and pressure drop. At the onset of the project, this was not required of the fabric filter vendor. The industry had been led to believe that a fabric filter was a flow-balancing, pressure-equalizing device. However, during the project, it was decided to conduct a flow model study of the fabric filter. A more detailed discussion of the fabric filter model will be addressed later.

FABRIC FILTER DESIGN

Coal being burned in Units 1-4 is low sulfur eastern coal with design specifications of: 0.6 to 0.8% sulfur; 10-20% ash; and 10,000-12,000 BTU/lb. Design gas flow is 754,000 ACFM each at 305°F. In 1977, early in the planning for the current particulate control program, it was decided to solicit bids for electrostatic precipitators and fabric filters. In June 1978, American Air Filter was issued a letter of intent to supply four fabric filters, one each for Units 1-4. Table No. 2 lists pertinent data of the fabric filter.

TABLE 2. FABRIC FILTER DESIGN INFORMATION

Fabric Filter Supplier	American Air Filter
Number of Compartments	12
Type of Cleaning	Reverse air
Air-to-Cloth Ratio-Design	
Gross	1.93:1
Net(1)	2.1:1
Net-Net(2)	2.31:1
Cloth area per Compartment	32,632 ft.^{2}
Filter Bags	
Per Compartment	312
Total	3,744
Filter Bag Configuration	3w6w3x26

(1) One compartment off-line for cleaning

(2) One compartment off-line for cleaning, and one down for maintenance

The fabric filter reverse air and outlet dampers are poppet-type and the inlet damper is a flat-plate butterfly damper. Due to site constraints and the desire to utilize existing chimneys, the inlet and outlet of the fabric filter are on the same side. Figure No. 3 illustrates the confined duct arrangement. The reverse air system has two 100% sized fans for each unit. The reverse air circuit is kept hot by circulating clean flue gas. When a compartment requires cleaning the reverse-air bypass dampers close, and the individual compartment reverse-air damper opens. A manually operated compartment ventilation system is also provided. Automatic control of the fabric filter is accomplished by an Allen-Bradley programmable controller. Pressure drop information is shown in Figure No. 4.

The fabric filter is bypassed via two Andco flap-door type dampers. The fabric filter will automatically be bypassed on high flue gas temperature and high differential pressure across the fabric filter. The fabric filter is manually bypassed on start-up and can be operator initiated for emergency or abnormal situations.

The filter bags are fiberglass with Teflon B coating. Additional information is shown in Table No. 3. In Unit No. 3, thirty-six acid resistant bags have been installed for test purposes. These bags are style Q78-S3016 with Filter Resources' acid resistant proprietary finish.

TABLE 3. FILTER BAG DATA

Bag Manufacturer	Filter Resources
Bag Style	Q79-S3016
Bag Finish	10% Teflon B
Weight	9.5 oz/yd^2
Weave	3 x 1 Twill
Count	54 x 30
Permeability	35-60(1)
Yarn Designation	
Fill	75 1/2
Warp	75 1/0
Bag Dimensions	
Diameter	11 3/4"
Length	34' 7"
Anticollapse Rings	
Number	8 per bag
Type	Cadmium plated carbon steel

(1) CFM/ft.^{2} @ 0.5 IWG

FABRIC FILTER FLOW MODEL STUDY

When the fabric filter was initially procured, a flow model study was not a requirement. After seeing results of the flow model conducted for the EPRI pilot plant located at the Arapahoe Plant, it was deemed appropriate to flow model the W. H. Sammis Plant fabric filter. American Air Filter was approached with this request, and they agreed that a flow model would be beneficial.

The model work was conducted by NELS Incorporated of St. Catherines, Ontario, Canada. The model was 1:12.57 scale and made of plexiglass. It incorporated all the ductwork from the air heater outlet to the fabric filter, the fabric filter, and ductwork from the fabric filter to the ID fan inlet. Structural members that affected gas flow, dampers, and all thimbles were included in the model. A second phase of the model addressed the ID fan outlet duct to and including eight diameters of the chimney.

The primary objectives of the modeling program were: minimize pressure drop; achieve acceptable flow distribution to the ID fans; determine acceptable flow and particulate distribution to the compartments; determine acceptable flow and particulate distribution through the tubesheets; minimize hopper reentrainment; and evaluate the system under bypass conditions. Unlike precipitator modeling which has acceptance criteria established by the industry, fabric filter flow modeling had no established industry guidelines. A target balance for flow within ±10% and particulate distribution within ±20% of theoretically equal flow was established. Through the tubesheet, a target balance having an RMS deviation less than 25% was established.

Vaning was added to minimize the pressure losses and to improve the flow and dust distributions. Flow distribution values were generally within or close to the target values. Dust distribution was generally outside the target values. It was recognized that dust distribution could not effectively be controlled without going to massive internal control structures and increased pressure losses. The system pressure loss is essentially constant for various operating configurations.

Perhaps the two most important findings of the program pertained to hopper reentrainment and system bypass. Flow patterns in the hoppers indicated severe reentrainment. The dust flows entering the hoppers were initially concentrated at the hopper inlet and continued to recirculate in the hopper without dispersing. This condition was rectified by installing ladder vanes and a false floor in the inlet duct and flow deflectors in the hopper.

The original outlet duct configuration with poppet-type bypass dampers had an unacceptably high pressure drop of 17.7 IWG for a full load bypass. The entire outlet duct and bypass duct was modified. The subsequent pressure drop was near that expected under normal operating conditions. (3, 4)

PREOPERATIONAL TESTING AND TRAINING

As the fabric filter installation for Unit 3 neared completion, approximately 4 months before start-up, a team comprised of plant and vendor personnel began checking out the various systems. Wiring was verified, and limit switches were set on all dampers which provided inputs to the programmable controller. The cleaning cycle was then operated in both the pressure and time initiated mode using the programmable controller. All other equipment was checked-out in the same manner. This attention was useful in that problems encountered with the reverse air fans, limit switches and control panels were detected and corrected before start-up.

In conjunction with the checkout activities, training was conducted by various vendors and Gilbert/Commonwealth at the plant site. This training was directed toward both operating and maintenance personnel.

Throughout the 4 month period prior to start-up, trips were taken by various engineering and plant supervisory personnel to operating installations. This first-hand observation and discussion opportunity is extremely beneficial. Learning from the experience of others allows valuable insight into potential problem areas and gives guidance for operating and maintenance personnel. This also establishes a line of communication to solve future problems that may be encountered.

Unit 3 came off line on June 22, 1982 for a scheduled turbine overhaul and boiler inspection. During this outage, final tie-in of the new ductwork was accomplished. Initial firing of the boiler began on August 28, 1982. Finally, on September 1, 1982, precoating of the fabric filter was ready to begin.

It was our intent to precoat the fabric filter on line rather than precoat with cold flyash. This was a change from the original thinking during the project. With American Air Filter's approval, the following criteria was established: flue gas temperature to be 305°F or greater; gas flow to be approximately 400,000 ACFM; fluidizing air and hopper heaters at least 24 hours prior to start-up; the unit had to be on total coal fire; all 12 compartments in service; and no cleaning until a 3 IWG pressure drop was experienced across a compartment. At 1:40 a.m., on September 1, 1982, the bypass dampers were closed and flyash laden flue gas was introduced into the fabric filter.

At start-up, the opacity monitor was not operable. The individual compartment differential pressure gauges were operable, but needed to be recalibrated. The primary indication that the fabric filter was operating was the flange-to-flange differential pressure recorder. Precoating continued until 4:00 a.m., when the first cleaning cycle was initiated.

Reverse air damper problems were experienced on several of the compartments. The damper shaft was hanging up on the guide bearings. With 9 of 12 compartments operating, the pressure drop was approximately 3.9 IWG at 140 MW. At 11:26 a.m., the fabric filter was cleaned down from a differential pressure of 4.3 IWG to 2.6 IWG. We have elected to maintain a differential pressure of 2.6 to 3.6 IWG. The design on the Bailey Network 90 implosion protection system needs to be reviewed and settings readjusted. In this interim period, we are overcleaning the fabric filter to minimize system pressure losses.

PRELIMINARY OPERATION

Since September 1, 1982, there have been approximately 15 boiler trips. These trips have been caused mainly by the boiler implosion protection system signals and equipment. To date, the fabric filter has not caused a unit trip.

On September 6, 1982, the fabric filter was inspected internally. At this time, 16 bags were found to have dislodged from the thimbles. Twelve of the 16 bags were discovered in Compartment B-1 which was the first compartment bagged. Some holes in the tubesheet and at the thimbles were also discovered. All bags were then retensioned.

The compartments were again inspected on September 24, 1982. It was observed that some bags needed retensioning, but on a random basis. Several holes in the tubesheets were observed. Leakage between the inlet plenum and the interior of Compartment B-1 was observed. This has been repaired.

Since September 1, 1982, thirteen bags have been removed. Seven of the bags had failed. Six of the bags were removed because there appeared to be problems with the bag. Of these, one was an acid resistant coated bag. These failures have been concentrated mainly in the cuff and first ring areas. The bags are being analyzed. Currently, we are attributing these failures to installation problems, normal infant mortality of the bags, and problems caused by holes in the tubesheet and back wall.

The opacity monitors were operable on September 13, 1982. Opacity has generally been running between 9-13%. The opacity is less than the 20% required opacity, but it is higher than anticipated. This has been attributed to instrument calibration, some instrument debugging problems, and possible overcleaning of the bags.

MAINTENANCE CONSIDERATIONS

The plant personnel are committed to a comprehensive preventative maintenance program. This is based on discussions with American Air Filter and various utilities with operating fabric filters. Checklists have been developed to aid in this program. Specific equipment and areas are highlighted, and space is provided to note observations. This data will be used to provide historical information to troubleshoot problem areas.

Because the filter bags are so critical to the operation of the fabric filter, a filter bag mapping program has been instituted. A form has been developed which shows a compartment with all of the thimbles. An alphanumeric matrix is utilized to locate the filter bags. When a compartment is inspected, the form is used to note observations such as retensioning requirements, bag blousing and bags dislodged from their thimbles. A second sheet is provided to note bag failures. On this sheet, a filter bag profile is shown. Recorded observations would be bag type (teflon or acid resistant coating), location of failure, description of failure and corrective action taken.

Expansion targets have been installed at the outside corners of the fabric filter. These are located exterior to the fabric filter so they can be easily observed. It was decided to install these targets for early detection of expansion problems or problems with the column sliding plates.

FUTURE PLA

While it is too early to fully assess the operation of the fabric filter, we are optimistic. Experience gained from this unit will be factored into the other three units. Several tasks have yet to be accomplished.

As previously discussed, the cleaning cycle will be optimized after adjustments to the Bailey Network 90 implosion protection system are completed. From industry experience, the cleaning cycle optimization could take several months.

The American Air Filter test program of the Filter Resources' Q78-S3016 acid resistant bags is scheduled to cover three years. Ohio Edison is contemplating its own filter bag test program on Unit 1. The primary purpose is to determine candidates for future filter bag replacement.

Reprogramming of the fabric filter programmable controller is required for two reasons. Currently, the cleaning cycle is programmed to stop at each compartment. If a compartment is isolated, the cleaning cycle will still stop at the compartment for its alloted time even though it is not physically cleaned. The program will be changed to skip an isolated compartment. Also, during the cleaning cycle, the outlet and reverse air dampers are moving simultaneously for a given period of time. The program will be changed to correct this.

At American Air Filter's request, a temperature survey was conducted on a compartment, B-6. They are concerned about the fabric filter temperature at low load operation due to low air-to-cloth ratio, low flue gas temperature, temperature stratification and potential acid dewpoint problems. The area of concern is primarily at or near the tubesheet elevation. We have already added extra insulation on the lower 8' of the compartment exterior wall. Flue stops have also been added in the insulation to prevent convection currents. Data from the test is currently being analyzed.

The work described in this paper was not funded by the U.S. Environmental Protection Agency, and therefore the contents do not necessarily reflect the view of the Agency and no official endorsement should be inferred.

REFERENCES

1. Fines Overhead, Utility Races to Meet Air Rules; Engineering News Record, August 5, 1982, pp. 26-27.

2. Ibid.

3. Ross, D. R., and Bowen, C.F.P; 1979. The Modeling of a Baghouse. Proceedings of the 4th International Fabric Alternatives Forum; Phoenix, Arizona, December 5-6. pp. (3-1) - (3-31).

4. Bowen, C.F.P; 1981. Gas Flow Model Study. Proceedings of the 5th International Fabric Alternatives Forum. Phoenix, Arizona, January 15-16. pp. (1-1) - (1-44).

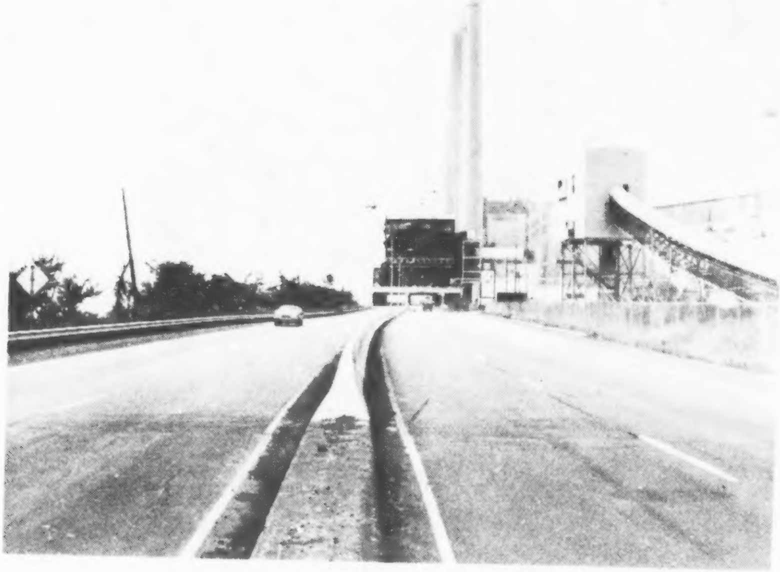

Figure 1. View of deck taken from the southbound lane of Route 7. Unit 1 fabric filter is in the background.

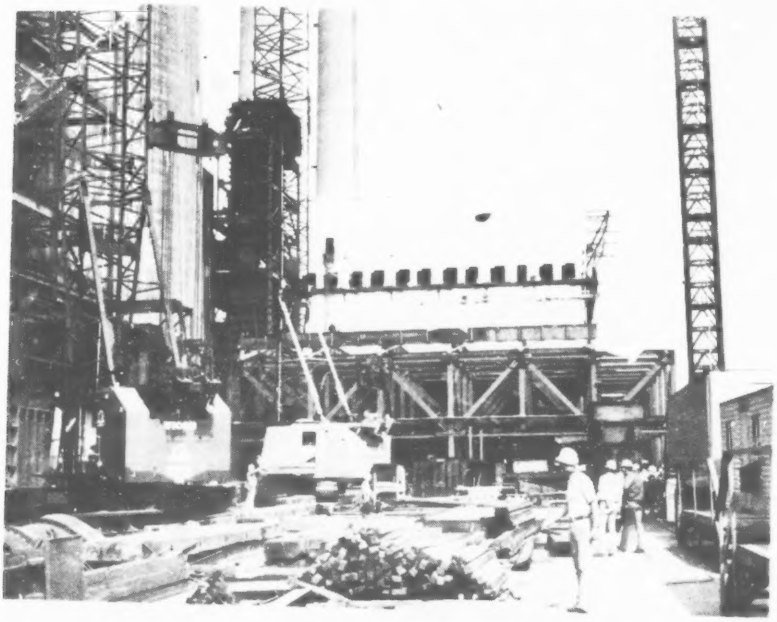

Figure 2. View from deck looking towards Unit 4 fabric filter. Structural steel and ductwork in middle of the picture is for Unit 5 precipitator.

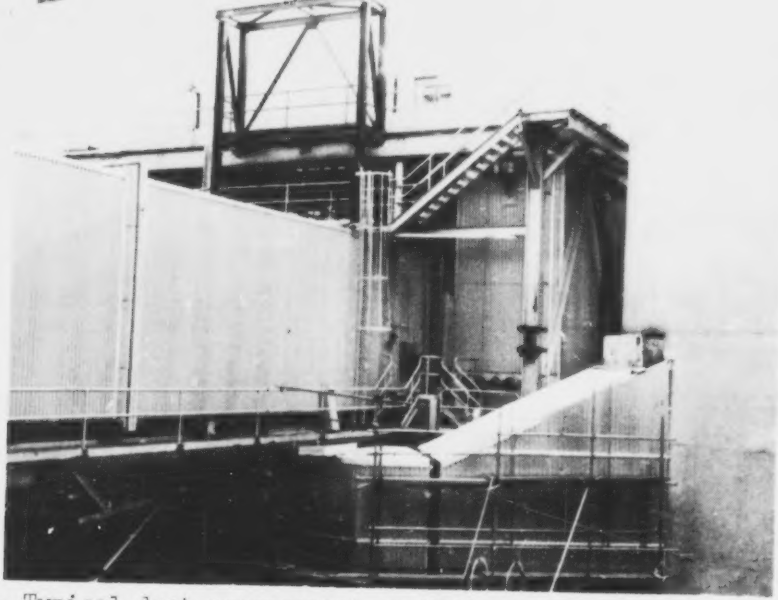

Figure 3. Typical duct arrangement on Units 1-4. Fabric filter inlet duct enters from the left. Fabric filter outlet duct is at top of picture. Duct entering the chimney is the ID fan outlet duct.

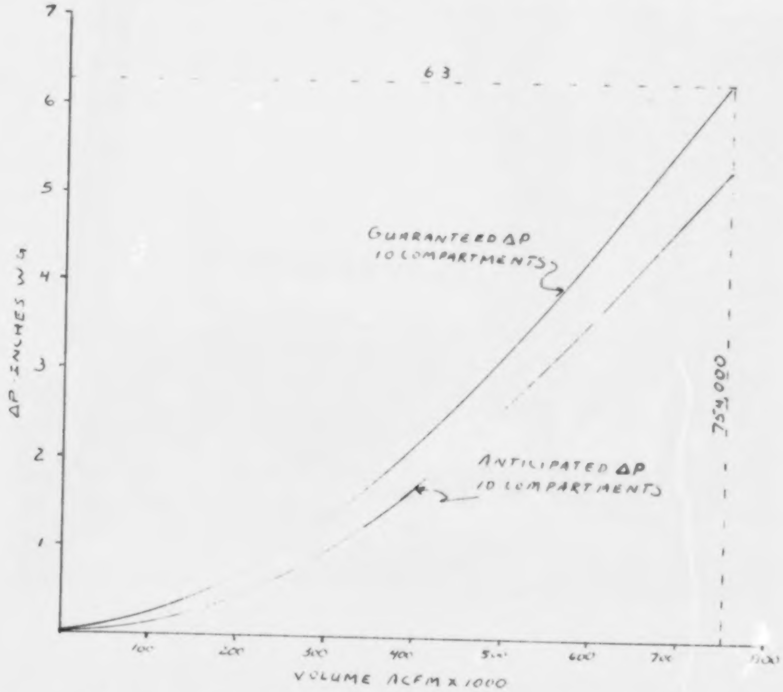

Figure 4. Guaranteed and anticipated fabric filter pressure drop with two compartments out of service.

RESULTS FROM THE FABRIC FILTER EVALUATION PROGRAM AT COYOTE UNIT #1

H. James Peters, Arthur A. Reisinger and W. Theron Grubb
Wheelabrator-Frye Inc.
Air Pollution Control Division
600 Grant Street
Pittsburgh, Pennsylvania 15219
and
Merrill Lewis
Montana Dakota Utilities
Beulah, North Dakota

ABSTRACT

The fabric filter at Coyote Unit #1 has been in service since May 1981 collecting lignite flyash and sodium-based spray dryer product as the second stage of the dry scrubbing system installed by the Wheelabrator-Frye Inc./Rockwell International Joint Venture.

A program is being conducted to evaluate the performance of acrylic, polyester, Nomex, and fiberglass filtration fabrics in full compartment trials. The unit uses predominantly acrylic fabric and operates at filter ratios of typically 3:1 using combination deflation air and mechanical shaking as the fabric cleaning method.

This paper highlights the results of the fabric evaluation program to date including comparisons of the pressure drop, throughput, replacement history, filtration parameters, and changes in physical properties of the various fabrics over the first year of operation. Discussion of the overall performance of the unit and economic and technical considerations for fabric selection is also covered.

BACKGROUND

In late 1976, prior to final equipment selection for the Coyote project, an extensive pilot program was undertaken to demonstrate the use of nahcolite and a fabric filter as an SO_2 and particulate collection process. The program was conducted at the Leland Olds Plant of Basin Electric Power Cooperative by Wheelabrator-Frye Inc. and Superior Oil under the sponsorship of the Coyote Project Utilities and their engineer, Bechtel. The resultant four months of tests proved to be very positive with respect to SO_2 removal and sorbent utilization as well as particulate collection. SO_2 removal in the range of 70-90 percent was achieved at stoichiometric ratios of 1.0 to 1.5(1). This compares favorably with reports (2,3) describing other testing of dry injection systems using nahcolite and trona.

Early in 1977 it became obvious that the lack of commercial availability of nahcolite would preclude a commercial installation of the process. As an alternative to the dry injection system utilizing nahcolite, testing was conducted by Wheelabrator-Frye and Rockwell International using a spray dryer upstream of the pilot baghouse as a means of injecting an alkaline material into the flue gas stream for SO_2 absorption. This two stage SO_2 and particulate removal system (4) proved to be technically and economically favorable and was selected for the Coyote Station.

PLANT DESCRIPTION

The 410 megawatt Coyote Station which has been on stream since the second quarter of 1981, is located in the city of Beulah in Mercer County, North Dakota and is fired with locally mined lignite fuel. The boiler is a balanced draft cyclone-fired unit with twelve cyclones and steam driven forced draft fans. The system is designed for lignite fuel having an average of 7,046 Btu per pound, 7% ash and 0.78% sulfur. During operation flue gas exits two air heaters and flows through four 46-foot diameter spray dryers into a 38-compartment fabric filter. Two axial flow induced draft fans discharge the filtered flue gas to a single stack. The flue gas temperature at the inlet to the fabric filter is in the range of 210°-$220^{\circ}F$. Gas temperatures beyond fabric capabilities are alarmed and gas flow is diverted through the fabric filter bypass system.

PILOT TESTING

Testing for the Coyote Station was first conducted in 1976 and examined the use of nahcolite as a dry absorbent in a pilot fabric filter incorporating twelve 11-1/2" diameter by 30 ft. bags with combination deflation air - mechanical shake cleaning. During the nacholite testing and in subsequent testing of the spray dryer dry scrubbing process, fabric filter data was gathered on various fiberglass, acrylic, and polyester fabrics and correlated with boiler and spray dryer operating conditions.

The resulting correlations allow estimates of filter fabric pressure drop during full scale operation through a simple model.

$$\Delta P = S_E V + K L T V^2$$

ΔP = fabric pressure drop at time T, in w.g.
S_E = effective residual drag coefficient, in w.g.-min/ft
V = filter velocity, ft/min
K = dustload drag coefficient, in w.g.-ft-min/grain
L = particulate loading, grains/ft^3
T = elapsed time since cleaning, minutes

The duration of exposure to flue gas during pilot testing was limited to at most a few months for each fabric, therefore no assessment of long term performance or bag life could be made. In the course of pilot testing no bag failures occured which were caused by flue gas conditions. All of the fabric types tested were deemed acceptable for the service.

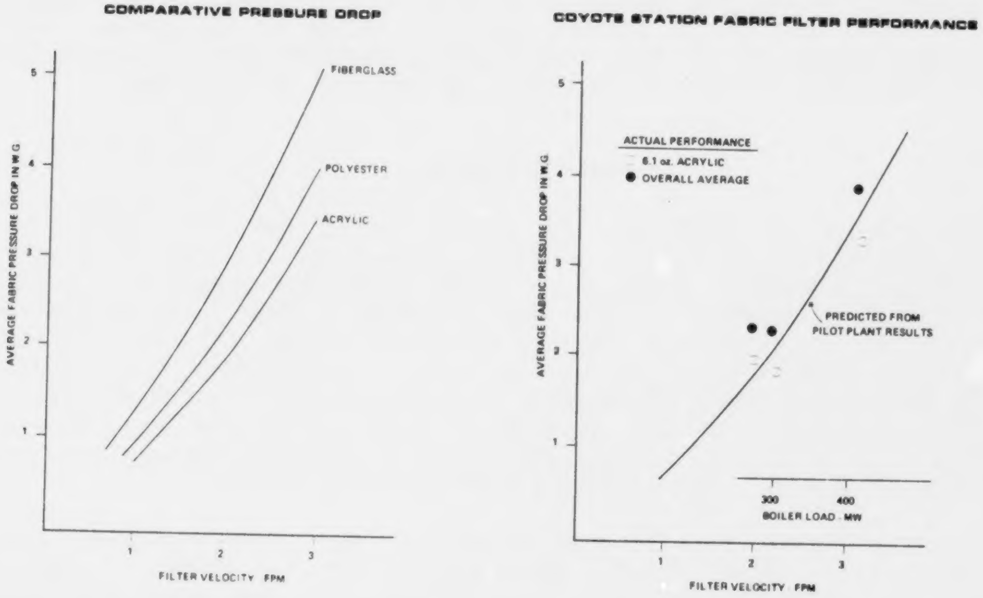

Figures 1 and 2. Pilot plant and actual operating pressure drop.

Figure 1 shows the predicted fabric pressure drop as a function of filter velocity for the lightweight acrylic, polyester, and fiberglass fabrics based on continuous cleaning cycles for the fabric and expected grain loading.

Figure 2 shows the predicted fabric pressure drop for the lightweight acrylic only with representative actual operating points from full scale operation. The approximate relationship between boiler load and filter velocity is also indicated. A comparison of the pressure drop versus the filter velocity from pilot unit correlations and full-scale operation shows the effectiveness of scale-up from pilot plants.

PROGRAM OBJECTIVES

Although the pilot work with various fabrics had been successful, due consideration was given to the process as a new application, and a long-term program to determine the best fabric for this system in terms of operating and replacement costs was initiated. A recommendation was made to the prime contractor and the Coyote partners to allow installation of several full-compartment trials of various candidate fabrics. This program would allow evalution of the fabrics in this new application and would enhance the selection of future replacement bags. The program began with the selection of fabric types and the number of full compartments of each which were to be installed.

In conjunction with the fabric selection, a monitoring program was established to review the operation of the entire collector for comparison with the pilot unit and to perform specific testing of the various fabrics. The primary objectives of this comprehensive program were to determine the fabric dimensional stability, filtration performance, and baglife.

FABRIC ALTERNATIVES

The process of selecting the proper fabric for the Coyote Station baghouse involved considerations of fabric durability, filtration performance (efficiency, throughput, drag, and cleanability), and economics. Since the design operating temperature was 180°F, synthetic fabrics were considered as alternatives to fiberglass fabrics, which were being utilized in all coal-fired boiler baghouses in the United States at that time. The synthetic fabrics had a lower cost, potentially better durability in the deflate/shake cleaning system, and lower operating pressure drop than fiberglass fabrics as indicated in pilot tests. Fabrics considered as alternatives were those made of acrylic (Dralon T), aramid (Nomex), and polyester fibers.

Polyester fabric was the most economical choice and performed well in the short pilot plant tests durations at up to 200°F. Laboratory exposure to 180°F/40% RH with and without SO_2 and with and without alkaline dust exposure resulted in no appreciable strength loss of the polyester fabrics. However, there was still a concern that with the high moisture content of the flue gas and the high alkalinity of the particulate, if the baghouse were to operate for extended periods of time in the 220-250°F range, the polyester fiber might be subject to hydrolysis resulting in severe strength loss and premature bag failure.

Dralon T homopolymer acrylic fabric had been successfully used on coal-fired boiler baghouses in Australia. Acrylic fiber is formed by addition polymerization and thus is not susceptible to hydrolysis as are polyester and Nomex, which are formed by condensation polymerization. The design operating temperature was safely below the maximum temperature rating of 284°F for Dralon T acrylic. The only concern regarding the use of acrylic fabric was dimensional stability. Extensibility problems had been previously encountered with acrylic fabrics in other filtration applications. These stability problems were discussed with fabric and bag suppliers who generally agreed that a stable acrylic fabric could be produced by proper heat-setting and finishing techniques.

Nomex fabric was considered, in spite of its high relative cost, because of its potential for increased cleanability and lower pressure drop compared to fiberglass, based on experience in the Southwestern Public Service Co. Harrington Station Unit #2 baghouse. In addition, Nomex fabric would be able to withstand the normal flue gas temperatures at the spray dryer inlet. Because of the alkalinity of the excess soda ash reagent, there was little concern about acid degradation of the Nomex fabric.

Fiberglass fabric was included based on successful operation in other coal-fired boiler baghouses and for full evaluation as a replacement fabric in the unlikely event that spray dryer operation could not provide the necessary flue gas cooling for the synthetic fabrics. Since deflate/shake cleaning was to be used, synthetic fibers were expected to provide superior bag life to fiberglass which has inherently poor flex abrasion resistance.

TABLE 1. NOMINAL PROPERTIES OF INITIAL FABRICS INSTALLED.

Fiber Type	Yarn Type	Weight (oz/yd^2)	Finish Type	Finish Code	No. Compartments
Acrylic	Spun	6.1	H_2O Repellant	E	19
Acrylic	Spun	10.0	H_2O Repellant	E	12
Nomex	Spun	5.5	Acid Resistant	F	1
Polyester	Filament/Spun	6.1	Heat-Set	G	1
Polyester	Woolen Spun	12.0	Acid Resistant	F	1
Glass	Filament/Text.	10.0	Teflon B (10%)	A	1
Glass	Filament/Text.	13.5	Acid Resistant	B	1
Glass	Filament/Text.	13.5	Acid Resistant	C	1
Glass	Filament/Text.	13.5	Acid Resistant	D	1

Based on all of the above considerations, acrylic was chosen as the primary fabric for use at Coyote. This choice was based on the expectancy of lower fabric pressure loss, increased bag life, and reduced cost compared to fiberglass fabric, without the potential risk of hydrolysis which might be encountered with polyester fabric. Special fabric finishing and rigorous quality control testing were utilized to minimize any potential stretching of the acrylic bags. Two different acrylic fabrics were selected: the 6 oz./yd^2 fabric which had been used for all pilot plant and laboratory evaluations and a 10 oz./yd^2 fabric similar to that used successfully for boiler applications in Australia and in many industrial applications. A list of the nine initial fabrics selected and their nominal properties is given in Table 1.

FABRIC FILTER OPERATION

The Coyote fabric filter is cleaned by a combination of deflation air and mechanical shaking. During cleaning, an individual compartment is isolated from gas flow and controlled reverse flow is used to collapse the bags to a partially open configuration. The bags are then cleaned by shaking action for 10-15 seconds, time is allowed for dust to settle, bags are gently reinflated and the compartment is placed back into filtration service.

In normal operation, overall fabric pressure drop (including inlet and outlet manifold and housing losses) is maintained by pressure drop initiation of the cleaning cycle at 6" w.g. At low loads, where the 6" setpoint would not be reached within several hours, cleaning cycles are initiated on 3-6 hour intervals. This maintains an average dust loading on the fabric and allows the fabric filter to easily accommodate rapid boiler load increases. Continuous cycles (each compartment cleans after one hour filtering time) are used at full boiler load to maintain approximately 4" fabric and 6" overall pressure loss at 3 ft/min filter velocity.

The fabric filter contributes significantly to the sulfur dioxide removal as the second stage of the flue gas desulfurization process. Residual sodium carbonate leaving the spray dryer continues to react with SO_2 during filtration. The fabric filter typically accounts for as much as 20 percent of the overall SO_2 removal.

The fabric filter performance as a particulate collection device is as anticipated. Particulate emissions have been measured and are well below the required new source performance standards.

In order to properly evaluate the overall performance of the fabric filter and the relative performance of the various fabrics, data on individual compartment pressure drop and relative flow was collected at periodic intervals.

Under steady operating conditions the pressure loss across the fabric was measured for each of the compartments immediately before and after the compartment was isolated for cleaning. Together with the individual compartment ΔP data, sufficient information on boiler and spray dryer operation was taken to estimate the total gas flow and particulate loading to the fabric filter.

Twelve compartments, including the nine alternative fabrics plus three additional acrylic compartments were outfitted with pressure taps to measure the pressure loss across the outlet valve opening. This measurement allows the flow rate through the compartment to be determined. To ensure meaningful comparisons the data was coordinated with the fabric filter cleaning cycle and taken both immediately before and after cleaning. The outlet valve ΔP data enables relative flow comparisons between any of the test fabrics. In combination with total gas flow data, a weighted average of the data allows the filter velocity for each of the fabrics to be established.

This individual compartment flow can also be compared with flow rates calculated directly from the outlet valve ΔP value based on generalized flow correlations developed during scale model flow studies of the outlet duct and valve air flow configuration. Good agreement was found between the model study correlation and flow rates derived from system operation and weighted average data.

With individual compartment ΔP and filter velocity data available as well as system operating data, effective residual drag and dust load drag coefficients can be determined for each individual fabric as had been done during pilot testing.

RESULTS OF FABRIC TESTING

During scheduled boiler outages, test compartments were inspected and sample bags removed for measurement of fabric strength and other fabric properties. In addition, control bags were measured to track dimensional stability, and several bags in each test compartment were tested for filter drag (5) and residual dust weight.

The results of Mullen Burst testing are presented in Figure 3. Results from measurements of M.I.T. flex vs. length of service for the fiberglass fabrics are given in Figure 4 and for the synthetic fabrics in Figure 5. Note that except for the polyester fabrics, the strength as measured by both tests stabilized at levels indicating good potential baglife. Of particular interest is the M.I.T. flex tests performed on the synthetic fabrics. This type of testing is typical for fiberglass filtration fabrics but not usually performed on synthetic bags. The M.I.T. flex values were a clear indicator of the progressive hydrolysis of the polyester which eventually led to failure and replacement. The absolute value of the M.I.T. flex test rather than the percentage loss appears to be a better indicator of potential bag failure.

Fabric in-situ drag measurements and residual dust weights were for the most part in agreement with pressure drop and relative flow measurements taken during operation, although the state of the bags at the time actually tested (elapsed time since cleaning, length of time out of service, ambient conditions, etc.) was not necessarily the same for each fabric style.

The lightweight acrylic and Nomex fabrics consistently indicated the highest relative flow (throughput), low drag values, and low residual dust weights. The 10 oz. acrylic and all of the fiberglass fabrics operated at higher drag, residual dust, and pressure drop with lower throughput.

Of interest is the low residual dust loadings found for the fabrics. Residual dust weight for the lightweight acrylic was as low as 7 lbs. This can be contrasted with as much as 50-100 lbs. for fiberglass fabrics in reverse air collectors filtering boiler flyash. The shaking action on the lightweight fabric maintains a low residual dust, and at the same time particulate collection efficiency is maintained at a high level. Residual dust weights for the 10 oz. acrylic and fiberglass fabrics in the Coyote fabric filter were roughly 50% greater than that of the lighter acrylic.

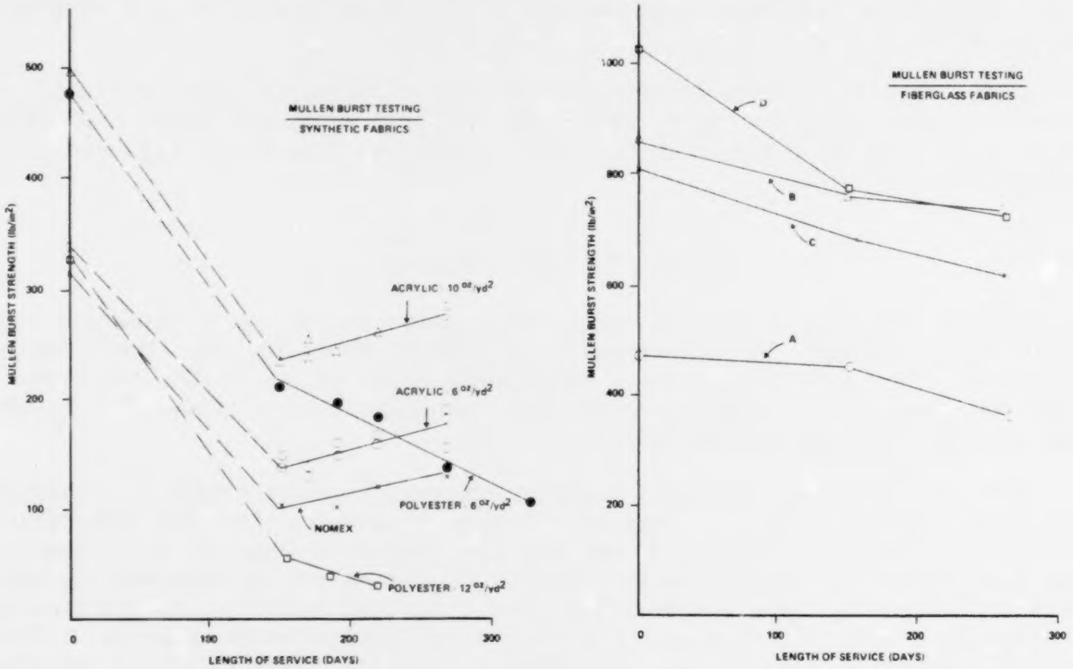

Figure 3. Results of Mullen Burst tests for synthetic and fiberglass fabric.

Overall performance of the lightweight acrylic fabric has been superior to the other test fabrics. Although a substantial decrease in Mullen burst strength of 50-60% was observed during the initial six months of operation, the fabric physical properties have stabilized at a level which should result in more than adequate bag service life. The few bag failures which did occur were due to random physical damage during installation and minor construction modifications.

The Nomex fabric has also performed very well to date. Fabric strength has stabilized at a level which indicates good potential baglife. A full compartment of Nomex has been in service for 27 months at the Southwestern Public Service Harrington #2 baghouse. The Nomex fabric has exhibited excellent cleanability, low pressure drop, and low filter drag as determined during single bag testing. The relative flow has been slightly lower than the lightweight acrylic based on compartment outlet valve ΔP measurements.

The 10 oz/yd^2 acrylic fabric has exhibited consistently higher pressure drop than the lightweight acrylic fabric. Single bag filter drag was higher than for the other fabrics and compartmental relative flow was lower than the 6 oz/yd^2 acrylic. The bulky yarn construction and resistance to shake cleaning of the heavier weight fabric apparently result in poor cleanability.

Fiberglass fabrics exhibit excellent strength retention after twelve months operation, as would be expected at the low operating temperature (relative to the 550°F capability of glass fabrics) and moderately alkaline conditions to which they have been exposed.

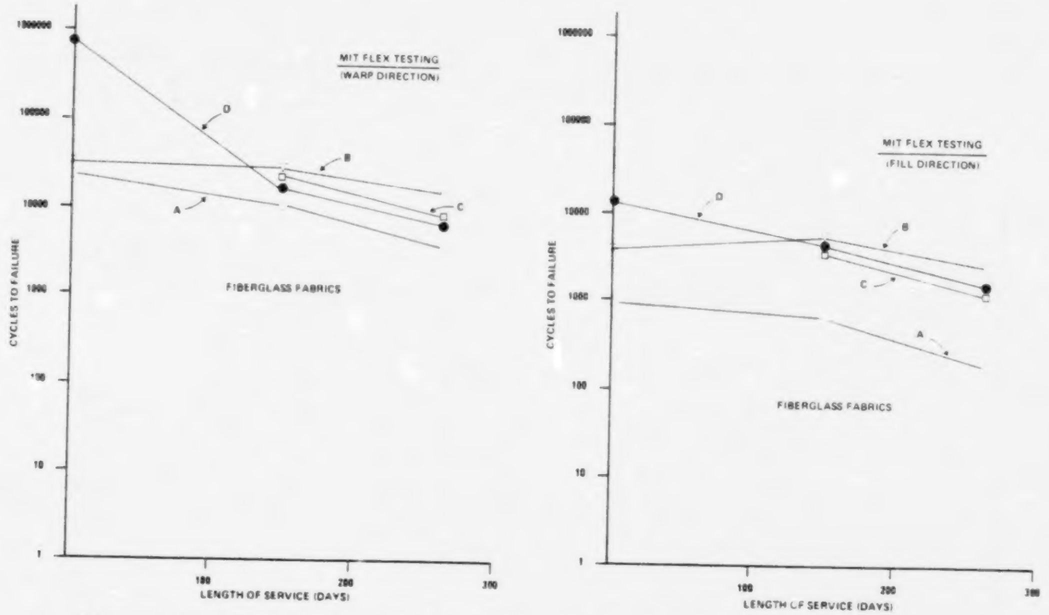

Figure 4. Results of M.I.T. flex tests for fiberglass fabrics.

Polyester fabrics experienced drastic loss of strength and high rate of failure due to chemical degradation of the polyester fiber. Exposure to 240-250°F operating temperatures in the presence of the typically high flue gas moisture content and moderate alkalinity resulted in hydrolysis of the fiber. If it had been known that actual operating temperatures would be 230-250°F rather than the 180°F design, polyester fabrics would likely have been omitted as candidates for evaluation.

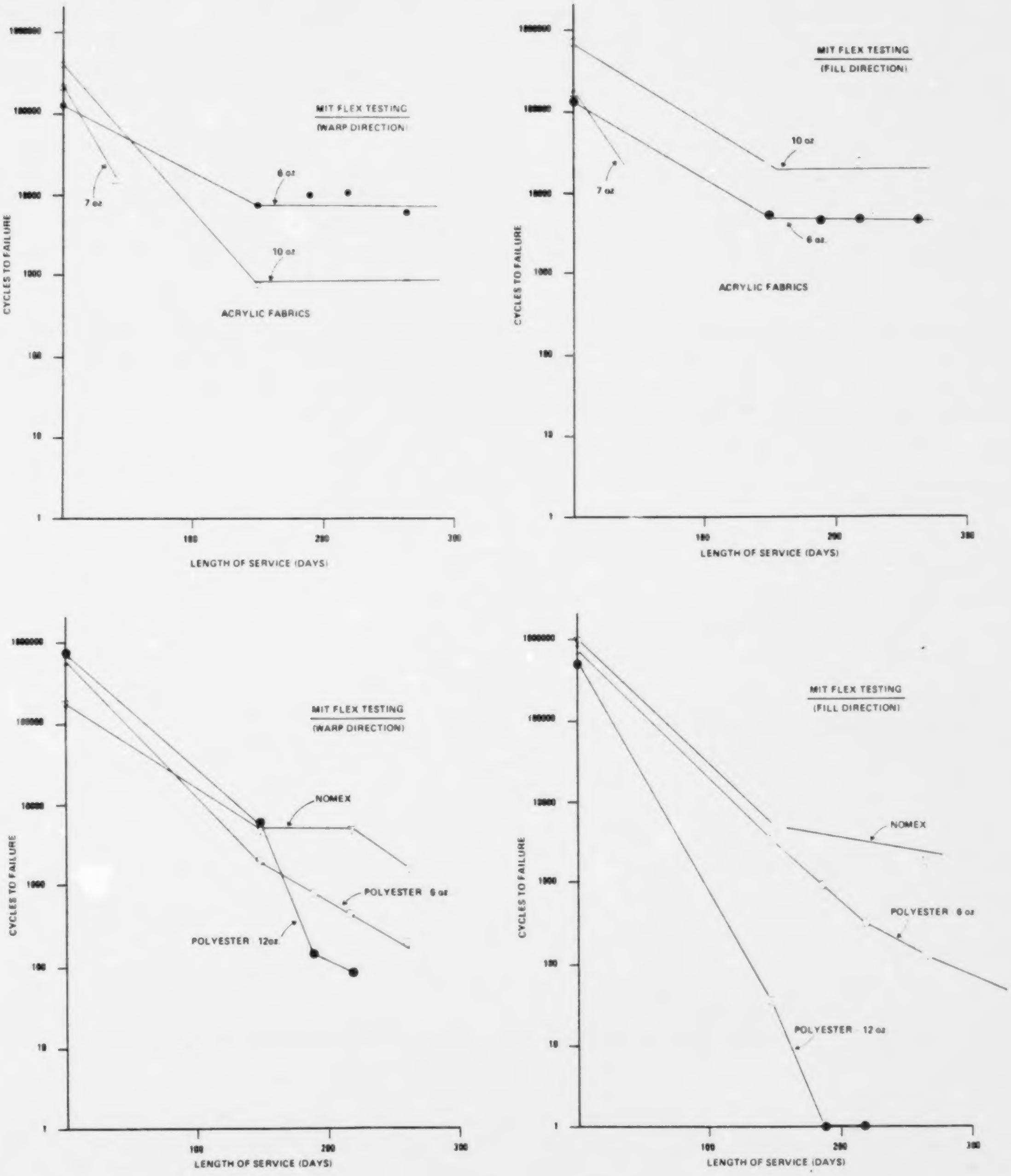

Figure 5. Results of M.I.T. flex test for synthetic fabrics.

The overall performance of the Coyote filtration fabrics has been excellent. Excluding the polyester fabrics only 35 failures have occurred in the first eighteen months for a failure rate of less than 0.5%. These failures (detailed in Table 2) are all due to miscellaneous physical damage which occurred during installation or as a result of minor construction modifications required inside the compartments after bag installation.

TABLE 2. BAG FAILURE SUMMARY.

Start-up through September 8, 1982 (excluding polyester bags*):

Primary bag failures	-	33
Secondary failures (damage by adjacent bag failure)	-	2
Total over sixteen months	-	35

Primary failures by fabric type:

	Number failed	Percent failed
Acrylic		
6 oz.	16	0.41
10 oz.	11	0.45
Fiberglass		
10 oz. - Finish A	1	0.49
13.5 oz. Finish B	0	0
13.5 oz. Finish C	0	0
13.5 oz. Finish D	4	1.96
Nomex		
5.5 oz.	1	0.49
Total	33	0.45

Causes of bag failure:

Specific physical damage:	
Abrasion against internals	18
Damage to bottom during installation	7
Top cuff damaged by bag clamp	2
Cause undetermined	6
Secondary failures:	2
Total	35

*Note: Both types of polyester bags were severely damaged due to hydrolysis of the fiber. Prior to total replacement 25 12 oz. bags and 29 6 oz. bags failed.

ACTUAL VS DESIGN

The fabric filter was designed for a nominal air-to-cloth ratio of 3-to-1 with two compartments cleaning and two compartments off-line for maintenance. Tests performed during the past eighteen months indicate that air-to-cloth ratios in a range of 2.5 to 3.8-to-1 have been achieved. During this time the fabric filter has maintained pressure losses of 4-8 inches (including manifold and housing losses) with stable pressure drop at each flow rate. During periods of reduced boiler load, the fabric filter pressure loss operates at the previous values for that specific load. Although fabric air-to-cloth ratios have been higher than anticipated the fabric filter has consistently operated without difficulty. Filtration performance (pressure drop, cleanability, and efficiency) has remained relatively stable in spite of a wide variety of boiler and FGD system operating conditions. Pressure excursions, due to boiler load swings, uneven gas distribution from spray dryers, fabric filter control or equipment malfunctions, etc., have only been temporary, and when system operation returned to normal, so did fabric pressure drop.

The higher temperature operation (230-250°F operation for much of the first twelve months compared to 180°F design) resulted in discoloration of the acrylic fabric as would be expected, but had no serious effect on fabric strength, expected service life or dimensional stability. The higher temperature did accelerate the hydrolysis failure of the polyester fabrics leading to their replacement with acrylic and at this time polyester is not considered a viable alternative for this application.

ECONOMICS

The use of acrylic fabric in lieu of fiberglass offers significant economic advantages due to:

- Lower fabric cost.
- Lower pressure drop at equivalent throughput.
- Less possibility of installation damages.
- Potentially longer bag life.

Bags fabricated of the six ounce acrylic fabric are priced 20% less than a nominal ten ounce fiberglass bag with 10% teflon finish yielding a clear economic advantage for the acrylic in capital costs. In addition, for the Coyote operation, assuming one inch of pressure loss is equivalent to $50,000 per year operating costs, lower pressure drop operation reflects significant savings. Longer fabric life may also be realized for the acrylic fabric.

Nomex can be considered a viable alternative fabric. However, the economics indicate that an additional year of baglife would be required of the Nomex assuming a three-year life for the acrylic, and also a one inch lower pressure loss. This remains to be substantiated through continued operation.

OUTLOOK

The fabric filter evaluation program at Coyote will continue through the life of the initial set of bags. Modifications to the cleaning action for the fiberglass bags are being considered in order to improve their relative performance. The basic objective of identifying an optimum fabric selection for eventual rebagging of Coyote has been satisfied by the superior performance of the lightweight acrylic.

After eighteen months of fabric filter operation at Coyote with superior performance in terms of low pressure drop at high filter velocities, fabric replacement experience and service life expectancy the combination deflation - mechanical shaker type fabric filter using synthetic bags is demonstrated to be an exceptional selection for the dry scrubbing application. In a side-by-side comparison the general serviceability of fiberglass bags with shaker cleaning is also demonstrated. Fabric filter operating temperatures can be maintained below the upper limits for the synthetic fabric even during periods of off-normal operation by the spray dryers. The ability to use acrylic instead of fiberglass offers significant economic advantages and potentially longer fabric life.

The work described in this paper was not funded by the U.S. Environmental Protection Agency and therefore the contents do not necessarily reflect the views of the Agency and no official endorsement should be inferred.

REFERENCES

1. Estcourt, V. F., Grutle, R.O.M., Gehri, D. C., and Peters, H. J., "Tests of a Two-Stage Combined Dry Scrubber/SO_2 Absorber using Sodium or Calcium", American Power Conference, Chicago, Illinois, April 1978.

2. EPRI Report FP-207, "Evaluation of Dry Alkalies for Removing Sulfur Dioxide from Boiler Flue Gases", October, 1976.

3. Muzio, L. J., Sonnichsen, T. W. et al., "Demonstration of SO_2 Removal on a Coal-Fired Boiler by Injection of Dry Sodium Compounds", EPA/EPRI Symposium on Flue Gas Desulfurization, Hollywood, Florida, May 1982.

4. U.S. Patent No. 4,197,298, "Sequential Removal of Sulfur Oxides from Hot Gases" issued to Wheelabrator-Frye Inc. and Rockwell International.

5. Grubb, W. T. and Banks, R. R., "Field Evaluation of the Drag of Individual Filter Bags", 4th Symposium on the Transfer and Utilization of Particulate Control Technology, Houston, Texas, October, 1982.

BAGHOUSE PERFORMANCE AND ASH CHARACTERIZATION AT THE ARAPAHOE POWER STATION

by: Robert S. Dahlin
Southern Research Institute
Birmingham, Alabama 35255

D. Richard Sears
U.S. Department of Energy
Grand Forks, North Dakota 58202

George P. Green
Public Service Company of Colorado
Denver, Colorado 80202

ABSTRACT

This paper presents the results of a field test conducted in March, 1981, on the Unit 3 baghouse of the Arapahoe Station of the Public Service Company of Colorado. The unit was burning a subbituminous coal from Routt County, Colorado, and was retrofitted with a baghouse in 1979. Baghouse performance was found to be excellent with an overall mass efficiency of 99.98 percent. The estimated cumulative collection efficiency of all particles smaller than two microns was 99.92 percent.

The average electrical resistivity of the fly ash was found to be 6 x 10^{11} ohm•cm at 266°F. This was consistent with the low level of SO_3 found in the flue gas ($\sim$ 0.3 ppm). The measured resistivity agreed reasonably well with that predicted by Bickelhaupt's technique using the analysis of the ash obtained by atomic absorption spectrometry. These results suggest that a high SCA and possibly flue gas conditioning would be required to obtain the same collection efficiency from an ESP.

A microanalytical characterization of ash elemental and mineral composition has been performed. Using SEM, detailed major element analyses for $\sim$ 240 individual ash particles have yielded concentration frequency distributions, composition as function of particle size, and inter-element concentration correlations. The results have been correlated with coal and ash mineralogy. Suggestions are made concerning possible application of this data to practical problems of fly ash control and disposal.

INTRODUCTION

The Grand Forks Energy Technology Center of the U.S. Department of Energy, through its contractor Southern Research Institute, is conducting a series of field tests to study the characteristics and control of fly ash from the combustion of low-rank Western coals. Emphasis is being placed on two types of coal: Western subbituminous coal and Texas lignite. The overall objective of the project is to provide data that will be useful in evaluating particulate control technologies for these coals.

To date, two field tests have been performed. The first field test, the subject of this paper, was conducted in March 1981, at Unit 3 of the Arapahoe Power Station of the Public Service Company of Colorado. The unit, retrofitted with a baghouse that was placed in service in May 1979, was burning a low-sulfur subbituminous coal from Routt County, Colorado. The second field test, which was jointly sponsored by DOE and EPRI, was completed in May 1982 at the San Miguel Station of the San Miguel Electric Cooperative located between San Antonio and Corpus Christi, Texas. Results of the San Miguel test will be reported elsewhere.

OBJECTIVES AND SCOPE

The primary objectives of the Arapahoe test were to evaluate the performance of the baghouse and characterize the fly ash. This information will be used, along with information from other power plants, in evaluating various particulate control technologies for low-rank Western fuels. In this case, the fuel is a low-sulfur Western subbituminous coal. Baghouse performance was evaluated in terms of mass efficiency, fractional efficiency, and pressure drop. The fly ash was characterized in terms of its particle size distribution, chemical composition, and electrical resistivity.

The scope of the test program encompassed the following elements:

(1) Determination of inlet and outlet mass loadings and mass efficiency by EPA Method 17,

(2) Measurement of inlet and outlet particle size distributions and fractional efficiency using calibrated cascade impactors,

(3) Documentation of boiler and baghouse operating conditions during testing,

(4) Sampling and analysis of coal by ASTM methods,

(5) Sampling and analysis of fly ash using glass fiber thimbles and a five stage cyclone assembly for sampling with analysis of major elements by Atomic Absorption Spectrometry (AA) and minor elements by Spark Source Mass Spectrometry (SSMS),

(6) Analysis of major flue gas components by Orsat apparatus with moisture determined by adsorption on Drierite dessicant,

(7) Determination of ash resistivity using an in situ point-plane probe,

(8) Analysis of particulate and gaseous organics by gas chromatography (GC) and high performance liquid chromatography (HPLC) of extracts of fly ash and XAD-2 resin exposed to flue gas in a SASS train,

(9) Measurement of SO_2 and SO_3 (H_2SO_4) levels in the flue gas by the Cheney-Homolya method,

(10) Collection of two metric tons of coal for use in the pilot-scale Particulate Test Combustor at Grand Forks,

(11) Mineral characterization of the coal by x-ray diffraction (XRD) of as-received coal and of oxygen plasma low temperature ashed (LTA) coal, as well as by chemical fractionation,

(12) Major element analysis of coal and size-fractionated ash by neutron activation analysis (NAA), and

(13) Detailed microanalytical characterization of size fractionated ash using scanning electron microscopy/electron microprobe (SEM).

Space limitations preclude detailed presentation of the entire effort here. Therefore, several phases of this study will appear elsewhere. See, for example, references 13 and 14 for a more complete exposition of the microanalytical results.

SITE DESCRIPTION

BOILER

The Unit No. 3 steam generator at Arapahoe is a vertically down-fired, dry-bottom boiler supplied by Babcock and Wilcox. The unit was placed in service in 1951, and now operates as an intermediate peaking unit and used for cycling duty. Nominal generating capacity is 46 megawatts. The design specifications and nominal operating conditions of the boiler are summarized in Table 1.

FUEL

At the time of the testing, the Unit No. 3 boiler was burning a low-sulfur subbituminous coal from Routt County, Colorado. Proximate and ultimate analyses of the coal performed after completion of the testing revealed that the coal was of somewhat higher quality than anticipated, being borderline between a subbituminous A and a high volatile C bituminous coal. Proximate and ultimate analyses of daily composite coal samples are given in Table 2.

TABLE 1. BOILER DESIGN AND NOMINAL OPERATING PARAMETERS

Manufacturer	Babcock and Wilcox
Generating Capacity	46 Megawatts
Year On-Line	1951
Duty Cycle	Cycling*
Firing Method	p-c vertical (down-fired)
Slagging Method	Dry bottom
Steam Header Temperature	900°F (482°C)
Steam Header Pressure	870 psig (6100 kPa)
Fuel	Western subbituminous coal
Heating Value	10,600 BTU/lb (5890 kcal/kg)
Moisture	8%
Ash	10%
Volatile Matter	40%
Fixed Carbon	42%
Sulfur	0.5%
Excess Combustion Air	15%
Fuel Feed Rate	46,800 lb/hr (21,200 kg/hr)
Combustion Air Flowrate	450,000 lb/hr (204,000 kg/hr)

*Generally base-loaded Monday through Friday; boiler designed for quick start-up and unit taken off line during low-load periods.

TABLE 2. PROXIMATE AND ULTIMATE COAL ANALYSES# (AS RECEIVED)

Date Sampled	3/3/81	3/4/81	3/5/81	Average
Proximate				
% Moisture	4.62	13.38	6.19	8.06
% Ash	9.31	10.46	9.94	9.90
% Volatile	43.63	34.82	41.74	40.06
% Fixed Carbon	42.44	41.33	42.13	41.97
BTU/lb	10,738	10,454	10,786	10,659
% Sulfur	0.49	0.48	0.48	0.48

TABLE 2. PROXIMATE AND ULTIMATE COAL ANALYSES[#]
(AS RECEIVED) (Cont'd)

Date Sampled	3/3/81	3/4/81	3/5/81	Average
Ultimate				
% Moisture	4.62	13.38	6.19	8.06
% Carbon	61.02	59.75	60.62	60.46
% Hydrogen	5.15	4.19	4.95	4.76
% Nitrogen	1.47	1.39	1.38	1.41
% Chlorine	0.07	0.07	0.04	0.06
% Sulfur	0.50	0.49	0.48	0.49
% Ash	9.32	10.46	9.93	9.90
% Oxygen[†]	17.85	10.27	16.41	14.84

[#] Analyses performed by Commercial Testing and Engineering, Inc. using standard ASTM methods.

[†] By difference.

Perhaps the most noteworthy feature is the low sulfur content (∿ 0.48%). The high moisture content on March 4 was believed to be due to snowfall during the preceding night. Otherwise, the composition of the coal appears to have remained fairly constant during testing.

BAGHOUSE

Unit No. 3 was retrofitted with a Joy-Western baghouse which was placed in service in May 1979. The baghouse is a reverse-air unit with Teflon-coated fiber glass bags. The design air-to-cloth ratio (A/C) was 2.0 acfm/ft^2 (0.010 m/s) with all compartments on line and 2.16 acfm/ft^2 (0.011 m/s) with one compartment out for cleaning, at a design gas flow of 315,000 acfm (149 m^3/s). Actual gas flows measured during the testing were significantly lower, with an average of 238,000 acfm (112 m^3/s), resulting in A/C values of 1.51 acfm/ft^2 (0.0077 m/s), and 1.63 acfm/ft^2 (0.0083 m/s) with all compartments on line and one compartment out, respectively. The discrepancy between the design and measured gas flows is a direct result of the conservative baghouse design.

The baghouse is divided into 14 compartments with 236 bags in each compartment. The bags are 8 in (20 cm) in diameter and 22 ft (6.7 m) in height. A schematic drawing of the baghouse is shown in Figure 1. The drawing also shows the locations of the inlet and outlet test ports. Table 3 gives a summary of the design parameters of the baghouse.

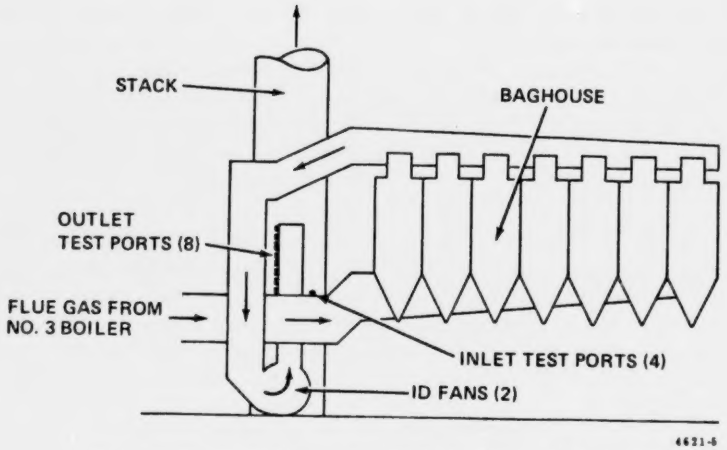
STACK
BAGHOUSE
OUTLET TEST PORTS (8)
FLUE GAS FROM NO. 3 BOILER
INLET TEST PORTS (4)
ID FANS (2)
4621-6

Figure 1. Schematic Side View of Baghouse

TABLE 3. BAGHOUSE DESIGN PARAMETERS

Supplier	Joy-Western
Year On-Line	1979
Design Gas Flowrate	315,000 acfm @ 290°F (149 m^3/s @ 143°C)
Design A/C Ratio	2.0 $acfm/ft^2$ (0.010 m/s)
(With One Compartment Off-Line)	2.16 $acfm/ft^2$ (0.011 m/s)
Cleaning Method	Reverse Air
Design Pressure Drop	6" H_2O (11.2 mm Hg)
Fabric	Teflon Coated Fiberglass
No. of Compartments	14
No. of Bags Per Compartment	236
Bag Diameter	8 in (20 cm)
Bag Length	22 ft (6.7 m)
Efficiency Guarantee	99.8 Percent

During the initial operation of the baghouse, minor discrepancies were noted such as thimble leaks and valve seatings that required adjustments. However, these repairs were expeditiously made and initial performance tests conducted.

After approximately two months of operation, the flange to flange pressure drop exceeded design to the point that reductions in unit load were required. In an effort to keep the baghouse on line, hand cleaning and beating of the bags became necessary on a regular basis to remove cake build-up on the inside of the bags. Several attempts were made by plant personnel to correct the pressure drop problem, such as replacing the original woven fiberglass teflon coated bag with a teflon B coated bag, and burning different types of coal. Attempts were also made to optimize cleaning cycles and model flow distribution patterns.

All efforts at optimizing the cleaning cycle, including adjusting reverse air periods, pressure-initiated cleaning cycles and continuous cleaning cycles, and installing the teflon B bags, did not improve the problem associated with the high flange to flange pressure drop. Ultimately, the pressure drop problems were resolved by the installation of sonic cleaning devices (1).

PROCEDURES AND RESULTS

MASS LOADING AND MASS EFFICIENCY

Inlet and outlet mass loadings were determined by isokinetically collecting suspended fly ash on in situ filters using the equipment and procedures specified in EPA Method 17 (2). Although Method 5 is usually required for compliance testing, Method 17 was deemed to be more appropriate for mass efficiency determinations. Method 17 gives a better representation of the true particulate concentration at actual flue gas conditions because it avoids the possibility of new particle formation by condensation. Each sampling run involved a traverse of the entire duct area.

The measured mass loadings and efficiencies are given in Table 4. Based on a total of six runs, the mean inlet and outlet loadings were 3.20 gr/dscf (7330 mg/m^3) and 0.00055 gr/dscf (1.26 mg/m^3). The standard deviations on the inlet and outlet loadings were 15.7% and 23.6% of the mean values, respectively. The mean mass efficiency was 99.983%, corresponding to a mean penetration of 0.017%. The standard deviation on the penetration was 19.0% of the mean value. Thus, at the 90% confidence level, the penetration is in the range of 0.012 to 0.023%, or the efficiency is in the range of 99.977 to 99.988%. This corresponds fairly well to the range of measured efficiency values.

The outlet mass loadings were comparable to those reported by Ensor et al (3) for the Kramer Station fabric filter, which was operating at an A/C value of 1.67 acfm/ft^2 (0.0085 m/s). The mass efficiencies were well above the design value, certainly due in part to the conservative design of the baghouse. The average emission rate was calculated to be approximately 0.001 lb/10^6 BTU (0.43 μg/J). The stack opacity recorded by the plant visiometer was essentially zero during all testing. Unit No. 3 was running at essentially 100% laod during all testing.

TABLE 4. MEASURED MASS LOADINGS AND EFFICIENCIES†

Run No.	Flue gas Flowrate acfm (m^3/s)	Temp. °F	Temp. (°C)	Mass Loading grains/dscf (mg/m^3) Inlet	Mass Loading grains/dscf (mg/m^3) Outlet	Baghouse Efficiency %
1	229,000 (108)	262	(128)	3.13 (7170)	0.00066 (1.5)	99.979
2	231,000 (109)	271	(133)	3.35 (7670)	0.00044 (1.0)	99.987
3	241,000 (114)	273	(134)	3.84 (8790)	0.00058 (1.3)	99.985
4	241,000 (114)	268	(131)	2.45 (5610)	0.00036 (0.82)	99.985
5	242,000 (114)	264	(129)	3.59 (8220)	0.00071 (1.6)	99.980
6	241,000 (114)	258	(126)	2.86 (6550)	0.00055 (1.3)	99.981

†Obtained by EPA Method 17.

PARTICLE SIZE DISTRIBUTION AND FRACTIONAL EFFICIENCY

Inlet and outlet particle size distributions were measured using modified Brink impactors at the inlet and University of Washington Mark III impactors at the outlet. Eight real impactor runs and two blank runs with filters ahead of the impactors were performed in separate sampling ports at the inlet. At the outlet, three complete traverses of duct area were performed, with no blank runs. The blank runs at the inlet did not indicate any appreciable substrate interference problems with the flue gas. Glass fiber substrates were used at the inlet and greased metal foils were used at the outlet.

The raw impactor data were reduced using an updated version of the Cascade Impactor Data Reduction System (CIDRS) originally described by Johnson, et al (4). The resulting inlet and outlet size distributions are given in Table 5 on the basis of cumulative percentages of particulate mass contained in particles smaller than various diameters. Based upon these results, it appears that submicron particles account for about 0.84% of the particulate mass at the inlet. At the outlet, about 7.7% of the particles by mass are smaller than 1 μm. The mass median diameter (mmd) of the inlet distribution is beyond the upper particle size limit of the modified Brink impactors. However, an extrapolation of the data using an osculating polynomial (5) suggests that the inlet mmd is about 20 μm. The mmd of the outlet distribution is about 4.5 μm.

Inlet and outlet differential mass distributions ($\Delta M/\Delta \log D$ versus D) were also computed using the same data reduction system. Fractional penetration values were computed as the ratio of outlet to inlet values of $\Delta M/\Delta \log D$ at various particle diameters. Figure 2 shows the fractional efficiency curve constructed from these calculations. The calculated fractional efficiency

TABLE 5. INLET AND OUTLET PARTICLE SIZE DISTRIBUTIONS†

Particle Diameter (μm)	Cumulative Percentage of Particulate Mass Contained in Particles Smaller Than Indicated Diameter (%)	
	Inlet	Outlet
0.4	0.36	2.1
0.6	0.48	3.8
0.8	0.64	5.7
1	0.84	7.7
2	3.0	19
4	12	43
6	18	64
8	23	79

†Average of eight inlet runs with Brink impactors and three outlet runs with University of Washington Mark III impactors.

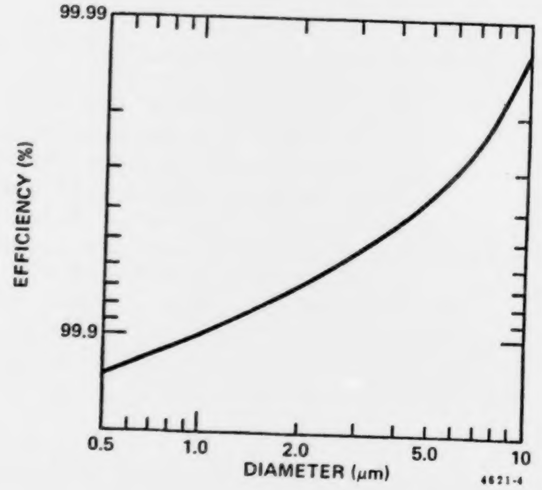

Figure 2. Fractional Efficiency Curve.

decreased steadily from 99.988% at 10 μm to 99.87% at 0.5 μm. The impactor data are not reliable below about 0.5 μm. Despite the apparent sensitivity to particle size, the baghouse still attained an estimated cumulative collection efficiency of 99.92% for all particles smaller than 2 μm. In absolute terms, this is well in excess of the fine particle collection efficiencies typically obtained with most conventional control equipment.

FLY ASH ANALYSIS

Fly ash from an inlet mass train thimble was ignited and then digested by standard acid attack for analysis by atomic absorption spectrometry. The results are given in Table 6. The results are reported as the weight percentages of the elements as their oxides, but this is not intended to imply that they actually occur in this form. Based on the relatively low alkali metal content of this fly ash, the ash would be expected to exhibit an inherently high electrical resistivity in the absence of any conditioning effects from flue gas species.

TABLE 6. CHEMICAL ANALYSIS OF FLY ASH OBTAINED BY ATOMIC ABSORPTION SPECTROMETRY ON A DIGESTED SAMPLE#

(weight percentage as oxide)

Li_2O	0.03
Na_2O	0.46
K_2O	1.3
MgO	1.4
CaO	5.1
Fe_2O_3	3.6
Al_2O_3	25.1
SiO_2	57.4
TiO_2	1.3
P_2O_5	1.0
SO_3	0.68
LOI†	1.8
Total	99.17

#The sample was taken from the thimble of a mass train which isokinetically sampled the flue gas at the inlet of the baghouse.

†Loss on ignition.

FLUE GAS COMPOSITION

The major flue gas components were determined by the standard Orsat method with water vapor determined gravimetrically by adsorption on Drierite dessicant. The average composition of the flue gas was as follows: 73% N_2, 4.8% O_2, 13.5% CO_2, and 8.7% H_2O. The oxygen level was somewhat higher than expected from the amount of excess air reportedly being used in the boiler, but this difference could be attributable to air inleakage ahead of the sampling ports.

Sulfur oxides were determined by the method of Cheney and Homolya (6). Sulfuric acid, which was originally present as either SO_3 or H_2SO_4, was collected by selective condensation in a temperature-controlled tube packed with a Pyrex glass plug. Sulfur dioxide was captured by absorption in a solution of 3% H_2O_2. The recovered condensate and the spent peroxide solution were analyzed for sulfate content by titration. Two of the eight analyses were performed by ion chromatography as a check on the titration. The two analytical techniques gave results that agreed to within an average percent difference of 15.8%.

The results of eight sampling runs yielded a mean SO_3 (H_2SO_4) concentration in the flue gas of 0.29 ppmv with a standard deviation of 0.039 ppmv. The mean SO_2 concentration was 391 ppmv with a standard deviation of 11.5 ppmv. At the concentration levels found in these analyses, the SO_3 (H_2SO_4) would be expected to have very little effect on the electrical resistivity of the ash.

ELECTRICAL RESISTIVITY OF ASH

Although the collector in this case is a baghouse, the electrical resistivity of this ash may be of interest to utilities considering various types of collectors for a new plant burning a similar coal. Electrostatic effects play an important role in current theories of filtration, so it is also reasonable to expect that the resistivity of the ash may influence its filtration characteristics. Indirect evidence of this effect has recently been obtained in an EPRI-sponsored study of fabric filtration (7).

An in situ point-plane probe was used to measure ash resistivity by the sparkover method. This procedure has been described in detail elsewhere (8). A series of nine measurements were made at the inlet sampling location. The mean value of sparkover resistivity was 6×10^{11} ohm•cm with a standard deviation of 4×10^{11} ohm•cm. The considerable scatter in the data is partly due to temporal and spatial fluctuations of flue gas temperature and SO_3 and moisture levels.

The measured resistivity was compared to that predicted by the technique of Bickelhaupt (9) using the ash composition given in Table 6 and assuming no conditioning effect of the SO_3. At the mean flue gas temperature during the in situ resistivity measurements (266°F/130°C) the predicted resistivity was 5×10^{11} ohm•cm at a flue gas moisture level of 8.7%. Thus, the predicted value of resistivity agreed with the mean in situ measurement to within 20% despite the considerable scatter in the in situ data.

PRESSURE DROP

The pressure drop across the baghouse was monitored throughout the test program. However, these pressure drop data were probably not representative of typical baghouse operating conditions at Arapahoe since the bags were cleaned during a plant outage that occurred about two weeks prior to the test program. Although the measured pressure drops were well below the design value of 6 in H_2O (11.2 mm Hg), excessive pressure drop has been a problem in the past as previously noted. During the test, the pressure drop typically varied from about 3.4 in H_2O (6.4 mm Hg) near the end of the cleaning cycle up to about 5.0 in H_2O (9.3 mm Hg) near the start of the cleaning cycle. The average pressure drop was estimated to be about 4.3 in H_2O (8.0 mm Hg).

DISCUSSION OF FIELD TEST RESULTS

The low-sulfur Routt County coal burned at Arapahoe produces a low-alkali, inherently resistive ash. In the absence of flue gas conditioning, a relatively large precipitator would be required to attain collection efficiencies comparable to those achieved by the Arapahoe baghouse. A comparable collection efficiency was reported by Lodge Cottrell (10) for the Dave Johnston Unit 1 cold-side precipitator without flue gas conditioning. The measured collection efficiency was 99.96% at a specific collection area (SCA) of 661 ft^2/1000 acfm (130 $m^2/m^3/s$). The sulfur content of the coal was in the range of 0.4 to 0.7%. With flue gas conditioning, the Pleasant Prairie Unit 1 precipitator achieved a measured efficiency of 99.96% (11). The SCA was 440 ft^2/1000 acfm (86.6 $m^2/m^3/s$) and the fuel was a low-sulfur (0.37%) Powder River Basin coal. The Pleasant Prairie precipitator was equipped with a sulfur burner that supplied roughly 5 ppmv of SO_3 to the flue gas ahead of the ESP. These results suggest that comparable efficiencies may be attainable in relatively large precipitators without conditioning and in somewhat smaller precipitators with conditioning. Efficiencies of 99.98% for the baghouse and 99.96% for the ESP correspond to penetrations varying by a factor of two. At the Arapahoe Station, however, baghouse penetrations also varied by a factor of two (0.012 - 0.023%) at the 90% confidence level. Consequently the baghouse and ESP efficiencies quoted above must be regarded as comparable within experimental uncertainty.

Excessive pressure drop, although not documented during this test, has been a problem at Arapahoe as it has at a number of other baghouse installations. The causes of this problem are generally not well understood. This is clearly an area in which additional research is required. The effects of electrostatic phenomena and the interactions of the filter cake with various flue gas species need to be investigated.

LABORATORY CHARACTERIZATION OF ARAPAHOE ASH

Baghouse inlet ash samples comprising five size-fractionated cuts were obtained using the 5-stage series multicyclone sampling/sizing system developed by SoRI (12).

Laboratory investigation of the multicyclone cuts included:

- Major element composition
- Particle size distribution within the cuts
- Scanning electron microscope investigation (including electron microprobe) study of particle size, morphology, and individual particle composition
- Statistical analysis of SEM data to develop inter-element correlations and composition-size correlations
- Auger spectrometry study of individual particles including application of secondary ion mass spectrometry (SIMS) and electron spectroscopy for chemical analysis (ESCA)

Major element analyses of the first four multicyclone stages were performed by x-ray fluorescence. No significant departures from bulk composition were observed (cf. Table 6 for the latter).

A quite different approach is provided by scanning electron microscopy/electron microprobe (SEM).* SEM analysis can be applied to individual ash particles. If sufficient particles are analyzed, the data can be subjected to on-line statistical analysis. Also, morphological information obtained by SEM may have relevance to ash collectability. E.g. Arapahoe ash in the >6.5 μm range is composed predominantly of typical spherical ash particles solidified from the molten state. Submicron Arapahoe ash, however, contains frequent hollow pleurospheres, particles with surface irregularities, and numerous non-spherical particles. The density and the surface interactions of such particles will differ from those of the larger, smooth spheres. This in turn may be important in filter cake formation and cohesion.

SEM determination of particle size and shape and SEM-electron microprobe analysis of major element composition were done on approximately 50 particles# from each of the five multicyclone stages. The data obtained from all five stages were combined to form a population of ∿ 240 particles and the data were analyzed using the SEM's on-line computational system.

Because of space limitations, we can present here only a few examples of the detailed composition information and correlation analyses. Additional information may be found in Refs 14 and 15 and in a forthcoming detailed report of the SoRI-GFETC field test results.

---

*GFETC employs a JEOL JSM 35 scanning electron microscope. X-rays are detected with a Kevex lithium-drifted silicon detector and the elemental analysis is performed by means of a Tracor Northern NS-880 x-ray analyzer. (Reference to specific brand names and models is done to facilitate understanding and neither constitutes nor implies endorsement by the Department of Energy.)

#To eliminate human bias in selection of particles to be measured and analyzed, photographs of SEM fields are overlaid with a grid. Random-number-generated grid coordinates are used to select particles for analysis.

Figure 3 displays frequency distributions for two constituents important in moderating ash resistivity: Na_2O and SO_3. Frequency distributions of this type can help one understand the range of particle resistivities presented to an ESP.

Figure 4 displays the same elemental concentrations as functions of particle size. At least in the case of SO_3, there is clearly an increased concentration in the 0-5 µm size range. Because this range includes sizes for which ESP efficiencies often are poorest, studies of this type may be useful in diagnosing successes and failures of various conditioning strategies.

An example of a well-defined inter-element correlation is that shown by Al_2O_3 versus SiO_2, Figure 5. This is the only example of a functional relationship which is preserved to a significant degree in data for each individual multicyclone stage. In this plot, as in all of the intervariable correlation plots, each datum represents a specific, individual, identifiable, serial-numbered ash particle. By tracking it back through the statistical system, each particle's concentration of other elements may be recovered. A major concentration of data in Figure 5 falls in a region bounded by 50-60 pct.SiO_2 and 25-35 pct.Al_2O_3. This lies within the range of compositions of dehydrated illite (16).

Using x-ray diffraction applied to low temperature, oxygen plasma ashed coal, species identified include α-quartz, calcite, and a clay, kaolinite. Possible minor constituents which could not be positively confirmed included dolomite and anorthite, $CaAl_2Si_2O_8$.

The thermal decomposition of kaolinite (and illite) proceeds through a sequence of stages. Above 1095°F mullite and cristobalite are formed (16, 17, 18). Clearly, mullite is found in some coal ash. Hulett and Weinberger have isolated spherical mullite skeletons in Eastern coal ash particles by removing the glass phases using a 1 pct.H_2F_2 etch (17). Stinespring and Stewart have discussed these transformations (18) and their relation to fly ash surface chemistry. X-ray diffraction of Arapahoe multicyclone ash confirms the presence of mullite and α-quartz, but not cristobalite. No other species are observed.

The SEM/microprobe analysis of individual particles does not distinguish phases--microprobe intensities contain contributions from surface atoms as well as atoms within the interior; the combined signal cannot be "unfolded" to reveal the relative contributions from several phases containing a common element. Figure 5 can best be understood as representing a population of ash particles containing dehydrated aluminosilicates (especially kaolinites or illites) which have been converted thermally at least in part to mixtures of mullite-like phases and quartz. The high SiO_2, descending leg of Figure 5, would correspond to ash particles high in SiO_2 to the exclusion of Al_2O_3-rich phases. In addition, all particles contain phases with measurable concentrations of some of the other eight "major" elements.

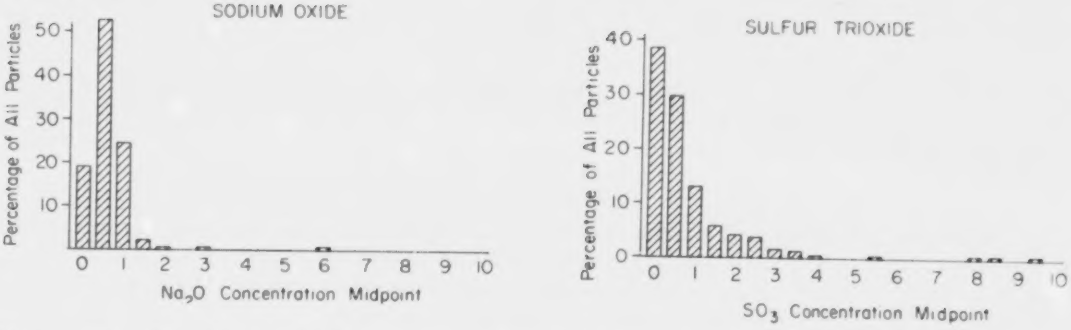

Figure 3. Examples of Frequency Distributions of Elemental Concentrations

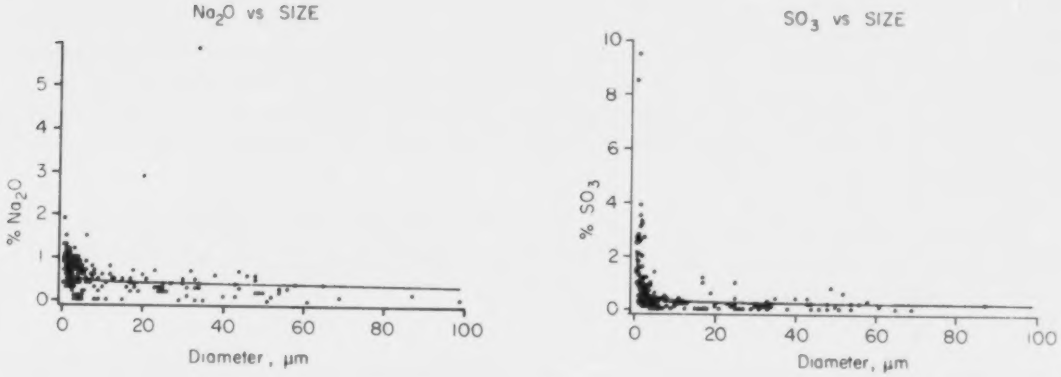

Figure 4. Examples of Concentration-Particle Size Correlations

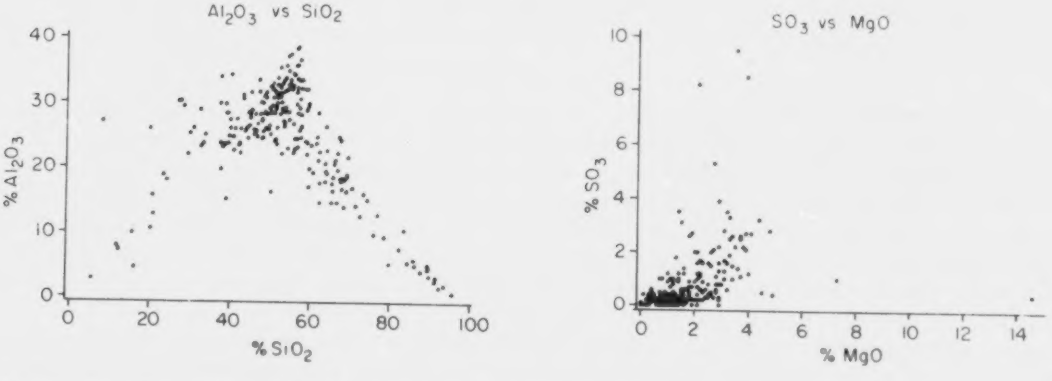

Figure 5. Examples of Inter-element Concentration Correlations

Ultimately it may be possible to employ detailed coal mineral analysis, in advance of pilot plant test burns, to predict the chemical species in the fly ash. This would be useful in planning ash disposal strategy, and possibly in predicting collector performance. Meanwhile, it is becoming possible to employ detailed ash characterization studies to predict aspects of ash properties beyond bulk resistivity.

For example: by using SEM's data it is possible to produce not only binary, but also ternary and higher order inter-element correlations and also to calculate various concentration-dependent properties of individual particles. In another paper in this symposium (19) this approach is used to calculate frequency distributions of resistivity and resistivity-particle size correlations.

In summary: Arapahoe ash characterization studies performed at GFETC have resulted in:

- Particle morphology information probably relevant to fabric filter performance.
- Detailed composition data for individual particles.
- Frequency distributions of individual elements, data maps of composition versus particle size, and inter-element concentration correlations.
- Identification of mineral species in coal and ash.
- Suggestions that these studies may be used to understand and predict ash behavior in particle collection devices such as ESPs.

ACKNOWLEDGMENTS

The authors gratefully acknowledge the contributions of the staff of Southern Research Institute who participated in the field test at Arapahoe. The field test personnel were supervised by Mr. G. H. Marchant, Jr. Mr. W. R. Dickson was responsible for the gas sampling and analysis and ash analysis. Other members of the test crew included: Messieurs W. S. Hall, T. F. Hammond, E. C. Landham, C. V. Lindsey, J. S. O'Neal, Z. A. Peich, D. Sanders, and T. A. White.

We also wish to acknowledge the contributions of GFETC staff who performed extensive microanalyses, microscopy and data analyses. Principal contributors were S. A. Benson, D. P. McColler, S. J. Miller, and D. K. Rindt.

This work was funded by the U.S. Department of Energy, Grand Forks Energy Technology Center, Grand Forks, North Dakota, under Contract No. DE-AC18-80FC10225.

DISCLOSURE

The work described in this paper was not funded by the U.S. Environmental Protection Agency and therefore the contents do not necessarily reflect the views of the Agency and no official endorsement should be inferred.

REFERENCES

1. Menard, A. R. and Richards, R. M. The Use of Sonic Horns as an Assist to Reverse Air Cleaning of a Fabric Filter Dust Collector. This Symposium, Session A-5.
2. Code of Federal Regulations. Title 40, Part 60, Appendix A. July 1, 1978. pp. 220-237.
3. Ensor, D. S., Cowen, S., Shendrikar, A., Markowski, G., Woffinden, G., Pearson, R. and Scheck, R. Kramer Station Fabric Filter Evaluation. EPRI-CS-1669. Electric Power Research Institute, Palo Alto, California, 1981.
4. Johnson, J. W., Clinard, G. I., Felix, L. G. and McCain, J. D. A Computer-Based Cascade Impactor Data Reduction System. EPA-600/7-78-042. U.S. Environmental Protection Agency, Research Triangle Park, NC, 1978. 592 pp.
5. Johnson, J. W., Pyle, B. E. and Smith, W. B. Extending Precision in a Computer-Based Cascade Impactor Data Reduction System. In: Proceedings of the Second Symposium on Advances in Particle Sampling and Measurement. EPA-600/9-80-004. U.S. Environmental Protection Agency, Research Triangle Park, NC, 1980. pp. 146-166.
6. Cheney, J. L. and Homolya, J. B. Sampling Parameters for Sulfate Measurement and Characterization. Environ. Sci. Technol. 13:584, 1979.
7. Felix, L. G., Merritt, R. L. and Smith, W. B. Particulate Emission and Operating Characterization of a Fabric Filter Pilot Plant. SoRI-EAS-82-549. Southern Research Institute, Birmingham, Alabama, 1982.
8. Nichols, G. B. Techniques for Measuring Fly Ash Resistivity. EPA-650/2-74-079. U.S. Environmental Protection Agency, Research Triangle Park, NC, 1974.
9. Bickelhaupt, R. E. A Technique for Predicting Fly Ash Resistivity. EPA-600/7-79-204. U.S. Environmental Protection Agency, Research Triangle Park, NC, 1979. 105 pp.
10. Smock, R. W. Cold-Side Precipitators Performing Well on Western Coal Power Plants. Electric Light and Power. 59(5):21, 1981.

REFERENCES (Cont'd)

11. Eskra, B. J. and McKinney, B. G. One Year's Operating Experience with SO_3 Conditioning on a Large Coal-Fired Unit's Electrostatic Precipitator. Paper presented at the 75th Annual Meeting of the Air Pollution Control Association, New Orleans, Louisiana. June 20-25, 1982.

12. Smith, W. B. and Wilson, R. R., Jr. Development and Laboratory Evaluation of a Five-Stage Cyclone System. EPA-600/7-78-008. U.S. Environmental Protection Agency, Research Triangle Park, NC, 1978.

13. Hart, F. C. and DeLaney, B. T. The Impact of RCRA (PL 94-580) on Utility Solid Wastes. FP-878. Electric Power Research Institute, Palo Alto, California, 1978.

14. Sears, D. R. Particulate Control for Low Rank Coals. In: DOE/GFETC/QTR-81/3-4. U.S. Department of Energy, Grand Forks, North Dakota, 1982.

15. Sears, D. R. Hydrocarbon and Trace Element Emissions from Combustion. In: DOE/GFETC/QTR-81/3-4. U.S. Department of Energy, Grand Forks, North Dakota, 1982.

16. Deer, W. A., Howie, R. A. and Zussman, J. Rock Forming Minerals. Vol. 3 Sheet Silicates. Longman, London, 1976.

17. Hulett, L. D. and Weinberger, A. J. Some Etching Studies of the Microstructure and Composition of Large Aluminosilicate Particles in Fly Ash from Coal Burning Power Plants. Environ. Sci. Technol. 14:965, 1980.

18. Stinespring, C. D. and Stewart, G. W. The Surface Chemistry of Aluminosilicate Particles--Application to Combustion Stream Chemistry. METC/RI-79/7. Morgantown Energy Technology Center Report. Morgantown, WV, 1979.

19. Sears, D. R., Benson, S. A., McCollor, D. P. and Miller, S. J. Fly Ash from Texas Lignite and Western Subbituminous Coal: A Comparative Characterization. This Symposium, Session C-4.

AN EVALUATION OF FULL-SCALE FABRIC FILTERS ON UTILITY BOILERS

by: John W. Richardson, John D. McKenna, John C. Mycock
ETS, Inc.
Roanoke, Virginia 24018

ABSTRACT

The objective of this EPA sponsored program was to determine the particulate emission concentrations of a coal-fired electric utility of greater than 100 MW output. Tests were also conducted to determine gaseous constituent concentrations of the flue gas and particle size via a cascade impactor.

Testing was conducted at Southwestern Public Service's Harrington Station, Unit 3, between July 6, 1981, and July 11, 1981. A total of three (3) outlet tests and one (1) inlet test were performed. Due to the absence of inlet test ports, inlet testing was done by bypassing the baghouse and testing at the outlet ports of the stack.

Emissions for Unit 3 are controlled by two (2) baghouse systems, an east and a west, each with its own operating control system and bypass dampers for start-ups, emergency operation and shutdown. Each system incorporates shake/deflate cleaning, and consists of 32 compartments with 204 bags per compartment for a total of 6,528 bags.

Average outlet concentration resulted in a lower than expected value of 0.007 lbs./10^6 Btu.* The loading of the inlet testing was 2.0 lbs./10^6 Btu giving a 99.65% collection efficiency for the baghouse. This emission rate is significantly lower than the existing Federal standard of 0.03 lbs./10^6 Btu. Particle sizing tests indicated that the mass geometric mean diameter for outlet tests 1 through 3 ranged from 7.5 to 13 μm with an extrapolated inlet mass diameter of 60 μm, and a baghouse collection efficiency of 99.86%.

This paper has been reviewed in accordance with the U. S. Environmental Protection Agency's peer and administrative review policies and approved for presentation and publication.

(*) Readers more familiar with the metric system may use the conversion factors at the end of this paper.

I. INTRODUCTION

This test series of Southwestern Public Service, Harrington Station Unit 3, was carried out as part of EPA Contract Number 68-02-3649, titled: An Evaluation Of Full-Scale Fabric Filters On Utility Boilers.

The purpose of this project is to evaluate and characterize the performance of three (3) full-scale fabric filter units controlling 100 MW or larger coal-fired power plants. Efforts are being made to select sites that are representative of different boiler and coal types, with control systems characteristic of modern fabric filters.

Three outlet particulate emission tests were conducted at SPS's Harrington Unit 3 during the week of July 6-11, 1981,to determine particulate emissions in lbs./10^6 BTU.

Baghouse and control room data, along with basic baghouse maintenance and operational data, were also obtained.

Test protocol followed that specified in the Federal Register. Diagrams of the stack and sampling ports may be found in Figures 1 and 2.

A total of four (4) outlet particulate tests and one inlet particulate test were performed. Run 1 was voided because an incorrect stack moisture content was assumed which resulted in the wrong size sampling nozzle being used. Runs 2, 3, and 5 (outlet tests) are considered valid tests. Run 4 was the inlet particulate test which was conducted by bypassing the baghouse and testing at the stack outlet ports. A summary of these test data may be found in Table 1.

II. DESCRIPTION OF PROCESS AND CONTROL DEVICES

SPS's Harrington Station Unit 3 consists of a tangentially fired, Combustion Engineering steam generator, capable of producing 2,700,000 pounds of steam per hour at 2500 psig, 1005°F superheat, and 1005°F reheat.

Pulverized Western coal averaging 8,475 Btu/lb., 0.3% sulfur and 5.5% ash is burned.

Particulate emissions are controlled by Wheelabrator-Frye, Inc. baghouses designed to operate at a flue gas flow of 1,650,000 ACFM at 313°F, with a minimum design efficiency of 98.6%.

There are two (2) baghouse systems at Harrington Unit 3, an east and a west system; each with its own operating control system and bypass dampers for start-up, emergency operation and shutdown. A schematic of the boiler and baghouse configuration may be found in Figure 3.

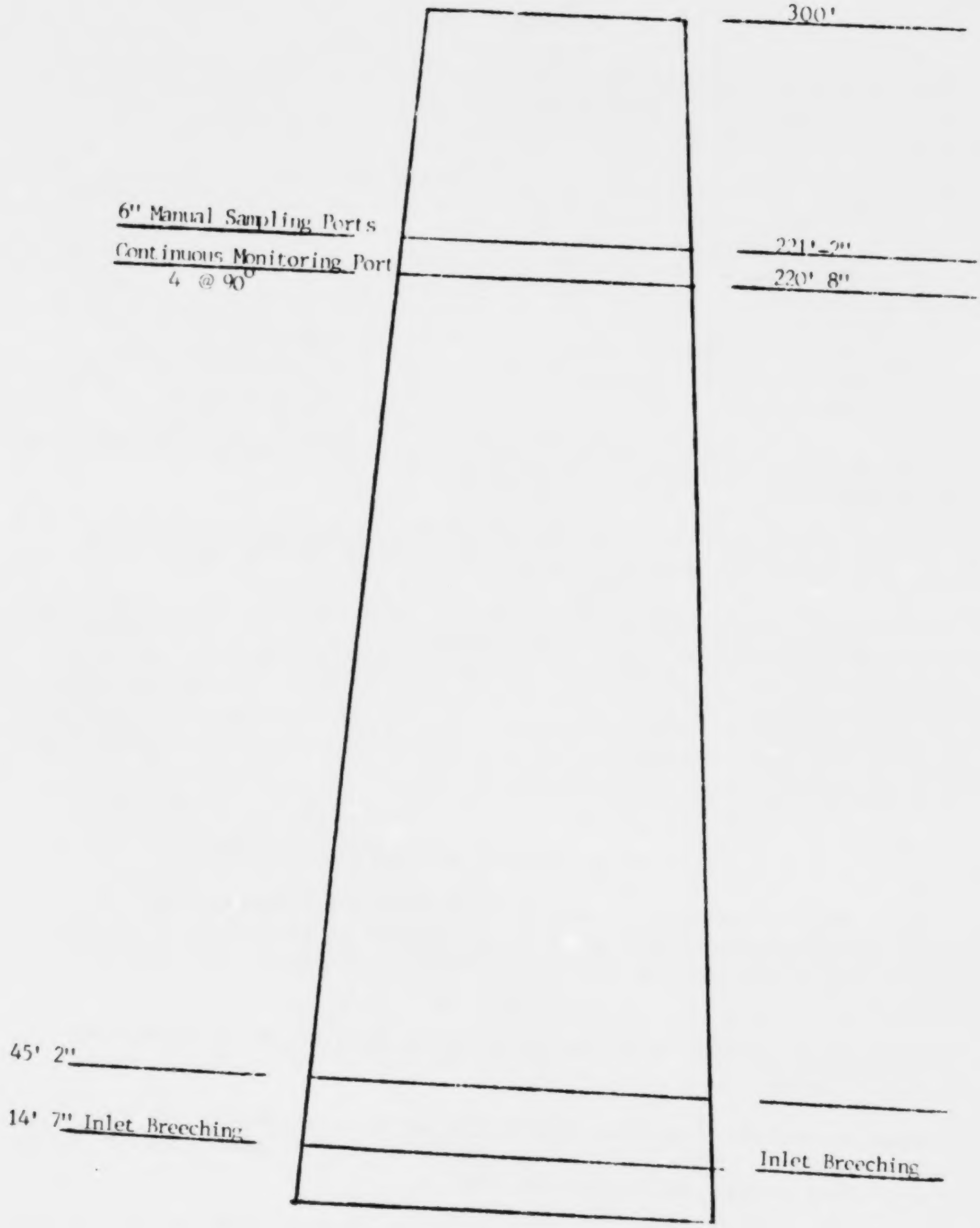
300'
6" Manual Sampling Ports
Continuous Monitoring Port
4 @ 90°
221'-2"
220' 8"
45' 2"
14' 7" Inlet Breeching
Inlet Breeching

Figure 1
Harrington Unit 3 Stack Configuration

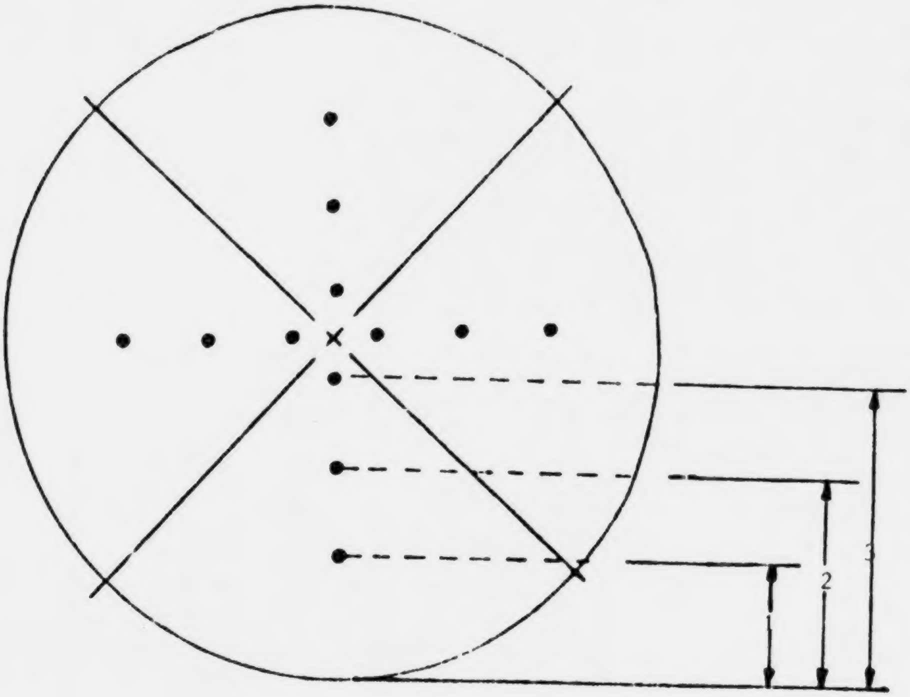

Traverse Pt.	Distance in Inches
1	56.3
2	81.8
3	119.2

Figure 2

Traverse Points Harrington Unit 3

TABLE I

DATA SUMMARY TABLE

Southwestern Public Service, Harrington, Unit 3

OUTLET EMISSION DATA

July 6 - 11, 1981

Run & Date	Particulate Emissions Outlet lbs/10^6 BTU	Particulate Emissions Outlet lbs/hr	Particulate Emissions Outlet gr/ACF	MW Production % Opacity	Flow Outlet ACFM DSCFM	Outlet Temp. ^oF	Orsat % CO_2 Inlet Outlet	Orsat % O_2 Inlet Outlet	Orsat % CO Inlet Outlet	Baghouse Differential Pressure in. H_2O	Stack Gas Moisture, % In: Out:
Run 1 7/8/81	---- VOID ----										
Run 2 7/9/81	0.009	35	0.0024	341 5.5	1,710,000 944,000	323	In:[a] — Out: 11.6	In: — Out: 6.5	In: — Out: 0.0	East BH: 6.98 West BH: 6.26	In: — Out: 10.6
Run 3 7/9/81	0.009	34.6	0.0022	350 5.5	1,740,000 912,000	323	In: — Out: 11.6	In: — Out: 6.5	In: — Out: 0.0	East BH: 8.1 West BH: 6.7	In: — Out: 14.3
Run 5 7/10/81	0.003	11.7	0.0008	349 5.6	1,710,000 938,000	323	In: — Out: 11.6	In: — Out: 6.5	In: — Out: 0.0	East BH: 7.1 West BH: 6.6	In: — Out: 10.2

INLET EMISSION DATA[b]

Run & Date	Particulate Emissions Inlet lbs/10^6 BTU	Particulate Emissions Inlet lbs/hr	Particulate Emissions Inlet gr/ACF	MW Production % Opacity	Flow Inlet ACFM DSCFM	Inlet Temp. ^oF	Orsat % CO_2 Inlet Outlet	Orsat % O_2 Inlet Outlet	Orsat % CO Inlet Outlet	Baghouse Differential Pressure in. H_2O	Stack Gas Moisture, % In: Out:
Run 4 7/9/81	2.0	7960	0.517	349 98	1,780,000 947,000	341	In: 11.6 Out: —	In: 6.5 Out: —	In: 0.0 Out: —	East BH: 5.4 West BH: 4.9	In: 10.7 Out: —

[a] Not tested

[b] Inlet test conducted by bypassing the baghouse.

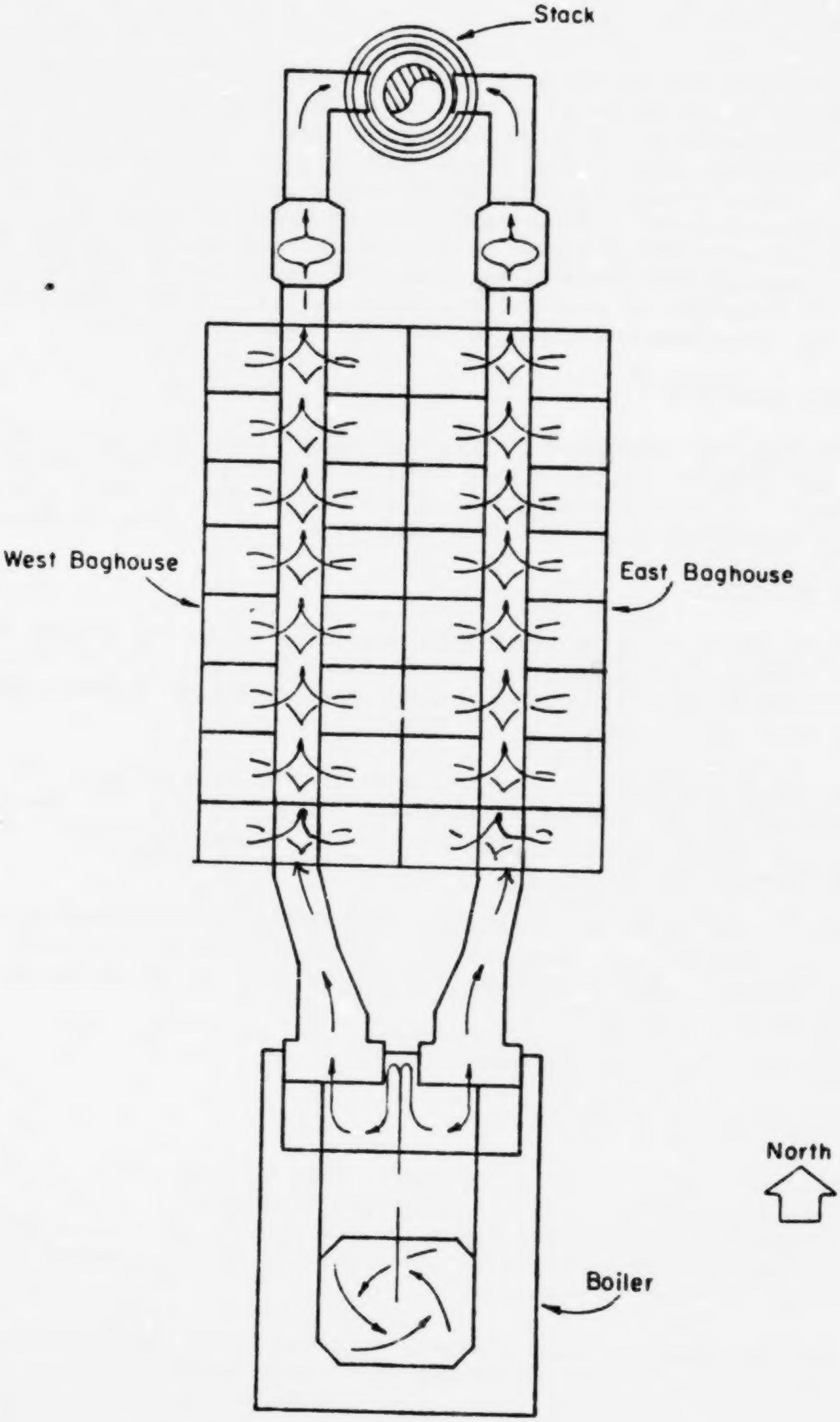
Stack
West Baghouse
East Baghouse
North
Boiler

Harrington No. 3 Flue Gas Flow
Figure 3

This shake/deflate cleaning system consists of 32 compartments with 204 bags per compartment for a total of 6,528 bags; each bag is 11.5 inches in diameter and 30 feet, six inches long. Bag spacing is 14.0 inches center-to-center, with a bag reach of two. Design air-to-cloth ratio is 2.81:1 gross, 2.90:1 with one compartment down and 3.0:1 with two compartments down. Total cloth area is 6.0 X 10^5 $ft.^2$ The baghouse is outfitted with 50% 14 ounce fiberglass acid resistant coating Criswell 449I625 bags and 50% Criswell 442 570C-2 10 ounce Teflon coated fiberglass bags. All bags are of caps and eye bolts design. Three and one-half inches of fiberglass insulation covers the baghouse exterior.

TEST PORT LOCATIONS

Sampling was conducted at four (4) ports spaced equi-distance around a 20.8 ft. diameter stack. Three traverse points were assigned to each of the four (4) ports, resulting in a twelve (12) point traverse particulate test. A diagram of the stack traverse points may be found in Figure 2.

TESTING METHODOLOGY

Particulate emission tests were conducted according to U.S. EPA Reference Method 5 procedures in conjunction with Methods 1, 2, 3 and 4. Each test included a 12-point traverse with a ten (10) minute sampling duration for each point.

Assembly and use of the impactor train followed state-of-the-art protocol and general Method 5 sampling train procedures.(1) Special precaution was taken to avoid rough handling of loaded impactors, overloading of the impactor and in the performance of hot leak tests.

Test 4 was an inlet particulate test conducted by bypassing the baghouse and directing the particulate directly to the outlet stack. Test 4 incorporated EPA Method 17 using a Norton AN-899 5.0 μm retention Alundum thimble.

SAMPLING EQUIPMENT AND PROCEDURES

Particulate

The particulate sampling equipment used is referred to as the "EPA Particulate Sampling Train", designed and developed by the EPA.(2) The "train" used in this testing was assembled by ETS, Inc. in accordance with construction details published by the EPA.(3) A schematic of the sampling train is shown in Figure 4.

The EPA sampling train consists of a stainless steel sampling nozzle, a Method 5 filter holder containing an 87 millimeter Schleicher and Scherell #1 HV High Purity Glass Filter, a series of four (4) Greenburg-Smith impingers, a check valve, a leakless vacuum pump, a dry gas meter,

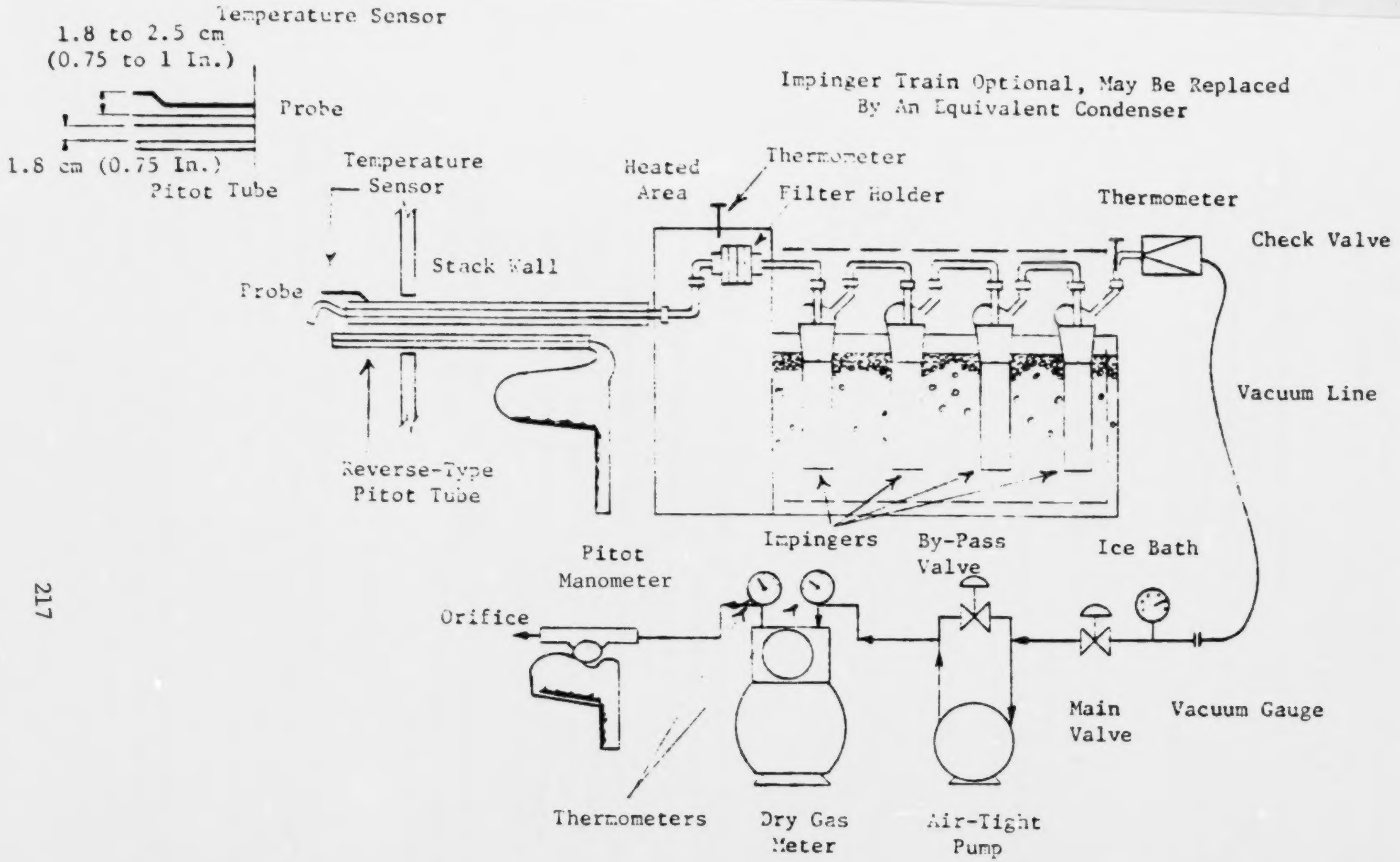
Temperature Sensor
1.8 to 2.5 cm
(0.75 to 1 In.)
Probe
1.8 cm (0.75 In.)
Pitot Tube
Impinger Train Optional, May Be Replaced
By An Equivalent Condenser
Temperature
Sensor
Heated
Area
Thermometer
Filter Holder
Thermometer
Check Valve
Stack Wall
Probe
Vacuum Line
Reverse-Type
Pitot Tube
Impingers
By-Pass
Valve
Ice Bath
Pitot
Manometer
Orifice
Main
Valve
Vacuum Gauge
Thermometers
Dry Gas
Meter
Air-Tight
Pump

Method 5 Sampling Train

Figure 4

and a calibrated orifice. The impingers and connecting tubes are made of Pyrex glass and are connected with glass ball and socket joints. The probe is made of type 316 stainless steel.

Using the Type "S" pitot tube, a velocity traverse is performed along all traverse axis during each particulate run. The velocity pressure at each sampling point is measured by means of an inclined manometer. A thermocouple is also attached to the pitot tube to measure gas stream temperature. Thermal potential is measured with an Omega portable potentiometer.

Prior to, and at the conclusion of, each run the complete sampling train including probe and nozzle is leak tested by plugging the nozzle with a rubber stopper and then applying a vacuum of 15 inches of mercury to the system. The maximum allowable leakage rate of 0.02 cfm was not exceeded in any of the leak tests.

During testing, isokinetic sampling conditions are achieved by maintaining the velocity of the stack gas entering the sampling nozzle equivalent to the stack gas velocity at each sampling point. The required velocity of the stack gas entering the sampling nozzle is obtained by adjusting the pressure drop across the calibrated orifice. The pressure differential across the calibrated orifice is measured by an inclined/vertical manometer with an inclined range of 0-1.0 inches of water and a vertical range from 1.0 to 10.0 inches of water.

At the completion of each test, the sampling nozzle,inside of the probe, inside of the thimble holder and front-half of the glass fiber filter holder were washed with acetone. The washings were collected in separate storage containers. The Alundum thimble and the glass fiber filter were removed from their respective fiber holders and stored in separate storage containers. The contents of the first three impingers were measured and discarded. The silica gel from the fourth impinger was transferred to a separate storage container. All storage containers were returned to the laboratory for analyses.

Tests to determine carbon dioxide, oxygen and carbon monoxide were conducted via an Orsat analysis according to EPA Method 3. A calibrated cylinder was run as a blank.

III. DISCUSSION OF RESULTS

During this test series, there were no deviations from normal operating conditions for Unit 3 that could be determined from the control room or baghouse control room data or conferences with the boiler operators. Control room data monitored during the test period compared closely with previous data.

Strip charts monitoring ash discharge, SO_2, O_2 and NO_x concentrations, percent opacity, baghouse outlet temperature and pressure drop were collected and the data were recorded. Flue gas volumes for the three (3) outlet and one inlet particulate tests were within an expected and consistent range.

Coal and ash samples were taken for analysis. Approximately five pound integrated coal samples were taken during each test, of which approximately one-half pound was analyzed for ash, sulfur, moisture and Btu content (proximate fuel analysis). Coal parameter concentrations remained within the expected and design range.

Outlet particulate emissions at Harrington Unit 3 averaged 0.007 lbs./10^6 Btu. Emission rates were also expressed in lbs./hr. and averaged 27.39 lbs./hr. for the three (3) outlet tests. The single inlet emission test performed by bypassing the baghouse resulted in an emission rate of 2.0 lbs/10^6 Btu or 7958.5 lbs./hr. Emission rates for outlet runs 2 and 3 were very close at 0.009 lbs./10^6 Btu (35.9 lbs./hr.), and 0.009 lbs./10^6 Btu (34.6 lbs./hr.), respectively, while outlet run 5 resulted in an unexpectedly low emission rate of 0.003 lbs./10^6 Btu or 11.7 lbs./hr. The inlet run performed at the outlet stack ports also resulted in a lower emission rate than expected when compared to previous test results conducted at SPS Harrington Unit 3.

Cascade impactor sampling was performed by Research Triangle Institute, July 8 and 9, 1981. A total of three (3) outlet and one (1) inlet impactor tests were performed. Figure 5 summarizes the cumulative mass size distribution results for the three (3) outlet impactor tests.

All outlet impactor tests including a blank had some stages with weight losses in spite of extended sampling times. The weight losses on the substrates were believed to be due to chemical reactions of the flue gas with the grease to form volatile materials, although the Apiezon-H grease has performed satisfactorily at other test sites. All of the outlet size distribution data were adjusted using the blank test substrate weights. The mass geometric mean diameter for outlet tests 1 through 3 ranged from 7.5 to 13 μm with an extrapolated inlet mass diameter of 60 μm, and a baghouse collection efficiency of 99.86%.

Southwestern Public Service has expressed concern that the results obtained during this series of tests do not represent typical operation of the Harrington Unit 3. The following paragraph is taken from a letter sent to EPA.

"SPS questions the validity of the data because there is substantial disagreement with previous testing by SPS and GCA on Harrington Unit 2 and by SPS on Unit 3. Additionally, results of the inlet grain loading test (Run 4) by ETS are lower than the theoretical values by 50%. Finally, it seems unreasonable that the lowest particulate loadings measured came the day after the bypasses had been opened the night before."

ETS agreed to include this paragraph in the paper to make the SPS reservations known, however, we feel that the emission levels measured are representative of the baghouse performance at the time of the test. Inlet

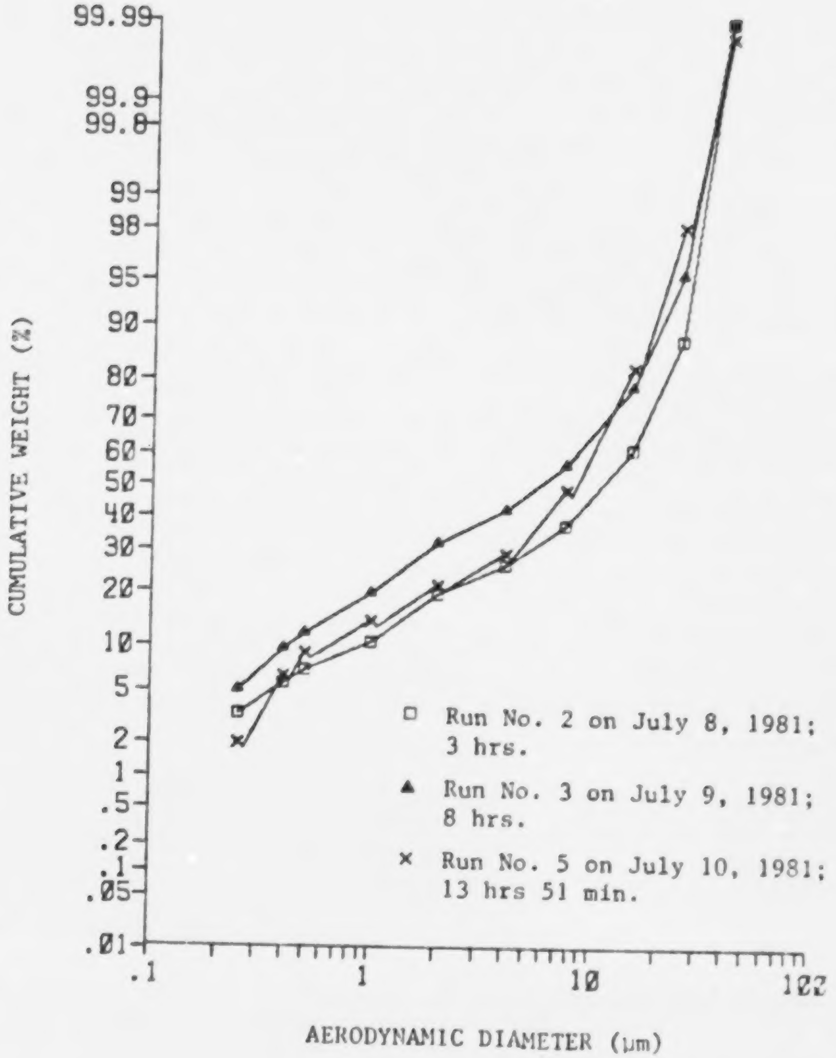

Figure 5 Cumulative mass size distribution for three outlet impactor samples.

testing may be suspect since the inlet sample was obtained at the stack outlet sampling ports after bypassing the baghouse. However, as can be seen in Table 2, the results of the outlet tests compare with emission tests conducted at other coal-fired utilities. This conclusion is also supported by facts such as the 15 hour sampling time required to obtain a representative impactor sample, a visual opacity reading between 0 and 5 percent during all the outlet tests, and the presence of an RTI quality assurance specialist during the entire testing program.

Bag analyses were performed at ETS' laboratory in Roanoke, Virginia. A battery of tests were performed including permeability, tensile strength, MIT flex, and Mullen Burst. A total of four (4) bags (2 used and 2 new) were tested.

Overall, the bag analyses conducted by ETS, Inc. indicate a greater percentage loss of strength in terms of MIT flex, Mullen Burst and tensile strength than previous tests performed by another firm. Permeability as received is essentially the same when comparing ETS's and the other firms' results. The cleaning procedures differ between the two laboratories but, in general, indicate approximately the same permeability improvement after cleaning. A more detailed comparison of the bag analyses may be found in Table 3.

It should be noted that ETS used a .04 in. jaw and four (4) pound weight and the other firm used a .03 in. jaw and four (4) pound weight when performing the MIT flex test. Another possible contributing factor to the differences is the other firms bag testing was done in April 1981, and the ETS bag analyses were performed in September 1981; thus, the bags were on stream longer before the ETS tests were conducted.

Laboratory analytical procedures incorporated were those mandated by the Federal Register Part II, Environmental Protection Agency, Revision to Reference Methods 1-8.

Second Test Location

Particulate emission tests were also conducted at Pennsylvania Power and Light's Brunner Island Station Unit 1 August 10-14, 1981 and August 30-September 4, 1982.

Unit 1 consists of a 345 MW Westinghouse turbine generator unit supplied by a continuous operating Combustion Engineering type CL pulverized coal-fired boiler; with a maximum rating of 2,100,000 lbs. of steam/hr. at 1005°F and 2750 PSIG at the superheater outlet and reheat rating of 1,947,000 lbs. steam/hr. at 1005°F and 600 PSIG.

Particulate control is handled by a Carborundum baghouse with a designed gas flow of 1,200,000 ACFM at 330°F.

The average particulate emission rate for five (5) outlet tests

TABLE 2

MASS PARTICULATE EMISSIONS OF VARIOUS COAL-FIRED POWER PLANTS

	SITE	EMISSIONS, gr/ACF
1.	SPS - Harrington Unit 3	0.002
2.	Colorado Ute, Nucla Station	0.003
3.	Northern States Power Riverside Station	0.003 - 0.006
4.	Nebraska Public Power Kramer Station	0.02
5.	Pennsylvania Power & Light Sunbury Station	0.005 - 0.006
6.	Pennsylvania Power & Light Brunner Island	0.0085
7.	Northern States Power Elk River	0.004
8.	SPS - Harrington Unit 2	0.017
9.	Colorado Ute Bullock Station	0.012

TABLE 3 - FABRIC TESTING RESULTS COMPARISON

Bag Type	Fabric Tests				Testing Co.[b]
	Flex (Fill)[a]	Mullen Burst[a]	Tensile[a]	Permeability[a]	
Acid Resistant (625) Used	Top - 48 Middle - 55 Bottom - 68	13 - 29% loss	Fill - 0-20% Warp - 1-17%	As received - 1.48-2.75 After wash - 48	Other Lab
	Top - 58 Middle - 57 Bottom - 71	32% loss	Fill - 43% Warp - 31%	As received - 1.2-2.1 After vacuum - 60.4	ETS, Inc.
Teflon - B Used	Top - 59 Middle - 50 Bottom - 49	2 - 20% loss	Fill - 0-16% Warp - 0-7%	As received - 2.31-2.75 After wash - 55	Other Lab
	Top - 84 Middle - 88 Bottom - 89	24% loss	Fill - 18% Warp - 27%	As received - 1.8-2.0 After wash - 46.4	ETS, Inc.
Acid Resistant (625) New	Fill - 2,500 Warp - 12,500	700 PSI	Fill - 300 Warp - 600		Other Lab
	Fill - 3,013 Warp - 10,400	619 PSI	Fill - 252 Warp - 465		ETS, Inc.
Teflon - B New	Fill - 500 Warp - 15,000	525 PSI	Fill - 130 Warp - 250		Other Lab
	Fill - 629 Warp - 9,946	343 PSI	Fill - 87 Warp - 228		ETS, Inc.

[a]

Test	Measurement Parameters
MIT Flex	cycles
Mullen Burst	lbs/sq. inch
Tensile	lbs/inch
Permeability	CFM/sq. ft.

[b] Other Lab - .03 in. jaws @ 4 lbs.
ETS, Inc. - .04 in. jaws @ 4 lbs.

performed in 1981 was 0.0364 lbs./10^6 Btu. Inlet emissions averaged 13.08 lbs./10^6 Btu.

A total of six (6) cascade impactor tests were performed, two (2) inlet, two (2) outlet, and two (2) blank runs. Mean extrapolated particle size was 54.3 microns at the inlet and 8.72 microns at the outlet. These impactor tests indicated that the baghouse collected more than 99.9% of the particulate matter in the flue gas.

This fabric filter characterization program continues and efforts continue to secure a third site for testing.

METRIC EQUIVALENTS

Readers more familiar with metric units may use the following equivalents to convert to that system:

Nonmetric	Times	Yields Metric
Btu	1055	J
in.	2.54	cm
in.^{2}	6.45	cm^2
^{o}F	5/9(^{o}F-32)	^{o}C
ft	0.30	m
ft^2	0.09	m^2
ft^3	28.32	liter
gr	0.06	g
lb	0.45	kg
micron	1.00	µm
oz	28.35	g

REFERENCES

1. Harris, D. Bruce. "Procedures For Cascade Impactor Calibration and Operation in Process Streams". EPA 600/2-77-004, (NTIS PB263623), January 1977.

2. "Code of Federal Regulations". Method 17, Title 40, Part 60, Appendix A.

3. Martin, Robert M. "Construction Details of Isokinetic Source Sampling Equipment". EPA report APTD-0581 (NTIS PB203060), April 1971.

Status of SPS Investigation of Harrington Station Unit 2 Fabric Filter System

Richard Chambers
Southwestern Public Service Company
P. O. Box 1261
Amarillo, Texas 79170

Dale Harmon
Industrial Environmental Research Laboratory
Environmental Protection Agency
Research Triangle Park, North Carolina 27711

ABSTRACT

This paper describes activities during the fourth year of the SPS/EPA fabric filtration study at Harrington Station. The scope of the overall study and its purposes were outlined in earlier papers.

During the fourth year of this project, sufficient information was available to make certain comparisons between Harrington Station's high air-to-cloth ratio (3.4 ft/min) shake/deflate fabric filter system and low air-to-cloth reverse air units. Specifically, comparison of bag life economics and pressure drop performance is addressed. Sizing of reverse air and shake/deflate baghouses is discussed in light of current operating data from Harrington Station and other installations.

Operation and maintenance costs are shown for the Harrington Unit 2 fabric filter system, and suggestions for improved shaker design are given. Plans to investigate sonic augmentation of bag cleaning are described.

This paper has been reviewed in accordance with the U.S. Environmental Protection Agency's peer and administrative review policies and approved for presentation and publication.

INTRODUCTION

Electric utility experience with fabric filtration for particulate control of coal-fired boiler emissions has increased dramatically over the last 5 years. Southwestern Public Service (SPS) established itself as a pioneer in utility fabric filtration with the construction of two shake/deflate baghouses in 1978 and 1980.

Since 1977, SPS, under contract to the Environmental Protection Agency, has been collecting data at Harrington Station, Unit 2; therefore, a great deal of information is available on the Unit 2 system. Results of this study have become increasingly important as other utilities, seeking solutions to emission control problems, look for design and performance specifications based on actual operating experience.

This paper presents information SPS has accumulated that will be of value to utilities evaluating the applicability of shake/deflate cleaning for a specific installation. Comparisons are made between shake/deflate and reverse air fabric filters in the areas of pressure drop, sizing, bag life and fabric replacement economics, and operation and maintenance costs.

The EPA study at Harrington Station is now into its fifth and final year. The results of this program are providing much needed knowledge of the effectiveness of a shake/deflate fabric filter system used in association with low sulfur western coal. A final report will be published at the conclusion of the study.

BAG LIFE

There is very limited data available to the utility industry regarding the bag life of various fabrics in reverse air and shake/deflate collectors because few collectors have been on line long enough to establish fabric life, especially on large units. According to a 1981 EPRI report (1), "Preliminary results from reporting utilities indicate bag lives in excess of two years, with several units exceeding three years." As more experience is gained, many of these collectors will undoubtedly achieve bag life in the 3 to 6 year range, but as yet no reliable fabric life predictions are available for reverse air units.

Harrington Unit 2, however, has been on line since 1978 and bag life data is available from this shake/deflate unit. Full compartment tests were done on a variety of fabrics to determine both their pressure drop performance and wear characteristics (2).

Of the fabrics tested at Harrington, the plied, 10-oz/yd^2 Teflon-coated materials have shown the best bag life and performance. These tests demonstrate that bag life in the 3.0 to 3.5 year range is obtainable in a shake/deflate collector employing suitable fabrics.

Recent testing on the Unit 2 filter has shown the possibility of extending bag life beyond the 3 to 3.5 year range. Fabric wear occurs mostly during the cleaning cycle where the fabric is subject to flexing and abrasion. Therefore, reducing the shaking time and increasing the filtration time between cleaning cycles should yield gains in bag life. Preliminary testing results have shown that reducing the shake times at Harrington from 20 to 5 seconds does not adversely affect pressure drop, implying satisfactory cleaning with just a 5-second shake. In addition, preliminary results of attempts to increase filtering time before cleaning look promising. With these changes, it is anticipated that bag life on Harrington 2 can be extended to 4 to 4.5 years.

The Harrington Unit 3 fabric filter operates at a design air-to-cloth ratio of 3.0 ft/min, compared to 3.4 ft/min for Unit 2. Although it is too early to determine what bag life the unit will eventually experience, after only 2 years of operation (start-up summer 1980), the fabric appears to be in better shape than the Unit 2 fabric after 2 years service. Most likely this is because the Unit 3 filter is cleaned less frequently due to its lower pressure drop. On this basis it is expected that the lower air-to-cloth ratio fabric filter on Unit 3 will exceed 4 years bag life on its first set of bags.

FABRIC REPLACEMENT COSTS FOR R/A AND S/D FABRIC FILTERS

In comparing fabric replacement costs for reverse air (R/A) and shake/deflate (S/D) collectors the following factors must be kept in mind:

1. The rather substantial price difference between ringed R/A and unringed shaker bags.
2. The larger number of R/A bags compared to a higher air-to-cloth shaker.
3. The higher wear rate of shaker bags vs. reverse air bags due to cleaning forces.

To quantify the interrelationship between these factors the levelized fabric replacement costs vs. bag life are considered for a 1100 MW unit equipped as follows:

1. R/A baghouse, a/c = 2.0 ft/min with 2 of 32 compartments out-of-service.
2. S/D baghouse, a/c = 2.7 ft/min with 2 of 32 compartments out-of-service.
3. S/D baghouse, a/c = 3.0 ft/min with 2 of 32 compartments out-of-service.
4. S/D baghouse, a/c = 3.4 ft/min with 2 of 32 compartments out-of-service.

For this analysis:

Bag installation cost = $8.30/bag
Bag dimensions = 33.5 x 1 ft
R/A bag cost = $61.60/bag (7 rings)
S/D bag cost = $48.50/bag (no rings)
Inflation = 5%
Cost of capital = 11%

The breakdown of replacement costs is shown in Table I.

TABLE I. FABRIC REPLACEMENT COSTS *

A/C (ft/min)	Cleaning	Fabric Cost ($)	Installation Cost ($)	Total Replacement Cost ($)
2.0	R/A	1,345,000	181,300	1,526,300
2.7	S/D	784,700	134,300	919,000
3.0	S/D	706,200	120,900	827,100
3.4	S/D	623,100	106,600	729,700

* at 1100 MW

The results of this analysis are shown in Figure 1.

The most striking result is the very rapid initial decline of all the curves. In the 1 to 5 year range of bag life, dramatic changes in replacement cost occur from year to year. These curves strongly point out the magnitude of the savings to be gained by optimizing fabric life.

The highest curve in Figure 1 is that for the reverse air unit. This happens because the reverse air filter has the larger number of bags (having the lowest air-to-cloth ratio) and the highest priced fabric. Although it is difficult to compare directly, reverse air cleaning is generally expected to be less damaging to the fabric and gives better bag life. The purpose of these curves is to indicate how much longer bag life needs to be to obtain the same fabric replacement cost as the shake/deflate units. The smallest of the shake/deflate units is the one with an air-to-cloth ratio of 3.4 ft/min. The pressure drop and resulting fan cost at this air-to-cloth ratio is estimated to be equivalent to the reverse air collector at a 2.0 ft/min air-to-cloth ratio (Figures 2 and 3). Since this collector has the same air-to-cloth ratio as Harrington, it could be assumed that bag life would be at least in the 3 to 3.5 year range (comparable to Harrington). As shown in the lower portion of Figure 1, a 3.0-year bag life on this unit is roughly equivalent to 5.5 years life on the reverse air system.

Bag life should increase on the shake/deflate units as the air-to-cloth ratio decreases since less cleaning will be required to maintain a given pressure drop. Comparing a 4-year bag life on the 3.0 ft/min air-to-cloth ratio shake/deflate collector with a reverse air unit gives a 6.3-year bag life to achieve equivalent fabric replacement costs.

The analysis discussed above makes a number of assumptions that may not actually be realized in practice. The intent, however, is not a definitive analysis, but to illustrate the interplay of the factors involved for a fairly reasonable set of assumptions. The one point that can be drawn from the analysis is that the shake/deflate design can be competitive with reverse air designs in terms of fabric replacement costs under certain conditions.

PRESSURE DROP AT HARRINGTON STATION

Figure 4 shows the pressure drop history of the Harrington Unt 2 baghouse (beginning after the first rebagging of the unit.) The pressure drops shown are flange-to-flange pressure drops, calculated at full load (a/c=3.4 ft/min) from operational data taken for each month. (Note: Pressure drops in Figure 2 are lower since they are tube-sheet pressure drops.) As Figure 4 shows, much variation in pressure drop occurs over an extended period of time due to variations in operating and filtration conditions.

The full-load flange-to-flange pressure drop has averaged 7.87 in. w.g. over the past 38 months of operation. At a reduced load (318 MW) and an air-to-cloth ratio of 3.0 ft/min, the pressure drop averaged 6.85 in. w.g. for this same period.

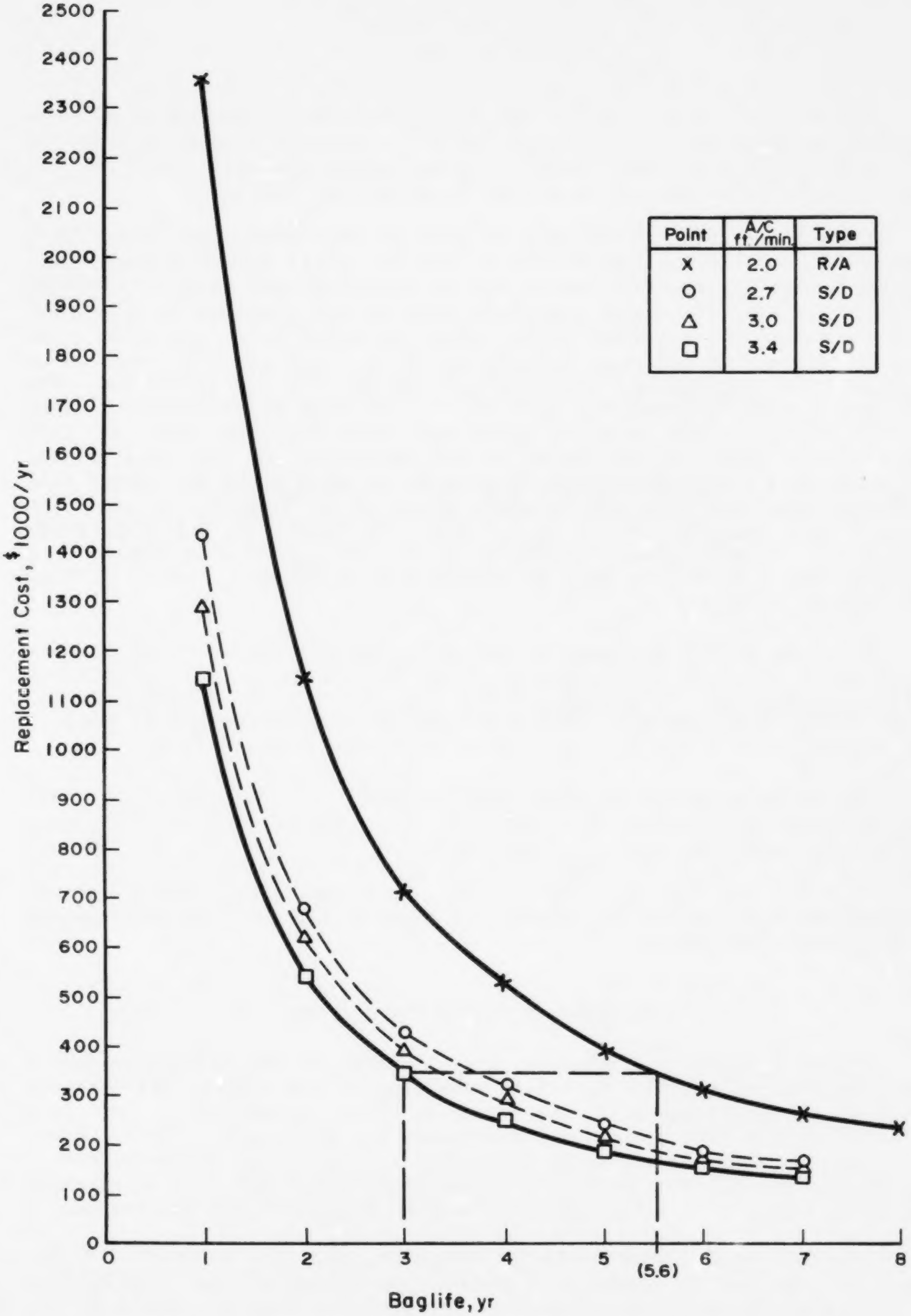

Figure 1. Levelized fabric replacement cost (1100 mw unit).

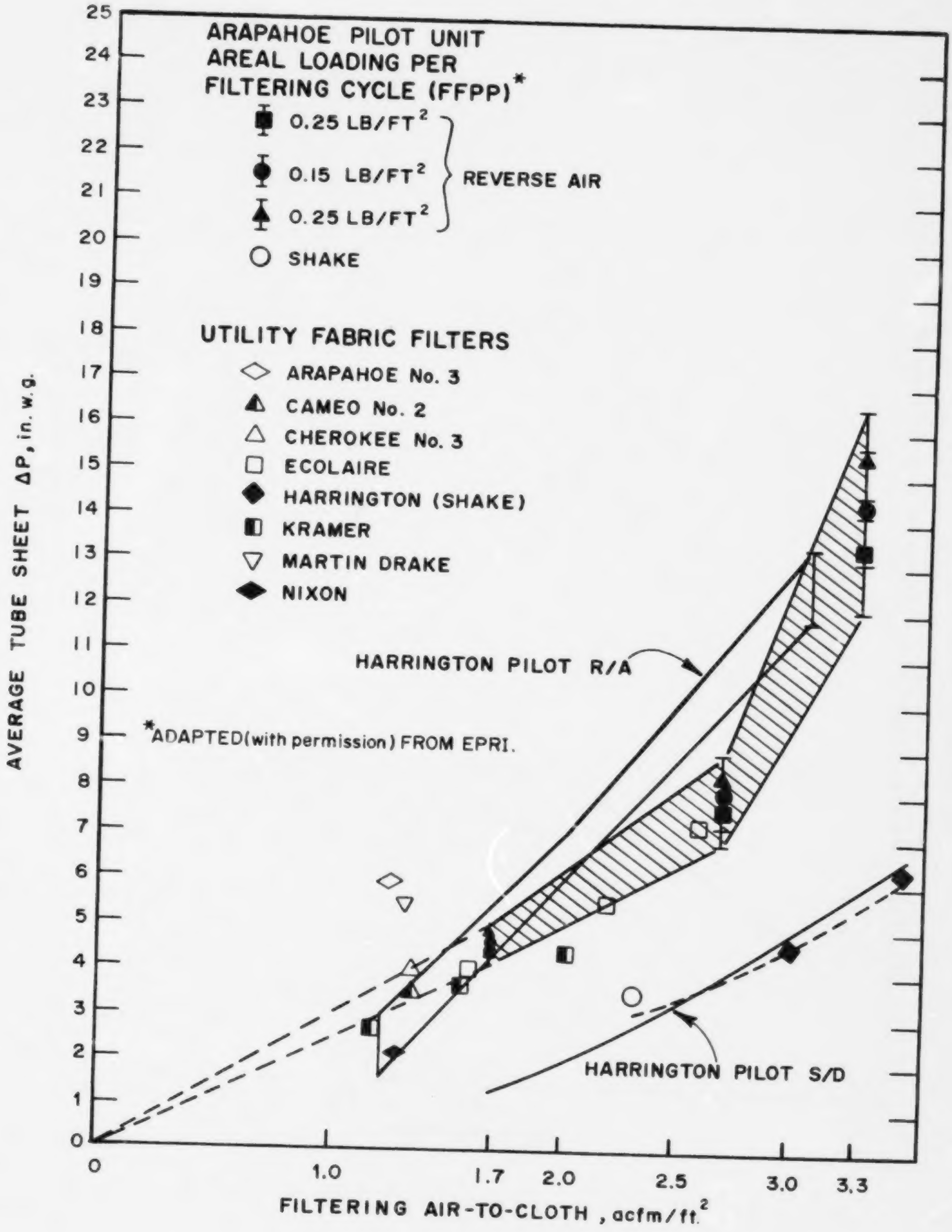

Figure 2. Comparison of EPRI/Harrington data.

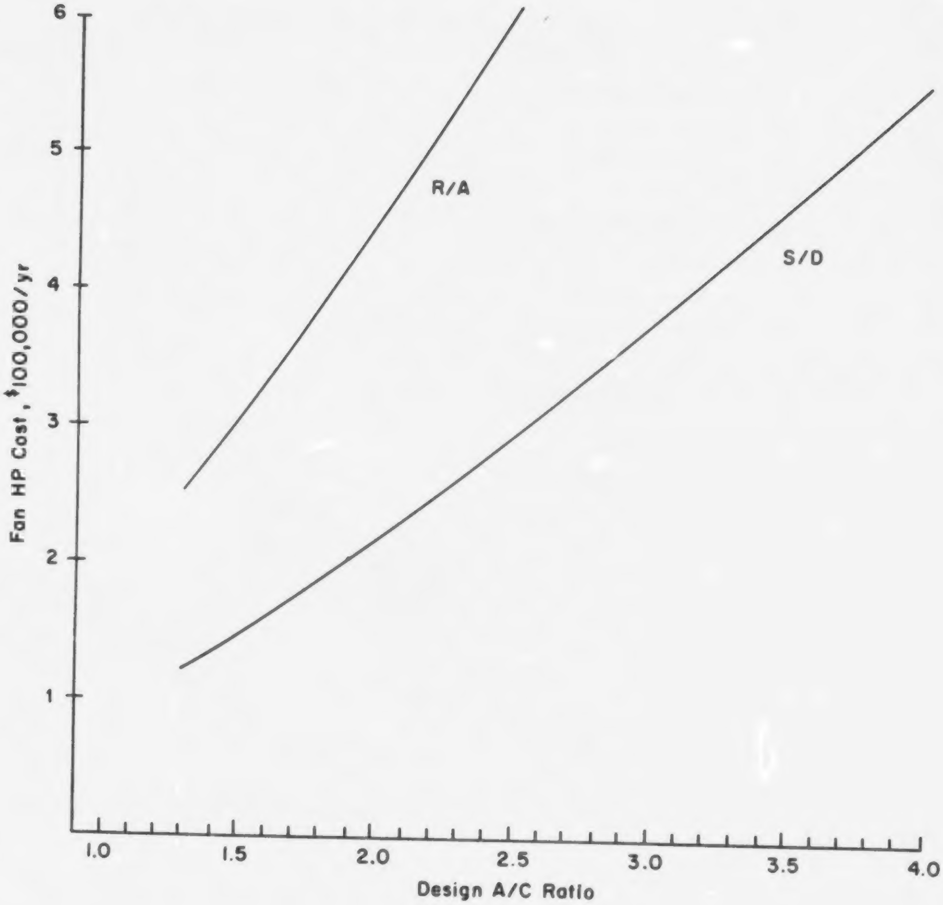

Figure 3. Fan horsepower costs for 1100 mw unit.

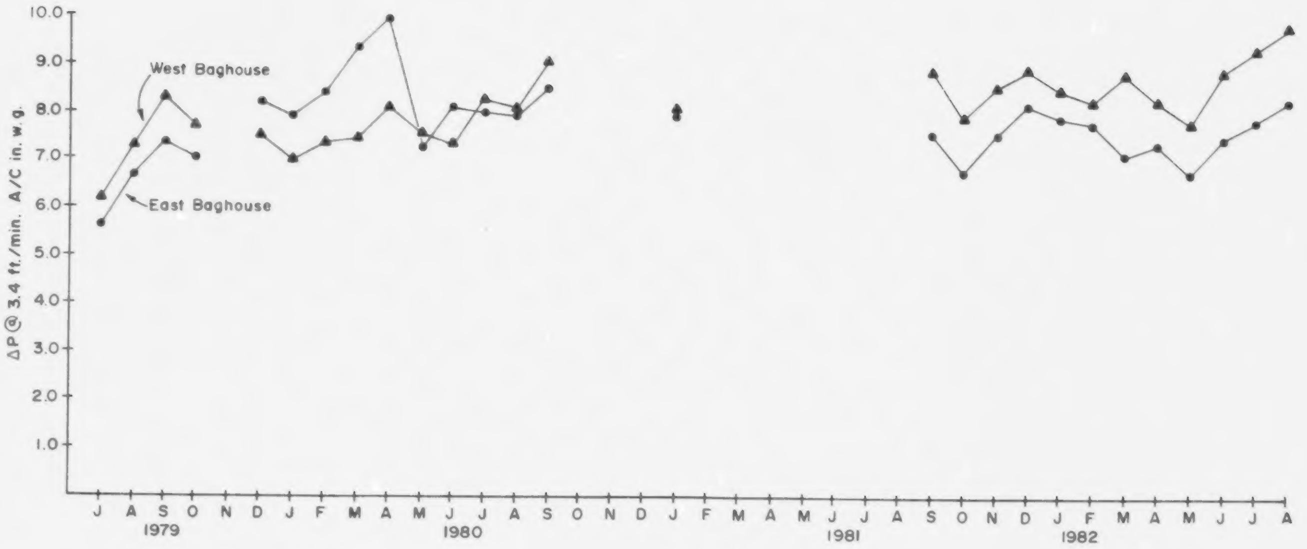

Figure 4. Monthly average full-load pressure drop.

Curve fitting the pressure drops versus air-to-cloth ratio over a long period of time has led to the following correlation for pressure drop:

$$\Delta P = 1.51V^{1.35} \tag{1}$$

where V is the air-to-cloth ratio in ft/min and ΔP is the pressure drop in in. w.g. The equation represents both of Harrington Station's fabric filters (Units 2 and 3) very well in predicting the average pressure drop at some given air-to-cloth ratio over a long period of time.

The pilot baghouse (3, 4) at Harrington Station has been able to essentially duplicate the performance of the prototype units at Harrington when operated in the shake/deflate mode. The pressure drop correlation developed for the pilot is almost identical to that for the prototype.

$$\Delta P = 1.60V^{1.35} \tag{2}$$

PRESSURE DROPS FROM OTHER UNITS

Care should be exercised when selecting collectors for comparisons of pressure drop due to the low capacity factor of some units. A baghouse on a small boiler that is used for peaking purposes only cannot be expected to give the pressure drops that a larger base loaded unit would give. Figure 5 shows the increase in pressure drop at Harrington Station at constant MW load with respect to time over a 38-hour period. This plot illustrates the effect that extended periods of high load can have on pressure drop.

Pressure drop data for the following comparison were taken from four sources:

1. Harrington Station.
2. EPRI data on utility baghouses.
3. EPRI's fabric filter pilot plant.
4. Harrington Station's pilot unit.

Figure 2 shows the tube sheet pressure drops and air-to-cloth ratios of these units. All of the shake/deflate data seem to correlate fairly well as shown in the lower right-hand corner of the graph. The pilot unit data from Harrington and EPRI agree well with each other and with operating experience from many of the reverse air prototype units below an air-to-cloth ratio of 2.0 ft/min. Above 2.0 ft/min, the Harrington pilot gives higher resulting pressure drops than the EPRI pilot, the Ecolare unit, and the Kramer.

ANNUAL I.D. FAN HORSEPOWER COSTS

To compare the I.D. fan horsepower costs associated with the pressure drops shown in Figure 2, costs for a 1100 MW unit are again considered based on the Harrington pilot work shown in Figure 2. Casing losses for

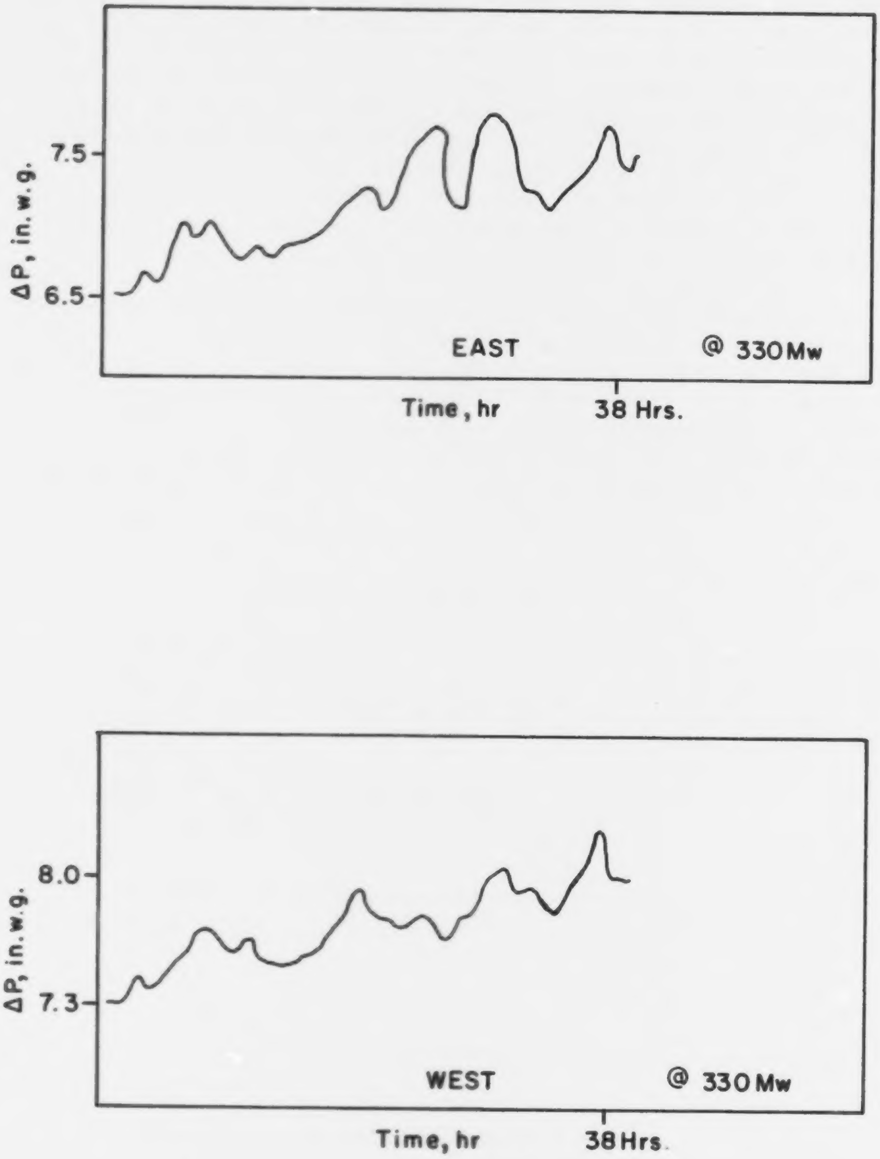

Figure 5. Pressure drop at constant load.

reverse air were approximated at 2.0 in. w.g. to obtain the total flange-to-flange pressure loss. In practice the casing losses vary between about 1.5 and 3.0 in. w.g. Since data was available for the kilowatt-hours associated with pressure drop across Harrington Unit 2, these numbers were used along with Harrington's busbar electrical cost of 19.17 mills/kWh. Strictly speaking, this means that Harrington's fan and fluid drive efficiencies are being assumed; in addition, a capacity factor of 0.70 was assumed. While these assumptions and the Harrington pilot projections are certainly only approximations of the real cases, they should serve the purpose here of a "ballpark" comparison of I.D. fan horsepower costs for shake/deflate and reverse air units at various air-to-cloth ratios. The resulting yearly costs of fan horsepower versus air-to-cloth ratio are shown in Figure 3.

The 2.7 ft/min air-to-cloth shake/deflate collector shows equivalent fan horsepower costs to reverse air at an air-to-cloth ratio of 1.6. As expected, the 3.0 ft/min air-to-cloth ratio shake/deflate unit has higher pressure drop and is equivalent to reverse air in fan costs at an air-to-cloth ratio of approximately 1.75 ft/min. The 3.4 ft/min air-to-cloth ratio shake/deflate case has even higher pressure losses and is equivalent to reverse air in fan costs at an air-to-cloth ratio of approximately 2.0 ft/min.

OPERATION AND MAINTENANCE COSTS

Operation and maintenance costs for Harrington Station's Unit 2 fabric filter system for a 3-year period are shown in Table II (in 1982 dollars) in terms of dollars per installed kilowatt per year.

TABLE II. OPERATION AND MAINTENANCE COSTS FOR HARRINGTON STATION UNIT 2

Year	Materials	Maint. Labor	Oper. Labor
81-82	0.055	0.167	0.192
80-81	0.248	0.179	0.215
79-80	0.570	0.170	—
Avg.	0.291	0.172	0.204

The material costs shown include bag purchases in 1979. The average O&M cost over this 3-year period is $0.667/kW/yr.

No data was available for R/A collectors to compare with these numbers. R/A O&M costs should vary from those of a S/D collector mainly for the following reasons:

1. Difference in bag replacement costs.
2. R/A fan horsepower pressure drop and maintenance, compared to the much smaller deflation fan on S/D collectors.
3. No shaker maintenance on R/A baghouses.

IMPROVEMENTS IN SHAKER DESIGN

Operating experience over the last 5 years at Harrington Station has pointed to several areas of improvement in shake/deflate design. These improvements, described below, are aimed at minimizing system cost and annual operation and maintenance costs.

1. Amplitude of shake: The distance the top of the bag is moved during a shaking cycle can profoundly affect bag life since the fabric may actually fold over and abrade against itself during cleaning. Maintaining shake amplitude at around 1 in. at reasonable shake frequencies could lengthen baglife considerably.

2. Deflation control should be established on flow rather than pressure drop. The deflation air-to-cloth ratio employed at Harrington is approximately 0.2 ft/min and produces a pressure drop in the 0.1-0.3 in. w.g. range. Control with this small pressure drop is difficult at best.

3. Multiple shakers should be used on larger compartments in an effort to keep the inertia of the shaking system to a minimum and reduce wear on bearings and supports.

4. Two-speed or variable-speed shaker motors might be of use in minimizing fabric wear. Under conditions where less cleaning is desirable the shaker motors could be put on low speed to lessen fabric damage.

5. Shaker tube bearings that are mounted in the compartment wall must be carefully designed for adequate wall stiffness to avoid any movement that could damage the bearings. In addition the shaker tube bearings need to be protected from overheating.

SONIC AUGMENTED CLEANING

A number of utilities are employing sonic horns to augment fabric cleaning. Therefore, EPA and SPS decided that a study of sonic augmentation was needed to determine its effectiveness compared to shaking and to look at the effects it has on fabric life. After consulting with the Fuller Co., six sonic horns were purchased and plans were made to suspend them evenly spaced beneath the two walkways in one compartment in the Unit 2 baghouse at Harrington Station.

During testing the horns will be activated during the deflation cycle for approximately 10 seconds. Both flow and pressure drop will be measured on the compartment and then compared with adjacent compartments. Testing will be done with and without shakers to determine the relative magnitude of the cleaning forces being generated by the sonic horns.

Fabric samples will be taken from the compartment at certain intervals and tested to determine if there is any difference in fabric wear between the two cleaning techniques.

CONCLUSIONS

Southwestern Public Service has gained a great deal of knowledge from the EPA/SPS fabric filter study that has been of immediate benefit in the proper operation of Southwestern's fabric filter systems. The research performed under this program has allowed SPS to identify the performance and wear characteristics of the commonly used fabrics and led to identifying a successful fabric for the unit in terms of both bag life and pressure drop. Fabric studies have revealed the mechanism of fabric wear under shake cleaning conditions that has been invaluable in understanding bag wear.

As useful as this program has been, fabric filtration in the utility industry still has a need for more fundamental research. Ash filtration properties are as yet very poorly understood and are beyond prediction, making accurate sizing of fabric filters difficult. Little research has been done in the area of designing fabrics specifically for utility filtration which would be a very fruitful area of research. Additional work is needed in the fluid mechanical design of baghouses to minimize casing losses and ensure good ash distribution.

As electric utilities convert to coal, the challenge of balancing environmental compliance with rising electric rates increases the significance of research in the field of fabric filtration. Studies such as the one conducted at Harrington Station can best yield results that reflect utility standards and regulatory interests.

REFERENCES

1. Operating History and Current Status of Fabric Filters in the Utility Industry, EPRI Report 1401. July 1981.

2. Chambers, R., Ladd, K., and Kunka, S. SPS Experience with Fabric Filtration. Paper presented at Fifth International Fabric Filter Forum, Phoenix, Arizona, January 1981.

3. Ladd, K., Hooks, W., Kunka, S.,and Harmon, D. SPS Pilot Baghouse Operation. In: Third Symposium on the Transfer and Utilization of Particulate Control Technology. Volume I. Control of Emissions from Boilers, EPA-600/9-82-005a, July 1982. (NTIS PB83-149583), pp 55-64, July 1982.

4. Chambers, R., Kunka, S., and Harmon, D. Update of SPS Pilot Baghouse Operation. Paper presented at Fourth Symposium on the Transfer and Utilization of Particulate Control Technology, Houston, Texas, October 1982.

UPDATE OF SPS PILOT BAGHOUSE OPERATION

Richard Chambers and Sherry Kunka

Southwestern Public Service Company
P. O. Box 1261
Amarillo, Texas 79170

Dale Harmon
Industrial Environmental Research Laboratory
Environmental Protection Agency
Research Triangle Park, North Carolina 27711

ABSTRACT

An option of the 1977 Environmental Protection Agency (EPA) contract with Southwestern Public Service Company (SPS) to assess the performance of a large prototype fabric filter system provided for the installation of a pilot baghouse. The pilot unit was placed in service in October 1979. This paper describes the test program being conducted in the pilot unit by SPS for the EPA. These test programs to date have primarily involved the evaluation of the filtration characteristics of a number of fabrics in both the shake/deflate and reverse air cleaning modes.

This paper has been reviewed in accordance with the U.S. Environmental Protection Agency's peer and administrative review policies and approved for presentation and publication.

INTRODUCTION AND BACKGROUND

In 1977, the Environmental Protection Agency (EPA) executed a contract with Southwestern Public Service Company (SPS) to assess the performance of a large fabric filter system used on a new utility boiler burning low sulfur Western coal. One option of this contract provided for the installation of a pilot filter system on-stream with Harrington Station Unit 2. The EPA elected to exercise this option in 1979, and SPS agreed to operate and maintain a pilot unit at Harrington Station.

The pilot unit is a Wheelabrator-Frye, Inc. Model 366, Series 11.5 RS Dustube Dust Collector. It has two six-bag compartments and initially was fitted with a Criswell Teflon-coated fabric; bags were 11.5 in. in diameter and 366 in. long. Cloth area per compartment is 549 ft^2. The unit is operated by a 480-V control panel and an instrumentation panel.

The pilot unit is installed at the southeast corner of the east baghouse on Harrington's Unit 2. Inlet flue gas to the pilot is pulled from the east inlet duct of the main baghouse and mixed with hot preheater flue gas through a mixing valve to maintain constant temperature. (See Figure 1.)

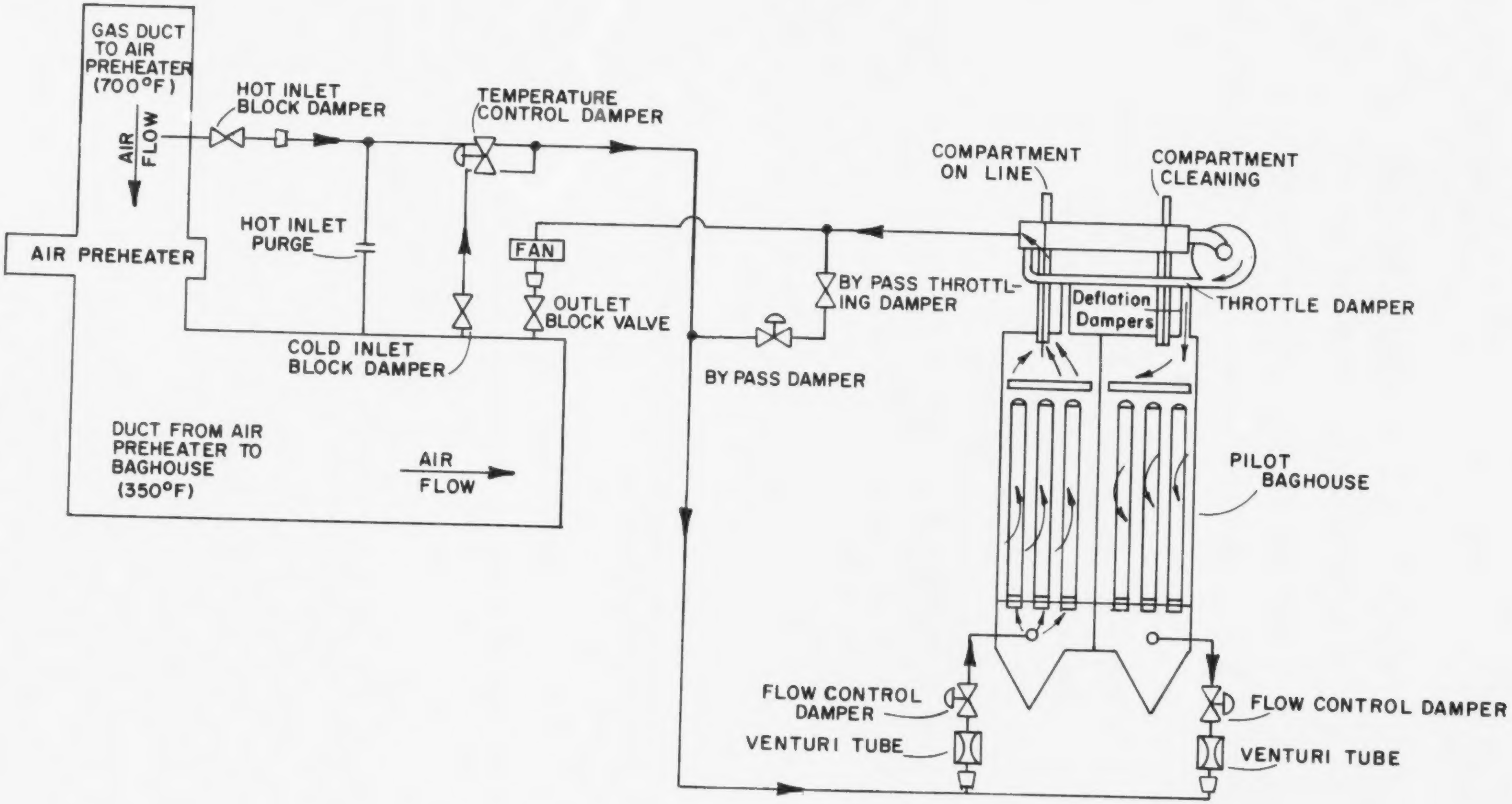
GAS DUCT TO AIR PREHEATER (700°F)
AIR FLOW
HOT INLET BLOCK DAMPER
TEMPERATURE CONTROL DAMPER
HOT INLET PURGE
AIR PREHEATER
FAN
OUTLET BLOCK VALVE
COLD INLET BLOCK DAMPER
DUCT FROM AIR PREHEATER TO BAGHOUSE (350°F)
AIR FLOW
BY PASS DAMPER
BY PASS THROTTLING DAMPER
COMPARTMENT ON LINE
COMPARTMENT CLEANING
Deflation Dampers
THROTTLE DAMPER
PILOT BAGHOUSE
FLOW CONTROL DAMPER
VENTURI TUBE
FLOW CONTROL DAMPER
VENTURI TUBE

Figure 1. Pilot baghouse schematic.

In October of 1979, the pilot baghouse was placed in service. Several initial problems had to be resolved before a satisfactory operating level could be attained (1). By July of 1980, the pilot unit was ready for testing of particulate and gaseous emissions. This first series of tests confirmed that flue gas composition and particulate loading for the pilot unit were comparable to those of the main baghouse.

The next series of tests, which are discussed in this paper, were designed to reflect the interests of both SPS and EPA. These areas of testing include scale-up studies with shake/deflate cleaning, reverse air fabric studies, and special interest studies, such as ringed bag testing and design equations. The pilot baghouse is now being prepared for an electrostatic enhancement program to be conducted at Harrington Station.

SCALE-UP WITH SHAKE/DEFLATE CLEANING

OVERVIEW

The first objective of the pilot baghouse study following start-up and check-out was to prove that suitable scale-up to the prototype unit existed. Data were collected over a 5-month period with the pilot unit operating in various modes considered to be representative of the prototype baghouse.

The fabric chosen for this initial program was W. W. Criswell's 442-57DC-2 (10-oz. Teflon-coated). Ideally, for comparison, the same fabric used in the prototype unit would be used in the pilot unit; however, this mode of operation was not possible due to the large number of fabrics being tested in the prototype (see Table I). The Criswell fabric was selected for the pilot unit because it represented the majority of fabrics in the prototype unit and had a proven performance record.

In the first phase of the pilot scale-up work, the unit was operated around the clock for 1 month at the design air-to-cloth ratio of 3.4 ft/min. Phase two called for alternating operation between high and low loads. Therefore, in June the pilot unit was run at air-to-cloth ratios of 2.8 and 3.4 ft/min, and in July at air-to-cloth ratios of 2.2 and 3.4 ft/min.

Because none of the above test methods attempted to cycle load with the boiler, an effort was made in the third phase of the scale-up study to simulate the daily load cycle. During August and September the pilot unit was run at an air-to-cloth ratio of 3.4 ft/min from 8:00 a.m. to 3:30 p.m. The air-to-cloth ratio was then reduced to 1.94 ft/min until the next morning.

OPERATING PARAMETERS

Cleaning cycle parameters and operating conditions for the scale-up study are:

TABLE I. PROTOTYPE FABRIC SUMMARY

West Baghouse

1 *	2 *
3 *	4 *
5 *	6 Menardi - Southern Teflon Test Bags
7 1 Nomex All-Spun; 2 Nomex Comb.; 5 Crisoflex 446; 4 Crisoflex 449; Bal. *	8 *
9 * (Warp-In)	10 *
11 *	12 *
13 *	14 *

East Baghouse

15 **	16 **
17 **	18 **
19 Original bags equipped with special shaker mechanism	20 Fabric Filters All-Filament Teflon
21 Criswell 442 Teflon B Test Bags	22 34 Acid Flex; 34 Tri-Treat Balance: Original Bags
23 Fabric Filters 502 Tri-Treat Test Bags	24 Globe - Albany Nomex
25 Criswell 449 Teflon B Test Bags	26 **
27 **	28 **

* Criswell 442 Teflon B; (10.5 oz.) (Rebagging complete).

** Criswell 449 Tri-Treat; (14 oz.) (Rebagging complete).

Inlet Temperature	400°F
Grain Loading	0.75-1.2 gr/acfm
Filtering Cycle	30 min.
First Null Period	20 sec.
Deflate	40 sec.
Shake	20 sec.
Settle "no-flow"	20 sec.
Cleaning Cycle	30 min.

DATA REDUCTION

Pressure drop data was collected throughout each filtration cycle by strip chart recorders. A typical filtration cycle is shown in Figure 2.

According to filtration theory the pressure drop, ΔP, across a single compartment fabric filter is given by

$$\Delta P = \Delta P_e + K_2 c V^2 t \qquad (1)$$

where

ΔP_e = effective ΔP after cleaning

K_2 = the specific resistance

c = grain loading

V = air-to-cloth ratio

t = filtration time.

The effective pressure drop after cleaning, ΔP_e, was determined by extrapolating the linear portion of the filtration curve shown in Figure 2 to zero time.

The specific resistance can be calculated by rearranging the equation above and setting ΔP equal to the terminal ΔP. Grain loading, however, was not measured on a regular basis during the testing program. Therefore only values of K_2c can be calculated from the data without some assumption about the absolute value and constancy of the grain loading. K_2c was calculated from

$$K_2 c = (\Delta Pt - \Delta P_e)/tV^2 \qquad (2)$$

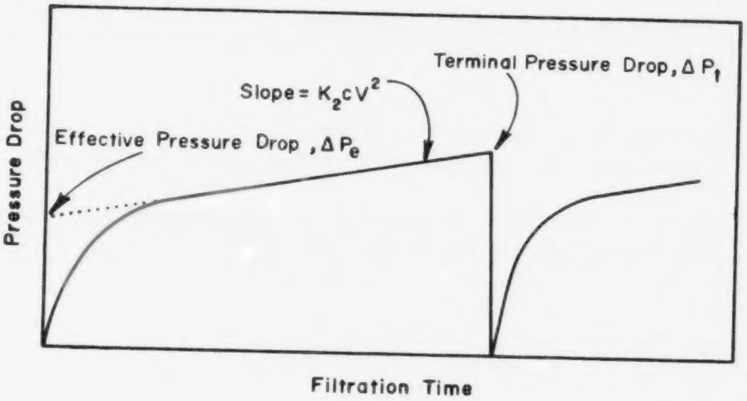

Pressure Drop
Terminal Pressure Drop, Δ P_t
Slope = K_2cV^2
Effective Pressure Drop , Δ P_e
Filtration Time

Figure 2. Typical filtration cycle.

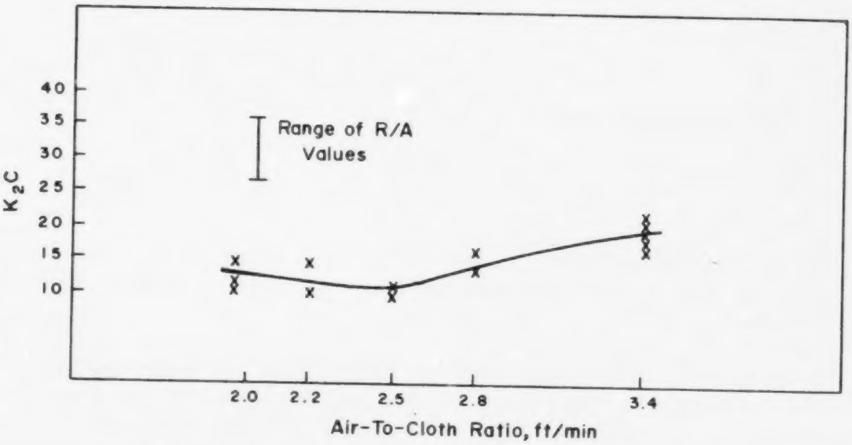

Figure 3. K_2C results.

For comparison with the prototype, the terminal and effective pressure drops were averaged to give an average cell-plate pressure drop. The pilot cell-plate pressure drop data cannot be simply compared to the prototype flange-to-flange pressure drops: one includes "casing" losses, and the other does not. Casing losses, of course, account for entrance effects into hoppers, pressure drops across dampers, duct losses, and other losses not associated with the fabric.

Casing losses across the Harrington fabric filters are given approximately by:

$$\Delta Pc = 0.156V^2 \qquad (3)$$

To put the pilot and prototype data on the same basis and allow direct comparison of the numbers, $0.156V^2$ was added to the average cell-plate pressure drop obtained from the pilot unit.

RESULTS

Table II shows the average flange-to-flange pressure drops from the pilot and prototype units for the 5 months of the study. The numbers agree remarkably well overall. The range of the flange-to-flange pressure drop values measured at each operating condition is shown in the last column of Table II. The pressure drops for the pilot and prototype units fall within a fairly narrow range for each operating condition except for June and August. In June the pressure drop on the east side of the prototype was unusually high, and in August the east side pressure drop was unusually high. No reason for these differences have been identified but it is suspected that operational problems are responsible rather than filtration phenomena.

TABLE II. SUMMARY OF SCALE-UP STUDY
WITH SHAKE/DEFLATE CLEANING

MONTH	A/C, ft/min	Prototype F/F[a]		Pilot F/F[a]		Range[b]
		East[b]	West[b]	East[b]	West[b]	
May	3.40	7.21	7.50	7.66	7.58	0.45
June	2.80	6.23	5.73	6.23	6.02	0.50
	3.40	8.08	7.27	7.59	7.12	0.96
July	2.20	4.61	4.84	4.29	4.57	0.55
	3.40	8.00	8.27	8.71	8.23	0.71
August	1.94	3.88	3.74	3.58	3.96	0.38
	3.40	7.86	7.97	9.18	8.26	1.32
September	1.94	4.11	3.99	4.34	3.73	0.61
	2.50	5.70	5.76	5.87	5.22	0.65
	3.40	8.48	8.85	8.80	8.81	0.33
Average						0.65

[a] Flange-to-flange pressure drop

[b] In. w.g.

One surprising result of the study was that cycling the pilot did not give any significant improvement in agreement of data. Apparently it is not necessary in pilot studies of this type to follow the load cycle since good results can be obtained by simply operating at the conditions of interest.

REVERSE AIR CLEANING

OVERVIEW

The next phase of the pilot program concerned reverse air cleaning studies on a number of different fabric types. A summary of fabrics studied in the pilot unit is shown in Table III.

TABLE III. PILOT FABRIC SUMMARY

Manufacturer[a]	Fabric Style	Finish	Weight oz/yd^2	Weave[b]
Ken	617F	CS-428	10	3x1 T
FF	502-1	AF	14	3x1 T
GA	877	Q78	14	3x1 T
FF	502-1	TC	14	3x1 T
MS	601	TC	10	3x1 T
FF	504-1	AF	10	3x1 T
FF	504-1	TC	10	3x1 T
MS	MS601T (7 Rings)	TC	10	3x1 T
MS	MS601T (5 Rings)	TC	10	3x1 T
MS	601	TC	10	3x2 T
MS	601	TC	10	Crowfoot
MS	601	TC	10	2x2 T
MS	509-N[c] (7 Rings)	TC	9	3x1 T

[a] MS - Menardi-Southern
FF - Fabric Filters
Ken - Kennecott
GA - Globe Albany
TC - Teflon Coating
AF - Acid Flex (I-625)

[b] Twill

[c] Napped

The reverse air study looked at the pressure drop performance of various fabrics having different weights and coatings as well as numbers of rings. In addition, several fabrics were examined with weave types that are not commonly encountered in utility filtration systems. The vast majority of fabric used today in baghouses has a 3x1 twill weave. To get an idea of how other weaves would react to utility filtration conditions, a 3x2 twill, a 2x2 twill, and a crowfoot weave fabric were examined. In addition, a napped fabric was evaluated to examine the effectiveness of napping as compared to texturizing in producing a filtration surface.

OPERATING CONDITIONS

The operating and cleaning cycle parameters employed during the reverse air testing are:

Operating

Inlet temperature	400°F
Grain loading	0.75-1.2 gr/acfm
Filtering cycle	60 min.

Cleaning

First settle	30 sec.
R/A settle	45 sec.
Second settle	30 sec.
R/A air-to-cloth	1.3-1.5

DATA REDUCTION

The reverse air data were reduced in the same way as the shake/deflate study, with one exception. To estimate the flange-to-flange pressure drop of a multicompartment prototype, 2.0 in. w.g. was added to the average cell-plate pressure drop instead of $0.156V^2$. Typically, the casing losses in a large reverse air collector are in the 1.5 to 3.0 in. w.g. range and 2.0 in. w.g. assumes fairly good design.

RESULTS OF REVERSE AIR STUDY ON STANDARD FABRICS

Results of reverse air on standard fabrics are shown in Table IV. All of the fabrics tested resulted in fairly high pressure drops. The measured cell-plate pressure drops ranged from 5.26 to 6.52 in. w.g. The flange-to-flange pressure drops for a multicompartment prototype were estimated from this data. These pressure drops ranged from 7.26 to 8.52 in. w.g. at an air- to-cloth ratio of 2.0 ft/min.

TABLE IV. RESULTS OF REVERSE AIR STUDY ON STANDARD FABRICS

Fabric Style	No. of Rings	Air-to-Cloth[a]	K_2c[b]	ΔP After Cleaning[c]	ΔP Before Cleaning[c]	Avg.[c] ΔP	F/F[d] ΔP
Ken-617F	6	2.30	32.29	6.31	7.78	7.05	9.05
		(2.00)	(Calculated	Values)		(5.84)	(7.84)
FF502-1AF	6	2.00	31.21	5.98	7.05	6.52	8.52
GA 877-Q78	6	2.00	27.36	4.81	5.70	5.26	7.26
FF502-1TC	6	2.00	33.89	5.84	7.00	6.42	8.42
MS 601-T	6	2.00	27.19	4.92	5.80	5.36	7.36
FF504-1AF	6	2.00	29.24	5.10	6.05	5.58	7.58
FF504-1TC	6	2.00	32.22	5.81	6.92	6.37	8.37

[a] ft/min

[b] $\frac{\text{in. w.g. min. ft. gr.}}{\text{lb}_m\ \text{cu. ft.}}$

[c] in. w.g.

[d] Estimated flange-to-flange

Unlike the remainder of the fabrics, the first test fabric (Ken 617F) was run at an air-to-cloth ratio of 2.3 ft/min. The results of this test indicated that the higher air-to-cloth ratio was not necessary to compensate for a short testing period. After the Kennecott test the air-to-cloth was lowered to 2.0 ft/min. To allow comparison with the rest of the fabrics, the Kennecott results were projected at an air-to-cloth ratio of 2.0 ft/min.

The data on the MS601-T and GA877-Q78 fabrics (see Table IV) must be viewed cautiously since neither came to equilibrium during the testing period. In both cases the pressure drop monotonically increased throughout the testing period. This phenomenon of slowly approaching operating equilibrium has also been observed for the MS601-T fabric in full-compartment testing on the Harrington prototype baghouses.

FF502-1AF and FF504-1TC fabrics had the same pressure drops. This result is again in agreement with full-compartment testing done on the shake/deflate Harrington filter. In these full compartment studies no difference has been noted between 10-oz. Teflon-coated fabrics and 14-oz. acid-resistant coated fabrics in terms of pressure drop.

The FF502-ITC fabric is a 14-oz. fabric with a 10 percent Teflon coating. This combination represents the "high-priced spread" in that the more expensive 14-oz. fabric and Teflon coating are combined. The fabric showed pressure drops in the same range as fabrics FF502-1AF and FF504-1TC. Testing of 14-oz. Teflon-coated materials in the prototype indicated reduced flow (10 percent), but the pressure drop was not substantially different than the commonly used FF502-1AF and FF504-1TC fabrics.

The FF504-1AF fabric is a 10-oz./yd^2 fabric with an acid-resistant coating. This fabric is essentially the "low-priced spread," combining the least expensive coating and fabric. The fabric exhibited one of the lower pressure drops observed in the pilot for the standard fabrics, 7.58 in. w.g. In the prototype this fabric has shown no lower pressure drop than the other fabrics. Baglife on this fabric is now approximately 20 months in two compartments in Unit 2. Observed wear on the fabric seems to indicate that inferior bag life will be obtained under shake/deflate conditions. The exact economic trade-off of bag cost versus bag life will be studied for this fabric to see if it offers an economic advantage despite its shorter bag life.

RING STUDY

The effect of various numbers of rings in a bag was studied using samples having five, six, and seven rings (equally spaced). The fabric chosen for this study was a 10-oz./yd^2 Teflon-coated material. Originally only MS601-T was to be used in the study, but its failure to come to equilibrium made it necessary to include data previously obtained on another 10-oz./yd^2 Teflon-coated material (FF504-1TC). The results obtained on these fabrics are shown in Table V.

TABLE V. RESULTS OF RING STUDY

Fabric Style	No. of Rings	K_2c[a]	ΔP After Cleaning[b]	ΔP Before Cleaning[b]	Avg. ΔP[b]	F/F ΔP[b,c]
MS601-T	5	36.70	5.76	6.94	6.35	8.35
FF504-1TC	6	32.22	5.81	6.92	6.37	8.37
MS601-T	6	27.19	4.92	5.80	5.36	7.36
MS601-T	7	31.74	5.65	6.68	6.16	8.16

[a] $\frac{\text{in. w.g. min. ft. gr.}}{\text{lb}_m \text{ cu. ft.}}$

[b] in. w.g.

[c] Estimated flange-to-flange

The pressure drops for the three fabrics that obtained equilibrium during the testing show very little difference. From this data it would appear that the number of rings in a bag do not have profound effects on pressure drop. Outside the range of five to seven rings in a 30-ft bag, however, some effect on pressure drop may occur.

NON-STANDARD FABRICS

One area of fabric filter research left virtually untouched in the utility industry is the effect of fabric weaves and construction on performance of filtration materials. To date only texturized 3x1 twill weaves have been employed to any extent on glass fabrics. Certain experiences with 3x1 and 3x2 twill Nomex fabrics at Harrington pointed to weave as being a potentially major factor in fabric performance.

Several fabric weaves and constructions that are uncommon to utility application were tested in the pilot unit. Table VI lists the results for these non-standard fabrics.

TABLE VI. RESULTS OF TESTING ON NON-STANDARD FABRICS

Fabric Style	No. of Rings	Weave	K_2c[a]	ΔP After Cleaning[b]	ΔP Before Cleaning[b]	Avg. ΔP[b]	F/F ΔP[b,c]
MS 3x2 T	6	3x2 T	32.51	5.05	6.71	5.61	7.61
MS-CF	6	Crowfoot	26.93	5.02	5.94	5.48	7.48
MS 2x2 T	6	2x2 T	16.07	3.09	3.57	3.33	5.33
MS509N	7	Napped	32.69	5.73	6.75	6.24	8.24

[a] $\frac{\text{in. w.g. min. ft. gr.}}{\text{lb}_m \text{ cu. ft.}}$

[b] in. w.g.

[c] Estimated flange-to-flange

The 3x2 twill and the crowfoot fabrics have significantly lower pressure drops than most of the fabrics in common use. No operational difficulties were encountered during the testing of either of these fabrics, but the crowfoot weave exhibited a rather strange phenomenon. Initially the pressure drop rose after start-up and leveled off at close to 5.5 in. w.g. For the last 3 days of the test period, however, the pressure drop decreased suddenly to approximately 4.3 in. w.g. To be sure of interpreting this data conservatively, the last few days of operation were ignored in the data analysis. Further analysis of the crowfoot fabric would certainly be wise.

The 2x2 twill fabric exhibited pressure drops below 2 in. w.g. for the first 4 days and increased slowly throughout the testing period. Only the last few days of testing were used to evaluate the 2x2 twill fabric. Since it did not come to equilibrium by leveling off in pressure drop, the data are not satisfactory. Again, more testing should have been done, but time was not available.

The seven-ringed napped fabric with a pressure drop of 8.24 in. w.g. failed to show any advantage over the 3x1 twill seven-ringed texturized fabric at a pressure drop of 8.16 in. w.g.

ADDITIONAL STUDIES

K_2c RESULTS

The K_2c values obtained during the scale-up period are shown versus air-to-cloth ratio in Figure 3.

K_2c decreases as the air-to-cloth ratio is lowered. At air-to-cloth ratios lower than 2.7 ft/min, however, no significant changes in K_2c are observed. If grain loading can be assumed constant, this implies that K_2 also decreases with air-to-cloth ratio and does not change significantly below an air-to-cloth ratio of 2.7 ft/min. The minor dip at an air-to-cloth ratio of 2.5 ft/min may be an anomaly. If not, it is due to settling out of heavier particles as the velocity gets lower and lower.

The range of K_2c values measured for reverse air cleaning on the various test bags is also shown in Figure 3. As shown, the K_2 values for reverse air cleaning are substantially larger than the K_2 values obtained for shake/deflate cleaning at the same air-to-cloth ratio (2.0 ft/min). Cleaning then is shown to influence K_2 as well as ash properties. This effect could reflect the length of time required to"repair" the ash cake after cleaning. Reverse air cleaning causes fissures in the ash cake along with some areas where cake has sloughed off. After cleaning, these areas are quick to rebuild with the result that any additional cake is generally distributed and influences the pressure drop increase. After shake/deflate cleaning, large areas of the cloth are stripped bare to the surface. The time required to repair these larger areas strongly influences the rate at which pressure drop can increase across the filter cake.

DESIGN EQUATIONS

The pilot data obtained in the scale-up and reverse air studies can be used to develop pressure drop relationships for use in design. The equations are:

$$\Delta P = 1.60V^{1.34} \quad \text{Shake/deflate} \tag{4}$$

$$\Delta P = 3.29V^{1.34} \quad \text{Reverse air} \tag{5}$$

Figure 4 shows a plot of pressure drop versus air-to-cloth ratio predicted from these equations.

Strictly speaking, these correlations apply only to one ash type, certain fabrics, and a given set of cleaning conditions. The data used in developing these correlations, however, represent the cloth used in over 90 percent of the baghouses in operation on utility boilers. In addition, the cleaning conditions employed are representative of those used by many installations. These equations then should be useful in modeling filtration of ashes similar to the Wyoming ash produced at Harrington Station.

Because the operating conditions during testing were deliberately chosen to simulate operations at high capacity factors, these correlations should not be used for peaking units and other low load applications.

CONCLUSIONS

The fabric filter pilot unit at Harrington Station has successfully demonstrated the ability of a pilot unit to model large scale fabric filter systems. The pressure drop model developed from the pilot unit describes both the Harrington fabric filters (Unit 2 and Unit 3) with good accuracy and should be a useful tool in design of units with similar fly ashes.

Although no direct comparison from pilot to prototype was available for the reverse air studies, there is no apparent reason that the reverse air equation should not be accurate for the ash type studied.

The experience gained from Harrington Station's pilot and prototype units indicates that the typical design goal of 6.0 in. w.g. flange-to-flange pressure drop can be obtained with a properly designed shake/deflate baghouse at an air-to-cloth ratio of approximately 2.7 ft/min. The reverse air study indicates the maximum air-to-cloth ratio for a reverse air baghouse on western ash is in the 1.5-1.7 ft/min range.

The reverse air fabric study points to the need for more research in the area of fabric weaves and construction. Shown below in Table VII are all the fabrics tested arranged according to increasing pressure drop.

6

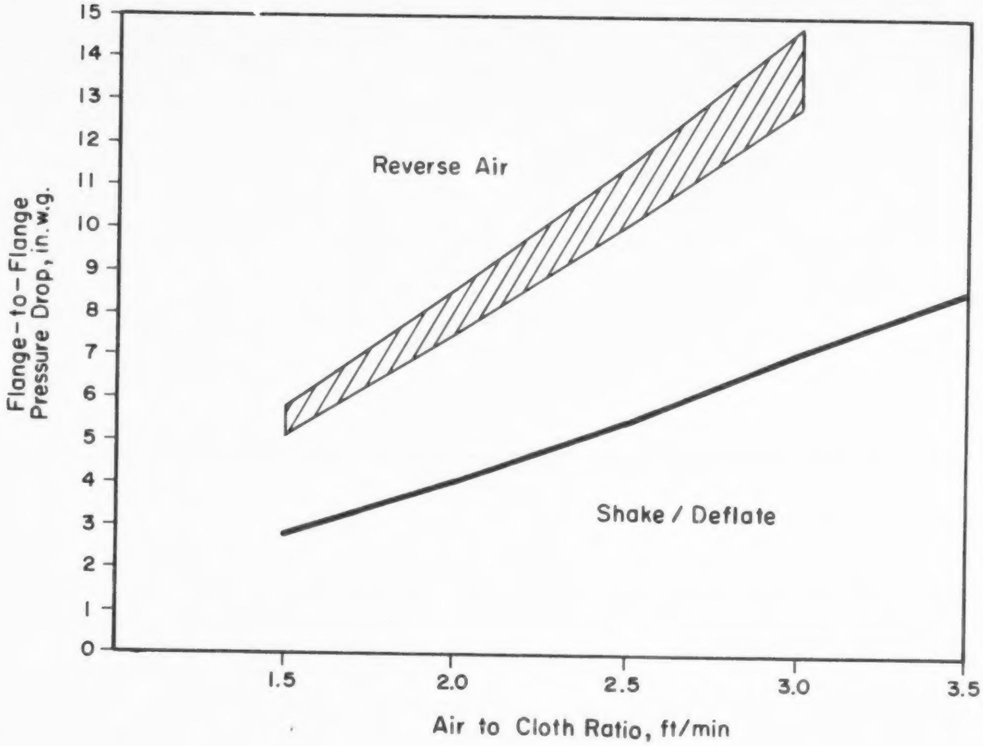

Figure 4. Plot of pressure drop vs. air-to-cloth.

TABLE VII. FABRICS BY PRESSURE DROP

Fabric	Weight oz/yd^2	Coating	Weave	F/F[a] ΔP	Comments
MS601-T	10	Teflon	2x2 Twill	5.33	Equilibrium not obtained
GA 877-Q78	14	Q78	3x1 Twill	7.26	Equilibrium not obtained
MS601-T	10	Teflon	3x1 Twill	7.36	Equilibrium not obtained
FF504-1AF	10	Teflon	Crowfoot	7.48	
MS601-T	10	Acid Flex	3x1 Twill	7.58	
Ken-617-F	10	Teflon	3x2 Twill	7.61	
MS601-T (7 Rings)	10	CS-428	3x1 Twill	7.84	Calculated
MS509N (7 Rings)	10	Teflon	3x1 Twill	8.16	
MS601-T (5 Rings)	10	Teflon	3x1 Twill	8.24	
FF504-1TC	10	Teflon	3x1 Twill	8.35	
FF502-1TC	10	Teflon	3x1 Twill	8.37	
FF502-1AF	14	Teflon	3x1 Twill	8.42	
	14	Acid Flex	3x1 Twill	8.52	

[a] Flange-to-flange, in. w.g.

The highest pressure drops recorded during tests were for the three most commonly used fabrics. Two of the non-standard weaves, the 3x2 twill and the crowfoot, did show significantly lower pressure compared to the commonly used types. Although the 2x2 twill fabric did not come to equilibrium, its behavior during the test program would indicate that it may also be a candidate for enhanced performance. The three lowest pressure drop fabrics are those that did not come to equilibrium during the testing period, and no clear conclusion can be drawn from the data about their performance.

These results demonstrate that better performance may be obtained if further research is aimed at developing fabrics especially suited for utility filtration systems. Considering the costs of premature bag replacement and the cost of high pressure drop, further studies could lead to greater cost-effectiveness.

REFERENCES

1. Ladd, K. L., Hooks, W., Kunka, S. L., and Harmon, D. SPS Pilot Baghouse Operation. In Third Symposium on the Transfer and Utilization of Particulate Control Technology: Volume I. Control of Emissions From Coal-Fired Boilers, EPA-600/9-82-005a (NTIS PB83-149583), pp 55-64, July 1982.

THE USE OF SONIC AIR HORNS AS AN ASSIST TO REVERSE AIR CLEANING OF A FABRIC FILTER DUST COLLECTOR

by: Alan R. Menard
R. Mark Richards
Public Service Company of Colorado
Arapahoe Station
Denver, Colorado 80201

ABSTRACT

A detailed summary of the installation, test program, and performance of sonic air horns used as an assist to reverse air cleaning of an operating FFDC is presented. Four sonic air horns were installed and tested on compartment number 11 of Public Service Company of Colorado's Arapahoe Unit #3 FFDC. The overall objective of the test program was to reduce the pressure drop across the tube sheet of the test compartment. Sonic cleaning reduced the compartment tube sheet differential pressure by approximately 27 percent; this was sufficient to warrant the purchase and installation of two (2) sonic air horns in each of the 14 baghouse compartments.

INTRODUCTION

The need to decrease the pressure drop across the filtering elements in a Fabric Filter Dust Collector (FFDC) is inherent to the reduction of its operating costs. Public Service Company of Colorado's Arapahce Unit #3 FFDC has experienced flange to flange pressure drops on the order of 10 inches VWC at full load as opposed to the design pressure drop of 6 inches VWC. Much of this discrepancy in pressure drop can be attributed to the formation of nodules (Reference 1) or cake on the inner surface of the filtering elements which is not removed during the reverse air cleaning cycle (Figure III-1). The formation of nodules or cake reduces the effective filtering area of the baghouse, which in turn, increases operating air-to-cloth ratio.

A solution was sought by Arapahoe Station personnel that would decrease the overall pressure drop of Arapahoe Unit #3 FFDC. Because the nodule/cake buildup on the filtering elements was felt to be directly related to the pressure drop problem, the use of sonic air horns used in conjunction with the reverse air cleaning cycle was thought to be a viable solution to the problem of fly ash removal. A test program was devised that would determine the effect of using sonic air horns during the reverse air cleaning cycle as a means of reducing the pressure drop across the filtering elements.

Four Fuller air horns were purchased and installed in compartment #11 of Arapahoe Unit #3 FFDC. Compartment #4, having the most similar flow characteristics to compartment #11, was used to collect base data for comparison purposes during the test period. The use of the sonic air horns made an appreciable improvement in the performance of the test compartment; significant enough to warrant the purchase and installation of horns in all 14 baghouse compartments.

This report summarizes the installation, test program and performance of sonic air horns used as an assist to reverse air cleaning of a FFDC.

TECHNICAL DISCUSSION

BAGHOUSE DESIGN AND HISTORY

Public Service Company of Colorado's Arapahoe Unit #3 FFDC was designed for 315,000 acfm flow with a 6-inch VWC pressure drop flange to flange, and a 2.16 operating air-to-cloth ratio. The boiler/turbine combination has a 48 MW capability and operates on low sulphur, sub-bituminous western coal. The baghouse is a reverse air cleaning type, consisting of two rows of seven modular compartments with inlet, outlet, and reverse air ducts located between the two rows of compartments (see Figure II-1). Each compartment contains a total of 236 bags which are arranged as shown in Figure II-2. The bags are 8 inch diameter, 22 feet long, woven fiberglass with teflon B coating. The baghouse was started up on May 18, 1979, and reached initial full load operation on May 21, 1979. For complete design specifications on Arapahoe Unit #3 baghouse, see Table 1.

After initial operation of the baghouse, several mechanical problem areas such as valve seating, air cylinder operation, and thimble leaks were recognized and repaired. With these problems solved, performance testing of the baghouse began. Originally, the baghouse was outfitted with 8-1/4 inch diameter Acme Mills woven fiberglass bags with teflon coating. After approximately two months of operation, the baghouse experienced flange to flange pressure drops in excess of the design pressure drop of 6 inches VWC at full load. Acceptable pressure drops could only be obtained by hand clapping and/or beating the bags to remove the cake buildup on the inside surface of the filtering elements. However, as the cake began to build up on the bags, the pressure drop would again exceed design levels. The baghouse manufacturer felt that the pressure drop problem could be solved by replacing the O.E.M. bags with Menardi Southern bags with teflon B coating.

Compartments 1 and 7 were outfitted with the Menardi Southern bags and a test program was initiated. The performance of the two compartments outfitted with the new bags was significantly better than the other compartments (Reference 2). It was decided to install the Menardi Southern bags in all 14 baghouse compartments. Eight-inch diameter bags were chosen as opposed to 8-1/4 inch diameter bags because of long lead times associated with obtaining the 8-1/4 inch diameter bags. This three percent reduction in filtering area was felt to be outweighed by the performance increase with the new bags.

During this time period, data acquisition and testing was initiated to optimize the operation of the baghouse. Different types of coal were burned. Although some coals increased operating flange to flange pressure drop, no coal was found that decreased pressure drop. Optimization of the cleaning cycle was also attempted. Multiple settling/reverse air periods, continuous

Table 1
ARAPAHOE UNIT 3 FFDC DESIGN SPECIFICATIONS

DESIGN CONDITIONS

Process	Power Generation
Suspended Material	Fly Ash
Fuel	Pulverized Coal
Gas:	
Source	Coal-Fired Boiler
Gas Flow (max. acfm)	315,000
Temperature (°F)	290
Outlet Loading (fr/acf)	0.007
Pressure Drop (in. VWC)	6.0
Design Pressure (in. VWC)	±20
Total Filter Area (sq ft)	156,995
Effective Filter Area (sq ft)±	145,781
Total Filter Ratio	2:1
Active Filter Ratio±	2.16:1
Reverse Air Flow:	
Total (max acfm)	16,700
Static Pressure (in VWC)	10.6
Reverse Air Fan (qty)	2 (1 on standby)

FFDC DATA

Type	Modular
No. of Units	2
No. Compartments/Units	7
Bags:	
Total Quantity	3304
Per Compartment	236
Material	Menardi Southern, Teflon B coating
Diameter (in.)	8
Length (ft)	22
Power Requirements	480V, 3 phase, 60Hz

Air Flow Regulation	Type	Qty
Hopper Inlet (Isolation)	Butterfly °	14
Reverse Air/Outlet Valve	Double Disc°	14
Reverse Air Control (Null) Damper	Butterfly °	1
Outlet Duct (Isolation)	Butterfly °	14
By-Pass Damper	Poppet °	2

±With one compartment out for cleaning and one compartment out for maintenance

°Pneumatic operated

Figure II-1 Arapahoe Unit 3 Baghouse Compartment Locations

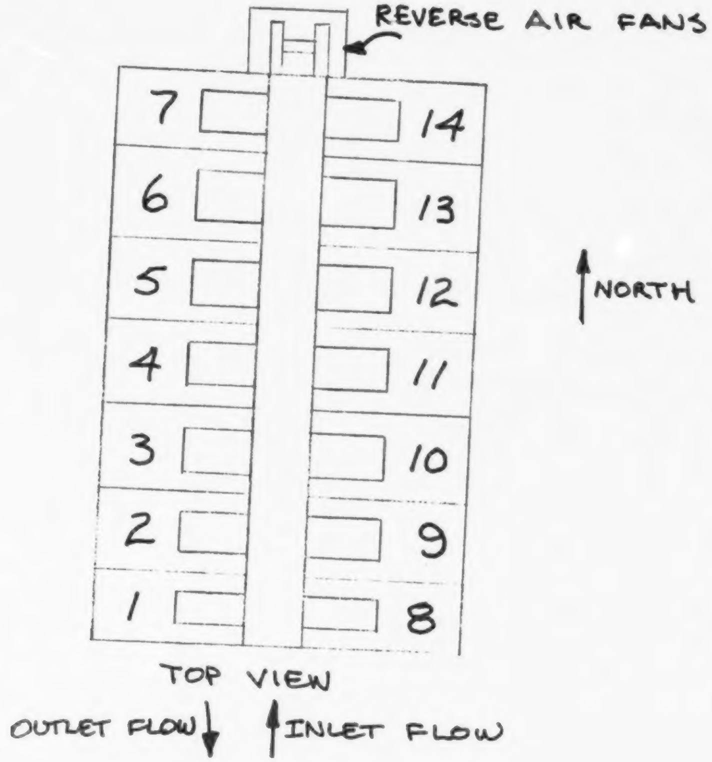

TOP VIEW

REVERSE AIR FANS
7
14
6
13
5
12
4
11
3
10
2
9
1
8
NORTH
OUTLET FLOW
INLET FLOW

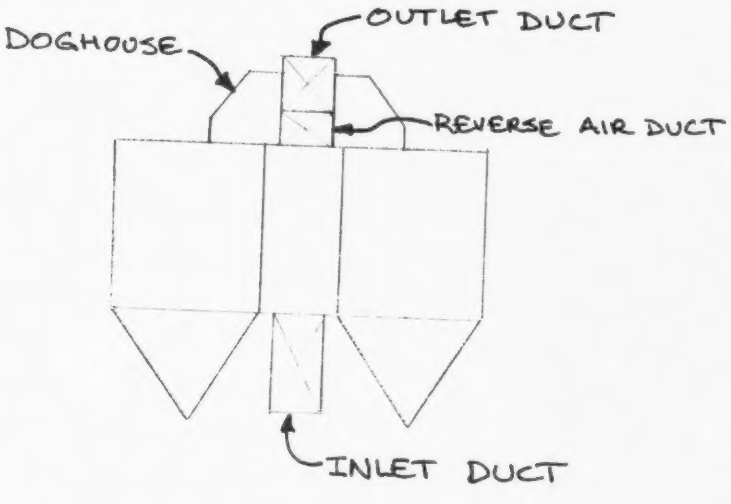

END VIEW

OUTLET DUCT
DOGHOUSE
REVERSE AIR DUCT
INLET DUCT

Figure II-2 Typical Compartment Filter Element Location

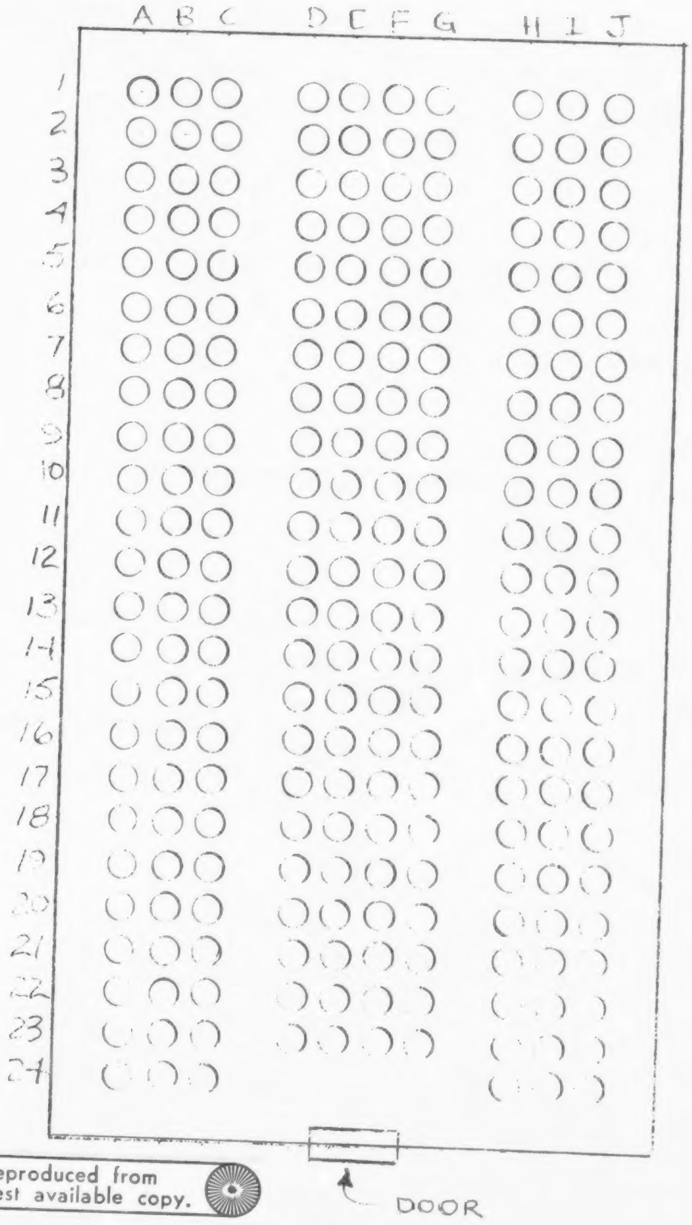
A B C
D E F G
H I J
1
2
3
4
5
6
7
8
9
10
11
12
13
14
15
16
17
18
19
20
21
22
23
24
DOOR

Reproduced from
best available copy.

cleaning as well as differential pressure initiation of the cleaning cycle were also tested. None of these experiments made any significant improvement in flange to flange pressure drop.

After approximately three months of operating with the new Menardi Southern bags, the pressure drop from the inlet flange to the outlet flange again exceeded the design specification of 6 inches VWC. To maintain a reasonable pressure drop, the bags still had to be periodically hand beaten to remove the cake/nodule buildup on the inside surface of the filtering elements. As a result of this, Arapahoe Station personnel, with assistance from the staff at EPRI's Emission Control Test Facility at Arapahoe Station sought a solution to the pressure drop problem. Because all attempts at optimizing the cleaning cycle and the switching to a different filtering element made no appreciable improvement on the overall flange to flange pressure drop, it was felt that the nodule/cake buildup on the filtering elements was directly related to the pressure drop problem. The use of sonic air horns as an assist to the reverse air cleaning cycle was felt to be a viable solution to the problem of cake buildup not being removed from the filtering elements with reverse air cleaning only. A test program was developed that would determine the effect of sonic cleaning on the nodule/cake buildup problem, and ultimately would determine if sonic cleaning would reduce the operating flange to flange pressure drop.

HORN INSTALLATION

Four sonic air horns were obtained on a trial basis for installation at Arapahoe Station from Fuller Company. Because of time limitations, a test program was devised that was somewhat limited in scope but would still determine the overall effectiveness of sonic cleaning. Arapahoe Station personnel, in conjunction with the staff at EPRI's Emission Control Test Facility at Arapahoe Station, assembled a list of critical parameters that would be monitored during the test period. During these initial discussions, decisions were made on horn placement, boiler loading, horn operation and special equipment needed to control horn operation.

Four Fuller air horns, model 310-64-1-0099-01 were installed in compartment 11 of Arapahoe Unit #3 FFDC. It was thought that the compartment should be divided into four equal quadrants, and a horn placed at the center of each quadrant. The location of the "Doghouse" containing the outlet and compartment isolation valves made this objective impossible and the horns were placed as shown in Figure II-3. Figure II-4 shows the installation of a typical horn through the roof of the compartment.

Each air horn requires 70-90 psig air at 50 scfm. The control air system that operates the existing air cylinders on top of the baghouse, at 80 psig, was adequate to supply the horns. However, it was felt that an air receiver tank was necessary to supply the four horns with a sufficient volume of air. A 30 cubic foot air receiver tank was purchased and installed on top of the baghouse. A one (1) inch diameter manifold was run from the receiver tank to the horns with one-half (½) inch copper tubing branching from the manifold to each horn.

Figure II - 3 Test Compartment Horn Locations

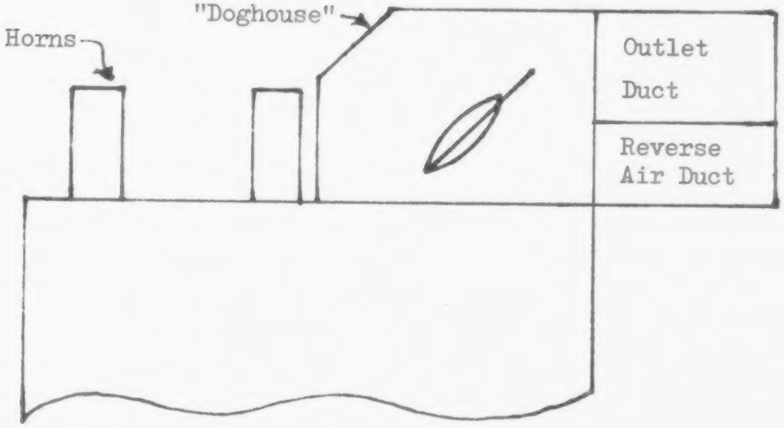
Horns
"Doghouse"
Outlet Duct
Reverse Air Duct

Side View

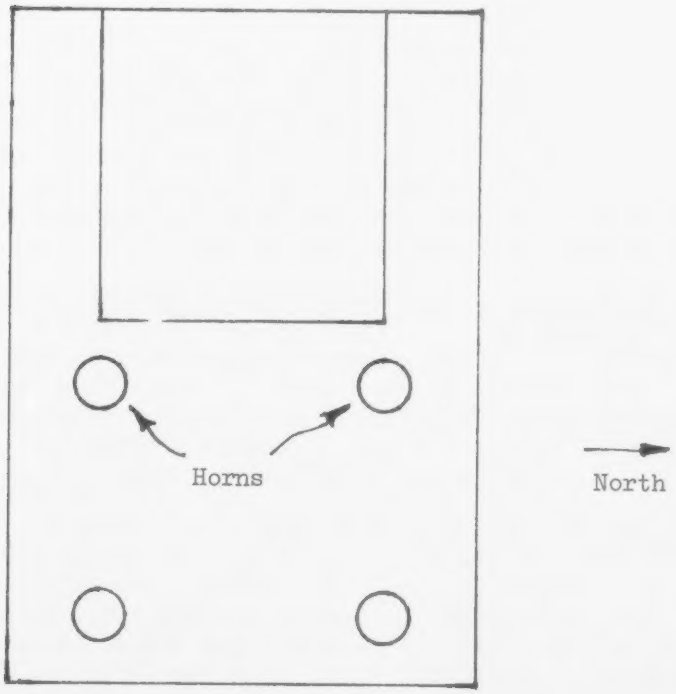
Horns
North

Top View

Figure II-4 Compartment Horn Installation

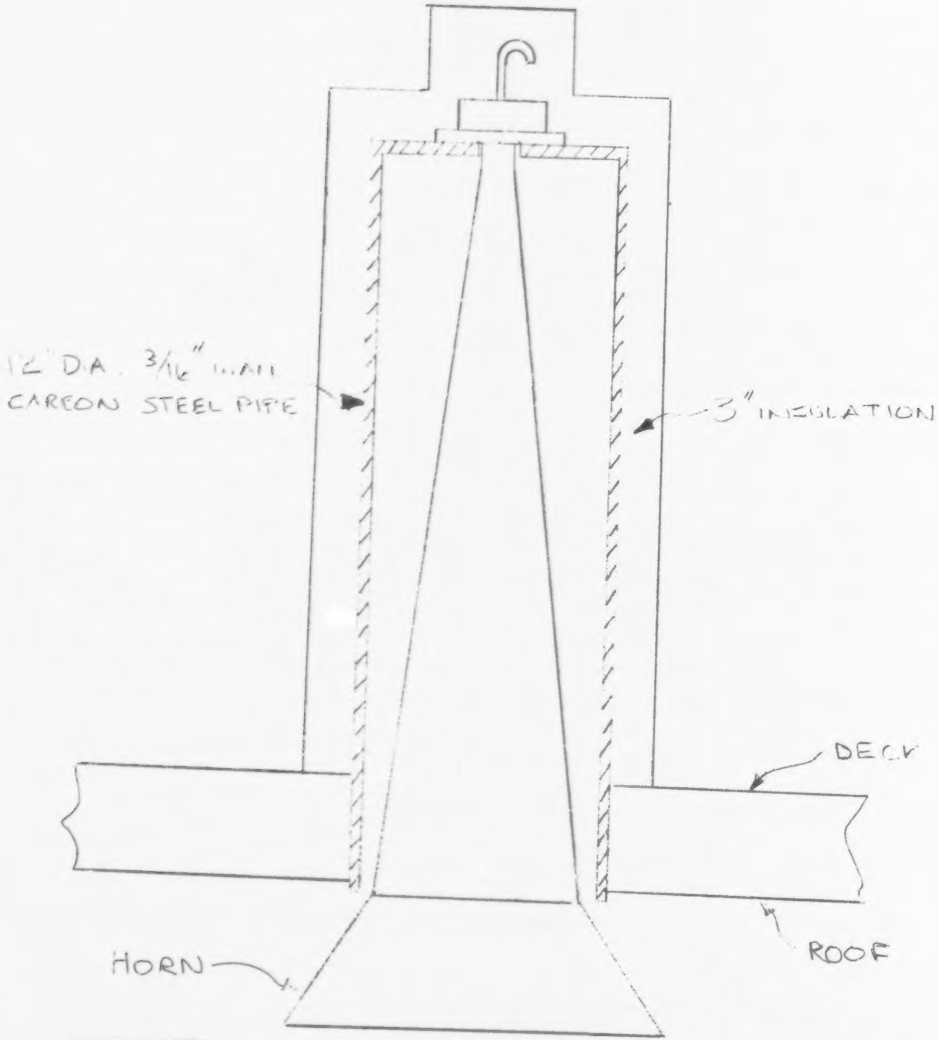
12" DIA. 3/16" WALL
CARBON STEEL PIPE
3" INSULATION
DECK
ROOF
HORN

Reproduced from
best available copy.

The question of when to operate the horns and for what duration during the cleaning cycle was discussed. Having limited experience with sonic air horns, three options were considered:

(1) Operate the horns during the initial settling period (no reverse air);

(2) Operate horns during reverse air cleaning;

(3) Operate horns during the final settling period.

Because of time limitations on the Fuller air horn trial period, it was not feasible to optimize horn operation. It was decided that option two would achieve the best results. The horns would be operated as an assist to the reverse air fan for a period of ten seconds. This proved to be the best method of horn operation and will be discussed later.

A means of controlling horn operation was devised. A normally closed solenoid valve was installed in the line exiting the air receiver tank that would open when horn operation was desired. At the baghouse control panel, reverse air damper movement (initiation of compartment clean) would initiate a primary timer. After 40 seconds, the first timer would initiate a second timer which operated the solenoid valve for a period of ten seconds. This system served to operate the horns at the approximate time the reverse air flow reached the compartment.

TEST PROGRAM

The objective of the test program was to determine the effect of sonic cleaning on flow and pressure drop in the test compartment. An increase in flow and a decrease in pressure drop in the test compartment was desired. Four Fuller air horns were installed on compartment #11 of Arapahoe Unit #3 FFDC and it was designated the test compartment. Compartment #4, having the most similar flow characteristics to compartment #11, was used to accumulate base data for comparison purposes. The following is a list of parameters that were monitored during the test period:

(1) Pressure drop across the thimble sheet of the test compartments;

(2) Exit flow of the test compartments;

(3) Flange to flange pressure drop;

(4) Inlet, outlet, reverse air, and compartments 4 and 11 exit gas temperature;

(5) Compartment ash pulling times;

(6) Bag weights - before and after cleaning.

For comparison purposes of data taken on different days, it was decided that a constant boiler load was essential. Variations in load would cause fluctuations in flow, pressure drop, etc., which would have made data interpretation and correlation more difficult. The unit was base loaded at 46 MW (full load) one (1) day per week during the test period. Although the horns continued to operate during periods of varying load, the majority of relevant data was taken during the periods of base loading. The instrumentation and recorders were installed and were ready for operation by February 22, 1982.

Before the test period began, bags were weighed in each of the test compartments before and after cleaning. Ash pulling times were also recorded. The recorders were placed in service to accumulate base data before any horns were operated.

It was decided to test the horns in successive combinations of 1, 2, or 4 horns to determine the minimum amount of horns required for successful sonic cleaning. On February 23, 1982, one horn was operated. On February 25, 1982, 2 horns and on March 29, 1982, 4 horns were tested. Ash pulling times were recorded each Monday.

During the test period, the baghouse was on a continuous clean cycle. There was a ten minute delay between each compartment clean, and it would take approximately 2.75 hours to clean all 14 compartments. Reverse air flow was held constant during the test program. For a complete log of the test program, see Appendix A.

TEST RESULTS AND DISCUSSION

Introduction

The use of sonic air horns as an assist to reverse air cleaning proved to be a viable solution to the problems of nodule/cake formation on the filtering elements and increased pressure drop in an operating FFDC. During the test period, bag weights, filter element cake thickness and tube sheet differential pressure were all reduced in the test compartment. In addition, flow through compartment 11 increased during the period of horn operation. Results indicated that two (2) horns per compartment were sufficient to adequately clean the compartment and maintain the reduction in pressure drop. As a result of this test program, Public Service Company of Colorado has purchased and installed two (2) sonic air horns in each of the fourteen (14) baghouse compartments at Arapahoe Station's Unit #3 FFDC. This section summarizes the performance of sonic air horns used as an assist to reverse air cleaning of a FFDC.

Discussion of Results

The overall objective of the test program was to reduce the pressure drop across the thimble sheet in the test compartment. The following parameters were monitored during the test program:

(1) Bag weights and samples;

(2) Compartment ash pulling times;

(3) Thimble sheet differential pressure;

(4) Test compartment exit flows.

A summary of the effect of sonic cleaning on each of the above listed parameters is presented below.

Bag Weights and Samples

Probably the most significant effect of sonic cleaning was on the filtering elements (bags) themselves. Before the sonic horns were operated, bags were weighed in both compartments 4 and 11. Bag weights ranged from 34 to 55 pounds with the average weight being approximately 46 pounds. At several points during the test program, the test compartments were isolated and bags were weighed. Compartment 4's filtering elements remained the same in weight while the bag weights in compartment 11 were dramatically reduced.

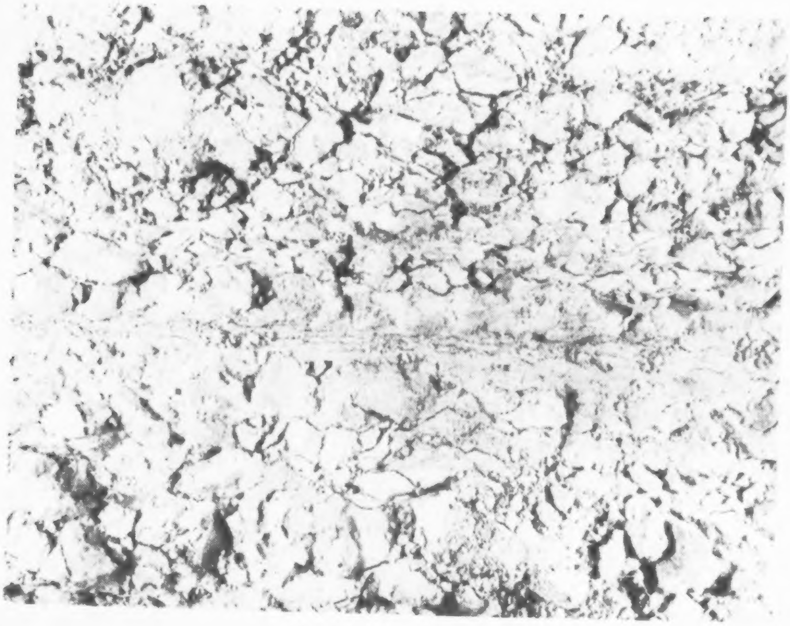

Figure III-1 Nodule/Cake Formation on a Typical Filtering Element - Without Sonic Cleaning

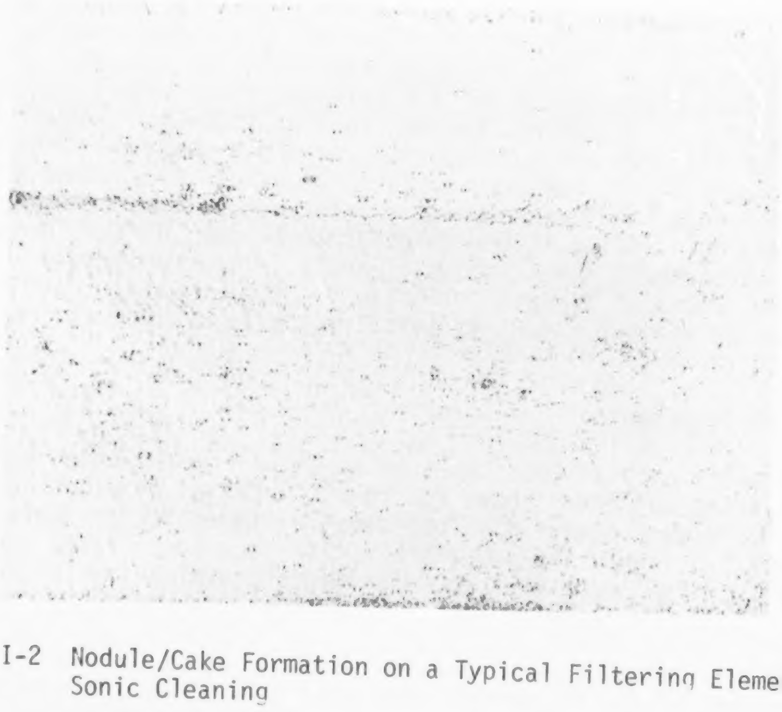

Figure III-2 Nodule/Cake Formation on a Typical Filtering Element - With Sonic Cleaning

Weights in the test compartment ranged from 12-1/2 to 25 pounds with the average weight being approximately 18 pounds. A new filtering element weighs approximately 9 pounds. The sonic air horns reduced the amount of fly ash cake buildup on the filtering elements an average of 76 percent. This reduction in weight has an added benefit. The filtering elements are tensioned to 50 pounds in the compartments. As bag weights approach 50 pounds, it is difficult to maintain proper bag tensioning which affects the way the bags collapse during reverse air cleaning. With the reduction in bag weights due to sonic cleaning, more uniform filtering element tensioning is possible. For a complete tabulation of bag weights taken during the test program see Table 2.

Samples of the filtering elements were taken in each of the test compartments before and after cleaning. Samples were cut from the top, middle and bottom of selected bags without disturbing cake buildup. The difference in nodule formation with and without sonic cleaning can be seen in Figures III-1 and III-2.

Compartment Ash Pulling Times

Another means of determining the effectiveness of sonic cleaning was to monitor the amount of time required to remove the fly ash from the compartment ash hoppers. An increase in the amount of time required to remove the ash from the hopper on the compartment with sonic horns would indicate that the cake buildup on the filtering elements was being removed. Ash pulling times before the test program began were recorded and are shown in Figure III-3. Figure III-4 shows compartment ash pulling times during one and two horn operation. Assuming that the curves in Figure III-4 would be similar in shape to the curves in Figure III-3 without sonic cleaning, ash pulling times in compartment 11 increased by approximately 90 percent. It was expected that after the majority of cake buildup in the test compartment had been removed by sonic cleaning, the ash pulling times for compartment 11 would decrease from the ash pulling times recorded when the horns were first operated. Figure III-5 shows the compartment ash pulling times after two weeks of continuous two hourn operation. The ash pulling time for compartment 11 should be slightly higher than normal because of the increase in flow through the compartment due to sonic cleaning (discussed below). However, the increased amount of fly ash collected in compartment 11 over the 2.75 hour time period between cleanings is difficult to measure and does not show up readily in the data.

Thimble Sheet Differential Pressure

The pressure drops across the tube sheet of compartment 4 and 11 were recorded on a two pen strip chart recorder. Data was recorded at full load before any horns were operated. Tube sheet differential pressure measured at that time was 6.5 inches VWC immediately after the compartment cleaned and would decay to 8.5-9 inches VWC immediately before cleaning (see Figure III-6).

On February 23, 1982, with the unit stabilized at 45 MW, one horn in the northeast corner of the compartment was operated. Pressure drop across the tube sheet in compartment 11 was reduced to 3.2 inches VWC immediately after

Table 2

BAG WEIGHTS

Bag #	Compartment	Weight	Comments
13G	4	46 lbs.	0 horns, before cleaning
20D	4	44 lbs.	0 horns, before cleaning
10C	4	34 lbs.	0 horns, before cleaning
20D	11	46½ lbs.	0 horns, before cleaning
15C	11	49 lbs.	0 horns, before cleaning
10G	11	52 lbs.	0 horns, before cleaning
19G	11	47 lbs.	0 horns, after cleaning
16H	11	49 lbs.	0 horns, after cleaning
11D	11	55 lbs.	0 horns, after cleaning
14D	4	45 lbs.	0 horns, after cleaning
18G	4	45 lbs.	0 horns, after cleaning
8H	4	37 lbs.	0 horns, after cleaning
5C	11	12½ lbs.	2 horns, after cleaning 3/1/82
5D	11	14 lbs.	2 horns, after cleaning 3/1/82
5G	11	15 lbs.	2 horns, after cleaning 3/1/82
5H	11	16½ lbs.	2 horns, after cleaning 3/1/82
12C	11	15 lbs.	2 horns, after cleaning 3/1/82
12D	11	14 lbs.	2 horns, after cleaning 3/1/82
12G	11	14½ lbs.	2 horns, after cleaning 3/1/82
12H	11	15 lbs.	2 horns, after cleaning 3/1/82
20C	11	19 lbs.	2 horns, after cleaning 3/1/82
20D	11	15½ lbs.	2 horns, after cleaning 3/1/82
20G	11	15½ lbs.	2 horns, after cleaning 3/1/82
20H	11	18 lbs.	2 horns, after cleaning 3/1/82
7C	11	18½ lbs.	2 horns, before cleaning 3/17/82
20D	11	18 lbs.	2 horns, before cleaning 3/17/82
13G	11	19 lbs.	2 horns, before cleaning 3/17/82
20D	4	36 lbs.	0 horns, before cleaning 3/17/82
20G	4	34½ lbs.	0 horns, before cleaning 3/17/82
8D	11	20 lbs.	2 horns, after cleaning 3/18/82
8H	11	24 lbs.	2 horns, after cleaning 3/18/82
12G	11	19 lbs.	2 horns, after cleaning 3/18/82
15C	11	22 lbs.	2 horns, after cleaning 3/18/82

15D	11	22½ lbs.	2 horns, after cleaning 3/18/82
17G	11	25 lbs.	2 horns, after cleaning 3/18/82
22D	11	24 lbs.	2 horns, after cleaning 3/18/82
22G	11	24½ lbs.	2 horns, after cleaning 3/18/82
3C	11	18 lbs.	4 horns, after cleaning
3H	11	22 lbs.	4 horns, after cleaning
8C	11	21½ lbs.	4 horns, after cleaning
8D	11	18 lbs.	4 horns, after cleaning
11G	11	17½ lbs.	4 horns, after cleaning
11H	11	21 lbs.	4 horns, after cleaning
17C	11	20 lbs.	4 horns, after cleaning
20G	11	24½ lbs.	4 horns, after cleaning
3C	4	40 lbs.	0 horns, after cleaning
3H	4	35½ lbs.	0 horns, after cleaning
11D	4	35½ lbs.	0 horns, after cleaning
11G	4	38 lbs.	0 horns, after cleaning
21C	4	34 lbs.	0 horns, after cleaning
21H	4	35 lbs.	0 horns, after cleaning

Figure III - 3 Compartment Ash Pulling Times - Pre Test Data

Note: Differences in ash pulling times between one curve and another are due to boiler load fluctuations and time between ash pulling cycles. The intent of the Figure is to show the time trends of the ash pulling cycle.

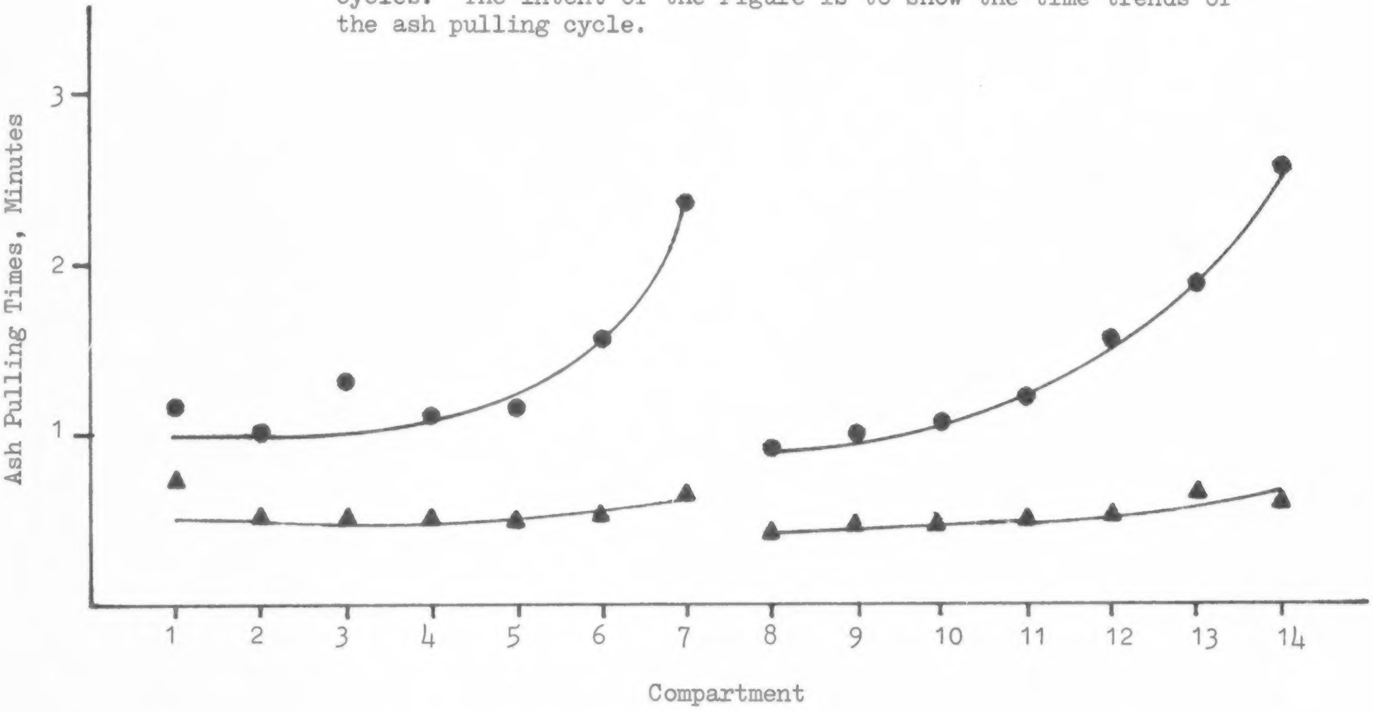

Figure III-4 Compartment Ash Pulling Times During One and Two Horn Operation

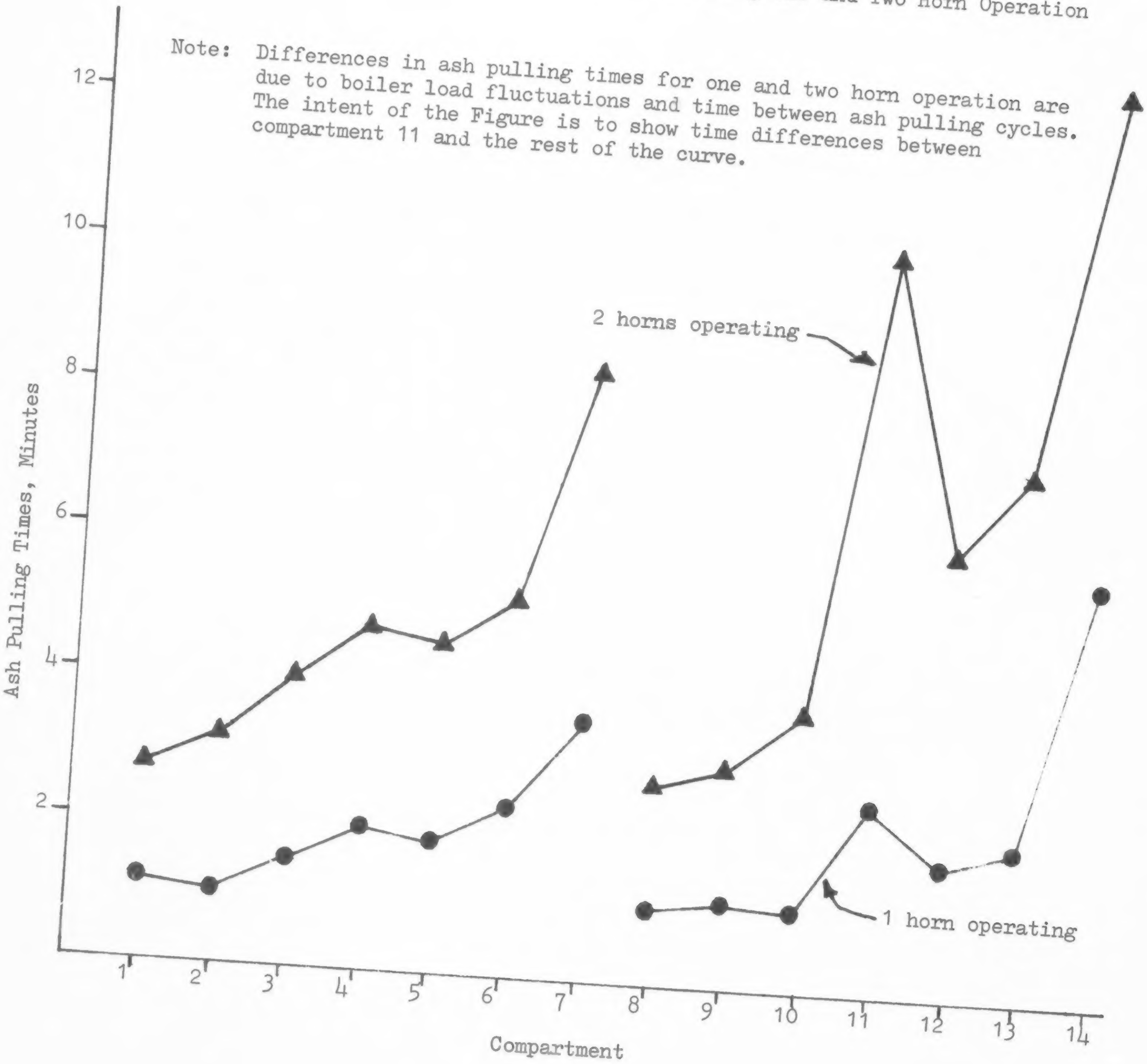

Note: Differences in ash pulling times for one and two horn operation are due to boiler load fluctuations and time between ash pulling cycles. The intent of the Figure is to show time differences between compartment 11 and the rest of the curve.

Figure III - 5 Compartment Ash Pulling Times After Two Weeks of Continuous Two Horn Operation

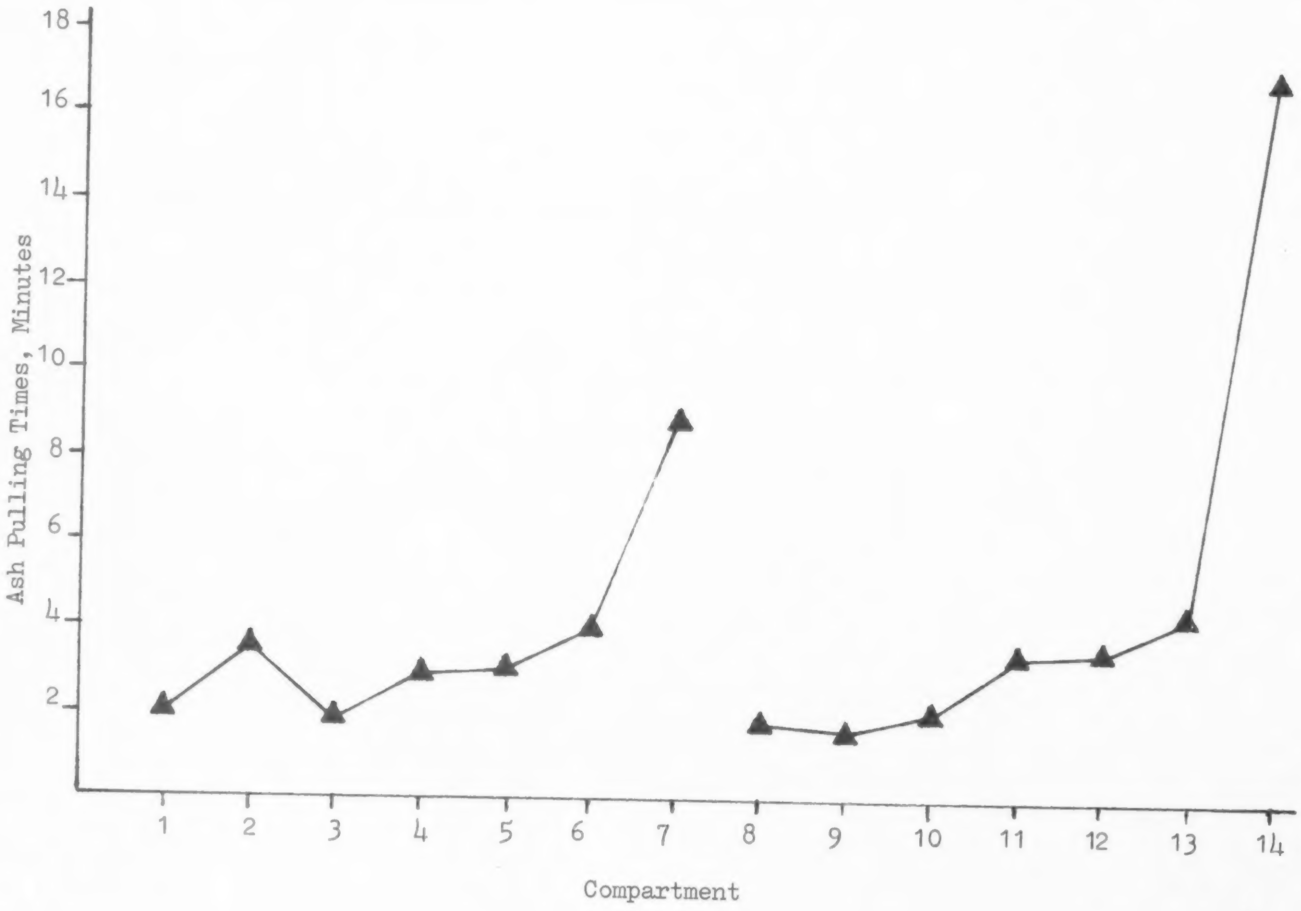

FIGURE III-6. COMPARTMENT TUBE SHEET PRESSURE DROP AT FULL LOAD - NO HORNS OPERATING

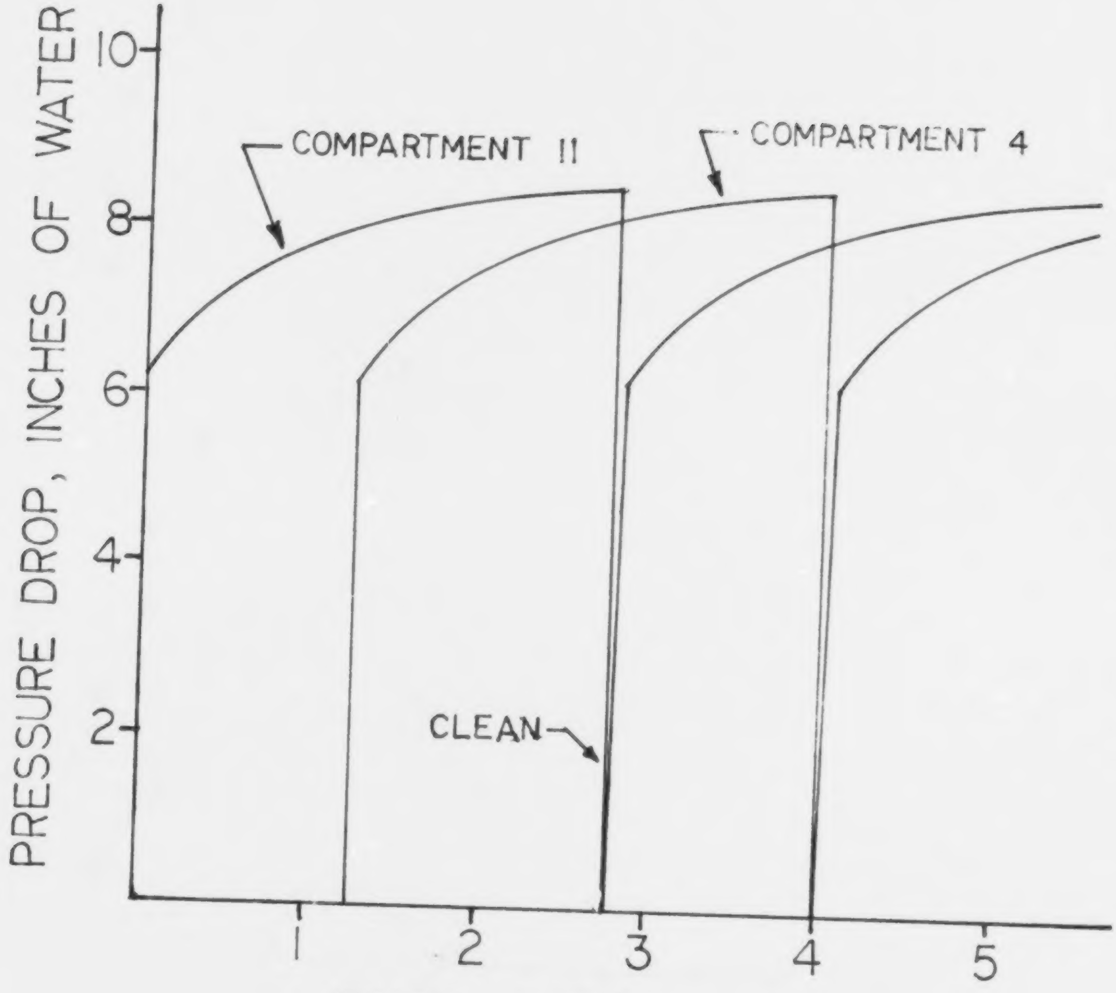

cleaning (see Figure III-7). It was assumed that the pressure drop across the tube sheet would increase at the same rate as in the compartment without sonic horns. Pressure drop increased at a more rapid rate until it was equal to the pressure drop in compartment 4 immediately before compartment 11 cleaned. This phenomenon can be explained because accompanying the decrease in pressure drop there was a substantial increase in flow through the test compartment. This indicates that a greater amount of fly ash was being collected in the compartment with sonic horns than in the other compartments, hence, the rapid increase in pressure drop.

On February 25, 1982, two horns, one in the northeast and one in the southwest corner of the test compartment were operated. Pressure drop across the tube sheet was reduced to 3.0 inches VWC immediately after the compartment cleaned. Again the increased rate of pressure drop decay was observed.

During this time period, unit 3 was loaded as P.S.Co. system requirements mandated. This served two purposes; first, to allow the baghouse test compartment to experience a more "real world" environment, and secondly to allow the test compartment time to seek its own steady state operating point. Pressure drop across the tube sheet increased to 4 inches VWC at full load immediately after cleaning after about one week of continuous two horn operation. This pressure drop remained the same for the remainder of the two horn test period (approximately 1 month). It was felt that steady state operation had been reached.

Figure III-8 shows tube sheet pressure drop versus time for two horn operation after steady state operation had been reached. The dashed line in the Figure represents a corrected pressure drop curve which assumes that the pressure drop decay would be similar to the curve of the compartment with no horns operating if sonic horns were installed in all fourteen compartments.

During baghouse operation without sonic horns, flange to flange pressure drop measured between 9 and 9.5 inches VWC or approximately ½ to 1 inch VWC higher than the tube sheet differential pressure immediately before the compartment cleaned. It is assumed that the flange to flange pressure drop curve would be similar in shape with the use of sonic horns in all fourteen compartments to the pressure drop curve without sonic horns. This would equate to a flange to flange pressure drop of 6.5 to 7 inches VWC if two sonic horns were installed in all fourteen compartments. This represents approximately a 27 percent decrease in flange to flange pressure drop if the horns were installed in all fourteen compartments.

We believe that this is a conservative estimate of performance improvement because of the significant increase in flow through the test compartment. A portion of the pressure drop through the compartment could be due to the fact that the test compartment flow was higher than the flow in the remaining 13 compartments (discussed below). When sonic horns are installed on all fourteen compartments, the flow will be more evenly distributed throughout the baghouse and the pressure drop across the tube sheets should decrease.

It is interesting to note that the horns were accidentally operated at

Figure III - 7 Compartment Tube Sheet Pressure Drop at Full Load - One Horn Operating

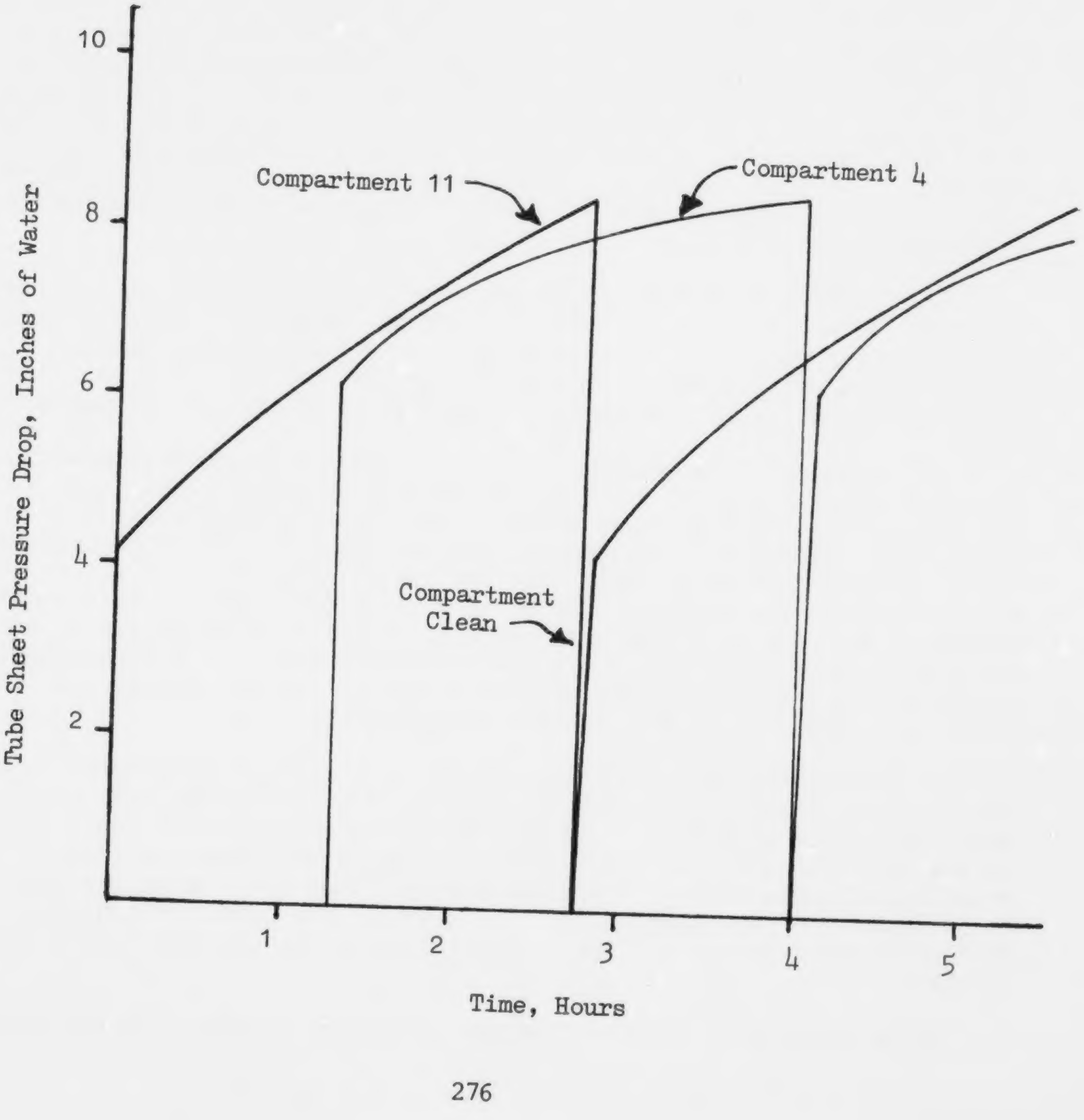

FIGURE III-8. COMPARTMENT TUBE SHEET PRESSURE DROP AT FULL LOAD - TWO HORN OPERATION

* Theoretical curve assumes the pressure drop curve would be similar in shape to the pressure drop curve with no horns operating if the sonic horns were installed on all fourteen compartments.

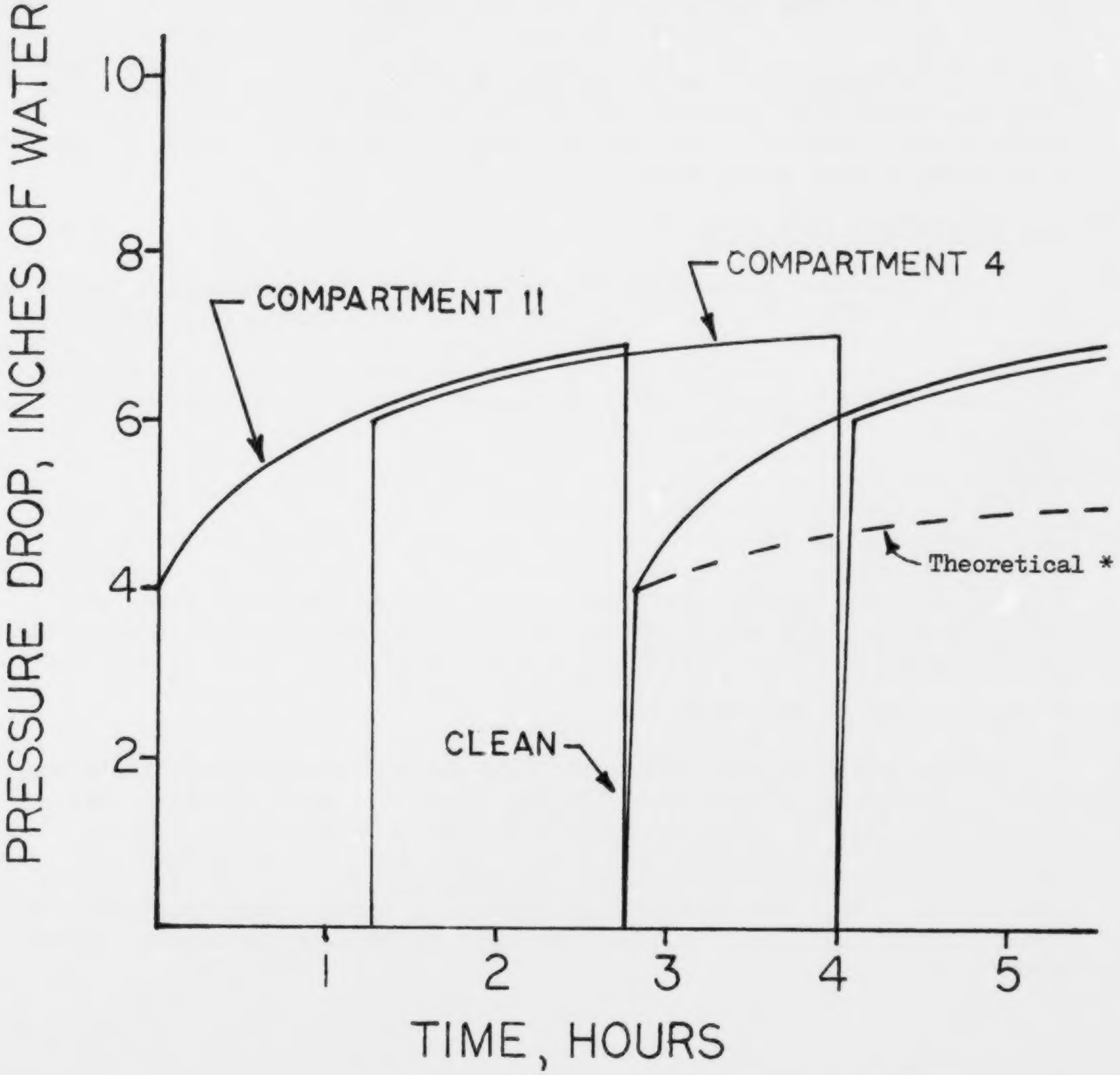

the wrong time during the two horn test period. Because of a mistaken adjustment in the timing sequence that operated the horns, the horns were operated during the initial settling period of the compartment clean (no reverse air). Pressure drop across the tube sheet in compartment 11 returned to its original no horn levels after two days of operating in this manner. With the timing sequence problem solved, the horns were again operated during the reverse air period. Tube sheet pressure drop returned to 4 inches VWC immediately after cleaning.

On March 29, 1982, all four horns in the test compartment were operated with the unit at full load. Pressure drop across the tube sheet of the compartment with sonic horns was 5 inches VWC immediately after cleaning as opposed to 7 inches VWC in the test compartment without sonic horns immediately after cleaning. The significance of this data is somewhat questionable because at the time the boiler was operating on a different coal than that which was used in the beginning of the test program. This new coal has been known to significantly increase the operating flange to flange pressure drop of the baghouse and on that day, flange to flange pressure drop was recorded at 9.5 to 10 inches VWC. It can be seen from Figure III-9 that the sonic horns did reduce the pressure drop across the tube sheet in the test compartment when compared to the pressure drop across the tube sheet of the compartment without sonic horns.

Test Compartment Exit Flows

Exit flows were measured in the outlet ducts of compartment 4 and 11 using a S-type pitot tube. Data was recorded at full load before any horns were operated and flow through both test compartments was from 23,600 acfm immediately after cleaning to 15,850 acfm immediately before each compartment cleaned (see Figure III-10). A summary of test compartment exit flows is presented in Table 3 and is also shown in Figures III-11, III-12, and III-13. It can be seen that flow through the test compartment with sonic cleaning did increase significantly and conversely, flow through the test compartment without sonic horns decreased. It is assumed that flow through the remaining compartments in the baghouse also decreased due to the 15.3 percent increase in flow through compartment 11. The greatest proportion of flow followed the path of least resistance; through the compartment with sonic cleaning. This would explain the rapid increase in tube sheet pressure drop noted earlier. With the installation of sonic horns in all fourteen (14) compartments, flow will be more evenly distributed and will return to the original no horn levels.

Because pressure drop across the tube sheet achieved steady state operation at an acceptable level with the use of two (2) sonic horns, it was decided that two (2) horns per compartment would be the minimum amount of horns required for successful sonic cleaning. Four (4) sonic horns per compartment would have the advantage of more rapid removal of the initial cake buildup. Once the initial cake buildup is removed from the filtering elements, four horns show no appreciable improvement in compartment performance.

Table 3 - Test Compartments Exit Flows - Immediately Before and After Cleaning

	Immediately After Cleaning		Immediately Before Cleaning	
	Compartment 11	Compartment 4	Compartment 11	Compartment 4
0 Horns	23,600 acfm	23,600 acfm	15,800 acfm	15,800 acfm
1 Horns	29,900 acfm	22,400 acfm	17,500 acfm	17,500 acfm
2 Horns	27,200 acfm	20,800 acfm	15,800 acfm	13,500 acfm
4 Horns	26,500 acfm	20,100 acfm	15,800 acfm	15,800 acfm

Figure III- 9 Compartment Tube Sheet Pressure Drop at Full Load - Four Horns Operating

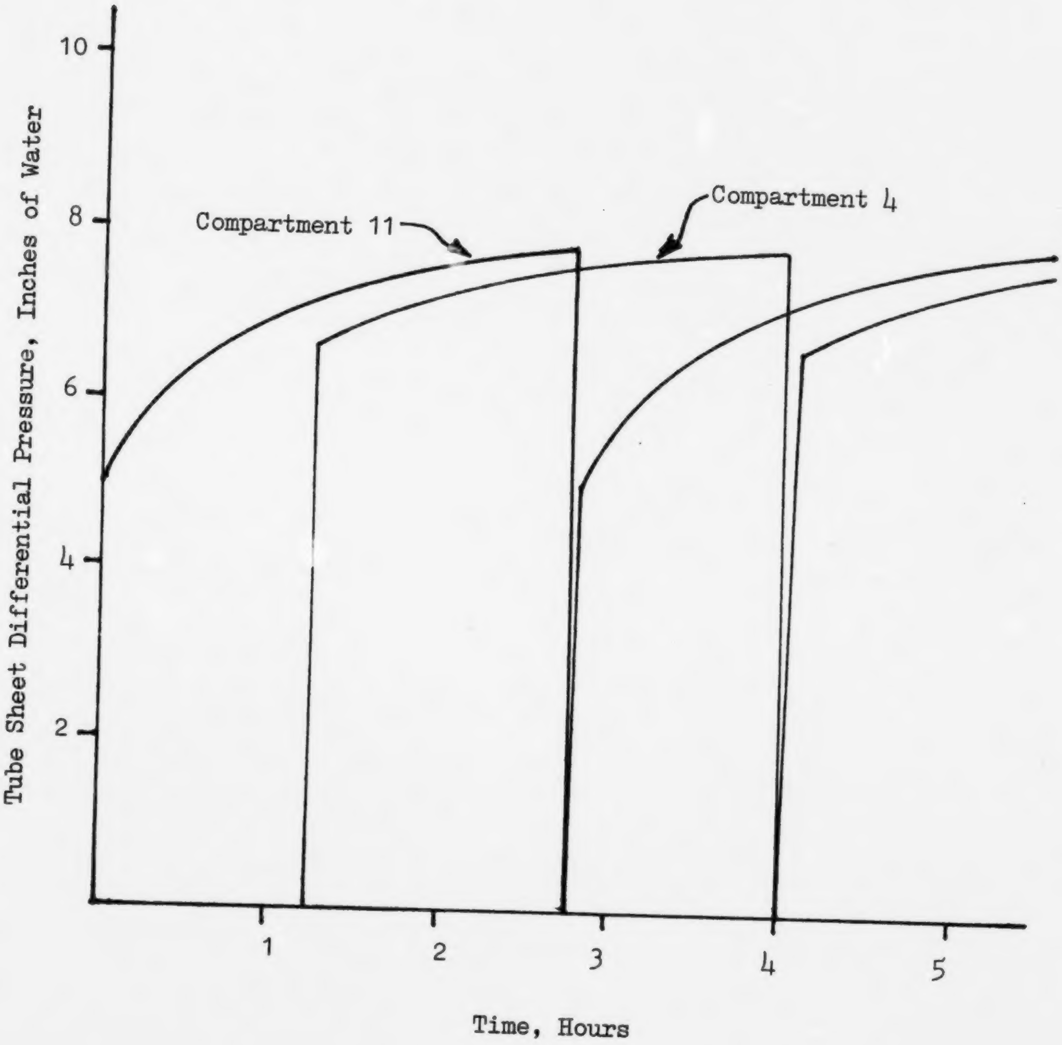

Figure III- 10 Compartments 4 and 11 Exit Flow vs Time - No Horns Operating

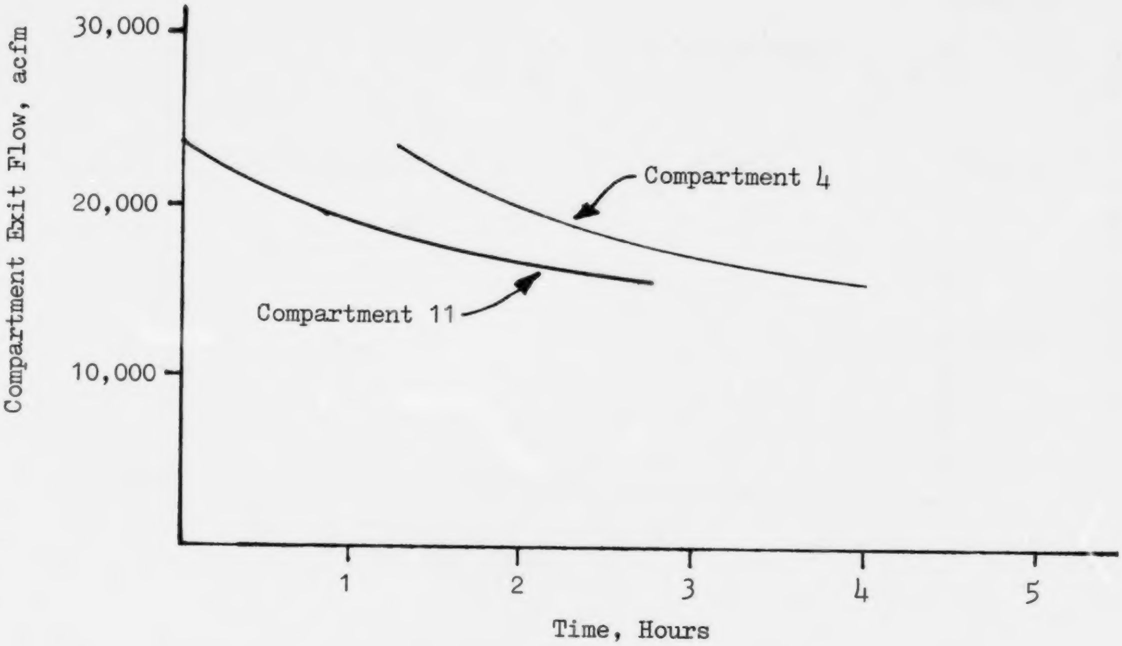

Figure III-11 Test Compartments Exit Flows vs Time - One Horn Operating

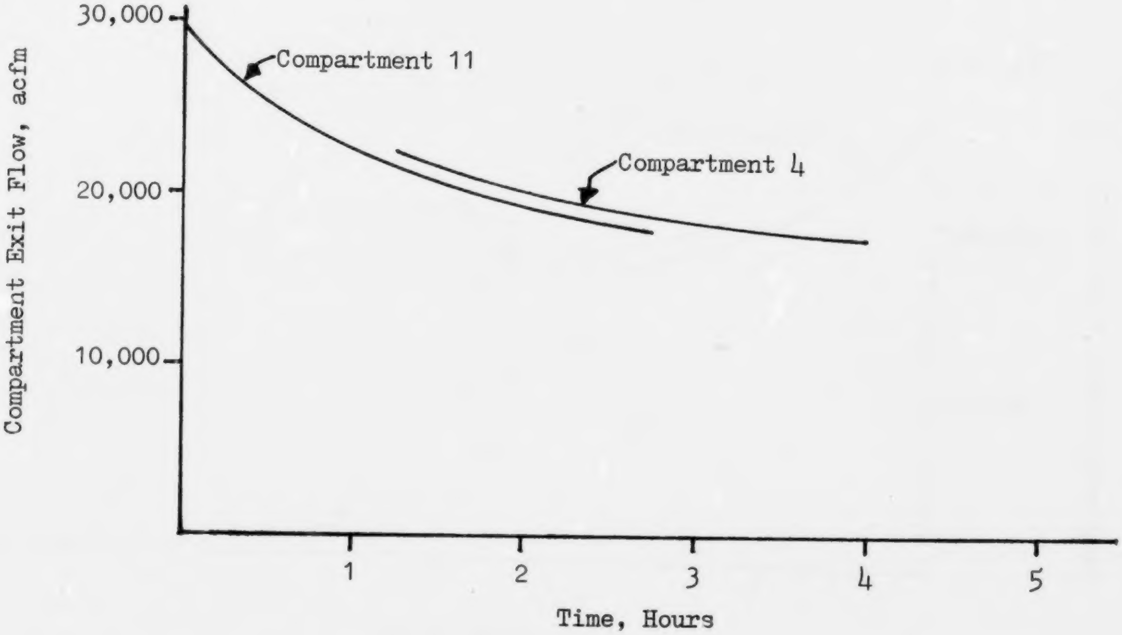

Figure III-12 Test Compartments Exit Flow vs Time - Two Horn Steady State Operation

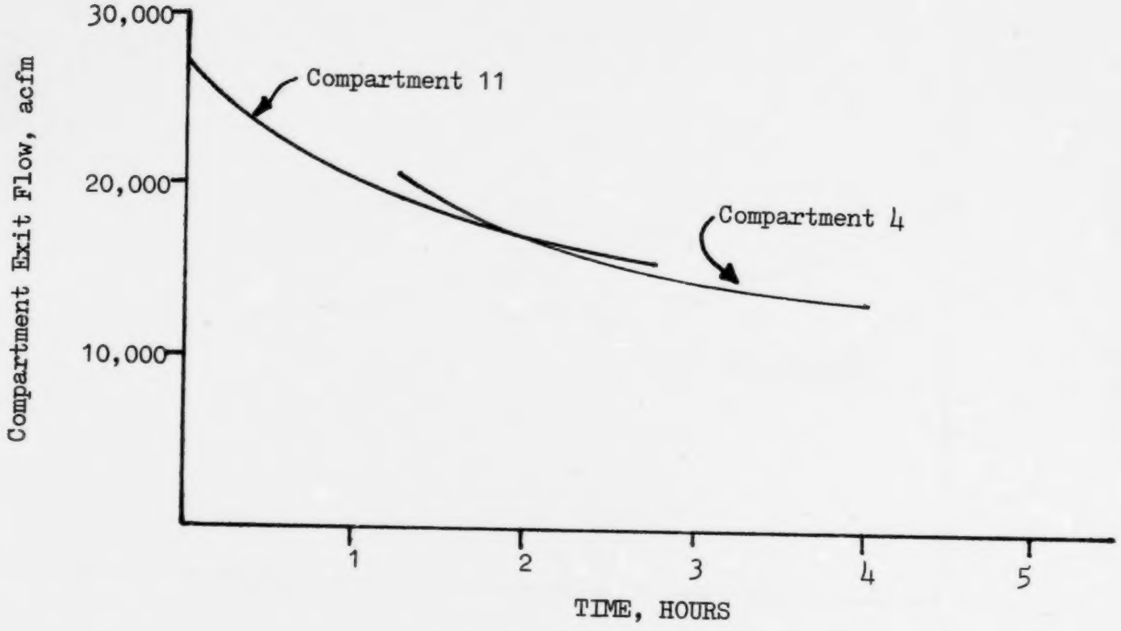

Figure III-13 Test Compartments Exit Flows vs Time - Four Horns Operating

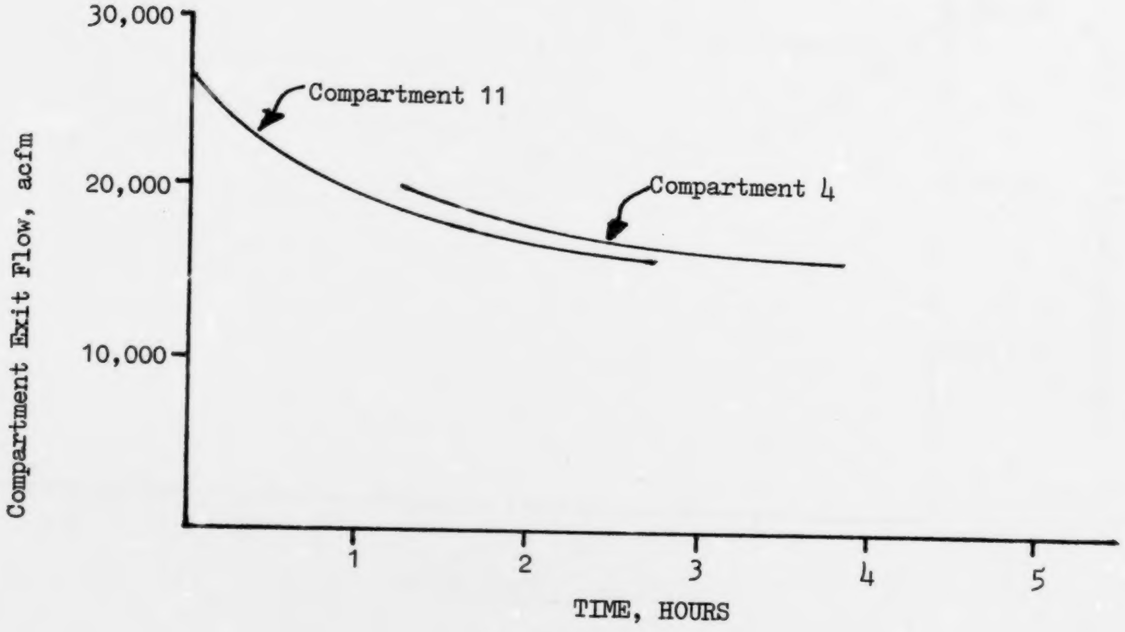

CONCLUSION

Because of boiler instabilities and resultant load limitations, along with the high costs associated with operating Induced Draft (ID) fans at high pressure drops, the need to reduce the operating flange to flange pressure drop of a FFDC is imperative. Assuming the 27 percent decrease in flange to flange pressure drop noted earlier, a savings of approximately $52,400 per year could be realized (Reference 3). It is estimated that the total cost of purchasing and installing two horns in each of the fourteen baghouse compartments would be $53,000. With the I.D. fan cost savings alone, this investment would pay for itself in one year. Added savings would be realized in the elimination of the costs associated with the labor required for periodically hand clapping the filtering elements to remove the cake buildup.

The use of sonic air horns as an assist to reverse air cleaning is an inexpensive and effective means of reducing the pressure drop across the tube sheet of an operating baghouse. As a result of the information obtained from this test program, Public Service Company of Colorado has purchased and installed two sonic air horns in each of the fourteen compartments on Arapahoe Unit #3 FFDC. Preliminary test results indicate a significant reduction in flange to flange pressure drop.

A test program has been initiated that will not only determine the net reduction in flange to flange pressure drop of Arapahoe Unit #3 FFDC, but will determine if higher operating air-to-cloth ratios are obtainable with the use of sonic cleaning. If higher air-to-cloth ratios are achievable while still maintaining acceptable pressure drops, significant capital savings could be realized on new baghouse installations through the reduction of the number of compartments and/or total filtering area required for the successful operation of a FFDC.

The work described in this paper was not funded by the U.S. Environmental Protection Agency and therefore the contents do not necessarily reflect the views of the Agency and no official endorsement should be inferred.

REFERENCES

1. "Nodular Deposits in Fabric Filters", Robert F. Lembach and Gaylord W. Penny, Journal of the Air Pollution Control Association, August, 1979.
2. Letter, Ronald F. Ross, Joy Industrial Equipment Company, to Gordon Schott, P. S. Co., April 8, 1980.
3. "Evaluating Baghouse Systems for Energy Efficiency", Plant Energy Management, February, 1982.

APPENDIX A

TEST LOG

Date	
2/22	Load 46 MW. Final setting up of horns. Obtained base data.
2/23	Load 45 MW. Operated 1 horn in NE corner of compartment. Dropped 3 inches in ΔP.
2/24	Load 45 MW. Continued 1 horn test. Pulled ash and timed.
2/25	Load 46 MW. Operated 1 horn NE corner. At 2:30 p.m. 2 horns operated NE and SW corners. Dropped 1 inch in ΔP.
2/26	Load 46 MW. Continued 2 horn test. Pulled ash and timed.
3/1	Load variable. Compartment isolated took bag weights. Compartment back in service. Continue with 2 horn test (NE and SW corners) for next two weeks.
3/2	Load variable. Continued 2 horn test.
3/3	Load variable. Continued 2 horn test.
3/4	Load variable. Continued 2 horn test.
3/5	Load variable. Continued 2 horn test.
3/8	Load 46 MW. Continued 2 horn test. Pulled ash and timed.
3/9	Load variable. Continued 2 horn test.
3/10	Load variable. Continued 2 horn test.
3/11	Load variable. Inspected compartment 4 for bag leaks. Found nothing wrong. Stood in compartment 4 while the horns operated in compartment 11 to see if there was any sound attenuation to explain the decrease in thimble sheet ΔP in #4. Felt no excess vibration while horns were operating.
3/15	Load 46 MW. Two horn test continues. Pulled ash and timed. Switched out wrong Agastat so horns were operating before reverse air. Horns had no effect on tube sheet ΔP. Agastats fixed.
3/16	Load variable. Continued 2 horn test.
3/17	Load variable. Continued 2 horn test. Took bag samples in 4 and 11. Weighed bags in both compartments. All data taken before cleaning.

3/18	Load variable. 2 horns operating. Cut samples and weighed bags in compartment 11 after cleaning. Took coal sample.
3/19	Load variable. 2 horns operating.
3/22	Load 46 MW. 2 horns operating. Pulled ash and timed.
2/23	Load variable. Continued 2 horn test.
3/24	Load variable. Continued 2 horn test.
3/25	Load variable. Continued 2 horn test.
3/26	Load variable. Continued 2 horn test.
3/29	Load 46 MW. Continued 2 horn test. At approximately 1:00 p.m. operating 4 horns.
3/30	Load variable. Continued 4 horn test.
3/31	Load variable. Continued 4 horn test.
4/1	Load variable. Continued 4 horn test.
4/2	Load variable. Continued 4 horn test.
4/5	Load 46 MW. Continued 4 horn test.
4/6	Load variable. Continued 4 horn test.
4/7	Horns shut off at 7:00 a.m. Weighed bags in compartment 11. No leaks found in compartment 11.
4/8	Load variable. No horns.
4/9	Load variable. No horns.
4/10	Load 46 MW. No horns. Pulled ash and timed.

"ELECTROSTATIC STIMULATION OF REVERSE-AIR-CLEANED FABRIC FILTERS"

by: D. A. Furlong and G. P. Greiner
ETS, Inc.
Suite C-103, 3140 Chaparral Dr., SW
Roanoke, VA 24018

D. W. Van Osdell
Research Triangle Institute
Research Triangle Park, NC 27709

L. S. Hovis
U. S. Environmental Protection Agency
Industrial Environmental Research Laboratory
Research Triangle Park, NC 27711

ABSTRACT

The concept of electrostatic stimulation of fabric filtration (ESFF) has been investigated on a slipstream of a pulverized-coal-fired boiler using reverse-air-cleaned, woven-fiberglass fiber bags. Operation was demonstrated using ESFF at a gas-to-cloth ratio (G/C) of 6 ft/min.[1] An un-electrified control house was simultaneously operated at a G/C of 3 ft/min. Under these conditions, the ESFF house maintained a pressure drop equal to or less than the control baghouse. In addition to reducing the filter cake pressure drop, ESFF was observed to apparently have long term benefits in preventing irremovable dust buildup in the fabric.

This paper has been reviewed in accordance with the U. S. Environmental Protection Agency's peer and administrative review policies and approved for presentation and publication.

---

[1] Readers more familiar with metric units may multiply ft/min by 0.305 for the equivalent m/min.

INTRODUCTION

This paper describes development activities from May 1981 to March 1982 using a pilot scale, slipstream fabric filter employing electrostatic stimulation of fabric filtration (ESFF).

The ESFF concept is based on laboratory scale tests at the Textile Research Institute (TRI) as reported by Lamb and Costanza.(1) The TRI concept of ESFF consists of applying an electric field parallel to the surface of the fabric through use of electrodes located at the upstream surface of the filter fabric. Figure 1 is a schematic of a TRI electrode "harness" located on the outside of a pulse cleaned bag and electrically connected so that alternate electrode wires are at high electrical potential, producing an electric field of 2 to 4 kV/cm.

A team composed of Research Triangle Institute (RTI), ETS, Inc., and TRI, under contract to the U.S. EPA, is evaluating this concept at pilot scale. The pilot scale program was started in October 1979. The first year's primary objective was to verify the TRI laboratory results under actual flue gas conditions. EPA, as manager, and RTI, as prime contractor, have directed the technical effort and performed initial electrical hardware development and construction. ETS, Inc. has designed, built, installed, and is operating the pilot unit. ETS and RTI are further developing the ESFF hardware. The pilot plant is installed on a slipstream of a pulverized-coal boiler at the E. I. DuPont de Nemours & Company plant, Waynesboro, Virginia.

The pilot unit was designed to operate in either the pulse-jet (outside collection) or reverse air (inside collection) cleaning mode. The baghouses were first operated as pulse-jet collectors. The principal conclusions of the pulse-jet work, as reported previously,(2,3) were:

1) At any given face velocity, the pilot ESFF baghouse had a reduced residual pressure drop and a reduced rate of pressure drop increase when compared to the pilot conventional baghouse.

2) The pilot ESFF baghouse could be operated in a stable fashion at face velocities up to about twice the stable operating conditions for the pilot conventional baghouse.

3) A reduction in total annualized cost of about 30 percent was estimated for an industrial boiler application utilizing an ESFF baghouse at twice the conventional face velocity.

4) Particulate emissions from the two baghouses were not significantly different.

5) The electrode configuration developed in the course of the study, a combination pulse-jet cage/electrode, located on the downstream side of the filter fabric, was feasible and had potential for commercial use.

In May 1981, the pilot plant was converted to reverse-air cleaning. This paper summarizes the development activities and reports preliminary results and conclusions based on the work from May 1981 to March 1982.

THE PILOT SYSTEM

The pilot system provides the capability of simultaneous monitoring of the ESFF effect through use of two identical baghouses receiving their inputs from a common slipstream. One baghouse is supplemented with electrical enhancement equipment; the other is not.

Figure 2 is an isometric drawing of the pilot unit, and Figure 3 is the system schematic. Each baghouse can accept up to 9 reverse-air cleaned bags each 20.3 cm (8 in.) in diameter and 224 cm (8 ft) long, or up to 13 pulse cleaned bags, 11.7 cm (4-5/8 in.) in diameter and 224 cm (8 ft) long.

The provision of parallel control and experimental units is an important feature of the pilot plant in that it permits operation in either of two modes, parallel or separate. In parallel operation, both baghouses have the same inlets, compensating for the cumulative effect of varying inlet conditions. Any differences between the two units, either intentional or unintentional, can be evaluated by parallel operation. Future work is planned where separate tests will be conducted in each baghouse after sufficient experience is in hand to negate the further need of a "control" baghouse.

The pilot unit is installed on a slipstream from an industrial boiler baghouse. Four pulverized-coal boilers are used with a normal load of about 160,000 kg/hr (350,000 lb/hr) of steam. The coal fed to the boilers changes frequently, with sulfur content varying from less than 1 percent to about 2 percent, and ash content ranging from 5 to 15 percent. The boilers are sometimes co-fired with No. 2 or No. 6 fuel oil. Inlet dust loadings at the pilot plant have varied from 0.6 to 5 g/scm (0.25 to 2 gr/scf); 0.7 g/scm (0.3 gr/scf) is typical. The mass mean diameter of dust particles averaged 6.3 μm.

ESFF TEST HARDWARE

The electrical power requirements of the ESFF system are very low. The power consumption measured by TRI and confirmed in the pilot system is about 1 W/m^2 (0.1 W/ft^2) of cloth. This ESFF power requirement is equivalent to approximately 0.1 in. of water pressure drop at a G/C of 6 ft/min.

The electrical system used in the pilot unit consisted of a variable DC power supply (0 to 20 kV at 5 mA) for each of five power supply networks. Current and primary voltage were measured separately in each network.

Current limiting and meter protection circuits were used.

The electrode designs utilized to date have been based on the combination cage/electrode developed during the pulse-jet work. Again, these cages were placed on the downstream (clean) side of the fabric, so as to not restrict cleaning of the bag and to avoid dirt buildup on the cage. These cages (patterned after the pulse-jet cage/electrode, constructed of welded 1/8-in. (0.318 cm) rods, and referred to as "rigid cages") exhibited two problems: first, fabric wear was observed at the insulator locations; and second, the wire spacing of 2.5 cm coupled with insulator limitations restricted field strength to about 4 kV/cm. New cages were fabricated using 34 1/8-in. diameter electrodes (1.68 cm spacing). These electrodes were held in place by woven fiberglass straps having sewn-in pockets. These cages are referred to as flexible cages, since the electrode/strap assembly is quite flexible prior to installation on the bags.

Fiberglass bags were used for the entire reverse-air test series. The bags were 20.3 cm (8 in.) in diameter and 224 cm (8 ft) long; no anti-collapse rings were used. These bags were made of J. P. Stevens Style No. 648, 17 oz (482 g) texturized fiberglass fabric with a 10 percent Teflon B finish. Each bag was tensioned to 40 lb (18 kg) using a conventional tensioning spring.

RESULTS AND OBSERVATIONS

Electrostatic stimulation of fabric filtration has two primary effects on filter behavior when compared to conventional filtration at the same G/C: (1) the average pressure drop is reduced through a combination of lower residual pressure drop and a reduced pressure drop rise during a filtering cycle; and (2) the ESFF baghouse can operate at a higher stable G/C.

To define and compare the effects on pressure drop rise during a filtering cycle, a figure of merit called PDR (pressure drop ratio) is used. PDR compares the beginning and ending ΔP across one cleaning cycle using electrostatic enhancement with the comparable ΔP change without electrostatic enhancement.

PDR is defined as:

$$\frac{(\Delta P_f - \Delta P_r)\ \text{ESFF}}{(\Delta P_f - \Delta P_r)\ \text{control}}$$

where ΔP is the pressure drop across the bags,

f refers to the final state (just prior to cleaning), and

r refers to the residual state (just after cleaning).

For an idealized filter cycle, in which the bag pressure drop increases linearly with time and for constant dust loading from ΔP_r to ΔP_f, it can be shown that:

$$PDR = \frac{(K_2)\ \text{ESFF}}{(K_2)\ \text{control}}$$

where K_2 is the specific cake resistance.

PDR, then, is the ratio of the flow resistance of a dust cake collected by an ESFF system to that collected by a conventional fabric filter.

Figure 4 presents typical pressure drop recordings for both the conventional and ESFF pilot baghouses in reverse-air operation. The rate of increase of pressure drop in the ESFF baghouse when compared to the conventional pilot baghouse is evident. PDR can be seen to vary depending on the length of the filter cycle, and thus is most useful for comparison of two baghouses operating with the same cleaning cycle. As the two baghouses were operating at the same face velocity when these data were obtained, the ESFF baghouse also has a reduced residual pressure drop. Thus, the ESFF effect is to produce a lower average pressure drop when operated at the same filtering velocity.

The reverse-air baghouse operation was started up with a break-in period of about 1 week at a G/C of 2 ft/min, with no electrical field in the ESFF baghouse. During this period, the two baghouses exhibited essentially identical pressure drop characteristics, indicating that the two baghouses could be analyzed as identical baghouses in parallel. The electrical field was then put on the bags, and was left on almost continuously for the next several months.

Figures 5 and 6 present a chronological summary of the results during May and June 1981, using reverse-air bag cleaning. Field strength and gas-to-cloth ratio were independent variables. The PDR and average pressure drop were measured for each filtering cycle and averaged for the day. The gas-to-cloth ratio was progressively increased from 2 to 6 ft/min for the ESFF baghouse; however, the control house could not operate stably above a G/C of 4.5 ft/min. Note also that on May 12 and 13, when the electric field was removed, the average ΔP of the ESFF house rapidly approached that of the control house. Note particularly, that from June 10 to June 30, a 21-day period of continuous 24-hour operation, the ESFF house operated at a G/C of 6 ft/min, with an average ΔP between 6.4 and 7.1 in. (16.3 and 18.0 cm) of water, while the control house operated at a G/C of only 3 ft/min and yet had an average ΔP of 7.4 to 8.3 in. (18.8 to 21.1 cm) of water. Stated another way, ESFF allowed a doubling of the velocity without a major change in pressure drop.

Figure 6 demonstrates the ability of an ESFF baghouse to operate at a higher stable G/C. Note that from June 9 to 13, the control baghouse demonstrated inability to operate stably at a G/C of 4.5 ft/min; subsequently, it was reduced to a G/C of 3 ft/min. Simultaneously, the ESFF baghouse operated at a G/C of 6 ft/min from June 10 to 30.

Based on these encouraging results, a series of tests were undertaken to evaluate the effects of field strength and gas-to-cloth ratio on pressure drop characteristics.

Figure 7 summarizes the evaluation of field strengths of 3 and 4 kV/cm on average ΔP over a G/C ratio range of 1 to 6 ft/min. This test series used the rigid cages; hence, fields above 4 kV/cm were not possible. These data show graphically the benefit derived from the ESFF effect. The conventional baghouse had a higher average ΔP where it was capable of stable operation. Increasing the electric field from 3 to 4 kV/cm does not appear to offer an advantage.

By the end of this test series, the disadvantages mentioned previously for the rigid cage had become evident, and it was necessary to install new bags in the ESFF pilot baghouse. Figure 8 is a chronological summary of testing with new bags and the new flexible cages at field strengths up to 6 kV/cm. After a break-in period at a G/C of 2 ft/min on July 26 through 28, the G/C was increased to 4 ft/min and an electric field of 4 kV/cm resulted in an immediate decrease in the average ΔP compared to the control house. Figure 9 summarizes the results of this initial approximately 1 month test period with the flexible cages. These results indicate two things. First, little or no benefit was derived from field strengths above 3 kV/cm. Second, note the results at 0 kV/cm. As the ESFF bags were relatively new while the conventional bags had been in use since the beginning of the test program, some difference in the ΔP response of the two bag sets at zero field was expected. However, the magnitude of the difference was surprising, and suggested that something other than the electric field might be causing at least a portion of the ΔP advantage being shown by the ESFF baghouse. An extensive investigation of the situation was undertaken, and several factors which served to exaggerate the advantage of the ESFF baghouse were identified. A concise explanation is still in the process of being defined; however, three contributing features stand out so far:

(1) As is well known, reverse-air baghouses are extremely sensitive to cleaning parameters. Although efforts had been made to favor the control house by cleaning it last, this, in fact, may have favored the ESFF house, possibly by giving it a pre-coat after cleaning. In addition, a slight leak below the tubesheet in the control baghouse, balanced by a similar sized leak above the tubesheet in the ESFF baghouse, raised the effective gas-to-cloth ratio in the conventional baghouse. These factors were quantified by experimentation, and their mathematical inclusion in the data analysis indicated that the ESFF baghouse at zero field still had a lower average ΔP than did the conventional baghouse. The same corrections reduce the size of the advantage which the data had indicated for the ESFF baghouse at the various field strengths.

(2) In May, as shown in Figure 5, the field was removed after 2 weeks

of operation, then the ΔPs at zero field strength were essentially equal. In September, after 2 months of operation, the ESFF bags are better even with no field. This certainly suggests the possibility of a long term, cumulative effect of the electric field by reducing the residual ΔP by avoiding the buildup of un-removable dust accumulations deep in the fabric weave.

(3) During the investigation into the zero field behavior, the ESFF bags were operated for approximately 2 months without the electric field. It was noted that, after this zero field operation, the low residual ΔP results which were obtained during the early operation were no longer observed. The hypothesis is that the long term lack of an electric field allows the fabric to build an interstitial dust layer which cannot be removed by normal means, leading to the increased residual ΔPs. A return to new fabric will try to verify this observation.

CONCLUSIONS

Although the evaluation of electrostatic augmentation of reverse-air-cleaned bags is not as yet complete, the observations to date of primary significance are:

(1) Starting with new fabrics, ESFF operation for an extended period (21 days) at a G/C of twice (6 vs. 3 ft/min) that of the control house was demonstrated at comparable or lower pressure drops (Figure 6).

(2) Interruption of the electric field for periods of 1 to 2 days did not eliminate most of the benefits of ESFF. Removal of the field for several months did diminish the benefits of ESFF upon reapplication of the field.

(3) ESFF appears to maintain the fabric in a "near new" condition relative to entrapped particles within the fabric. It is, of course, these entrapped particles that result in the residual ΔP after cleaning. This observation is consistent with earlier work, indicating that under ESFF conditions more particulate is captured near the upstream side of the fabric, and penetration into the fabric is reduced. Thus ESFF prevents, or at least significantly retards, the buildup in residual ΔP.

FUTURE WORK

Both the rigid and the flexible cages are recognized to have practical and economic limitations for full-scale filter use; hence, electrode design is continuing. The most promising concept at this time for reverse-air-cleaned applications appears to be a "woven" electrode, although this has not as yet been tested in the pilot system. Woven electrodes consist of conductive yars woven into the warp of the fabric at the desired electrode spacing. Yarns consisting of stainless steel filaments, graphite filaments, or a graphitized high temperature nylon are now being investigated. These conductive yarns, and the techniques for weaving them, have been previously used to produce anti-static fabrics for both filtration applications and for carpets. Woven electrodes in both glass and Teflon fabrics are being investigated.

ACKNOWLEDGEMENTS

This work was supported by EPA Contract 68-02-3186 from Industrial Environmental Research Laboratory, Research Triangle Park, NC. The assistance provided by E. I. duPont de Nemours and Company, Inc. is gratefully acknowledged. The pilot unit was located at their Waynesboro, Virginia, plant. Teflon® fabric was donated to the test program by DuPont.

REFERENCES

1. Lamb, G. E. R., and P. A. Costanza. A Low-Energy Electrified Filter System, Filtration and Separation 17:319, 1980.

2. Van Osdell, D. W., G. P. Greiner, G. Lamb, and L. S. Hovis, "Electrostatic Augmentation of Fabric Filtration", In proceedings of the Third Symposium on the Transfer and Utilization of Particulate Control Technology, Volume I. Control of Emissions from Coal-Fired Boilers, EPA-600/9-82-005a, July 1982.

3. Greiner, G. P., D. A. Furlong, D. W. Van Osdell, and L. S. Hovis. "Electrostatic Stimulation of Fabric Filtration", JAPCA, 31:1125-1130, 1981 (presented at the 74th Annual Meeting of the APCA, Philadelphia, Pennsylvania, June 1981).

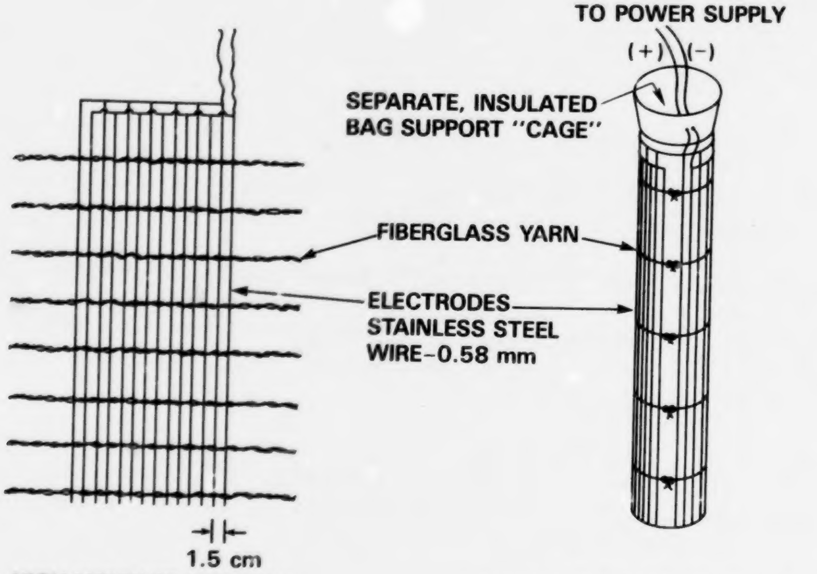
TO POWER SUPPLY
(+)
(−)
SEPARATE, INSULATED BAG SUPPORT "CAGE"
FIBERGLASS YARN
ELECTRODES STAINLESS STEEL WIRE−0.58 mm
1.5 cm

HIGH VOLTAGE HARNESS

HARNESS INSTALLED ON BAG

Figure 1

TRI HARNESS

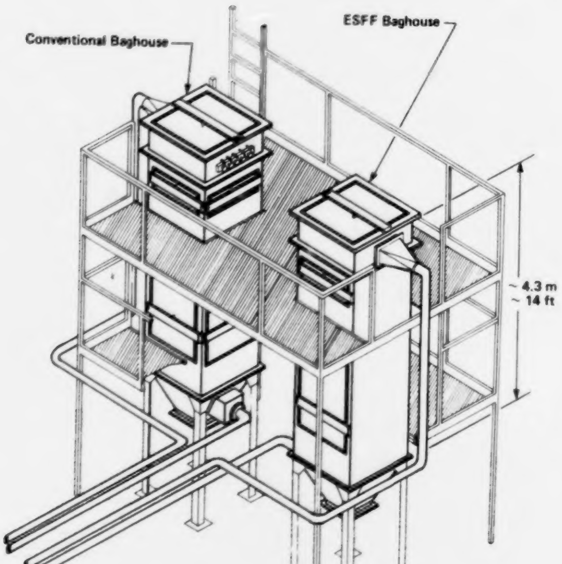
Conventional Baghouse
ESFF Baghouse
~ 4.3 m
~ 14 ft

Figure 2

PILOT PLANT

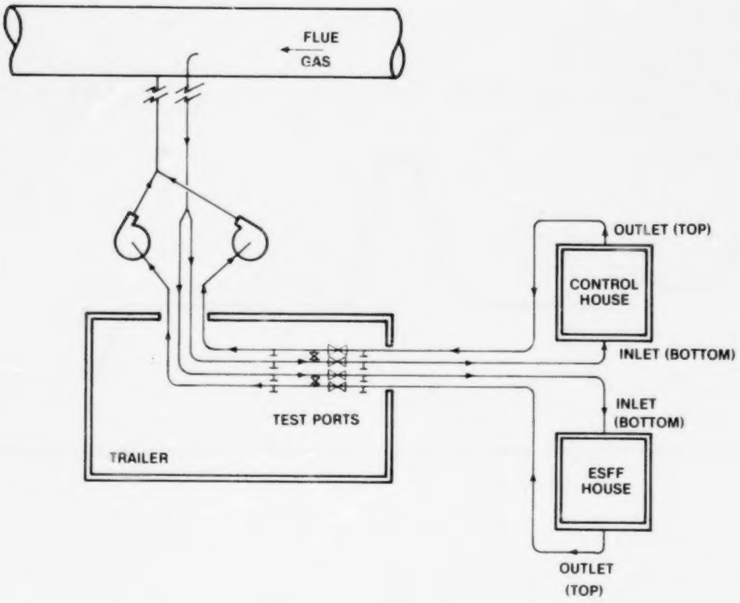
FLUE
GAS
OUTLET (TOP)
CONTROL HOUSE
INLET (BOTTOM)
INLET (BOTTOM)
TEST PORTS
TRAILER
ESFF HOUSE
OUTLET (TOP)

Figure 3

SYSTEM SCHEMATIC

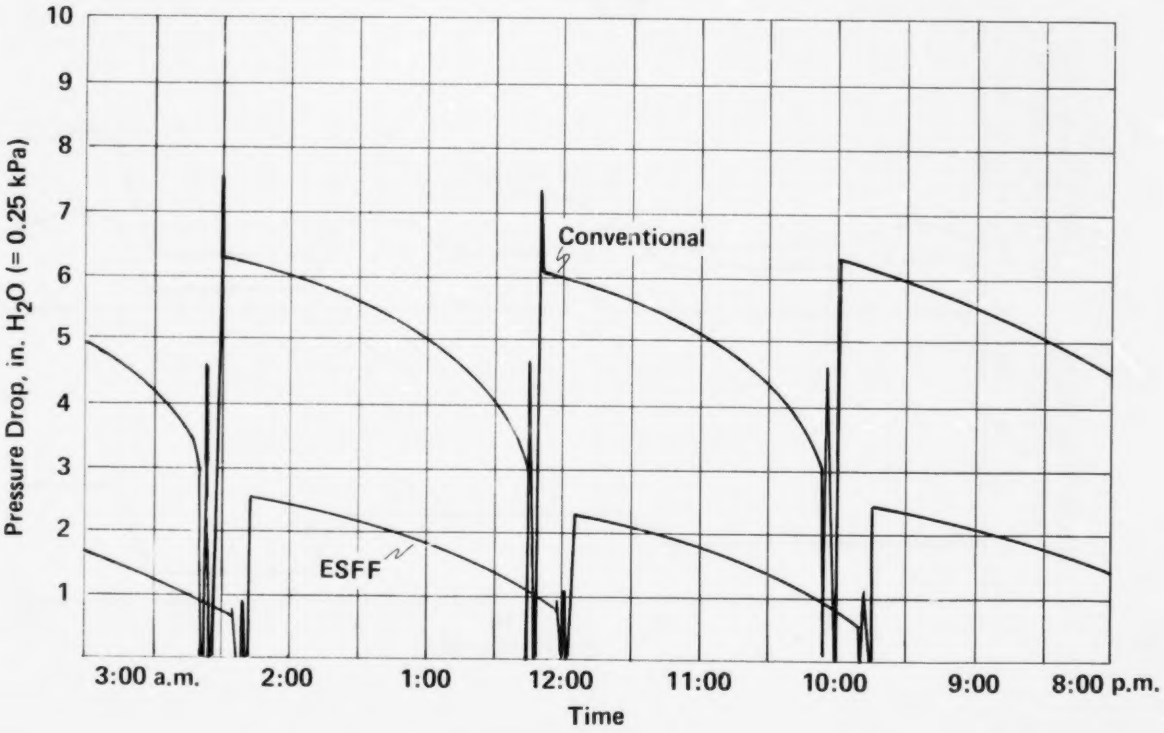

Figure 4

REVERSE AIR PILOT BAGHOUSE PRESSURE DROP TRACE

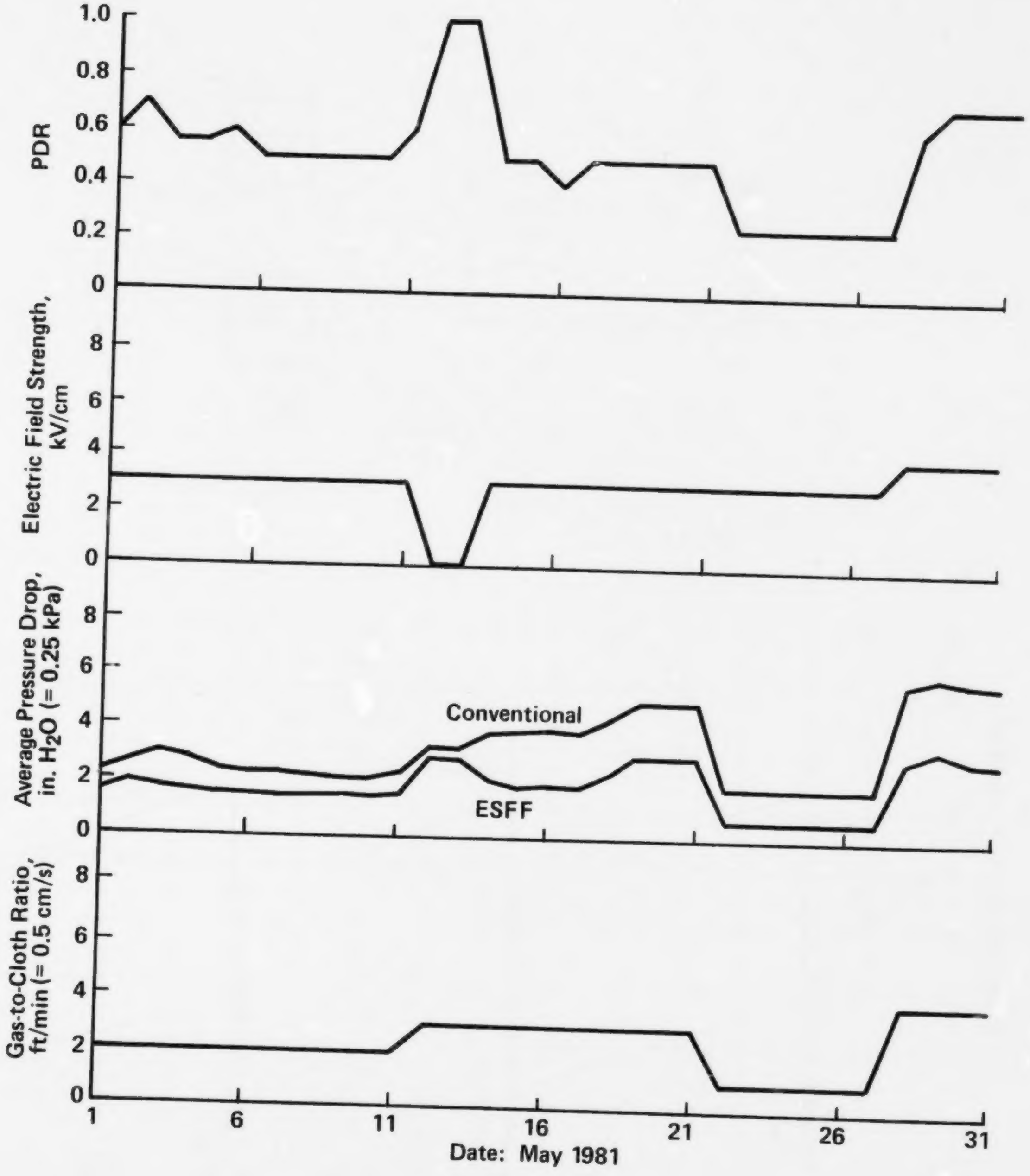

Figure 5

ESFF CHRONOLOGICAL SUMMARY, MAY 1981

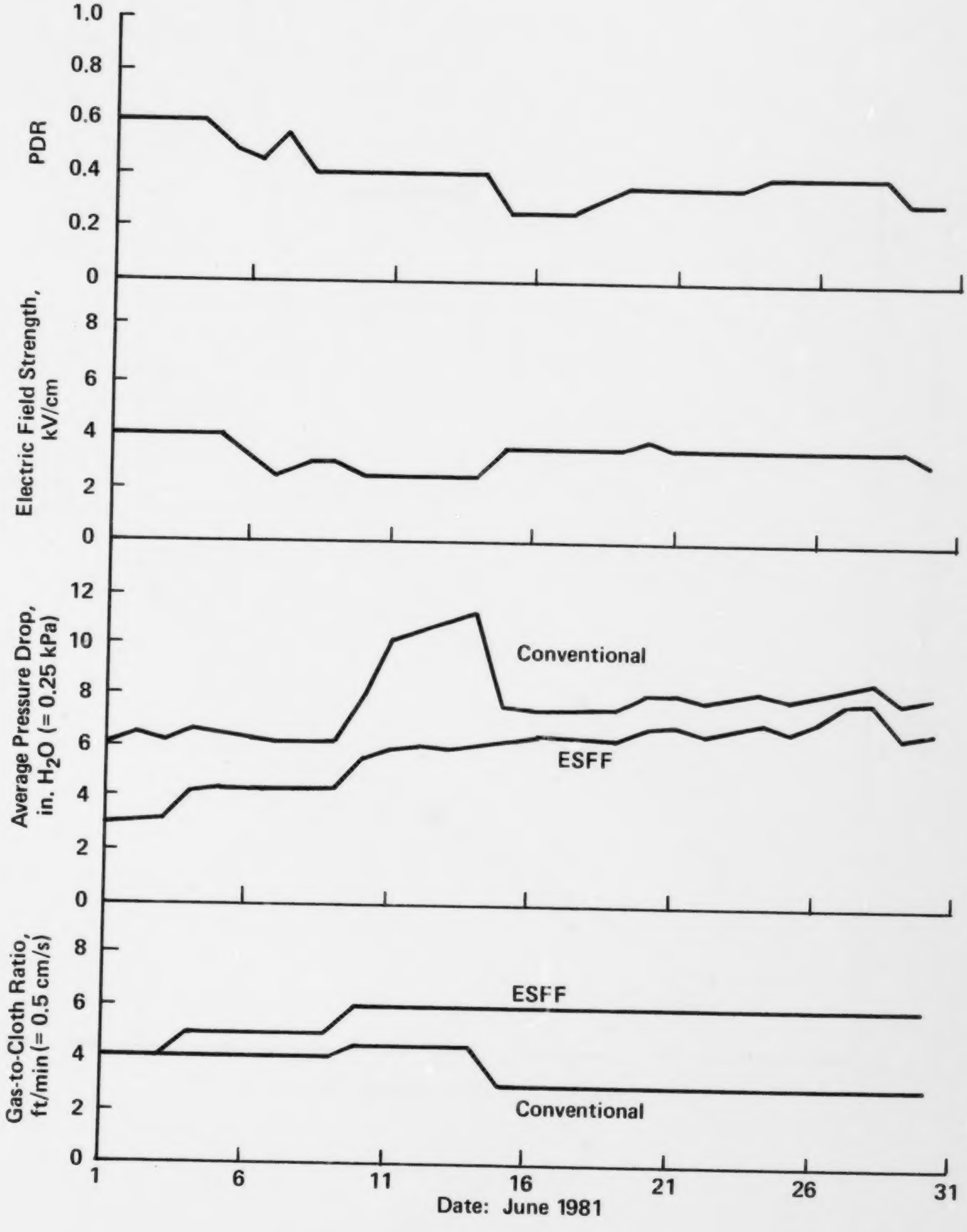

Figure 6

ESFF CHRONOLOGICAL SUMMARY, JUNE 1981

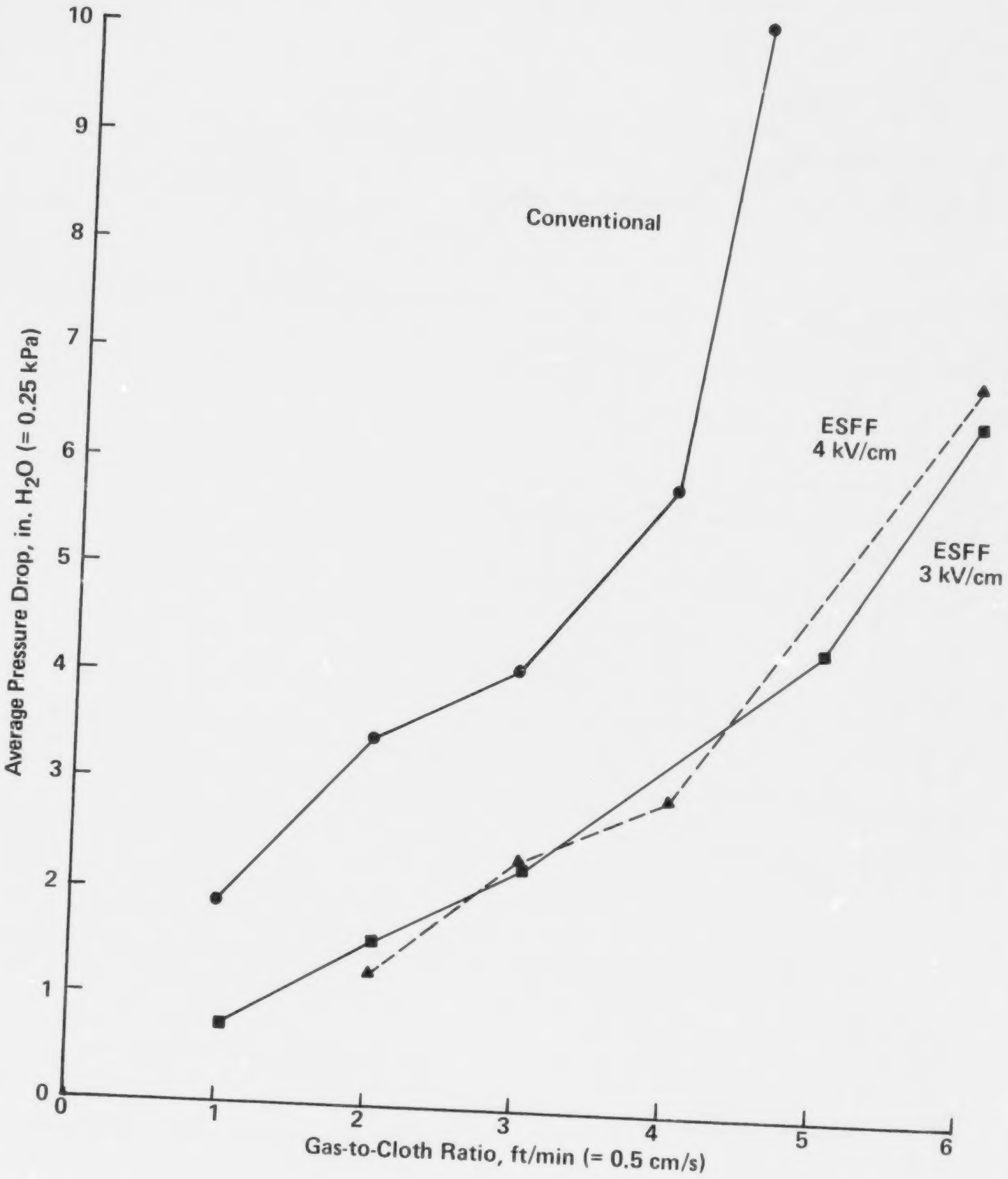

Figure 7

DELTA P AVG. VS G/C RATIO
RIGID CAGE
APRIL 24 TO JULY 15

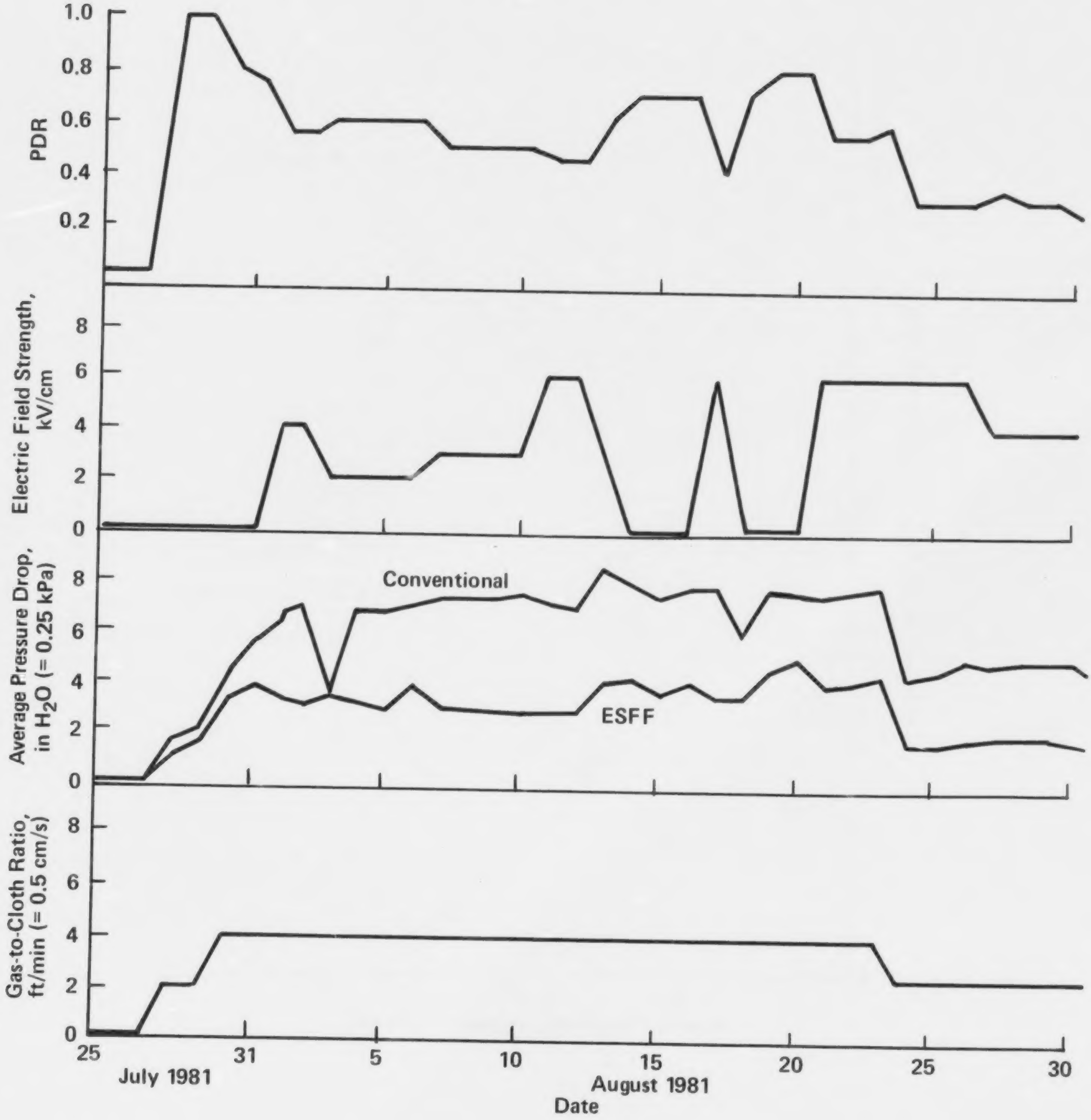

Figure 8

ESFF CHRONOLOGICAL SUMMARY, JULY 25 – AUGUST 31, 1981

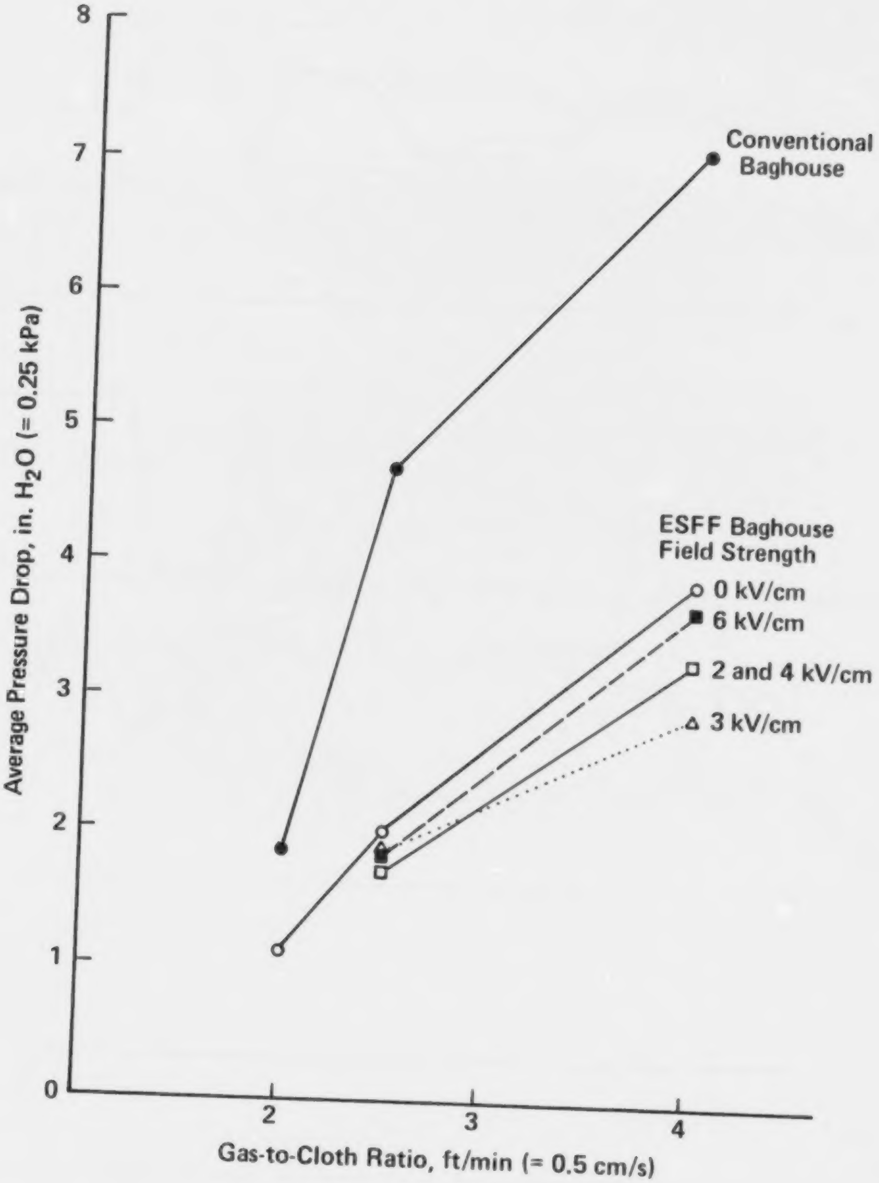

Figure 9

DELTA P AVG. VS G/C RATIO
FLEXIBLE CAGE
JULY 27 TO SEPT. 21

ELECTRICAL STIMULATION OF FABRIC FILTRATION: ENHANCEMENT BY PARTICLE PRECHARGING

by: George E. R. Lamb, Richard I. Jones and William B. Lee
Textile Research Institute
Princeton, New Jersey 08540

ABSTRACT

The reductions in pressure drop that accompany the establishment of a strong electric field near a filter fabric appear to be due to three separate mechanisms. One is the formation of a more porous dust cake due to dust capture in the low packing density regions of the fabric. A second mechanism is attraction of particles to the bag wall which causes the bag to act like a precipitator. The thickness of dust cake is then greater near the entrance than at the end of the bag, and this results in a lower pressure drop. The third mechanism involves attraction of particles to the bag electrodes. The dust is then deposited in bands with relatively thin deposits in between. Measurements and visual inspections of the dust deposits indicate that the second and third effects are enhanced when the aerosol is charged. A particle charger of new design appears to be particularly suitable for this purpose, and is found to cause major changes in filtration performance.

This paper has been reviewed in accordance with the U.S. Environmental Protection Agency's peer and administrative review policies and approved for presentation and publication.

INTRODUCTION

A number of investigations have been directed to the development of systems for electrically stimulated fabric filtration (ESFF). Some have taken the approach of establishing an electric field near the filter (1-4). Others have sought to improve performance by adding charges to the aerosol particles (5-7). In a few cases, both effects have been combined (8,9).

When electric fields are applied in the vicinity of the filter, performance is improved by virtue of the increased capture efficiency of single fibers in the presence of a field (10). This causes the dust cake to form closer to the surface of the fabric. The cake is then more easily removed when the filter is cleaned, and less dust is retained (10). If, in addition, the upstream surface of the filter has a nap, the dust cake will form in the nap and be more porous. (The nap is the fuzzy region on the surface of some fabrics where the fiber volume fraction is smaller than in the interior.) Both these effects will allow the filter to run at lower pressure drop than without the electric field. Penetration is usually reduced by ESFF. This, intuitively, is also an expected result of the better single fiber efficiency, but an indirect mechanism may involve reduced seepage because of the upstream shift of the dust deposits.

The results in Table 1 illustrate these effects. They were obtained with a series of bags made of Teflon® felts with increasing degrees of nap. It can be seen that, as the nap becomes more pronounced, not only overall pressure drop levels are reduced, but also pressure drop ratios (PDR). If ΔP_f is the pressure drop just before a filter is cleaned, and ΔP_i the pressure drop just after, then the PDR is defined as the ratio of $(\Delta P_f - \Delta P_i)$ when the electric field is applied to the corresponding value with no field. The table also shows that the field reduces penetration.

TABLE 1. EFFECT OF SURFACE LOW-DENSITY LAYER ON PRESSURE DROP REDUCTION

Av. field (kV/cm)	Control			Low nap			High nap		
	$\Delta P_i, \Delta P_f$ (mm H_2O)	PDR	Eff. (%)	$\Delta P_i, \Delta P_f$ (mm H_2O)	PDR	Eff. (%)	$\Delta P_i, \Delta P_f$ (mm H_2O)	PDR	Eff. (%)
0	7, 23	---	98.03	7, 22	---	98.04	5,17	---	96.83
2	6, 16	0.63	98.80	7, 15	0.53	98.93	3,9	0.50	98.51
4	7, 15	0.50	98.88	5, 12	0.47	99.13	3,4	0.08	98.76

Charging the aerosol upstream of the bag has also been found to result in lower pressure drops and lower penetrations, but few workers have taken account of the loss of dust which occurs either in the precharger or in the duct from precharger to baghouse. In such cases, it is difficult to assess the effects of charging on bag performance. One study (7), in which the dust collected by the bag was weighed, showed no difference in specific cake resistance with precharging. The lower pressure drop was due to reduced dust loading.

EXPERIMENTAL

In order to study the effects of precharging without interference from reduced dust loading, the charger design shown in Figure 1 was adopted.

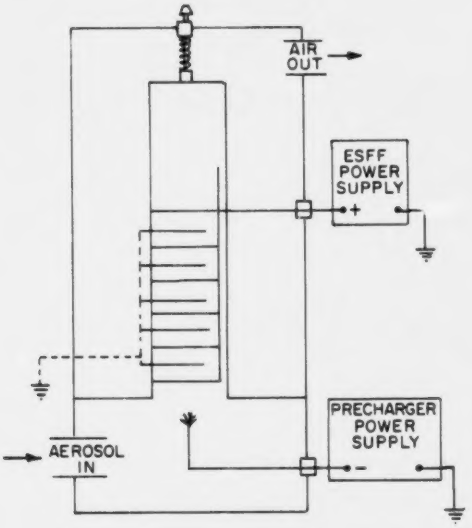

Figure 1. Location of "lightning rod" precharger in reverse air baghouse.

The charger, a metal rod provided with wire bristles at the upper end, was positioned by means of an insulated support, so that its tip was just below the entrance to the bag in a one-bag laboratory baghouse. With this arrangement it was expected that all dust would enter the bag because of the high air velocity at the bag entrance. The bags used were provided with electrodes on the upstream surfaces.

Table 2 lists results obtained with a Teflon® felt bag provided with so-called "printed" electrodes, which in this case consisted of narrow bands of a conducting elastomer composition. The use of "printed" electrodes is a technique undergoing trial. If successful, it should permit a length of fabric to be fitted with an electrode pattern more easily and cheaply than would be the case with wire electrodes. The results in Table 2 may be taken as an indication that such electrodes can provide electrical stimulation as effectively as wires. The question to be examined in the future is one of durability.

The results in Table 2 show that, when aerosol precharging is combined with an electrified bag, reductions in PDR of almost an order of magnitude can be obtained. It is clear that, when bag electrodes and precharger are raised to potentials of opposite signs, the pressure drop reductions are greater than when the signs are the same. It can also be seen that, with this bag, activating the precharger and not the bag electrodes causes only a minor reduction in pressure drop.

TABLE 2. PRESSURE DROP RATIOS WITH ESFF AND PRECHARGED AEROSOL

Teflon® bag with printed electrodes. Inlet concentration 4.8 g/m³.
Face velocity 6 ft/min (3 cm/s).

Bag field (kV/cm)	Precharger voltage (kV)	$\Delta P_i, \Delta P_f$ ($mm\ H_2O$)	PDR
0	0	16,110	
0	-9	16,107	0.97
+2	0	15, 83	0.72
+2	-9	14, 28	0.15
-2	0	15, 60	0.48
-2	-9	15, 41	0.28
-3	0	15, 52	0.39
-3	-9	15, 35	0.21
+2	+9	16, 39	0.24
-2	+9	17, 31	0.15

Figure 2 shows results obtained with woven glass bags having sewn-in 150 μm bare copper wire electrodes. It can be seen that, as before, without a potential on the precharger, the reductions in the pressure drop are modest. With the precharger activated, PDR values fall considerably lower.

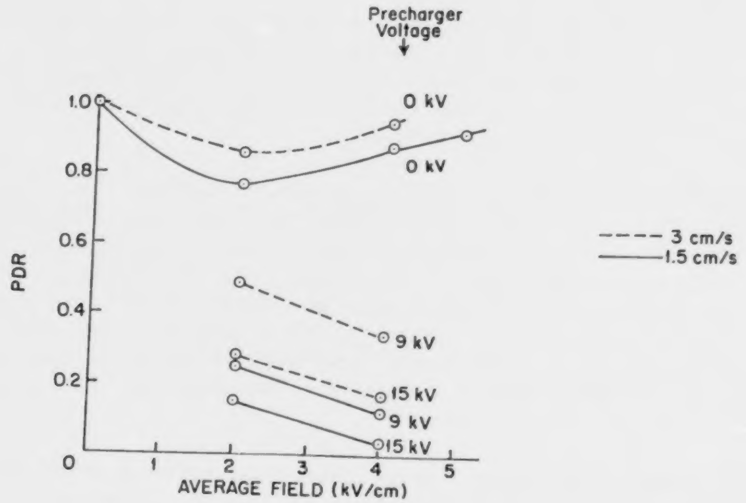

Figure 2. Dependence of PDR on bag field after extended run. Top curves: no precharger.

In order to study the mechanism by which precharging reduces pressure drop, the bag support was modified to allow the bag to be removed easily from the baghouse. The sewn seam of the bag was replaced with an overlap held closed by clamps. With this arrangement, the bag(after being removed from the baghouse) could be carefully opened and the dust cake could be examined. Visual inspection immediately showed that nonuniform distribution of the dust deposit occurred both in the longitudinal and in the tangential direction. Deposition was heavier at the lower end of the bag and on the electrodes, as shown in Figure 3.

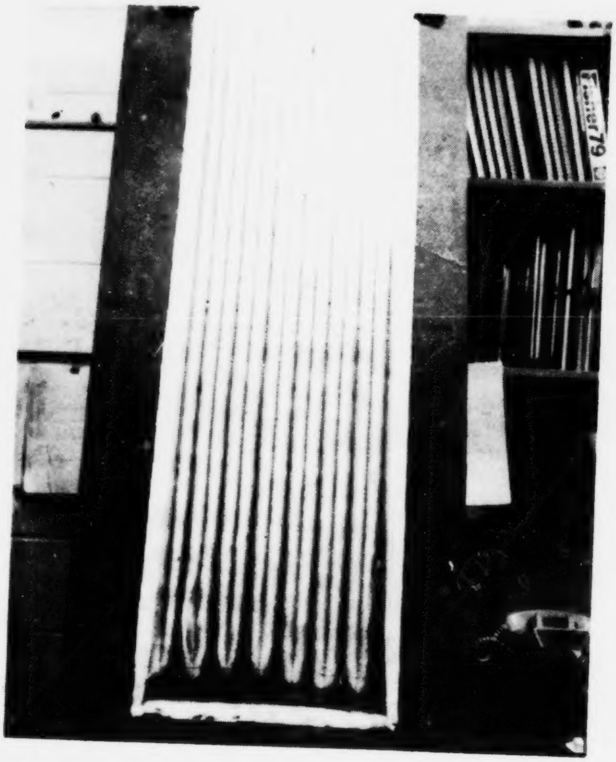

Figure 3. Dust deposition pattern with 4 kV/cm field and -15 kV precharger potential.

Mass distribution with respect to bag height was measured by placing a mask at a series of positions over the opened bag and aspirating the dust from the area within the mask. The dust was collected on a filter and weighed. This was done for various combinations of bag fields and precharger potentials. The results are plotted in Figure 4: in all cases more dust collects at the bottom than at the top of the bag. When this occurs with no voltage applied, the cause is assumed to be settling by gravity; but with an applied field, the tendency for early deposition is increased. Values of PDR are listed alongside the curves. It should be noted that these were values obtained from the pressure drop reached after 15 minutes, starting from an almost clean bag. The bag was cleaned by vacuuming each time so as to allow measurement of the dust deposit areal densities plotted in Figure 4. The PDRs in Figure 4 must therefore not be regarded as typical of values that would be obtained after prolonged conditioning. They nevertheless bear a certain relationship to the curves. It can be seen that curves with greater slopes tend to correspond to lower PDR. Deviations from this trend must be attributed to nonuniformity in distribution in a tangential direction, such as shown in Figure 3, which is a photograph of the opened bag after being run 15 minutes with an average +4 kV/cm field between wires and a -15 kV potential on the precharger (+4,-15). It can be seen that: (1) Most of the dust collects on the positive wires. (2) The amount collected, as plotted in Figure 4, is greatest at the bottom and diminishes with distance up the bag. (3) Some

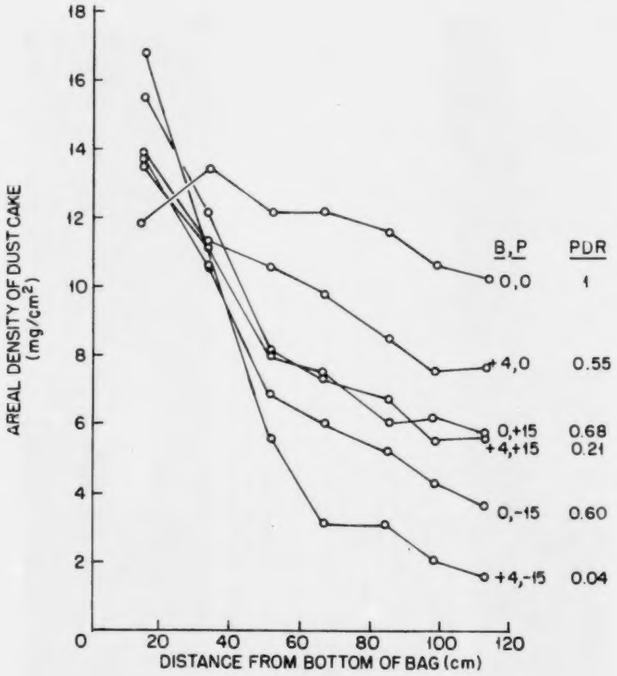

Figure 4. Distribution of dust mass with respect to distance from the bottom of the bag. B and P indicate average field on bag in kV/cm and voltage on precharger in kV, respectively.

collection occurs on the ground wires. This may be dust that, having deposited on the positive wires, is reentrained after gaining a positive charge. (4) Spaces between wires are left essentially clean.

Photographs taken of the bag surface and dust deposits are shown in Figures 5, 6, and 7. In all these photographs, pieces of adhesive tape had been stuck to the clean bag over portions of some of the electrodes. The patterns of dust deposition on the tape lead to some interesting conclusions about the motion of dust particles during filtration, as discussed below. Figure 5 shows the bag surface after vacuuming (a) and with a dust cake laid at no applied voltage (b). No dust has collected on the pieces of adhesive tape because there is no air flow normal to the tape. Figure 6 shows dust deposited with a 4 kV/cm field between bag electrodes and +15 kV (a) and -15 kV (b) on the precharger. In both cases the dust forms visible bands on the wires, but the bands are sharper when bag voltage and precharger voltage are of opposite sign. An interesting feature of this figure is that dust was deposited on the adhesive tape in an amount apparently equal to that elsewhere on the band. This indicates that particle velocities due to the field near the wires are much greater than the gas velocity. The bag is thus acting like a precipitator. Figure 7 shows the appearance of the dust deposits when only a bag potential was applied (a). Here there are still visible bands, but they are more diffuse and dust is again deposited on both the electrodes and the adhesive tapes. When only the precharger was activated (b and c), the dust deposit was uniform, and there was some deposition on the tapes, presumably of dust driven to the wall by space charge effects.

After each of the 15-minute runs specified in Figure 4, the bag was weighed and the mass of dust determined. Table 3 shows that no matter what the combination of bag and charger potential, the mass collected in 15 minutes was always the same. Thus the changes in pressure drop were not to any extent due to reduced total dust loading. This appears to disagree with the data in Figure 4. In that figure the total mass of dust should be proportional to the area under each curve, and the lower curves appear to enclose smaller areas. The explanation must be that the sharp upswings to the left of the lower curves were plotted with too few points to show accurately the amount in those regions. Figure 3 shows that heavy deposition occurs within a few centimeters of the bottom of the bag; the telephone (12 cm high) to the right of the photograph gives an idea of scale.

TABLE 3. MASS OF DUST COLLECTED ON BAG IN 15 MINUTES

Bag field (kV/cm)	Precharger voltage (kV)	Mass of dust collected (g) in two trials
0	0	30, 31
+4	0	33, 31
+4	-15	27, 29
+4	+15	37, -
0	-15	35, 27
0	+15	32, 31

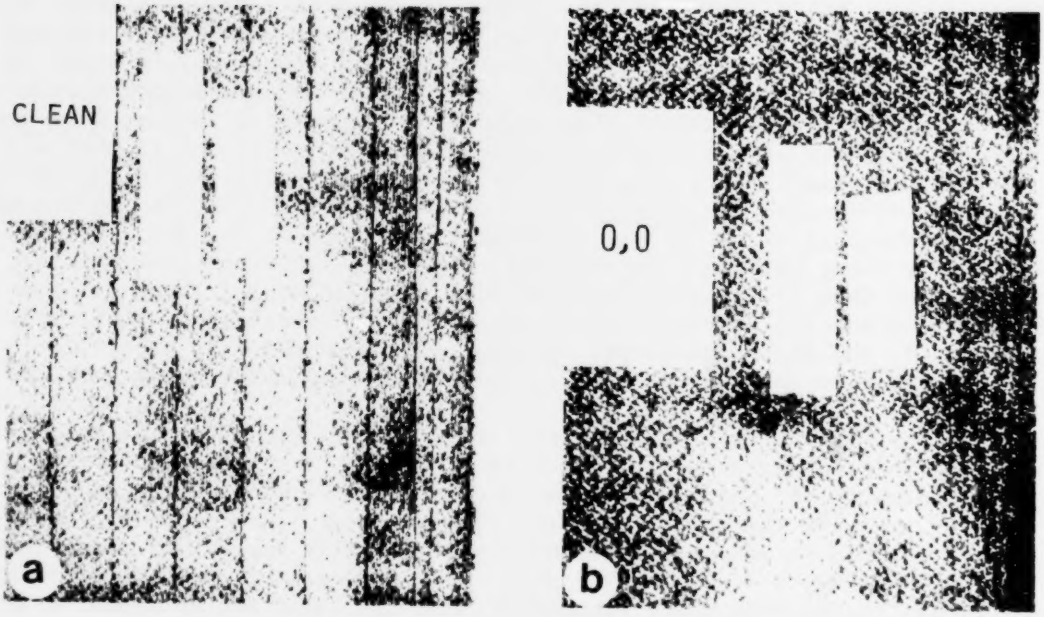

Figure 5. Appearance of the inner surface of the bag:
a) after vacuum cleaning through a wire screen; and
b) with an average of 7.5 mg/cm^2 of fly ash deposited with no electric field or precharging.
No fly ash has deposited on the tape in either case. In Figures 5, 6, and 7, horizontal bands are due to anticollapse rings inside the bag.

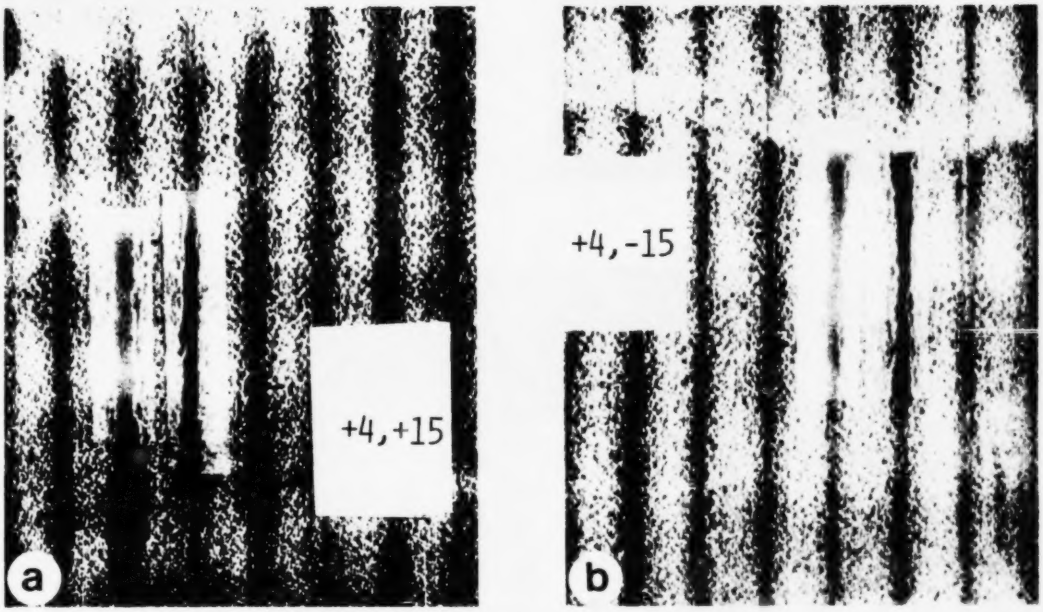

Figure 6. Appearance of the inner surface of the bag:
a) after deposition with 4 kV/cm between bag electrodes and +15 kV on the precharger; and
b) after deposition with 4 kV/cm between bag electrodes and -15 kV on the precharger.

Points to note: (1) Dust collects on tape.
(2) Bands are narrower with negative precharging.

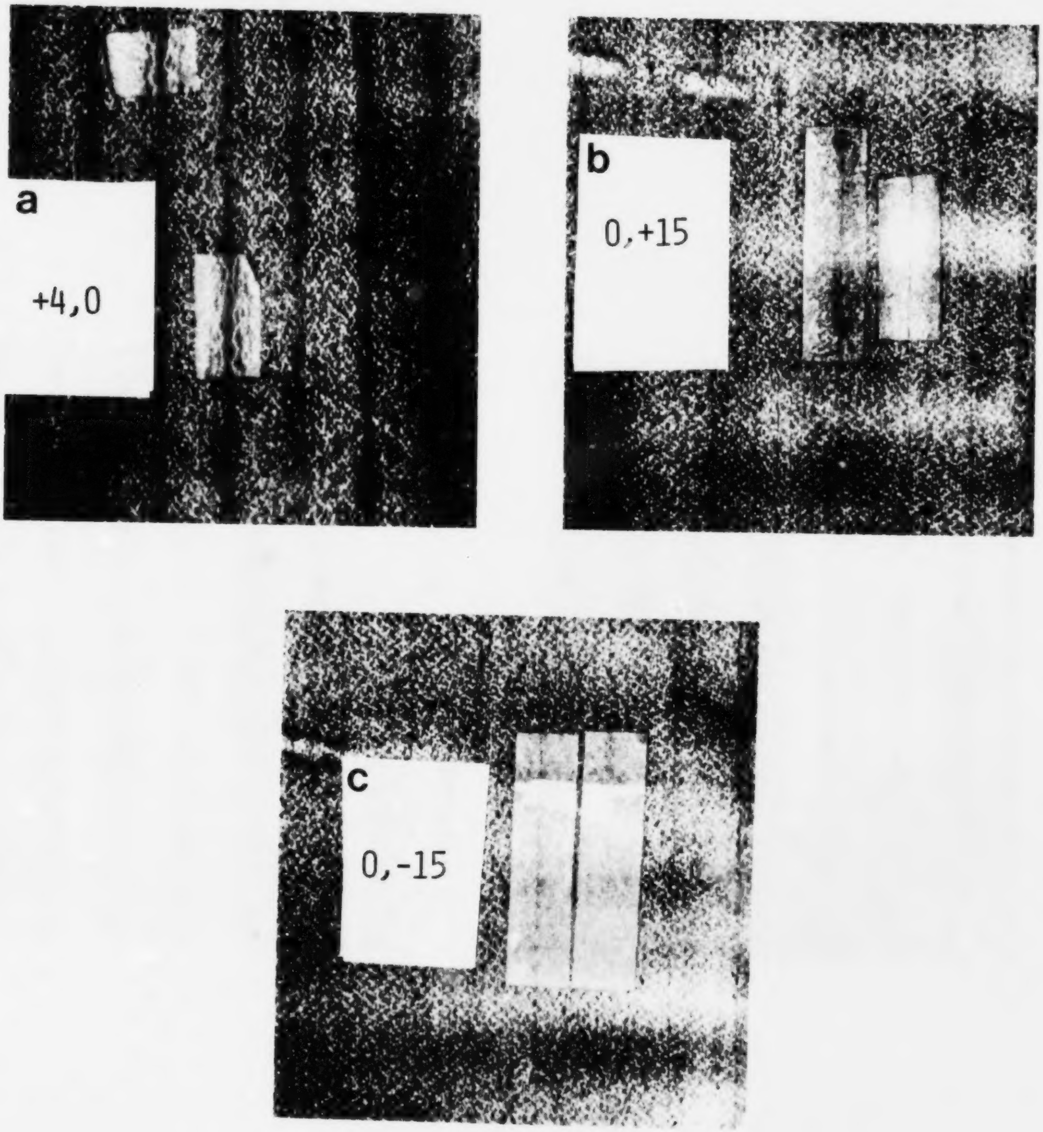

Figure 7. Appearance of inner surface of bag:

a) after deposition with 4 kV/cm between bag electrodes and no precharging. Dust deposits in bands on both sets of electrodes and on tapes.

b) with positive precharging only. Faint bands are visible on grounded electrodes, including area covered by tape.

c) with negative precharging only. No bands are visible.

Any technique capable of reducing pressure drop offers several possible benefits: one can choose to operate at a lower energy consumption level, allow longer intervals between cleanings, or, by raising face velocities, use fewer bags. A recent study (11) has shown that the third of these options gives the largest savings in operating costs, and it may be assumed that in any future commercial development of ESFF, face velocities will be higher than those in present practice. However, limits to face velocity are also imposed by falling efficiency. The possible increases in face velocities attainable in the combined bag electrode/precharger mode were explored by making measurements of efficiency at a series of velocities. Figure 8 shows efficiencies obtained with no field (0,0), with +4 kV/cm average field between electrodes (+4,0), and with +4 kV/cm and -15 kV on the precharger (+4,-15). There is a clear enhancement of efficiency at all velocities. The bag used was the same one in Figures 3 to 7, made of textured woven glass. Long-term tests in a pilot plant will be needed to determine the maximum velocity at which stable operation is possible. It is reasonable to assume, however, that with a precharger/electrified bag combination, considerable increases in face velocity will be possible.

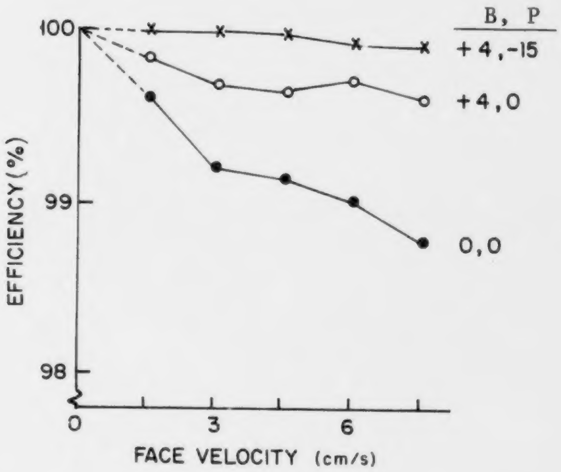

Figure 8. Dependence of efficiency on face velocity for woven glass bag with and without ESFF. B and P indicate the same quantities as in Figure 4.

CONCLUSIONS

Use of a precharger of new design in conjunction with electric fields generated by electrodes in the bag walls has led to reduced pressure drop and lower dust penetration. The reduction in pressure drop is due at least partly to lessened uniformity of the dust cake, which is heavier at the bottom of the bag and on the electrodes. The improved performance was not due to reduced dust loading, since no changes in total mass collected on the bag were observed. With this type of precharger/electrified bag combination, it should be possible to operate a baghouse at face velocities several times higher than those of current practice.

REFERENCES

1. Iinoya, K. and Makino, K. Application of electric field effects to dust collection filters. Aerosol Science 5: 357, 1974.

2. Rivers, R. D. Non-ionizing electrostatic air filters. ASHRAE Journal 37: February 1962.

3. Frederick, E. R. Some effects of electrostatic charges in fabric filtration. In Proceedings: Symposium on Use of Fabric Filters for the Control of Submicron Particulates, EPA-650/2-74-043 (NTIS PB 237629), May 1974.

4. Bergman, W., Hebard, H., Taylor, R., and Lum, B. Electrostatic filters generated by electric fields. Paper presented at the Second World Filtration Congress, London, England, September 1979.

5. Lundgren, D.A. and Whitby, K.T. Effect of particle electrostatic charge on filtration by fibrous filters. I & E C Process Design and Development 4:345, 1965.

6. Helfritch, D.J. Performance of an electrostatically aided fabric filter. CEP 54: August 1977.

7. Hovis, L.S., Abbott, J.H., Donovan, R.P., and Pareja, C.A. Electrically charged flyash experiments in a laboratory shaker baghouse. In Third Symposium on the Transfer and Utilization of Particulate Control Technology, Vol. I, EPA-600/9-82-005a (NTIS PB83-149583), July 1982.

8. Penney, G.W. Electrostatic effects on fabric filtration. Vol. I, EPA-600/7-78-142a (NTIS PB288576), September 1978.

9. Lamb, G.E.R. and Costanza, P.A. Electrical stimulation of fabric filtration - Effects of electrode current. Textile Res. J. 51:389, 1981.

10. Lamb, G.E.R., Costanza, P.A., and Turner, J. H. Role of filter structure and electrostatics in dust-cake formation. Textile Res. J. 50: 661, 1980.

11. Van Osdell, D. W., Ranade, M. B., Greiner, G. P. and Furlong, D. F. Electrostatic Augmentation of Fabric Filtration: Pulse-Jet Pilot Unit Experience, EPA-600/7-82-062 (NTIS PB83-168625), November 1982.

ESFF AS A FIELD EFFECT

By: L. S. Hovis and G. H. Ramsey
Industrial Environmental Research Laboratory
U. S. Environmental Protection Agency
Research Triangle Park, North Carolina 27711

and

R. P. Donovan
Research Triangle Institute
P. O. Box 12194
Research Triangle Park, North Carolina 27709

ABSTRACT

Evidence to suggest that the mechanism on which ESFF (electrostatic stimulation of fabric filtration) depends is an electric-field-only mechanism (as opposed to a Coulomb mechanism that depends on both electric field and electric charge) includes:

1. A room-temperature high-humidity factorial experiment in which both external electric field and fly-ash electrical charge were independent variables.
2. Selected experiments carried out at low relative humidity and room temperature.
3. Enhanced filtration measurements made with a 60-Hz ac electric field applied to the bag electrodes.
4. Published precharging data of others in which enhancement vanishes at high relative humidity.

All of the data collected in EPA/IERL's Research Triangle Park laboratory (items 1-3, above) refer to experiments in which pulverized coal fly ash was the dust source. Dusts from other sources were used in the experiments of item 4.

This paper has been reviewed in accordance with the U. S. Environmental Protection Agency's peer and administrative review policies and approved for presentation and publication.

ESFF (electrostatic stimulation of fabric filtration), an acronym coined by reseachers at Textile Research Institute(1), refers to a technique for improving fabric filtration performance by applying an external, nonionizing electric field parallel to the fabric surface during the filtration process. The improved performance manifests itself as a reduced drag and reduced penetration (although not all researchers report a reduced penetration--Reference 2, for example).

Typical explanations of the observed enhancement invoke Coulomb capture forces between the electrically charged dust particles and the externally applied surface field, expecially on the low-fiber-density upstream surface of the fabric.(1) Particles collected on these low-fiber-density surfaces do not contribute as much to fabric drag as those collected in the more tightly packed interstices of the bulk fabric. Qualitatively, this model of ESFF portrays the action of the electric field as enhanced upstream capture of electrically charged dust at low-fiber-density surface sites.

In such a model, particle charge is expected to be a variable of first order significance since the Coulomb force experienced by a particle approaching the fabric depends on both particle charge and the electric field in the region through which it passes. Other electrical forces exist, however, such as polarization forces; and other non-Coulomb-force-field-dependent mechanisms could be significant. This paper reviews data that support ESFF effects based on mechanisms other than Coulomb capture.

HIGH HUMIDITY FACTORIAL

This experimental series used both fly-ash electrical charge and an external electric field at the fabric surface as independent variables in a factorial experiment measuring the performance of a pulse-jet baghouse. Dependent variables of the experiment included pressure drop across the bags (ΔP), outlet fly-ash concentration (C_o), and an effective cake resistance (K_2'). The last quantity was calculated from increase in ΔP during a filtration cycle and the corresponding increase in fly-ash mass on the bags, determined by carefully demounting and weighing.

In the context of this factorial experiment, high relative humidity means 52 to 59 percent. The specific value itself is not important except as an indication that the electrical resistivity of the fly ash/fabric filtration media would be low enough to dissipate the electrical charge deposited along with the collected fly ash without significant charge accumulation in/on the dust cake. Since the maximum current carried to the bags by the fly ash under any of the test conditions was 150 to 200 nA, having the bag electrode current in the 150- to 200-μA range, three orders of magnitude higher, ensures that the field at the bag surface depends primarily on the voltage applied to the electrodes. Thus, keeping the relative humidity greater than 50 percent kept the electical resistivity of this particular test fly ash/fabric combination low enough to avoid the complications brought about by an electric field component attributable to deposited charge.

The details of the experimental procedure and apparatus appear elsewhere.(3) The key conclusions are summarized in Figures 1 through 4, the first two of which plot normalized K_2' and ΔP_D as a function of precharger current (Figure 1) and field voltage (Figure 2). Figure 1 shows that K_2' does not change with increasing fly-ash electrical charge, as measured by the corona precharger current. (The average charge/mass of the fly ash varied over the range ±0.2 μC/g to -2.0 μC/g as the power supply current varied over the range plotted.) The dashed line in Figure 1 plots the normalized ΔP_D values corresponding to these precharger power settings. ΔP_D is the final pressure drop (ΔP_F) minus the residual pressure drop (ΔP_R) in one filtration cycle. The reduction in ΔP_D with increasing precharger current is the electrical enhancement effect attributed to precharging.(4-6) Since K_2' (which depends on the ratio $\Delta P_D/M_D$, where M_D is the increase in fly-ash mass on the bag that caused ΔP_R to increase to ΔP_F) does not change, Figure 1 implies that the ΔP_D decrease has been compensated by a similar decrease in M_D. Figure 3, which compares the normalized ΔP_D curve with the corresponding normalized M_D curve, shows that that is exactly what has happened and that the electrical enhancement described by the reduced values of ΔP_D are achieved by reducing the M_D on the bags. The precharger acts as a collecting prefilter, a conclusion reported at the previous symposium for both pulse-jet(7) and shaker baghouse(8) experiments.

The field voltage dependencies (Figures 2 and 4) tell a different story. Figure 2 shows that the normalized K_2' and the normalized ΔP_D decrease together as a function of external field voltage. Figure 4 confirms that M_D is independent of field voltage meaning that the mass of fly ash reaching the bags is independent of bag electrode voltage. These plots show, therefore, that the permeability of the deposit has increased, resulting in a decrease in cake airflow resistance, because of the field.

The mechanism by which this increase in permeability takes place cannot be further specified other than to say that Coulomb forces do not dominate the mechanism. This conclusion follows from the observation that charging the fly ash to a high charge-to-mass ratio (Q/M) does not alter the magnitude of the permeability enhancement; that is, the reduction in K_2' brought about by the external field is the same for the lowest Q/M fly ash as for the highest. A mechanism that depended on Coulomb forces primarily should produce increasing response with increasing Q/M at constant field. That the fly-ash deposit does not exhibit this property leads to the conclusion that ESFF, in this experimental setup at least, depends upon electrical interactions other than Coulomb attraction.

While the capability of the precharger to add charge to the fly ash that reaches the bags is indisputable (the bag electrodes can be used to measure the increased current contributed by the precharger), the distribution of this charge by particle size is not known. Conceivably, all the charge could be added to a size fraction of the fly ash that proves insignificant in ESFF. Two additional experiments are planned to further clarify the conclusions:

1. Charge spectrometry by the Millikan apparatus.

2. Charge neutralization by operating the precharger in the ac mode.

The first supplementing experiment will measure the distribution of charge among the various sizes of fly-ash particles; the second will attempt to neutralize the natural charge now present on the fly ash so as to achieve a data point of even lower Q/M than when the precharger is OFF.

LOW HUMIDITY OBSERVATIONS

When the high humidity factorial experiment is not carried out at "high humidity," by definition significant electrical charge can accumulate on the bags because the charges carried by the fly ash do not leak off as readily as when operating at high humidity. The cage voltage(9) is one measure of accumulating bag charge. At operating relative humidity of 35 percent or less, the cage voltage (cage voltage is the voltage on the electrically isolated support cage of a pulse-jet bag, as read by a high impedance voltmeter such as an electrometer) generally builds up to values exceeding ±1000 V dc, suggesting that the net electric field at the fabric surface now has a component attributable to accumulating charge in addition to the applied field that dominated the high humidity case.

Furthermore, because these charges will drift in the externally applied field, they distribute themselves so as to neutralize the external field over much of the fabric surface similar to the action described by Walkenhorst in his metallic fiber filter.(10) Figure 5 sketches an extension of the Walkenhorst model to a fabric filter as envisioned here.

Laboratory observations confirm that the ESFF effect diminishes at low relative humidity and that charge accumulation increases. However, because experiments correlating cage voltage with K_2' and other performance measures are incomplete, this evidence is only speculative at present. Should the interaction depicted in Figure 5 prove valid, then a low frequency field reversal as discussed by Walkenhorst(10) should restore the ESFF interaction.

AC ESFF

A third general experimental approach is to examine ESFF as a function of field frequency. The reason such observations are significant is that Coulomb forces depend on field direction, while other field dependent mechanisms such as dielectrophoresis do not. Dielectrophoresis, the net attractive force experienced by a polarized neutral body in an electric field gradient, depends on the direction of the field gradient alone. The net force is always in the direction of increasing field strength; thus, reversing the polarity of the field does not change the direction of the net polarization force in the typical ESFF experimental configuration. The net Coulomb force under ac operation, however, is zero for time periods long compared to 1/f, where f is the ac frequency.

To date, the only frequency investigated has been 60 Hz. At 60 Hz, the ESFF mechanism appears intact and operative, although limitations in available power supplies have restricted the available field strength. A fly-ash fabric combination that yielded a pressure drop ratio (PDR) of 0.6 with 8000 V dc across electrodes 1.8 cm apart produces a PDR of 0.7 with 5000 V rms (60 Hz). The PDR is the ratio of ΔP_D with an electric field to ΔP_D without a field. Face velocity during both measurements was approximately 5 cm/s.

While the observation of an ac ESFF effect suggests that polarization is a significant mechanism, Coulomb forces cannot be ruled out until much higher frequency data are available.

FIBROUS FILTER ELECTRICAL ENHANCEMENT

Other researchers have reported electrically enhanced fibrous filtration through the use of prechargers(11), electric fields across the media (12), or both (13). Calculations of the single-fiber collection efficiency of an electrically charged particle flowing past a charged fiber(14) predict that the addition of this Coulomb force to the classical capture mechanisms influences single-fiber efficiency primarily at Stokes numbers below about 2 (Figure 6). For typical filter parameters, this conclusion implies that Coulomb forces are important only for particles less than about 5 μm diameter.

These Coulomb-force-based predictions agree reasonably well with published data, using either a precharger (Figure 7) or an external field across the filter (Figure 8). In these two plots, overall filter efficiency is the ordinate and particle diameter, the abscissa.

Figures 7 and 8 represent an electrical enhancement of fibrous filtration attributable to a Coulomb force. What will be argued next is that these enhancements are not ESFF-type enhancements as described in References 1, 2, and 3 and, in fact, exhibit behavior different from the reported ESFF enhancement. Furthermore, the behavior exhibited by the electrically enhanced fibrous filters is consistent with Coulomb force enhancement, while that exhibited in the ESFF experiments is not.

No significance is attached here to the fact that the primary enhancement criterion differs between the two types of filters. For the fibrous filter, collection efficiency is the primary measure of performance; for fabric filters, it is pressure drop, drag, K_2', or some normalized ratio describing filter energy consumption. What is crucial is that the enhancement of each depends differently on certain independent variables.

Take the data in Figure 8 first. Bergman et al.(12) report that the enhancement depicted in Figure 8 largely disappears if the dust source is passed through a charge neutralizer prior to the filter. This behavior is consistent with a Coulomb force which depends on both particle charge and the electric field at the collector. With fabric filters, as described in the high humidity factorial experiment, increasing the particle charge produced no discernible effect on K_2'. While increasing the particle charge is not identical to the Bergman et al.(12) experiment, a Coulomb-force-dominated variable should respond to any change in particle charge. That it did not do so in the fabric filter experiment led to the conclusion that Coulomb forces do not dominate the ESFF enhancement observed in the high humidity factorial experiment.

The charge neutralization experiment planned as continuing work is similar to the experiment reported by Bergman, who concluded that "natural" particle charge was essential for the electrical enhancement he observed and as a Coulomb mechanism would require.

The precharger-induced enhancement represented in Figure 7 is reported by Yu and Teague(11) to disappear when carried out at high humidity or with conductive dusts. This observation agrees with a model picturing charge accumulation on the filter as the source of the electric field at the filter surface that is required for the Coulomb capture force to be present. When these charges are allowed to leak off, the field disappears, and the Coulomb force vanishes as does the enhancement. These observations are consistent with the hypothesis that this fibrous filtration enhancement is Coulomb-force dominated.

The ESFF data presented earlier exhibit just the opposite behavior. It is at high humidity--no surface charge accumulation--that the ESFF enhancement is most pronounced. Charge accumulation seems to be associated with diminished ESFF, although this conclusion is very tentative at present.

What the preceding paragraphs have attempted to do is to review the properties of a type of electrically enhanced filtration thought to be dominated by Coulomb forces (i.e., fibrous filtration) and then show that certain dependencies of these filters differ from those observed with ESFF and that, furthermore, those differences can be understood by attributing the electrical enhancement of fibrous filtration to Coulomb forces and the electrical enhancement of fabric filtration of fly ash to some unspecified but nonCoulomb mechanism.

CONCLUSIONS

The evidence cited supports the existence of a non-Coulomb mechanism of ESFF. While the evidence is neither conclusive nor exclusive (in that some experiments remain to be done before the conclusion becomes solidly established and nothing presented rules out the existence of conditions under which Coulomb forces could be significant in ESFF), the data make a non-Coulomb mechanism or mechanisms the most likely explanation of the ESFF phenomenon observed in the EPA/IERL-RTP in-house laboratories. The data do not distinguish between an electrical polarization mechanism and other non-Coulomb mechanisms. They do suggest that the magnitude of the electrical charge on the incoming fly ash is not an important variable, a surprising conclusion in view of the recognized dominance of Coulomb forces in most electrified systems.

REFERENCES

1. Lamb, G. E. R. and Costanza, P. A. A low-energy electrified filter system. Filtration and Separation. July/Aug.:319-322, 1980.

2. Greiner, G. P., Furlong, D. A., VanOsdell, D. W., and Hovis, L. S. Electrostatic stimulation of fabric filtration. J. Air Pollut. Control Assoc. 31:1125-1130, 1981.

3. Donovan, R. P., Hovis, L. S., Ramsey, G. H., and Ensor, D. S. Electric-field-enhanced fabric filtration of electrically charged flyash. Aerosol Science and Technology. 1:385-399, 1982.

4. Ariman, T., and Helfritch, D. J. Pressure drop in electrostatic fabric filtration. In: Second Symposium on the Transfer and Utilization of Particulate Control Technology, Vol. III. EPA-600/9-80-039c (NTIS No. PB-81-144800) (Sept.), 1980. pp. 222-236.

5. Chudleigh, P. W., and Bainbridge, N. W. Electrostatic effects in fabric filters during build-up of the dust cake. Filtration and Separation. 17:309-311, 1980.

6. Iinoya, K., and Mori, Y. Experimental advances in fabric filtration technology in Japan--effects of a corona precharger and relative humidity on filter performance. In: Second Symposium on the Transfer and Utilization of Particulate Control Technology, Vol. III. EPA-600/9-80-039c (NTIS No. PB-81-144800) (Sept.), 1980. pp. 237-250.

7. Donovan, R. P., Hovis, L. S., Ramsey, G. H., and Abbott, J. H. Pulse-jet filtration with electrically charged flyash. In: Third Symposium on the Transfer and Utilization of Particulate Control Technology, Vol. I. EPA-600/9-82-005a (NTIS No. PB-83-149583) (July), 1982. pp. 11-22.

8. Hovis, L. S., Abbott, J. H., Donovan, R. P., and Pareja, C. A. Electrically charged flyash experiments in a laboratory shaker baghouse. In: Third Symposium on the Transfer and Utilization of Particulate Control Technology, Vol. I. EPA-600/9-82-005a (NTIS No. PB-83-149583) (July), 1982. pp. 23-34.

9. Donovan, R. P., Ogan, R. L., and Turner, J. H. Electrostatic effects in pulse-jet fabric filtration of room temperature flyash. In: M. P. Freeman and J. A. Fitzpatrick (eds.), Theory, Practice and Process Principles for Physical Separations. Engineering Foundation, New York, New York, 1981. pp. 445-466.

10. Walkenhorst, W. Deliberations and studies on the filtration of dust-laden gases with special allowance for electric forces. Staub-Reinholt Luft. 29(12):1-13, 1969.

11. Yu, H. S., and Teague, R. K. Performance of electrostatic fiberbed. In: Extended Abstracts of the 1st Annual Conference of the American Association for Aerosol Research, Santa Monica, California. February 17-19, 1982. pp. 19-3-19-4.

12. Bergman, W., Hebard, H. D., Taylor, R. D., and Lum, B. Y. Electrostatic filters generated by electric fields. In: Proceedings of The Second World Filtration Congress, 1979.

13. Ho, C. P., the Bahnson Co., Winston-Salem, N.C.

14. Loeffler, F. The influence of electrostatic forces and of the probability of adhesion for particle collection in fibrous filters. In: Proceedings: Symposium on New Concepts for Fine Particle Control. EPA-600/7-78-170 (NTIS No. PB-292-095) (August), 1978. pp. 206-236.

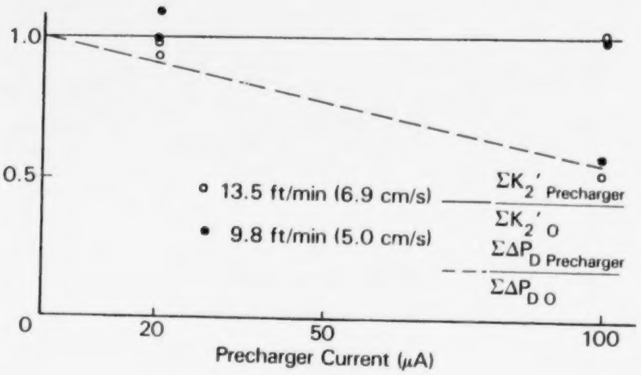

Figure 1. Normalized K_2' and ΔP_D as a function of precharger current. (Each Σ value is summed over three values of field voltage.)

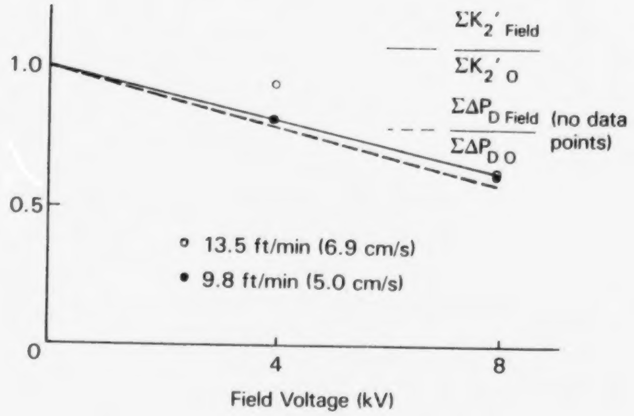

Figure 2. Normalized K_2' and ΔP_D as a function of field voltage. (Each Σ value is summed over three values of precharger current.)

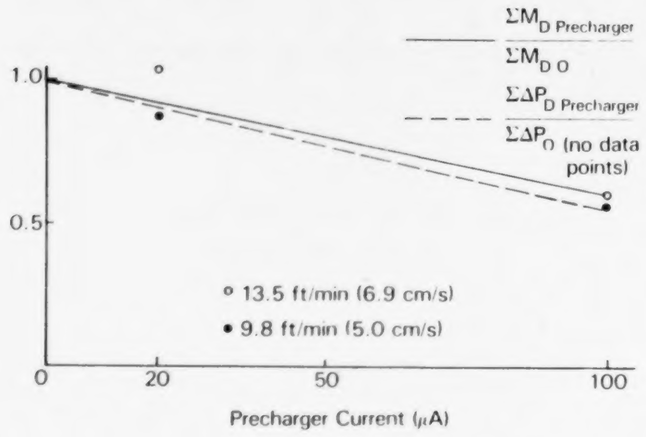

Figure 3. Reduction in dust mass (M_D) deposited on bags because of particle precharging.

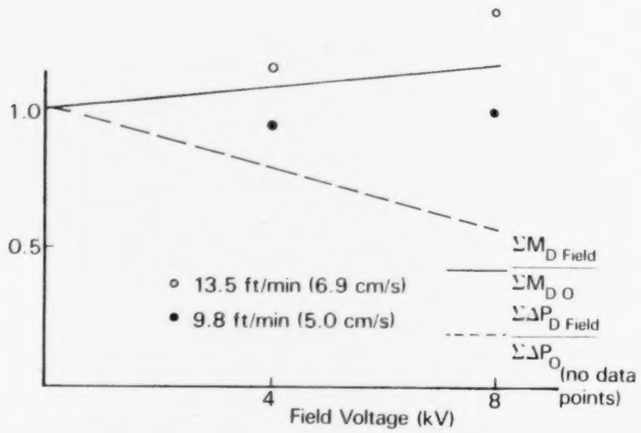

Figure 4. Independence of dust mass and field voltage.

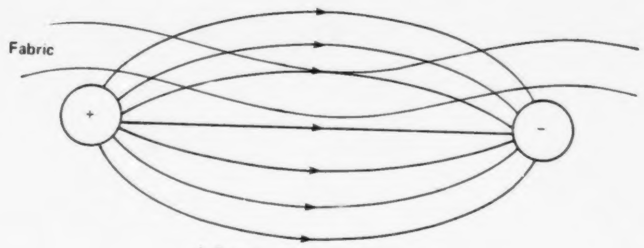

a) Starting field lines ($\epsilon_{fabric} \sim 1$)

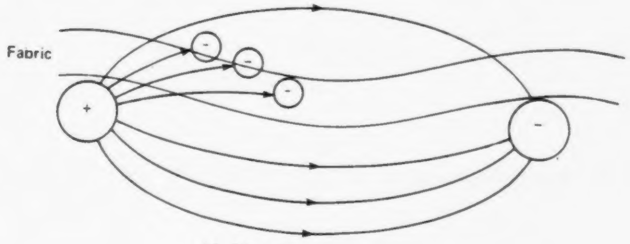

b) After charge accumulation

Figure 5. Predicted influence of charge accumulation on the surface electric field.

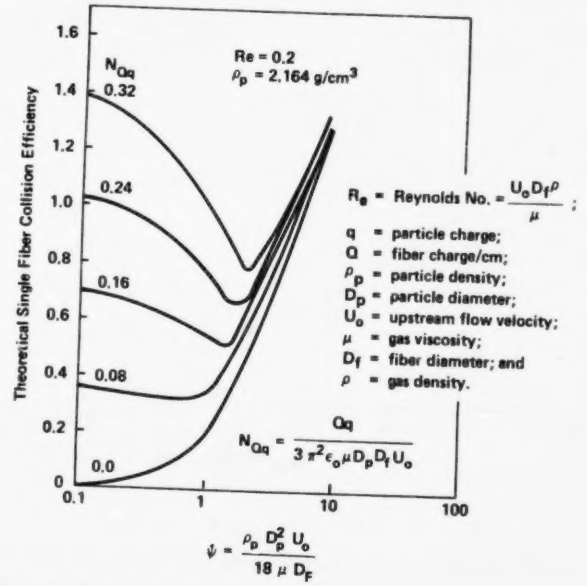

Figure 6. Theoretical single-fiber collision efficiencies. (Inertia, interception, and gravity with electrostatic forces, Lamb's flow field.) (Loeffler, 1978).

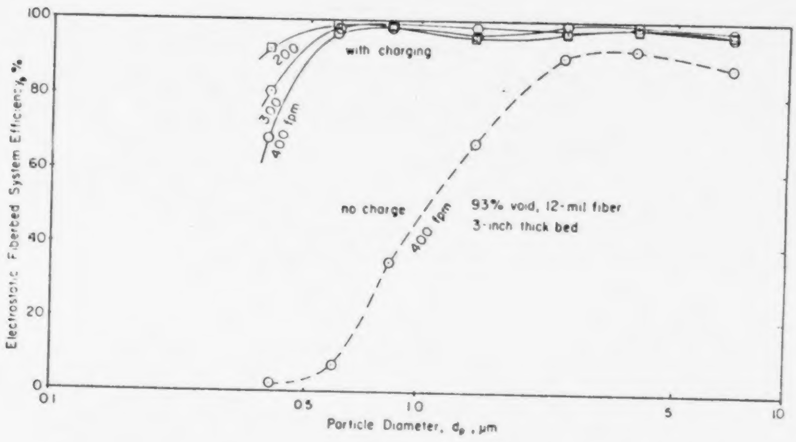

Figure 7. Fractional efficiency of electrostatic fiberbed. (Yu and Teague, 1982).

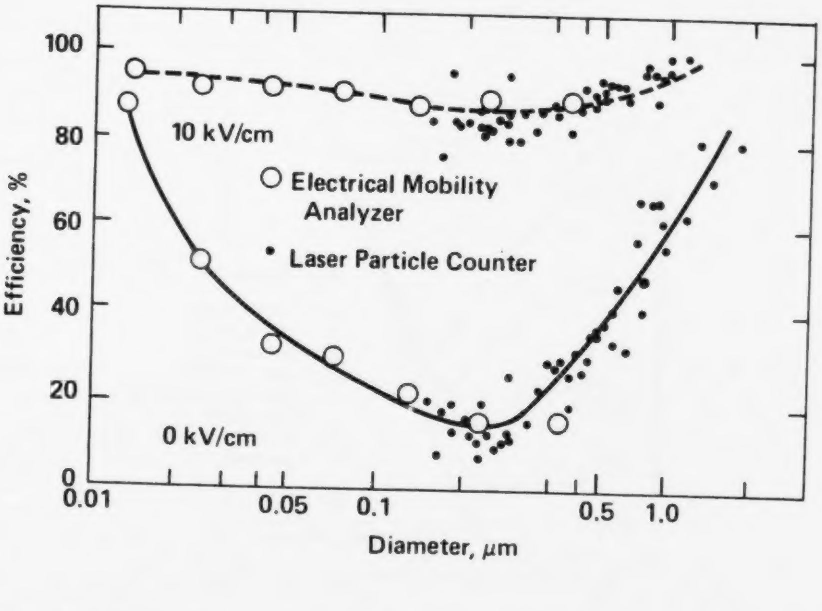

Figure 8. Filter efficiency as a function of particle size with and without an electric field using naturally charged aerosols. (Bergman et al., 1979).

ELECTRICAL ENHANCEMENT OF FABRIC FILTRATION: PRECHARGING VS. BAG ELECTRODES

by: R.P. Donovan
Research Triangle Institute
Research Triangle Park, NC 27709

and

L.S. Hovis and G.H. Ramsey
Industrial Environmental Research Laboratory
U.S. Environmental Protection Agency
Research Triangle Park, NC 27711

ABSTRACT

Two distinct approaches to achieving electrically enhanced fabric filtration are: 1) upstream precharging in a corona discharge; and 2) dust filtration in an external electric field applied by electrodes woven into or positioned adjacent to the bag. Both techniques have demonstrated performance enhancement by some measure, but the mechanisms of enhancement may differ; clearly the hardware does.

This paper reviews the hardware options and configurations available with each basic approach and summarizes various mechanisms whereby each approach brings about an electrical enhancement, including those which dominate in combined precharger/bag electrode systems. From this background, guidelines for matching configurations to source properties are suggested, as well as a hybrid electrostatic precipitator (ESP)/fabric filter design incorporating features that enable it to operate as either an electric-field aided baghouse or a hybrid ESP/baghouse.

This paper has been reviewed in accordance with the U.S. Environmental Protection Agency's peer and administrative review policies and approved for presentation and publication.

As used in this paper, electrical enhancement of fabric filtration refers to any technique for improving filter performance by the use of high voltage electrodes, in either an ionizing or non-ionizing mode, at the fabric surface or some upstream location. Even this restricted definition of electrical enhancement now encompasses a growing number of configurations and mechanisms. Rather than simplify and clarify choices, on-going research is uncovering more mechanisms and options by which the performance of fabric filters can be improved electrically. This paper reviews the present state of understanding and design options now available.

The two basic variables that high voltage can control in particle collection by a fabric filter are dust particle electrical charge and fabric electric field (collector electrical charge).

Early electrical enhancement work concentrated on directly controlling only one or the other of these quantities, while more recent research includes arrangements for controlling each independently. With the more elaborate control capability has come not only more variation in control options, but also improved understanding of the full range of electrical enhancement mechanisms.

CORONA PRECHARGING

Typical hardware for controlling dust charge consists of a corona precharger located upstream of the bags. Conventional wire-duct geometry--a high voltage wire positioned along the centerline of a circular duct which also serves as the low voltage electrode--lends itself to easy incorporation in most installations, new or old. The role of the precharger is to add electrical charge to the dust which certain researchers imply enhances fabric filtration, although no plots of dust drag or dust cake resistance versus collected dust charge/mass are in the literature. What typically appears is a plot of ΔP, drag, or change of drag with dust load versus a measure of corona power supply output or, more commonly, a comparison of precharger ON and precharger OFF performance characteristics. Such data alone leave unanswered questions regarding the enhancement mechanisms.

One obvious collection mechanism is electrostatic precipitation in the precharging section--the precharger is a single-stage electrostatic precipitator, albeit a low efficiency unit in most designs. Thus, dust charged by the wire can be trapped in the same applied electric field that created the corona conditions.

Even charged dust that is not trapped in the precharger section can be precipitated on the duct walls or the baghouse walls prior to reaching the bags. The electrical force driving the charged dust to the walls can be the mutual repulsion between species with charge of the same sign (space charge precipitation) or can be an image force created in the wall by each charged dust particle. The latter is likely to be important only at low charge densities, while the former dominates in high charge density regions more typical of particulate control equipment design.

Regardless of capture mechanism, the effect is to reduce the rate at which dust arrives at the fabric, thus slowing the rate at which ΔP or drag increases but not necessarily changing the dust cake specific resistance (K_2). Thus, this enhancement mechanism is that of a prefilter. From a mass viewpoint alone, a cyclone upstream of the bag does the same. (A cyclone prefilter would affect the size distribution of the dust reaching the bags differently than an ESP prefilter.)

A drawback of any prefilter concept is that two control sections must be operated and maintained, including cleaning. Dust collected by the precharger must also be accounted for and removed. Some clever schemes exist for minimizing this extra cost. For example, in the Apitron® (1) design (Figure 1), the same air pulse that cleans the fabric also cleans the corona wire and duct. The discharge from both sections is to a common hopper so that, in principle, one cleaning action regenerates both sections.

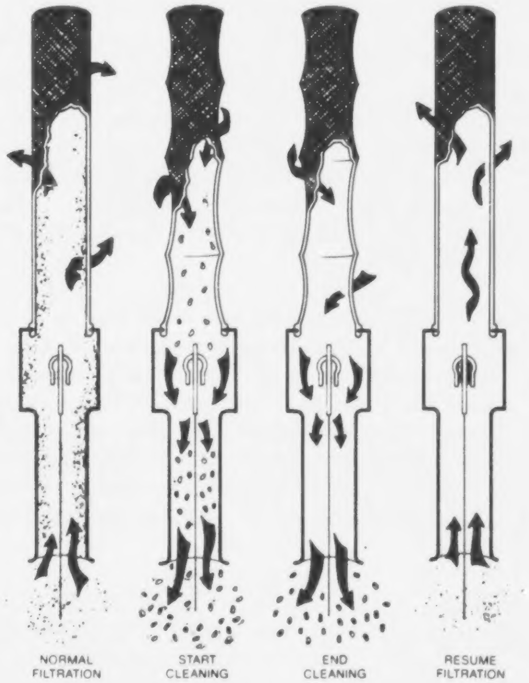

Figure 1. Apitron® design and operation (1).

An alternative approach described by Lamb (2) is to locate the precharger at the bag mouth so that the precipitated dust is collected on the bag surface. In this arrangement, bag cleaning action is all that is necessary since both the precipitated dust and the filtered dust are collected on the bag surface.

At the opposite extreme is the use of a conventional electrostatic precipitator (ESP) in series with a conventional baghouse. This option exists in the field where regulations dictate upgrading of existing ESP equipment. Simply adding a downstream baghouse while continuing to operate the ESP would, in the context of electrical enhancement of fabric filtration, cause the ESP to serve as a precharger for the dust entering the baghouse in addition to performing its usual collection function. Here, however, particulate control is clearly a tandem operation; both the ESP and the baghouse would be operated and maintained as independent units. Because of the reduced load, the ΔP buildup across the fabric would be very slow, independent of any charge-dependent increase in dust-cake permeability.

At least three cases of precharger/baghouse coupling thus exist. Table 1 classifies prechargers according to location with respect to the fabric collection surface of the downstream baghouse. The role of a precharger is to add electrical charge to the dust. All prechargers are assumed to perform this function satisfactorily and to succeed in having most of the dust particles at near-saturation charge when they leave the precharger section. Then, depending on the length of the run between the precharger and the geometry of the intervening duct work, more or less charge is lost in transit.

For the close-coupled case, virtually all charge added to the dust by the precharger ends up on the bag surfaces as the dust is collected. For the independent units, considerable loss of charge and dust will occur by collision with the walls. Dust that contacts the walls but is subsequently reentrained will probably have lost most of its charge. The quantity of charge reaching the fabric surface is likely to be a small fraction of that carried away from the precharger by the dust.

No charge data exist for these two extreme cases. For the second case listed in Table 1--the remote coupled--some measurements of charge deposited on the bag do exist. By comparing these measured values with the total charge that would be collected if all the particles collected carried the saturation values of charge corresponding to the operating conditions of the precharger, the observed charge is typically 2 to 5 percent of what is calculated to leave the precharger. (The procedure for calculating expected charge per particle follows conventional ESP procedures and is outlined in the Appendix of Ref. 3.)

Field coupling (Table 1) refers to a field component being present at the fabric surface because of the location of the precharger. While a field component at the fabric can be created not only by applying a voltage to the corona wire but also by the charges added to the dust leaving the precharger, the field coupling in Table 1 refers only to the direct coupling--that component that is present when corona power is ON but no dust is flowing--and only the close-coupled case produces such a fabric surface field component.

Common cleaning (Column 2, Table 1) implies that an additional separate cleaning action is not required to remove the dust collected by the precharger. For the separate units case (No. 1, Table 1), the ESP hoppers must be emptied and the collection plates rapped. Common cleaning is not possible. For the close-coupled unit, there is no collection surface other than

TABLE 1. TYPES OF PRECHARGER-BAGHOUSE COUPLINGS

	Electrical Coupling		Common Cleaning	Electrical Enhancement of*	
	Charge	Field		S; $\Delta S/\Delta t$	K_2'
1. Two independent separate units (ESP upstream of the baghouse)	Yes (small)	No	No	Yes	? (No data available)
2. Remote-coupled units (Precharger in the hopper inlet)	Yes	No	Yes/No (Geometry dependent)	Yes	Yes/No (Dust conductivity and size dependent)
3. Close-coupled units (Precharger at the bag mouth)	Yes (high)	Yes	Yes	Yes	Yes...but†

---

[*] S = drag = $\Delta P/V$; K_2' = measured specific cake resistance = $\Delta S/\Delta M$ (where M = dust mass/unit area).

[†] Yes, assuming uniform dust distribution, but dust distribution is known to be highly non-uniform.

the fabric. When the fabric is cleaned, both the baghouse and the ESP collectors are being cleaned, since they are the same.

The remote-coupled unit (Case 2, Table 1), as operated at EPA/RTP, does not require additional cleaning because virtually all of the precipitated dust collects in the hopper or the baghouse walls. No additional cleaning is required as these surfaces slough off their dust loads in normal operation without a special trigger. The precharger walls do not accumulate any dust because of the high gas flow-through. Other larger remote installations may not operate this way, and aperiodic rapping might be required.

The evidence showing filtration to be electrically enhanced consists of reduced S and $\Delta S/\Delta t$ in all cases. Only for the close-coupled case is $\Delta S/\Delta M$ unambiguously reduced. This reduction in $\Delta S/\Delta M$ appears to result primarily from a highly non-uniform dust distribution along the bag length, the greatest dust areal density being adjacent to the precharger end of the bag, where the precharger contribution to the fabric surface electric field is concentrated (2).

In the remote-coupled configurations, reports of K_2' enhancement conflict. Ariman and Helfritch (4), Chudleigh and Bainbridge (5), and Iinoya and Mori (6) present data which show enhanced K_2', while Donovan et al. (3) and Hovis et al. (7) fail to find such a result. The key to this difference apparently lies in the capability of certain collecting systems to accumulate electrical charges as they collect dust, thereby building up an electric field on the fabric surface. Filtration of charged dust in the presence of this self-induced electric field produces a reduced K_2'. If, however, the collecting surface is conductive, so that no significant electric field builds up, the K_2' enhancement does not occur. At room temperature, increases in the relative humidity from 48 percent to 58 percent can convert a K_2' enhancing system to a non-enhancing system as reported in the data published by Chudleigh and Bainbridge (5). Because of high flyash resistivity, utility baghouses operate under conditions that favor a K_2' reduction in either the independent or remote-coupled configurations, but this result also depends on particle size being small (see Refs. 8 and 9).

Corona wires in all precharger versions must be cleaned, especially those which are located between the bags and the hopper, such as the Apitron® or a bottom-feed close-coupled case. During cleaning, the dust removed from the bag cascades through the electric field on its way to the hopper, adding an extra opportunity for dust collection on the corona wires. A top-feed design avoids this potentially deleterious interaction.

FIELD ELECTRODES

The role of field electrodes is to create a strong external electric field throughout the volume occupied by the filtration media and the near upstream volume of the fabric. Orientation of the electric field can be either in the direction of gas flow through the filter--roughly perpendicular to the fabric surface--or in the plane of the fabric surface--roughly perpendicular to the direction of gas flow (Table 2). Different authors have preferred different orientations based on analyses of a single fiber in an electric field. For example, Havlicek (10) argues for the electric field in the direction of the gas flow; Lamb et al. (11) prefer the electric field perpendicular to the gas flow. Without discussion, Zebel (12) solves only the case of electric field parallel to the gas flow.

In practice, both orientations have been used successfully. The practical advantages of building the electrodes into a cage or the fabric itself have resulted in more experience with the electric field in the plane of the fabric than along the direction of gas flow, but limitations in this arrangement, chiefly with respect to power consumption with low resistivity dusts or fabrics, may lead to more research with the alternative orientation and arrangement. Primary emphasis here will be on configurations that orient the field in the plane of the fabric--the ESFF (electrical stimulation of fabric filtration) orientation developed at Textile Research Institute (11, 13).

TABLE 2. FIELD ELECTRODE OPTIONS

Electric Field Perpendicular to Fabric Surface

  a) center-line wire electrode (inside-out flow)
  b) enclosing cage or housing wall (single bags)

Electric Field in the Plane of the Fabric Surface

  a) electrodes upstream (dirty side)
  b) electrodes downstream (clean side)
  c) electrodes woven into the fabric

Even after the selection of the field orientation in the plane of the fabric, options exist. The electrodes can be upstream (wholly on the dirty-gas side of the fabric), downstream (wholly on the clean-gas side of the fabric), or incorporated into the fabric itself (part upstream, part downstream, and part within).

The option recommended by Lamb and Costanza (14) (and still the preferred from a field strength viewpoint) is the upstream location in which the electrodes, an array of parallel wires of alternating polarity, are positioned immediately in front of the fabric but not quite touching it. This location creates a high electric field in the near-upstream region of the fabric just prior to dust collection. The electrical enhancement is greater when the fabric surface has a heavy nap finish which causes many surface fibers to protrude into the upstream region. In the presence of an electric field these fibers become more efficient capture centers than without the electric field. Since dust collected in this low fiber density region makes a smaller incremental contribution to fabric drag than dust collected deeper within the fabric, the net result of turning ON the field is a lower K_2'. This model of ESFF has been dubbed "the tall trees" model (15), and represents a depth redistribution of collected dust mass. Areal mass density, averaged over dimensions large with respect to fiber-to-fiber separation, is assumed constant in this model. Dust mass distribution as a function of depth into the filter is postulated to account for the improved performance.

A major advantage of the upstream location is that the electric field in the near-upstream volume from the fabric is not attenuated by fabric electrical properties. When the electrodes are shifted to the downstream clean side, a layer of fabric shields this critical near-upstream volume from the electrostatic field. With conductive fabrics (or conductive dusts which become an important part of the filtration media as the dust accumulates in and on the fabric), a significant reduction in the electrical field in the near-upstream volume could occur. The "tall trees" model predicts that such a reduction in field in this region should reduce the magnitude of the enhancement per unit applied voltage between the electrodes.

In some reports switching from a high resistivity fabric such as Teflon to a lower resistivity material such as polyester does in fact degrade the observed electrical field enhancement, confirming qualitatively this prediction of the tall trees model. By other accounts, however, this fabric dependence is not observed. And, in the initial pilot-scale work on an industrial boiler (16), switching from upstream electrodes to downstream electrodes (Teflon fabric) had little effect on the electrical enhancement. Thus, attenuation of the electrical field appeared unimportant here.

The major advantage of downstream electrodes is that they can be easily incorporated into the support cages of outside-in bag filters, allowing ESFF to be implemented with only minor modifications in the conventional hardware. Rather than require the design of a special electrode harness as in the upstream option, the downstream option can be implemented by the simple addition of electrical insulators between appropriate cage members. This arrangement has been shown to perform with impressive economic advantage on a pulverized-coal-fired industrial boiler (16), even though the fabric used in this demonstration was the relatively expensive Teflon felt.

Electrodes woven into the fabric are a third option seemingly well matched to the requirements of reverse-air cleaned baghouses. In this configuration yarns made of conductive fibers become part of the fabric weave. Choice of suitable weave pattern allows the conductive yarn to face primarily upstream if that is deemed desirable or to be incorporated in any of the variety of weaves available to textile processing. A major advantage of this configuration is that it minimizes user preparation and demands. In routine service the plan is to install and handle the ESFF bags much the same as conventional bags. The only differences would be that the fabric is special and an electrical contact, perhaps no different from conventional mechanical attachment, however, must be made at each end of the bag. In operation the ESFF power supplies must be monitored.

Experience with this option is limited to laboratory operation at present but already some striking differences are apparent, the most pronounced of which is preferred deposition of the collected dust on the electrodes, as reported by Lamb (2). This mechanism of enhancement is a surface redistribution phenomenon--the deposited dust does not coat the fabric surface uniformly as in conventional filtration but piles up on the electrodes creating a distinct striped deposition pattern in the early stages of filtration. The dust pattern mirrors the electrode geometry, although one electrode polarity generally appears to collect more dust than the other.

This kind of deposition pattern leads to an electrical enhancement attributable to non-uniformity in dust deposition between electrodes, similar to that previously reported by Penney (17) and by Chiang et al. (18). This type of deposition non-uniformity is also similar to that previously associated with the close-coupled precharger. When the woven-in electrodes are in the warp direction (along the bag axis) of a vertically suspended bag, the deposition non-uniformity is in the lateral direction (the concentration gradient is maximum in the horizontal direction). When combined with a close-coupled precharger (deposition non-uniformity in the vertical direction), as in Lamb's configuration, the resultant two-directional non-uniformity produces dust deposits of drastically reduced K_2' as compared to either single-direction non-uniformity alone or the uniform deposition case (2).

Because of the parallel flow paths through a bag, the dust distribution that results in the highest net drag is the uniform distribution. Any departure from uniformity produces a lower net drag because the flow through the region of reduced drag increases with respect to the flow through all other regions. This argument assumes that drag is proportional to areal mass density. Decreasing the mass density in one area decreases that area's drag and correspondingly increases the drag of all those areas to which the displaced mass has been added.

Figure 2 illustrates the parallel flow concept. These curves, adapted from Dennis et al. (19), plot net filter drag as a function of dust loading for two distributions (Figure 3): 1) the uniform loading case, and 2) a highly non-uniform loading case. The non-uniform case assumes that the dust deposits on the fabric in increments of areal density equal to 700 g/m^2 so that the fabric consists of two areas: a loaded area and an unloaded area. As deposition continues, the size of the loaded area (dust load always equals 700 g/m^2) grows uniformly with time. In the uniformly loaded case, the dust load per unit area increases uniformly with time.

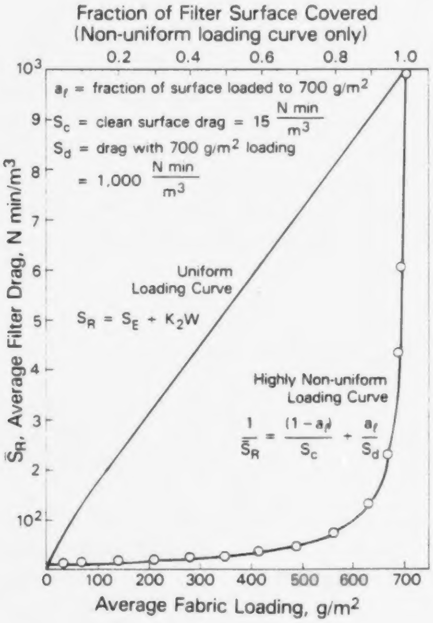

Figure 2. Impact of non-uniform dust loading upon drag (19).

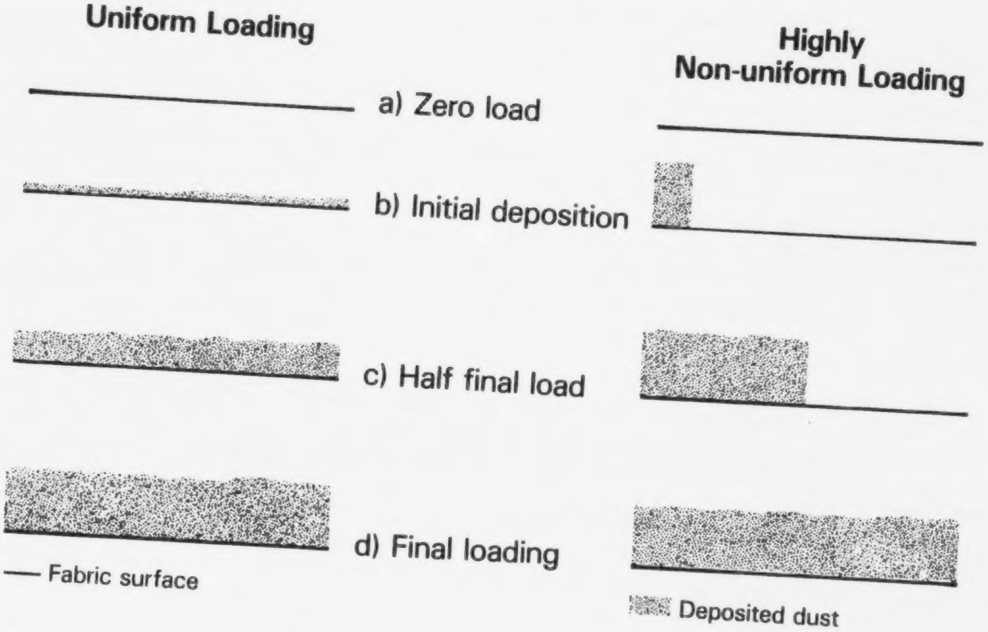

Figure 3. Loading schematic.

The curves of Figure 2 show that, for the drags assumed for the loaded and unloaded areas, the net filter drag of the highly non-uniform case is not only lower than that of the uniformly loaded case but (over much of the range of dust loads) dramatically so. Not until the non-uniform case begins to run out of area does its dS/dM exceed that of the uniform case. This rapid rise in S brings the two curves together at the same final loaded condition (the non-uniform case becomes uniform at 700 g/m^2 loading when all its area is loaded), but the route over which that same end point is reached differs dramatically.

Non-uniform loading via electrical forces has the effect of changing the conventional uniform loading drag characteristic into one more like the non-uniform loading curve illustrated in Figure 2. Chiang et al. (18) have mathematically modeled pressure drop reduction for both step changes in dust cake areal density and bell-shaped distributions in support of non-uniform deposition as a mechanism of electrically enhanced fabric filtration.

This non-uniform loading mechanism is distinct and independent from the tall trees mechanism. Both the tall trees model and the non-uniform loading model can predict the observed results, and some experimental confirmation of each now exists in the literature. Which dominates when is important in choosing hardware for electrical enhancement.

One further option should be resurrected--that of the electric field aligned parallel to the gas flow (perpendicular to the fabric surface). An embodiment that is both easy to implement and compatible with reverse-air baghouse design is the suspension of a corona wire down the center of a bag which is itself either conductive or else incorporates conductive electrodes woven into its fabric. This configuration can operate in either an ionizing or non-ionizing mode; its main advantage, however, is that it is compatible with dusts which otherwise, with electrodes in the plane of the fabric, would draw prohibitively large currents. Note, however, that such a configuration creates the highest field and the highest field gradient in the vicinity of the corona wire. This feature means that this configuration will probably be most effective when operated as an electrostatic precipitator (ESP), generating its own charges for the dust and drifting this charged dust by Coulomb forces to the fabric surface for capture. In this mode the equipment then operates as a conventional wire-duct ESP in which the collector surface is a fabric filter and the air flow is through the collector plate rather than parallel to it. It is in effect a hybrid ESP/fabric filter.

SUMMARY OF MECHANISMS

Mechanisms capable of predicting electrically enhanced filtration include:

1. Prefiltering, because of electrostatic precipitation.
2. The "tall trees" model, a depth distribution effect.
3. Non-uniform deposition, a surface distribution effect.

Other candidate mechanisms, such as electroclamping (20), exist.

Comparing these mechanisms with the choices of precharger configurations (Table 1) and field electrode configurations (Table 2) leads to certain general conclusions:

1. Prefiltering applies only to precharger location; the close-coupled precharger minimizes its significance.
2. The tall trees model depends strongly on fabric properties and electrode location. It postulates enhanced dust capture by upstream fibers, so depends on any variable that contributes an electrical capture force such as fiber-scale electric field in the upstream region, and dust electrical charge. This mechanism is compatible with either Coulomb forces or polarization forces.
3. Non-uniform deposition also depends on electrical forces but responds over a bigger volume--the electrical forces in the upstream regions remote from the near-fabric-surface volume, most likely Coulomb forces, are important. Distinct from the tall trees mechanism, it does not depend on fabric surface finish and should be less dependent on fabric properties, a distinct advantage.

Any specific hardware design for electrical enhancement depends on understanding the mechanism by which the electrical enhancement occurs. In general this understanding does not yet exist. What typically is known is that electrifying a given conventional operation produces certain improvements in performance. Reports of such improvements are frequently accompanied by speculation as to the enhancement mechanism, such as those previously listed, but established proof is scarce.

Against such a background and with the uncertainties it implies, a few tentative guidelines can be suggested (Tables 3 and 4).

TABLE 3. PRECHARGER DESIGN CONSEQUENCES

Configuration	Dust	Remarks
K_2' Reduction		
Close coupled	Any	Non-uniform deposition
Any	Small ($\leq$ 3-5 μm), nonconductive	Coulomb force aided (field self-created by collected particles)
No K_2' Reduction		
Remote or separate	Any size, conductive	No self-created field
Remote or separate	Large ($\geq$ 5 μm), nonconductive	Inertial capture forces dominate Coulomb forces

TABLE 4. ELECTRODE DESIGN CONCLUSIONS

1. Downstream electrodes, incorporated into the support cage, match up best with outside-in filters.
2. Woven-in electrodes are the preferred configuration for inside-out filtration.
3. Upstream filters, while electrically advantageous, do not justify their added cost at present.

1) While any of the precharger locations described can serve as a prefilter, the close-coupled configuration is the only one guaranteed to decrease the dust-cake resistance because it is the only one which precipitates dust on the bag surface and capitalizes on the non-uniform deposition mechanism (2, 17, 18). For the special category of non-conductive small particles

(less than say 3 to 5 μm), the self-induced electric field at the fabric surface could also produce a reduced K_2' using any of the precharger configurations (8, 9, 21).

2) With remote or separate precharger configurations, the only guaranteed mechanism of electrical enhancement is that of a prefilter. Only when filtering small non-conductive dust particles is the electrical enhancement likely to include a K_2' reduction (9). The prefilter function is itself often worthwhile, especially if it entails no additional cleaning hardware, hoppers, or dust removal, as is true in the EPA/RTP pulse-jet baghouse.

3) When corona prechargers are used, they will be subject to operating limitations similar to those of existing ESPs with regards to back corona. Note, however, that poor particle charging and low-efficiency collection can be better tolerated in a precharger than in an ESP. Thus, a precharger should not be ruled out simply because an ESP has been ruled out.

4) Bag electrodes that create an electric field in the plane of the fabric are simple to build and use when they are incorporated into the bag or as part of the cage. This consideration favors the electrode/cage assembly for pulse-jet operations and woven-in electrodes for reverse air (printed electrodes, not yet successfully developed, also share this advantage [2]).

The performance advantages cited for upstream electrode placement do not justify their added expense. Ruggedness and long field life would need to be included in any demonstration to alter this conclusion.

5) Configurations that favor non-uniform deposition such as the woven-in electrode fabric and the close-coupled precharger described by Lamb (2) appear less dependent on fabric properties and electrode location than those relying on the tall trees mechanism; that is, dust non-uniformities (large with respect to fiber or dust particle dimensions) are less dependent on fiber or dust properties than those that depend on dust-cake porosity changes. The fields and electrical charges needed to create gross non-uniformities are easier to reproducibly create in the laboratory than the fiber-scale fields and charges.

6) A practical field-electrode configuration compatible with conductive dust ESFF, while not yet demonstrated, appears to be available based on a variation of one embodiment contained in Sharlit's patent (22) or as discussed by Frederick (23). This concept is the suspension of a corona wire down the centerline of a reverse-air bag. The counter electrode is the bag itself (coated with conductive particles) or electrodes woven into the bag. No conductive path forms between the high voltage and the bag electrodes. When in corona, this configuration operates as a hybrid ESP/fabric filter.

ACKNOWLEDGEMENTS

It is a pleasure to acknowledge the contribution of George E.R. Lamb and his coworkers at Textile Research Institute who hosted one of the authors (R.P. Donovan) for an extended visit during which certain of the ideas expressed in this paper were crystallized or refined.

REFERENCES

1. Helfritch, D.J. Apitron®. Product Brochure, Apitron Division, American Precision Industries, 12037 Goodrich Drive, Charlotte, NC 28217, 1979.

2. Lamb, G.E.R. Influence of particulate precharging on the performance of an electrically stimulated fabric filter (ESFF). Paper presented at World Filtration Congress III, The Filtration Society, Downingtown, PA. September 14-16, 1982.

3. Donovan, R.P., Hovis, L.S., Ramsey, G.H., and Abbott, J.H. Pulse-jet filtration with electrically charged flyash. In: Third Symposium on the Transfer and Utilization of Particulate Control Technology, Vol. I. EPA-600/9-82-005a (NTIS PB 83-149583), July 1982.

4. Ariman, T. and Helfritch, D.J. Pressure drop in electrostatic fabric filtration. In: Second Symposium on the Transfer and Utilization of Particulate Control Technology, Vol. III. EPA-600/9-80-039c (NTIS PB 81-144800), September 1980.

5. Chudleigh, P.W. and Bainbridge, N.W. Electrostatic effects in fabric filters during build-up of the dust cake. Filtration and Separation. 309-311, July/August 1980.

6. Iinoya, K. and Mori, Y. Experimental advances in fabric filtration technology in Japan--effects of a corona precharger and relative humidity on filter performance. In: Second Symposium on the Transfer and Utilization of Particulate Control Technology, Vol. III. EPA-600/9-80-039c (NTIS PB 81-144800), September 1980.

7. Hovis, L.S., Abbott, J.H., Donovan, R.P., and Pareja, C.A. Electrically charged flyash experiments in a laboratory shaker baghouse. In: Third Symposium on the Transfer and Utilization of Particulate Control Technology, Vol. I. EPA-600/9-82-005a (NTIS PB 83-149583), July 1982.

8. Loeffler, F. The influence of electrostatic forces and of the probability of adhesion for particle collection in fibrous filters. In: T. Ariman (ed.), Novel Concepts, Methods and Advanced Technology in Particulate-Gas Separation. University of Notre Dame, 1978.

9. Yu, H.S. and Teague, R.K. Performance of electrostatic fiberbed. Paper presented at 1st Annual Meeting of the American Association for Aerosol Research, Santa Monica, CA. February 1982.

10. Havlicek, V. The improvement of efficiency of fibrous dielectric filters by application of an external electric field. Int. J. Air and Water Poll. 4(3/4): 225-236, 1961.

11. Lamb, G.E.R., Costanza, P.A., and O'Meara, D.J. Electrical stimulation of fabric filtration. Part II: Mechanism of particle capture and trials with a laboratory baghouse. Textile Research Journal. 48(10): 566-573, October 1978.

12. Zebel, G. Deposition of aerosol flowing past cylindrical fiber in a uniform electric field. J. Colloid Sci. 20, 1965.

13. Lamb, G.E.R. and Costanza, P.A. Electrical stimulation of fabric filtration. Textile Research Journal. 47(5): 372-380, May 1977.

14. Lamb, G.E.R. and Costanza, P.A. A low-energy electrified filter system. Filtration and Separation. 319-322, July/August 1980.

15. Greiner, G.P. Electrical stimulation of fabric filtration. Paper presented at APCA 74th Annual Meeting, Philadelphia, PA. June 1981.

16. Greiner, G.P., Furlong, D.A., VanOsdell, D.W., and Hovis, L.S. Electrostatic stimulation of fabric filtration. J. Air Pollut. Control Assn. 31:10, 1125-1130, October 1981.

17. Penney, G.W. Using electrostatic forces to reduce pressure drop in fabric filters. Powder Technology. 18: 111-116, 1977.

18. Chiang, T-K., Samuel, E.A., and Wolpert, K.E. Theoretical aspects of pressure drop reduction in a fabric filter with charged particles. In: Third Symposium on the Transfer and Utilization of Particulate Control Technology, Vol. III. EPA-600/9-82-005c (NTIS PB 83-149609), July 1982.

19. Dennis, R., et al. Filtration model for coal flyash with glass fabrics. EPA-600/7-77-084 (NTIS PB 276489), August 1977.

20. VanOsdell, D.W., Donovan, R.P., Furlong, D.A., and Hovis, L.S. Permeability of dust cakes collected under the influence of an electric field. Paper presented at The Fourth Symposium on the Transfer and Utilization of Particulate Control Technology, U.S. Environmental Protection Agency, Houston, Texas. October 11-15, 1982.

21. Bergman, W., Hebard, H.D., Taylor, R.D., and Lum, B.Y. Electrostatic filters generated by electric fields. Proceedings of The Second World Filtration Congress. 1979.

22. Sharlit, I.B. Filter system. U.S. Patent 3,577,705 (to Hitco), May 4, 1971.

23. Frederick, E.R. Some effects of electrostatic charges in fabric filtration. J. Air Pollut. Control Assn. 24(12): 1164-1168, December 1974.

PERMEABILITY OF DUST CAKES COLLECTED UNDER THE INFLUENCE OF AN ELECTRIC FIELD

By: D. W. VanOsdell and R. P. Donovan
Research Triangle Institute
P. O. Box 12194
Research Triangle Park, North Carolina 27709

D. A. Furlong
ETS, Inc.
Roanoke, Virginia 24018

L. S. Hovis
Industrial Environmental Research Laboratory
U. S. Environmental Protection Agency
Research Triangle Park, North Carolina 27711

ABSTRACT

The reductions in dust cake flow resistance and residual pressure drop that can be achieved by electrostatic stimulation of fabric filtration (ESFF) have been documented. The changes in the dust deposition characteristics which cause these improvements are not well understood. This paper presents results from three investigations into the nature of dust deposits collected with ESFF. Permeability data collected at various axial positions along ESFF and conventional bags were the basis of the first study. The second study concerned the deposition patterns of dust collected on a laboratory filter when ESFF was in use, and the third, the resistance to compression of the collected dust with and without an electric field.

These investigations gave evidence that ESFF caused the formation of a residual dust deposit which was not axially uniform (the permeability at the bottom of the bag was half that at the top) and was more easily removed than a conventional dust deposit. In the laboratory, it was shown that ESFF caused newly collected dust to form very nonuniform deposits. The dust tended to collect near the electrodes, in patterns which have not been observed in the pilot units. In the third study, the ESFF electric field was found to improve the resistance to consolidation of the dust cake collected in a pulse-jet pilot unit.

This paper has been reviewed in accordance with the U. S. Environmental Protection Agency's peer and administrative review policies and approved for presentation and publication.

INTRODUCTION

The use of electrostatic fields to improve the performance of fabric filters is a topic of considerable research interest today. Numerous researchers have investigated the topic, applying electrostatics in different ways. Particle charging, accumulation of charge on the fabric filter, and the application of external electric fields (either perpendicular or parallel to the gas flow) have all been used singly or in combination during this research. In all cases, it has been found that the performance of the filter has been improved in the sense that the drag due to the collected particles was reduced. Generally, an improvement in collection efficiency was also noted. Although much has been learned about the beneficial effects of ESFF, the mechanisms by which it operates in a baghouse are not well understood. The experimental evidence is difficult to reproduce and sometimes contradictory. One important question is whether the ESFF filter deposit is nonuniform at the size scale of the bag, at the scale of the electrode spacing, or at the scale of the particles. Treating the filter as an assembly of resistances in parallel, at any scale, can account for the ESFF effect mathematically.(1) Another question is whether the reduced dust cake drag attributed to ESFF is due to the structure of the dust cake as collected, or to some other phenomenon related to the electric field.

This paper describes three experiments with electrostatically stimulated fabric filtration (ESFF) which cast light on the mechanisms by which ESFF causes reduced filter drag. All three experiments utilized the same concept of ESFF--no particle charging and an electric field applied at the filter surface and oriented parallel to the surface. This concept was initially developed by the Textile Research Institute(2,3,4) and was extended to pilot scale by the Research Triangle Institute (RTI) and ETS, Inc.(5,6)

The first experiment to be described was conducted on bags from the Waynesboro ESFF pilot unit. The permeability of the cleaned bags (both ESFF and conventional) was determined at the top, bottom, and middle areas of the bags. In addition, the particle size distribution of the dust collected at the top and bottom of an ESFF bag was determined. The second experiment considered the appearance of dust deposits collected with and without electric fields. A small laboratory filter was used to remove resuspended fly ash from an air stream, the pressure drop characteristics were measured, and the filter deposits photographed. The third experiment investigated the compressibility of dust collected with and without an electric field. This experiment was conducted on a pilot-scale pulse-jet fabric filter operating on fly ash resuspended in ambient air.

FILTER BAG AXIAL PERMEABILITY MEASUREMENTS

EXPERIMENTAL ARRANGEMENT

The experiments reported in this section were conducted on bags from the pilot-scale ESFF baghouse located at Waynesboro, Virginia. This baghouse has been described in earlier papers(5,6), and only a brief description is presented here. The pilot unit included two identical baghouses operated as parallel units with identical inlets. One baghouse utilized ESFF; the other was conventional. The pilot unit was operated on a slipstream from an industrial boiler house. A schematic diagram of the pilot unit is given in Figure 1. The boiler burned pulverized coal, and the coal supply was highly variable; the average sulfur content was about 1.3 percent and the ash content was about 13 percent. Boiler operation was continuous. The average inlet temperature to the baghouse was about 155° C (310° F), with an average dust loading of about 0.9 g/sm^3 (0.4 gr/scf).

The pilot baghouses (both conventional and ESFF) each contained four bags in a dirty-gas-inside, reverse-air-cleaned configuration. The filter bags were made of J. P. Stevens 648 fabric, a 570 g/m^2 (16.8 oz/yd^2) woven fiberglass cloth with a 10-percent Teflon® B coating. The initial permeability of the fabric was 18 to 28 cm/s at 0.125 kPa (35 to 55 ft/min at 0.5 in. H_2O). The electrostatic augmentation of the ESFF bags was provided by a vertical array of 3.2-mm (0.125-in.) wires, connected to provide alternating grounded and high negative potential electrodes (Figure 2).

TEST PROGRAM

The pilot baghouses were used to test the long-term behavior of reverse-air-cleaned fiberglass bags under ESFF conditions. The operational results of this test have been reported(5), and this paper discusses permeability results obtained after the bags had been removed from the baghouses. Results from two bag sets are reported. One bag set (to be referred to as JF) was in use during January and February 1982. The second set (June) was in use during June 1982. All bags were conditioned at 1 cm/s (2 ft/min) and were operated at about 2 cm/s (4 ft/min). The electrical field was applied to the ESFF bags from start-up and was maintained continuously at about 3 kV/cm. During the JF test period, the conventional baghouse was used as a control on the ESFF experiment. During the June test, both baghouses were in use in different ESFF arrangements, and control bags were not available.

The permeability tests reported here were run on a standard bag permeability test apparatus.(7) The JF bags were in a "just-cleaned" state when tested. The June bags were removed before cleaning, taken to the laboratory to remove dust samples, then extended to allow the remaining dust cake to fall off prior to permeability testing. Permeability tests were run on the fabric in an "as-received" condition and following vacuum cleaning at 3.75 kPa (15 in. H_2O) vacuum and at 7.5 kPa (30 in. H_2O) vacuum. These tests were done for both the conventional and ESFF bags.

The particle size distribution tests were run on dust samples from the top and bottom of the June bags by resuspending and analyzing the dust in a Bahco apparatus.

RESULTS

The results of the permeability tests are presented in Table 1, and the results of the Bahco size analysis in Figure 3. Features of these results which merit special attention are discussed below.

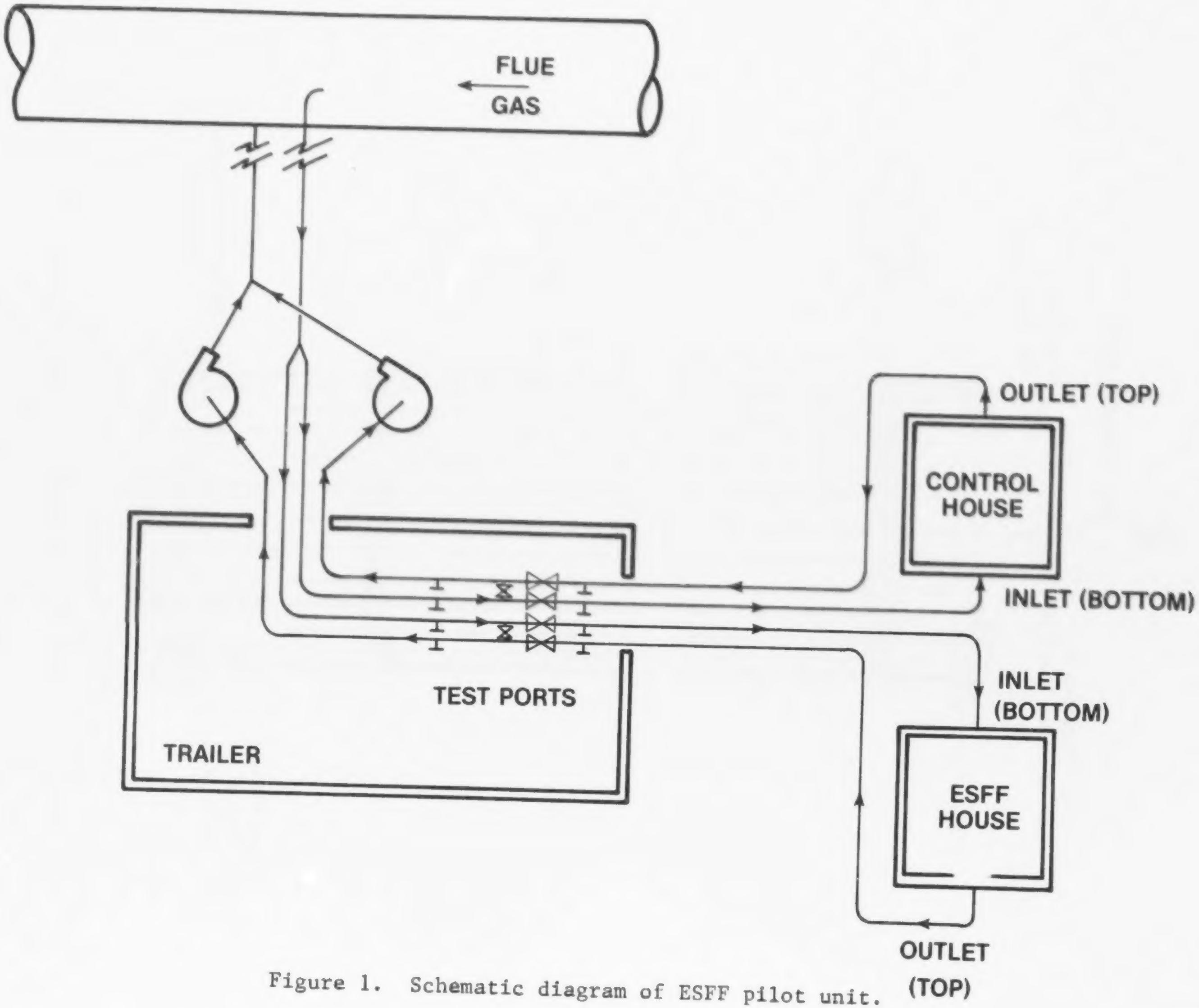
FLUE
GAS
OUTLET (TOP)
CONTROL HOUSE
INLET (BOTTOM)
INLET (BOTTOM)
ESFF HOUSE
OUTLET (TOP)
TEST PORTS
TRAILER

Figure 1. Schematic diagram of ESFF pilot unit.

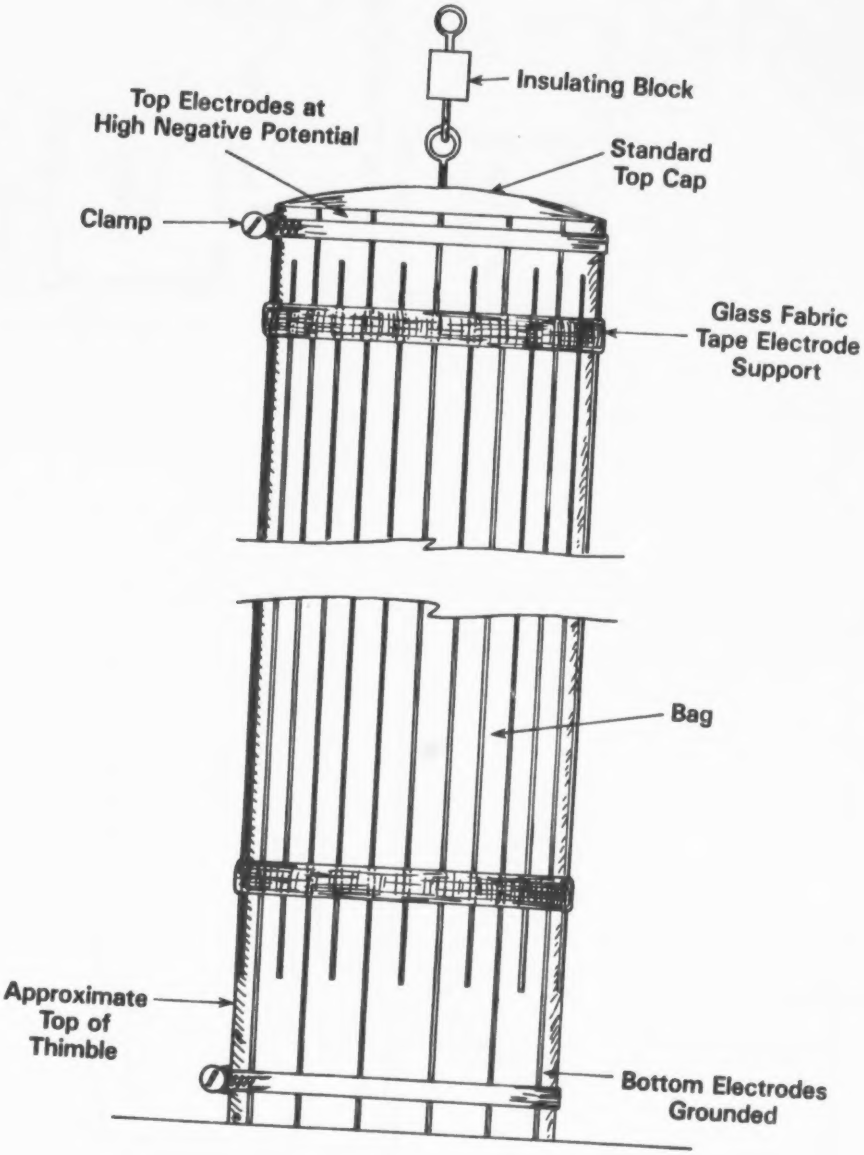
Insulating Block
Top Electrodes at High Negative Potential
Standard Top Cap
Clamp
Glass Fabric Tape Electrode Support
Bag
Approximate Top of Thimble
Bottom Electrodes Grounded

Figure 2. Pilot-unit reverse-air bag electrode array.

TABLE 1. PERMEABILITY RESULTS FOR ESFF AND CONVENTIONAL BAGS*

Sample Descriptor	Permeability Results—ft/min @ 0.5 in. H_2O ΔP (cm/s @ 0.125 kPa ΔP)		
	January-February (JF)† Conventional Bag	January-February (JF)† ESFF Bag	June‡ ESFF Bag
As received:			
Top	3.8 (1.9)	5.5 (2.8)	4.5 (2.3)
Middle	2.6 (1.3)	3.6 (1.8)	N.M.§
Bottom	3.3 (1.7)	1.6 (0.8)	3.6 (1.8)
Vacuumed @ 3.75 kPa (15 in. H_2O):			
Top	3.8 (1.9)	11.8 (6.0)	11.5 (5.8)
Middle	5.5 (2.8)	6.7 (3.4)	N.M.§
Bottom	2.9 (1.5)	4.4 (2.2)	10.5 (5.3)
Vacuumed @ 7.5 kPa (30 in. H_2O):			
Top	7.4 (3.8)	13.6 (6.9)	17.5 (8.9)
Middle	8.3 (4.2)	9.7 (4.9)	N.M.§
Bottom	5.7 (2.9)	7.5 (3.8)	12.5 (6.4)

* All test work performed by ETS, Inc.

† January-February results from one bag.

‡ June results are average from two bags.

§ N.M. = not measured.

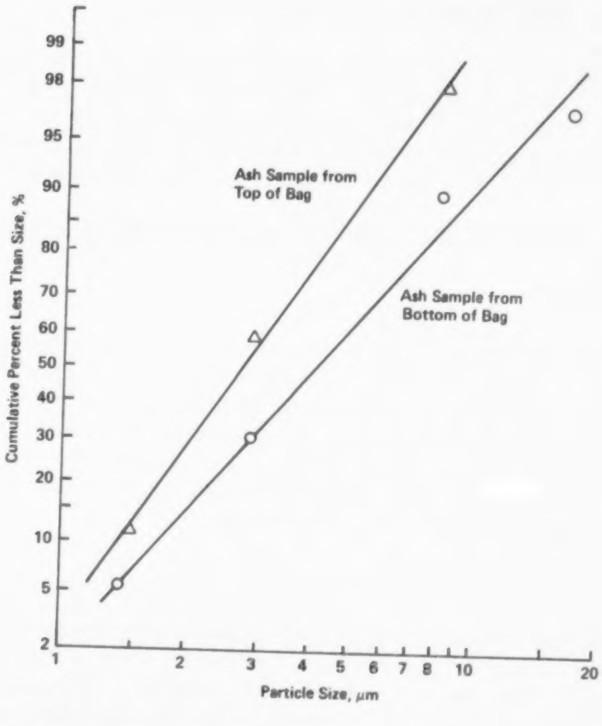

Figure 3. Bahco size distribution of dust from top and bottom of June ESFF bag.

Axial Variation of Permeability of ESFF Bag

The permeability at the top of the ESFF bag was consistently greater than at the bottom, both before and after vacuuming and for both ESFF bags. This is especially evident for the JF ESFF bag. The permeability of the JF conventional bag was lowest at the bottom, highest in the middle or top, and did not vary as much between positions as did the JF ESFF bag.

Magnitude of Permeability

The average of the three permeability measurements for the ESFF bag in the as-received state was 11 percent greater than that of the conventional bag. It was 87 percent above the conventional bag permeability after the first vacuuming and 44 percent higher after the second.

Ease of Cleaning

The JF ESFF bag had an average permeability before vacuuming of 3.6 ft/min (1.8 cm/s). Following vacuuming at 3.75 kPa, the average permeability had risen to 7.6 ft/min (3.8 cm/s), an improvement of 11 percent. For the JF conventional bag, the same treatment increased the permeability from 3.2 ft/min (1.6 cm/s) to 4.1 ft/min (2.0 cm/s), an increase of 28 percent.

Axial Variation of Dust Deposit Size Distribution

The size distribution of the dust at the top of the ESFF bag differs from that at the bottom (Figure 3). Mass mean diameter at the bag top was 2.6 μm and at the bottom, 3.7 μm. As no corresponding data are available for the conventional pilot plant bags and others(8) report similar trends for conventional baghouses, this variation cannot be ascribed to the ESFF effect.

DUST COLLECTIONS ON A LABORATORY FILTER

EXPERIMENTAL APPARATUS

The laboratory filter deposition study was conducted on the apparatus shown in Figure 4. As shown, the filter is oriented face downward and is 10 cm square. The electric field was provided by six parallel electrodes spaced 2 cm apart and located on the clean side of the filter. The test dust was resuspended fly ash, fed by a screw feeder into a sonic air jet, blown against an impaction plate, and then into the inlet duct. The tests were conducted with ambient air as the carrier gas.

TEST PROGRAM

Fly ash from the Waynesboro pilot unit, resuspended in a sonic air jet at about 4 g/m^3 (1.8 gr/ft^3), was fed to the filter at a face velocity of 2 cm/s (4 ft/min). Cascade impactor size analysis indicated a mass median aerodynamic diameter of about 3.1 μm for the resuspended ash. An extractive charge-to-mass measurement based on a filter within a Faraday cup indicated an average net positive charge on the resuspended ash of 0.57 μC/g. The

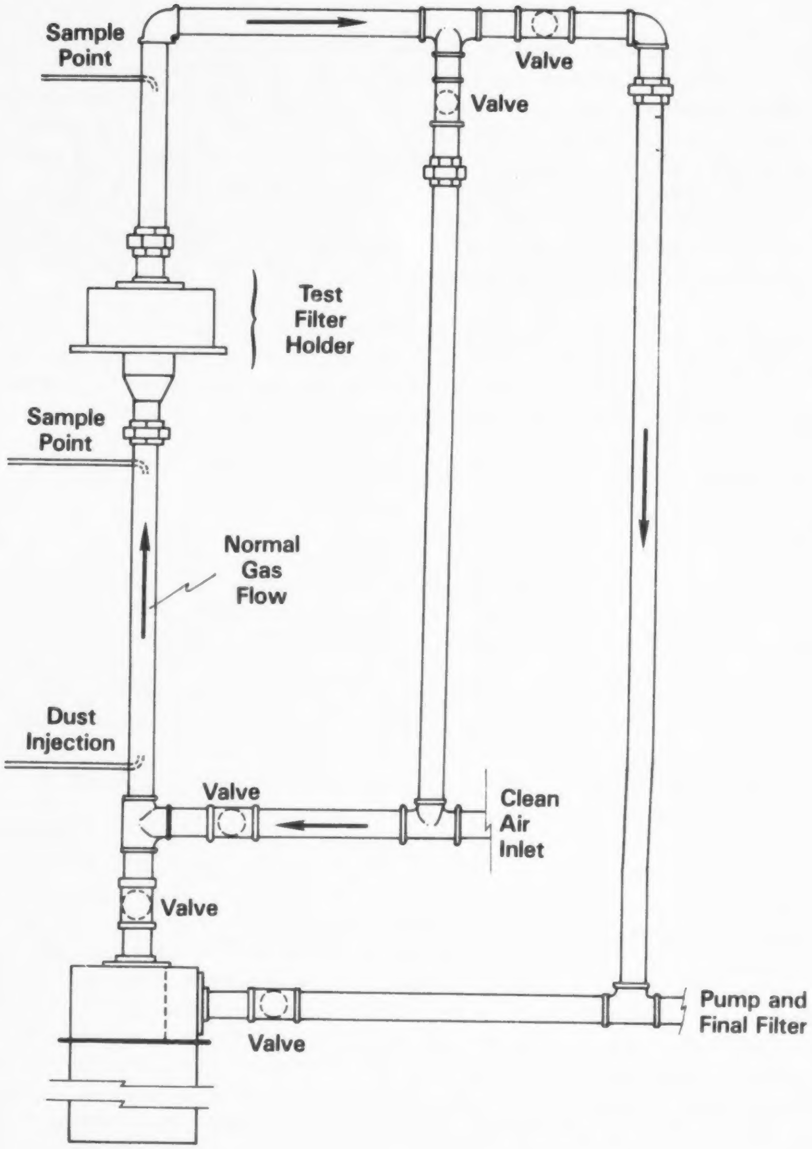
Sample Point
Valve
Valve
Test Filter Holder
Sample Point
Normal Gas Flow
Dust Injection
Valve
Clean Air Inlet
Valve
Pump and Final Filter
Valve

Figure 4. Laboratory filtration apparatus.

filter was of glass fiber, and a new filter was used for each test. The filter was weighed before and after the run to get an approximate measure of the cake mass. Run time was 100 min for these experiments, and the total dust cake mass was between 4 and 5 g.

RESULTS

The dust accumulations on the filter were nonuniform when the electric field was ON, becoming increasingly nonuniform as the field increased. Figure 5 is a photograph of the dust cake when collected with the field OFF. The faint surface lines were produced by turning the field ON after the dust cake was collected, with clean gas flow through the filter. Figure 6 shows a deposit collected with an electric field of 1 kV/cm, and Figure 7, a deposit collected with a 4-kV/cm electric field. The pressure drop behavior of each deposit is shown in Figure 8; as expected, the dust cakes with the field ON have a lower pressure drop than with the field OFF at any given time.

Dust samples from the positive and negative electrodes of a 4-kV/cm run were analyzed by a Coulter counter, along with a sample from between the electrodes. The size distribution curves from the three sites were identical; the mean diameter was 2.37 μm from the Coulter analysis.

INFLUENCE OF AN ELECTRIC FIELD ON DUST CAKE COMPRESSIBILITY

INTRODUCTION

The compaction of filter dust cakes due to the increasing pressure drop across the cake has been described.(9) Increased interparticle adhesion within a particle bed due to an external electric field has also been documented and discussed.(10,11) Increased interparticle adhesion has the potential of being an important ESFF mechanism. If a large fraction of the pressure drop across a filter cake is caused by the continual compression of the cake, then interparticle forces which prevent or reduce cake compression would reduce the net pressure drop much as is observed with ESFF. Some evidence for a mechanism of this sort can be observed in a pilot unit pressure drop characteristic curve. Figure 9 compares the ΔP for the buildup of a dust cake collected with the electric field ON to a conventional field-OFF curve. While the reduced ΔP of the field-ON curve is evident throughout, the field-ON curve exhibits a continually increasing slope which includes a series of steps at high pressure drops--indicating dust cake consolidation by discrete cake collapses. The field-OFF curve also shows these steps but not as many and they are reduced in magnitude. This difference between the two curves suggests that the field may increase interparticle adhesion sufficiently to support a more porous dust cake initially but that at least part of this advantage can be lost through cake compression. The discussion below reports a test series which investigates the drag of dust cakes collected with and without an electric field when subjected to stress from increased filter ΔP.

EXPERIMENTAL APPARATUS

The experiments were conducted on a small pulse-jet fabric filter located at the Industrial Environmental Research Laboratory of the U. S.

Figure 5. Patch filter dust cake collected at 0 kV/cm.

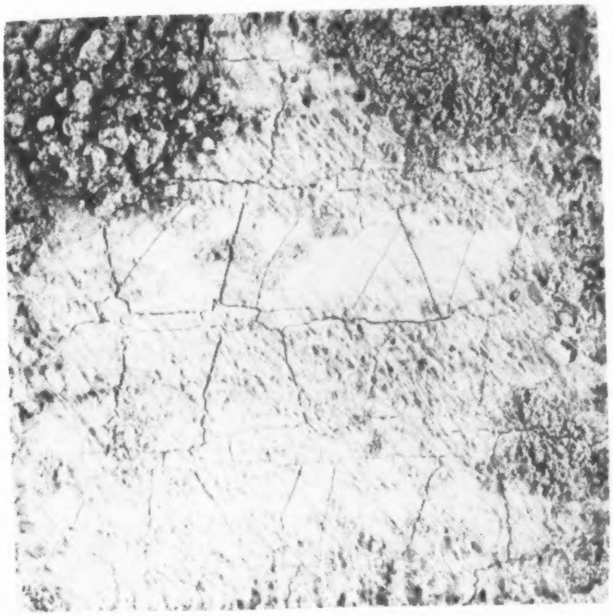

Figure 6. Patch filter dust cake collected at 1 kV/cm.

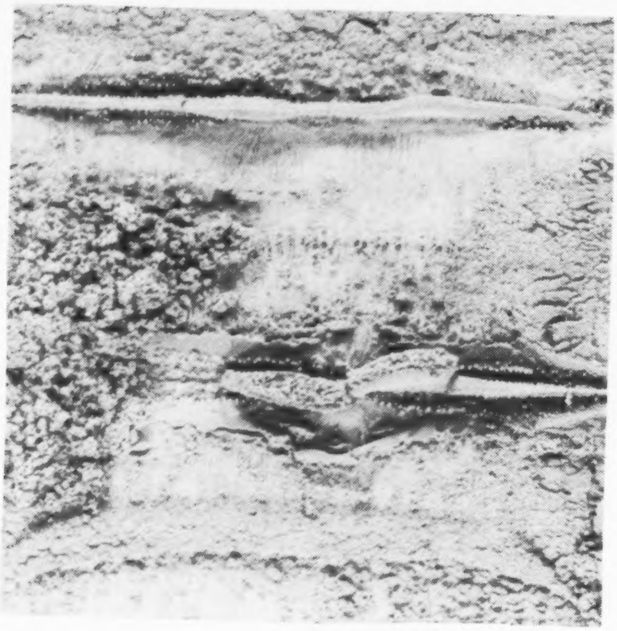

Figure 7. Patch filter dust cake collected at 4 kV/cm.

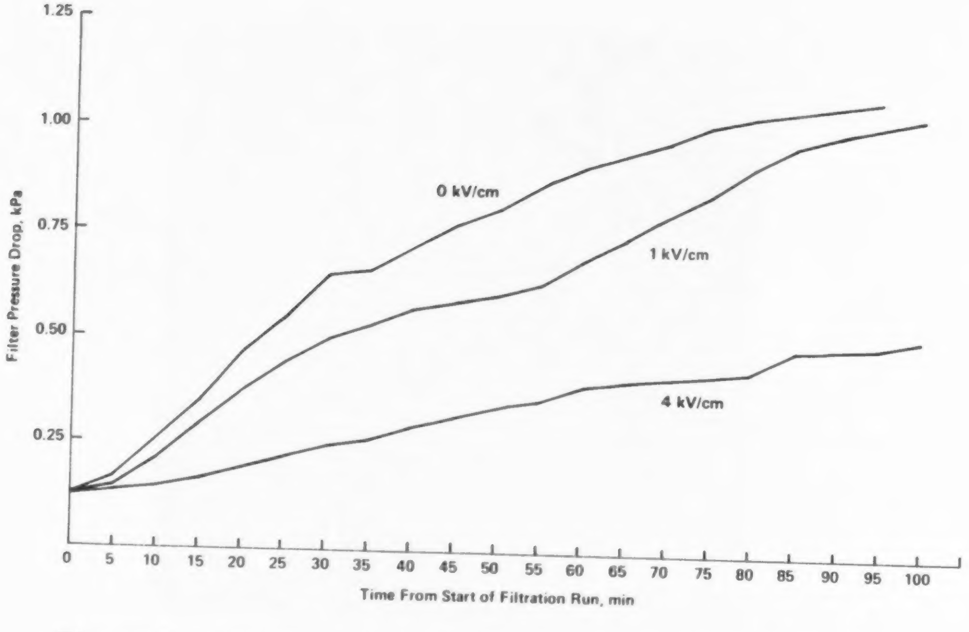

Figure 8. Pressure drop characteristics of laboratory filter at constant dust rate.

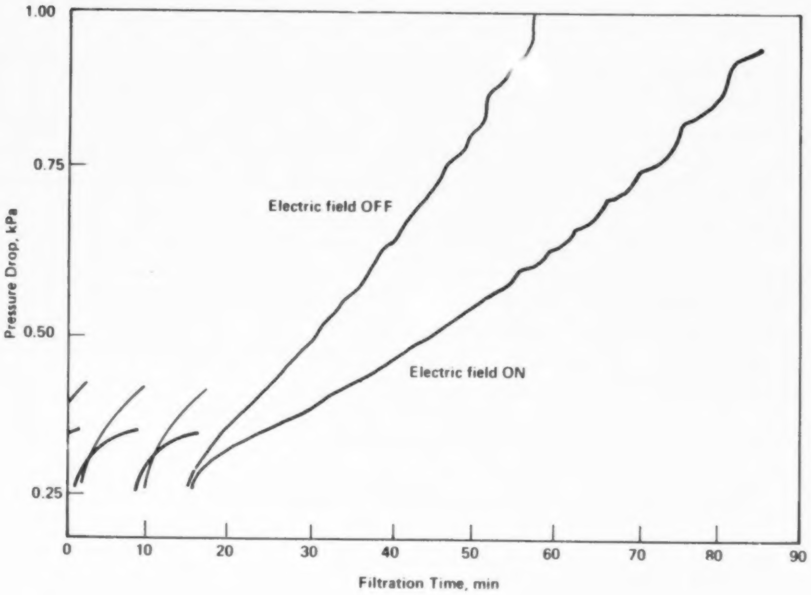

Figure 9. Long filtration time pressure drop curve.

Environmental Protection Agency in Research Triangle Park, North Carolina. This particular pilot baghouse has been described previously.(12) In summary, the baghouse used 11.4-cm-diameter (4.5-in.) bags, 122 cm (4 ft) long, made of Teflon® felt. The test dust was resuspended fly ash at a concentration of about 6.4 g/m^3 (2.8 gr/ft^3). Three bags were in use. All of the work was at ambient conditions using air as the carrier gas.

TEST PROGRAM

The test program was a three-step procedure. First, a dust cake was formed on the bags--with or without an electric field depending on the test. The dust cake was built until a predetermined pressure drop had been reached at the initial face velocity of 8.5 ft/min. The ESFF effect caused the dust cake in the field-ON condition to require more time (and more fly ash) to build than was required for an equivalent ΔP dust cake in the field-OFF condition. Once the dust layer was in place, the dust feed was stopped. The dust cake was then stressed by increasing the flow rate to reach a new, higher, predetermined ΔP. The flow rate at the increased stress level varied from test to test; only the ΔP was fixed. Following a fixed time period at the high ΔP level, the flow rate was reduced to the initial flow rate (the flow rate at which the cake was built) and the ΔP recorded. The change in ΔP at the initial flow rate is then indicative of the amount of cake compression which took place during the stress period.

RESULTS

The results of this test program are presented in Table 2. The August 6th data, which followed a thorough bag cleaning by vacuuming, permits a fairly clear interpretation. Depositing a dust layer with the electric field ON results in a layer which proves more compressible under a fixed field-OFF ΔP loading (Run 5) than a similarly stressed layer deposited with the field OFF (Run 6). In fact, the post-stress ΔP across a layer treated as in Run 5 (deposit field ON, stress field OFF) is very close to what would be predicted for depositing the same quantity of dust with the field OFF. It is as though the air stress step eliminated the drag differences between the field-ON and field-OFF depositions. However, it is notable that leaving the field ON during the air stress step largely preserves the reduced drag of the field-ON deposit.

CONCLUSIONS

In summary, the results of these three experiments are:

1. The residual permeability of an ESFF bag varied axially to a greater extent than that of a conventional bag. The ESFF bag was more easily cleaned by vacuuming and had a greater average permeability.

2. The dust deposits collected with ESFF can be very nonuniform; nonuniformities of this scale have not been observed in pilot unit operation.

3. A given pressure drop caused less dust cake consolidation with ESFF than without; the reduced drag due to ESFF can be eliminated by sufficient dust cake compression.

TABLE 2. STRESS DATA FOR FIXED ΔP LEVELS

Run	Date	Deposit ΔP kPa (deposit time)	Stress ΔP kPa	Flow at high stress m^3/min	Field status		Change in ΔP after stress kPa	Remarks
					Deposition	Stress		
1	7/28	0.91 (~14 min)	1.74	4.87	Off	Off	0.31	0.25 kPa overshoot on high stress level.
2	7/28	0.91 (~28 min)	1.74	5.64	On	On	0.17	
3	7/29	0.85 (~28 min)	1.87	Unstable	On	On	0.30	Unstable layer; repeated stress cycling produced continuously increasing ΔP.
					[Bags Vacuumed, 7/30/82]			
4	8/6	0.67 (28 min)	1.50	6.06	On	On	0.24	
5	8/6	0.62 (23 min)	1.50	6.20	On	Off	0.40	
6	8/6	0.62 (12 min)	1.50	6.20	Off	Off	0.21	
7	8/6	0.62 (14 min)	1.50	6.20	Off	On	0.19	Bag voltage read as 0 by MOD COMP but had appropriate bag current for field On.

The conclusions which can be drawn from these experiments are tentative because the range of applicability is limited and the number of experiments small. Nevertheless, these experiments do increase the understanding of the effect of ESFF on dust deposits and indicate fruitful subjects for further study.

BAG PERMEABILITY VARIATION

The vertical variation in "cleaned-bag" permeability evidenced by the ESFF bag--and the lack of variation for the conventional bag--can be explained in several ways. First, the difference could be due simply to a smaller residual deposit of fly ash at the top of the ESFF bag--the electric field causes the dust to be collected at a lower average height in this bottom-feed unit. A second explanation would be that the same amount of fly ash was present but that it was collected and held in a more porous structure at the top than at the bottom. Another explanation would be that the dust fractionates within the bag due to the electric field and that the fraction at the top has characteristics which differ from those of the bottom fraction. The top-to-bottom size difference noted supports this third mechanism, but the phenomenon occurs in conventional bags as well, and the present test data are very limited. The low permeability at the bottom of the ESFF bag in the as-received condition is a strong indication that more of the residual dust is at the bottom of the ESFF bag than for the conventional bag. This implies that most of the dust collects at the bottom of the bag. The improved cleanability of the ESFF bag is consistent with the premise that ESFF causes the dust to collect on the upstream side of the fabric and not penetrate as deeply into the fabric. This combination of the first and second hypotheses--more dust at the bottom of the bag and collected in deposits more on the upstream side of the fabric when compared to the conventional bag--seems best supported by the data.

NONUNIFORM DUST DEPOSITS

The extreme nonuniformity shown by the laboratory dust cake deposited in the presence of an electric field would certainly be adequate to account for the observed ESFF effect. However, ESFF has also been observed with dust deposits having no clear nonuniformity. This has been true for the pilot units, and it may be that bag cleaning and the redeposition of the cake prevents the extreme pattern shown by the laboratory filter. The size distribution analysis indicates that the nonuniformity of the deposits is probably not due to fractionation bv particle size.

INTERPARTICLE ADHESION

The experiment on increased interparticle adhesion due to the electric field demonstrates clearly that the reduced drag of an ESFF dust cake can be eliminated by compressing the layer. That compression removes the reduced drag advantage for ESFF argues that this ESFF effect is more of a bulk structural effect than just nonuniform deposition. The fact that the compression is reduced by keeping the electric field ON is an indication that electrostatic forces are increasing interparticle adhesion. The role of the clamping in producing the initial reduced drag--the ESFF effect itself--was not addressed by the experiment.

REFERENCES

1. Chiang, T- K., Samuel, E. A., and Wolpert, K. E. Theoretical aspects of pressure drop reduction in a fabric filter with charged particles. In: Third Symposium on the Transfer and Utilization of Particulate Control Technology, Volume III, EPA-600/9-82-005c (NTIS PB 83-149609), July 1982. pp. 250-260.

2. Lamb, G. E. R., and Costanza, P. A. Electrical stimulation of fabric filtration. Textile Research Journal. 47:372, 1977.

3. Lamb, G. E. R., Costanza, P. A., and O'Meara, D. J. Electrical stimulation of fabric filtration, Part II. Textile Research Journal. 48:566, 1978.

4. Lamb, G. E. R., and Costanza, P. A. A low-energy electrified filter system. Filtration and Separation. 17:319, 1980.

5. VanOsdell, D. W., Greiner, G. P., Lamb, G. E. R., and Hovis, L. S. Electrostatic augmentation of fabric filtration. In: Third Symposium on the Transfer and Utilization of Particulate Control Technology, Volume I, EPA-600/9-82-005a (NTIS PB 83-149583), July 1982. pp. 35-44.

6. Furlong, D. A., Greiner, G. P., VanOsdell, D. W., and Hovis, L. S. Electrostatic stimulation of fabric filtration--an update. Paper (No. 82-32.2) presented at the 75th Annual Meeting of the Air Pollution Control Association, New Orleans, Louisiana, June 20-25, 1982.

7. ASTM D737-66.

8. Smith, W. B., Cushing, K. M., and Carr, R. C. Performance of a 10 MW fabric filter pilot plant and comparison to full-scale units. Paper No. 82-59.6 presented at the 75th Annual Meeting of the Air Pollution Control Association, New Orleans, Louisiana, June 20-25, 1982.

9. Rudnick, S. N., and First, M. W. Dust cake compaction in fabric filtration. Paper No. 78-62.7 presented at the 71st Annual Meeting of the Air Pollution Control Association, Houston, Texas, June 25-30, 1978.

10. Dietz, P. W., and Melcher, J. R. Momentum transfer in electrofluidized beds. Air Pollutants--NO_x and Particulate Emissions. AIChE Symposium Series, No. 174, 74:166.

11. Dietz, P. W. Cohesive force and resistivity between electrostatically precipitated particles. Journal of Electrostatics. 6:273, 1979.

12. Turner, J. H. EPA research in fabric filtration: annual report on IERL-RTP in-house program. EPA-600/7-77-042 (NTIS PB 267441). U. S. Environmental Protection Agency, Research Triangle Park, North Carolina, May 1977. 39 pp.

"HIGH VELOCITY FABRIC FILTRATION FOR INDUSTRIAL COAL-FIRED BOILERS"

by: Gary P. Greiner and Shannon Delaney
ETS, Inc.
Suite C-103, 3140 Chaparral Dr., SW
Roanoke, VA 24018

Lou S. Hovis
U.S. EPA
IERL, MD-61
Research Triangle Park, NC 27711

ABSTRACT

Two parameters which dramatically affect the technical/economic performance of a fabric filter system are gas/cloth (G/C) ratio (or filtering velocity) and bag life.

Under an EPA sponsored contract, ETS, Inc. has been conducting a study of state-of-the-art and experimental fabrics and finishes in full-scale baghouses operating on coal-fired boilers at the Kerr Finishing Plant, Travelers Rest, South Carolina. The objective of the study is to operate, test, and evaluate performance at G/C ratios up to 10/1 and screen various fabrics with respect to pressure drop, collection efficiency, and fabric strength characteristics necessary for technical/economic analysis. Included in the program are some revolutionary fabrics which hold promise of technological breakthroughs.

This paper will discuss evaluation methodology, performance results, and future program plans.

This paper has been reviewed in accordance with the U. S. Environmental Protection Agency's peer and administrative review policies and approved for presentation and publication.

INTRODUCTION

ETS, Inc., through the sponsorship of EPA's Industrial Environmental Research Laboratory, has been conducting a pioneering program for the application of fabric filters to industrial coal-fired boilers since 1973. Many of the early lessons concerning this application were learned during the pilot program and subsequent full-scale implementation. Fabric compatibility, cleaning modes, component requirements and specifications, achievable filtering velocities, and emission capabilities all were evaluated, defined, and submitted to the industry. This information and the success of the full-scale systems did much to accelerate the application of fabric filters to industrial coal-fired boilers.

Now the program, continuing its pioneering approach, is seeking to extend the capabilities of the fabric filter system in this application through higher filtering velocities (G/C ratios) and longer fabric life, while maintaining required emission levels.

SITE AND EQUIPMENT DESCRIPTION

The present program is being conducted at the Kerr Finishing Plant in Travelers Rest, South Carolina. Figure 1 shows the general site layout. Baghouse No. 1 controls emissions from a 60,000 lb(*)/hr, Babcock & Wilcox (B&W) stoker boiler. Baghouse No. 2 controls emissions from a bank of four boilers (one 30,000 lb/hr and three 20,000 lb/hr). The coal used at this site is typical Eastern low sulfur coal. The operation is cyclic depending on production requirements, and is shut down each weekend.

The current project consists of two programs. The first, referred to as the High G/C Program, utilizes Baghouse No. 1 and seeks to raise the stable filtering velocity operating point to provide lower overall cost. The second, referred to as the Fabric Evaluation Program, utilizes Baghouse No. 2 and seeks to evaluate the bag strength characteristics versus exposure time of various fabric and finish candidates that could be applicable to both pulse jet and reverse air collectors.

HIGH G/C PROGRAM

Boiler Description

The No. 1 baghouse is applied to a Babcock & Wilcox coal-fired boiler rated at 60,000 lb/hr steam. A stoker grade coal (1½ X 1/4 in.) is fed to a spreader type Detroit stoker from a central weighing scale into three stoker sections and onto a riser type dump grate. Normal maximum boiler operation provides 52,000 lb/hr steam at 160 psig and saturation temperature. A multi-cyclone is located on the boiler outlet, but no economizer or fly ash reinjection is provided. The combustion air flow is provided by a combination of forced draft, overfire air, and induced draft fans. Normal operation produces 25-40,000 acfm and 400-450°F flue gas.

(*) Readers more familiar with metric units may use the conversion factors at the end of this paper.

Baghouse Description

The No. 1 baghouse accommodates up to 648 bags with a nominal size of 5 in. diameter X 104 in. long, having a total cloth area of 6800 sq ft for a maximum filtering velocity of 5.8 fpm with all bags installed. Its cleaning energy is supplied by 80-100 psi compressed air pulses assisted by low-pressure reverse-flushing air. The original design had 18 separate bag plenums and outlet dampers, but with common inlet and hopper areas. This provided a semi-off-line cleaning mode, but not of the type seen in today's modular collectors. It also lacked the ability to monitor and control the flow through each section. Modifications were performed to sectionalize the inlet and hoppers. The sectional inlet dampers, test ports, flow monitors, and differential pressure (ΔP) manometers permit the control and monitoring of the gas flow into each section. The resultant system provides a high degree of cleaning mode flexibility. Cleaning can be on-line, pulse jet only; on-line, pulse jet with varying amounts of reverse-flush assist; or off-line variations of the above. Normal operation is to take an individual cell off-line by closing the outlet damper, and allowing a minimum volume of reverse gas to flow, primarily to block the forward leakage flow and pulse the bags. This most closely simulates today's modular off-line cleaning pulse jet collectors.

Fabric Description

All fabric in baghouse No. 1 is a form of Teflon® fiber felt, supplied by the E. I. Dupont de Nemours Company. A description of the fabrics and bags utilized is shown in Table 1. The prior EPA program utilized a full house of 23 oz Teflon® felt bags. Section C, containing these original bags, has been retained to provide reference with past operation. Section F contains an experimental 17 oz Teflon® felt bag set that is constructed in an asymmetrical manner, such that most of the felt is on the outside of the bag. Sections A, B, D and E contain bag sets of experimental Teflon® fiber felt of varying weights and construction. A characteristic of Teflon® is that it physically shrinks with increasing temperature. This results in not only a smaller bag, but also a lower in-use permeability as shown in Figure 2. Heat setting at sufficient time and temperature will minimize this problem; however, these characteristics must be accounted for in the initial fabric and bag specifications. Note that the original Teflon® bags were not oversized as much as the newer bags (4-7/8 in dia. versus 5-1/4 in.). This was due to a lack of understanding of the actual shrinkage rate at the time (in 1976) that these bags were constructed. Unfortunately, all of these fabric styles were not obtainable at the beginning of the test program; they were installed as they became available. The installation dates are included in Table 1.

® Dupont TFE Fluorocarbon fiber

TABLE 1. BAG AND FABRIC DESCRIPTION

Description		Wt. oz/yd^2	Perm fpm	Mullen Burst psi	Tensile St. lbs/in Width		Bag Size dia. X length, in.	Initial Installation Date
Baghouse Section[a]	Fabric (Teflon®)				Warp	Fill		
A	Exp. (Y1)	21	36	354	87	78	5¼ X 108	10/81
B	Exp. (X)	23	21	340	88	70.5	5¼ X 108	07/81
C	XT 2363 (Std)	27	27	306	115	93	4-7/8 X 108	01/77
D	Exp. (Y2)	19	42	324	84	74	5¼ X 108	10/81
E	Exp. (X)	23	21	340	88	70.5	5¼ X 108	07/81
F	Exp. (Asym)	17	59	231	83	61	5¼ X 108	05/81

[a] Location of section shown in Figure 4.

TECHNICAL OBJECTIVES

The program's primary objective was to develop methods of raising the stable filtering velocity operating level and, after demonstrating that stability, define the effect on drag, efficiency, and bag life. The mechanisms evaluated for raising the G/C ratio were:

Cleaning energy; i.e., pulse jet versus reverse air versus combinations;
Cleaning mode - on-line versus off-line;
Cleaning frequency; and
Fabric type and style.

PARAMETERS MONITORED AND APPROACH

The following describes the evaluation methods employed and the parameters monitored.

Section Drag

The parameter used to define stable operation was average section drag, which is the average tube sheet ΔP during a filtering cycle divided by the section G/C:

$$S\ (\text{Avg}) = \frac{\Delta P\ (\text{Avg})}{G/C}$$

A section was defined as having short term stability if no consistent upward movement in the average drag was observed over a minimum 2-3 day evaluation period.

The three cells of each section have pressure taps, so all 18 cells of the baghouse may be monitored for pressure drop. Generally, the middle section is monitored, and the ΔP is registered on a 15 in. W.G. Magnehelic gauge. There is one Magnehelic for each section. The G/C ratio is monitored by an Annubar located at each section inlet, and the flow is registered on an incline manometer. The instruments are located on a panel at the inlet test level.

The initial evaluation approach was to establish the cleaning variable to be tested, adjust each section inlet damper to produce equal section G/C, and monitor section ΔP. A method which proved more reliable was to adjust for equal section ΔP and monitor section flows. Since the total gas volume fluctuated with steam load demand, the average G/C typically varied between 5 and 8. The drag values were recorded several times each day. Each condition was evaluated long enough to establish only short term stability or instability. At various times during the test program, snapshots of ΔP versus G/C were obtained by varying the G/C from 6 to 10 for short periods and monitoring ΔP. This aided in verifying long term data, and also gave a fabric drag versus exposure time profile.

Efficiency

Collection efficiency was to be determined at regular intervals during the program. Due to the common outlet, testing of individual sections requires taking all other sections off-line. This has proved somewhat difficult and provided questionable results. Due to budget constraints, additional testing was deferred until optimum high G/C operation is achieved and additional funds are available. No individual fabric emission testing has been done. Both baghouses have been tested and have met compliance.

Fabric Characteristics

Bags were periodically removed from the baghouse for laboratory testing. Mullen Burst was monitored to define fabric strength retention. Permeability was monitored to define retention of flow characteristics.

RESULTS AND CONCLUSIONS

Time and funds dictated a fairly rapid initial evaluation of the magnitude of the effect of the available options. Having the fabrics enter the evaluation at different times further complicated the evaluation; however, certain trends were consistently found.

Effect of Cleaning Energy on Fabric Drag

The original baghouse utilized two 1½ in. diameter pulse jet valves per cell to pulse 18 bags each. In order to achieve the higher G/C desired without incurring high damper pressure drop losses, bags were removed as shown in Figure 3. Since all active bags were now located in four rows per cell, the cleaning energy supplied to each bag could easily be increased by 50% by removing one blow pipe per valve. The operating mode with four pipes is referred to as the High Pulse Jet mode, and with six pipes, the Medium Pulse Jet mode. A much lower level of cleaning energy was obtained by eliminating the pulse jet and cleaning with reverse air only.

Table 2 shows the relative drag values observed during the three cleaning energy levels. A significant effect was seen on all fabric types.

TABLE 2. EFFECT OF CLEANING ENERGY ON FABRIC DRAG

		Typical Drag	
Fabric Type	R.A. Only	Med. P.J.	High P.J.
Std. Teflon®	Unstable	1.5	1.0
Asym. Teflon®	Unstable	1.2	0.8
Exp. Teflon®	1.1	0.8	0.5

The experimental felts are grouped as shown, since no significant difference was observed between styles during this experiment. Note that both the standard and asymmetrical felts did not produce a stable operating point with reverse air only. This may be due to their longer bag set exposure or differences in construction.

Effect of Cleaning Mode on Fabric Drag

Off-line cleaning is accomplished by activating a cell's outlet damper, which closes to block the forward gas flow, pulsing all the bags in that cell at one time, and maintaining the cell off-line for 15 seconds before reopening the outlet damper and resuming normal flow. On-line cleaning was established by allowing the pulse jet cleaning to continue, but deactivating the outlet dampers from the cleaning cycle. High energy cleaning was employed throughout this experiment.

Table 3 shows the relative drag values observed during the two cleaning modes and at high and low filtering velocities.

TABLE 3. EFFECT OF CLEANING MODE ON FABRIC DRAG

G/C Ratio	Typical Drag			
	≤5		>6	
Cleaning Mode	Off-Line	On-Line	Off-Line	On-Line
Fabric Type				
Std. Teflon®	1.0	1.0	1.0	1.5 (Unstable)
Asym. Teflon®	0.8	1.0	0.8	1.5 (Unstable)
Exp. Teflon®	0.5	1.0	0.5	1.2 (Unstable)

This evaluation confirmed past operating experience at Kerr in that stable operation at high G/C and with on-line cleaning is not possible. The low G/C evaluation was not run over a long enough time to determine if long term stability could be maintained. The dramatic effect on drag is assumed to be due to the reduction of re-entrainment in the off-line mode.

Effect of Cleaning Frequency on Fabric Drag

Theoretically, one tries to establish cleaning frequenty at the minimum level that produces a reasonable stable pressure drop. This then should minimize compressed air usage and extend bag, pulse jet, and damper component life. Prior experience with the standard Teflon® felt and asymmetric felt was that a 6-minute cleaning frequency is required with the medium cleaning energy level; most data with those fabrics are at that cleaning frequency. Initial evaluation of the new experimental fabrics indicated that a lower cleaning frequency could be used: most data on those fabrics was collected at the 20-minute cleaning frequency. With all sections employing high energy cleaning, the results of Table 4 were obtained.

TABLE 4. EFFECT OF CLEANING FREQUENCY ON FABRIC DRAG

Cleaning Frequency	Typical Drag	
	6 Min.	20 Min.
Fabric Type		
Std. Teflon®	1.0	1.2
Asym. Teflon®	0.8	1.0
Exp. Teflon®	0.5	0.5

Note that the fabric drag was not reduced by increasing the cleaning frequency on the experimental felts. The pressure drop rise between cleaning has been both very low and extremely linear, indicating the possibility of further extending the cleaning frequency. The short term increase in fabric drag of the standard and asymmetric felts under high cleaning energy and 20-minute cleaning was quite modest. Note that sufficient test duration was not allowed to verify long term stability and that the more rapid rise of pressure between cleaning indicates that the optimum cleaning frequency may be somewhere between 6 and 20 minutes.

Effect of Fabric Construction on Fabric Drag

Due to the variables of bag history, cleaning energy, and cleaning cycles employed, direct comparisons of the various Teflon® felt constructions have been difficult. Earlier tables have shown the Teflon® styles for reference to indicate the relative effect of the cleaning variable under study. The indicated trends are both real and significant.

Table 5 provides relative drag values for the four major felt constructions now under evaluation. Experimental construction X differs from construction Y in that Y was designed to have a 50% higher initial permeability. Two different weight bags of construction Y were fabricated (styles No. 402 and 403). No significant difference was seen between the two in the drag results.

All of the prior evaluations were run with the system inlet having a high degree of dilution due to ambient air in-leakage in the boiler stack, expansion joints, and emergency dilution damper. This produced an inlet grain loading of approximately 0.2 gr/acf. In-leakage was minimized through most of these areas. While this has reduced the average G/C, the boiler load fluctuates sufficiently over the course of a day that the same G/C range of 6 to 10 can still be evaluated with the reduced cloth area. Also, boiler operation has provided some variation in grain loading with some data being obtained at 0.5 to 0.8 gr/acf. With this, the standard fabric drags are now more in line with industrial experience at 4-5 G/C. The short term ΔP versus G/C evaluations show a constant drag over this range.

TABLE 5. EFFECT OF FABRIC TYPE ON FABRIC DRAG (short term evaluation)

	Typical Drag	
Inlet Loading (gr/acf)	0.2 - 0.3	0.5 - 0.8
Std. Felt	1.0	1.6
Asym. Felt	0.8	1.4
Exp. Construction X	0.5	1.1
Exp. Construction Y	0.5	0.8

The drag data previously shown were a result of short term evaluations which did not allow full stabilization of fabric condition and were intended only for relative comparisons of fabric types. From May to August 1982, an evaluation at fixed conditions revealed the results contained in Table 6. While these drags are higher than previously reported, they were consistent under normal boiler operation and represent what might typically be expected. To further evaluate the drag values, the system was operated at relatively constant conditions and modes over an extended period of time. The baghouse was operated with the stack cap bypass damper closed, the Vortex damper control on automatic off-line cleaning, a cleaning frequency of 6 minutes, and a typical grain loading of 0.5 to 0.6 gr/acf. This evaluation produced the data of Table 6.

TABLE 6. EFFECT OF FABRIC TYPE ON FABRIC DRAG (long term evaluation)

Fabric Type	Typical Drag
Standard Felt	1.6 - 1.7
Asym. Felt*	-
Exp. Teflon Const. X	0.95- 1.0
Exp. Teflon Const. Y1	0.9 - 0.95
Exp. Teflon Const. Y2	1.1 - 1.2

CONCLUSIONS AS TO HIGH G/C CAPABILITY

The primary thrust of the evaluation to date has been to identify parameters that produce lower drag values or improve pressure drop stability so that higher G/C levels may be achieved with reasonable and stable pressure drops. By necessity, the G/C levels have varied with the boiler load, and specific evaluations have been short. Future program activity is to select the optimum system and fabric parameters and evaluate them over a longer period.

The results to date indicate that the optimum system operation is with higher energy, off-line pulse jet cleaning, a cleaning frequency of 6-20 minutes, and experimental Teflon® felt Construction Y. Short term stability up to a G/C of 10 has been demonstrated. During the long term evaluation, the system was operated in a manner that allowed the section pressure drops to self balance and the section gas volume flows to be dictated by their fabric drags. This resulted in the experimental felt Construction Y running typically at 7-9 G/C with no instability observed and a drag typically less than 1.0 even at the highest inlet grain loadings during high boiler loads. Mullen Burst tests on samples from the above test bags showed only a modest drop in strength for all fabrics except experimental Construction Y1.

A longer term evaluation of the above conditions is recommended and, if successful, could double the present filtering velocity now common in this application.

FABRIC EVALUATION PROGRAM

Boiler Description

The No. 2 baghouse is applied to a bank of four coal-fired boilers with a common manifold supplying a natural draft stack. The first three boilers were built in 1928 by Walsh & Weidner Boiler Company and are equipped with Combustion Engineering underfeed retort spreader type stokers and side dump grates. The boilers are rated at 22,500 lb/hr steam at 250 psig and saturation temperature. The fourth boiler was built by Combustion Engineering in 1941 and is equipped with Combustion Engineering underfeed retort spreader type stoker and side dump grates. It is rated at 30,000 lb/hr steam at 250 psig and saturation temperature. All four boilers are provided with force draft fans, and generally two boilers at a time are operated. Outlet flue gas is directed to the baghouse from the manifold. Normal operation produces 40,000 acfm and 400 - 450°F flue gas.

---

* Note: Asymmetric felt was not included in this evaluation.

Baghouse Description

The No. 2 baghouse is identical to No. 1, except its cleaning method is reverse air plenum pulse instead of pulse jet. The collector incorporates 648 bags with a nominal size of 5 in. diameter and 104 in. long, having a total cloth area of 6800 sq ft. Normal filtering velocity is 5-6 fpm. Its cleaning energy is supplied by a 4000 acfm fan at 10 in. W.G. pressure through cell outlet poppet dampers that simultaneously stop the normal forward gas flow through one cell, and introduce the reverse pulse of heated ambient air. A typical cleaning cycle is 10 seconds of reverse flushing followed by 5 seconds of delay before moving to the next cell. This produces a bag cleaning frequency of 4.5 minutes. The house was divided into six sections and is instrumented in the same manner as house No. 1.

Fabric Description

The fabric being evaluated consists of four bag sets: three woven glass with varying finishes and one Nomex® felt with an acid resistant finish. The woven glass bags all have the same basic fabric construction, one that is presently being used in both pulse jet and reverse air collectors on coal-fired boilers. Three different finishes are being evaluated on the glass bags: an experimental Teflon® based finish developed by Dupont, and two state-of-the-art finishes, Burlington's style I615, 10% Teflon B®, and Burlington's style I625, Acid Flex®. The Nomex® bag set utilized Globe Albany's 16 oz Nomex® felt with Permagard® finish that has shown success in Europe.

Fabric specifications are shown in Table 7. The locations of the various fabrics in the baghouse are shown in Figure 4. A test cell incorporating all fabric types was established to normalize any biased effects of section location.

TECHNICAL OBJECTIVE

This program's primary objective was to evaluate the operational characteristics and service life of the various fabrics while exposed to normal operating conditions of the Kerr coal-fired boiler and baghouse system.

TABLE 7. WOVEN GLASS FABRIC ANALYSIS

ALL FABRICS

Fiber:	Glass
Construction:	
Weave	3 X 1 Twill
Count	W44 X F24
Warp Yarn	DE 37-1/0 - (Singles Construction)
Fill Yarn	DE 75-1/0 - (Plied, 2 Texturized, 1 Untexturized)

Virgin Cloth Perm ≈ 90 fpm @ 0.5 in. W.G.

	A, Acid Flex®	B, Teflon B®	X, Exp'tal
Fabric Finisher	Burlington	Burlington	Clark-Swabel
Perm, Avg.	77.8	56.1	47.5
LOI, wt%	4.6	9.5	9.6
Oz/yd^2			
- Treated	12.6	14.3	13.6
- Untreated	12.0	12.9	12.3
Thickness, in.	0.0144	0.0142	0.0158

Virgin Cloth Perm ≈90 fpm

PARAMETERS MONITORED AND APPROACH

The following describes the evaluation methods employed and the parameters followed.

Fabric Drag

Filtering velocities were maintained as equal as possible between test sections throughout the evaluation by monitoring the inlet Annubars and manually adjusting the section inlet dampers. Normal filtering velocities were maintained in the 4-6 fpm range. Section tube sheet ΔP was recorded daily to compute average fabric drag values. Fabric permeability was monitored on bags that were periodically removed for testing.

Fabric Properties

To evaluate the effect of operational exposure on bag life, the fabric strength characteristics were monitored. Test bags were scheduled for removal after exposure times of 1 hour, 1 day, 1 week, 1 month, 3 months, 5 months and 7 months. Fabric testing included Tensile, Mullen Burst, MIT Flex, Loss on Ignition (LOI), and visual and microscopic inspection.

Efficiency Testing

Mass efficiency tests by EPA Method 5 were scheduled to be run after stabilization of the system. Although difficult, individual section emission testing was scheduled to provide comparative data between fabric types. Testing currently has been deferred due to budget constraints.

BAG CONDITIONING AND OPERATING HISTORY

Conditioning of the bags was initiated on May 14, 1981, and continued for the next 4 weeks. The flow was maintained at the low (1.5 - 2.5) G/C for an extended time to both obtain some data at low G/C and ensure that system control would prevent biasing of any fabric. The flow, temperature, and section pressure drop were carefully monitored, and the bags were inspected visually.

Due to intermittent boiler operation and long weekend shutdowns, 7 full days of exposure required 1 month of calendar time (early in the program). The plant was then shut down for the month of July. After resuming operation, the baghouse was set to operate at 4-5 fpm. Malfunctions in the damper system of section C, the experimental Teflon® finish, resulted in lower filtering rates in that section for 3 weeks. Again, due to limited plant production which reduced the boiler needs, it would take approximately 3 months to obtain the next 2 months exposure time. The 3 month test bags were scheduled for removal on October 16. Unfortunately, a severe boiler upset caused a fire in the baghouse, and all the experimental Teflon® finished bags and the test bag cell were destroyed on October 12. The baghouse remained off-line until new experimental Teflon® finish bags could be obtained. The evaluation was restarted on May 5, 1982.

RESULTS AND OBSERVATIONS

The cyclic nature of the baghouse during this evaluation dramatizes the need for fabrics that can survive many start-ups, shutdowns, and their resultant dew point excursions. Normal boiler operation was start-up on the 2nd shift Sunday, and shutdown on the 2nd shift Friday. Due to production limitations, several shorter operating cycles were run. In addition, baghouse auxiliary component malfunctions forced the baghouse off-line at times. Needless to say, this type of application intensifies the need for preheat and purge capabilities (which exist) and fabrics that can resist acid condensation.

ΔP Evaluation

Through June 25, the plant's summer shutdown, the filtering velocities were held constant and, for all practical purposes, the ΔP levels of all sections were the same. Following the shutdown, Section C (exp. finish) ran at lower G/C ratios and higher ΔP levels as a result of cleaning system problems. These problems were intermittent, recurring throughout August. After correction, its ΔP was comparable to that of the other section.

No significant differences in fabric drag could be seen during the evaluation between sections. Average drags ranged from 1.5 to 2.0, reflecting the low energy cleaning system being employed.

Fabric Strength Tests

Results to date are plotted on Figures 5 through 8 and Table 8. The test plan calls for the removal of three bags of each type after 1 hour, 24 hours, 1 week, 1 month, 3 months, 5 months, and 7 months of exposure time. After removal, the top, middle, and bottom of each bag is tested for its strength characteristics. The tests include permeability, tensile strength, flex strength, and burst strength. Tests have been completed through 7 months of exposure. In addition, all but the experimental bags have seen over 6 months additional off-line exposure. It has been determined that there is no significant difference in the strength characteristics of the top, middle, and bottom of any of the bags. Note that increases in the value of a given parameter versus on-line time are not expected. These increases are attributable to variations in the initial strength characteristics of the bags, finish protection effectiveness, bag location, or (in the case of permeability) handling.

The new, 1 hour, 24 hour, 1 week, and 1 month Acid Flex®, Teflon B,® and Nomex® data were obtained before the October 12 fire. The 3-month data were obtained from bags off-line for 6 months and were obtained in May 1982, after restart-up. All the experimental Teflon data were obtained on replacements for the original experimental Teflon bags. This evaluation began in May 1982, and the replacement bags have strength characteristics similar to those of the original bags.

Permeability

As previously stated with regard to the high G/C program, fabric permeabilities were taken in the laboratory and in-situ cake conditions have been altered by removal from the baghouse (removal from cages) and transferred to the laboratory. Again, this type of evaluation relies on examining the relativity of the data rather than the absolute values.

As can be seen in Figure 9, the greatest decrease in the permeability of all four fabrics occurs in the first hour of operation. Another substantial decrease takes place from 1 hour to 24 hours. The Acid Flex® bag set had the highest initial permeability, starting 35% higher than the other woven glass fabrics. However, it drops to the level of the other fabrics (25-30 fpm) within 1 hour. The Nomex® fabric starts with the lowest value; however, it exhibits the least decrease in permeability, and is higher than the other fabrics up to 3 months. All the fabrics are in the range of 4 to 10 fpm within 1 month. Dirty as received permeability values of 4 to 10 are normal for fabrics operating at 4-8 in. W.G. pressure drops at 4-6/1 G/C. At 3 months, all the woven fabrics have roughly the same permeability. From 5 months on, all fabrics are essentially the same and reflect the sameness in fabric drag seen in the field. Note that no severe blinding has occurred in any of the fabrics through 7 months.

Flex Strength

Figure 5 is a plot of the flex strengths for the woven glass fabrics. The Nomex® felt is considerably higher than any of the woven glass fabrics (initial value around 47,000).

The Nomex® showed its greatest decrease in flex strength between 24 hours and 1 week (from 42,000 to 9,000). The Nomex bag set showed dramatic loss of strength between 5 and 7 months, and several field failures occurred during this period. The Teflon B® fabric's initial superiority was eliminated within 1 day, and this may be of significance to the finisher. Also, the Teflon B® had the lowest flex value by 1 month and continued to have the lowest at 5 months, although only slightly less than Acid Flex®. The Acid Flex® fabric showed its greatest decrease to be between 24 hours and 1 week. The experimental Teflon® finished bags, although starting at a lower value, have shown much less strength deterioration, and bags tested at 5 and 7 months show virtually no reduction in flex strength.

When the 1 month old bags were removed for testing, the samples located on the outside walls were very wet. Table 8 is a summary of the flex results for the wet Acid Flex®, Teflon B®, and experimental Teflon® fabrics. The experimental Teflon® showed no significant decrease in flex strength. The Acid Flex® showed a significant loss of flex strength only in the middle of the bag, and the Teflon B® showed virtually a total loss of flex strength. These are good indications of the finish's ability to encapsulate the fiber and resist moisture and acid attack.

Mullen Burst

Figure 6 shows the Nomex® to have: the lowest initial burst value, as is typical of felts; a slow decline in strength; stability between 1 and 5 months; and rapid deterioration between 5 and 7 months. Of the glass fabrics, Acid Flex® and Teflon B® show similar burst characteristics with over 40% strength loss at 1 month, and only a slight decline to 7 months.

TABLE 8. WET BAG FLEX DATA FOR
1-MONTH OLD BAGS

Fabric	Number Of Flexes		
	Top	Middle	Bottom
Acid Flex®	811	37	467
	1384	34	588
Teflon B®	31	9	43
	26	14	24
Experimental Teflon®	1025	1242	614
	1587	912	820

The experimental Teflon® started with the same burst value as the other woven fabrics (as expected, since all were fabricated with the same basic fabric construction), but has shown superior retention of strength.

Tensile Strength

The Nomex® fabric shows noticeably lower (typical of felts) tensile strength (Figures 7 and 8) than the Glass fabrics, but significant deterioration after 5 months. The Glass fabrics show similar trends to each other, with the greatest decrease occurring between 24 hours and 1 week. The experimental Teflon® again has the highest value after 3 months.

General Observations

The study, by design, represents a short evaluation period when put in the context by seeking greater than 2 years of bag life. The data are unique in that they are the first documented evaluation of how rapidly strength characteristics are lost (i.e., hours, days).

Fabric filters typically show an early strength loss of 50%, at which time they reach a plateau until the end of the bag life cycle. The Acid Flex® and Teflon B® appear to be at this level within 1 week, and are reasonably stable through 7 months on-line exposure plus the extended off-line. The experimental Teflon B® finish was designed to improve fabric strength retention and has been successful through 7 months, indicating that its finish may be protecting the fabric better.

The Nomex® bag set with its Permagard® 6 finish showed superiority over the 1 month life previously obtained on untreated Nomex® but insufficient life to be practical in this application.

CONVERSION FACTORS

Readers more familiar with metric units may use the following factors to convert to that system:

Non-metric	Times	Yields Metric
°F	5/9 (°F-32)	°C
ft	30.48	cm
ft^2	0.09	m^2
ft^3	28.32	L (liter)
gr	0.06	g
in.	2.54	cm
$in.^2$	6.45	cm^2
lb	0.45	kg
oz	28.35	g
yd	91.44	cm

Reproduced from
best available copy.

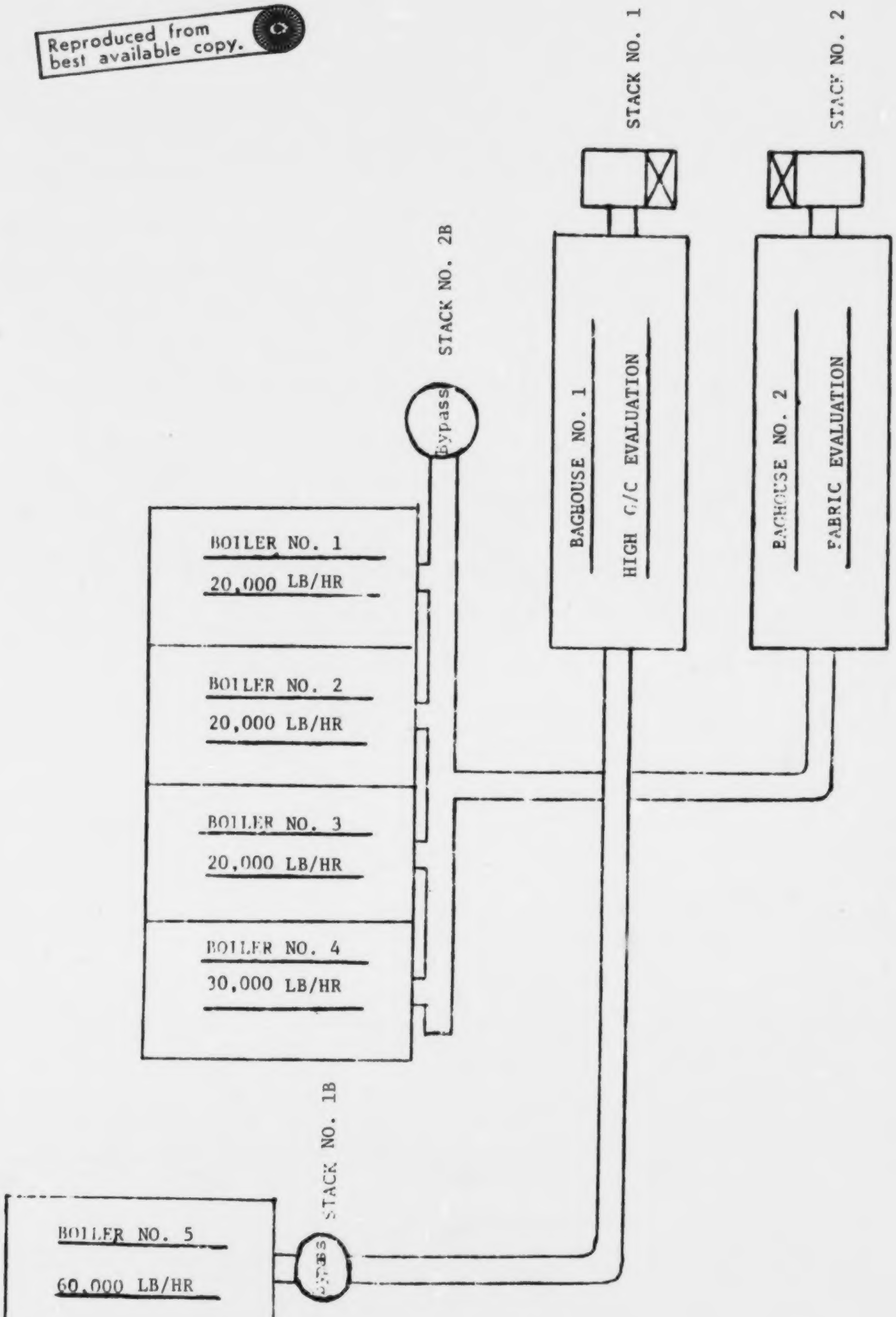
STACK NO. 1
STACK NO. 2
STACK NO. 2B
Bypass
BAGHOUSE NO. 1
HIGH G/C EVALUATION
BAGHOUSE NO. 2
FABRIC EVALUATION
BOILER NO. 1
20,000 LB/HR
BOILER NO. 2
20,000 LB/HR
BOILER NO. 3
20,000 LB/HR
BOILER NO. 4
30,000 LB/HR
STACK NO. 1B
BOILER NO. 5
60,000 LB/HR

Figure 1. Kerr site layout.

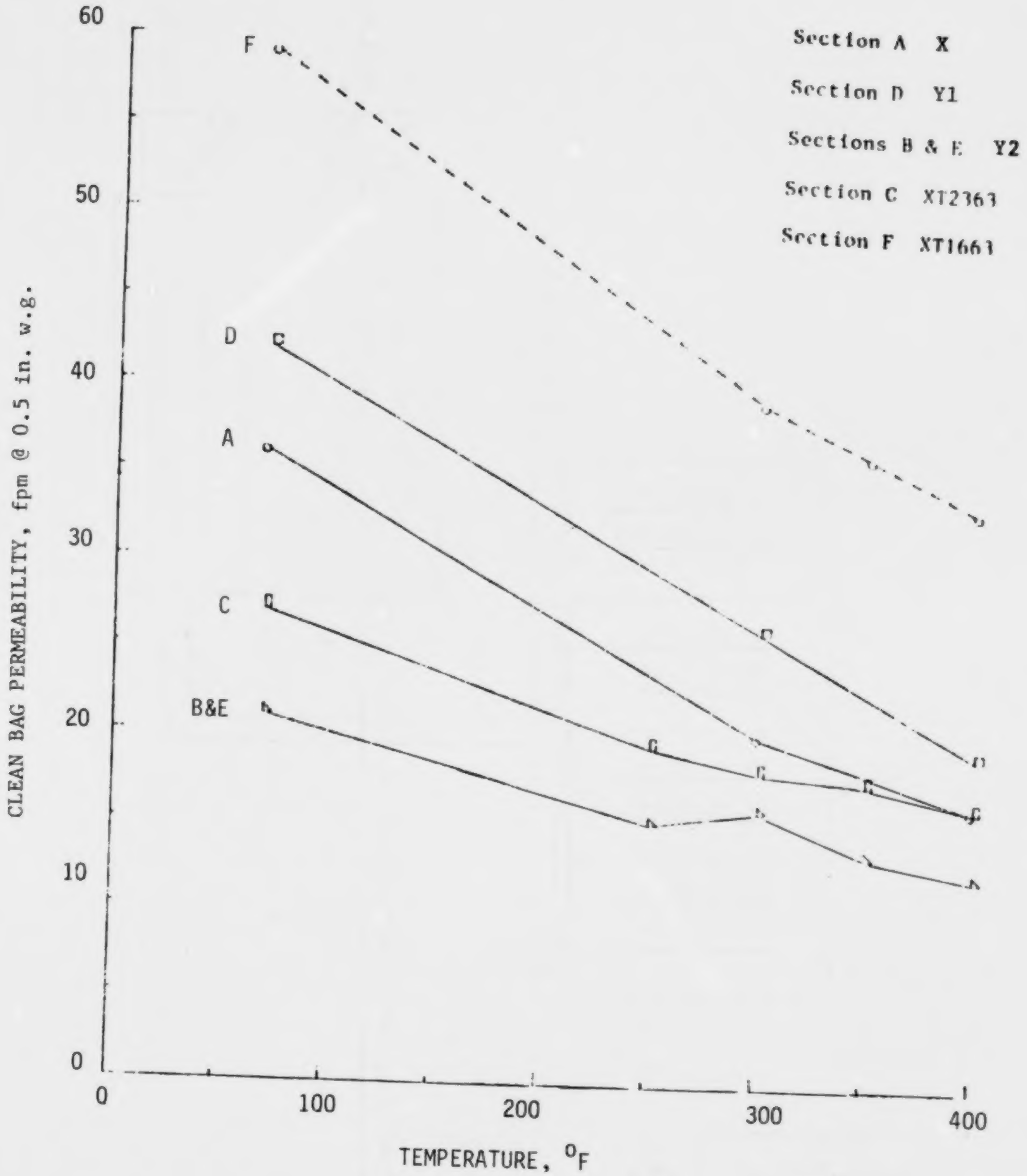

Figure 2. Permeability vs. temperature.

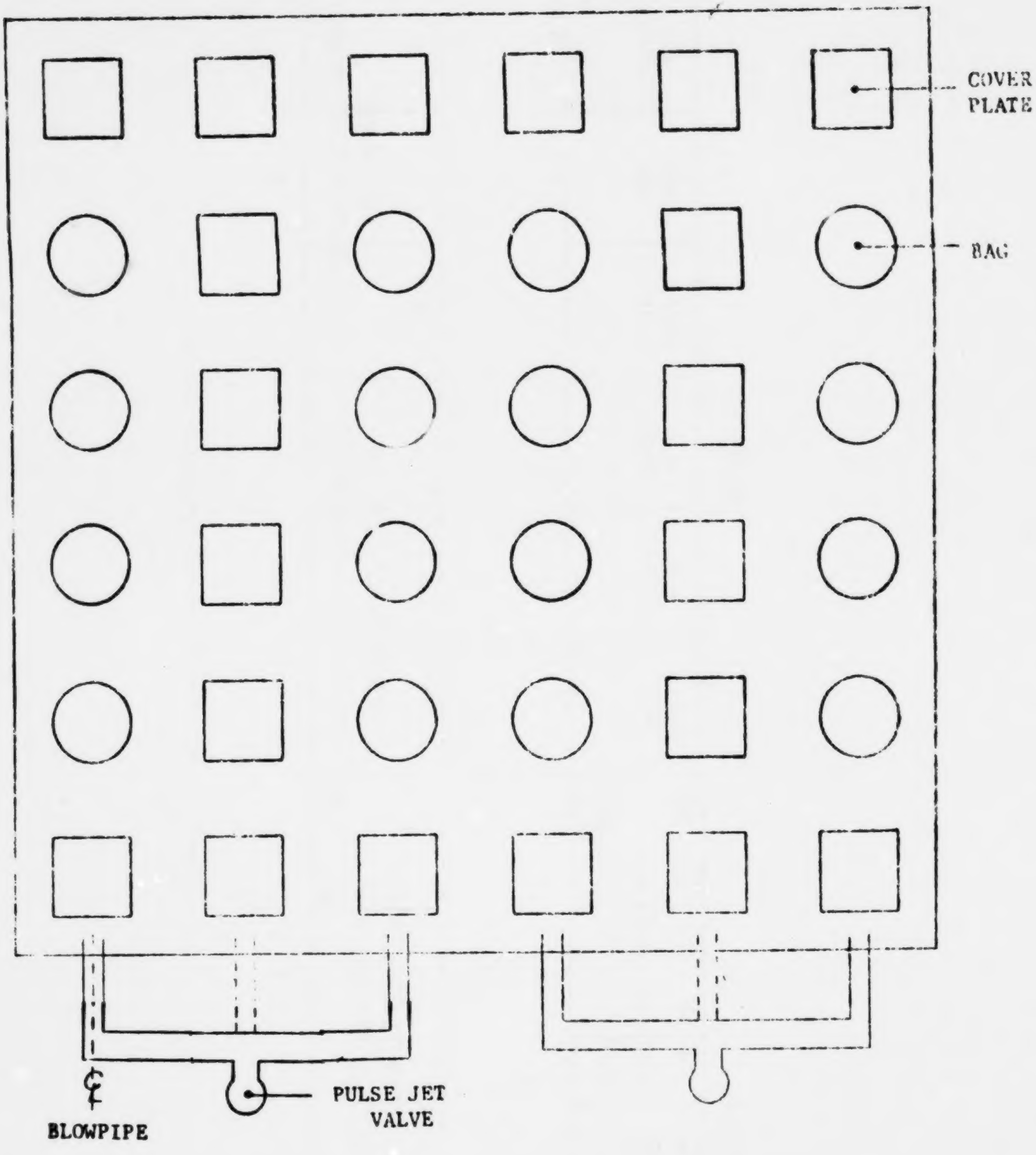
COVER PLATE
BAG
BLOWPIPE
PULSE JET VALVE

Figure 3. High gas-to-cloth cell bag layout.

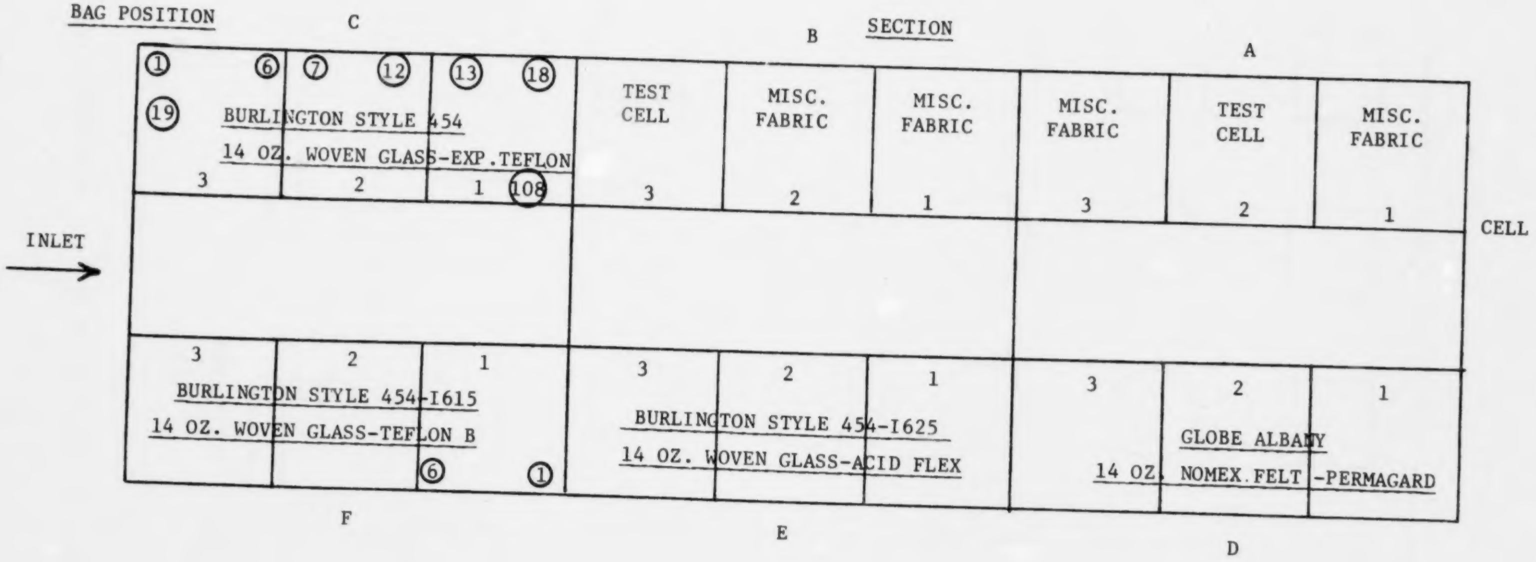
BAG POSITION
C
B
SECTION
A
①
⑥
⑦
⑫
⑬
⑱
⑲
BURLINGTON STYLE 454
14 OZ. WOVEN GLASS-EXP.TEFLON
3
2
1
108
TEST CELL
3
MISC. FABRIC
2
MISC. FABRIC
1
MISC. FABRIC
3
TEST CELL
2
MISC. FABRIC
1
CELL
INLET
3
2
1
BURLINGTON STYLE 454-I615
14 OZ. WOVEN GLASS-TEFLON B
⑥
①
3
2
1
BURLINGTON STYLE 454-I625
14 OZ. WOVEN GLASS-ACID FLEX
3
2
1
GLOBE ALBANY
14 OZ. NOMEX.FELT -PERMAGARD
F
E
D

Figure 4. Kerr Baghouse - cell schematic - system 2.

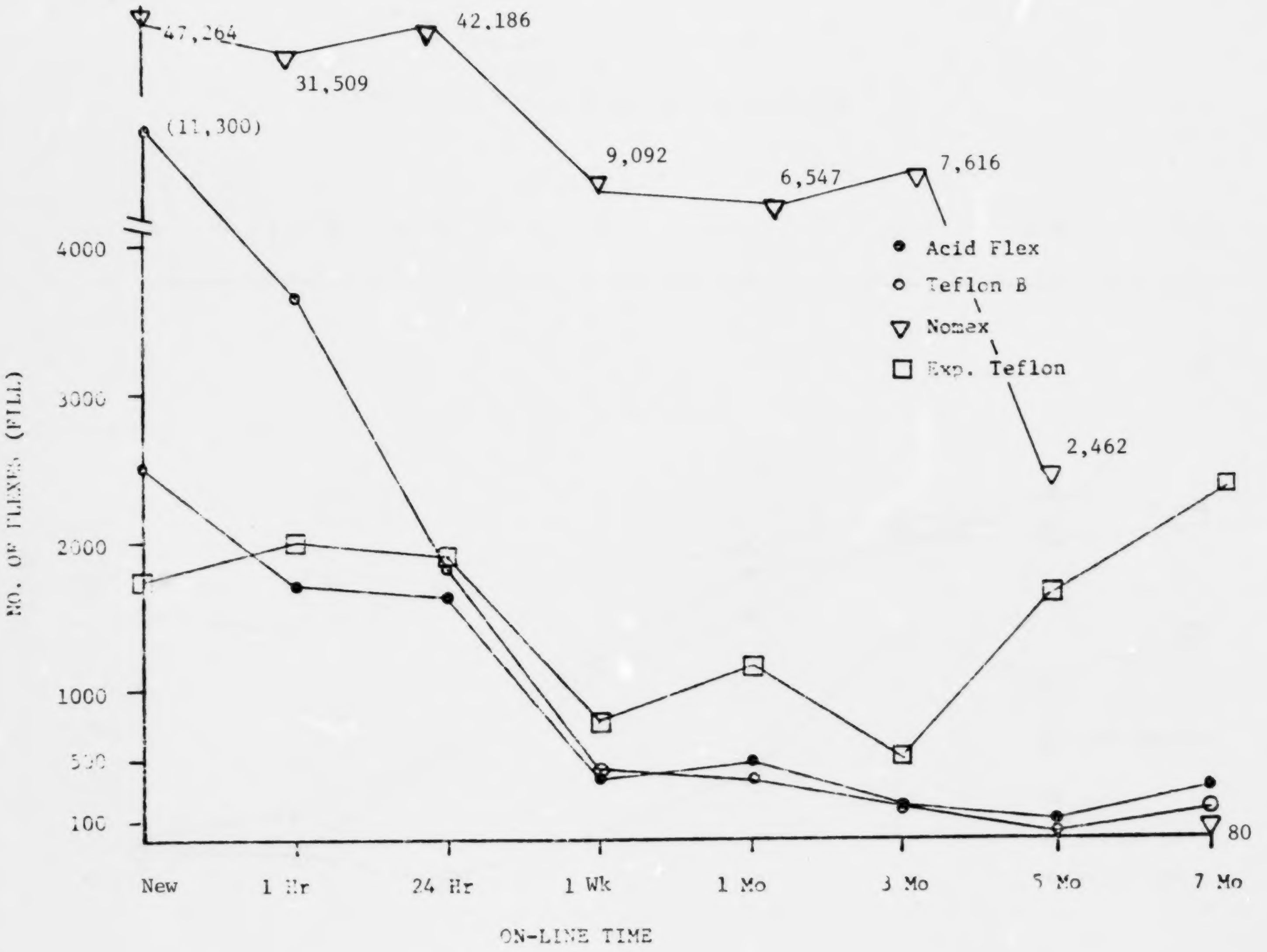

Figure 5. MIT Flex (fill) vs. on-line time
Kerr baghouse No. 2
fabric evaluation program.

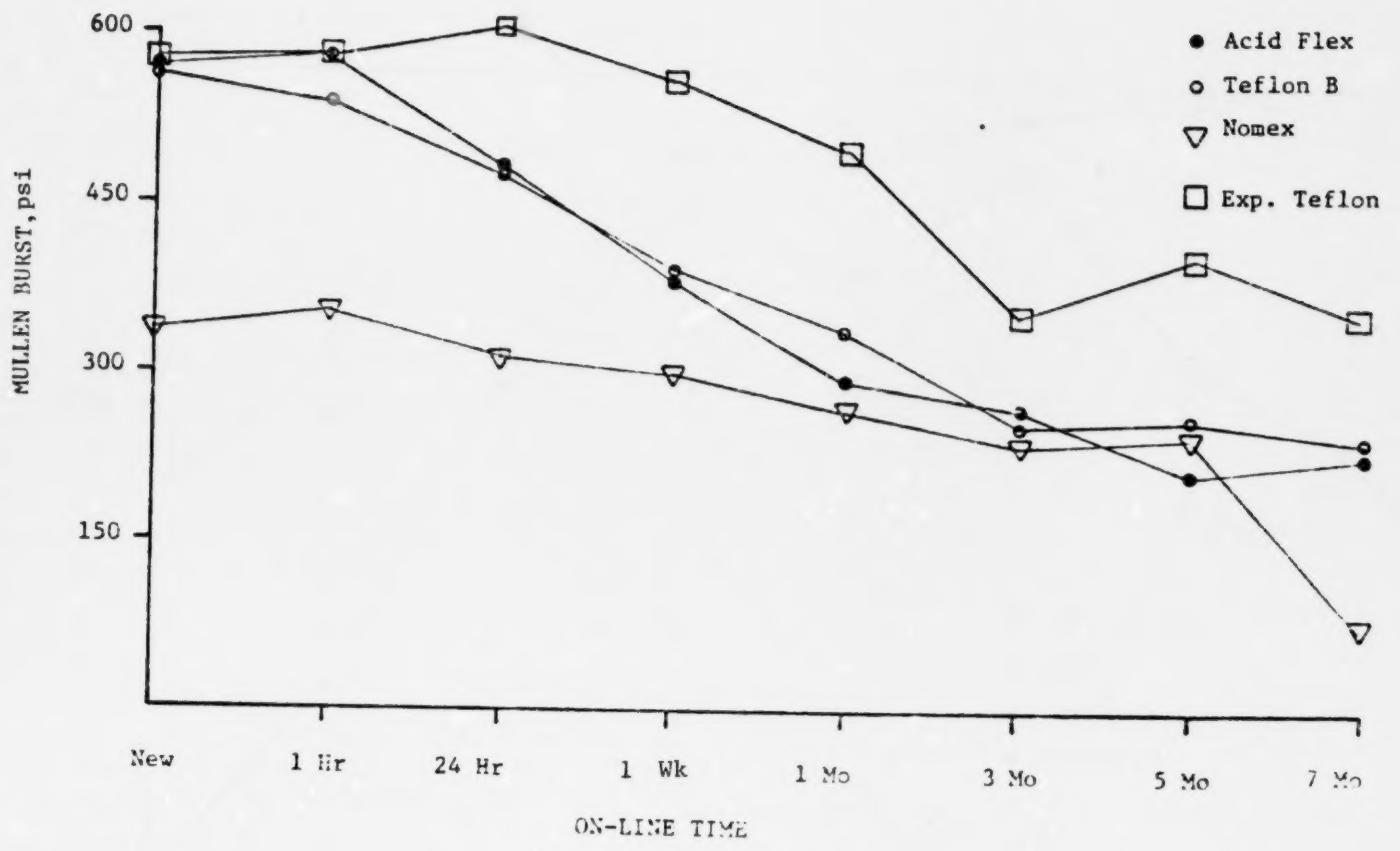

Figure 6. Mullen Burst vs. on-line time
Kerr baghouse No. 2
fabric evaluation program.

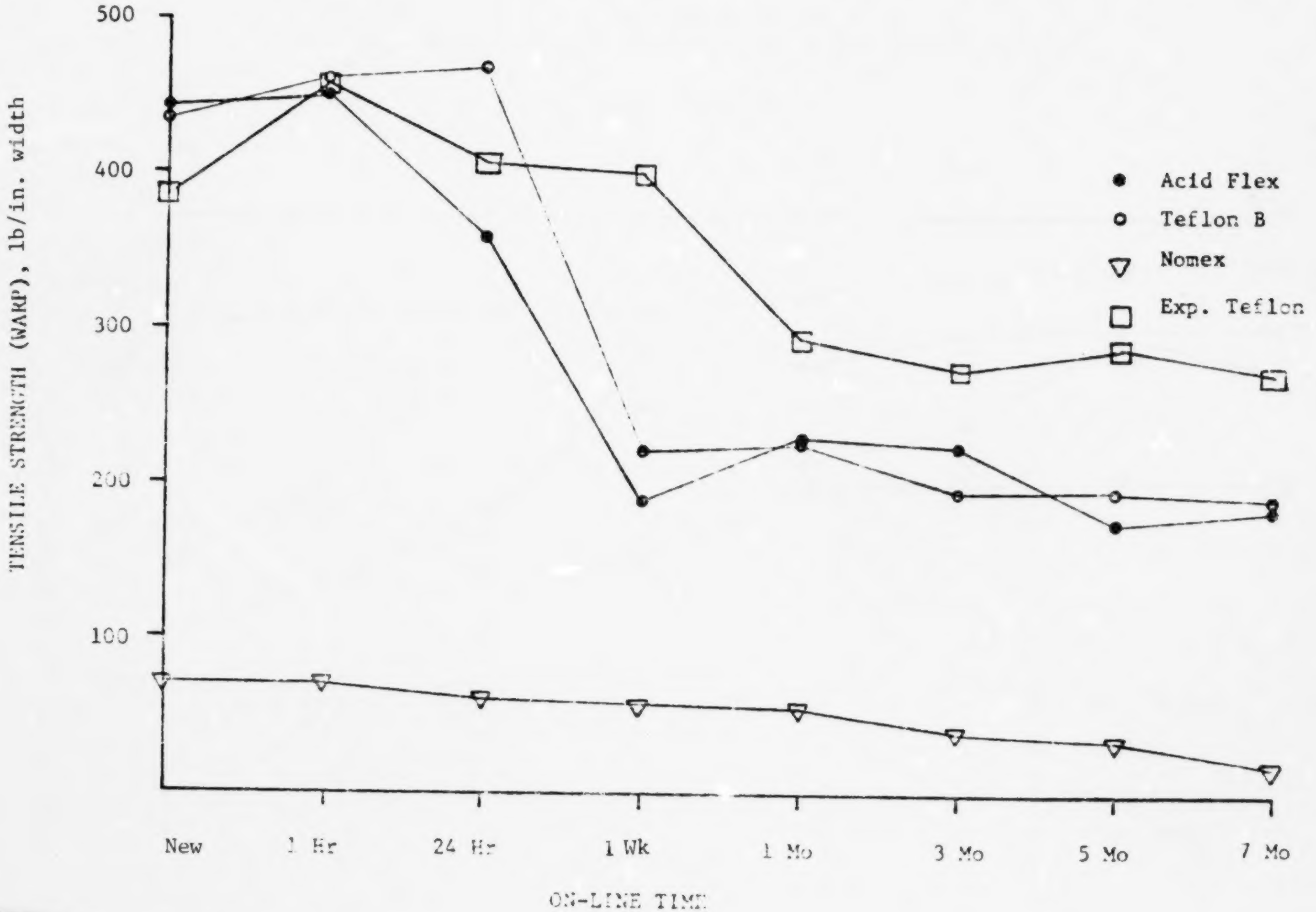

Reproduced from best available copy.

Figure 7. Tensile strength (warp) vs. on-line time Kerr baghouse No. 2 fabric evaluation program.

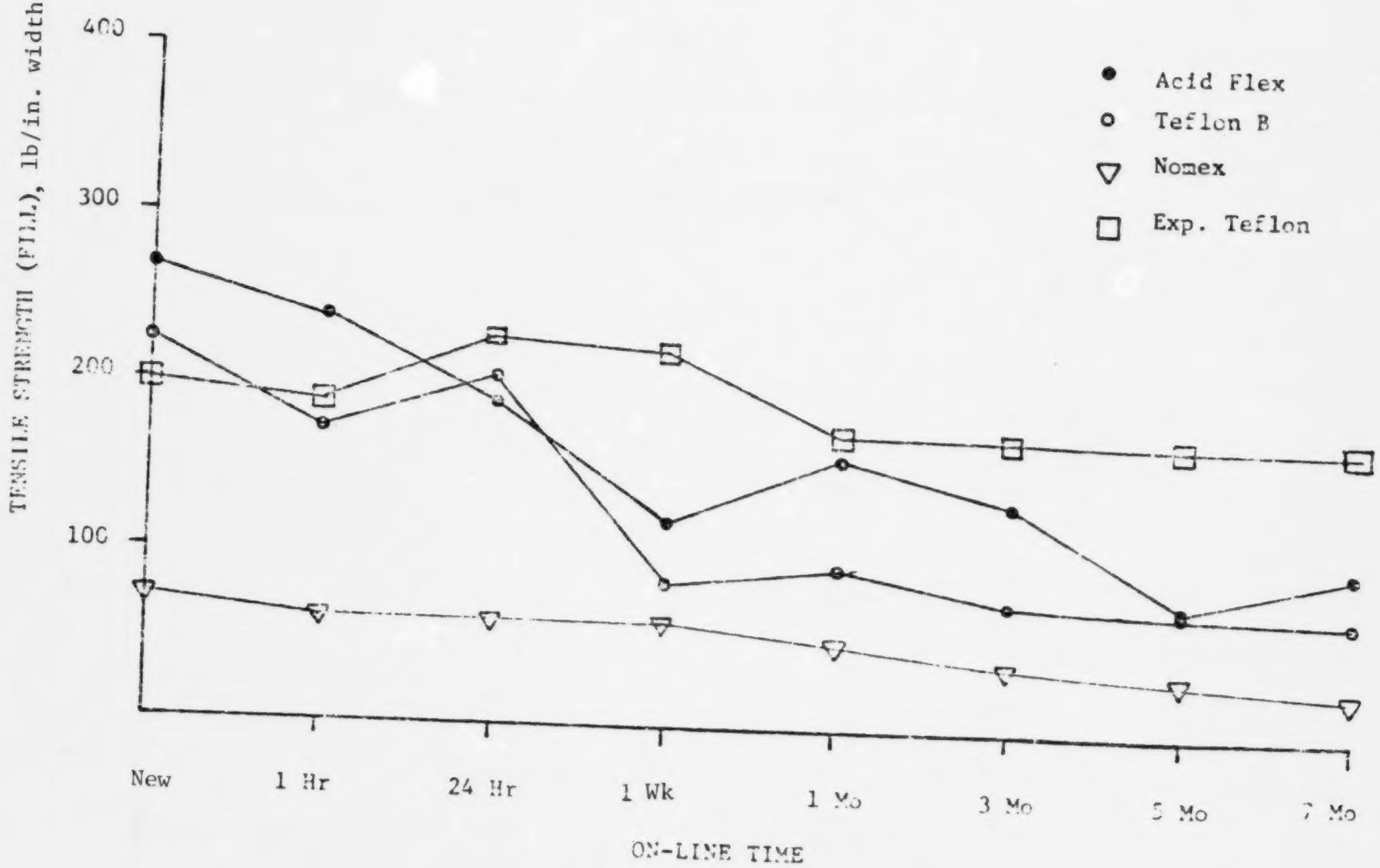

Figure 8. Tensile strength (fill) vs. on-line time
Kerr baghouse No. 2
fabric evaluation program.

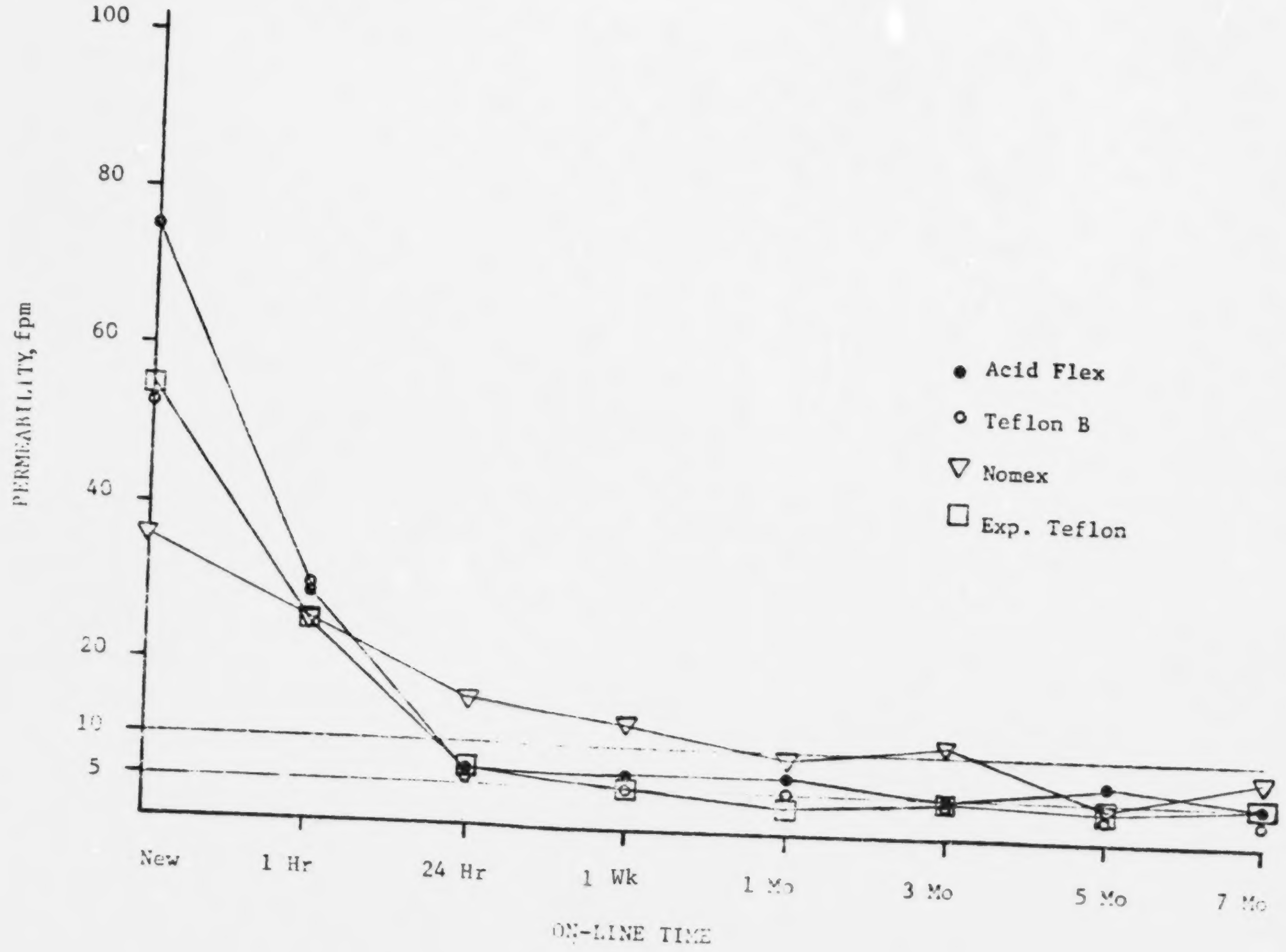

Figure 9. As received permeability vs. on-line time
Kerr baghouse No. 2,
fabric evaluation program.

OPTIMIZING THE LOCATION OF ANTI-COLLAPSE RINGS IN FABRIC BAGS

By: John G. Musgrove
Bechtel Power Corporation
P. O. Box 2166
Houston, Texas 77252-2166

ABSTRACT

The number and placement of anti-collapse rings in fabric filter bags are frequently left to the bag manufacturers. Bag manufacturers do not analyze operating requirements for determination of ring location but merely subdivide the bag into sections of approximately equal length. Bags whose section lengths are equal are suspected during reverse air cleaning of having greater collapse (deflection) in lower sections than in higher sections.

An analysis has been developed to predict the amount of collapse (deflection) in all sections of a bag undergoing reverse air cleaning. The methodology uses the catenary principle of a uniformly loaded suspension cable to determine deflection. A computer program utilizing this methodology has been developed to analyze the forces on a warp thread in a bag and to determine the location of anti-collapse rings to assure equal bag collapse in all sections. A companion program has been developed to predict bag section collapse for bags with established ring locations.

ACKNOWLEDGEMENTS

Special thanks is given to Research-Cottrell for providing the laboratory space and support personnel for conducting the full scale test program: Stephen Zierak, Southwest Regional Sales Manager; Stefan Negrea, Vice President of Engineering for the Air Pollution Control Division; Dennis Helfritch, Program Manager with Cottrell Environmental Sciences; and Chet Gorski and Mike Adams, laboratory technicians with Cottrell Environmental Sciences.

Thanks is also given to Houston Lighting & Power Company for providing spare filter bags for use in the test program: Soli Irani, Program Manager.

The assistance provided by Research-Cottrell and Houston Lighting & Power Company should in no way constitute their endorsement or agreement with the scope or results of this study. The scope and conclusions are solely those of the author.

INTRODUCTION

Fabric filter bags for reverse-air-cleaned baghouses, such as have been installed on utility steam electric generating stations, have anti-collapse rings located at intervals along their lengths to prevent excessive collapse during reverse air cleaning, Figure 1.

During flue gas cleaning or forward flow, the bag flexes outward uniformly, being restrained by the circumferencial stresses in the fill fibers. During the reverse-air cleaning mode, the bag collapses in a multi-lobe pattern, Figure 2. The fill fibers are no longer under tension and the stresses are taken by the warp fibers. The fibers at the inside diameter of the lobes undergo tension and form parabolic curves, Figure 3. Thus, the warp fibers form a family of hyperbolic curves, which is the basis for this study. A single section can therefore be presumed to form a hyperbolic shape, Figure 4.

The deflection caused by reverse air flow in each section is believed to increase from the top of the bag to the bottom of the bag as the tension decreases (1). If the original bag tension is inadequate and the ash loading on the inside of the bags is high, the deflection in the bottom section may be so great as to cause "pancaking", wherein opposite sides of the bag touch each other, Figure 5. This excessive deflection decreases bag life through excessive bag flexures and through abrasion of the bag by ash falling down through the bag.

The parabolic shape each fiber assumes under the uniform loading of the reverse air flow is identical to the catenary shape taken by a suspension cable under uniform loading. The purpose of this study is to develop a mathematical model to predict the amount of bag deflection at the initiation of reverse air cleaning so that the anti-collapse rings may be spaced so as to permit equal deflection of each bag section during reverse air cleaning. This study examines the catenary principle and applies it to the warp fibers of filter bags.

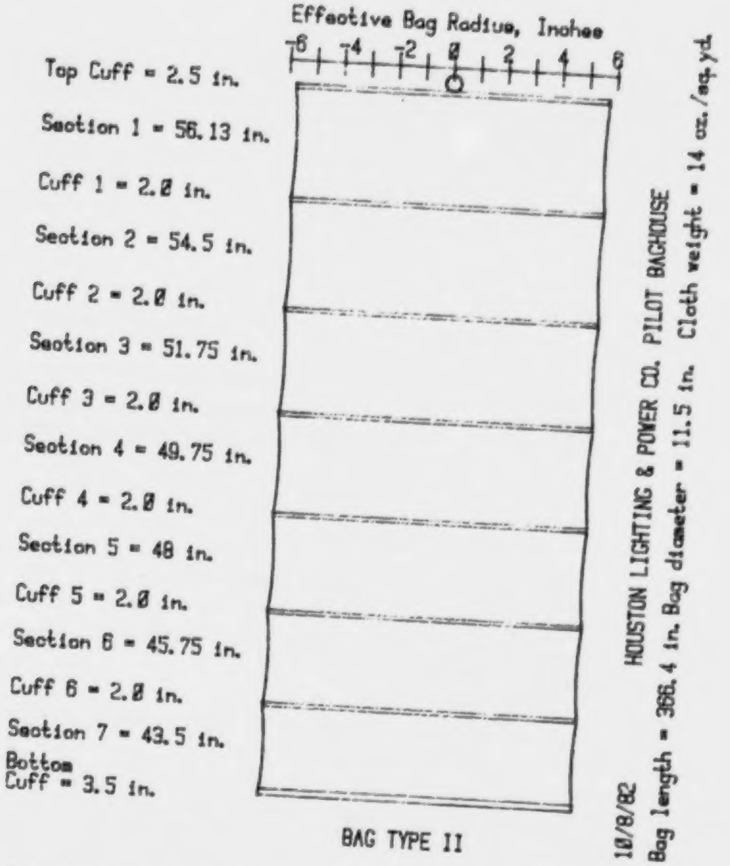
Effective Bag Radius, Inches
-6 -4 -2 0 2 4 6
Top Cuff = 2.5 in.
Section 1 = 56.13 in.
Cuff 1 = 2.0 in.
Section 2 = 54.5 in.
Cuff 2 = 2.0 in.
Section 3 = 51.75 in.
Cuff 3 = 2.0 in.
Section 4 = 49.75 in.
Cuff 4 = 2.0 in.
Section 5 = 48 in.
Cuff 5 = 2.0 in.
Section 6 = 45.75 in.
Cuff 6 = 2.0 in.
Section 7 = 43.5 in.
Bottom Cuff = 3.5 in.
BAG TYPE II
HOUSTON LIGHTING & POWER CO. PILOT BAGHOUSE
10/8/82
Bag length = 366.4 in. Bag diameter = 11.5 in. Cloth weight = 14 oz./sq.yd.

Figure 1. Filter bag with anti-collapse [illegible]gs.

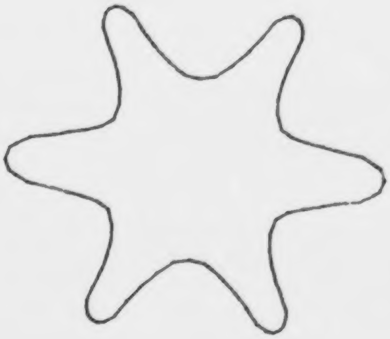

Figure 2. Plan view of collapsed bag section.

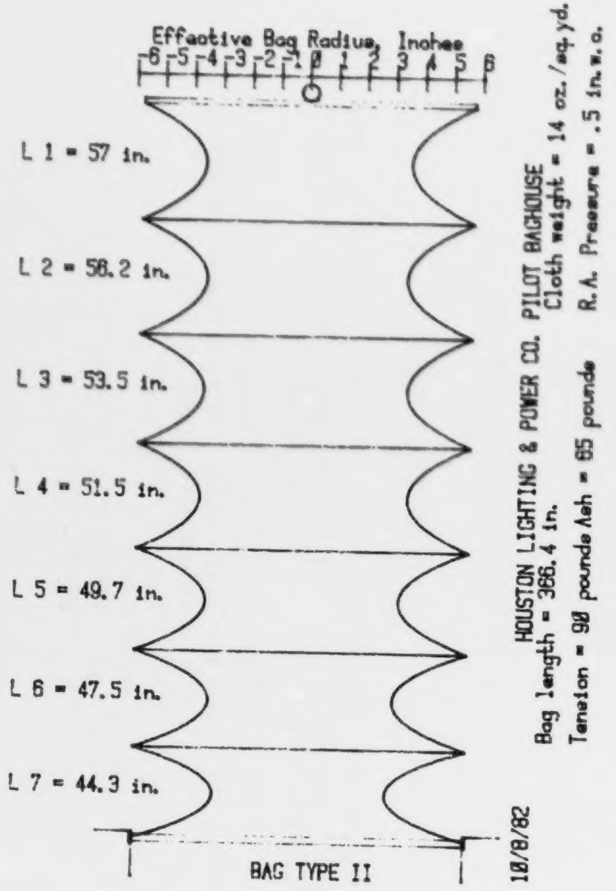

Figure 3. Section view of collapsed bag.

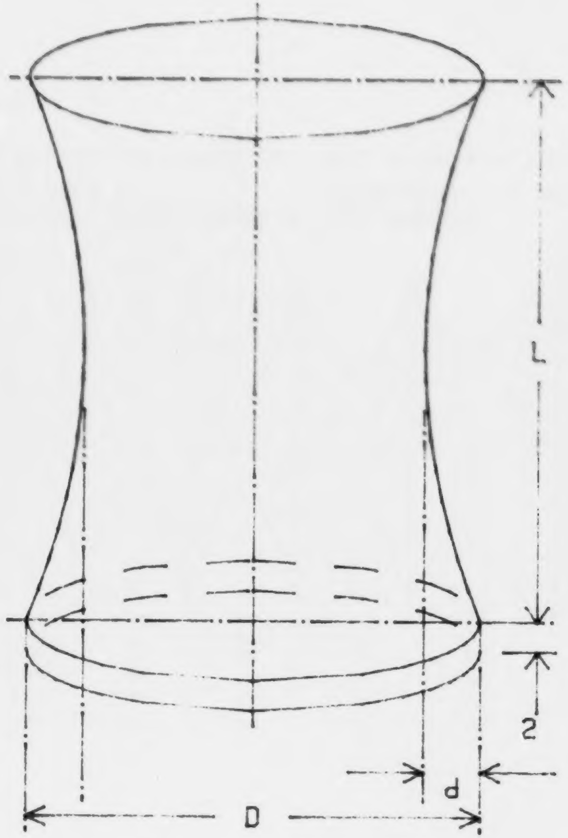

Figure 4. Downward view of collapsed bag section.

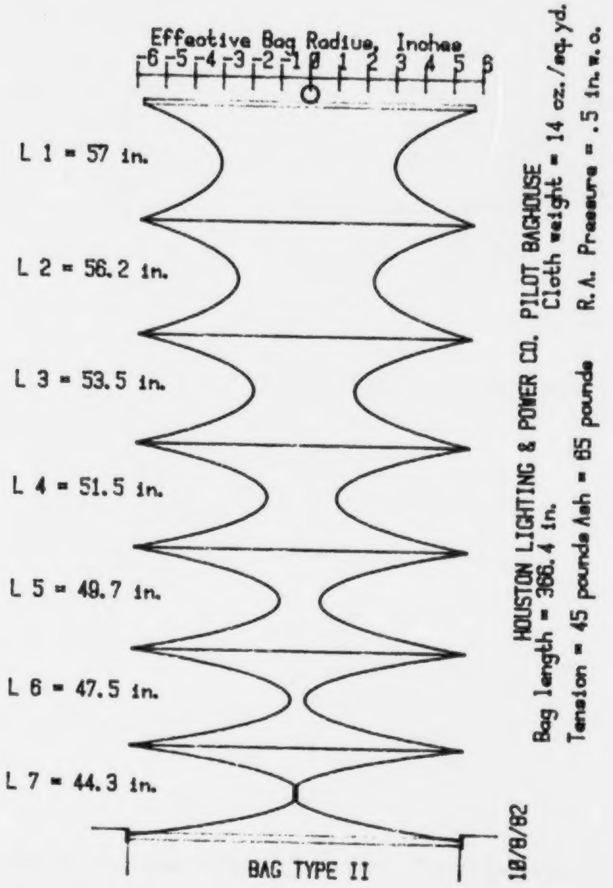
Effective Bag Radius, Inches
-6 -5 -4 -3 -2 -1 0 1 2 3 4 5 6
L 1 = 57 in.
L 2 = 56.2 in.
L 3 = 53.5 in.
L 4 = 51.5 in.
L 5 = 49.7 in.
L 6 = 47.5 in.
L 7 = 44.3 in.
HOUSTON LIGHTING & POWER CO. PILOT BAGHOUSE
Bag length = 366.4 in.
Cloth weight = 14 oz./sq.yd.
Tension = 45 pounds Ash = 65 pounds
R.A. Pressure = .5 in.w.c.
10/8/82
BAG TYPE II

Figure 5. Section view of "pancaking" bag section.

CATENARY SUSPENSION

The equations for determining stress and sag of a single cable under uniformly distributed load (2) are derived from the configuration of Figure 6. The forces and dimensions are as follows:

No load (initial configuration):
- ℓ = horizontal distance between supports
- L = developed length of cable
- f = sag of cable

Loaded Cable:
- T = tension in cable at support caused by superimposed loads

- q = weight of cable per unit length (assumed uniform)
- a = angle between horizontal and tangent to cable at support
- V = vertical component of T at support
- H = horizontal component of T at support
- Δf = increased sag in cable due to superimposed loads

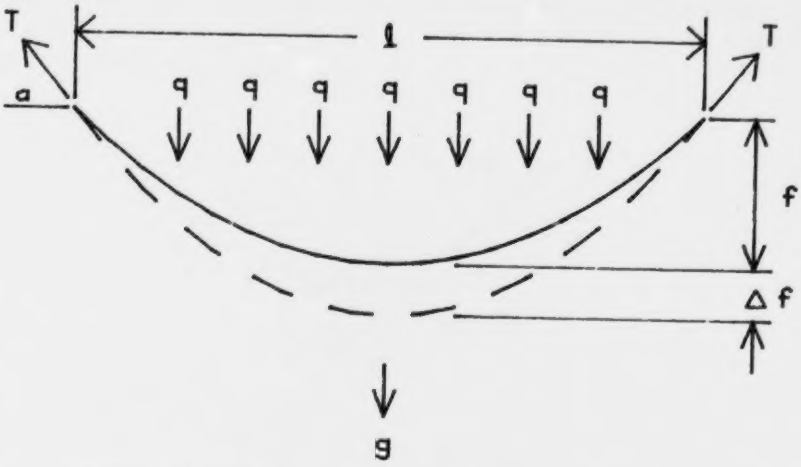

Figure 6. Catenary suspension force diagram.

The operational equations are:

$$L = \ell*[\ 1 + (8/3)*(f^2\ /\ell^2)],\ \text{in.} \qquad (1)$$

$$T = [(q*\ell^2/8*f)]*\ \text{SQR}\ [1 + 16*(f^2/\ell^2)],\text{oz.} \qquad (2)$$

$$\tan a = 4*(f +\!- \Delta f)/\ell \qquad (3)$$

$$V = T \sin (a),\ \text{oz.} \qquad (4)$$

$$H = T \cos (a),\ \text{oz.} \qquad (5)$$

The assumptions for these equations are that the initial sag, f, and distance between supports, ℓ are known, that the cable loading, q, is uniform, and that the unloaded cable weight and resulting tension are negligible compared to those of the loaded cable.

INITIAL MATHEMATICAL MODEL

CATENARY FORCES

The approach to determining fabric deflection is to assume the warp fibers undergo uniformly distributed loading, but in a vertical plane rather than a horizontal plane, Figure 7. The fiber is assumed to have a diameter of .0227 inches and therefore an area/inch of .0227 in^2/in. The fabric is assumed to have a count of 44 fibers per inch.

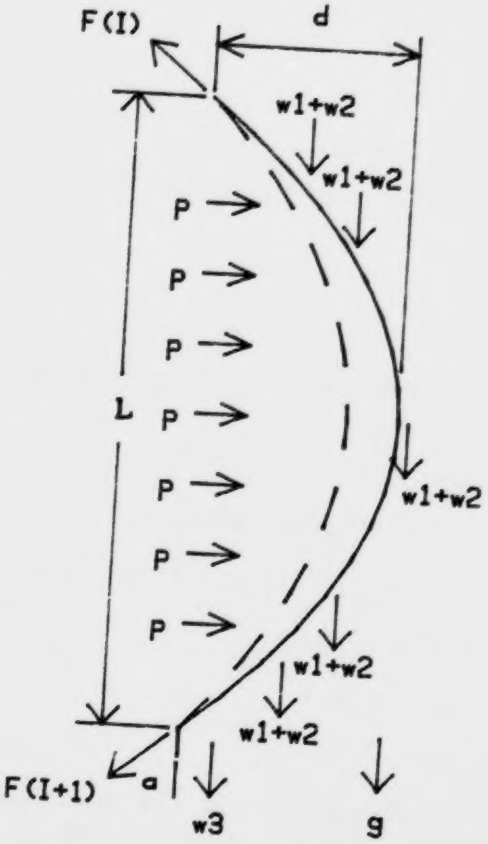

Figure 7. Bag warp fiber catenary force diagram.

The forces that translate from the suspension cable are:

- $\ell = L$ = vertical distance between rings, in.
- $L = S$ = developed length of collapsed fiber, in.
- $f = d$ = deflection of fiber from ring diameter, in.
- $T = F$ = tension force in fiber, oz.
- $q = p$ = force of reverse air, $oz/in^2/in$.
- $a = a$ = angle between vertical and tangent to fiber
- $V = F_H$ = horizontal component of F at ring, oz.
- $H = F_V$ = vertical component of F at ring, oz.

Additional forces to consider include:

- $W1$ = unit weight of cloth, oz/in.
- $W2$ = unit weight of ash, oz/in.
- $W3$ = unit weight of ring and ring cuff, oz.

Equations 1 through 5 can thus be rewritten as:

$$S = L [1 + (8/3)*(d^2/L^2)] \tag{6}$$

$$F = [(p*L^2)/(8*d)] * SQR [1 + 16*(d^2/L^2)] \tag{7}$$

$$\tan a = 4 * d/L \tag{8}$$

$$F_H = F * \cos (a) \tag{9}$$

$$F_V = F * \sin (a) = p * L^2/2 \tag{10}$$

Additional equations developed here include:

$$F_{VN} = F_{VN+1} + W3 + S_N *(W1 + W2) \tag{11}$$

Where N denotes the bag section undergoing analysis.

The tension in the thread is thus:

$$T_N = SQR [(F_{HN})^2 + (F_{VN})^2] \tag{12}$$

BAGHOUSE FORCES

The tension in the warp fiber is further influenced by the thermal expansion of the baghouse casing, the reverse air force in the bag cap and the weight of the accumulated ash. The tension due to thermal expansion is:

$$T4 = (T8-T6) * L' * K9 * (C_{E2} - C_{E1}) \tag{13}$$

Where:
T8 = operating temperature, F

T6 = ambient temperature during bag hanging, F

L' = casing length $(\sim L + 16)$, in.

K9 = tensioning spring constant, lb/in.

C_{E2} = Coefficient of thermal expansion of steel, in/in/F

C_{E1} = Coefficient of thermal expansion of glass (3), in/in/F

The relaxation of tension due to the reverse air force on the cap is:

$$T5 = A * .5781 * \pi * (R9)^2/16 \qquad (14)$$

Where:
A = reverse air pressure, in. wg

R9 = bag radius, in.

The weight of ash per inch of fiber is:

$$W6 = 80 * T1 * \pi * D9 * (L9-6)/1728 \qquad (15)$$

Where:
T1 = thickness of ash layer, in.

D9 = bag diameter, in.

L9-6 = effective bag length (less ring cuffs)

The total fabric tension just prior to reverse air cleaning is:

$$T3 = T + T4 + T2 \qquad (16)$$

Where:
T2 = upward force on bag cap

The total fabric tension just after start of reverse air cleaning is:

$$T9 = T + T4 - T5 \qquad (17)$$

The tension created by the weight of the ash itself is not included in T3 and T9 because it is a force that acts solely downward from within the bag. That is, since the support spring will deflect and relax the tension at the bottom as the tension at the top increases, the net effect within the bag is negligible and assumed to be zero.

OPERATING EQUATIONS

The four fundamental equations for analysis then become

$$F_{H_N} = F2(I) = p* [L (I)]^2/2 \qquad (18)$$

$$F_{V_N} = F1(I) = T9 * (16/1660)-K1 * (W1 + W2) - W3 * (I-1) \qquad (19)$$

$$F = F(I)= SQR [(F1(I))^2 + (F2(I))^2] \qquad (20)$$

$$D(I) = p* L(I)^2/(4 * SQR [(2* F(I))^2- (p * L(I))^2] \qquad (21)$$

The initial modeling effort, in using the catenary principles, had no method for relating tension prior to uniform loading of the fiber to tension following such loading since the catenary principal assumed initial tension to be negligible. Development of this relationship was made by the measurement of actual deflection under loading of two different fabric filter bags.

LABORATORY TESTING

Research-Cottrell was kind enough to provide a high-bay test structure and technical support for measuring the deflections of a filter bag undergoing reverse air pressure. The bags were provided from spares purchased by Houston Lighting & Power Company as part of a separate pilot baghouse test program. The pilot test program was performed under a contract with Cottrell Environmental Sciences.

LABORATORY TEST FACILITY

The test facility was erected in Research-Cottrell's forty-foot high precipitator electrode test bay. Individual fabric bags, each 30'-6" long and 11.5" in diameter were hung by a spring scale from the upper bay supports. The bottom of the bags were attached to a single thimble which was restrained by chains linked to earth anchors. The thimble was sealed at the bottom and connected to a vacuum pump. An inclined manometer permitted measurement of the differential pressure across the bag. A fixed scale was placed adjacent to the thimble to indicate any bag movement due to application of the air pressure, and a tape measure was hung beside the bag, attached only at the top, to indicate the amount of bag shortening due to application of reverse air pressure. A standard workman's scaffold was erected around the bag and boards placed on it to permit convenient reading of the support scale load and the convenient measurement of the collapsed diameter of each section.

To assure attainment of reverse air pressures of up to 1 inch water guage (in. wg) a tube of plastic film (5 mils thick) was installed over the bag as it was hung to simulate the resistance of the dust cake. The weight of the ash was simulated by hanging masses of approximately equal weight onto the rings to simulate a uniform loading along the bag length.

Bag deflection was measured by use of a standard outside diameter caliper and a measuring rule to obtain the average minimum collapsed diameter of the bag.

Test Program

A total of ten test runs were conducted, as indicated in Table 1.

TABLE 1 - TEST PARAMETERS

Run, Number	Bag Type, Number	R.A. Pressure, in. wg	Initial Tension, pounds	Ash Load, pounds
1	2	0.5	100	0
2	2	1.0	98	0
3	2	0.5	63	0
4	2	1.0	65	0
5	2	0.5	51	65.25
6	2	1.0	51	65.25
7	2	0.5	85	65.25
8	2	0.85	72	65.25
9	3	1.0	63	65.25
10	3	1.0	95	65.25

The data from Runs 1 through 4 indicated greater deflection at the top of the bag than at the bottom of it. These data were subsequently discarded as being the result of anomolies due to light loading (no ash) and the influence of the plastic bag.

Test Runs 5 through 10 produced acceptable results - deflections increasing down the bag - and were used in the subsequent analysis. Appendix I presents the summary of test results.

DATA CORRELATION

TENSIONING DUE TO REVERSE AIR

The test program clearly identified a factor missing from equation 17, the tension created by the collapse and shortening of the bag sections. In order to calculate this tension, the resulting deflections were assumed to be solely restrained by this tension. Figure 8 presents the relative distance between rings as a percentage of the fiber length, a strong correlation. The total bag reduction in length was apportioned to each section in proportion to its unloaded length. Figure 9 presents the average reduced lengths for each test reverse air pressure and the average for all the tests.

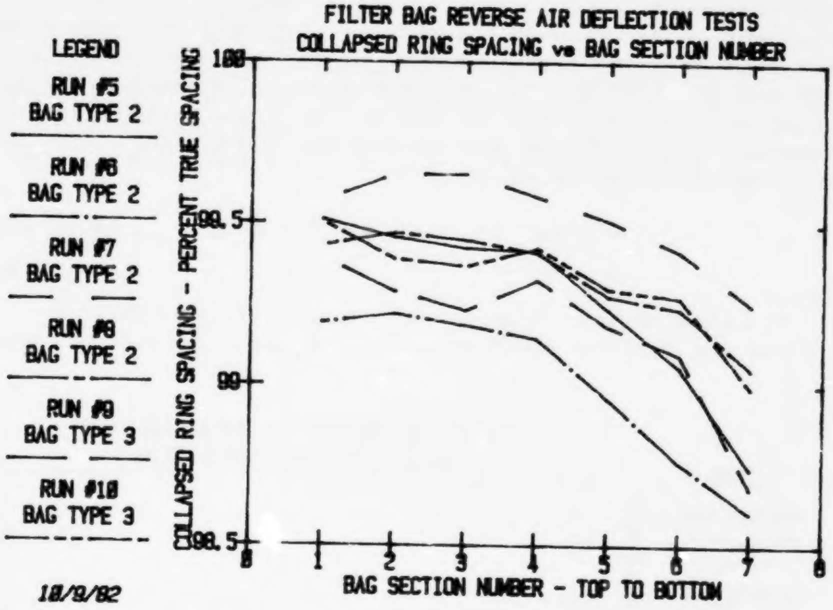

Figure 8. Bag section shortening due R.A. pressure.

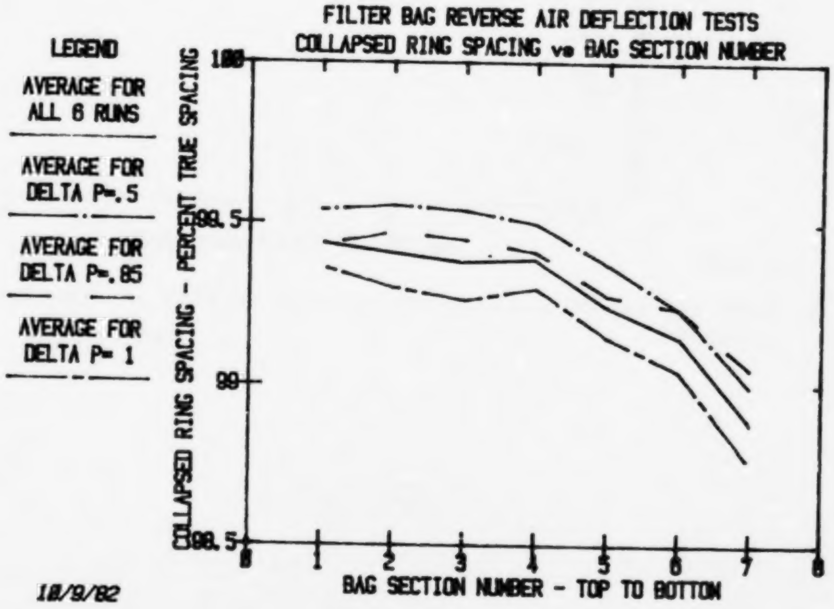

Figure 9. Average bag section shortening due to R. A. pressure.

The shape of the curves suggested an exponential relationship for the percentage shortening, one minus the reduced length. Figure 10 depicts the exponential curves for each of the three test reverse air pressures. Unfortunately, the data of the 0.85 in. wg case do not fall between those of 0.5 in. wg and those of 1.0 in. wg., perhaps due to measurement error or insufficient data at that test condition. A single exponential curve was then generated, Figure 11, to approximate the shortening of the bag sections. The relationship obtained is:

$$L = (1 - [(.01) * (.005 * \exp((I-1) * 0.844) + .5673)]) * S \qquad (22)$$

Where:

L = distance between rings as a factor of fiber length S

I = the bag section under analysis, numbered starting at the top

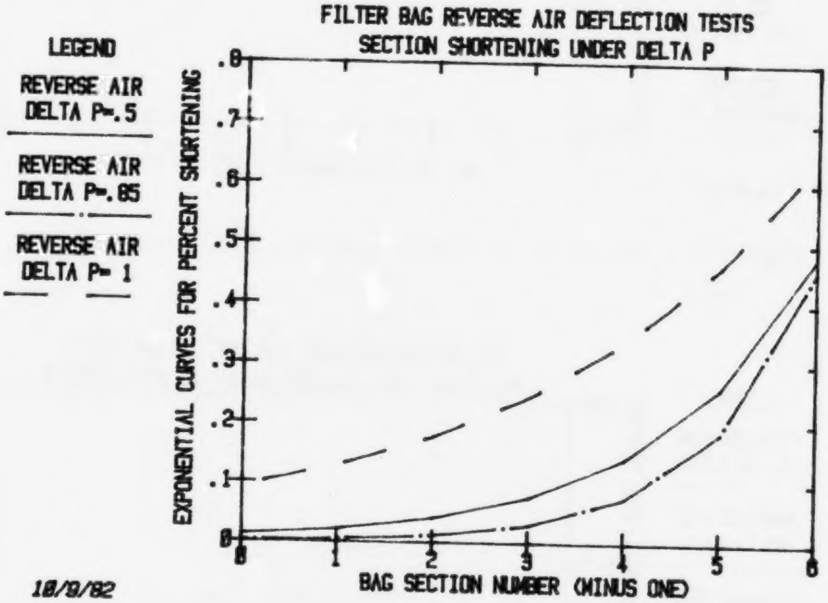

Figure 10. Averaged exponential curves for bag section shortening due to R. A. pressure.

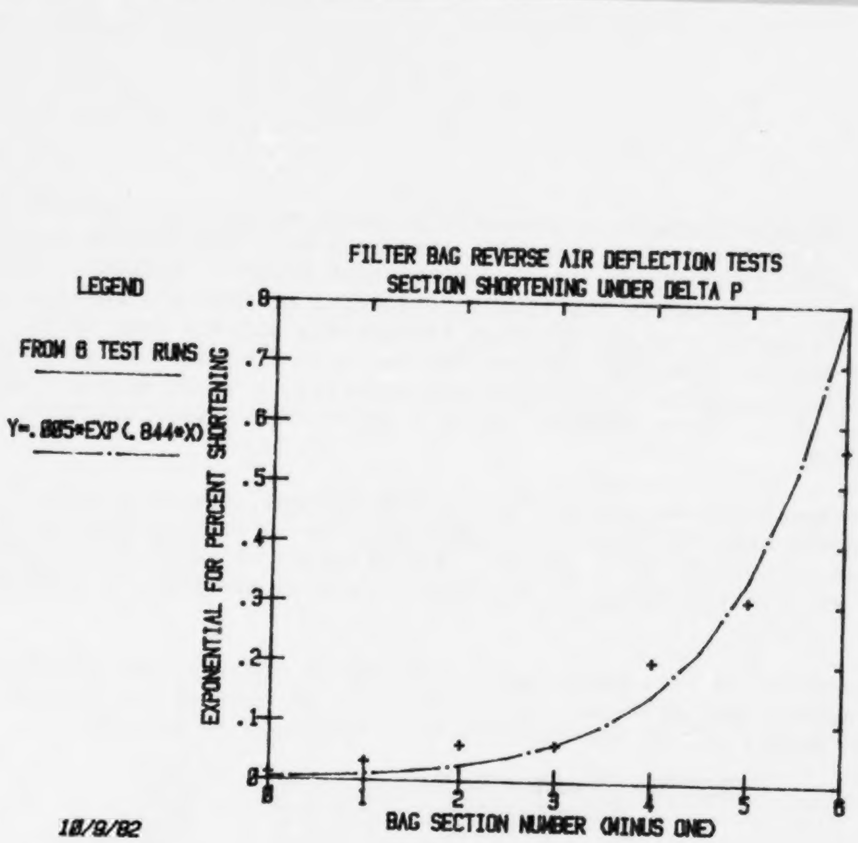

10/9/82

Figure 11. Overall average exponential curve for bag section shortening due to R.A. pressure.

FINAL MATHEMATICAL MODEL

By knowing the section deflections and the shortening caused by them, the tensions resisting the deflection can be calculated using equations 22, 6, 8 and 10. Equation 10 was modified to include a pressure factor which was varied to provide absolute equality. The pressure factors thus obtained, as a function of bag section I, can be closely approximated by:

$$F9\ (I) = .07833 + .00607 * I \tag{23}$$

Once the estimation of increased tension was obtained by the summation of the values for each section, equations 10, 11, and 12 were then iteratively calculated (with a new pressure factor in equation 10) to obtain a deflection equal to that measured in the test program. The new pressure factor for equation 10 is 0.673.

The computer program 'DEFLEC' of Appendix II performs the computations of the equations to calculate deflections of filter bags when the section lengths are known. Table 2 presents a sample printout of program 'DEFLEC'. Computer program 'RINGOP' of Appendix III is a modification of 'DEFLEC' which assumes equal section lengths to start and then iteratively adjusts them until all bag sections produce equal deflections for the stated conditions of initial tension, ambient/operating temperature differential, support spring constant, and ash cake thickness and weight. Table 3 presents a sample printout of program 'RINGOP'.

Figure 12 presents the deflections of two bag designs, one with equal ring spacings and one with optimized ring spacings, for an initial tension of 60 pounds and an ash weight of 57 pounds. The benefits of equal deflection can be observed and are the result of designing the ring spacings to assure equal deflection.

The work described in this paper was not funded by the U.S. Environmental Protection Agency and therefore the contents do not necessarily reflect the views of the Agency and no official endorsement should be inferred.

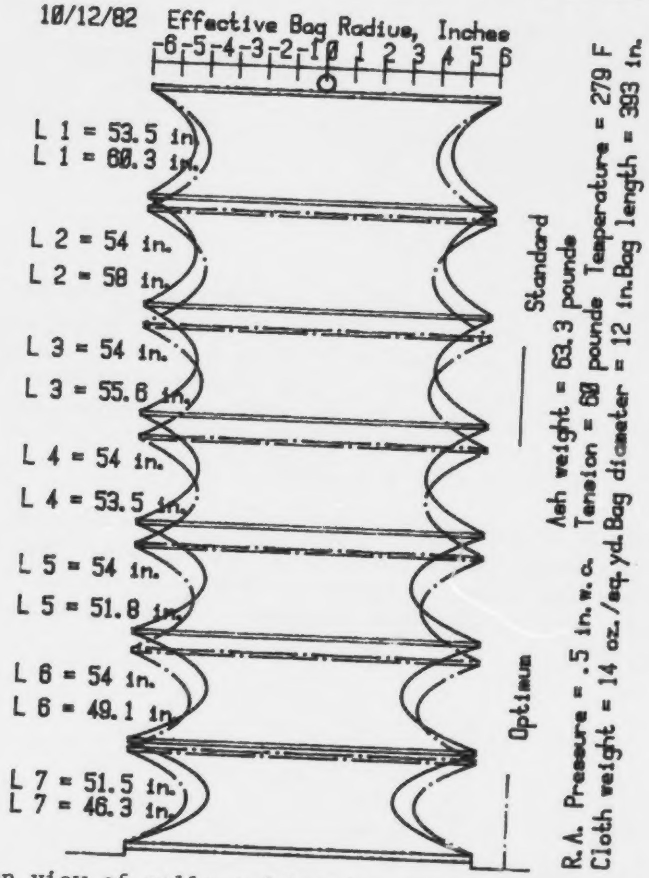

Figure 12. Section view of collapsed bag for both standard and optimum spacing of anti-collapse rings.

TABLE 2. SAMPLE OUTPUT OF PROGRAM "RINGOP".

```
This is program RINGOP to determine the optimum location of anti-collapse rings
in filter bags to assure equal deflection in each section during reverse air cleaning
11/2/1982

   Bag          Bag        Operating        Ambient         Dia. of         Tension
 Length,     Diameter,   Temperature,     Temperature,    Ring wire,      Prior to RA,
 inches       inches      Degrees F        Degrees F        inches          pounds
  396.0        11.50         300              80             .1875           95.7



  Weight      Initial    Forward Gas      Total Ash      Reverse Air        Tension
 of cloth,   Tension,     Pressure,        Weight,        Pressure,       Start of RA,
oz./sq.yd.    pounds       in.w.c.         pounds          in.w.c.          pounds
   14          60.0         4.00            40.8             .50            139.5

Number of Rings =  1
Deflection greater than 1/3 diameter; further analysis terminated.

  Weight      Initial    Forward Gas      Total Ash      Reverse Air        Tension
 of cloth,   Tension,     Pressure,        Weight,        Pressure,       Start of RA,
oz./sq.yd.    pounds       in.w.c.         pounds          in.w.c.          pounds
   14          60.0         4.00            40.8             .50            141.2

Number of Rings =  2
Deflection greater than 1/3 diameter; further analysis terminated.

  Weight      Initial    Forward Gas      Total Ash      Reverse Air        Tension
 of cloth,   Tension,     Pressure,        Weight,        Pressure,       Start of RA,
oz./sq.yd.    pounds       in.w.c.         pounds          in.w.c.          pounds
   14          60.0         4.00            40.8             .50            142.6

Number of Rings =  3
Deflection greater than 1/3 diameter; further analysis terminated.
```

Reproduced from
best available copy.

TABLE 2. SAMPLE OUTPUT OF PROGRAM "RINGOP" (CONT.)

```
   Weight       Initial     Forward Gas     Total Ash     Reverse Air      Tension
  of cloth,     Tension,     Pressure,       Weight,       Pressure,     Start of RA,
 oz./sq.yd.      pounds       in.w.c.        pounds         in.w.c.         pounds
     14           60.0         4.00           40.8            .50           143.4

Number of Rings =  4
Section 1 = 84.05 inches long (effectively); its deflection = 2.705 inches
Section 2 = 80.55 inches long (effectively); its deflection = 2.698 inches
Section 3 = 77.8 inches long (effectively); its deflection = 2.742 inches
Section 4 = 75.05 inches long (effectively); its deflection = 2.795 inches
Section 5 = 71.55 inches long (effectively); its deflection = 2.797 inches
Tension at the bottom of the bag (at the start of cleaning) =  91.3 pounds.

Measured (fabricated) section lengths are as follows (assuming 2 inch ring covers)
Section 1 = 83.175 inches long
Section 2 = 78.8 inches long
Section 3 = 76.05 inches long
Section 4 = 73.3 inches long
Section 5 = 70.675 inches long


   Weight       Initial     Forward Gas     Total Ash     Reverse Air      Tension
  of cloth,     Tension,     Pressure,       Weight,       Pressure,     Start of RA,
 oz./sq.yd.      pounds       in.w.c.        pounds         in.w.c.         pounds
     14           60.0         4.00           40.8            .50           143.2

Number of Rings =  5

Section 1 = 70.041 inches long (effectively); its deflection = 1.881 inches
Section 2 = 67.666 inches long (effectively); its deflection = 1.88 inches
Section 3 = 65.291 inches long (effectively); its deflection = 1.88 inches
Section 4 = 64.416 inches long (effectively); its deflection = 1.971 inches
Section 5 = 61.916 inches long (effectively); its deflection = 1.971 inches
Section 6 = 59.416 inches long (effectively); its deflection = 1.972 inches
Tension at the bottom of the bag (at the start of cleaning) =  90.6 pounds.
```

TABLE 2. SAMPLE OUTPUT OF PROGRAM "RINGOP" (CONT.)

```
Measured (fabricated) section lengths are as follows (assuming 2 inch ring covers)
Section 1 = 69.166 inches long
Section 2 = 65.916 inches long
Section 3 = 63.541 inches long
Section 4 = 62.666 inches long
Section 5 = 60.166 inches long
Section 6 = 58.541 inches long


  Weight       Initial    Forward Gas    Total Ash    Reverse Air     Tension
 of cloth,     Tension,    Pressure,      Weight,      Pressure,    Start of RA,
oz./sq.yd.     pounds      in.w.c.        pounds       in.w.c.        pounds
   14           60.0        4.00           40.8          .50          141.9

Number of Rings =  6
Section 1 = 60 inches long (effectively); its deflection = 1.393 inches
Section 2 = 58.25 inches long (effectively); its deflection = 1.393 inches
Section 3 = 56.5 inches long (effectively); its deflection = 1.394 inches
Section 4 = 55.5 inches long (effectively); its deflection = 1.434 inches
Section 5 = 54.625 inches long (effectively); its deflection = 1.486 inches
Section 6 = 52.75 inches long (effectively); its deflection = 1.487 inches
Section 7 = 50.875 inches long (effectively); its deflection = 1.489 inches
Tension at the bottom of the bag (at the start of cleaning) =  88.9 pounds.

Measured (fabricated) section lengths are as follows (assuming 2 inch ring covers)
Section 1 = 59.125 inches long
Section 2 = 56.5 inches long
Section 3 = 54.75 inches long
Section 4 = 53.75 inches long
Section 5 = 52.875 inches long
Section 6 = 51 inches long
Section 7 = 50 inches long
```

TABLE 3. SAMPLE OUTPUT OF PROGRAM "DEFLEC".

```
This is program DEFLEC to determine the filter bag
deflection in each section during reverse air cleaning

Number of rings =  6

   Bag          Bag        Operating        Ambient         Dia. of        Tension
 Length,     Diameter,    Temperature,    Temperature,    Ring wire,    Prior to RA,
 inches        inches     Degrees F       Degrees F        inches         pounds
  396.0        11.50         300              80            .1875          95.7

  Weight       Initial     Forward Gas     Total Ash     Reverse Air       Tension
 of cloth,     Tension,     Pressure,       Weight,       Pressure,     Start of RA,
 oz./sq.yd.     pounds       in.w.c.        pounds         in.w.c.         pounds
    14          60.0         4.00            10.2           .50            141.5
Section 1 = 54.375 inches long (effectively); its deflection = 1.147 inches
Section 2 = 55.75 inches long (effectively); its deflection = 1.234 inches
Section 3 = 55.75 inches long (effectively); its deflection = 1.264 inches
Section 4 = 55.75 inches long (effectively); its deflection = 1.296 inches
Section 5 = 55.75 inches long (effectively); its deflection = 1.329 inches
Section 6 = 55.75 inches long (effectively); its deflection = 1.365 inches
Section 7 = 52.375 inches long (effectively); its deflection = 1.237 inches
Tension at the bottom of the bag (just prior to cleaning) =119.5 pounds.


   Bag          Bag        Operating        Ambient         Dia. of        Tension
 Length,     Diameter,    Temperature,    Temperature,    Ring wire,    Prior to RA,
 inches        inches     Degrees F       Degrees F        inches         pounds
  396.0        11.50         300              80            .1875          95.7

  Weight       Initial     Forward Gas     Total Ash     Reverse Air       Tension
 of cloth,     Tension,     Pressure,       Weight,       Pressure,     Start of RA,
 oz./sq.yd.     pounds       in.w.c.        pounds         in.w.c.         pounds
    14          60.0         4.00            20.4           .50            141.5
Section 1 = 54.375 inches long (effectively); its deflection = 1.147 inches
Section 2 = 55.75 inches long (effectively); its deflection = 1.247 inches
Section 3 = 55.75 inches long (effectively); its deflection = 1.292 inches
Section 4 = 55.75 inches long (effectively); its deflection = 1.34 inches
Section 5 = 55.75 inches long (effectively); its deflection = 1.392 inches
Section 6 = 55.75 inches long (effectively); its deflection = 1.449 inches
Section 7 = 52.375 inches long (effectively); its deflection = 1.332 inches
Tension at the bottom of the bag (just prior to cleaning) =109.4 pounds.
```

TABLE 3. SAMPLE OUTPUT OF PROGRAM "DEFLEC" (CONT.)

```
   Bag           Bag        Operating      Ambient        Dia. of       Tension
 Length,      Diameter,   Temperature,   Temperature,   Ring wire,    Prior to RA,
 inches        inches      Degrees F      Degrees F       inches        pounds
  396.0         11.50         300             80           .1875          95.7

  Weight       Initial    Forward Gas     Total Ash    Reverse Air      Tension
 of cloth,     Tension,    Pressure,       Weight,       Pressure,    Start of RA,
oz./sq.yd.     pounds       in.w.c.        pounds        in.w.c.        pounds
   14           60.0         4.00           30.6           .50          141.5
Section 1 = 54.375 inches long (effectively); its deflection = 1.147 inches
Section 2 = 55.75 inches long (effectively); its deflection = 1.26 inches
Section 3 = 55.75 inches long (effectively); its deflection = 1.321 inches
Section 4 = 55.75 inches long (effectively); its deflection = 1.387 inches
Section 5 = 55.75 inches long (effectively); its deflection = 1.461 inches
Section 6 = 55.75 inches long (effectively); its deflection = 1.544 inches
Section 7 = 52.375 inches long (effectively); its deflection = 1.444 inches
Tension at the bottom of the bag (just prior to cleaning) = 99.3 pounds.
```

```
   Bag           Bag        Operating      Ambient        Dia. of       Tension
 Length,      Diameter,   Temperature,   Temperature,   Ring wire,    Prior to RA,
 inches        inches      Degrees F      Degrees F       inches        pounds
  396.0         11.50         300             80           .1875          95.7

  Weight       Initial    Forward Gas     Total Ash    Reverse Air      Tension
 of cloth,     Tension,    Pressure,       Weight,       Pressure,    Start of RA,
oz./sq.yd.     pounds       in.w.c.        pounds        in.w.c.        pounds
   14           60.0         4.00           40.8           .50          141.5
Section 1 = 54.375 inches long (effectively); its deflection = 1.147 inches
Section 2 = 55.75 inches long (effectively); its deflection = 1.273 inches
Section 3 = 55.75 inches long (effectively); its deflection = 1.351 inches
Section 4 = 55.75 inches long (effectively); its deflection = 1.438 inches
Section 5 = 55.75 inches long (effectively); its deflection = 1.538 inches
Section 6 = 55.75 inches long (effectively); its deflection = 1.652 inches
Section 7 = 52.375 inches long (effectively); its deflection = 1.575 inches
Tension at the bottom of the bag (just prior to cleaning) = 89.2 pounds.
```

TABLE 3. SAMPLE OUTPUT OF PROGRAM "DEFLEC" (CONT.)

```
   Bag           Bag         Operating       Ambient        Dia. of        Tension
 Length,      Diameter,    Temperature,   Temperature,     Ring wire,    Prior to RA,
 inches        inches       Degrees F      Degrees F        inches         pounds
  396.0        11.50          300             80             .1875          95.7

  Weight       Initial     Forward Gas     Total Ash     Reverse Air       Tension
 of cloth,     Tension,     Pressure,       Weight,       Pressure,     Start of RA,
oz./sq.yd.     pounds        in.w.c.        pounds         in.w.c.         pounds
   14           60.0          4.00           51.0           .50            141.5
Section 1 = 54.375 inches long (effectively); its deflection = 1.147 inches
Section 2 = 55.75 inches long (effectively); its deflection = 1.287 inches
Section 3 = 55.75 inches long (effectively); its deflection = 1.382 inches
Section 4 = 55.75 inches long (effectively); its deflection = 1.493 inches
Section 5 = 55.75 inches long (effectively); its deflection = 1.622 inches
Section 6 = 55.75 inches long (effectively); its deflection = 1.777 inches
Section 7 = 52.375 inches long (effectively); its deflection = 1.733 inches
Tension at the bottom of the bag (just prior to cleaning) = 79.1 pounds.
```

```
   Bag           Bag         Operating       Ambient        Dia. of        Tension
 Length,      Diameter,    Temperature,   Temperature,     Ring wire,    Prior to RA,
 inches        inches       Degrees F      Degrees F        inches         pounds
  396.0        11.50          300             80             .1875          95.7

  Weight       Initial     Forward Gas     Total Ash     Reverse Air       Tension
 of cloth,     Tension,     Pressure,       Weight,       Pressure,     Start of RA,
oz./sq.yd.     pounds        in.w.c.        pounds         in.w.c.         pounds
   14           60.0          4.00           61.2           .50            141.5
Section 1 = 54.375 inches long (effectively); its deflection = 1.147 inches
Section 2 = 55.75 inches long (effectively); its deflection = 1.301 inches
Section 3 = 55.75 inches long (effectively); its deflection = 1.415 inches
Section 4 = 55.75 inches long (effectively); its deflection = 1.552 inches
Section 5 = 55.75 inches long (effectively); its deflection = 1.717 inches
Section 6 = 55.75 inches long (effectively); its deflection = 1.922 inches
Section 7 = 52.375 inches long (effectively); its deflection = 1.926 inches
Tension at the bottom of the bag (just prior to cleaning) = 69.1 pounds.
```

REFERENCES

1. Jensen, R.M., "Potential Improvements in Baghouse Design," Proceedings of the Fifth International Fabric Alternatives Forum, Scottsdale, Arizona, January 15-16, 1981.

2. Gaylord and Gaylord, "Structural Engineering Handbook", McGraw-Hill Book Co., New York, 1979.

3. Personal telephone call to Steve McCluskey of Burlington Mills, 3-16-81.

APPENDIX I - TEST RESULTS

```
This is data for Run  5  of the bag deflection testing.
The Bag Type is #  2
The bag is 366.4 in. long, 11.38 in. in diameter and weighs 252 oz.
The initial bag tension was  51 pounds.
The bag tension at the start of R.A. cleaning was 215 pounds.
The R.A. pressure was  .5 inches w.g.
The support spring constant was 90 pounds/inch.
The ash weight was 65.40 pounds.
The bag length prior to R.A. application was 31.4479 feet.
The bag length after R.A. application was 31.3646 feet.

The bag section dimensions are as follows:
                 Measured
Ring 1       1.50 in. long,         Effective(arc)     Effective(straight)
Section 1   56.13 in. long,          1.50 in. long.
Ring 2       2.00 in. long,         57.00 in. long,       56.99 in. long.
Section 2   54.50 in. long,           .25 in. long.
Ring 3       2.00 in. long,         56.25 in. long,       56.24 in. long.
Section 3   51.75 in. long,           .25 in. long.
Ring 4       2.00 in. long,         53.50 in. long,       53.49 in. long.
Section 4   49.75 in. long,           .25 in. long.
Ring 5       2.00 in. long,         51.50 in. long,       51.49 in. long.
Section 5   48.00 in. long,           .25 in. long.
Ring 6       2.00 in. long,         49.75 in. long,       49.74 in. long.
Section 6   45.75 in. long,           .25 in. long.
Ring 7       2.00 in. long,         47.50 in. long,       47.49 in. long.
Section 7   43.50 in. long,           .25 in. long.
Ring 8       3.50 in. long,         44.38 in. long,       44.36 in. long.
                                     3.50 in. long.

Bag deflections are as follows:
Section     Dia. at deflection
Section 1;     6.625 in.         Catenary deflection    Equalizing deflection
Section 2;     6.438 in.             2.375 in.               1.783 in.
Section 3;     6.540 in.             2.469 in.               1.846 in.
Section 4;     6.688 in.             2.418 in.               1.811 in.
Section 5;     6.188 in.             2.344 in.               1.761 in.
Section 6;     5.875 in.             2.594 in.               1.929 in.
Section 7;     5.438 in.             2.750 in.               2.031 in.
                                     2.969 in.               2.169 in.
```

APPENDIX I - TEST RESULTS (CONT.)

```
This is data for Run  6  of the bag deflection testing.
The Bag Type is #  2
The bag is 366.4 in. long, 11.38 in. in diameter and weighs 252 oz.
The initial bag tension was  51 pounds.
The bag tension at the start of R.A. cleaning was 261 pounds.
The R.A. pressure was 1.0 inches w.g.
The support spring constant was 90 pounds/inch.
The ash weight was 65.25 pounds.
The bag length prior to R.A. application was 31.4583 feet.
The bag length after R.A. application was 31.3229 feet.

The bag section dimensions are as follows:
                Measured           Effective(arc)      Effective(straight)
Ring 1       1.50 in. long,         1.50 in. long.
Section 1   56.13 in. long,        57.00 in. long,        56.98 in. long.
Ring 2       2.00 in. long,          .25 in. long.
Section 2   54.50 in. long,        56.25 in. long,        56.23 in. long.
Ring 3       2.00 in. long,          .25 in. long.
Section 3   51.75 in. long,        53.50 in. long,        53.48 in. long.
Ring 4       2.00 in. long,          .25 in. long.
Section 4   49.75 in. long,        51.50 in. long,        51.48 in. long.
Ring 5       2.00 in. long,          .25 in. long.
Section 5   48.00 in. long,        49.75 in. long,        49.73 in. long.
Ring 6       2.00 in. long,          .25 in. long.
Section 6   45.75 in. long,        47.50 in. long,        47.48 in. long.
Ring 7       2.00 in. long,          .25 in. long.
Section 7   43.50 in. long,        44.38 in. long,        44.36 in. long.
Ring 8       3.50 in. long,         3.50 in. long.

Bag deflections are as follows:
Section      Dia. at deflection     Catenary deflection     Equalizing deflection
Section 1;       5.250 in.             3.063 in.                2.226 in.
Section 2;       5.438 in.             2.969 in.                2.169 in.
Section 3;       5.604 in.             2.886 in.                2.117 in.
Section 4;       5.688 in.             2.844 in.                2.090 in.
Section 5;       5.313 in.             3.031 in.                2.207 in.
Section 6;       5.063 in.             3.156 in.                2.282 in.
Section 7;       5.125 in.             3.125 in.                2.264 in.
```

Reproduced from
best available copy.

APPENDIX I - TEST RESULTS (CONT.)

```
This is data for Run  7  of the bag deflection testing.
The Bag Type is #  2
The bag is 366.4 in. long, 11.38 in. in diameter and weighs 252 oz.
The initial bag tension was  85 pounds.
The bag tension at the start of R.A. cleaning was 203 pounds.
The R.A. pressure was  .5 inches w.g.
The support spring constant was 90 pounds/inch.
The ash weight was 65.25 pounds.
The bag length prior to R.A. application was 31.4583 feet.
The bag length after R.A. application was 31.4323 feet.

The bag section dimensions are as follows:
                 Measured              Effective(arc)      Effective(straight)
Ring 1       1.50 in. long,             1.50 in. long.
Section 1   56.13 in. long,            57.00 in. long,         57.00 in. long.
Ring 2       2.00 in. long,              .25 in. long.
Section 2   54.50 in. long,            56.25 in. long,         56.25 in. long.
Ring 3       2.00 in. long,              .25 in. long.
Section 3   51.75 in. long,            53.50 in. long,         53.50 in. long.
Ring 4       2.00 in. long,              .25 in. long.
Section 4   49.75 in. long,            51.50 in. long,         51.50 in. long.
Ring 5       2.00 in. long,              .25 in. long.
Section 5   48.00 in. long,            49.75 in. long,         49.75 in. long.
Ring 6       2.00 in. long,              .25 in. long.
Section 6   45.75 in. long,            47.50 in. long,         47.50 in. long.
Ring 7       2.00 in. long,              .25 in. long.
Section 7   43.50 in. long,            44.38 in. long,         44.37 in. long.
Ring 8       3.50 in. long,             3.50 in. long.

Bag deflections are as follows:
Section      Dia. at deflection        Catenary deflection     Equalizing deflection
Section 1;        6.938 in.                 2.219 in.                 1.676 in.
Section 2;        7.438 in.                 1.969 in.                 1.500 in.
Section 3;        7.646 in.                 1.865 in.                 1.426 in.
Section 4;        7.436 in.                 1.970 in.                 1.501 in.
Section 5;        7.244 in.                 2.066 in.                 1.569 in.
Section 6;        7.063 in.                 2.156 in.                 1.632 in.
Section 7;        6.813 in.                 2.281 in.                 1.719 in.
```

APPENDIX I - TEST RESULTS (CONT.)

```
This is data for Run  8  of the bag deflection testing.
The Bag Type is #  2
The bag is 366.4 in. long, 11.38 in. in diameter and weighs 252 oz.
The initial bag tension was  72 pounds.
The bag tension at the start of R.A. cleaning was 211 pounds.
The R.A. pressure was  .9 inches w.g.
The support spring constant was 90 pounds/inch.
The ash weight was 65.25 pounds.
The bag length prior to R.A. application was 31.4792 feet.
The bag length after R.A. application was 31.4063 feet.

The bag section dimensions are as follows:
                Measured           Effective(arc)     Effective(straight)
Ring 1       1.50 in. long,         1.50 in. long.
Section 1   56.13 in. long,        57.00 in. long,        56.99 in. long.
Ring 2       2.00 in. long,          .25 in. long.
Section 2   54.50 in. long,        56.25 in. long,        56.24 in. long.
Ring 3       2.00 in. long,          .25 in. long.
Section 3   51.75 in. long,        53.50 in. long,        53.49 in. long.
Ring 4       2.00 in. long,          .25 in. long.
Section 4   49.75 in. long,        51.50 in. long,        51.49 in. long.
Ring 5       2.00 in. long,          .25 in. long.
Section 5   48.00 in. long,        49.75 in. long,        49.74 in. long.
Ring 6       2.00 in. long,          .25 in. long.
Section 6   45.75 in. long,        47.50 in. long,        47.49 in. long.
Ring 7       2.00 in. long,          .25 in. long.
Section 7   43.50 in. long,        44.38 in. long,        44.36 in. long.
Ring 8       3.50 in. long,         3.50 in. long.

Bag deflections are as follows:
Section      Dia. at deflection     Catenary deflection     Equalizing deflection
Section 1;       6.250 in.               2.563 in.               1.908 in.
Section 2;       6.500 in.               2.438 in.               1.825 in.
Section 3;       6.646 in.               2.365 in.               1.776 in.
Section 4;       6.667 in.               2.354 in.               1.768 in.
Section 5;       6.330 in.               2.523 in.               1.882 in.
Section 6;       6.438 in.               2.469 in.               1.846 in.
Section 7;       6.229 in.               2.573 in.               1.915 in.
```

Reproduced from
best available copy.

APPENDIX I - TEST RESULTS (CONT.)

This is data for Run 9 of the bag deflection testing.
The Bag Type is # 3
The bag is 366.4 in. long, 11.25 in. in diameter and weighs 256 oz.
The initial bag tension was 63 pounds.
The bag tension at the start of R.A. cleaning was 229 pounds.
The R.A. pressure was 1.0 inches w.g.
The support spring constant was 90 pounds/inch.
The ash weight was 65.25 pounds.
The bag length prior to R.A. application was 31.3646 feet.
The bag length after R.A. application was 31.2813 feet.

The bag section dimensions are as follows:

	Measured	Effective(arc)	Effective(straight)
Ring 1	1.50 in. long,	1.50 in. long.	
Section 1	54.25 in. long,	55.13 in. long,	55.11 in. long.
Ring 2	2.00 in. long,	.25 in. long.	
Section 2	51.50 in. long,	53.25 in. long,	53.24 in. long.
Ring 3	2.00 in. long,	.25 in. long.	
Section 3	50.00 in. long,	51.75 in. long,	51.74 in. long.
Ring 4	2.00 in. long,	.25 in. long.	
Section 4	50.00 in. long,	51.75 in. long,	51.74 in. long.
Ring 5	2.00 in. long,	.25 in. long.	
Section 5	49.00 in. long,	50.75 in. long,	50.74 in. long.
Ring 6	2.00 in. long,	.25 in. long.	
Section 6	47.63 in. long,	49.38 in. long,	49.36 in. long.
Ring 7	2.00 in. long,	.25 in. long.	
Section 7	47.00 in. long,	47.88 in. long,	47.86 in. long.
Ring 8	3.50 in. long,	3.50 in. long.	

Bag deflections are as follows:

Section	Dia. at deflection	Catenary deflection	Equalizing deflection
Section 1;	6.250 in.	2.500 in.	1.865 in.
Section 2;	6.021 in.	2.615 in.	1.940 in.
Section 3;	5.962 in.	2.644 in.	1.959 in.
Section 4;	6.313 in.	2.469 in.	1.844 in.
Section 5;	5.896 in.	2.677 in.	1.981 in.
Section 6;	5.771 in.	2.740 in.	2.021 in.
Section 7;	4.808 in.	3.221 in.	2.316 in.

APPENDIX I - TEST RESULTS (CONT.)

```
This is data for Run  10  of the bag deflection testing.
The Bag Type is #  3
The bag is 366.4 in. long, 11.25 in. in diameter and weighs 256 oz.
The initial bag tension was  95 pounds.
The bag tension at the start of R.A. cleaning was 241 pounds.
The R.A. pressure was 1.0 inches w.g.
The support spring constant was 90 pounds/inch.
The ash weight was 65.25 pounds.
The bag length prior to R.A. application was 31.3854 feet.
The bag length after R.A. application was 31.3438 feet.

The bag section dimensions are as follows:
                 Measured           Effective(arc)      Effective(straight)
Ring 1       1.50 in. long,         1.50 in. long.
Section 1  54.25 in. long,         55.13 in. long,        55.12 in. long.
Ring 2       2.00 in. long,          .25 in. long.
Section 2  51.50 in. long,         53.25 in. long,        53.24 in. long.
Ring 3       2.00 in. long,          .25 in. long.
Section 3  50.00 in. long,         51.75 in. long,        51.74 in. long.
Ring 4       2.00 in. long,          .25 in. long.
Section 4  50.00 in. long,         51.75 in. long,        51.74 in. long.
Ring 5       2.00 in. long,          .25 in. long.
Section 5  49.00 in. long,         50.75 in. long,        50.74 in. long.
Ring 6       2.00 in. long,          .25 in. long.
Section 6  47.63 in. long,         49.38 in. long,        49.37 in. long.
Ring 7       2.00 in. long,          .25 in. long.
Section 7  47.00 in. long,         47.88 in. long,        47.87 in. long.
Ring 8       3.50 in. long,         3.50 in. long.

Bag deflections are as follows:
Section      Dia. at deflection     Catenary deflection     Equalizing deflection
Section 1;      6.750 in.                2.250 in.                1.696 in.
Section 2;      6.417 in.                2.417 in.                1.809 in.
Section 3;      6.475 in.                2.388 in.                1.789 in.
Section 4;      6.708 in.                2.271 in.                1.710 in.
Section 5;      6.313 in.                2.469 in.                1.844 in.
Section 6;      6.359 in.                2.446 in.                1.828 in.
Section 7;      5.641 in.                2.805 in.                2.062 in.
```

Reproduced from
best available copy.

APPENDIX II - COMPUTER PROGRAM "DEFLEC"

```
10 REM This is program DEFLEC developed by J. Musgrove of Bechtel Power Corporation, Houston, TX
20 REM This program was developed as part of 'Optimizing the Location of Anti-Collapse Rings
30 REM in Fabric Filter Bags,' Paper 89, presented to The Fourth Symposium on the
40 REM Transfer and Utilization of Particulate Control Technology
50 REM Houston, Texas, October 11-15, 1982
60 REM This program listing is current as of November 2, 1982
70 PRINTER IS 701,140
80 OPTION BASE 1
90 DIM L(9),F(9),F1(9),F2(9),D(9),L1(9),D1(9),F9(9),P9(9),T(9),T1(1)
100 MAT L=ZER@ MAT F=ZER@ MAT F1=ZER@ MAT F2=ZER
110 MAT D=ZER@ MAT L1=ZER@ MAT D1=ZER@ MAT F9=ZER
120 MAT T=ZER@ MAT T1=ZER@ MAT P9=ZER
130 PRINT "This is program DEFLEC to determine the filter bag"
140 PRINT "deflection in each section during reverse air cleaning"
150 PRINT
160 CLEAR
170 DISP "What is the bag diameter, inches"
180 INPUT D9
190 R9=D9/2
200 DISP "What is the total bag length, inches?"
210 INPUT L9
220 DISP "How many anti-collapse rings are in the bag?"
230 INPUT I2
240 PRINT "Number of rings = ";I2
250 L8=L9-6-.25*I2
260 K=I2+1
270 REDIM L(K),F(K),F1(K),F2(K),D(K),L1(K),D1(K),F9(K),P9(K),T(K)
280 DISP USING 290 ; K
290 IMAGE "Input all ",2D," individual section lengths (excluding ring cover dimensions)"
300 DISP "top to bottom.  Be sure to separate data by commas (i.e. 56,52,55,60)"
310 MAT INPUT L
320 L(1)=L(1)+.875
330 L(K)=L(K)+.875
340 FOR Z=2 TO I2
350 L(Z)=L(Z)+1.75
360 NEXT Z
```

APPENDIX II - COMPUTER PROGRAM "DEFLEC" (CONT.)

```
370 PRINT @ PRINT
380 DISP "What is the bag support spring constant, lb/in?"
390 INPUT K9
400 DISP "What is the operating temp., F?"
410 INPUT T8
420 DISP "What is the ambient temp., F, during initial bag tensioning?"
430 INPUT T6
440 T7=T8-T6
450 DISP "What is the weight of the bag material, oz./sq.yd.?"
460 INPUT C
470 DISP "What is the number of fill yarns per inch of fabric (44 is typical)?"
480 INPUT C1
490 C2=C1*D9*PI
500 C3=1/C1
510 DISP "What is the diameter of the ring wire, inches?"
520 INPUT R
530 DISP "What is the reverse air pressure, in. H2O?"
540 INPUT A
550 T4=T7*(L9+16)*K9*.0000038
560 T5=A*.5781*PI*R9^2/16
570 CLEAR
580 DISP @ DISP @ DISP @ DISP @ DISP
590 DISP "DO NOT DISTURB!!!"
600 DISP "PROGRAM IN PROGRESS"
610 FOR I1=1 TO 3
620 FOR I3=1 TO 6
630 A2=4
640 T2=A2*.5781*PI*R9^2/16
650 P=A*.5781*C3
660 T8(1)=0
670 FOR I=1 TO K
680 Y6=.005*EXP((I-1)*.844)
690 Y7=Y6+.5673
700 Y8=Y7/100
710 Y9=1-Y8
720 L2(I)=Y9*L(I)
```

APPENDIX II - COMPUTER PROGRAM "DEFLEC" (CONT.)

```
730 D9(I)=SQR(.375*L2(I)*(L(I)-L2(I)))
740 A9=ATN(4*D9(I)/L2(I))
750 F9(I)=.07833+.00607*I
760 T(I)=F9(I)*L(I)*P/(2*SIN(A9))
770 T8(1)=T8(1)+T(I)
780 NEXT I
790 T=60*(I1+3)/4
800 A1=80
810 T1=.015625*I3
820 W2=A1*T1*C3*16/1728
830 W5=R^2*PI^2*.284*16*12/(4*C2)
840 W1=C/(9*C1*144)
850 W4=8*W1
860 W3=W4+W5
870 W6=T1*PI*D9*(L9-6)*A1/1728
880 T3=T+T4+T2
890 T8(1)=T8(1)*C2/16
900 T9=T+T4-T5+T8(1)
910 PRINT "   Bag             Bag          Operating        Ambient          Dia. of        Tension"
920 PRINT " Length,        Diameter,     Temperature,     Temperature,      Ring wire,    Prior to RA,"
930 PRINT " inches           inches        Degrees F        Degrees F         inches         pounds"
940 PRINT USING 950 ; L9,D9,T8,T6,R,T3
950 IMAGE 2X,3D.D,8X,DD.DD,10X,3D,12X,3D,10X,D.4D,9X,3D.D
960 PRINT @ PRINT @ PRINT
970 PRINT "  Weight        Initial      Forward Gas      Total Ash       Reverse Air      Tension"
980 PRINT " of cloth,      Tension,      Pressure,        Weight,         Pressure,     Start of RA,"
990 PRINT "oz./sq.yd.       pounds        in.w.c.         pounds           in.w.c.         pounds"
1000 PRINT USING 1010 ; C,T,A2,W6,A,T9
1010 IMAGE 4X,2D,9X,3D.D,8X,2D.2D,10X,3D.D,11X,D.2D,10X,3D.D
1020 GOSUB 1220
1030 PRINT USING "K" ; CHR$(27);"&17V"
1040 NEXT I3
1050 PRINT USING "K" ; CHR$(11)
1060 NEXT I1
1070 PRINT USING "K" ; CHR$(11)
1080 CLEAR
```

Reproduced from
best available copy.

APPENDIX II - COMPUTER PROGRAM "DEFLEC" (CONT.)

```
1090 DISP "    J   000   BBBB"
1100 DISP "    J  O   O  B   B"
1110 DISP "    J  O   O  BBBB"
1120 DISP " J   J  O   O  B   B"
1130 DISP "  JJJ    000   BBBB"
1140 DISP ""
1150 DISP ""
1160 DISP " EEEEE  N   N  DDDD"
1170 DISP " E      NN  N  D   D"
1180 DISP " EEE    N N N  D   D"
1190 DISP " E      N  NN  D   D"
1200 DISP " EEEEE  N   N  DDDD"
1210 END
1220 PRINT
1230 FOR I=1 TO K
1240 P9=P*.673
1250 F2(I)=P9*L(I)/2
1260 ON I GOTO 1270,1280,1290,1300,1310,1320,1330
1270 K1=0 @ GOTO 1340
1280 K1=L(1) @ GOTO 1340
1290 K1=L(1)+L(2) @ GOTO 1340
1300 K1=L(1)+L(2)+L(3) @ GOTO 1340
1310 K1=L(1)+L(2)+L(3)+L(4) @ GOTO 1340
1320 K1=L(1)+L(2)+L(3)+L(4)+L(5) @ GOTO 1340
1330 K1=L(1)+L(2)+L(3)+L(4)+L(5)+L(6) @ GOTO 1340
1340 F1(I)=T9*(16/C2)-K1*(W1+W2)-W3*(I-1)
1350 F1=T9*(16/C2)-L8*(W1+W2)-W3*(I-1)
1360 F(I)=SQR(F1(I)^2+F2(I)^2)
1370 F=SQR(F1^2+F2(I)^2)*(C2/16)
1380 IF F1<0 THEN F=-F
1390 D(I)=P9*L(I)^2/(4*SQR((2*F(I))^2-(P9*L(I))^2))
1400 NEXT I
1410 MAT L1=ZER
1420 MAT D1=ZER
1430 FOR J=1 TO K
1440 L1(J)=INT(1000*L(J))/1000
```

APPENDIX II - COMPUTER PROGRAM "DEFLEC" (CONT.)

```
1450 D1(J)=INT(1000*D(J))/1000
1460 PRINT "Section";J;"=";L1(J);"inches long (effectively); its deflection =";D1(J);"inches"
1470 IF D1(J)>R9 THEN GOTO 1480 ELSE 1490
1480 PRINT "                This section is pancaking!!"
1490 NEXT J
1500 PRINT USING 1510 ; F
1510 IMAGE "Tension at the bottom of the bag (just prior to cleaning) =",3D.D," pounds."
1520 IF F<0 THEN GOTO 1530 ELSE 1540
1530 PRINT "BAG IS BLOWING INTO THIMBLE DUE TO EXCESSIVE ASH OR INSUFFICIENT TENSION!!"
1540 RETURN
```

APPENDIX III - COMPUTER PROGRAM "RINGOP"

```
10 REM This is program RINGOP developed by J. Musgrove of Bechtel Power Corporation, Houston, TX
20 REM This program was developed as part of 'Optimizing the Location of Anti-Collapse Rings
30 REM in Fabric Filter Bags,' Paper 89, presented to The Fourth Symposium on the
40 REM Transfer and Utilization of Particulate Control Technology
50 REM Houston, Texas, October 11-15, 1982
60 REM This program listing is current as of November 2,1982
70 REM "This program RINGOP determines the optimum location of anti-collapse rings"
80 REM "in filter bags to assure equal deflection in each section during reverse air cleaning"
90 PRINTER IS 701,140
100 OPTION BASE 1
110 DIM L(9),F(9),F1(9),F2(9),D(9),P(9),F9(9),T(9),T8(1),L2(9)
120 PRINT "This is program RINGOP to determine the optimum location of anti-collapse rings"
130 PRINT "in filter bags to assure equal deflection in each section during reverse air cleaning"
140 MAT L=ZER@ MAT F=ZER@ MAT F1=ZER@ MAT F2=ZER
150 MAT D=ZER@ MAT P=ZER@ MAT F9=ZER
160 MAT T=ZER@ MAT L2=ZER@ MAT T8=ZER
170 CLEAR
180 DISP "What is today's date? mm/dd/yyyy"
190 INPUT A$
200 PRINT A$
210 PRINT @ PRINT
220 CLEAR
230 DISP "What is the bag diameter, inches"
240 INPUT D9
250 R9=D9/2
260 DISP "What is the total bag length,   inches?"
270 INPUT L9
280 DISP "What is the bag support spring  constant, lb/in?"
290 INPUT K9
300 DISP "What is the operating temp., F?"
310 INPUT T8
320 DISP "What is the ambient temp., F,   during initial bag tensioning?"
330 INPUT T6
340 T7=T8-T6
350 DISP "What is the weight of the bag   material, oz./sq.yd.?"
360 INPUT C
```

APPENDIX III - COMPUTER PROGRAM "RINGOP" (CONT.)

```
370 DISP "What is the number of fill yarns per inch of fabric (44 is typical)?"
380 INPUT C1
390 C2=C1*D9*PI
400 C3=1/C1
410 DISP "What is the diameter of the ring wire, in.?"
420 INPUT R
430 DISP "What is the reverse air          pressure, in. H2O?"
440 INPUT A
450 P=A*.5781*C3
460 T4=T7*(L9+16)*K9*.0000038
470 T5=A*.5781*PI*R9^2/16
480 CLEAR
490 DISP @ DISP @ DISP @ DISP @ DISP
500 DISP "DO NOT DISTURB!!!"
510 DISP "PROGRAM IN PROGRESS"
520 FOR I1=1 TO 3
530 FOR I3=1 TO 6
540 A2=4
550 T2=A2*.5781*PI*R9^2/16
560 T=60*(I1+3)/4
570 A1=80
580 T1=.015625*I3
590 W2=A1*T1*C3*16/1728
600 W5=R^2*PI^2*.284*16*12/(4*C2)
610 W1=C/(9*C1*144)
620 W4=8*W1
630 W3=W4+W5
640 W6=T1*PI*D9*(L9-6)*A1/1728
650 T3=T+T4+T2
660 PRINT "   Bag           Bag         Operating       Ambient        Dia. of        Tension"
670 PRINT " Length,      Diameter,    Temperature,    Temperature,     Ring wire,     Prior to RA,"
680 PRINT " inches         inches      Degrees F       Degrees F        inches          pounds"
690 PRINT USING 700 ; L9,D9,T8,T6,R,T3
700 IMAGE 2X,3D.D,8X,DD.DD,10X,3D,12X,3D,10X,D.4D,10X,3D.D
710 PRINT @ PRINT @ PRINT
720 FOR I2=1 TO 6
```

APPENDIX III - COMPUTER PROGRAM "RINGOP" (CONT.)

```
730 L8=L9-6-.25*I2
740 T8(1)=0
750 K=I2+1
760 REDIM L(K),F(K),F1(K),F2(K),D(K),P(K),F9(K),T(K),L2(K)
770 FOR J=1 TO K
780 L(J)=L8/K
790 NEXT J
800 FOR Z1=1 TO K
810 Y6=.005*EXP((Z1-1)*.844)
820 Y7=Y6+.5673
830 Y8=Y7/100
840 Y9=1-Y8
850 L2(Z1)=Y9*L(Z1)
860 D9(Z1)=SQR(.375*L2(Z1)*(L(Z1)-L2(Z1)))
870 A9=ATN(4*D9(Z1)/L2(Z1))
880 F9(Z1)=.07833+.00607*Z1
890 T(Z1)=F9(Z1)*L(Z1)*P/(2*SIN(A9))
900 T8(1)=T8(1)+T(Z1)
910 NEXT Z1
920 T8(1)=T8(1)*C2/16
930 T9=T+T4-T5+T8(1)
940 GOSUB 1160
950 NEXT I2
960 PRINT USING "K" ; CHR$(11)
970 NEXT I3
980 PRINT USING "K" ; CHR$(11)
990 NEXT I1
1000 PRINT USING "K" ; CHR$(11)
1010 PRINT A$
1020 CLEAR
1030 DISP "     J   OOO   BBBB"
1040 DISP "     J  O   O  B   B"
1050 DISP "     J  O   O  BBBB"
1060 DISP " J   J  O   O  B   B"
1070 DISP "  JJJ    OOO   BBBB"
1080 DISP ""
```

APPENDIX III - COMPUTER PROGRAM "RINGOP" (CONT.)

```
1090 DISP ""
1100 DISP " EEEEE  N   N  DDDD"
1110 DISP " E      NN  N  D   D"
1120 DISP " EEE    N N N  D   D"
1130 DISP " E      N  NN  D   D"
1140 DISP " EEEEE  N   N  DDDD"
1150 END
1160 PRINT @ PRINT
1170 PRINT "  Weight       Initial     Forward Gas    Total Ash     Reverse Air     Tension"
1180 PRINT " of cloth,     Tension,     Pressure,      Weight,       Pressure,    Start of RA,"
1190 PRINT "oz./sq.yd.     pounds       in.w.c.        pounds        in.w.c.        pounds"
1200 PRINT USING 1220 ; C,T,A2,W6,A,T9
1210 PRINT
1220 IMAGE 4X,2D,9X,3D.D,8X,2D.2D,10X,3D.D,11X,D.2D,11X,3D.D
1230 J9=0
1240 PRINT "Number of Rings = ";I2
1250 FOR I=1 TO K
1260 P9=P*.673
1270 F2(I)=P9*L(I)/2
1280 ON I GOTO 1290,1300,1310,1320,1330,1340,1350
1290 K1=0 @ GOTO 1360
1300 K1=L(1) @ GOTO 1360
1310 K1=L(1)+L(2) @ GOTO 1360
1320 K1=L(1)+L(2)+L(3) @ GOTO 1360
1330 K1=L(1)+L(2)+L(3)+L(4) @ GOTO 1360
1340 K1=L(1)+L(2)+L(3)+L(4)+L(5) @ GOTO 1360
1350 K1=L(1)+L(2)+L(3)+L(4)+L(5)+L(6)
1360 F1(I)=T9*(16/C2)-K1*(W1+W2)-W3*(I-1)
1370 F1=T9*(16/C2)-L8*(W1+W2)-W3*(I-1)
1380 F(I)=SQR(F1(I)^2+F2(I)^2)
1390 F=SQR(F1^2+F2(I)^2)*(C2/16)
1400 IF F1<0 THEN F=-F
1410 F1=F1*C2/16
1420 D(I)=P9*L(I)^2/(4*SQR(ABS((2*F(I))^2-(P9*L(I))^2)))
1430 IF D(I)>D9/3 THEN GOTO 1650
1440 NEXT I
```

APPENDIX III - COMPUTER PROGRAM "RINGOP" (CONT.)

```
1450 X1=AMAX(D) @ X2=AMAXROW
1460 Y1=AMIN(D) @ Y2=AMINROW
1470 Z=X1-Y1
1480 IF Z<.1 THEN 1540
1490 L(X2)=L(X2)-.125 @ L(Y2)=L(Y2)+.125
1500 J9=J9+1
1510 IF J9>200 THEN 1530
1520 GOTO 1250
1530 PRINT "Iterative limit reached at 200"
1540 FOR J=1 TO K
1550 L(J)=INT(1000*L(J))/1000
1560 D(J)=INT(1000*D(J))/1000
1570 PRINT "Section";J;"=";L(J);"inches long (effectively); its deflection =";D(J);"inches"
1580 NEXT J
1590 PRINT USING 1600 ; F1
1600 IMAGE "Tension at the bottom of the bag (at the start of cleaning) = ",3D.D," pounds."
1610 IF F1<0 THEN GOTO 1620 ELSE 1630
1620 PRINT "BAG IS BLOWING INTO THE THIMBLE DUE TO EXCESSIVE ASH OR INSUFFICIENT TENSION!!"
1630 GOSUB 1670
1640 RETURN
1650 PRINT "Deflection greater than 1/3 diameter; further analysis terminated."
1660 RETURN
1670 L(1)=L(1)-.875
1680 L(K)=L(K)-.875
1690 FOR Z2=2 TO I2
1700 L(Z2)=L(Z2)-1.75
1710 NEXT Z2
1720 PRINT
1730 PRINT "Measured (fabricated) section lengths are as follows (assuming 2 inch ring covers)"
1740 FOR Z2=1 TO K
1750 PRINT "Section";Z2;"=";L(Z2);"inches long"
1760 NEXT Z2
1770 RETURN
```

PULSE JET ON-LINE CLEANING FILTER FOR FLY ASH

by: Wayne G. Wellan
Carter-Day Company
Minneapolis, Minnesota 55432

ABSTRACT

This paper describes the development and performance of on-line cleaning by pulse jet filters with needled felt. This pulse jet filter design is in operation on various types of coal-fired boilers. Considerable research and testing was involved in finding a fiber that would endure continuous pulsing, high temperatures, and a sulfur environment. Additional research was required to develop the proper filter media in the areas of needling and scrim design. Also, analysis of various types of fly ash was conducted to determine particle size and shape, and what effect it has on the performance of the filter.

INTRODUCTION

Eight years ago it was decided by our management that Carter-Day should develop a filter for the flue gas filtration market, specifically industrial and utility coal-fired boilers. The market trends at that time showed a tremendous growth due to the oil embargos and increase in prices of oil and gas. Also, other people in the baghouse manufacturing industry had tested a reverse air fiberglass baghouse with success.

Our first test site was a power plant at Granite Falls, Minnesota operated by Northern States Power. This power plant generated 50 megawatts of electricity from a pulverized coal-fired boiler. They burned a blend of western and Kentucky coal. This plant is a peaking station. They operate 8 to 16 hours per day. Therefore, they pass through the acid dew point on start-up and shut-down, which is a severe test for the fiber. We installed two slip-stream filters. One was a 24RJ96 filter, the other was a high velocity filter. The volume on the RJ filter was 2,500 cfm and the volume for the high velocity filter was 3,000 cfm. These units were put on stream in February, 1974.

Some of the first fibers we evaluated were Nomex, Polyimide, Kynol, Draylon T, Orlon, CS treated Nomex, acrylics, woven fiberglass, which all failed. We also tried teflon felt. This withstood the high temperature gas and sulfur conditions, but had very poor collection efficiency due to the on-line cleaning. Extensive testing was conducted on stainless steel fibers in an air laid web and also in a sintered construction, and none of these were successful. We also evaluated a woven fiberglass bag in the RJ filter which was in the round bag configuration. This did withstand the operation for a few months, but the bags eventually failed. Tests were also conducted on the high velocity filter using teflon in a felt and pile construction. None of these were successful.

We then installed a 48RF96 filter and a standard Pulse Jet filter, 14PJ96, at the Dairyland Co-op Power Generating Station at Alma, Wisconsin. This is an 80 megawatt power generating system that has a pulverized coal-fired boiler which burned high sulfur eastern coal, low sulfur western coal, and petroleum coke. This plant is a base loaded utility station which operates 24 hours a day. The RF filter was designed to handle 3,500 cfm and the volume for the Pulse Jet is 600 cfm. The slip-stream filters are designed to operate around the clock. We have our own ash conveying system which is tied into their system. These filters are operated unattended, other than having the filter pressure drop, air flow and cleaning pressure recorded and mailed to us once a week. Both of these systems are designed for on-line cleaning. We did not have a backup filter for off-line cleaning. Our design and premise of this whole program is with on-line cleaning. So, the bags are pulsed while the flue gas is entering the filter. We again tried some of the same felt we had at Granite Falls which failed in the same manner. We also evaluated other medias such as Kermel, carbon, graphite, ceramics, and Hyglass, which all failed. We have evaluated a newer Hyglass with a 3/4 inch mesh round cage design, and failed after 9 months of operation.

During this testing interval we came upon our new fiber called Ryton and we installed 3 bags in our Pulse Jet unit and proceeded to life test the bags. After 9 months we found that there was no deterioration or failures.

We acquired additional fiber to completely fit out the Pulse Jet filter and the RF filter at Alma. These bags were evaluated initially for collection efficiency and also for bag life. The collection efficiency was not satisfactory on the first set of bags and were replaced with a heavier weight Ryton in order to meet the new proposed EPA code, 0.03 to 0.05 lbs per million BTU. We also changed the bag frame by adding additional vertical and hoop wires to reduce the flexing of the media, which would cause the media to fail. We tested the new media and our collection efficiency did improve. Our results were .018 pounds per million BTU.

We continued testing the bags to determine bag life, and after 2 years without any bag failures, we proceeded to work with our fiber supplier to get a commitment to supply us with fiber for future jobs.

When we first contacted Phillips they were in the development stages of their fiber grade Ryton resin; therefore, they were not ready to release their fiber for commercial use. Carter-Day got involved and developed a method to spin the Ryton resin into fiber for the baghouse systems that are currently in operation.

You probably have seen Ryton advertised in various magazines. There are 2 different types of Ryton resin. One is their molding grade resin which is solely used for injection molding, and the other is fiber grade resin. The molded grade resin cannot be spun into fiber. It is a highly cross-linked resin which makes the fiber brittle.

FIBER TESTING

During the course of this program we developed a laboratory accelerated acid and temperature test to evaluate fibers for the flue gas environment. The fibers are wicked in an acid solution of 75% H_2SO_4 at 350°F for 3 hours. Then tensile tests are conducted on individual fibers and are compared to fibers before the acid treatment.

This test procedure has worked out quite well to screen out new fibers, and also serves as a quality control check on production lots of Ryton fiber. If the Ryton fibers are not processed properly they will deteriorate in a flue gas environment in a very short time.

Another procedure we use to evaluate fibers is our laboratory microscope with a special lens. This enables us to see any deterioration caused by acid attack and also shows us high stress concentration in the fiber caused by over crimping the fiber during the fiber spinning process.

In addition to the lab tests, bags are removed from the slipstream filters, and from various installations in the field. Physical tests are conducted on these bags such as tensile, tear, and mullen burst. See Figure 1. From this data we can project the bag life in various flue gas conditions. Also, all new production lots of Daytex felt are checked for physical strength, and one or two bags from each production lot is placed in our slip-stream filter.

NEEDLING AND SCRIM TECHNOLOGY

During the test program on our slip-stream filters, we were able to evaluate the long term effect on the filter bags. After 2 1/2 years in a flue gas environment, we have seen evidence of delamination of the fiber from the scrim which is related to how well the felt is needled. So, our next step was to evaluate the needling technology and develop ways to improve the process. After a long series of tests we were able to come up with an optimum procedure that doubled the tensile and mullen burst strength of the felt. The Ryton felt that is currently being produced is needled with the latest technology.

The main mode of failure is caused by flexing which is accelerated by the sulfuric acid and high temperature environment. In order to exceed the 2 year bag life, we had to improve the needling and scrim design. The scrim is a woven screen made of a fluorocarbon base fiber. This is placed in the center of the felt to give it additional strength for flexing. A series of tests were conducted on various scrim designs to improve the strength of the felt. These series of tests were conducted at the same time we evaluated the needling techniques. So, with the combination of better needling and a stronger scrim we will exceed our 2 year guarantee.

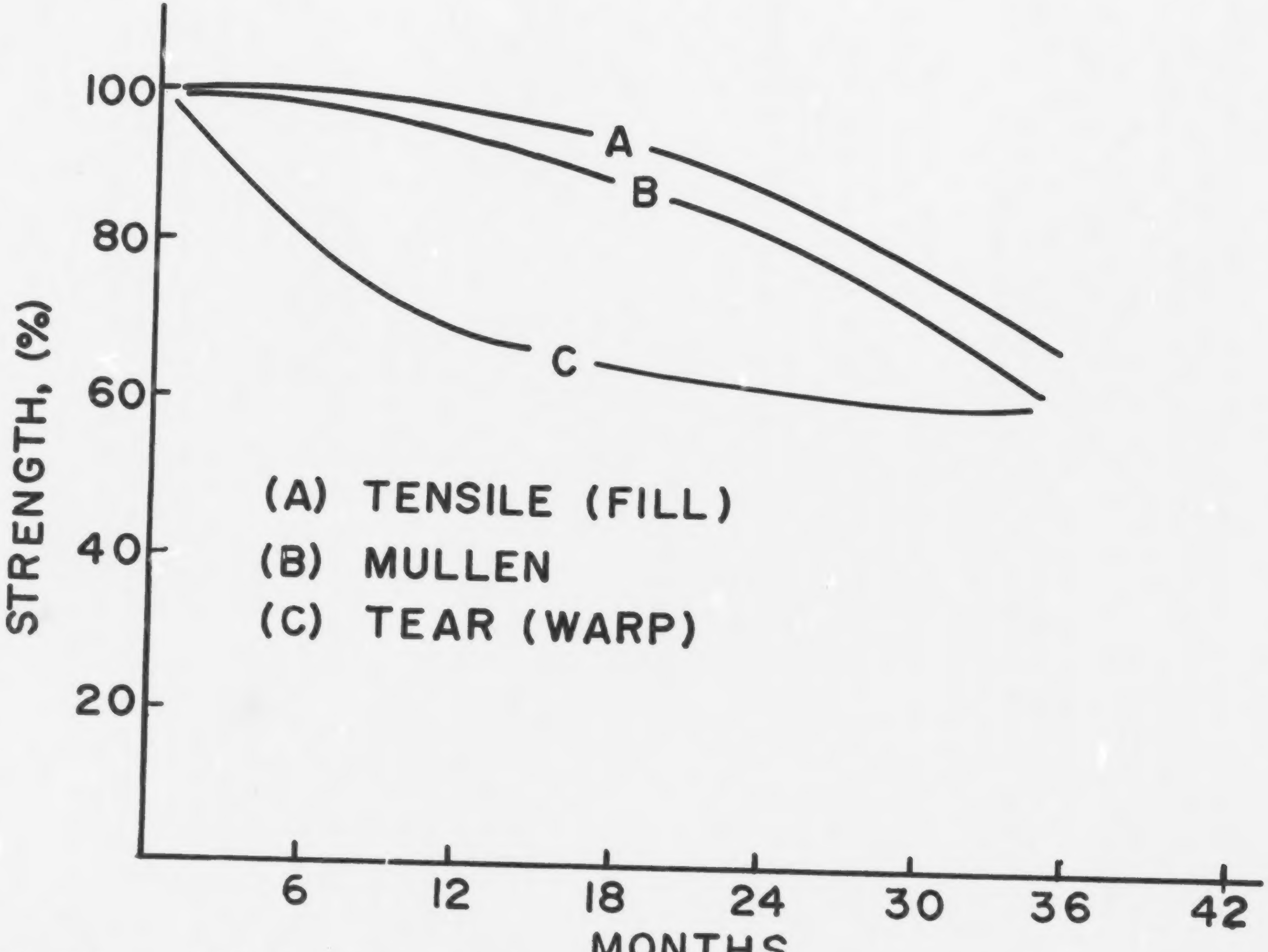

FIGURE 1- AGING EFFECTS OF DAYTEX IN A FLUE GAS ENVIRONMENT

"What is Daytex"

This is the filter media developed by Carter-Day for fly ash applications, and consists of:

1. Ryton fiber - (Polyphenylene Sulfide) resin developed by Phillips Chemical.

2. Scrim - fluorocarbon support grid optimized by Carter-Day.

3. Needling technology - optimized by Carter-Day.

PARTICLE SIZE VS FILTER PERFORMANCE

One of the other areas that determine a successful operating filter system on fly ash is knowing the particle size and shape. We have done extensive work in analyzing various fly ashes from boilers around the country, and also reviewed the operating performance of the baghouse at these locations. From this we compared it to the data we have accumulated from our field installations and slip-streams, and are able to recommend the proper baghouse size for future fly ash applications.

We classify the various fly ashes into 3 major groups. One is fly ash from an inefficient fired stoker, such as dump grates, some underfeed stokers, or a stoker that is operating with high excess oxygen, or upset conditions. Under these conditions, the stoker will create a very fine soot or unburned hydrocarbons which are sub-micron. See Figure 2. Therefore, you have to reduce your air to cloth ratio in order to maintain 2 - 5 inches of pressure drop across the baghouse.

Another type of stoker we refer to is an efficient operating stoker, such as a traveling grate, where there is no upset conditions in the fire bed. This type of stoker will produce large unburned carbon particles, 100μ to 200μ MMD. See Figure 3. This type of fly ash is very easy to filter, therefore we can size our baghouse to operate at a higher air to cloth ratio.

The other major type of fly ash is from a pulverized coal-fired boiler. The particle size will range from 4μ to 8μ MMD when burning western coal and 10μ to 20μ MMD when burning other coals. See Figure 4. The biggest concern is the spherical shape of the particles which can bleed through the media during the cleaning cycle if the media is not designed properly. The Daytex will eliminate the seepage of these particles during the cleaning cycle.

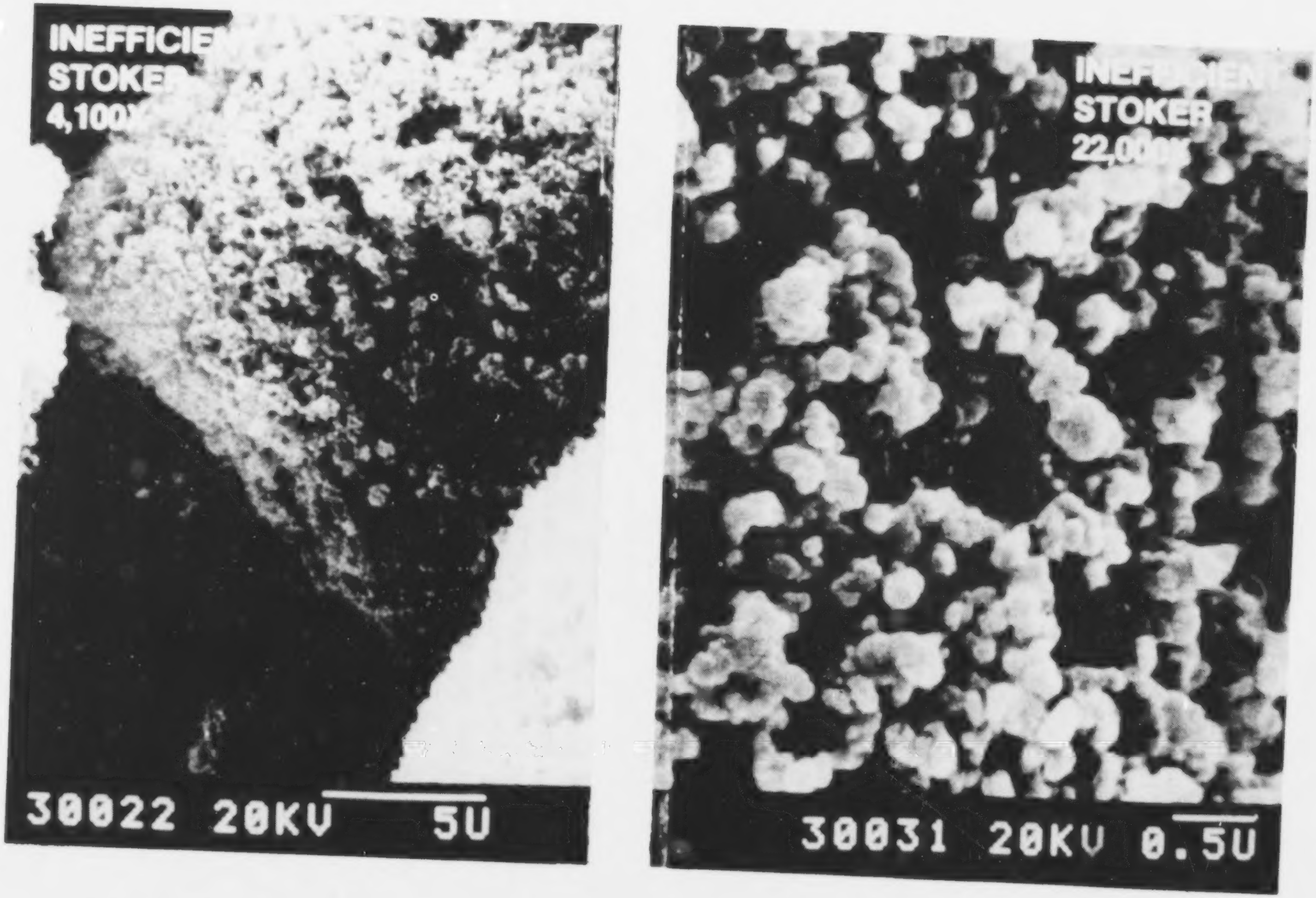
INEFFICIE
STOKE
4,100
30022 20KV 5U
STOKER
22,00
30031 20KV 0.5U

FIGURE 2-FLY ASH FROM INEFFICIENT FIRED STOKER

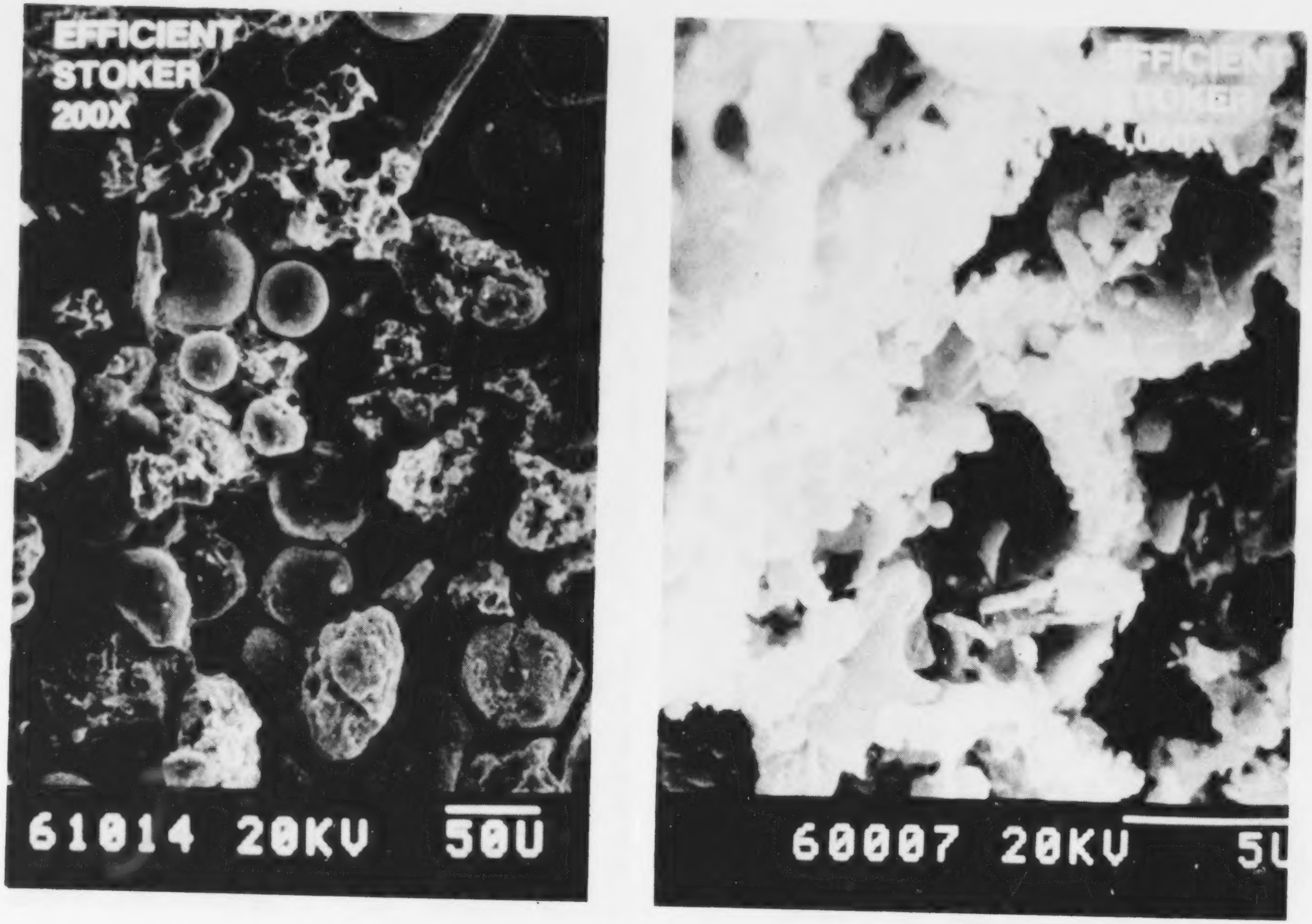
EFFICIENT
STOKER
200X
61014 20KV 50U
FFICIENT
TOKER
4,000X
60007 20KV 5U

FIGURE 3 - FLY ASH FROM EFFICIENT FIRED STOKER

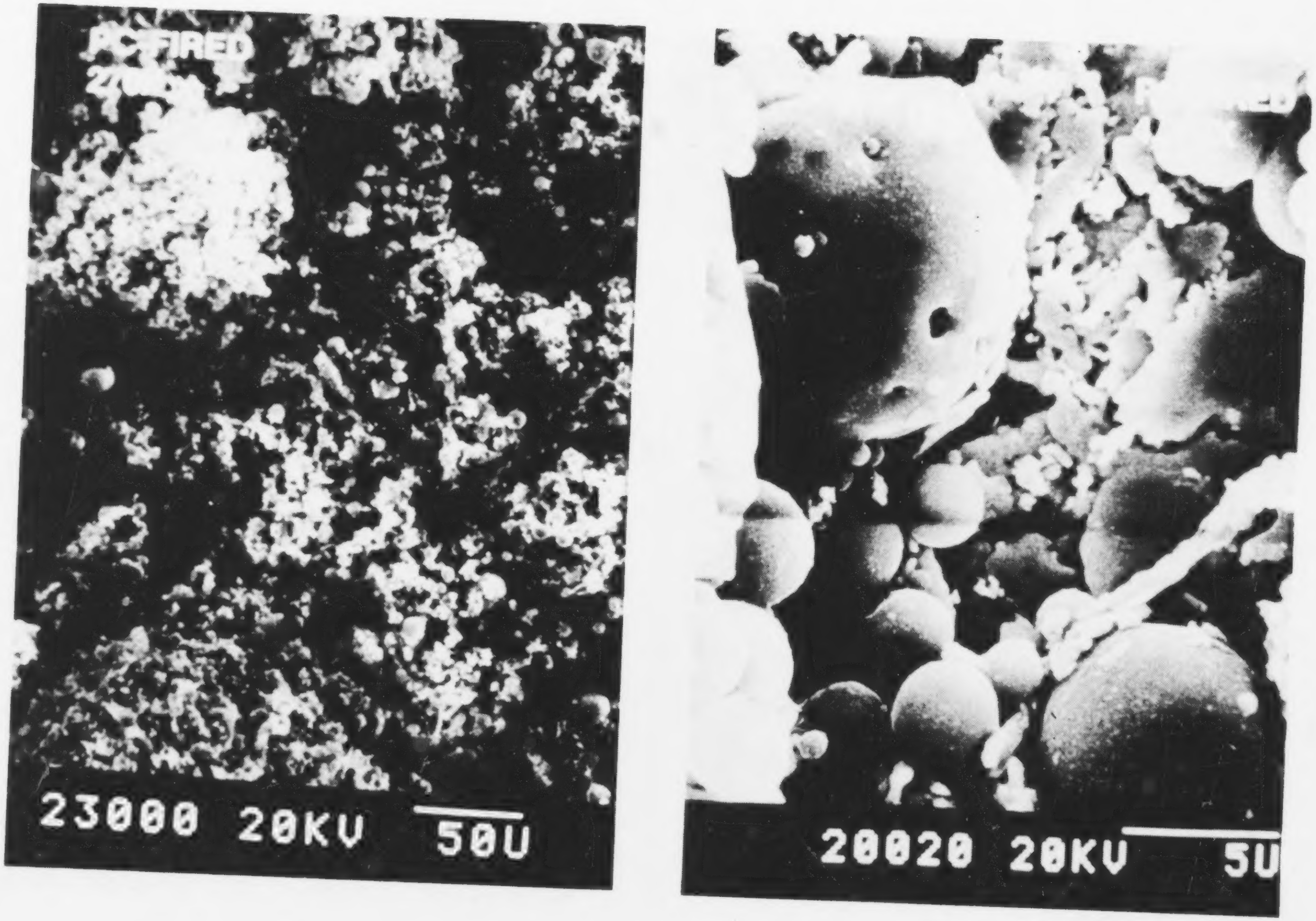
P-C FIRED
23000 20KV 50U
20020 20KV 5U

FIGURE 4 - FLY ASH FROM P-C FIRED

BAGHOUSE DESIGN FEATURES

The filter used for the industrial and utility boiler applications is the RF filter. See Figure 5. The gases enter at the bottom of the filter, and the fly ash is collected on the outside of the filter tube. The dust cake is released from the filter tube by a high energy pressure wave. This pressure wave is released from a quick opening diaphragm valve, then passes through special orifices on a rotating manifold. The cleaning system is a high volume, low pressure design (7.5 psi).

The weight of the Daytex filter tube is 22-25 oz/yd^2 and has proven to have excellent acid and temperature resistance up to 400°F. The length of the filter tubes are 8 to 14 feet and are removed from the top side of the filter.

SUMMARY

Ryton fiber with proper needling and scrim design is an excellent felt for the Pulse Jet filters on industrial and utility coal-fired boilers.

The particle size and shape of the various fly ashes has a major effect on the performance of the baghouse.

As for bag life, none of the bags at the Coors facility have failed, which have been in service for 33 months.

The RF filter system can operate with "on-line cleaning" or "off-line cleaning."

The work described in this paper was not funded by the U.S. Environmental Protection Agency and therefore the contents do not necessarily reflect the view of the Agency and no official endorsement should be inferred.

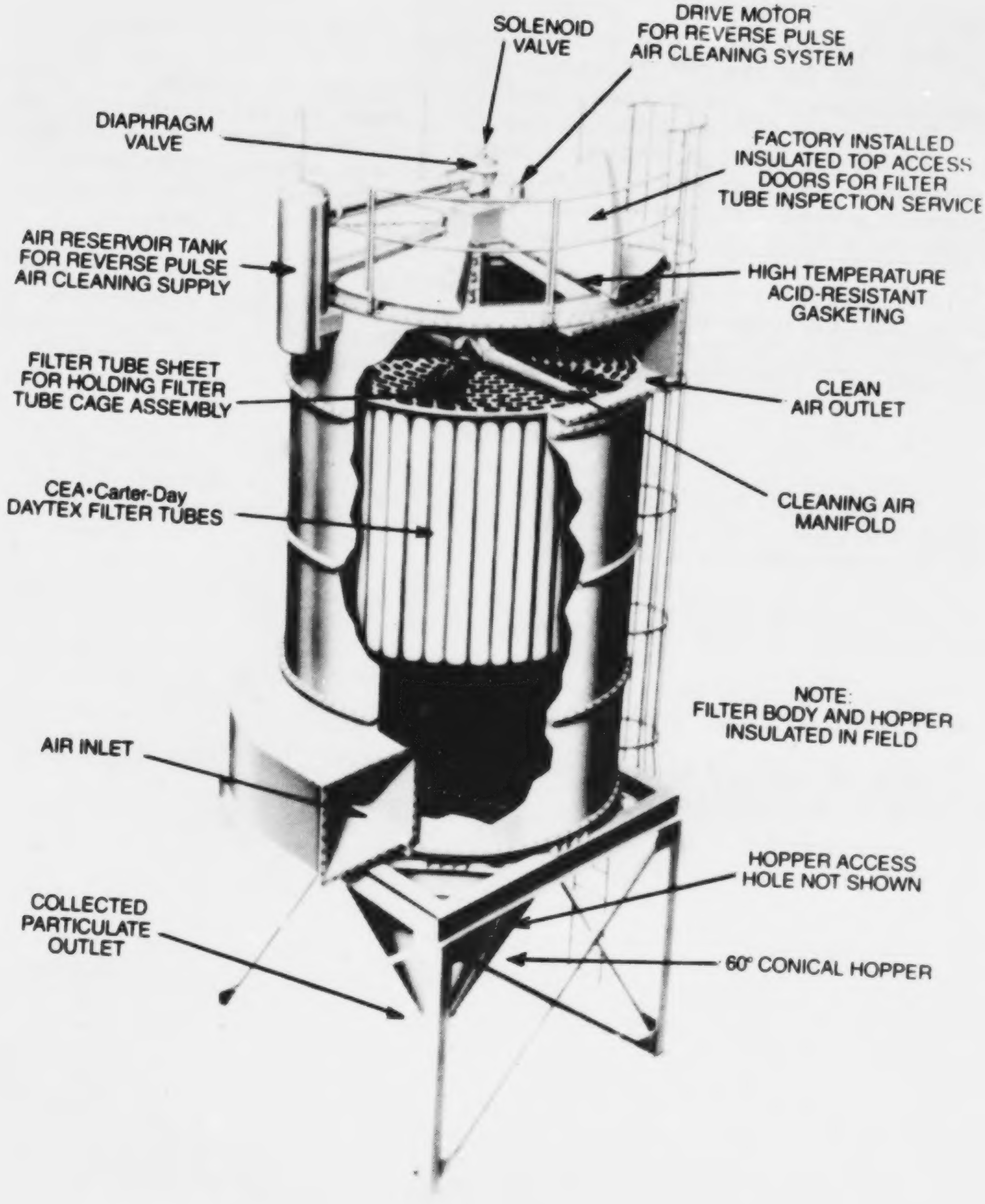
SOLENOID VALVE
DRIVE MOTOR FOR REVERSE PULSE AIR CLEANING SYSTEM
DIAPHRAGM VALVE
FACTORY INSTALLED INSULATED TOP ACCESS DOORS FOR FILTER TUBE INSPECTION SERVICE
AIR RESERVOIR TANK FOR REVERSE PULSE AIR CLEANING SUPPLY
HIGH TEMPERATURE ACID-RESISTANT GASKETING
FILTER TUBE SHEET FOR HOLDING FILTER TUBE CAGE ASSEMBLY
CLEAN AIR OUTLET
CEA•Carter-Day DAYTEX FILTER TUBES
CLEANING AIR MANIFOLD
NOTE: FILTER BODY AND HOPPER INSULATED IN FIELD
AIR INLET
HOPPER ACCESS HOLE NOT SHOWN
COLLECTED PARTICULATE OUTLET
60° CONICAL HOPPER

FIGURE 5 - CARTER-DAY RF FILTER FOR COAL FIRED BOILERS

TOP INLET VERSUS BOTTOM INLET BAGHOUSE DESIGN

by: Robert M. Jensen
Bechtel Power Corporation
San Francisco, California 94119

ABSTRACT

This paper compares top inlet with bottom inlet baghouse designs for bags that collect on the inside. The comparison includes performance data for top inlet baghouses in service with comparable bottom inlet performance.

The paper explains why pressure loss predictions for top inlet may be more reliable than for bottom inlet. Other advantages claimed for top inlet are higher cloth ratio for the same pressure loss as bottom inlet; use of longer bags; better utilization of unreacted reagent after a spray dryer; and more efficient cleaning with the reverse air.

The most important advantage of top inlet design may be the apparent ability for all bags to operate at a constant face velocity in contrast to bottom inlet bags in which the face velocity diminishes with time on line after each cleaning.

. . . .

Until a few years ago it was assumed that no correlation existed between the pressure loss of a baghouse on coal-fired flue gas and the properties of the coal burned and its ash. We now have ample evidence that a correlation does exist but we do not know what it is. One consequence of this situation is that we cannot predict accurately the pressure loss for a baghouse on coal-fired flue gas.

We do know that a correlation exists between pressure loss and particle size. We know that pressure loss increases as the median particle size decreases. Anything that causes the median particle size to decrease will increase pressure loss and should be avoided.

For baghouses on coal-fired flue gas, it is possible that the degree of unpredictability of pressure loss is the same, or nearly the same, as the degree of unpredictability of the amount of shift in particle size toward the smaller size caused by hopper fallout and reverse gas recirculation. If we eliminate the size shift, we may also eliminate the uncertainty in predictions of pressure loss. One way to avoid, or reduce, the shift may be to use top inlet instead of bottom inlet baghouse design.

Bottom inlet baghouses decrease the median particle size entering the bags by allowing coarse particles to fall out on entering the hopper and by recirculating the reverse gas flow with its fines back to the inlet duct. This shift toward smaller particles can be avoided if we eliminate hopper fallout and if we filter the reverse gas in a separate system.

This paper compares top inlet baghouse design with bottom inlet baghouse design for cylindrical bags that collect on the inside. The schematic arrangements of these two types of baghouses are shown for the filtering mode in Figure 1 and for the cleaning mode in Figure 2.

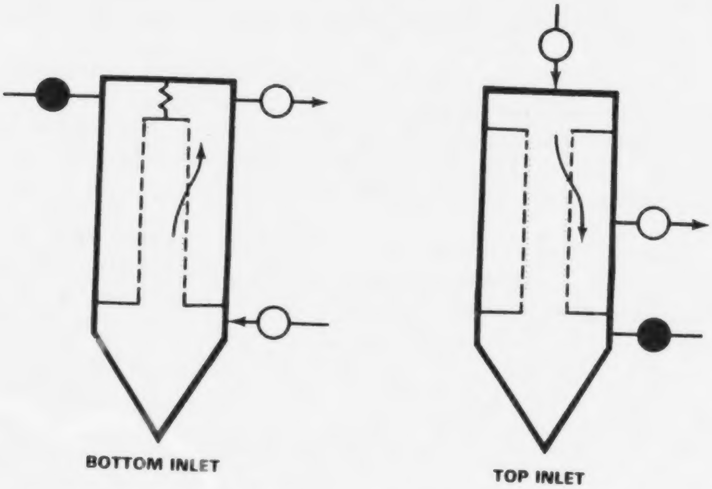

Figure 1. Filtering mode.

When reliable application data are available, a bottom inlet baghouse can be designed with assurance that it will work within the predicted pressure loss and not exceed the allowable emission limit. Reliable application data have been available for many years for a great variety of industrial applications. Until recently, it has been assumed that baghouses can be used to remove fly ash from coal-fired flue gas using design criteria that have been satisfactory for similar materials and operating conditions. This assumption is now in question as a consequence of the inability of some baghouses on coal-fired flue gas to meet predicted pressure loss and, in some cases, to stay within allowable emission rates.

One reason for this situation may be the highly variable nature of fly ash. Another reason may be some undesirable inherent characteristics of bottom inlet baghouses.

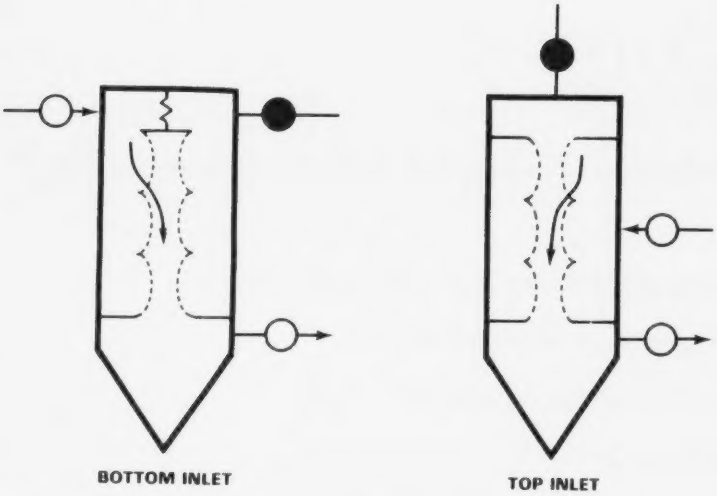

Figure 2. Cleaning mode.

Two of these undesirable characteristics of bottom inlet baghouses are, first, the unavoidable fallout of coarse material when the dirty gas enters the hopper and, second, the unavoidable dead end at the top of the bag. They cannot be corrected for obvious reasons. An explanation of why they are undesirable follows.

Consider the formula used for the pressure loss across cloth and cake:

$$\Delta P = k_1'V + k_2' \times \frac{C_i}{7000} \times t \times V^2 + k_3'V \qquad (1)$$

where

ΔP = the pressure loss across the cloth and cake in one compartment just before cleaning, inches of water gauge (in. wg)

C_i = grain loading at bag inlet, grains/actual ft^3 (gr/acf)

t = time between cleanings, minutes

V = air-to-cloth ratio = face velocity, ft/min, fpm

k_1' = resistivity of new cloth (negligible), $\frac{\text{in. wg}}{\text{(fpm)}}$

k_2' = resistivity of filter cake, $\frac{\text{in. wg}}{(\text{fpm})(\text{lb/ft}^2)}$

$$= \frac{k \times \eta_g}{\delta_p} \times \left(\frac{Ap}{\bar{V}p}\right)^2 \times \frac{1 - e}{e^3} \qquad (2)$$

k_3' = resistivity of cloth and cake after cleaning, $\frac{\text{in. wg}}{(\text{fpm})}$

where

k = Kozeny-Carman constant, dimensionless

= 5 (generally accepted value)

η_g = gas viscosity, lb(mass)/ft · sec

δp = specific particle density, lb/ft^3

Ap = surface area of particle, ft^2

$\bar{V}p$ = volume of particle, ft^3

e = porosity = void fraction = $1 - \alpha$

$\alpha = \frac{\text{bulk density of particle}}{\text{specific density of particle}}$, dimensionless.

The terms $k_1'V$ and $k_3'V$ are usually neglected; $k_1'V$ because it is very small and $k_3'V$ because it is the pressure loss immediately after cleaning which does not have to be guaranteed and is not used in evaluations. Our basic formula is thus:

$$\Delta P = k_2' \times \frac{C_i}{7000} \times t \times V^2 \ . \qquad (3)$$

If we assume spherical particles and typical values for the terms in Equation (2), we can solve for k_2' for different particle sizes. The relationship of k_2' and particle size is shown in Figure 3. For the assumed conditions, Figure 3 shows that k_2' is less than unity and therefore reduces pressure loss for particles greater than 10 microns and that k_2' and pressure loss increase rapidly as the particle size gets smaller below 10 microns.

The value of k_2' used in Equation (3) is usually the median particle size entering the baghouse. It should be the median particle size for the size distribution entering the bottom of the bag. We do not know and we cannot determine the particle size distribution entering the bag. This is true for a number of reasons.

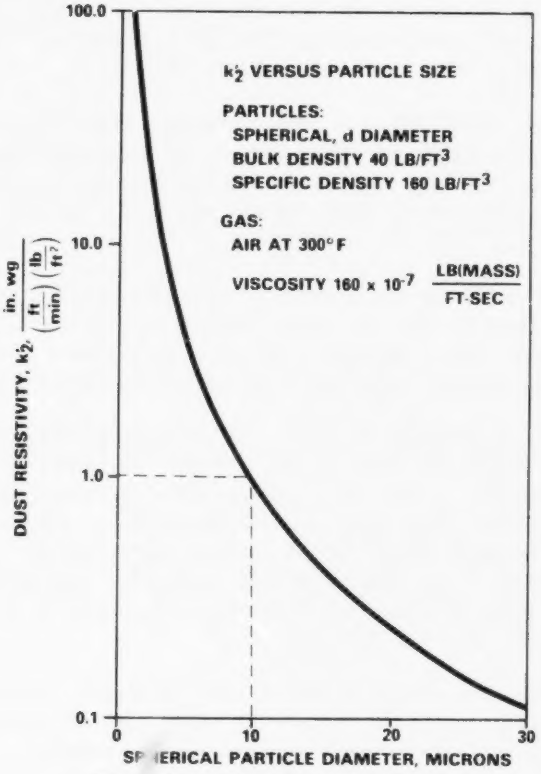

Figure 3. Variation of k_2 with particle size.

When writing a baghouse specification or when designing a baghouse it is customary to calculate the grain loading entering the baghouse. This is done by calculating the total ash, using the coal burn rate and the percentage of ash in the coal. An estimate is then made for the amount of total ash that will become fly ash. This gives us an approximate rate for the quantity of fly ash.

The gas volume entering the baghouse is also an approximation. It includes estimates of inleakage, airheater leakage, ash hopper evaporation, and margin. The number of grains per actual cubic foot is thus the result of dividing one approximation by another.

On the other hand, if we are working with a baghouse in service we can make a traverse of the inlet duct and determine grain loading and particle size distribution entering the baghouse or a compartment. This information does not serve our purpose for several reasons. First, it differs from the conditions at the inlet to the bags. Second, it may not include the fly ash that is recirculated during reverse air cleaning. And third, it includes the coarse fraction that will fall out when entering the hopper.

We cannot determine the grain loading and particle size distribution entering the bags because we cannot prevent nor measure hopper fallout. The gas flow rate into a compartment varies; it is highest immediately after cleaning and lowest immediately before the next cleaning. Hopper fallout will therefore vary because of the variable inlet velocity.

As the gas flow rate into a compartment diminishes, so will the gas velocity entering the bottom of the bags. A lowered velocity entering the bags means a reduced ability to carry solid particles. As a consequence, hopper fallout increases and the mean particle size entering the bags diminishes.

A bottom inlet design is thus seen to cause a shift in the particle sizes entering the bags toward the smaller sizes. As the median size of the particles entering the bags diminishes, k_2' increases and so does pressure loss. This is an undesirable inherent characteristic of bottom inlet designs.

Another inherent characteristic of bottom inlet design is the dead end at the top of the bag. When the dirty gas enters the bottom of a bag, it has a certain vertical velocity. As the gas passes through the bag, the volume remaining and rising in the bag diminishes and, therefore, so does the vertical velocity. As the vertical velocity diminishes, so does the ability to carry solid particles. As the vertical velocity approaches zero at the top of the bag, only the smallest particles will be carried upward. As a result, fines accumulate at the top of the bag.

Several investigators report that they have determined experimentally that there is no accumulation of fines in the top of bottom inlet bags. In each of these experiments there was a time lapse between taking the bags out of service and inspection of the bag. During that time, the compartment was opened to the atmosphere, it was cooled and purged by pulling outside air into it, and there was reverse flow through the cloth and down-flow in the bags. During this time there was a gradual reduction in temperature, which reduced the chimney effect in the bags. This time was equivalent to a null period which some favor as part of a cleaning cycle to allow dust to fall. It is very likely that some dust fell out of the bags during the cool-down period. It is possible that the predicted accumulation of fines in the top of the bag fell out during this period.

The actual inspection of the bags necessitated some agitation of the bottoms of the bags by the people moving about on the tubesheet. Sampling the cake on the inside of the bags by cutting swatches with the bags in place or removing the bags and cutting them open would also dislodge and/or redistribute the dust cake.

The conclusion that these experiments prove that there is no accumulation of fines in the tops of bottom inlet bags is not warranted. These experiments are inconclusive; they do not prove that there is no accumulation of fines at the top of bottom inlet bags.

The value of k_2' at the top of the bag may be higher if the median particle size is smaller. The path of least resistance for gas flow will then be through another part of the bag where k_2', and therefore flow resistance, is lower. In other words, the face velocity, or cloth ratio, is variable over the length of the bag.

None of the conventional cleaning methods is effective in removing the fines from the top of the bag. During cleaning, some of the fines stick to the top of the bag, some agglomerate and fall to the hopper, and some float in the motionless gas until the bag goes on line again, at which time they return to the bag.

Shaking the top of the bag will cause some agglomeration, but some fines will still remain to go back on the bag. One or more deflation flows during a shake/deflate cleaning cycle will help to move the dislodged material to the hopper. However, deflation flow will take the path of least resistance, which is in the lower part of the bag, and therefore is not effective for removing fines from the top of the bag.

In some baghouses, reverse air cleaning has not been effective either. It, too, takes the path of least resistance through the lower part of the bag, bypassing the top of the bag.

The dead end at the top of the bag is thus seen to be a cause of ineffective cleaning that entails pressure loss, increased frequency of cleaning, and reduced bag life. There is no way to avoid this because the submicron material will not settle by gravity. A half-micron size particle of fly ash in still air will reach its terminal velocity in a fraction of a second. At that velocity, it will take weeks for it to settle by gravity 30 feet from the top of the bag to the hopper. It actually will not settle any distance because its fall will be opposed by the convection currents, or chimney effect, in the bag.

We can assume that the accumulation of fines in the dead end will cause some cloth area at the top of the bag to go blind. Loss of filter area for this reason would necessitate a higher cloth ratio and therefore a higher pressure loss in the balance of the bag if nothing else changed. What actually happens can be inferred from the curve shown in Figure 4, which is typical for bottom inlet bags.

If we assume reasonable values for k_2' and C_i and if we take values of ΔP and t from the curve, we can solve Equation (3) for V, cloth ratio. If we then plot V versus the same time span, we have the relationship shown in Figure 5. Although k_2' and C_i are also likely to vary with time, we can assume that k_2' will probably increase as the size of the particles entering the bags becomes smaller and that its increase will be offset, to some extent, by a decrease in C_i. It is probably safe to assume that the shape of the curve in Figure 4 is caused mostly by changing cloth ratio and that Figure 5 is a reasonable representation of the variation of cloth ratio with time on line.

Figure 5 confirms the well-known fact that the gas flow rate through a bottom inlet compartment decreases while on line. The total flow through a baghouse is therefore the sum of the variable flows through the compartments. This can be illustrated by the electrical analogy of Figure 6.

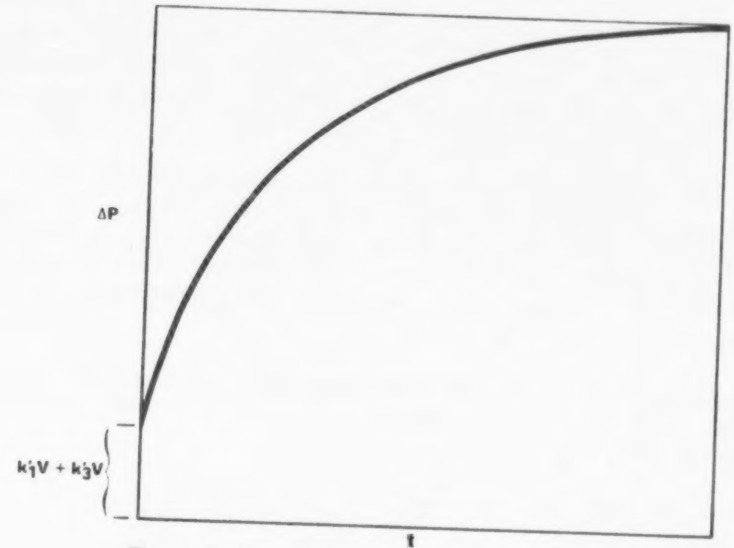

Figure 4. Pressure loss versus time on line for bottom inlet baghouses.

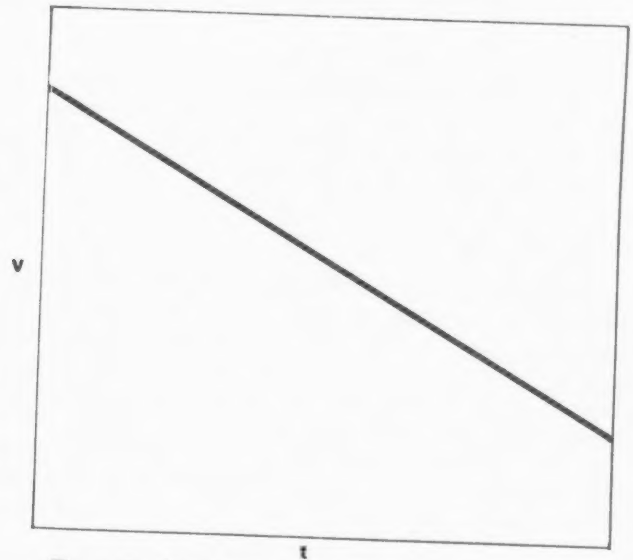

Figure 5. Cloth ratio versus time on line for bottom inlet baghouses.

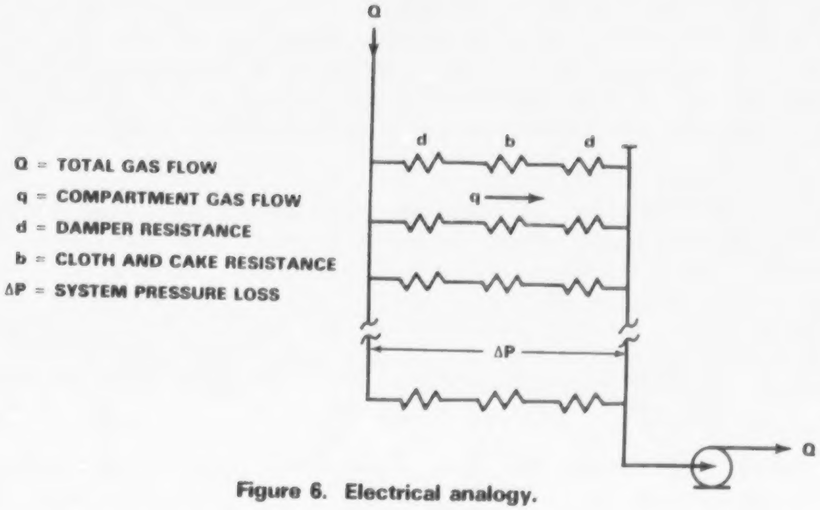

Figure 6. Electrical analogy.

In this diagram, Q is the sum of all the compartment flows, q, which varies depending on how long each compartment has been on line since its last cleaning. The system pressure loss, ΔP, will vary with Q, the number of compartments in service, and during the cleaning cycle. However, at any one moment, the sum of the resistances of the two dampers and the cloth and cake for any compartment will be the same as the system ΔP.

The pressure loss across the cloth and cake, b, will vary as shown by Figure 4. As b increases, q decreases and, as q decreases, so does the resistance through the two dampers, d. Baghouses are said to be "self-leveling" in the sense that the gas seeks the compartment with the lowest pressure loss. This may explain the initial steepness of the curve in Figure 4 when the bags are newly cleaned. Note that "self-leveling" for bottom inlet baghouses is on a compartment basis.

Figure 5 also illustrates the well established fact that cloth ratio for bottom inlet baghouses diminishes with the time on line. The design cloth ratio may be the average cloth ratio of an on-line compartment for the time span between cleanings. This average may be different for each compartment. Variable cloth ratio over the length of each bag and in every compartment is a consequence of this undesirable inherent characteristic of the bottom inlet design. Variable cloth ratio is undesirable because it means that the cloth is not filtering at a constant rate. For bottom inlet baghouses, cloth ratio can be thought of as the baghouse size; it is not the face velocity except momentarily at various places in some bags in one compartment when the baghouse is in service.

Remember, cloth ratio is the amount of gas to be cleaned divided by the area of the cloth used to clean it, or:

$$V = \frac{CFM}{ft^2} = \frac{ft}{min} = \text{face velocity.} \qquad (4)$$

If V diminishes between cleanings as shown by Figure 5, it could be because CFM diminishes or ft^2 increases. We know that cloth area does not increase and therefore CFM must decrease. However, if the bag goes blind at the top, we are reducing ft^2 which would make V increase. If the bag goes blind at the top and if V decreases, we conclude that CFM diminishes at a rate that compensates for the reduction in filtering cloth area at the top of the bag.

We thus have a vicious circle. As the compartment flow diminishes, the velocity entering the bag diminishes and the proportion of fines entering the bag increases. This accelerates the blinding at the top of the bag which accelerates the reduction in the rate of flow which reduces the velocity entering the bag, and so on. This may explain why the curve in Figure 4 shows the rate of ΔP increase slowing down as the compartment nears the time for its next cleaning. This vicious circle is unavoidable with bottom inlet baghouses.

Top inlet baghouses do not have the two undesirable inherent characteristics of bottom inlet baghouses. There is no hopper fallout and there is no dead end in the bag. As a result, the relationship of pressure loss versus time on line is as shown by the plots of data from top inlet baghouses in service in Figure 7. The data sources are described in the references.

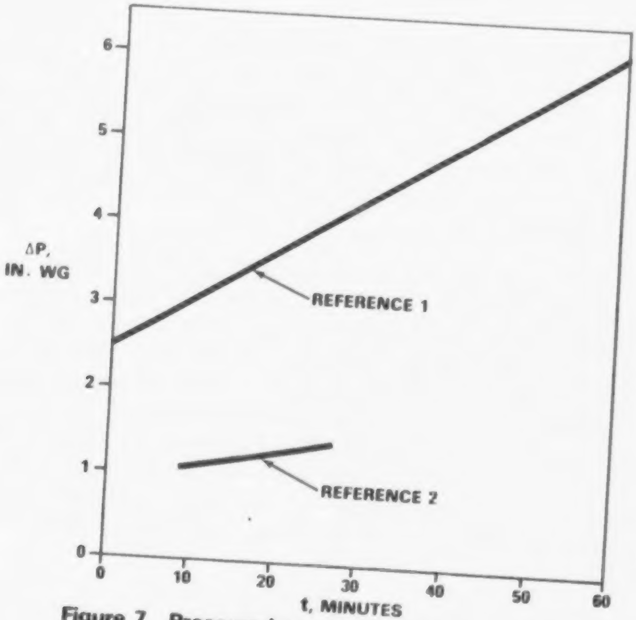

Figure 7. Pressure loss versus time on line for top inlet baghouses.

Substituting values from Figure 7 in Equation (3) and solving for the corresponding cloth ratio, we have the relationship for cloth ratio versus time on line as shown in Figure 8.

Figure 8 shows that top inlet baghouses probably operate at constant cloth ratio. If so, this would mean that every bag and every compartment would have the same face velocity regardless of how long it has been on line. For this to be so, we have to infer several things. First, k_2' does not vary over the length of the bag. Second, the rate of gas flow is the same in all compartments all the time on line. Third, top inlet baghouses may be self-leveling on a per bag basis rather than on a compartment basis as is the case for bottom inlet baghouses.

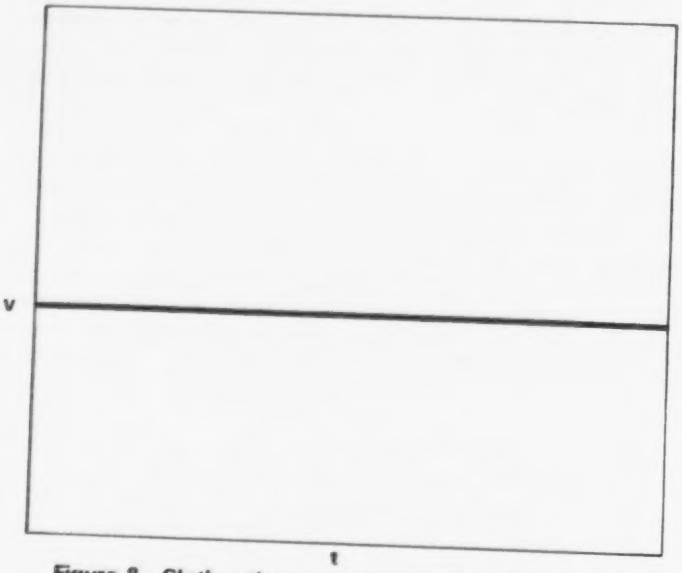

Figure 8. Cloth ratio versus time on line for top inlet baghouses.

These inferences should be checked experimentally. The bases for them are as follows:

For k_2' to be constant, the permeability, or porosity, of the filter cake must be the same in all bags, over the length of each bag, and in all compartments even though the cake gets thicker with time on line. This is possible within limits. Contrary to some reports in the literature, there is no hopper fallout with top inlet. As the vertically downward velocity in the bag diminishes, we have a downward velocity component approaching zero and a constant horizontal velocity component (face velocity) with a resultant component approaching the horizontal. In other words, the particles move toward the bag and reach the bag before they fall out of the bottom of the bag.

With no hopper fallout, the cake will have the full range of particle sizes and the median size will be larger. With coarse material in the cake, it will be more porous, k_2' will be smaller, and pressure loss will be smaller. For a typical grain loading leaving a coal-fired boiler and for a typical cleaning cycle, the filter cake will usually be only two or three hundredths of an inch thick. With a porous cake and a small pressure differential across it, there may be a negligible increase in k_2' as the cake builds from say 0.01 inch to 0.02 inch. In addition, there is very little likelihood of cake collapse, which would make it less porous. The first inference is thus plausible.

The second and third inferences are related. For the flow to be the same in all compartments all the time, the resistance to flow must be the same in all compartments all the time. This is possible if k_2', C_1, and V are all constant, which may be the case for top inlet bags. For this to be so, we have to assume that the cake in every bag is of uniform thickness, composition, or porosity over the full length of the bag. This is possible if cake deposition in the bag is uniform as a consequence of the gas seeking the path of least resistance in each bag.

As dirty gas enters the top of a clean bag, it will deposit cake at the top. The path of least resistance will then be below that cake. As the cake builds, the path of least resistance moves down the bag. This process probably happens very quickly over the length of the bag. The result may be a cake of uniform porosity for the full length of the bag. Any deviation from uniformity may be immediately corrected as the gas seeks the easiest way out. The self-leveling process may thus be on a per bag basis for top inlet. This could be a very significant difference from the per compartment basis for bottom inlet.

There is a possibility that top inlet bags perform differently from bottom inlet bags. Figure 9 may be evidence for this difference in performance. Both curves are for baghouses in service on cement kiln exhausts. The top inlet baghouse has a nominal cloth ratio of 3 ft/min and the bottom inlet baghouse has a nominal cloth ratio of 2 ft/min. These pressure losses were measured across cloth and cake in one compartment.

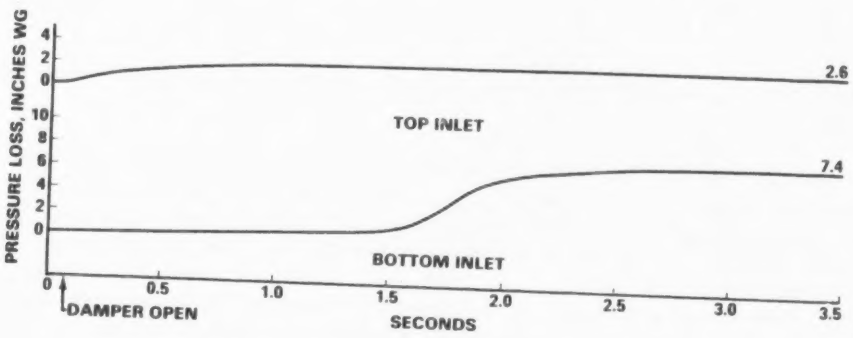

Figure 9. Initial Pressure Loss Versus Time (Reference 3)

Note the abrupt rise in pressure loss for the bottom inlet compartment and the gradual rise for the top inlet compartment. Note, too, that the pressure loss after the first three seconds on line for the bottom inlet compartment is about three times the loss for the top inlet compartment. During this test, the pressure loss for the bottom inlet compartment rose to 8.6 to 9.0 in. wg when it was on line and one of the other compartments was in the cleaning mode. The pressure loss in the top inlet compartment rose to 3.1 to 4.5 in. wg when it was on line and one of the other compartments was in the cleaning mode.

The bottom inlet curve may be a confirmation of the theory that fines floating in the top of a bottom inlet bag jump back on the bag as soon as it goes back on line after cleaning. The top inlet curve may be a confirmation that the filter cake formation in a top inlet bag is at a uniform rate.

The most significant difference between top and bottom inlet designs is the fact that the bottom inlet design has hopper fallout and dead ended bags and that the top inlet design has neither. Top inlet has other advantages that are certainly worth consideration.

Some evidence exists that top inlet baghouses will operate at a higher cloth ratio for the same pressure loss as bottom inlet baghouses or that they will operate at a lower pressure loss for the same cloth ratio as bottom inlet baghouses. This is illustrated by Figure 10.

Figure 10 shows that top inlet provides a saving in capital cost at the same pressure loss or a saving in operating cost (ΔP) at the same cloth ratio when compared with bottom inlet.

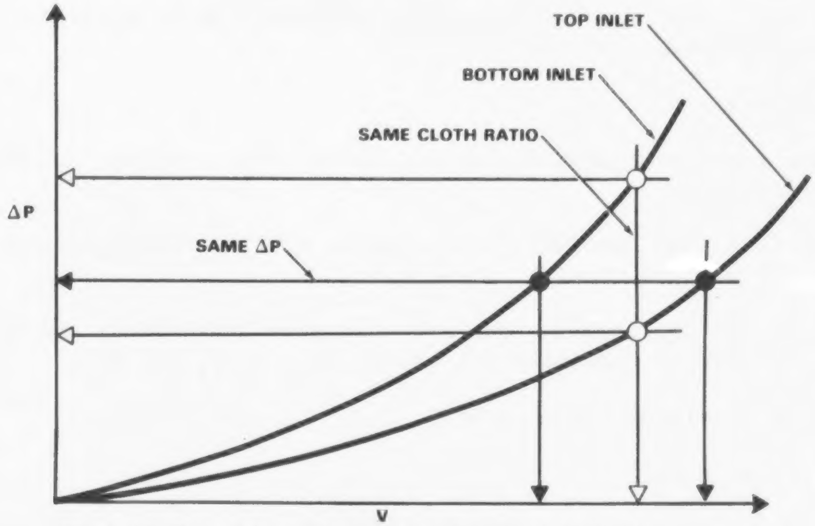

Figure 10. Comparison of top versus bottom inlet baghouses.

Top inlet bags can be longer than bottom inlet bags because they do not have a dead end to go blind. Making bottom inlet bags longer accelerates the rate of blinding at the top and aggravates the vicious circle described earlier. Contrary to common belief in the field of fabric filtration, high entrance velocity at the bag inlet is not necessarily the cause of bag failure at the inlet end. Failure of bottom inlet bags near the bottom at low (240 fpm) inlet velocity is more likely caused by inadequate bag tension. On the other hand, top inlet bags are in service on cement kiln exhausts that have inlet velocities of approximately 680 fpm that do not fail from abrasion at the inlet.

One advantage of longer bags is the lower cost per square foot of cloth and lower installation labor cost per square foot of cloth. In addition, longer bags mean fewer bags and less plan area.

If the baghouse is to be used downstream of a spray dryer, the hopper fallout in a bottom inlet design will contain some unreacted material that would remove additional sulfur dioxide if it got into the cake on the bags. With a top inlet design, this material would not be wasted.

To sum up:

Bottom inlet baghouses

- Suffer unnecessary pressure loss because particle size entering the bags is reduced in several ways, and smaller particles entail higher pressure loss.
- Operate at variable cloth ratio within each bag and among compartments.
- Are difficult to clean because of the accumulation of fines in the dead end top of the bag.

Top inlet baghouses

- Have lower pressure loss because the filter cake contains the full range of particle sizes.
- May operate at a constant cloth ratio within each bag and in all compartments all the time.
- Clean more readily because the cake includes the coarse particles and because the reverse flow does not bypass the top of the bag.
- Can operate at higher cloth ratios.
- Can use longer bags.
- Improve utilization of reagent and fly ash alkalinity in dry flue gas desulfurization systems.

The work described in this paper was not funded by the U.S. Environmental Protection Agency and therefore the contents do not necessarily reflect the views of the Agency and no official endorsement should be inferred.

ACKNOWLEDGEMENTS

In addition to the persons listed in the references, the author is most grateful to John Musgrove, William Lane, Ernest Purcell, and Betty Winkelman, all of the Bechtel Power Corporation, for their assistance in various ways in the preparation of this paper. Their assistance does not imply that they agree or disagree with this paper.

REFERENCES

1. Estopinal, E., and Noone, G., of Columbian Chemical Co. Data from carbon black baghouse in Mohave, California. Top inlet bags are 10-in. diameter, 31 ft 6 in. long. Private communication.
2. Graham, H., of Giant Portland & Masonry Cement Co. Data from cement kiln exhaust baghouse in Harleyville, South Carolina. Top inlet bags are 8-in. diameter, 62 ft 10 in. long. Private communication.
3. Brumagin, C., of Fuller Co. and Foster, R., of Whitehall Cement Manufacturing Co. Data from cement kiln exhaust baghouses in Cementon, Pennsylvania. Top inlet bags are 11.5-in. diameter, 37 ft 10 in. long. Private communication.

UPGRADE OF FLY ASH COLLECTION CAPABILITY AT THE CROMBY STATION

by: T.J. Ingram
R.J. Biese
Gilbert/Commonwealth
Reading, Pennsylvania

R.O. Jacob
Philadelphia Electric Company
Philadelphia, Pennsylvania

ABSTRACT

A description is given of measures to upgrade the dust collection capability of 28-year old Cromby Unit 1 in the interim period before installation of an SO_2 scrubber. A novel approach was taken to enhance the performance of outdated equipment, resulting in continued usage of existing mechanical collectors, upgraded electrostatic precipitators and the addition of a sidestream baghouse to accomplish the objective. The equipment was installed and started up within a year of writing specifications, and compliance was attained. The paper discusses some problems experienced, notably bag blinding which has resulted in a severe maintenance problem; steps in progress to resolve the problem are discussed.

INTRODUCTION

In August 1979, Philadelphia Electric Company signed a consent agreement with the Environmental Protection Agency and the Pennsylvania Department of Environmental Resources to bring Unit 1 at their Cromby Station into compliance with particulate emission limitations of 0.65 lb per million Btu input pending installation of a wet particulate scrubber and an SO_2 scrubber. Gilbert/Commonwealth (G/C) was consulted to make recommendations for achieving this goal and to do the engineering.

This 28-year old unit utilized mechanical dust collectors and electrostatic precipitators in series to remove dust from the flue gas, and it was found that emissions would have to be reduced by approximately 50 percent to attain the limitation of 0.65 lb/MMBtu. Although this limit is not strict by today's new source standards, the old and worn equipment, typical of such units, was not judged capable of achieving this performance with simple reconditioning. On the other hand, extensive replacement was not warranted because the scrubber installation would be complete within four years.

The program instituted was one of compromises, which was necessitated by a schedule calling for compliance by April 1981, and by the usual space limitations in an older plant. By the time initial tests could be run to establish base performance, there were only sixteen months remaining to the compliance date. To meet it, a gas flow model study was conducted, the existing equipment was reconditioned and modernized, and a small baghouse was added on a side stream.

Overall success of the program was demonstrated by achieving compliance. However, there has been a problem with early blinding and shortened bag life. A number of measures have been taken and the solution of this problem is well on the way to resolution.

PROBLEM DEFINITION

HISTORY

Cromby Unit 1 went into service in 1954. It is a 165 megawatt (MW) unit, designed to burn eastern pulverized coal in a front-fired, radiant, Babcock & Wilcox boiler. The original design was for pressurized operation and omitted induced draft fans. However, before construction was complete it was recognized that there were operating circumstances where a negative pressure in the boiler would be required for periods of time and reduced size induced draft fans were included. Casing leaks eventually forced continuous use of these fans and reduced power output. However, full size fans have recently been installed in conjuction with the installation of the SO_2 scrubber.

This unit was one of only three in the Philadelphia Electric system that operated on coal when this project was begun in 1979. It was, therefore, considered economical to maintain it in service to take advantage of the cheaper fuel, and to find means to comply with imposed environmental regulations.

INTERIM CONSENT DECREE

As a result of discussions with the regulating authorities a consent order was issued which required Cromby 1 to burn lower sulfur coal and to reduce particulate emissions during the interim period to a maximum of 0.65 lb/MM/Btu input while the particulate and SO_2 scrubbing system was being installed.

A series of tests performed in October 1979 showed average particulate emissions of 1.08 lb/MM/Btu input which was well in excess of the established limit.

An upgrade schedule for achieving compliance by April 1981 was submitted in accordance with the consent order.

THE SITUATION

EXISTING EQUIPMENT DESCRIPTION

The flue gas cleanup equipment that existed at the plant at the beginning of the modifications was unique by today's standards. In each of two parallel gas streams, between two tubular air heater stages, there was a mechanical collector (Figure 1) to remove most of the ash. The mechanical collector was the horizontal multi-tubular type. The flue gas entered the tubes through vanes which imparted a spin. The ash, being heavy, was thrown toward the wall and exited along with some gas through an annulus in the tube about half way through. It then dropped into a collecting duct and was drawn off through two sets of cyclones in series by a conveying fan. The conveying gas was reintroduced to the main gas stream just upstream of a precipitator as shown in Figure 2.

The ash transport gas from the mechanical collectors was approximately eight percent of total gas flow. Ash removed from this stream by the cyclones dropped into a dust silo through rotary valves. Ash collected in the precipitator hoppers was picked up by a stream of flue gas drawn from the precipitator inlet plenum and carried to small cyclones by a secondary conveying fan. The clean secondary stream was then combined with the clean primary ash collection stream before emptying into the precipitator inlet.

The precipitator, or actually two precipitators in parallel, were old units, each having 31 gas passages 8-3/4 inches wide, and two fields of collecting plates 20 feet tall by 9 feet long. The collecting plates were constructed of double sheets of expanded metal, and were rapped from the

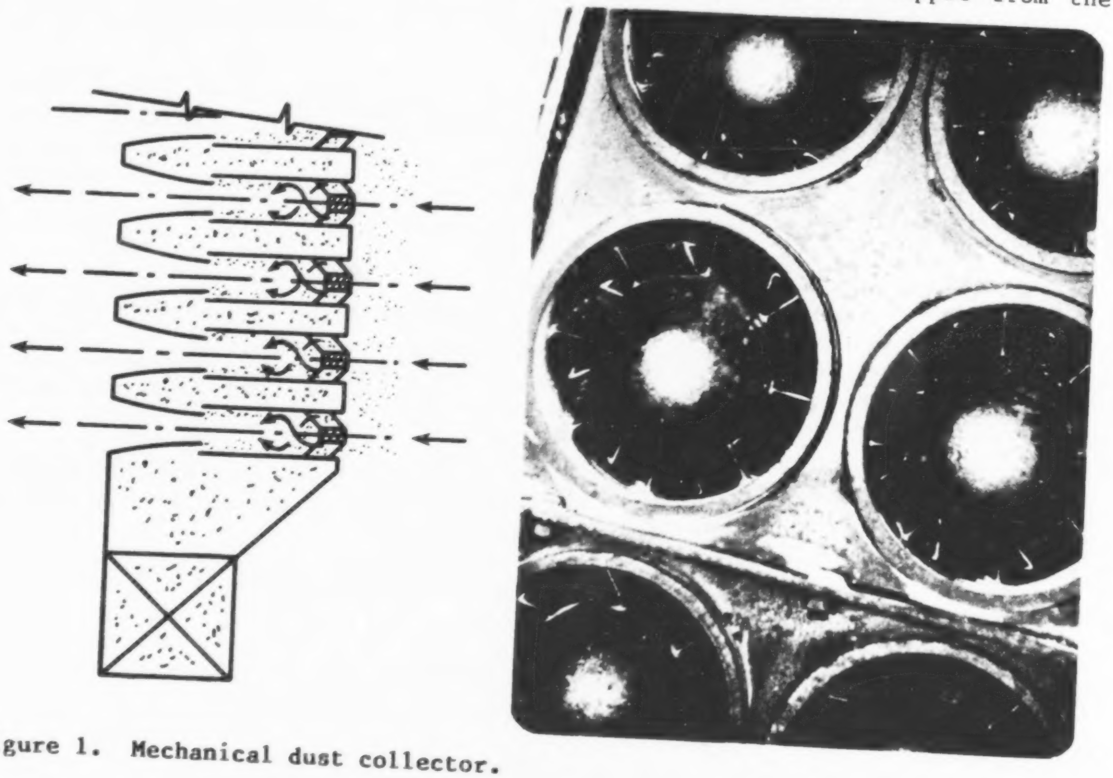

Figure 1. Mechanical dust collector.

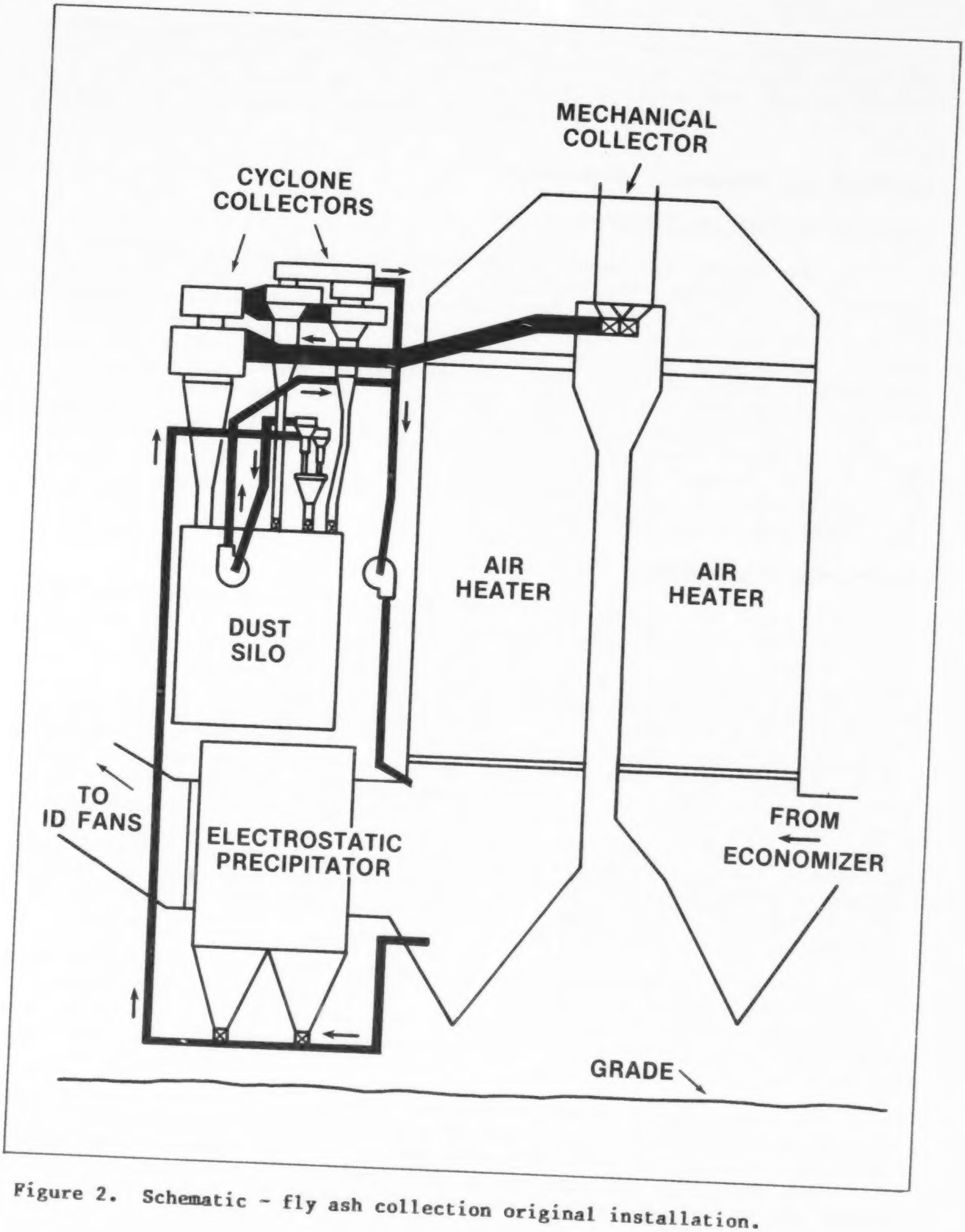
MECHANICAL COLLECTOR
CYCLONE COLLECTORS
AIR HEATER
AIR HEATER
DUST SILO
TO ID FANS
ELECTROSTATIC PRECIPITATOR
FROM ECONOMIZER
GRADE

Figure 2. Schematic - fly ash collection original installation.

side by magnetic impulse rappers. The discharge electrodes were weighted wire type, using air vibrators for rapping. Power was supplied from transformers through mechanical rectifiers. Single perforated plates were installed at both the inlet and outlet to obtain satisfactory gas distribution.

POTENTIAL FOR PERFORMANCE IMPROVEMENT

Condition of Existing Equipment

At the outset, the existing equipment was examined to determine the potential for upgrade. The mechanical collectors were found to be badly worn: several of the spinners showed advanced wear, and there were holes in a number of the tubes. The precipitator had several wires broken or missing, and a heavy ash buildup on those remaining. The collecting plates were heavily coated with ash. The perforated plates front and rear had some buildup, though were not plugged. The lower stabilizing frame was subject to sway. There were many ash deposits in the inlet and outlet indicating problems with gas distribution, and there were several leaks in the casing. The largest primary cyclones had inspection ports, and when examined appeared to be in satisfactory condition. The smaller ones, having no inspection ports, were not examined.

Improvement Requirements

The emission limitation of 0.65 pounds of particulate per million Btu's required about 90 percent overall removal efficiency of the dust control equipment. The results of the initial tests indicated overall efficiency of just under 88 percent, so the required improvement, at least on the surface, did not appear to be too difficult to obtain. Average efficiency of the mechanical collectors was 79 percent and of the precipitators 57 percent. The question then was, could the existing equipment be suitably modified or overhauled; or should it be replaced with new equipment, in view of the age of the equipment and the required performance increase? Although only a nominal overall improvement was actually required, in order to be sure that all tests would show compliance and in order to maintain a desired low particulate carryover for the future scrubber downstream, a somewhat higher target for overall efficiency was set. In fact, it was decided to try to upgrade the existing equipment to get the best possible performance improvement.

There were three choices for the mechanical collector. One, it could be completely overhauled with new tubes and low pressure drop spinners to minimize wear. Two, it could be completely overhauled as originally furnished with high pressure drop spinners to maximize performance. Or three, it could be gutted and not used.

The precipitator presented another problem. It suffered from a very low specific collection area, about 89 square feet per thousand ACFM, and a very high velocity of about 9.2 feet per second. In addition, the aspect ratio was only 0.9. The deposits of ash observed in the inlet and outlet during the initial inspection, and a brief examination of the ductwork configuration, indicated that a gas flow model study should be made to determine changes to improve the velocity distribution through the precipitator. It was also obvious from the type of power supplies and controls that much improvement could be made with modern electrical gear. Finally, it appeared that the rappers were not doing an adequate job of cleaning the electrodes. The wires that remained in the unit were in many cases kinked or bent so that clearances to the plates were considerably decreased. The condition of the precipitator casing was also questionable because of the number of holes that were observed during inspection.

Alternatives for Improvement

There was a valid question as to whether it might be more economical to install either new additional precipitator capacity or a baghouse, rather than upgrade the old equipment. There were also several other considerations in determining an alternative. The station suffered from a severe space limitation, typical of many backfits. Upon looking at a photograph of the plant before these modifications were made (Figure 3), it is obvious that there was no space available to put a longer precipitator between the ductwork coming from the air heater and the ID fan inlet. There was also a concrete deck extending part way over the existing precipitator which

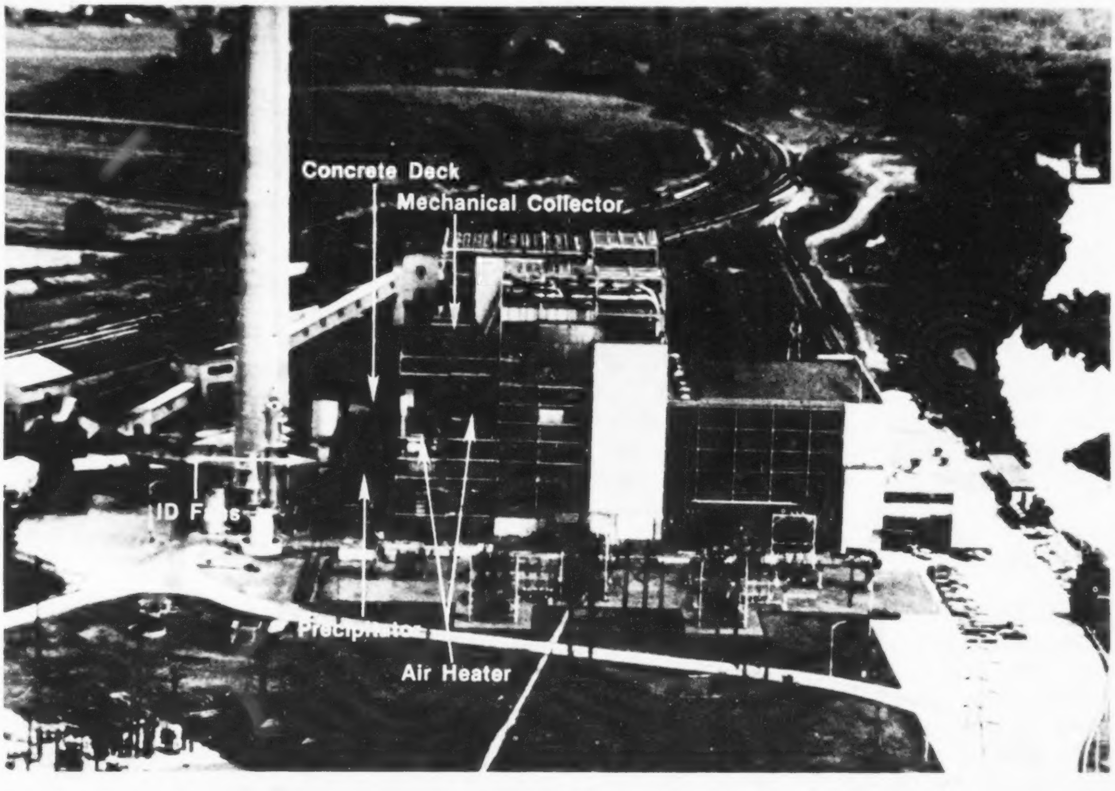

Figure 3. Cromby Station before modification.

effectively blocked installation of equipment above. Space upriver from the precipitator was obstructed by the No. 2 Unit and the area downriver from the precipitator was limited due to space allotment for the new scrubber, as well as to an existing substation. In addition to the space limitations, there were severe schedule restrictions. The consent agreement had stipulated that compliance must be achieved by April 1981, which left only about 16 months to make any improvements, to test to make sure those improvements were in fact doing the job intended and, if not, to make further improvements. There were also, of course, requirements for a minimum duration outage to make the modifications because of the cost of replacement generation.

SELECTED ALTERNATIVE

As a result of all these considerations, G/C recommended that the mechanical collector be refurbished, the precipitator upgraded, and a pulse-jet baghouse added to polish the dust conveying gas stream from the mechanical collectors (Figure 4). This option required replacement of the conveying fan to overcome the additional pressure drop imposed by the baghouse. G/C engineers were confident that the difficult schedule could be met. Looking back from the compliance date of April 1, 1981, testing the unit was planned for the end of February, which called for start-up around January 1. Since it was already mid-December 1979, only a little over a year remained to complete the project.

Several specific measures were considered for improving precipitator performance. Power could be maximized by replacing all wires with a later design and using heavier weights, replacing the old transformer-rectifiers with modern types having solid-state controls, and installing stabilizing insulators for the lower guide frame. Rapping could be improved by replacing all rappers with new magnetic impulse type having solid-state controls. Effective gas velocity could be improved by optimizing distribution and relocating the dust conveying gas duct discharge downstream of the precipitator. This would require installation of a baghouse to remove dust passed by the cyclones. It would have the effect of increasing the SCA and decreasing the velocity through the precipitator by about eight percent. The latter was felt to be critical because the scalping velocity was probably being exceeded.

PROGRAM EXECUTION

SCHEDULE

The planned schedule is shown in Figure 5. After the base performance test results were analyzed in mid-December 1979, the specification was written for model testing. It was decided that these test results were needed before the precipitator contract could be awarded, so a date of March 9, 1980 was requested for a preliminary report. In order to assure completion by the end of the year, it was necessary to award contracts for all major equipment by April 1. Although the initial stages occurred about a week late, the contracts were awarded on time. Erection was accomplished during a

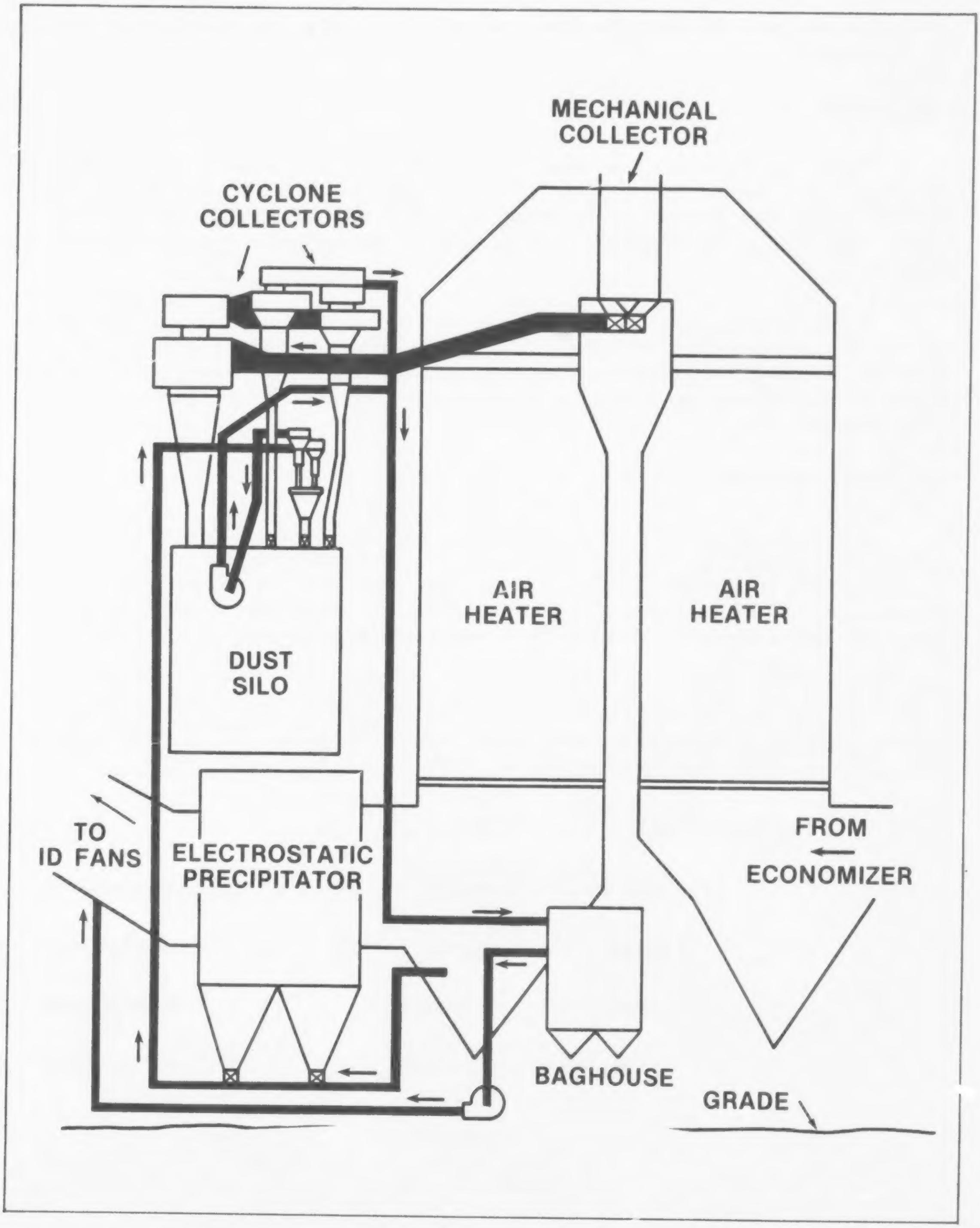
MECHANICAL COLLECTOR
CYCLONE COLLECTORS
AIR HEATER
AIR HEATER
DUST SILO
TO ID FANS
ELECTROSTATIC PRECIPITATOR
FROM ECONOMIZER
BAGHOUSE
GRADE

Figure 4. Schematic - fly ash collection modified installation.

five-week outage, followed by checkout and test prior to start-up at the end of the year.

MODEL STUDY

The first task was the model study which was necessary to determine if modifications would be required in the gas flow path. Accordingly, the specification was issued on December 24, 1979 and bids were due January 11, 1980. The study was subsequently awarded to NELS, Inc., of St. Catharines, Ontario.

Surprisingly, the velocity distribution which had been anticipated to be very bad turned out to be quite good, with RMS deviation of about 12 percent. Although it appeared improvement might still be made, NELS' experiments with turning vanes did not indicate sufficient improvement to justify the installation.

EQUIPMENT CONTRACTS

With the short bid time allotted, it was expected that it would be difficult to evaluate all the bids and award the contracts on schedule. However, with the number of bids received, the work was completed on time. Philadelphia Electric internally expedited its procurement process and the required approvals for purchase were immediately prepared.

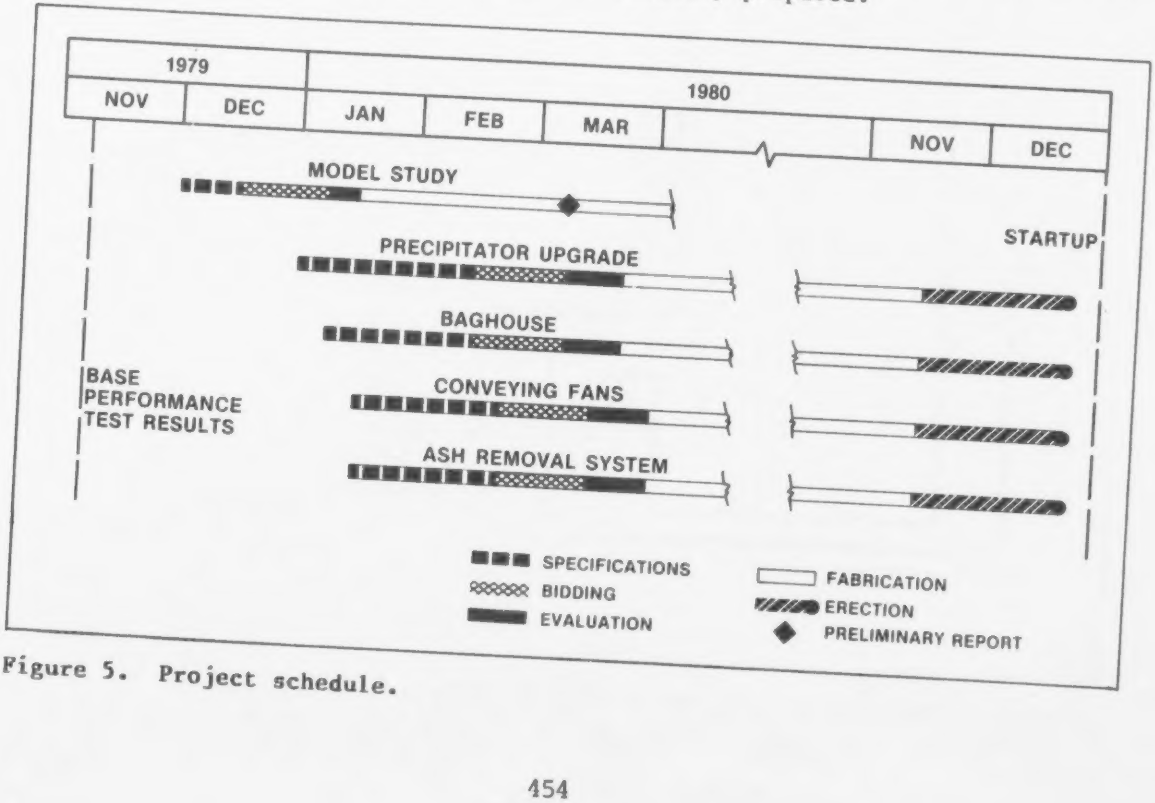

Figure 5. Project schedule.

Precipitator

The precipitator upgrade work was awarded to Belco Pollution Control Company. Their proposal covered the work requested, plus some innovative ways to increase sectionalization and improve rapping.

Shortly after Belco began design, the scrubber engineer informed the project engineers that the new ID fans which were to be installed to handle the scrubber pressure drop would impose a vacuum of about 20 inches of water on the precipitator. Accordingly, it was necessary to make an examination to see if the negative pressure could be withstood especially in view of the poor condition of the casing. Belco made this examination and recommended adding stiffeners on the inside of the casing. This was necessary since the outside of the casing between the precipitators was not accessible. To install the stiffeners, the collecting plates next to the walls would be slid or swung out of the way far enough to gain access to the casing wall. Belco subsequently was awarded an addition to their contract for this work, which was scheduled to take place concurrently with the other modifications.

Baghouse

Enviro-Systems & Research was awarded the baghouse. They proposed a four-module, pulse-jet unit with a gross air-to-cloth ratio of 3.86/1. Design dust loading was 3 grains per actual cubic foot. The bags were to be nominal 5 inch by 10 foot fiberglass having an acid resistant finish, with a fabric weight of 16 ounces per square yard, and a double-beam weave.

Other Equipment

The new single-inlet, airfoil vane, main conveying fans (one operating and one spare) were awarded to Westinghouse-Sturtevant. A vacuum ash conveying system was awarded to Allen-Sherman-Hoff.

DELIVERY, ERECTION AND START-UP

Equipment delivery and installation turned out to be a real challenge for both the project expediters and the field workers. It is a credit to all concerned that there was good cooperation among Philadelphia Electric's engineering, production, construction and start-up personnel, G/C engineers, United Engineers (the construction manager) and the vendors. There were many long days worked through the 1980 Christmas holidays in order for the equipment to be placed in service on schedule.

Erection was made more difficult by the weather. The winter was one of the area's colder ones, with several days during the erection and start-up periods being around 0^{o}F. Besides making work arduous, moisture condensation inside the equipment was a problem, making start-up tedious.

The unit went back into service on December 31, 1980. Because it had been a long cold winter and the work had been done very rapidly, a number of problems were revealed immediately after start-up. There was excessive sparking in the precipitator and there were problems with stuck butterfly dampers and malfunctioning controls in the baghouse. There were also problems with the ash system, primarily because the weather was below freezing and there was moisture in the ash lines which resulted in plugging. It was found that the sparking in the precipitator was caused by bits of welding rod and other debris which had been dropped inside the precipitator and which lodged in the expanded metal collecting plates. There were also some warped collecting plates next to the outside walls which had been bent when they were swung out of the way during installation of the casing stiffeners. The debris was easily removed; however, it was decided that the collecting plates, since they were expanded metal, could not be satisfactorily straightened. Therefore, it was necessary to remove a number of wires in the affected gas passages and to weld steel strips to the perforated plate ahead of those gas passages which were short on wires in order to restrict the amount of dirty gas that would flow through them. Although this was undesirable because it increased the velocity through the remainder of the precipitator, the project staff felt it was necessary in order to obtain satisfactory performance.

The sticking baghouse inlet and outlet dampers were trimmed in order to keep them from binding and much time was spent on the controls in order to secure proper cleaning sequences. Although the baghouse is equipped with hopper heaters, the ash lines plugged repeatedly because of moisture and improperly installed controls.

Start-up of the baghouse was done carefully. Since it was on a side stream, its use was not necessary until the unit was burning coal, so flow was not established during light-off with No. 2 oil. The conveying fan was started and the baghouse dampers were opened after two of the four mills were operating. Meanwhile, the baghouse hopper heaters had been on for over a day.

COMPLIANCE TESTING

Problems with the equipment were corrected to the point that the unit could be tested for compliance. This was done early in March of 1981; fortunately, the results were nearly as anticipated. The unit averaged a little over 0.5 pounds of particulate per million Btu's during three tests. This worked out to a little over 93 percent overall efficiency.

UNIT PERFORMANCE AND PROBLEMS

Concurrently with the compliance tests, the unit was also tested for equipment performance. These results are compared with the base data tests in Figure 6.

Although the unit passed the required tests, all was not completely satisfactory. As shown in Figure 6, the mechanical collector had actually decreased in performance, probably because of the lower loss spinners, and was performing at 67 percent. However, the precipitator, bent plates and all, was performing at up to 85 percent efficiency. The baghouse was

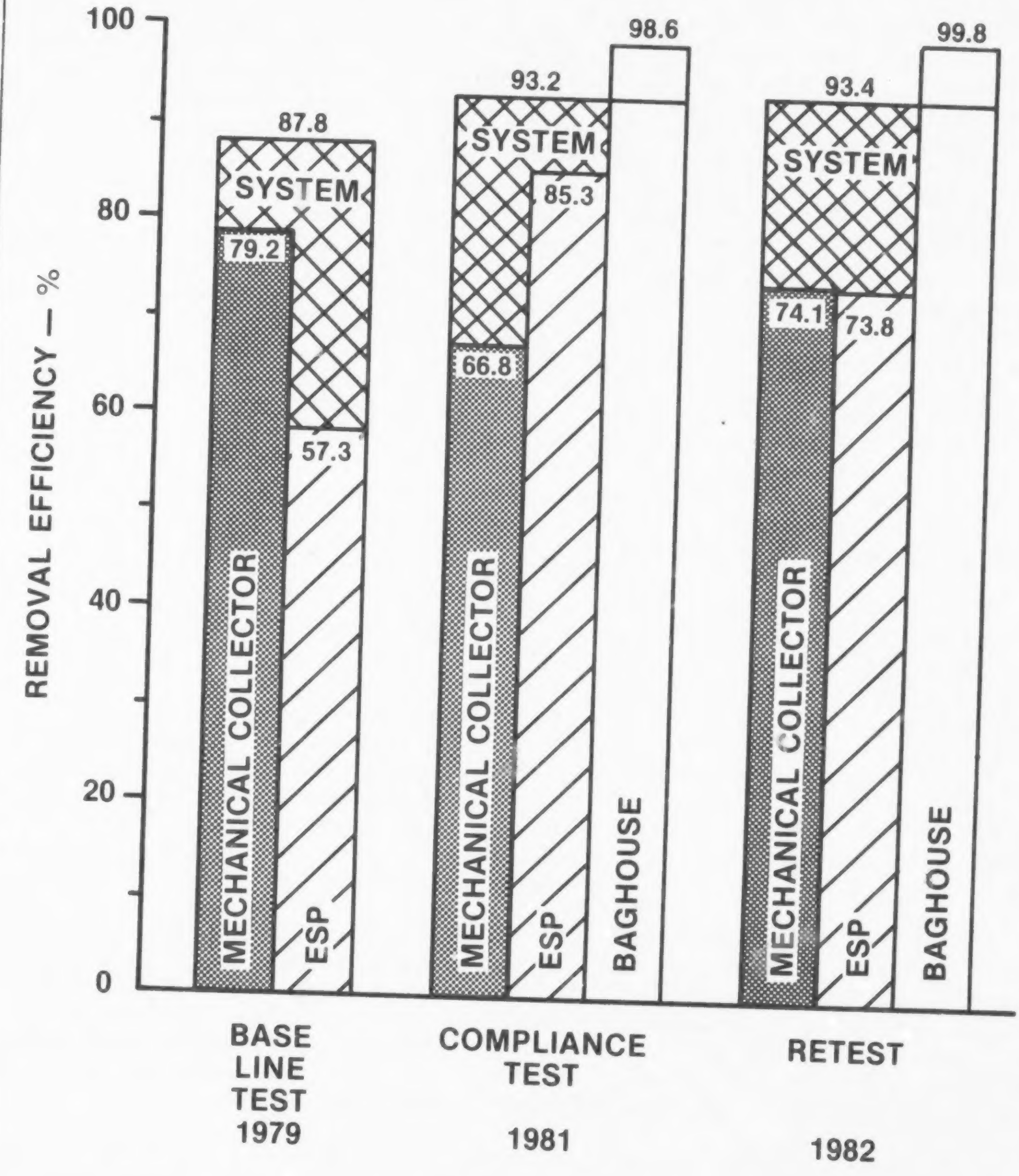

Figure 6. Performance test results.

reaching 98.6 percent efficiency, but was experiencing early high pressure drop and it was difficult to remove the cages and bags for inspection. The latter problem was finally traced to an internal cuff in the bags combined with oversized cage end caps, which prevented cages from being extracted from the bags. This delayed an investigation of exactly what was causing the high pressure drop because a bag could not be removed with the baghouse in service. By the time a bag could be removed and sent to the laboratory for investigation, the bags were completely blinded, after less than four months use. A further investigation by TexLab, Inc., of trial bags of different material indicated that not only the original bags but also two Huyglas and two Teflon felt bags were blinded with fine particulate which was penetrating the cloth to the degree that it could not be removed with normal cleaning. Tests for particle size distribution were made indicating a mean particle size of about seven microns, by Bahco analysis. There was also a significant quantity of fines. The reason for this is apparent when one examines the system schematic in Figure 4. The baghouse receives the finest particulate because the gas has previously passed through cyclone collectors. Cyclones, being most efficient on large particles, leave the small particles to be removed by the baghouse. Although this was anticipated, the number of fines was larger than expected. In order to alleviate the problem, it was decided that a partial bypass around the large cyclones would be installed, taking dust directly from the mechanical collectors so that more of the coarse particulate would be introduced to the baghouse, at the slight expense of higher dust loading.

The testing program had also disclosed that the secondary cyclones which remove the ash conveyed from the precipitator hoppers were passing a large quantity of material and in fact appeared to be leaking. Therefore, when a 12-week outage was scheduled for the end of 1981 to install new ID fans, a number of different tasks were planned to improve the interim modifications. The baghouse had to be rebagged, and it was decided that the original fabric was still the most suitable choice for this, but with a revised bag cuff design. Also, new cages having smaller diameter end caps were furnished by the vendor, and the partial bypass around the cyclones was installed. The secondary cyclones were scheduled for refurbishment. When they were dismantled, a great deal of pluggage and erosion was found.

Once again start-up took place around the first of a year, in late January 1982. The baghouse was precoated using pulverized limestone and started using similar procedures to the previous year. However, this time a program was followed to establish the best cake possible in order to keep the fines from penetrating the cloth. The baghouse was started with on-line cleaning, and pulse air pressure was set at 55 psig. Cleaning was initiated when overall pressure drop reached about 5 inches of water.

Initially, things looked much better than they did the year before, and a new test was performed the end of February. Overall performance results were very good, indicating that the unit was emitting about 0.35 pounds particulate per million Btu's or again a bit over 93 percent efficiency. However, the baghouse, in spite of the work done on it, again began to creep up in pressure drop until the bags again blinded. Although the cyclone bypass appeared to have increased the mean particle size to the baghouse, it had apparently done nothing to decrease the overall high number of fines.

At the time of this writing the baghouse has recently returned to service (9/20/82) after a one week outage during which new woven fiberglass bags were installed, Staclean diffusers were installed, the pulse pipe sequence was changed to random and the pulse air pressure setting was raised to 110 psig.

Additional measures which may be implemented, if found necessary, are to enlarge the pulsing system and to use bags made of a felted fabric.

CONCLUSION

The modification program was successful in achieving compliance with the required emission limit. The blinding problem, although troublesome, appears to be solvable. The large amount of work that was performed in a short period of time demonstrates that a cooperative effort can accomplish a great deal. The fact that the unit is in compliance at full rated load points to the real success of the project.

The work described in this paper was not funded by the U.S. Environmental Protection Agency and therefore the contents do not necessarily reflect the views of the Agency and no official endorsement should be infered.

HIGH SULFUR FUEL, FABRIC FILTER STARTUP EXPERIENCE

by: Phil Hanson
Power Production Manager
City Power and Light Department
Independence, Missouri 64056

Larry Adair
Project Manager/Senior Engineer
Phelps and Phillips
Independence, Missouri 60455

Robert N. Roop
Product Manager
Research-Cottrell, Inc.
Somerville, New Jersey 08876

Robert B. Moyer
Manager Fabric Filter Applications
Research-Cottrell, Inc.
Somerville, New Jersey 08876

ABSTRACT

The long term operation of fabric filters on low sulfur fuels has been, with a few exceptions, well demonstrated. Similar experience on high sulfur coals has not yet been gained. As utilities continue to convert to coal, reliability of fabric filters for high sulfur coal service will be of paramount concern.

The City of Independence, Missouri, recently put into service a fabric filter designed for three to five percent sulfur coal flue gases. Details of the design will be discussed. Anticipating the opportunity to test in real

world conditions, a bag evaluation program was initiated and is in progress. Physical and mechanical properties of the bag fabric are being tested to determine the effects of high sulfur service and a possible relationship to bag life. Results of that bag test program, as obtained to date, and its implications will be presented.

PLANT HISTORY

The two unit Missouri City Power Station, now owned and operated by the City of Independence, Missouri, was originally owned and operated by the N.W. Electric Power Cooperative, Cameron, Missouri, a member of Associated Electric Cooperative, Inc., Springfield, Missouri. Two identical generating units of 22 MW each were put into operation in 1954 at a site located adjacent to the Missouri River approximately eight miles northeast of Independence.

Foster Wheeler boilers each generated 220,000 lbs/hr of steam by oil and coal firing to drive Westinghouse turbine generators. Mechanical cyclones provided particulate collection. In addition to the boilers, turbine generators and their auxiliary equipment, the site included coal and oil unloading and storage facilities, ash pond, cooling water intake structure, well water storage reservoir, railroad sidings, transmission lines and a substation for power transformation and distribution. The substation and transmission lines remain the property of N.W. Electric Power Cooperative, Inc.

Air Pollution emission limitations entitled "Air Quality Standards and Air Pollution Control Regulations for the Kansas City Metropolitan Area" were adopted by the Missouri Air Conservation Commission on January 5, 1969, and were applicable to the Missouri City Plant. The state cited the Missouri City Plant for violation of visible emission limitations on March 25, 1970.

The N.W.E.P.C. was granted variance to burn coal by the Air Conservation Commission of the Missouri Department of Natural Resources (DNR), but soon afterwards the EPA issued an administrative order requiring compliance with the regulations by the installation of electrostatic precipitators.

In early 1975, N.W.E.P.C. requested that the state variance and the federal administrative order for ESP's be withdrawn. The request was based on escalating coal prices. While at the time, coal was costing $0.62 per million BTU and oil $1.80 per million BTU, it was projected that coal would increase to $1.77 per million BTU by 1978. Considering the projected rapid escalation of coal cost, the cost of ESP's and the limited use of the Missouri City Plant, N.W.E.P.C. wanted to revert to oil firing to comply with the air pollution regulations. The DNR and EPA amended their orders to allow for such.

In September, 1975, the Missouri City station experienced an electrical fire which destroyed the plant's high voltage switchgear and much of the adjacent plumbing, wiring and mechanical systems. The N.W.E.P.C. decided not to repair the damages and closed the plant; Associated Electric Cooperative had available other generating equipment better suited to its system.

During the middle 70's rapidly escalating oil and natural gas prices prompted a need for the City of Independence to look for additional base and intermediate load coal-generated capacity. The city was operating three coal-fired units at its Blue Valley Station and several oil and/or gas-fired combustion turbines throughout its system. Phelps, Hogland & Phillips Engineering Company was hired to study the City's power needs and various possible power supplies. These studies and much negotiating resulted in the City's purchase of the Missouri City Power Station in 1979. Engineering for renovation of the plant and the installation of necessary particulate collection equipment to permit coal firing was awarded to Phelps, Hogland & Phillips.

FABRIC FILTER SELECTION

Three major factors contributed to the selection of a fabric filter for controlling particulates from the Missouri City Power Station:

UNKNOWN COAL SUPPLIES

Engineering to provide quick reactivation of the plant was begun as soon as it became apparent Independence would become the new owner. The contract to provide air pollution control equipment was directly on the critical path, but at that time the City had no long term coal supply with a well defined quality. The ability of the boilers to burn a variety of fuels dictated that the air quality system also have that capability.

ALLOWANCE FOR FUTURE REQUIREMENTS TO REDUCE SULFUR EMISSIONS WITHOUT HARMING PARTICULATE COLLECTION

The City's Blue Valley Power Station had been restricted on allowable sulfur emissions. A need to make further restrictions to control ambient air quality in the Kansas City area was a possibility. Any reductions requiring the burning of low sulfur coal would not inhibit the collection capability of a fabric filter.

ON-LINE MAINTENANCE

Since one of the reasons the Missouri City plant was being renovated by the City was to replace oil and gas-fired generation, outages that required utilizing combustion turbines would be costly; continuity of service with on-line maintenance of the air pollution control equipment was an important criterion. However, funds for renovation were not unlimited. The flexibility of a single multicompartment baghouse to serve both units while providing the capability of on-line maintenance was a good fit.

The specification for the fabric filter was published for bidding on September 4, 1979, with bids received November 5, 1979. The contract was awarded in December, 1979. Construction began in January, 1981 and was completed in December, 1981. Start-up was in late March, 1982; testing was conducted in July, 1982.

FABRIC FILTER DESIGN

The contract was placed with Research-Cottrell (R-C) for complete system responsibility. R-C work commenced at the discharge of the existing I.D. fans atop the roof of the boiler house, included dismantling of the tie-duct between the fan and the old stub stacks, and terminated at the discharge of two new booster I.D. fans into a new common chimney.

The scope encompassed design, engineering, fabrication and erection of the inlet ductwork, including modulating I.D. fan discharge dampers from the existing fans, bypass system, fabric filter, discharge ductwork, booster I.D. fans, ash handling equipment, insulation and the erection of all supplied equipment.

The gas cleaning equipment for the unit is a Research-Cottrell reverse air fabric filter consisting of eight (8) modules, 4 deep x 2 wide. Each module contains 336 filter bags, 23' long x 8" diameter, which result in a total filter area of 126,928 ft^2 (111,062 ft^2 with one module off). Gas-to-cloth ratio with 8 modules on line is 1.78 ACFM/ft^2 cloth and 2.27 ACFM/ft^2 with 7 modules on line including R/A flow. Filter bags are constructed of 14 oz./yd^2 woven fiber glass cloth with an acid resistant finish of polymer/silicone-graphite-teflon. Table 1 shows the fabric filter design data and Table 2 describes the filter bags.

TABLE 1. FABRIC FILTER DATA

	Design
Flue Gas Volume (ACFM)	226,000
Temperature (^{O}F)	310
Inlet Dust Loading (Gr/ACF)	4.64
Gas-to-Cloth Ratio (Gross)	1.78:1
Net (w/o Reverse Air)	2.035:1
Net (w/Reverse Air)	2.27:1
Outlet Loading (Gr/ACF)	0.010
Number of Compartments	8
Gross Cloth Area	126,928
Total Bags	2688

TABLE 2. FABRIC FILTER BAGS

TYPE:	Fiberglass (ECDE) with Acid Resistant Finish
SPEC:	Weight - nominal 13.5 oz/yd^2 Permeability - 40-55 CFM/sq. ft. @ 0.5" W.G. Count - 44 x 24 Weave - 3 x 1 twill Fiber Thickness - 0.015 in. Weave - Warp: 37 1/0(F) Fill: 75 1/2(T) + 75 1/0(F)
DESIGN:	Bag Size - 8" dia. x 23'-0" (L/D = 34.5:1) Bottom Attachment - Snap Ring Top Design - Banded Top With Disposable Cap Rings - 4 carbon steel anti-collapse rings/bag

Cleaning of the modules is accomplished by a reverse air system which pulls clean gas from the common outlet duct and discharges it into an isolated module, collapsing the filter bags and dislodging the collected particulate. Reverse air (gas) is supplied by two (2) reverse air (R/A) fans (one operating, one standby), each rated at 26,000 ACFM requiring 125 HP motors.

System booster fans are located downstream of the fabric filter and are rated at 135,600 ACFM, 300 HP each. Each fan's inlet louvre damper is positioned and operated by a Bailey Control System. The Bailey Control signal is based on the static pressure at the outlet side of the boiler I.D. fans.

Hopper ash removal is accomplished by a Hydro Ash System. Ash is pneumatically conveyed from each hopper in sequence, mixed with the vacuum-producing water and gravity-flowed to a nearby ash pond. The controls sequence the compartment discharge feeder immediately after the compartment cleaning cycle.

The fabric filter is designed to treat 226,000 ACFM of flue gas at 310°F. The collection efficiency is to be 99.8% (based on a minimum inlet loading of 4.64 GR/ACF) with one (1) module out of service. System pressure drop is guaranteed to be 8 in. W.C. or less across the baghouse, ductwork and dampers.

FABRIC FILTER STARTUP

PRE-COATING

Since the plant's flyash is generated from burning high sulfur fuel, it was Research-Cottrell's recommendation that the filter bags be pre-coated to add protection for the bag fabric. An inert, moderate particle size diameter, low sulfur ash was chosen for the pre-coat. The selected ash was trucked to the site and conveyed via 4" diameter hoses to individual compartments using a blower on the truck.

The pre-coat operation was started with one booster fan operating, all compartment inlet dampers closed, and the baghouse bypass dampers closed. Ash was injected to each compartment through the hopper access door. Initially there was little increase in ΔP on module photohelic gauges using this method. It was obvious some ash was getting onto the bags because the shutting of the outlet dampers caused ash to fall back into the hoppers. This method was continued until the ash truck was empty. There was an ash level in each hopper up to the door. Continued operation of the booster fan and air lancing of the ash in the hoppers re-entrained it in the air flow to the bags. The second booster fan was then operated with minimal inlet damper opening and 90% on the first fan damper. One compartment inlet damper at a time was opened (also one bypass damper) and air lancing of the hoppers continued. This operation was maintained until at least three-quarters of the ash was held on to the bags.

After all hopper doors and inlet and outlet dampers were closed, there was no evidence that a significant amount of ash fell off the bags. It took only a very short time to pull the remaining ash from hoppers through the ash system. The maximum ΔP indicated on any module during this pre-coat procedure was 1" W.C.

INITIAL BAGHOUSE OPERATION

The following conditions were required for initial baghouse operation: one boiler operating at full load (20MW), for a minimum of one (1) hour at steady state conditions.

Baghouse conditions prior to putting first module on line are summarized below:

- One booster fan operating with damper 60% open (Note: at this time fan damper operation was in manual and was not being controlled at desired 1" W.C. boiler outlet pressure).
- Bypass damper open
- Outlet dampers open
- Inlet dampers closed
- Reverse air (R/A) dampers closed
- Reverse air (R/A) fans off
- Hopper heaters on (24 hrs.)
- Module ΔP = 0" W.C.

The No. 1 module was placed on-line by opening the inlet damper. Indicated module ΔP increased to 0.5". After approximately 1-1/2 hours of operation, no obvious increases in ΔP were noted. At this time Module No. 5 was placed in service, a ΔP of 0.5" was observed.

After about one more hour of operation, Modules No. 2 and No. 6 were placed into service. One bypass damper was then closed. The ΔP across in-service modules rose to 1". Modules No. 3 and No. 7 were placed in service followed by the remaining modules No. 4 and No. 8.

The time taken to bring all modules in service and to close the second bypass damper was five hours.

After closing of the last bypass damper the increase in module ΔP became more obvious. Within one hour, the maximum ΔP was up to 3".

At this time, modules with the highest pressure drop were nulled (outlet damper closed) one at a time and then placed back on line. The effect was significant. When each compartment was placed back on line its pressure drop had been reduced to between 0.5" and 1". The conclusion was that most of the new filter cake could be removed during a null without reverse flow and therefore the bags were not blinding. No reverse air was used during this time.

After approximately 32 hours of operation the baghouse was placed back into the bypass mode and the modules were taken out of service (inlet and outlets closed) in order to begin startup of the second boiler.

When the second boiler was up to full load and operating at stable conditions with no oil for one hour, the baghouse was placed back into service for both boilers. The normal startup method just described was employed with minor exceptions. All inlet and outlet dampers were opened. Time for modules to stabilize was allowed and then both bypass dampers were closed.

Indicated ΔP across the modules began increasing at a faster rate than with just one boiler as would be expected. After a short period when ΔP had increased to around 2", nulling was tried to see what effect it would have. Little or no effect was observed. At this time a reverse air fan was started.

Initial operation with the R/A fan, with manual control cleaning of a module, showed when cleaning was started at 3.5" to 4" ΔP, cleaning for a few seconds would drop the ΔP in the clean module by 1". During this period great difficulty in opening the reverse air dampers was encountered due to high static pressure in the closed reverse air duct. After overcoming the static pressure, R/A poppets would surge open nearly half way. Cleaning in this method resulted in puffing even with long settling times.

REPAIRS AND MODIFICATIONS

Stack puffing was deduced to be caused by the in-rush of gas into a module from the R/A system when a R/A poppet opened. The expansion of the gas in the system and lag time before the fan automatically throttled-down would force gas out the inlet duct into the other modules. A stack puff would then occur. This puff was eliminated when the module inlet damper was closed at the start of cleaning. Although satisfactory, a different solution was sought.

To reduce the R/A duct static pressure and the initial, fully opened damper-related surge, modifications were made to the fan damper control system within the Bailey controls. Originally one damper set point existed which controlled the dampers to maintain a given fan motor current. With all R/A dampers closed (between cleaning periods), the dampers would open fully in response to a control signal to increase fan current. This philosophy resulted in high static pressure in the R/A duct, and full volume condition when cleaning started. A device was backfit into the Bailey system to supersede this setpoint until a R/A poppet was fully open. The device drives the R/A fan damper fully closed. When the R/A poppet is fully open (limit switch contact made), damper control seeks the motor amp set point and R/A volume increases.

Because the fan dampers are not totally gastight, enough gas is still passed to develop a moderate static pressure in the R/A duct. A second modification was made to bleed off this additional gas and keep the static pressure low. Three 4-inch pipes were installed between the R/A and outlet ducts. These allowed a small volume to bleed off but did not affect the cleaning volume. Experimentation indicated only one pipe was necessary; caps were screwed onto the other two.

TUNING

Initial cleaning adjustments were made June 8-10, 1982 at 75% boiler load. Final tuning was accomplished during the week of July 12-16 at 100%.

Full 100% load operation was observed at this time and final adjustments were made. Figure 1 shows operation of the cleaning system with a 4.5" W.C. start-cleaning set point, 60% opening of R/A inlet damper and approximately 45 seconds of R/A cleaning time per compartment. Figure 2 shows the same 4.5" W.C. start point but with longer cleaning time (180 seconds indicated) and R/A inlet damper 100% open.

In figure 1, it can be seen that the inverval between cleaning cycles decreases with time and that the clean cloth ΔP increases from 2.8 to 3.8. After adjustment to the R/A cleaning duration and flow, clean-down has consistantly held between 3.0-3.5" ΔP and the duration between cleaning cycles has remained the same.

PERFORMANCE

On July 14, 1982, the fabric filter system was tested for compliance and performance. Fuel analysis for the tests and design values are noted in Table 3. The inlet test ports for ΔP readings were located just downstream of the boiler #2 I.D. fan discharge after combining the flows from boilers 1&2. The outlet pressure taps are located just beyond the outlet flange of the baghouse prior to the inlet of the new booster fan inlets.

TABLE 3. FUEL ANALYSIS

Constituents	Range %	Design %	Average As Tested %
Sulfur	2.0 - 4.1	2.7	4.05
Ash	5.0 -19.0	12.8	11.88
Moisture	2.0 -17.0	7.4	8.75
Carbon	57.6 -70.5	64.6	67.97
Hydrogen	3.5 - 5.0	4.7	4.87
Nitrogen	.7 - 1.8	1.4	0.8
Oxygen	5.5 - 9.0	6.4	10.53
Heat Value (BTU/#)	10,500-13,500	11,700	12,800

At maximum tested gas flow of 210,000 ACFM, the maximum system ΔP was measured at 6.9" W.C., when the first compartment was isolated during the cleaning cycle. This ΔP is dependent on the ΔP utilized to initiate the cleaning cycle and was within the guaranteed value. A summary of performance data is included in Table 4.

TABLE 4. FABRIC FILTER PERFORMANCE DATA

	Design	Tested*
Flue Gas Volume (ACFM)	226,000	210,000
Temperature	310°F	342°F
Inlet Dust Loading (Gr/ACF)	4.64	2.025
Gas-to-Cloth Ratio (Gross)	1.78:1	1.65:1
(Net)	2.035:1	1.89:1
Outlet Loading (Gr/ACF)	0.010	0.0081
Removal Efficiency (%)	.998	.996
Opacity (%)	20	3
System ΔP ("W.C.)	8.0	6.9

*Average of 4 runs

BAG TESTING PROGRAM

For this first baghouse to see high sulfur fuel utilizing a bag finish of polymer/silicone-graphite-teflon, it was determined that a bag fabric testing program would be undertaken. The acid-resistant-finish fiberglass cloth had shown excellent life on low sulfur with occasional high sulfur exposure at United Power Association's Elk River station, but Independence would be the first high-sulfur-only exposure. The testing program was designed to examine bags in operation for increasing periods of time to determine the cumulative effect of high sulfur exposure. Standard fabric tests including weight, permeability, breaking strength, Mullen burst, MIT flex and LOI were run. In addition, the pH of the dust cake was measured.

Bag weight and permeability measurements can be indicative of bag blinding. Breaking strength, Mullen burst and MIT flex tests are measures of chemical, physical or thermal degradation of the cloth. LOI (loss on ignition) shows the presence or absence of the finish. For comparison purposes, new bags are used as the base for determination of any degradation. Weight and permeability are measured with the dust cake on the fabric and after it is removed by vacuuming and washing. Figures 3, 4 and 5 graphically summarize the MIT flex tests and breaking strength results. All of the test results are enumerated in Table 5.

TABLE 5. CITY OF INDEPENDENCE TEST REPORT

	NEW	APRIL	JULY	AUGUST	SEPTEMBER
Weight (oz/yd^2)	13.5				
Top		18.4/13.6	23.3/13.6	23.2/13.6	22.2/13.7
Bottom		18.1/13.7	22.2/13.6	22.3/13.6	22.1/13.7
Permeability (cfm/ft^2)	47.0				
Top		4.73	1.79	1.73	1.93
Bottom		5.20	2.65	2.19	2.06
Strength (psi) (WARP/Fill)	592/292				
Top		601/280	424/191	385/162	384/149
Bottom		599/278	431/193	380/159	393/151
Mullen Burst (lb/in^2)	805				
Top		725	538	470	476
Bottom		739	537	448	485
MIT (cycles) (WARP/Fill)	40,038/3,517				
Top		35,020/1,625	6,705/631	4,659/584	4,785/515
Bottom		36,881/1,643	6,666/629	4,779/589	4,465/513
L.O.I.	4.6	4.5	4.6	4.3	4.4
pH*	-	9.8	3.72	3.7	

*Surface pH on bag after cleaning cycle

Note: Values in "new" condition reflects fabric tested to determine initial values and not published data.

The permeability in the "as received" condition averaged between 1.8 - 2.65 CFM/sq. ft. for bags tested during the last three test periods. These values correspond with values obtained from Research-Cottrell's Elk River installation employing identical acid-resistant-finish bags. At these permeabilities, the differential across the cloth is a maximum of 4" dirty and approximately 2½" immediately after cleaning.

After vacuuming the "as received" fabric, the vacuumed permeability ranged between 11.2 - 12.6 cfm/ft^2. This is somewhat lower than expected. Under microscopic examination, the cloth interstices show nodules with a high sulfate content which had encapsulated the surface filaments thus preventing proper dust release. The low pH of the dust cake solution supports this observation. However, as previously stated, it appears that it is not significantly affecting the cloth resistance while operating within the baghouse. The washed permeability returned to the values in the "new condition".

The L.O.I. of the acid-resistant finish is specified at a minimum of 4% by weight of the greige goods. Since after seven months of operation, the tested L.O.I. values exceeded the minimum of 4%, the results clearly indicate its stability.

The M.I.T. flex cycle tests are indicative of the number of flexes-to-failure which provides a comparison with other fabric flex tests. This M.I.T. flex endurance test is probably the most misinterpreted and misunderstood test as applied to bag life in baghouses today.

Many variables affect M.I.T. flex-to-failure. These variables consist of yarn construction, twist levels, method of texturizing, finishing, treatment procedures, finish cure time/temperature, operation time and temperature in a baghouse, removal efficiency of volatile matter and embedded abrasive particles within the yarn structure.

A fabric with a high flex value compared to a fabric with a low flex value does not necessarily mean that one is superior to the other. A good way to compare one fabric to another is to evaluate the percent loss of M.I.T. flex cycles based upon the environment to which the fabric is exposed.

Fiberglass is the primary fabric in the utility and industrial fly ash particulate market. That fabric will usually stabilize after 4-6 months of operation at approximately 50% reduction in M.I.T. flex cycles compared to new fabric. This reduction is primarily caused by physical and thermal deterioration upon first exposure to flue gas.

Upon reaching equilibrium, the fabric M.I.T. cycles will remain virtually constant until the fiber begins to show additional fatigue or breakdown due to chemical, thermal, or additional physical deterioration. Upon drastic degradation from equilibrium, the rate of fiber fatigue/breakage due to physical deterioration may indicate that the fabric is about to fail and bags should be considered for replacement.

If chemical or thermal deterioration also occurs, the equilibrium value of flexes will be lower than fabric flex values caused by physical deterioration only. Chemical and thermal deterioration usually occurs rapidly and can be easily measured. Once chemical or thermal adverse conditions cease to exist, fabric degradation stops. Physical deterioration generally occurs where movement in the fabric exists.

For example, reverse air cleaning causes local physical damage at the flex zone. Chemical deterioration occurs throughout the entire fabric.

By comparing flex values, between "flex fold" and "non-flex fold" areas, levels of chemical vs physical deterioration can be established. As an example, consider the flex cycle from the July test. The new fabric flex cycle was 3517. Assuming the normal 50% reduction to reach equilibrium, 1759 flex cycles would have been expected. However, due to chemical, thermal and physical deterioration, the actual equilibrium norm was at 630 cycles, (test on flex fold position), which equates to an additional 32% loss.

$$\frac{3517 - 630}{3517} = 82\%;\ 82\% - 50\% = 32\% \text{ additional reduction}$$

Therefore, we can presume that the fabric deteriorated the equivalent of 1129 additional flex cycles due to chemical and physical deterioration (1759 - 630 = 1129). From further testing of the fabric on the "off-fold" section, we obtained a flex cycle value of 790 cycles vs the 630 cycles from the "on fold" section. Subtracting this "off-fold" value from the equilibrium norm we can speculate that the difference in flex cycle loss was due strictly to chemical attack (1759 - 790 = 969 flexes) or 86% of the additional loss was due from chemical deterioration $1 - \frac{1129 - 969}{1129} = 86\%$ and 14% was due to physical deterioration (1.00 - .86 = 14%).

BAG FAILURES

Knowing that most baghouse outlet loadings usually are below 0.005 GR/ACF on utility applications, it was quite surprising to observe loadings up to 0.0081 Gr/ACF during the performance test. Approximately a week after the performance tests were conducted, the boilers came down. During an inspection of the baghouse 34 failed bags, over 1½% of the total installed quantity, were found.

To date, a total of 93 bags have been replaced due to mechanical fiber fractures, as shown in the photomicrograph Figure 6. Of the 93 bags replaced, 34 were completely failed where the bag had actually separated from the cap, and the additional 59 appeared ready to separate; the top band was visible, but was still in contact with the cap. (Figure 7). It appears from numerous microscopic examinations that when the caps were installed in the bags by the bag manufacturer, the packers apparently pulled on the top cuff area incorrectly when seating the band and fabric against the cap seat, thus severing the fibers.

Further inspection revealed that this top band was not wrapped with a protective cover nor was the body of the bag folded over to give a separate layer of fabric between the band and bag body.

To date, ten complete examinations have been performed on used bags and two new spare bags and only four of the ten did not reveal this fiber fracture. In one instance, several yarns had all 1632 filaments severed, all in the position coinciding with the band top edge. All fractures were at the top interior side of the bags, thus making it impossible to observe the defects without removing the cap and cutting the fabric at the band.

Observing the fractured filaments also in the new spare bags confirms that the damage originated prior to installing the bags in the baghouse.

A survey of bag suppliers was undertaken to question methods of installing these bands in bags. The majority responded that their standard construction for 8" or 12" dia. bags includes a pre-wrapped band or the bag body folded over to protect the bag itself from the band. As a recommendation to end users and O.E.M.'s to eliminate problems such as this, specifications issued to bag manufacturers should specifically require that all bands and ring covers be independently wrapped or that multiple layers of fabric exist between any metal object and the bag body itself.

CONCLUSIONS AND RECOMMENDATIONS

1. The City of Independence fabric filter is surpassing all performance guarantee requirements while high sulfur fuel is being burned. The air quality system has not caused any boiler outages.

2. Startup was uneventful with only minor modifications required.

3. Pre-coating the bags with inert flyash appears to have reduced the degree of bag blinding from chemical attack to a nominal level.

4. Reduction in MIT flexes-to-failure and tensile strength occurred after startup. An equilibrium condition has been reached.

5. Continued monitoring of bag condition is recommended to predict baglife.

6. Bag construction specifications should include provisions to prevent any metal and hardware contact with the bag cloth.

ACKNOWLEDGEMENT

Research-Cottrell wishes to acknowledge the Environmental Consultant Company of Phoenix, Arizona for their assistance in performing physical/mechanical, chemical tests and for the photo micrographs of bag fabric.

DISCLAIMER

Findings and projections regarding fabric filter performance and durability which appear herein are strictly for the purpose of scientific and technical inquiry and should not be construed as representations or warranties regarding characteristics of fabric filter systems marketed by Research-Cottrell.

The work described in this paper was not funded by the U.S. Environmental Protection Agency and therefore the contents do not necessarily reflect the views of the Agency and no official endorsement should be inferred.

Figure 1

City of Independence
Interval Between Cleaning Cycles
Decreased Down to Near 20 Minutes Between Cycles

7/12/82

4.5" ΔP Initiation of cleaning
60% Inlet damper opening RA fan
45 Sec. (indicated) RA poppet opening

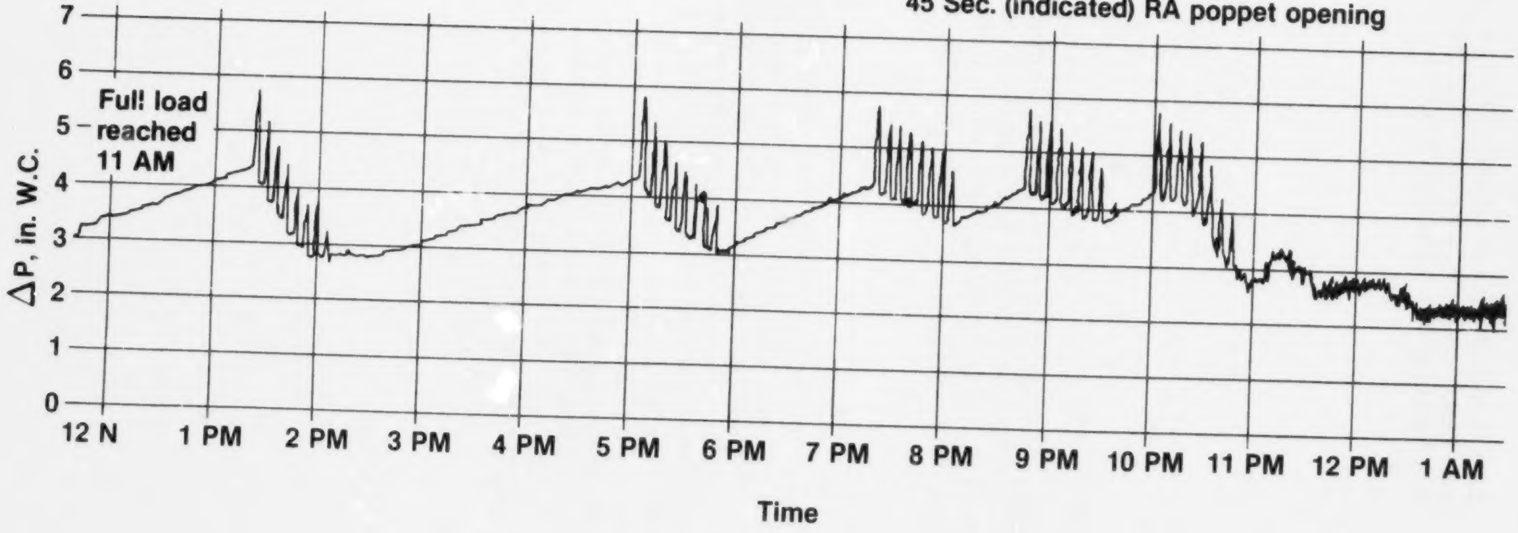

Figure 2

City of Independence

Cleaning Cycle After Final Tuning

7/14/82

4.5″ Δ P Initiation
100% Inlet damper opening RA fan
180 Sec. (indicated) RA poppet opening

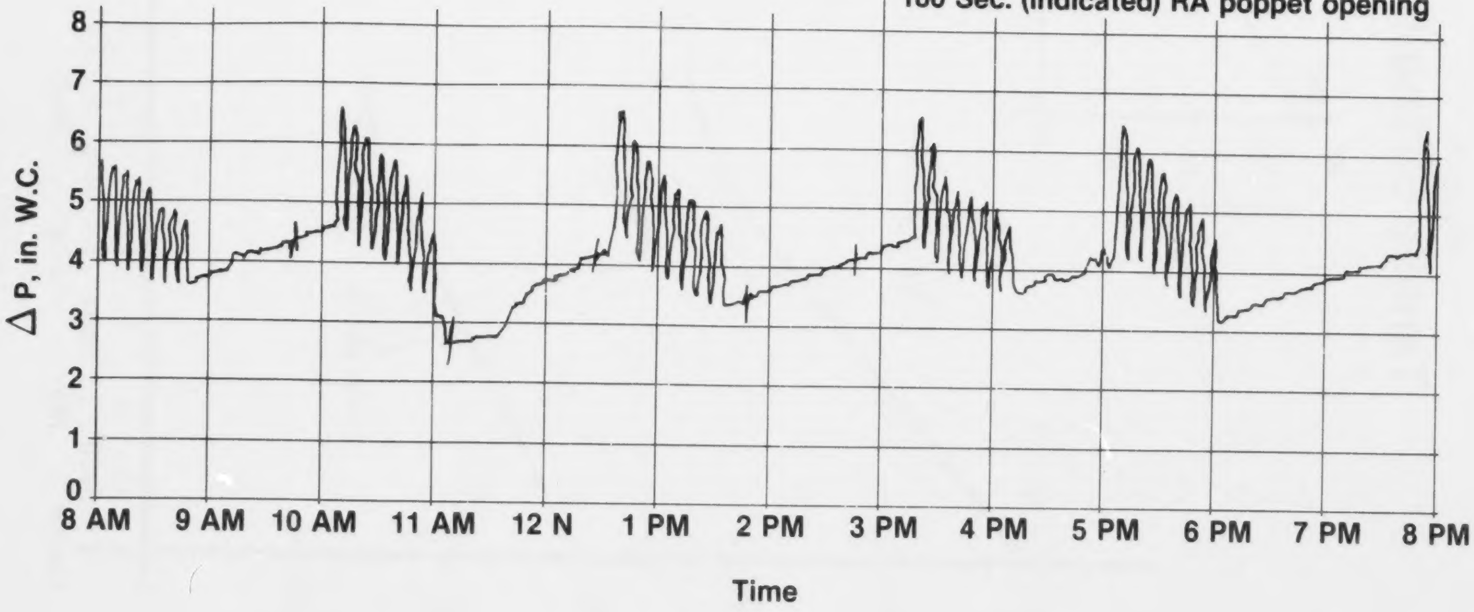

Figure 3

Tensile Strength

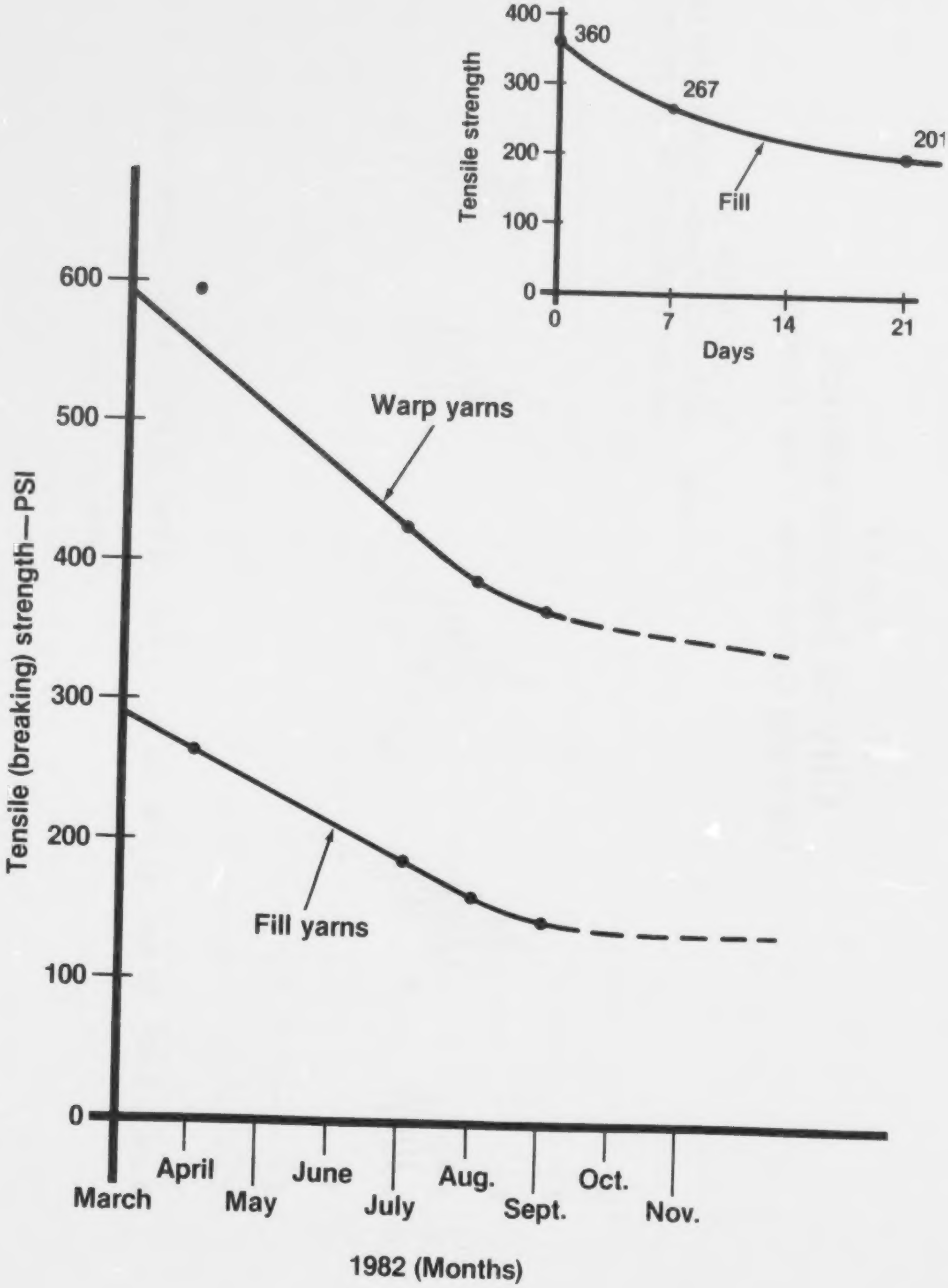

Figure 4

MIT Flex to Failure
(Filling Yarns)

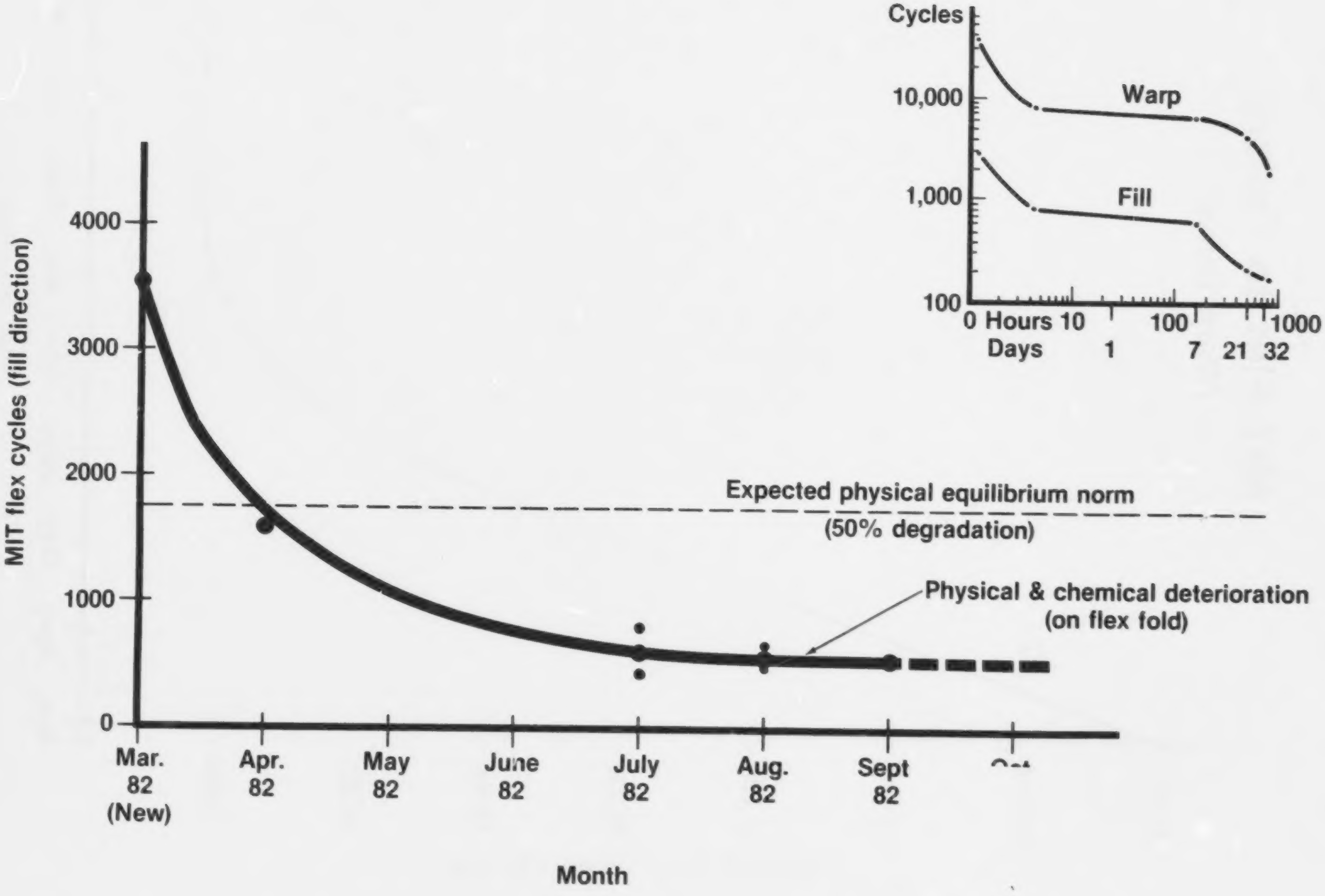

Figure 5

MIT Flex to Failure

(Warp Yarns)

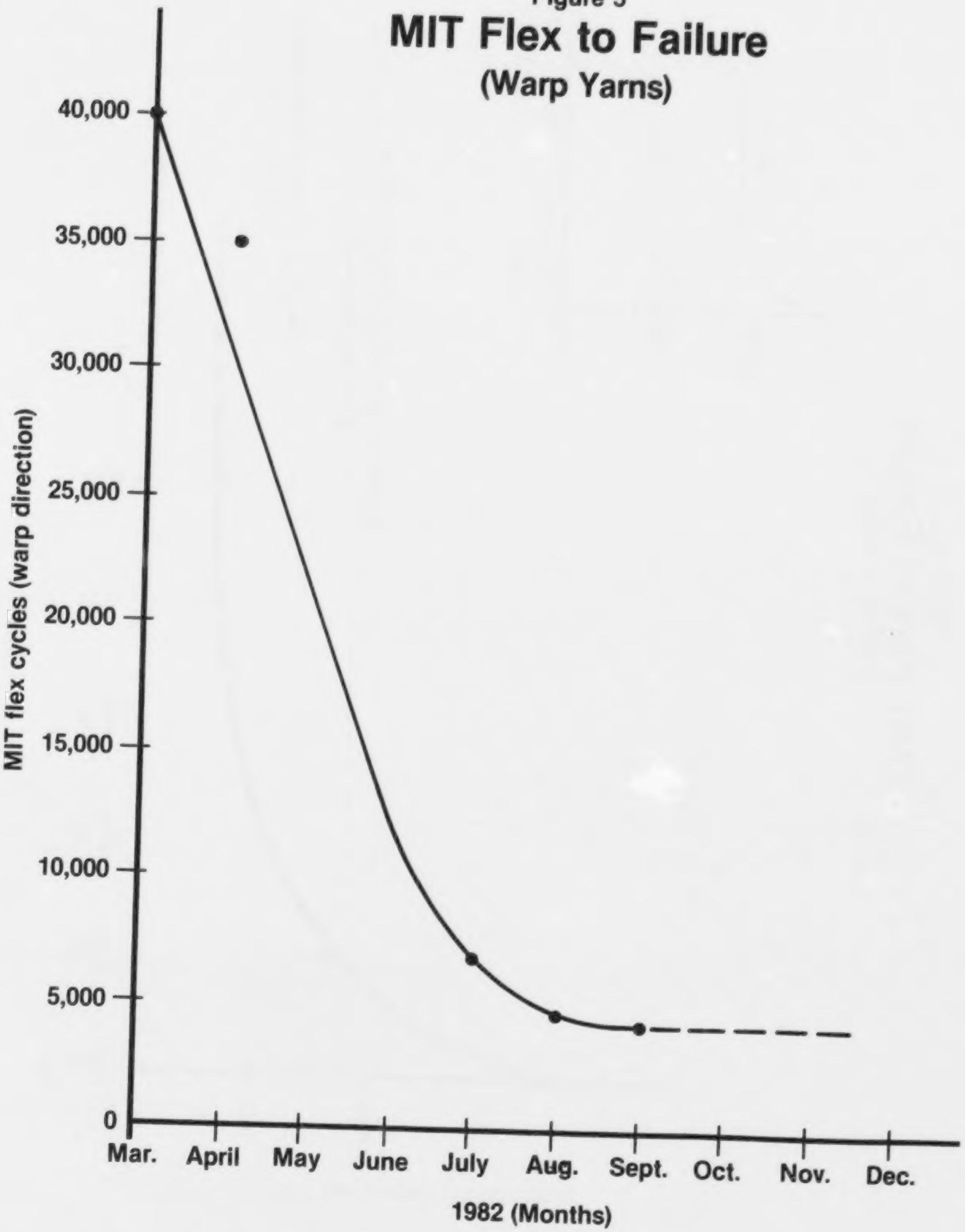

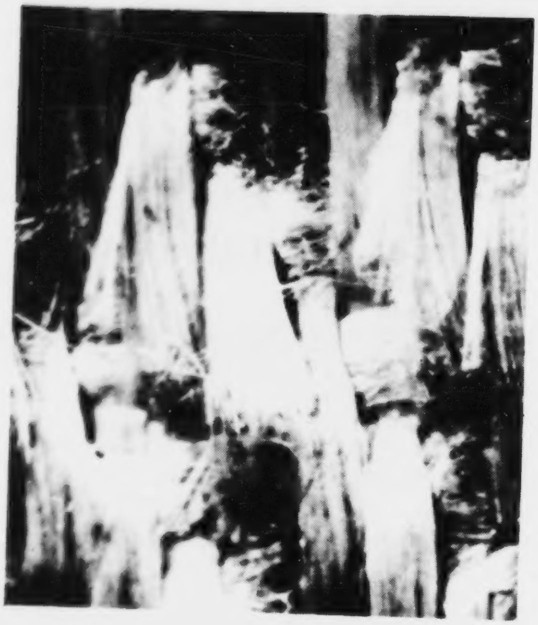

FIGURE 6. GLASS FIBER FRACTURE

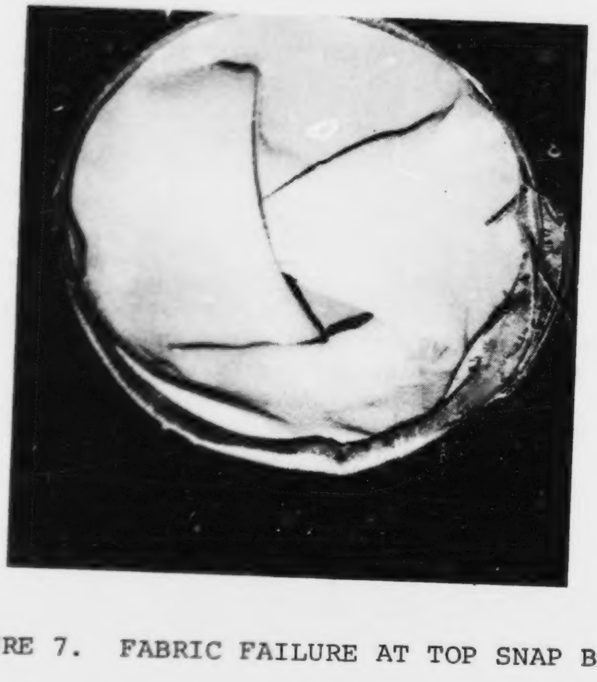

FIGURE 7. FABRIC FAILURE AT TOP SNAP BAND

FUNDAMENTAL STRATEGIES
FOR
CLEANING REVERSE AIR BAGHOUSES

by: GENERAL ELECTRIC ENVIRONMENTAL SERVICES, INC.

M.G. KETCHUCK
M.A. WALSH
O.F. FORTUNE
M.L. MILLER

ADAPCO

M.A. WHITTLESEY

ABSTRACT

In order to choose among the various cleaning cycle strategies, (Batch, Continuous, and Distributed) used for utility reverse air cleaned baghouses, it is necessary to understand the fundamentals of the cleaning process. This paper describes both analytical and experimental investigation of fundamental mechanics common to all cleaning strategies.

INTRODUCTION

Considerable debate has occured as to what is the best way to clean reverse air baghouses. Continuous cleaning, Batch cleaning and Distributed cleaning are all being used in operating utility baghouses with varying degrees of success. GEESI's operating experience indicates that a Batch cleaning provides both reasonable pressure losses, and makes provision for normal upsets in plant operating conditions, such as wet coal piles, steam soot blowing, low load flame stabilization, oil/gas supplemental firing, minor boiler tube leaks, etc.

Another issue which generates considerable discussion is whether it is better to allow a very heavy filtercake to build up on fabric filter bags before cleaning them, or to clean them, lightly loaded, as frequently as possible. Thick filtercakes seem to produce better cleaning in practice, but if overdone can lead to slack bags and fabric damage.

In order to insure that our baghouse cleaning cycles are fully optimized, GEESI has committed to on-going experimental and analytical programs designed to gain more insight into the fundamentals of reverse air cleaning, and to get factual answers to the above questions.

In this paper we would like to report the results of two of these programs:

(1) An analysis of the basic mechanics of the reverse air cleaning process, using the DELTAP computer program.

(2) Experimental measurements, using load cells, of the change in bag tensioning during the cleaning process.

THE FINITE ELEMENT MODEL

Observation of filter bags in reverse gas type fabric filter units has long established that the phenomenon of filter bag collapse and suspension spring bottoming occur during cleaning. To gain further insight into the interdependent effects of the reverse gas flow and the static/dynamic response of the total suspension system a Finite Element model was developed utilizing the ANSYS program. The following parameters were studied to determine the effects on filter bag cleaning, filter bag life, and structural loadings on the fabric filter structure.

- Reverse Air Flow
- Internal Decompression
- Initial Tension
- Dynamic Snap Back

The Finite Element model shown in Figure 1 reflects the stiffness of the suspension support structure, the suspension spring, suspension hardware, and the thimble/tube sheet structure. The fabric filter bag was modeled as two dimensional spars spanning ring nodes. In the Dynamic Analysis portion of the study the ring mass was lumped at the ring nodes and the dust mass was attached to the ring nodes via breakable links. The breakable links offered the ability to study various dust shedding schemes ranging from simultaneous release at all node points to a cascade release as dust cake from upper levels impinged upon lower regions of the filter bags. A gap element was utilized to analyze the effect of slack bags.

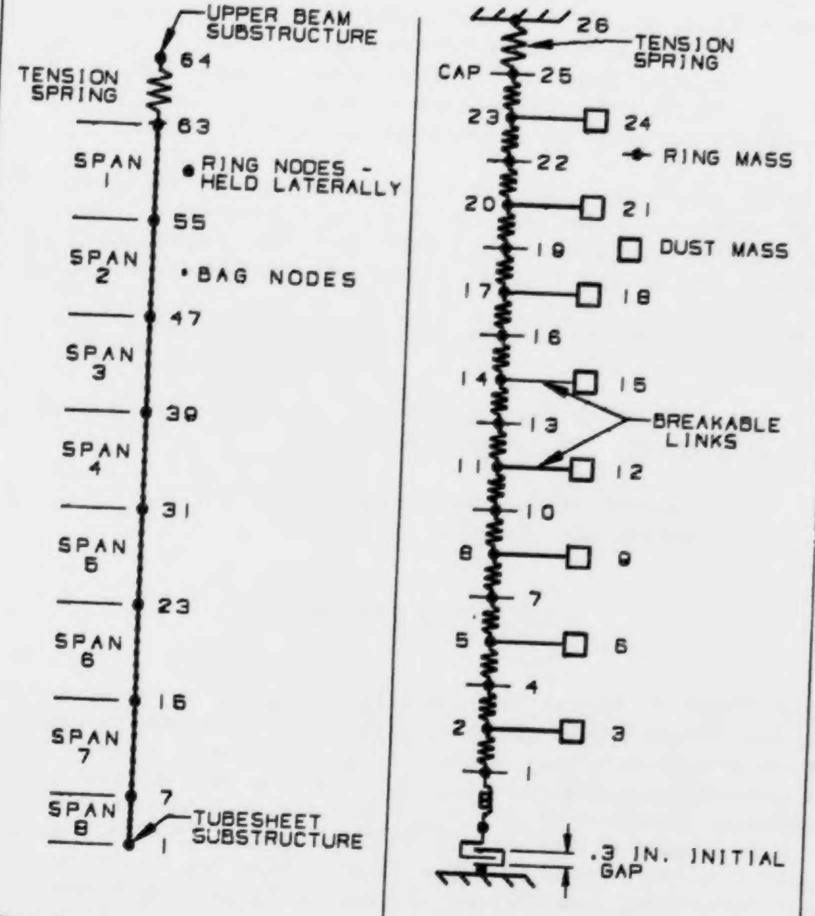
UPPER BEAM SUBSTRUCTURE
64
TENSION SPRING
63
SPAN 1
RING NODES - HELD LATERALLY
55
SPAN 2
BAG NODES
47
SPAN 3
39
SPAN 4
31
SPAN 5
23
SPAN 6
15
SPAN 7
7
SPAN 8
TUBESHEET SUBSTRUCTURE
1
26
TENSION SPRING
CAP
25
23
24
22
RING MASS
20
21
19
DUST MASS
17
18
16
14
15
13
BREAKABLE LINKS
11
12
10
8
9
7
5
6
4
2
3
1
.3 IN. INITIAL GAP

Bag Pressurization Model Used To Determine Deflections And Tensioning Spring Loads

Snap Back Dynamic Analysis Model

Figure 1. Finite Element Modelling Schematics

REVERSE GAS FLOW/INTERNAL DECOMPRESSION

The effects of Reverse Air Flow and Internal Decompression were studied utilizing the Finite Element model combined with a fluids approach. The collapse of the filter bag under the external pressure loading of reverse gas flow was studied using a Static Analysis to determine the deformed filter bag geometry and the bag spring rate.

A Dynamic Analysis was performed to determine the vertical mode frequency response, as it was initially felt that the rapid load increases in the suspension spring was possibly related to dynamic response of the Bag-Spring System as the dust cake detached and rapidly unloaded the filter bag and springs. The results of the Modal Analysis are shown in Table 1. It is important to note that even in the case where the filter bag lower span is collapsed, the fundamental frequencies are well above the observed frequency of oscillation of .125 to .167 HZ, and therefore, would not make significant contributions to the observed peaks in filter bag loadings.

TABLE 1. MODAL ANALYSIS SUMMARY

Case	Description	Mode	Freq.(HZ)
a	Bag assumed to be connected to a rigid tubesheet and rigid upper support beam.	1 2 3	5.58 12.77 20.92
b	Bag supported on a flexible tubesheet and upper support beam.	1 2	5.49 7.58
c	Bag supported by a flexible upper beam and unsupported at the bottom (i.e. bottom bag span collapsed).	1 2 3	2.58 9.01 16.69

A Fluids Analysis approach was used to study the effects of the falling dust plug. The effect is similar to that of a piston and cylinder, however, in this case the cylinder walls (the filter bag) has permeability and the piston (the dust plug) has porosity. Figure 2 shows the concept used in this portion of the study

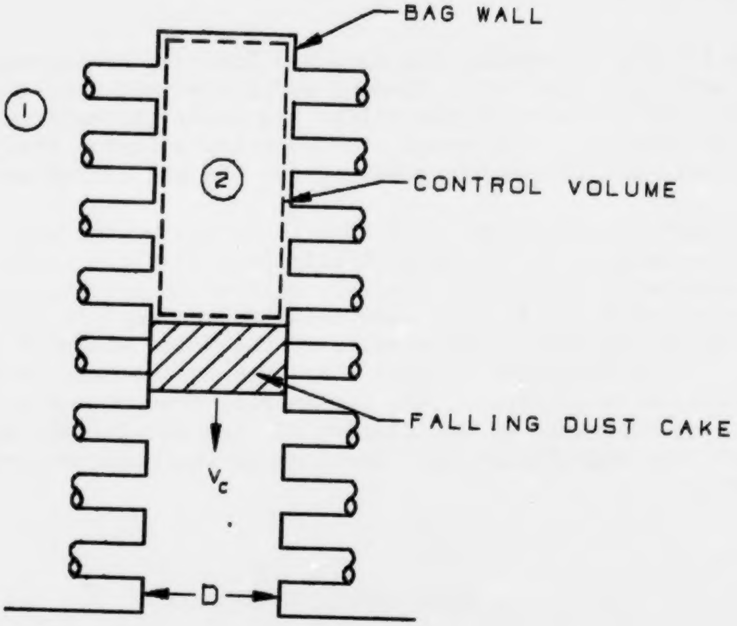

Figure 2. Schematic of Pressure Relationships For Fluid Analysis Model

The solution to the problem involved establishing equivalent "G" loadings on the spar elements, deformed filter bag geometry behind the falling dust plug, and inputing the stress strain properties of the filter bag material. Due to the nonlinear material properties, large deformations of the bag structure, and stress stiffening effects, an iterative procedure was required to converge on the solution.

Initially the reverse gas pressure loading was applied and the structure was allowed to deform to equilibrium geometry. The dust cake release was initiated at the top of the filter bag, and as shown in Figure 3 the porous dust plug began to fall towards the filter bag outlet. As the dust plug cascaded down the length of the filter bag the incremental dust mass was released. Maximum suspension spring loading occurred as the porous dust plug cleared the bottom of the filter bag. The results of one analysis is shown in Figure 4. Clearly, spring loadings of 2 to 3 times the initial filter bag tension can occur due to the internal decompression behind the falling porous dust plug.

Filter bag suspension spring, suspension hardware, and support structures must be designed to accommodate these increased loadings and proper design considerations must be made to eliminate structural failure due to low cycle fatigue.

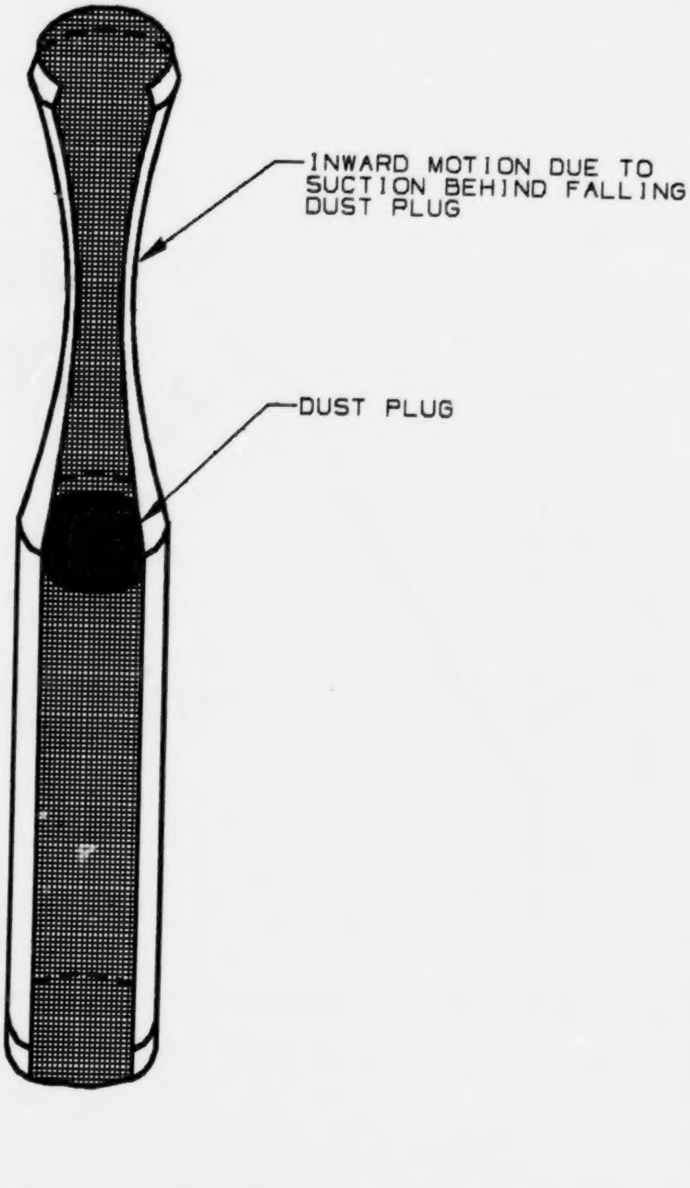
INWARD MOTION DUE TO SUCTION BEHIND FALLING DUST PLUG
DUST PLUG

Figure 3. Idealization of the Falling Dust Cake Upon Cleaning

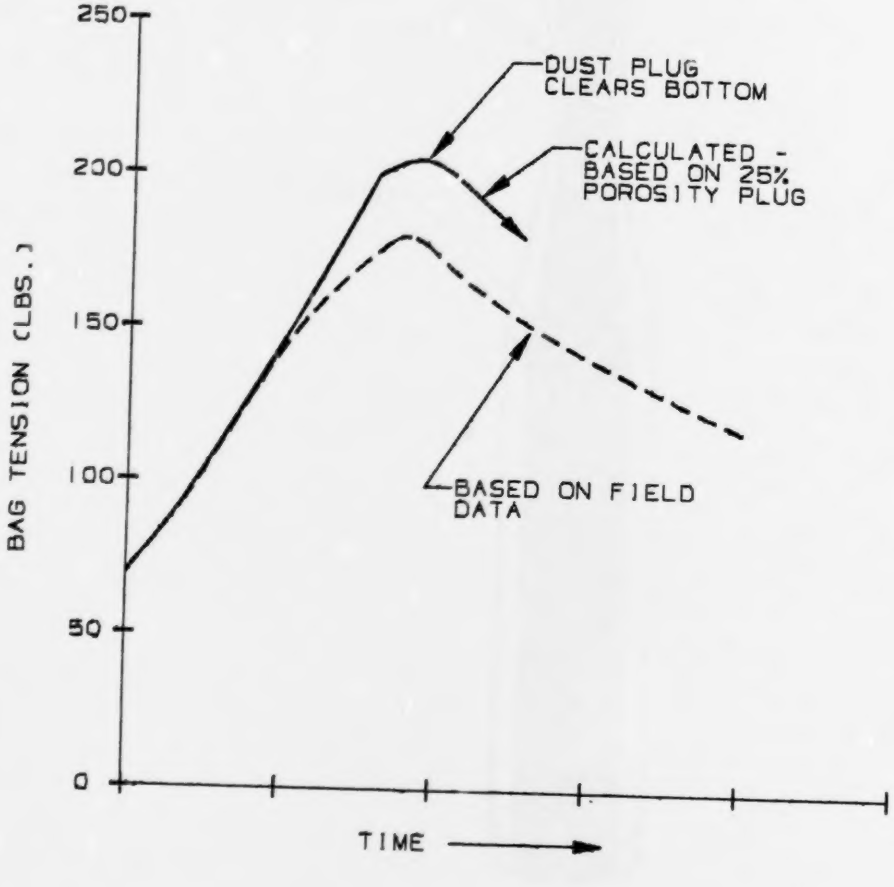

Figure 4. Comparison Between Calculated and Field Measured Peak Spring Tension

INITIAL BAG TENSION

The effects of Initial Bag preload on the filter bag deformed geometry and filter cake fracture was studied using the Finite Element model developed. The case of a fabric bag pretensioned to 75 lbs. ± 15 lbs. was studied. The results of the analysis are presented in Figure 5. Nodal displacements for the upper most and lowest span are presented for both the 90 lbs. and the 60 lbs. tension cases, thereby bracketing the initial target tension of 75 lbs.

The effect on filter bag nodal displacement and subsequent cake cracking appears to be narrowly banded. This indicates that the requirement for precise initial bag tension is currently over emphasized by equipment specifications and in fact may be detrimental from a maintenance point of view, as the requirement for precision filter bag tension breeds complicated hardware with increased cost.

However, the case for an adequate magnitude of initial tension should not be diminished as too low an initial tension can lead to early filter bag failure.

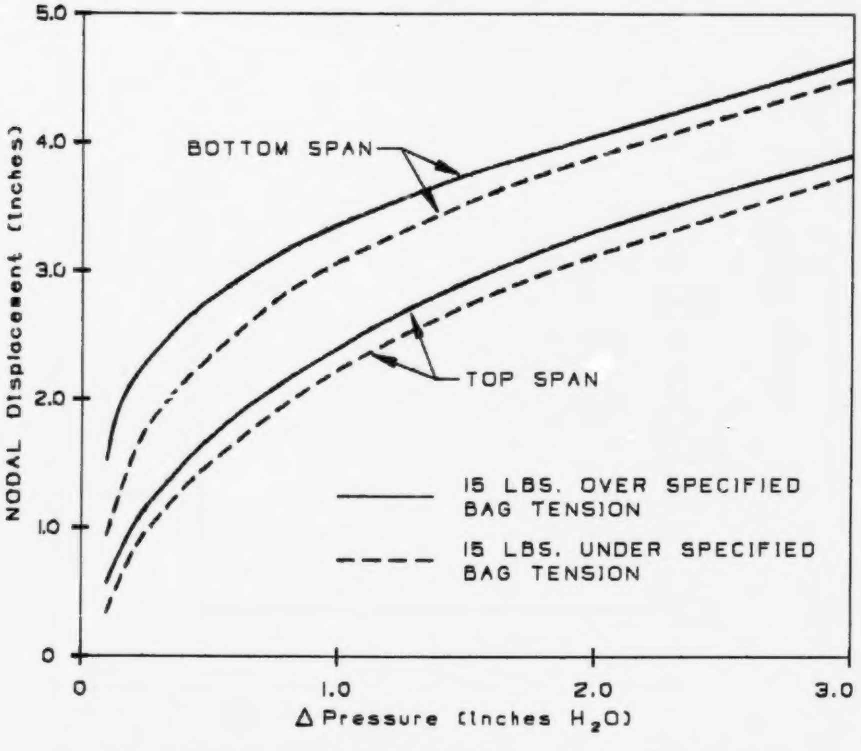

Figure 5. Maximum Span Displacements for the Top and Bottom Spans Versus Δ P for A Range of Bag Tensions

DYNAMIC SNAP BACK

The effect of a low initial filter bag tension may result in the lower region being untensioned and slack. In order to study this condition the Finite Element model was modified by placing a Gap Element in the bottom bag span. The filter bag model was then subjected to an initial dust cake loading with the bottom span in a slack condition. The dust cake was released and the filter bag was allowed to respond.

Figure 6 shows the force-time history response of the bottom span. The fabric material is subjected to a severe, short duration pulse loading. The effect on subsequent filter bag spans diminishes as one moves up the bag. At the upper suspension point the peak load is non existent and the system oscillates about the new equilibrium without the dust loading.

As previously discussed, the precise magnitude of initial bag tension is unimportant, but to avoid damaging effects to filter bag material sufficient minimum tension must be applied to prevent Dynamic Snap Back.

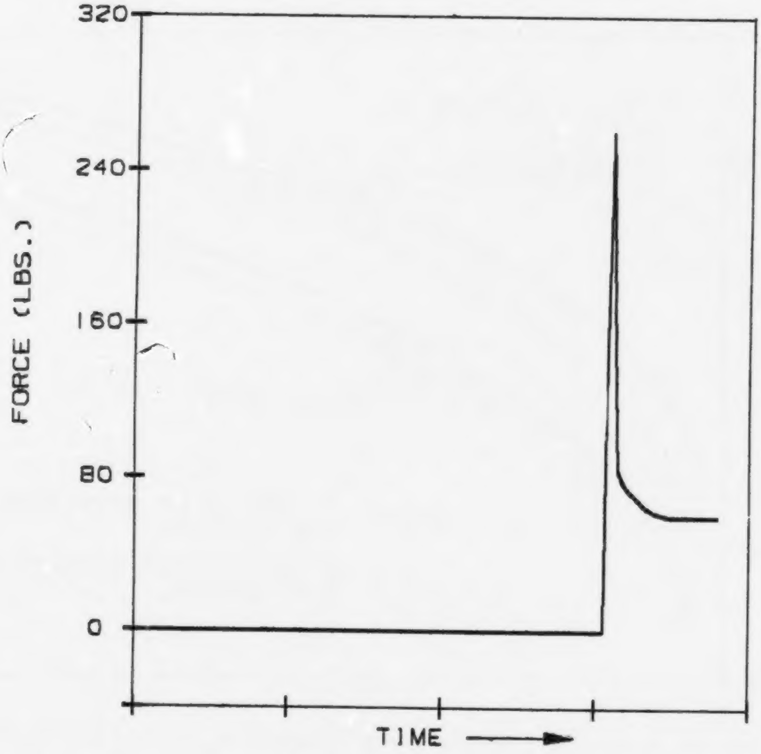

Figure 6. Snap-Back Analysis -- Force Time History For the Bottom Bag Span

EXPERIMENTAL FIELD DATA

Visually observed tension spring and bag movements along with the Finite Element model predictions of bag, tension spring, bag support structures and filter cake responses during the reverse air cleaning cycle prompted field "Insitu" testing to further quantify and support the proposed theories.

Testing was performed at a utility flyash baghouse operating at a flue gas temperature of 270°F., with cleaning cycle initiation at a baghouse compartment pressure drop of approximately 4 inches H_2O. The three acid resistent coated filter bags tested were 12 inches diameter and 34 ± feet long. Testing was accomplished via the setup schematically shown on Figure 7, where a specifically designed load cell was placed in the bag suspension system between the tensioning hardware and the top bag cap. Therefore, monitoring of the spring/top of bag forces was enabled.

A typical measured bag tension history is shown on Figure 8, with the outlet, reverse air, and reverse air relief valve movements shown. Several important items to note include:

(1) The gradual rise in spring tension at the onset of the reverse air valve opening.
(2) The sharp gradient starting at the reverse air valve fully opened position.
(3) The high (approximately 2.5 times initial bag tension) peak spring/top of bag tension.
(4) The spike-like peak duration most probably due to the force generated by the falling dust cake.

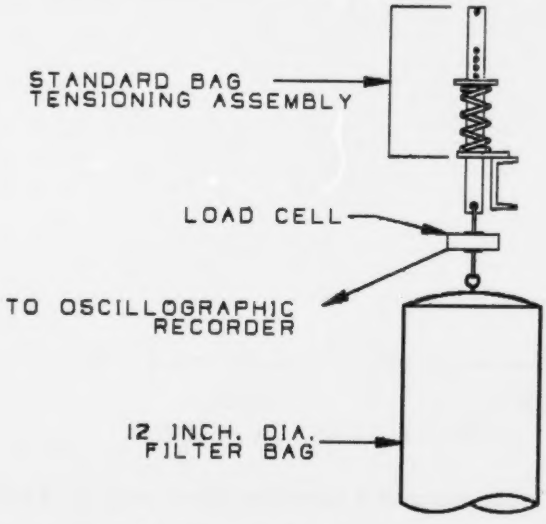

Figure 7. Schematic of Bag Tension Measurement Setup

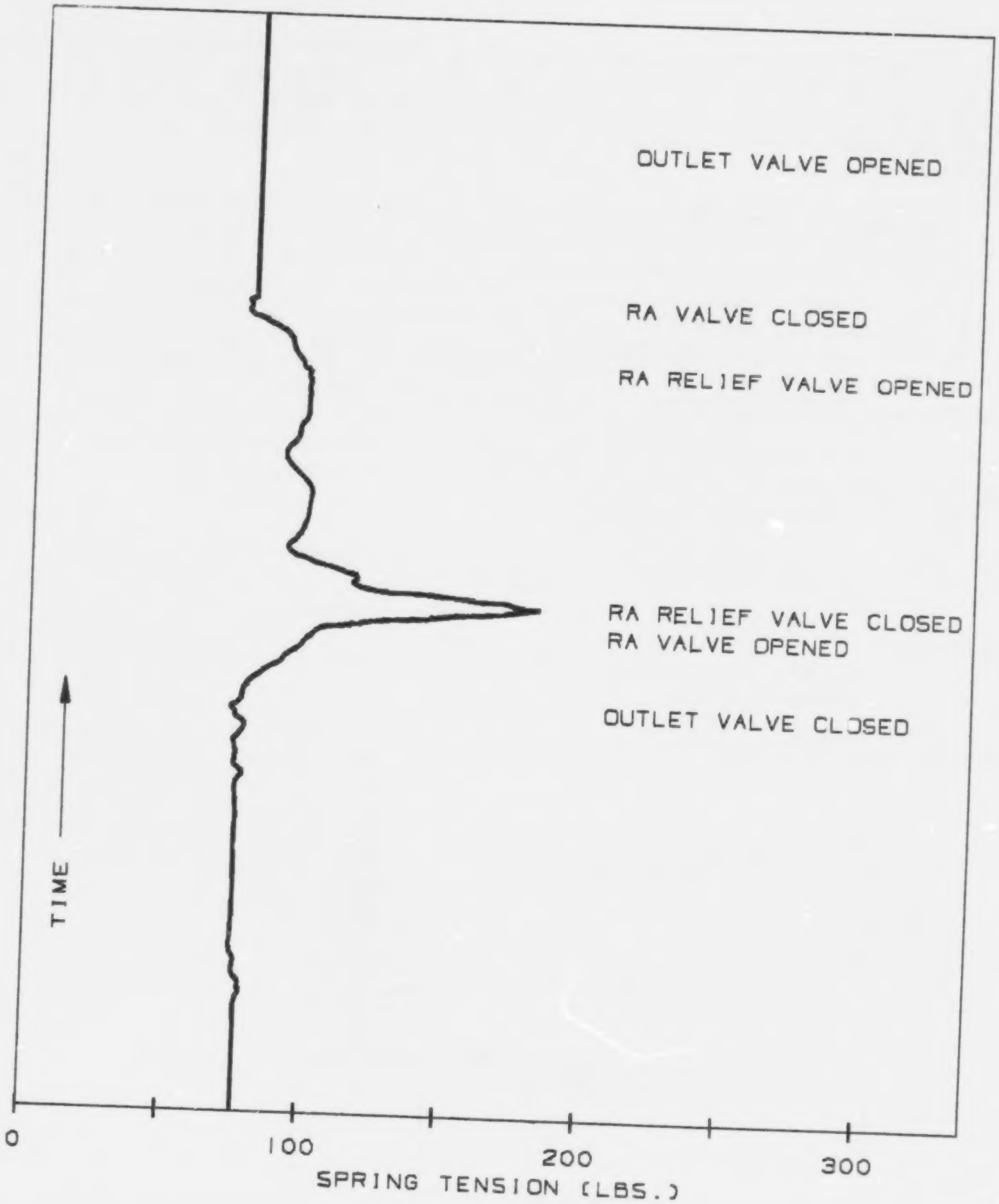

Figure 8. Typical Bag Response During Cleaning

CONCLUSIONS

Both reverse gas flow and the falling porous dust plug contribute to filter bag loadings during typical cleaning cycles.

The internal decompression effect contributes significantly to structural loadings. Proper attention in the design process is required to insure against low cycle fatigue failure of the suspension structure and hardware.

The effect of variances in initial tension is narrow banded making economic justification for hardware capable of precision adjustment difficult. Precision adjustment hardware breeds maintenance headaches.

The magnitude of initial tension is extremely important in reducing dynamic snap back of the fabric filter bag and damage to the material fibers.

The work described in this paper was not funded by the U.S. Environmental Protection Agency and therefore the contents do not necessarily reflect the views of the Agency and no official endorsement should be inferred.

DESIGN CONSIDERATIONS FOR BAGHOUSE - DRY SO_2 SCRUBBER SYSTEMS

by: Owen F. Fortune
and
Richard L. Miller
General Electric Environmental Services, Inc.
Lebanon, Pennsylvania 17042

ABSTRACT

The combination of a reverse air cleaned baghouse and a dry sulfur dioxide scrubber is attractive because of the ease with which the baghouse can remove over 99.9% of the high solids loading in the gas stream exiting the scrubber, and because sulfur dioxide scrubbing continues to occur in the filter-cake on the bags. However, in order to avoid having gypsum deposits shortening the usable life of the bags, close attention has to be paid to several design considerations. Among them are system response to boiler tube leaks, approach to saturation temperature, reheat system, avoidance of condensation in reverse air cleaning system, plant maintenance problems, changing boiler loads, and changing sulfur dioxide concentrations. Experience-based design strategies to deal with these issues are discussed in this paper.

INTRODUCTION

In less than ten years, the reverse-air cleaned, fiberglass bag fabric filter has become accepted, reliable technology for power plant dust emissions compliance. In the last few years, the utility baghouses' role has been expanded to become part of unified fly ash/sulfur dioxide removal systems. When a "wet" SO_2 scrubber is used, the baghouse remains immediately downstream of the air preheaters, and design modifications are not needed. However, when a "dry" spray absorber SO_2 removal system is used, the baghouse(s) are placed between the scrubber outlets and the induced draft fans, and must be designed to function for the dust loadings and close approach to saturation temperature of the spray absorber exit flows.

In 1980, we at General Electric Environmental Services, Inc. (GEESI) and Anhydro A/S of Copenhagen, contracted to supply the City of Marquette, Michigan, acting through Lutz, Daily, and Brain, with a spray absorber/baghouse system for their new 44 Megawatt Shiras No. 3 plant. Some of the system design parameters are given in Table 1, and the completed unit is shown in Figure 1. Since Shiras No. 3 will be coming on-line in the next month, it is timely to recount the issues that were considered in the design of the baghouse, and how they would apply to spray absorber/baghouse systems for boilers as large as 800 megawatts.

TABLE 1. CITY OF MARQUETTE SHIRAS NO. 3

- PROCESS

    44 Megawatts
    226,000 CFM at 265° F to spray absorber
    167,000 CFM at 175° F to baghouse
    1500 PPM SO_2
    15% Ash
    80% SO_2 removal guaranteed

- Baghouse

    75' x 45' in plan; 62' high baghouse compartments
    168 bags per compartment
    bags are 12 inch diameter x 35 feet long
    140,000 square feet of filtering surface

- Spray Absorber Vessel

    36' diameter x 71' high
    Central 7800 RPM rotating wheel atomizer
    200 HP vertical AC motor

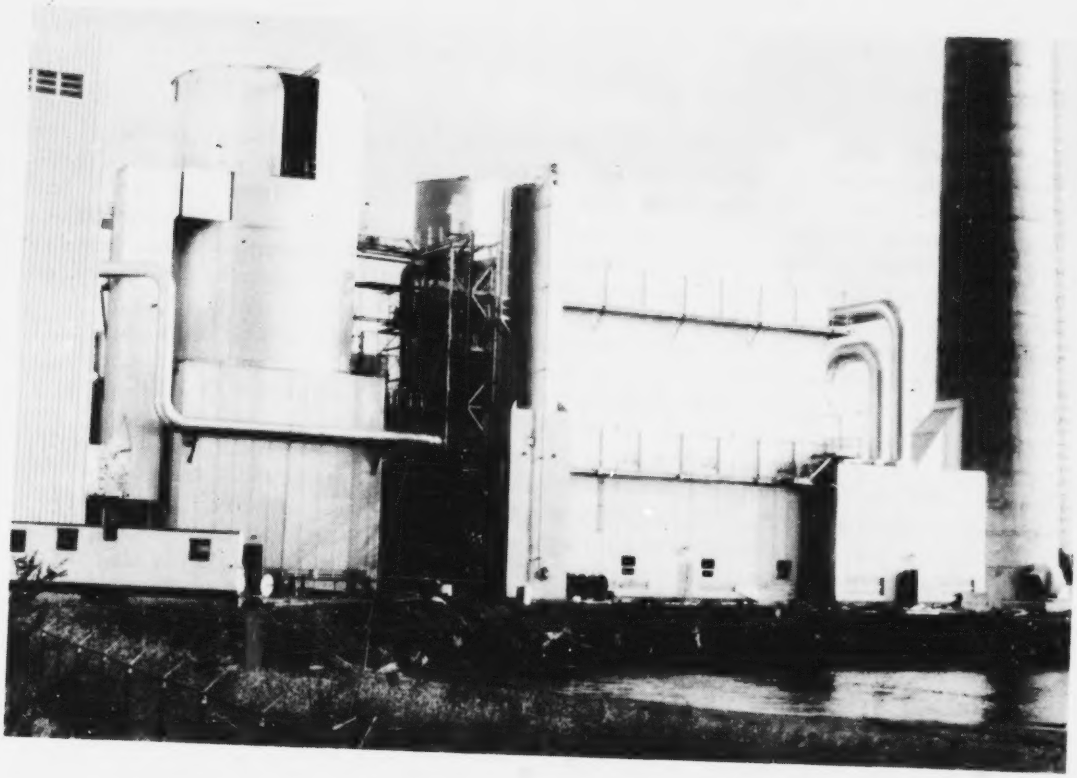

Figure 1. GEESI Spray Absorber/Baghouse System, City of Marquette, Michigan Shiras No. 3 Station

CHOICE BETWEEN BAGHOUSE AND ELECTROSTATIC PRECIPITATOR

Perhaps the first issue to be considered is why one should use a baghouse instead of an electrostatic precipitator in the first place. Since the gas temperature and humidity out of the spray absorber are essentially constant regardless of boiler load, it would seem to simplify the process of sizing of a precipitator for this application. Also, the very high gas moisture content is beneficial to the electrostatic precipitation process. Indeed, it seemed that SCAs in the range of 400-500 would be sifficient to insure dust emission levels under 0.03 lb/MBTU.

However, in investigating the issue, we found two strong reasons that will almost always weigh the decision in favor of a baghouse for a new power plant. The first is that the dust removal equipment must be capable of maintaining compliance, even if the SO_2 removal system is off-line. For low sulfur western coals, this means SCAs in the 600-800 range. Compared to precipitators in that size range, a baghouse will almost always be the more economical choice (1).

The second strong argument for teaming baghouses with spray absorbers is that about three times as much SO_2 is removed from the gas passing through a baghouse as through a precipitator operating at the same approach temperature. In other words, a baghouse will account for about 12% of the total SO_2 removal across the system, while a precipitator will only account for about 4% of the reductions in SO_2 emissions.

This may seem like a small consideration, but present worth evaluation factors on the order of ten million dollars per ton per hour of lime consumed are currently being used for utility boiler SO_2 scrubbing systems. For an 800 MW boiler burning 1% sulfur coal, approximately 6 tons of lime will be consumed each hour at full load. Thus, being able to operate with an 8% reduction in lime consumption would result in operational savings valued in today's dollars at 5 million dollars.

If the station were burning a 3% sulfur eastern coal, the lime consumption would increase by a factor of six (as required SO_2 removal efficiency increases from 70% to 90%). Thus, the financial incentives towards using a baghouse become even more pronounced, even though a smaller precipitator sizing (i.e., 450 SCA) would be appropriate.

Some air pollution equipment vendors (2) maintain that precipitators can be reliably operated at lower approach to saturation temperatures than baghouses, but other vendors, including GEESI, who use central rotating atomizers for fragmenting and dispersing the lime slurry into the boiler gas flow, have not had this problem (3,4,5,6).

Once the decision has been made to use a baghouse, the two main baghouse design factors to be considered are:

(a) To properly size the baghouse to handle the higher density, higher dust loading, gas exiting the spray absorber(s),

and

(b) To design the system so that operation will always be safely above the saturation temperature.

BAGHOUSE SIZING

At first glance, the fact that the gas entering the baghouse will be 100° to 150° F cooler than the gas exiting the air preheaters - and, hence, seems to have only 80% its flow volume - would argue that no modifications need to be made to the usual baghouse sizing procedures for the spray absorber FGD application. Reality is, however, that

(a) the mass flow rate of the boiler gas is increased by as much as 6% by the water evaporated in the spray absorber(s), and

(b) a considerable amount of new solids are formed in the spray absorber, due to the combination of the gaseous sulfur dioxide and calcium from the atomized slurry, to form calcium sulfite and calcium sulfate. In addition, as much as 25% reductions in lime consumption are realized in a recycle process by first slurrying and then reinjecting as much as 50% of the solids collected in the spray absorber and baghouse hoppers.

(c) Finally, the density of the gas entering the baghouse has increased by at least 20%, and will influence the baghouse pressure drops proportionately.

These factors can combine to easily double the dust loading to the baghouse and, thus, result in either substantially higher baghouse pressure losses, or substantially larger baghouses.

A positive factor in holding down baghouse sizes is to design the spray absorber so that a considerable portion of the solids enter and formed in the vessel are captured in the spray absorber hopper. The standard Anhydro reaction vessel is shown in Figure 2. A tapered inlet scroll and guide vanes are used to set up a cyclonic gas flow pattern which is reinforced by the rotary momentum of the atomized slurry spray and a near horizontal flow exit is positioned at two-thirds the height of the conical hopper. The controlled cyclonic flow pattern, combined with the Vortex holding effect of the exit duct, results in

(a) solids mechanical collection efficiencies of from 45% to 55%,

and

(b) several hours of hopper storage time to insure vessel maintainability.

The use of this type of spray absorber vessel, rather than a vessel that passes on all, or most, of the solids to the baghouse(s), reduces the baghouse inlet dust loading to levels similar to that at the air preheater exit. For instance, in the Shiras No. 3 design, the maximum load dust loadings are:

STATION	DUST LOADING (tons/hour)
Air Preheater Exit	4.4
Spray Absorber Vessel Exit	5.2
Baghouse Inlet	5.3

Hence, sizing the baghouse using arbitrary rules (such as gross air-to-cloth ratios of 1.5:1 or 2.0:1 net-net with reverse air), that ignore the processes occurring in the FGD vessels is poor practice. It is necessary to understand the consequences to the baghouse(s) of the various different types (multi

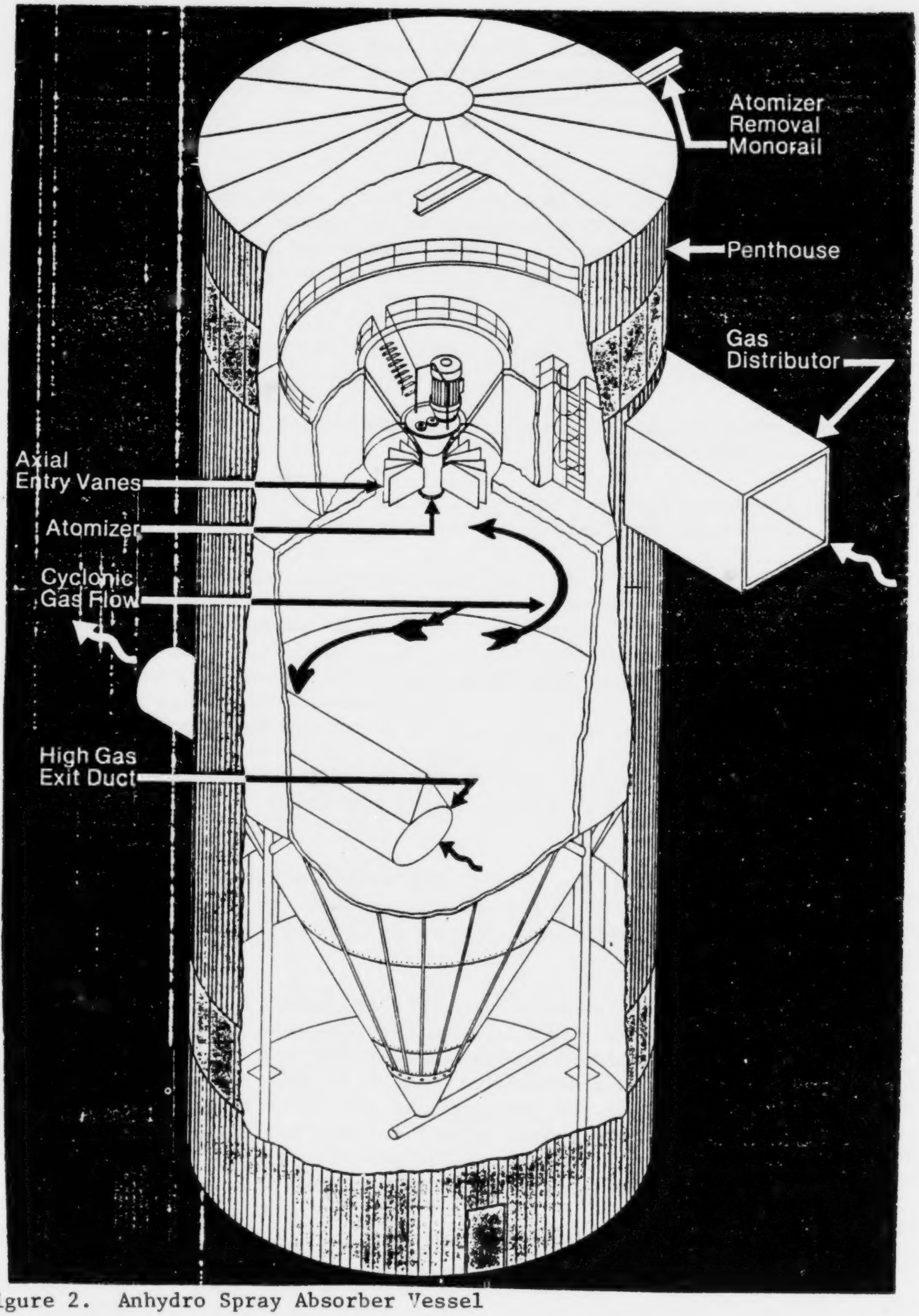
Atomizer Removal Monorail
Penthouse
Gas Distributor
Axial Entry Vanes
Atomizer
Cyclonic Gas Flow
High Gas Exit Duct

Figure 2. Anhydro Spray Absorber Vessel

two-fluid nozzle, multi-rotating atomizer, and central rotating atomizer) of atomizer and hopper configurations, worst case coal sulfur content, and their resulting impact on baghouse design.

REHEAT

Another factor which can have a significant impact on baghouse design is the practice of adding hotter gas to the spray absorber exit flow for fear of sub-dewpoint operations occurring in the baghouse or induced draft fans. Many different ways of "reheating" the FGD vessel outlet flows have been proposed. A few of the more logical ones are:

- Bypass of part of the economizer outlet flow around both the air preheaters and spray absorber vessels.
- Bypass of part of the air preheater outlet flow around the spray absorber vessels.
- Reheat of baghouse exit gas, using a "waste" steam heat exchanger to elevate temperature.

Considering that air pollution control manufacturers have been able to demonstrate stable rotating atomizer spray absorber operation at 20° F approach temperatures, and that about 10° F of reheating occurs across an induced draft fan operating at a 20" W.G. head, and that a well built baghouse - particularly one whose compartments have been pressure tested before being insulated - will have a temperature drop of less than 10° F, it is difficult to see why it is necessary to boost the spray absorber exit temperature before entering the baghouse when the boiler is operating at, or near, full load. Particularly since doing so will decrease the amount of SO_2 removed across the baghouse and, hence, the amount of lime consumed in the spray absorber.

However, as the mass flow through the system decreases, thermal losses through the baghouse will increase and can reach 15 to 20° F, even in a low inleakage, well insulated system. And at low boiler, lime consumption is less of an issue.

These factors argue for selection of a low capital cost, minimal capacity (10° F) reheat system. GEESI feels that the best way of supplying this reheat capacity is to bypass a few percent of the economizer outlet around the air preheaters. This insures that 450° F to 650° F temperature differential is available to elevate the baghouse gas inlet temperature with little capital cost beyond thermocouples, well insulated ductwork, and isolation and modulation dampers. Neither steam piping and valves nor electric heaters need be purchased and maintained.

PREVENTION OF THERMAL LOSSES

Using baghouse gas temperatures 20° F above saturation reinforces the importance of minimizing air inleakage, and external and internal insulation during construction of the baghouse is emphasized. Pressure leak testing of the compartments before they are insulated, durable door gasketing and door insulation shields, and minimizing the number of baghouse expansion joints, all become even more important than they are for straight fly ash collection baghouses.

In particular, the issue of compartment internal insulation becomes of greatly increased interest and concern. If a compartment with uninsulated internal walls is taken off line for inspection, then the wall temperature in the adjoining compartments will go below the gas dewpoint and there will be condensation on the on-line compartment side of the wall. This argues that full height internal insulation is needed on compartment walls to prevent wall and tubesheet corner condensation.

In a similar manner, heating the bottom of the baghouse hoppers to prevent condensation and insure free flowing ash removal becomes more important than in a straight fly ash baghouse, as does the importance of emptying the hoppers once a shift. In areas with severe winter climates, consideration should be given to insulated hopper enclosures in order to minimize the worst case sizing of the hopper heaters.

LOW LOAD OPERATION

For boilers larger than 200 MW, it is probable that more than one structural baghouse will be used per boiler. Discussions have appeared in the literature (7) recommending that at low load, entire baghouses be taken off-line and isolated in order to minimize thermal losses due to having greatly reduced mass flow rate per square foot of insulated external wall in each baghouse. It is true that a baghouse with, say, a 10° F loss at 100% boiler load, will have about an 18° F loss at 25% load. However, this low load condition can be compensated for by either operating the on-line spray absorber vessels at a higher approach temperature, or using a minimal capacity reheat system.

The reason that this is preferable to simply isolating baghouses, or compartments, is that a typical sized, 4000-bag fabric filter will have about two tons of water vapor in it when brought off line. Within a few hours, all of the water will condense as the baghouse cools down, unless an automatic auxiliary purge system is added to the baghouse to replace the trapped boiler gas with ambient air. Then, when boiler load increases, the baghouse must be reheated before being brought back on line.

It is difficult to see what is gained through this elaborate procedure, which significantly increases the capital cost of the baghouse by adding massive (i.e., 15' x 12') inlet and outlet isolation guillotine dampers, as well as the new ductwork and many-compartment dampers of the automated purge system, while doing nothing to improve system performance.

RESPONSE TO SYSTEM UPSETS

The presence of a spray absorber upstream of a baghouse protects the baghouse against the consequences of many of the minor upsets that occur in boiler operation during the course of a year. For instance, a properly designed spray absorber system minimizes the consequences of minor boiler tube leaks, since it will reduce the amount of recycle, or dilution, water as the boiler gas humidity rises in order for the spray absorber outlet temperature to stay at the specified approach to saturation temperature. Also, if one air preheater wheel stops turning, the ability of the spray absorber system to reduce the gas temperature by at least 150° F, will keep the average gas temperature entering the baghouse below 500° F and, hence, not even require bypass of the baghouse.

Operational upsets in the spray absorber systems - such as a lime slurry valve failing open - that could adversely impact the baghouse by causing sub-dewpoint operating conditions, can be controlled by vessel outlet temperature and humidity monitoring. For example, the GEESI Two-Loop Control system, shown in Figure 3, would respond by closing off the vessel recycle flow, as well as simply alarming the failure.

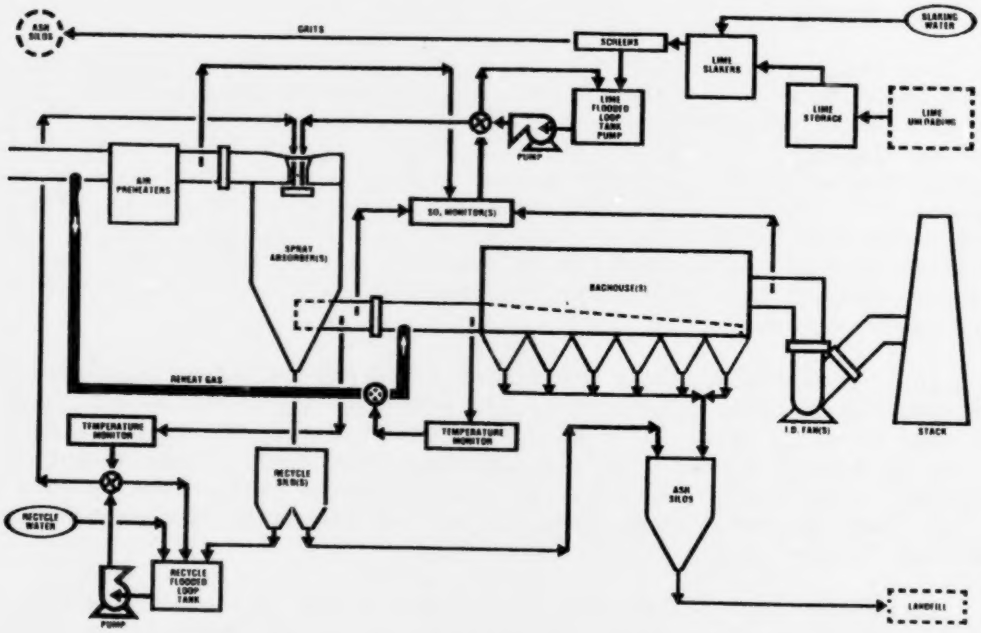
ASH SILOS
GRITS
SCREENS
SLAKING WATER
LIME SLAKERS
LIME FLOODED LOOP TANK PUMP
LIME STORAGE
LIME UNLOADING
PUMP
AIR PREHEATERS
SPRAY ABSORBER(S)
SO_2 MONITOR(S)
BAGHOUSE(S)
STACK
I.D. FAN(S)
REHEAT GAS
TEMPERATURE MONITOR
TEMPERATURE MONITOR
RECYCLE SILO(S)
ASH SILOS
RECYCLE WATER
RECYCLE FLOODED LOOP TANK
PUMP
LANDFILL

DRY FLUE GAS DESULFURIZATION SYSTEM
SPRAY ABSORBER/FABRIC FILTER

Figure 3. GEESI Two-Loop Control System

BAG FABRICS AND COATINGS

It will still be necessary for the baghouse to be able to reduce dust emissions to below 0.03 lbm/MBTU, regardless of whether or not the spray absorber is on-line. Thus, the bag fabric must be able to withstand gas temperatures above 300° F, as well as near saturated gas operation at 140 to 170° F. These dual requirements lead to fiberglass remaining as the most cost effective bag material in utility fabric filters.

Since baghouse dust inlet loadings will be higher in the combined SO_2/particulate removal system, GEESI believes that 13-1/2 ounce, rather than 9-1/2 ounce, fabric should be used because of its greater durability, as shown by flex testing.

The value of the bag coating now chiefly lies in its ability to act as a lubricant between glass fibers. Thus, even in the combined systems' highly alkali filter cakes, the so-called "Acid Resistant" coatings are preferred, since they flow more evenly during application and, hence, cover a higher percentage of the glass fiber surface area than do the earlier coatings, such as silicone-graphite-teflon, or pure Teflon-B.

BAGHOUSE MAINTENANCE CONSIDERATIONS

The operation of either a wet or dry SO_2 scrubbing system imposes a significant load on a plant's Maintenance and Operations Departments and, hence, it is of increased importance that baghouse maintenance issues be minimal.

The best way to insure this is to invest the time needed to keep the system automatic temperature, SO_2, and humidity monitors in good calibration. In particular, humidity sensors require periodic attention. GEESI believes that, at present, extractive sampling monitors give the most reliable information from dust laden flows. Thus, care should be taken that insulation and heat tracing of the sampling lines is adequate, as well as frequently checking the system's calibration.

The payoff for doing this will be avoidance of hopper pluggage and bag damage problems caused by sub-dewpoint operation.

SUMMARY

One very general conclusion that can be drawn from working out the design of a composite dry spray absorber/baghouse system is that the same factors which lead to good straight baghouse design, simply become more important for the composite system:

- Sharply evaluate the design point dust loading, mean particle size, gas density, etc., for sizing the baghouse, rather than just relying on rule-of-thumb formulas.

- Use and maintain gas temperature and humidity sensors to avoid sub-dewpoint operation for even short periods of time.
- Use insulation on compartment internal walls to prevent localized condensation.
- Heat hopper bottoms to head off potential pluggage problems.
- Pressure test compartments during erection to eliminate sources of ambient air inleakage due to skipped welds, or poor door gasketing.
- Instrument the system so that a mimi-computer can control feedback loops to avoid operational problems. Set up agreed upon calibration procedures to insure that the computer inputs are reliable.
- Use fiberglass bags with protective coatings.

A baghouse designed along these lines should be a high-reliability component in a composite spray absorber SO_2 removal/fabric filter system.

The work described in this paper was not funded by the U.S. Environmental Protection Agency and therefore the contents do not necessarily reflect the views of the Agency and no official endorsement should be inferred.

REFERENCES

1. Campbell, K.S., et al., Economics of Fabric Filters Versus Precipitators. Electric Power Research Institute FP-775, June, 1978.

2. Wilkinson, J. M. and Tonn, D. P., Baghouse vs. Precipitator for Dry Scrubber Systems -- Pilot Study Results. 4th International Coal Utilization Exhibition & Conference, Houston, Texas, December 1981, Vol. 3, p. 168.

3. Parsons, E. L., Hemenway, L. F., Kragh, O. T., and Brna, T. G., SO_2 Removal by Dry FGD. Proceedings: Symposium on Flue Gas Desulfurization -- Houston, October 1980, Vol. 2, p. 801.

4. Parsons, E. L., Boscak, V., Brna, T. G., and Ostop, R. L., SO_2 Removal by Dry Injection and Spray Absorption Techniques. Third Symposium on the Transfer and Utilization of Particulate Control Technology, March 1981: Volume 1. Control of Emissions from Coal Fired Boilers, p. 303.

5. Samuel, E. A., Lugar, T. W., Lapp, D. E., and Fortune, O. F., Dry FGD Pilot Plant Results: Lime Spray Absorption for High Sulfur Coal and Dry Injection of Sodium Compounds for Low Sulfur Coals. Paper presented at 1982 Symposium on Flue Gas Desulfurization, Hollywood, Florida.

6. Meyler, J. A. and Felsvang, K., One Year of Operation of the Riverside Dry Scrubber. Paper presented at the 44th American Power Conference, April, 1982.

7. Kaplan, S. M., et al., Dry Scrubbing at Northern States Power Company Riverside Generating Plant. Paper presented at 1982 Symposium on Flue Gas Desulfurization, Hollywood, Florida.

RESULTS OF BAGHOUSE AND FABRIC TESTING AT RIVERSIDE

By: H. W. Spencer III, Y. J. Chen, M. T. Quach
Joy Manufacturing Company
Western Precipitation Division
Los Angeles, California 90039

ABSTRACT

This paper presents the results of one year of baghouse and fabric testing at the Riverside Dry FGD Demonstration Facility during 1981. Operating parameters and baghouse performance data are summarized. The results of the fabric evaluation test are discussed. Pressure drop measurements are reported and pressure drop predictions for various fabric filters based on the experimental data are compared. Pressure drop predictions are compared with overall baghouse pressure drop. Good agreement between the predicted values and the actual measurements are reported. Measurements reported in the paper cover operation with three different coals.

INTRODUCTION

This paper presents the results of one year of baghouse and fabric testing at the Riverside dry FGD demonstration facility during 1981. The Riverside dry FGD demonstration facility is located in Minneapolis, Minnesota, at Northern States Power's Riverside Station. Operating parameters and baghouse performance data are summarized for the period January, 1981 to December 1981. During this period, the Western Precipitation reverse air baghouse was successfully operated downstream from the NIRO spray dryer.

EQUIPMENT DESCRIPTION DRY FLUE GAS DESULFURIZATION PLANT

Figure 1 is a schematic of the JOY/NIRO dry FGD Demonstration Plant. The design conditions and technical data for the fabric filter portion of the plant are given in Table I.

PROGRAM OBJECTIVES

The objectives of the JOY/NIRO test program at Riverside are listed below:

1. Confirming the scale-up factors from pilot to full-scale operation.
2. Confirming the sensitivity of various operating parameters in a full-scale system.
3. Demonstration of the system's operational flexibility, including turn-down, start-up, shut-down, and normal operation.
4. Demonstration of long-term, low-temperature operation.
5. Evaluation of various fabric filter media with dry FGD application.
6. Demonstration of operation with various fuels, including low sulfur Western coal and higher sulfur Eastern or Midwestern coals.
7. Demonstration of particulate and SO_2 removal capabilities with either a baghouse or an electrostatic precipitator.
8. Characterization of particulate matter emitted from the system.
9. Determining the characteristics of the dry FGD waste product with respect to disposal and utilization.
10. Characterization of the system operation and maintenance costs.
11. Optimization of energy and reagent consumption.
12. The establishment of system availability and reliability data.
13. The development of operating and maintenance procedures.
14. The training of power plant operators.

During 1981, a majority of these objectives were met. The test and operating record for the facility during 1981 is given in Figure 2. As shown, tests were conducted with three fuels having sulfur contents ranging from .8% to 3.2%. The characteristics of these fuels are summarized in Table II. Photomicrographs of isokinetically-collected dust samples at the inlet of the SDA and the inlet of the baghouse are displayed in Figures 3 and 4. Larger particle sizes were found at the baghouse inlet with the high sulfur fuel. This is most likely explained by the higher alkalinity of the slurry that was being spray-dried. Typical operating conditions for each of the coals are given in Table III. The Bahco particle size measurements of the baghouse dust samples contained in this table are consistent with the photomicrograph data. Dust loadings given in the Table were measured at the inlet of the baghouse.

Typical operating baghouse parameters with and without the spray dryer in service are given in Table IV. When the spray dryer is in operation, the baghouse runs at a considerably lower temperature than for a non-FGD installation. Dust loadings are higher and collection efficiencies are also higher. Data in Table IV shows increased emissions with broken bags. Bag failures are discussed later in this paper and were confined to certain types of bags. Figures 5 and 6 are the plots of the operating parameters during selected periods which include the high sulfur tests.

FABRIC EVALUATION

One of the major emphases of the JOY test program is to evaluate a variety of fabric materials in search of materials with longer life, lower cost, and lower pressure drop characteristics. The bag arrangements in the twelve compartment baghouses for the first phase and second phase of the test programs are given in Figures 7 and 8. The design characteristics for each of these materials are given in Table V. All the bags tested were fiberglass except for the ones in Compartment 9, which were polyester. The polyester bag type was not in service long enough for full test evaluation due to its temperature limitation.

The test program was planned to evaluate the fabric strength and bag life. New bags and bags which have been in service for certain periods of time were removed for evaluation tests, including weight tests, breaking strengths, Mullen burst, MIT flex test and permeability tests. In-situ bag weights were measured to check the dust build-up trends on the bag surface. A representative sample of in-situ bag weight of three bag types is plotted in Figure 9. Significant variation was found between bag material types with the texturized fiberglass bags having a much higher residual dust layer than the non-texturized bags. Very little variation was seen between the front and back of compartments. Measurements of the variation in bag weight from compartment to compartment was also made and again, there was no significant difference.

An example of decrease in breaking strengths and Mullen burst strengths with time is plotted in Figure 10. This plot is for a non-texturized lightweight teflon-finished fiberglass bag. As shown in a later plot, this bag had low failure rates even though there was a measurable decrease in the strength of the bag.

In Figure 11, the permeabilities of bag samples and corresponding bag materials weights are compared for as received, vacuumed, and washed samples.

The data shows that washing restored original permeabilities and weights. Vacuuming the material only partially restored the permeability. As expected, the permeabilities of the material in service are considerably less than the new materials.

BAG LIFE

Bag life is a major factor in determining the economics of fabric filters for utility applications. Figure 12 presents the cumulative bag failure rate as experienced at Riverside. Two of the bag materials, which have teflon coatings, showed very low failure rates; failures were apparently limited to bags damaged during initial installation. However, two bag materials with silicone, graphite, teflon tri-coated finish had unacceptable failure rates. The finish apparently did not protect the bags as well as the teflon coating. The bags with high failure rates also have lower strength in terms of MIT flex cycles. Fabrication errors also contributed to the failures which occurred at the top and lower bands, ring cover stitchings and outer ring cover areas. The tri-coated bags have now been removed from the Riverside baghouse. We are continuing to monitor the life of the teflon-coated bags and other bag materials.

BAGHOUSE PRESSURE MEASUREMENTS

One of the major factors controlling the design of a fabric filter is minimizing pressure drop. The Riverside baghouse has been instrumented to measure flange-to-flange pressure drop, and pressure drop across the individual compartments, outlet valves and inlet dampers. Pressure drop has been monitored over a range of air-to-cloth ratios by reducing the number of compartments in service under various boiler loads. Pressure drop was measured during full flow periods, settling periods (when one compartment is out for cleaning), and reverse air cleaning (when one compartment is out for cleaning with the reverse air flow), corresponding to the gross, net and net-net air-to-cloth ratios respectively. A sample trace of flange-to-flange pressure drop is given in Figure 13.

Individual compartment flow rate and pressure drop were measured for determination of filter drag, which is the ratio of compartment pressure drop and air-to-cloth ratio. By measuring the dust concentration to the baghouse and assuming uniform distribution of the dust between all compartments, the incremental areal cake density was calculated for each compartment. The incremental areal cake density is equal to the quantity of dust collected per unit area between the cleaning cycles. A knowledge of the dependence of the filter drag on areal cake density can be used to determine the effective drag coefficient, S_E, and specific dust-resistant coefficients K_2 for each specific bag material as shown in Figure 14. Knowledge of these coefficients can be used to predict pressure drops as a function of air-to-cloth ratio, dust concentrations, and cleaning cycles. In Figure 14, filter drag is plotted as a function of the incremental areal cake density for Type B bag materials at Riverside. Residual drag, which is the real drag of a filter after cleaning, is plotted at the incremental areal cake density just prior to cleaning instead of at the zero incremental areal cake density. The extrapolation of the filter drag curve at zero cake density point, S_E, does not coincide with the measured residual drag value, however, it is within the expected range. The slope of the curve determines the value of K_2. Another method using a computer model developed by Western Precipitation was used to reduce the data and calculate the effective drag, S_E, and specific dust-resistant coefficient K_2. The pressure drops prediction based on these coeffficients as a function of air-to-cloth ratio is presented as an example in Figure 15. Two pressure drop comparisons are given. The solid curves show pressure drops across different kinds of material without taking into account the effect of cleaning process. Considerable differences are found at higher air-to-cloth ratios. The open symbols compare the pressure drop including the effect of the cleaning process of a multi-compartment system. In this case, only minor differences between different materials are found.

In Figure 16, total baghouse pressure drop at Riverside is plotted as a function of air-to-cloth ratio and compared with computer predictions. Data are given for three coals with and without SDA operation. There is no apparent trend with respect to the three different coal types. The data shown correspond well with pilot plant data and with the computer-predicted pressure drops.

SUMMARY

In summary, the baghouse at Riverside has operated well. Baglife for teflon-coated bags has been good, pressure drops have been predictable and reproducible. The baghouse as a particulate collector for dry scrubber should be considered as a demonstrated technology.

REFERENCES

1. Kaplan, Steven M., Chen, Yang-Jen, Sannes, Carl A., Jr., "Dry Scrubbing at Northern States Power Company Riverside Generating Plant," EPA/EPRI Symposium on Flue Gas Desulfurization, May 17-20, 1982, Hollywood, Florida.

2. Spencer, H. W. III, Brown, Bert, Chen, Yang-Jen, "Experience with Baghouse for Dry FGD Service," 74th APCA Meeting, June 21-26, 1981, Philadelphia, Pennsylvania, Paper No. 81.95.

The work described in this paper was not funded by the U.S. Environmental Protection Agency and therefore the contents do not necessarily reflect the views of the Agency and no official endorsement should be inferred.

TABLE I

THERM-O-FLEX FABRIC FILTER DATA SUMMARY

PLANT NAME: Northern States Power Company
Riverside Generating Plant

LOCATION: Minneapolis, Minnesota

DESIGN CONDITIONS (FGD)*

Gas Volume (max acfm)	420,000 (540,000)
Design Temperature (°F)	500
Outlet Loading (gr/10^6 Btu)	210
Pressure Drop (in. VWC)	6
Design Pressure (in. VWC)	-30 to +20
Total Filter Area (sq. ft.)	321,200
Total Filter Ratio	1.31:1 (1.68:1)

TECHNICAL DATA

No. of Fabric Filters	1
No. of Rows	2
No. of Compartments/Row	6
Filter Bags:	
Total	3000
Per Compartment	250
Diameter (in.)	12
Length (ft.)	35

* Values in parenthesis are for non-FGD system operation. Where none are shown, values can be assumed to be the same.

TABLE II

FUELS USED IN SDA/BH TESTING

	Normal	Hi-Sulfur	Low-Sulfur
	85% Colstrip (Rosebud, Montana) (McKay Seam) 15% Petroleum Coke	Illinois Coal	Sarpy Creek Coal (Sarpy Creek, MT) (Robinson Seam)
Average			
Sulfur %	1.37	3.19	0.79
Ash %	8.33	10.36	9.20
Moisture %	22.0	12.76	25.33
BTU/lb.	9,500	10,930	8,614

TABLE III

TYPICAL OPERATING CONDITIONS

	HI-S	Sarpy Creek	Colstrip
• ΔT Ad. Sat. (°F)	19.2	17	17.3
• Product Moisture % BH	1.17	1.72	1.34
• Feed Rate (GPM)	136.5	140.35	121.85
• Feed Solid %	35.49	42.42	44.77
• Dust Loading (gr/ACF)	10.2	11.8	9.9
• Bulk Density (tapped) (lb/ft^3)	50.0	62.5	56.2
• Bahco Mass Mean (μm)	17	9.4	8.4
• Flow Rate (ACFM)	390,560	347,200	379,950

TABLE IV

BH Operating Range

—With SDA:	
• Inlet Temperature (°F)	140 — 175
• Inlet Gas Volume (ACFM)	219,000 — 444,000
• Inlet Dust Loading (gr/ACF)	4.27 — 12.1
• Outlet Dust Loading (gr/ACF)*	0.0010 — 0.0192*
• Efficiency (%)*	99.85* — 99.99
—Without SDA:	
• Inlet Temperature (°F)	270 — 310
• Inlet Gas Volume (ACFM)	182,000 — 458,000
• Inlet Dust Loading (°F)	1.2 — 2.9

*High outlet loading and low efficiency are due to broken bags.

TABLE V

FABRIC SPECIFICATIONS

	Avg. Wt. Oz./Sq. Yd.	Finish	Material
FABRIC A	8.4	Silicone Graphite Teflon	Glass
FABRIC B	9.3	Teflon	Glass
FABRIC C	8.8	Teflon	Glass
FABRIC D	8.4	Grafosil	Glass
FABRIC E	9.3	--	Polyester
FABRIC F	9.5	Teflon B	Glass
FABRIC G	13.5	Acid Res.	Glass
FABRIC H	9.5	Teflon B	Glass
FABRIC J	9.5	Acid Res.	Glass
FABRIC K	9.5	Teflon	Glass

FIGURE 1

FLOW DIAGRAM - DRY SCRUBBING SYSTEM AT RIVERSIDE

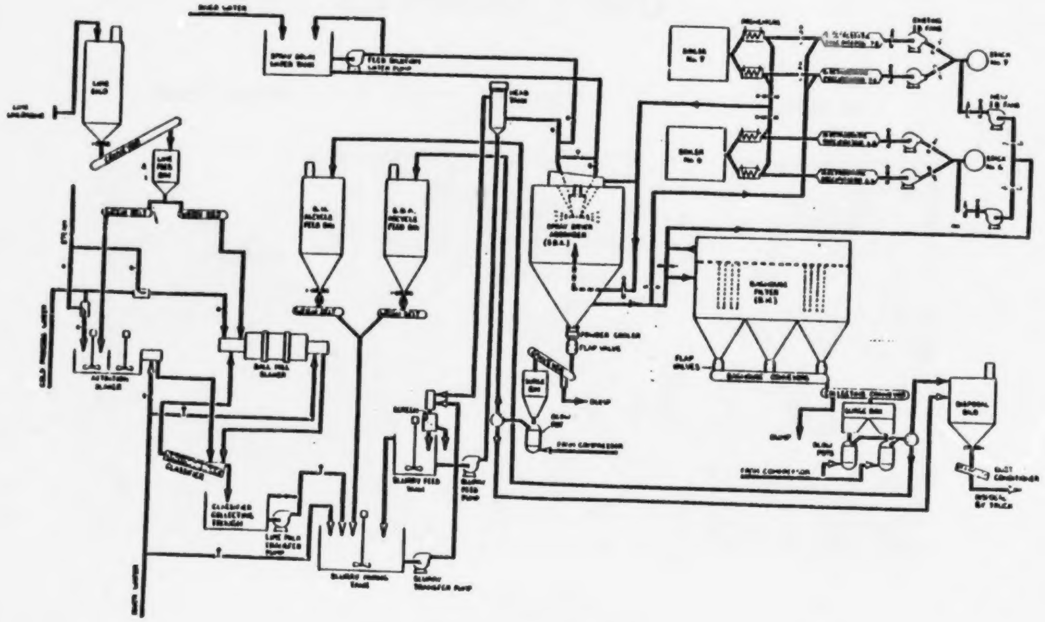
HEAD TANK
SPRAY DRYER ABSORBER (S.D.A.)
BAGHOUSE FILTER (B.H.)
POWDER COOLER
FLAP VALVE
FLAP VALVES
DUMP
FROM COMPRESSOR
DISPOSAL SILO
DUST CONDITIONER
DISPOSAL BY TRUCK

FIGURE 2

TESTING & OPERATION RECORD

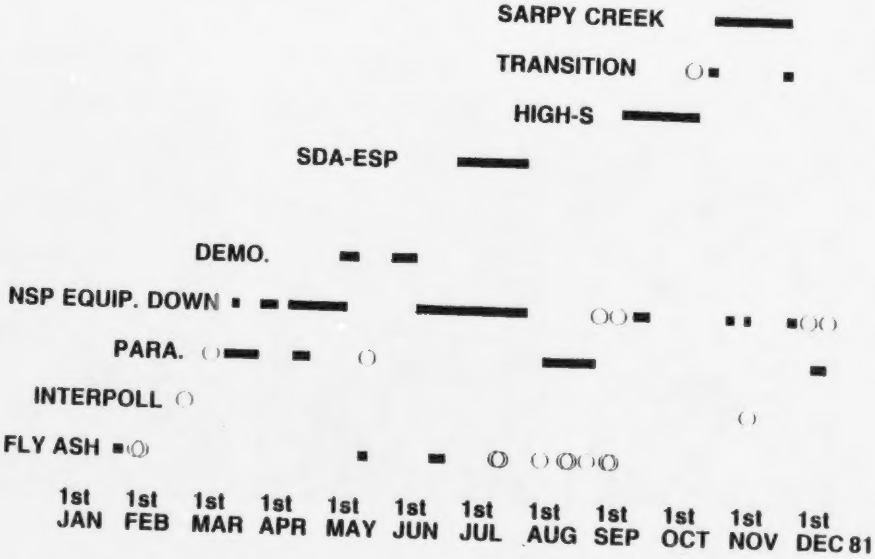

Note: ○ One day event

FIGURE 3

BH INLET
DUST SAMPLES

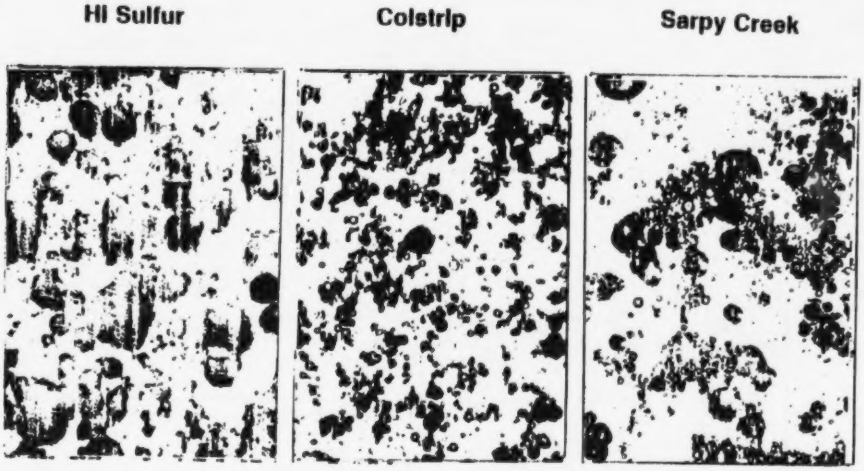
HI Sulfur
Colstrip
Sarpy Creek

FIGURE 4

SDA INLET
DUST SAMPLES

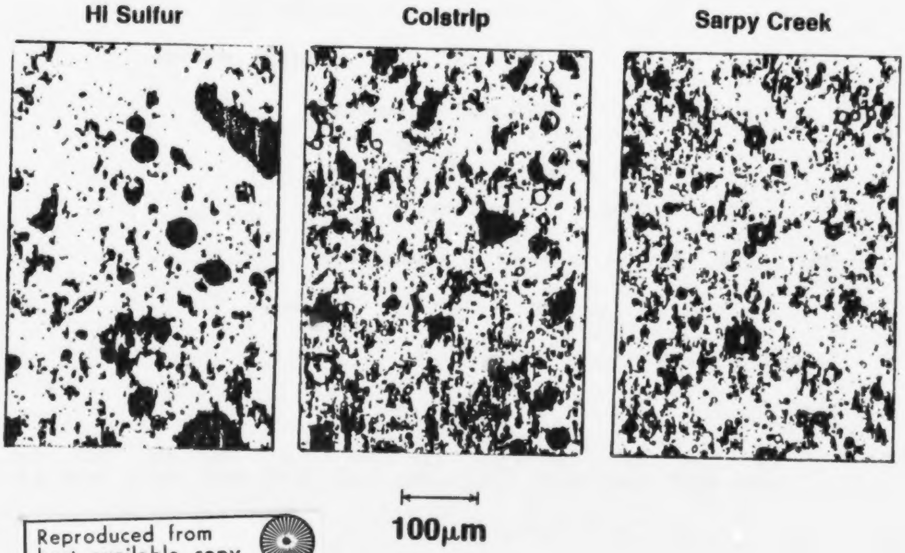
HI Sulfur
Colstrip
Sarpy Creek
100µm

Reproduced from
best available copy.

FIGURE 5

FGD OPERATION PARAMETERS

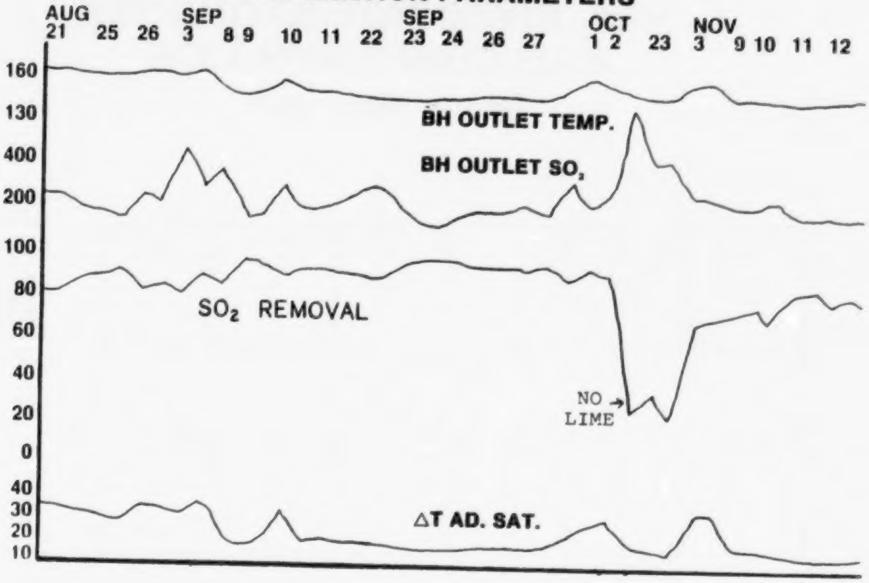

FIGURE 6

BH OPERATION PARAMETERS

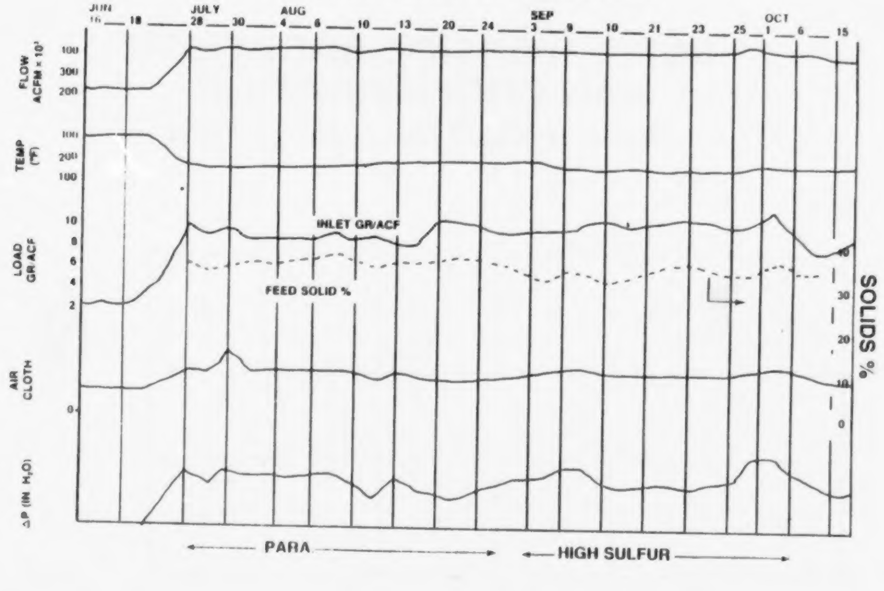

FIGURE 7

NSP, RIVERSIDE BAGHOUSE BAG CONFIGURATION

March - Dec., 1981

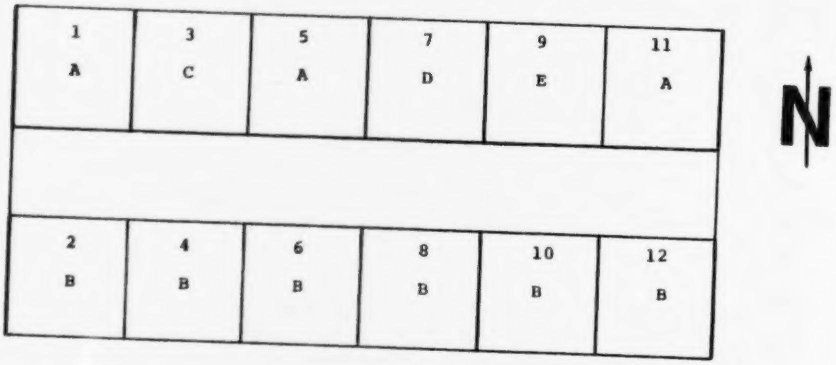

1
A
3
C
5
A
7
D
9
E
11
A
2
B
4
B
6
B
8
B
10
B
12
B
N

FIGURE 8

NSP, RIVERSIDE BAGHOUSE BAG CONFIGURATION

Second Start-up — June, 1982

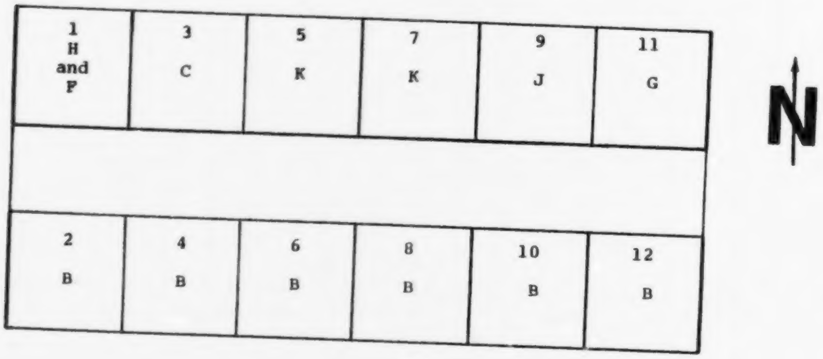

1
H
and
F
3
C
5
K
7
K
9
J
11
G
2
B
4
B
6
B
8
B
10
B
12
B
N

FIGURE 9

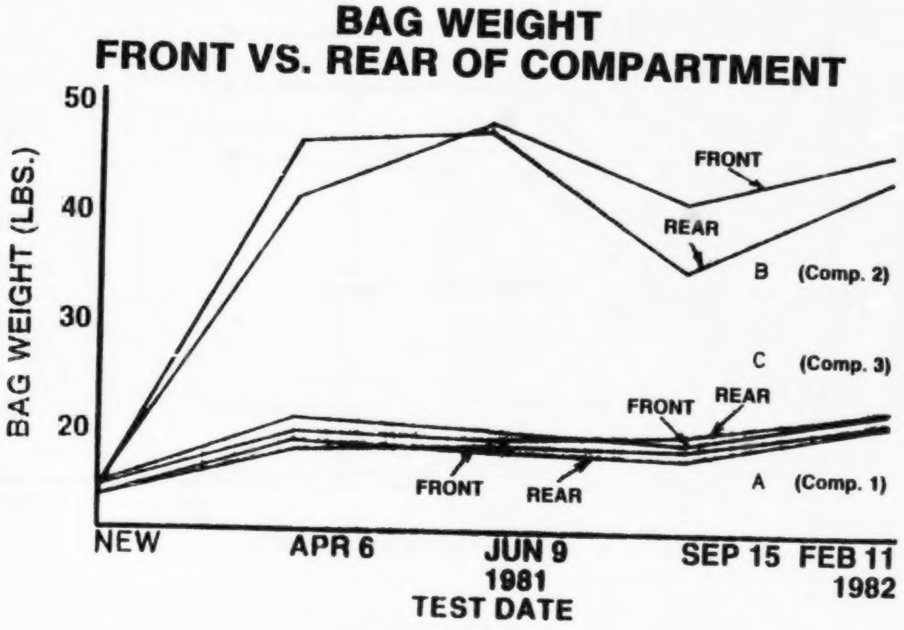

FIGURE 10

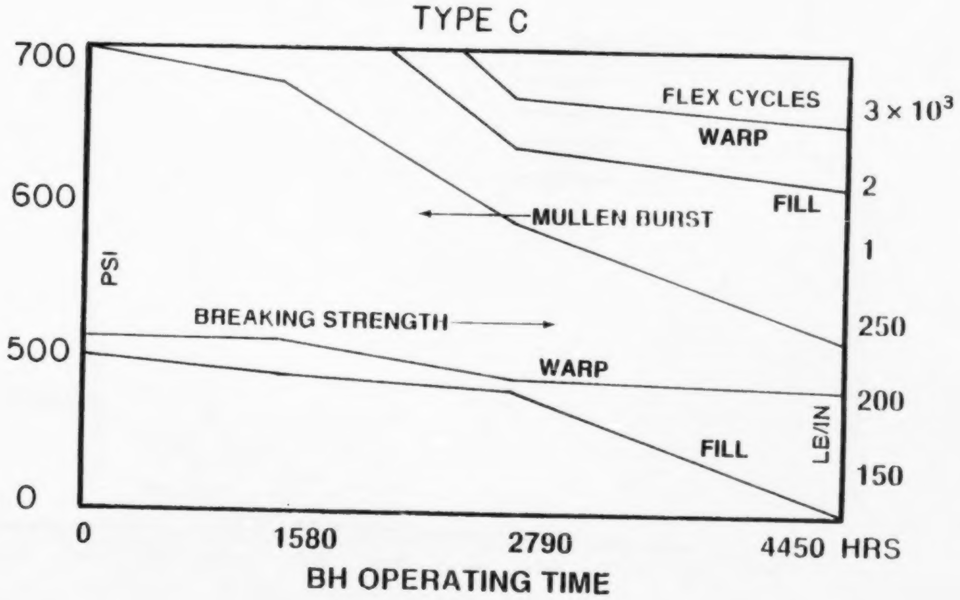

FIGURE 11

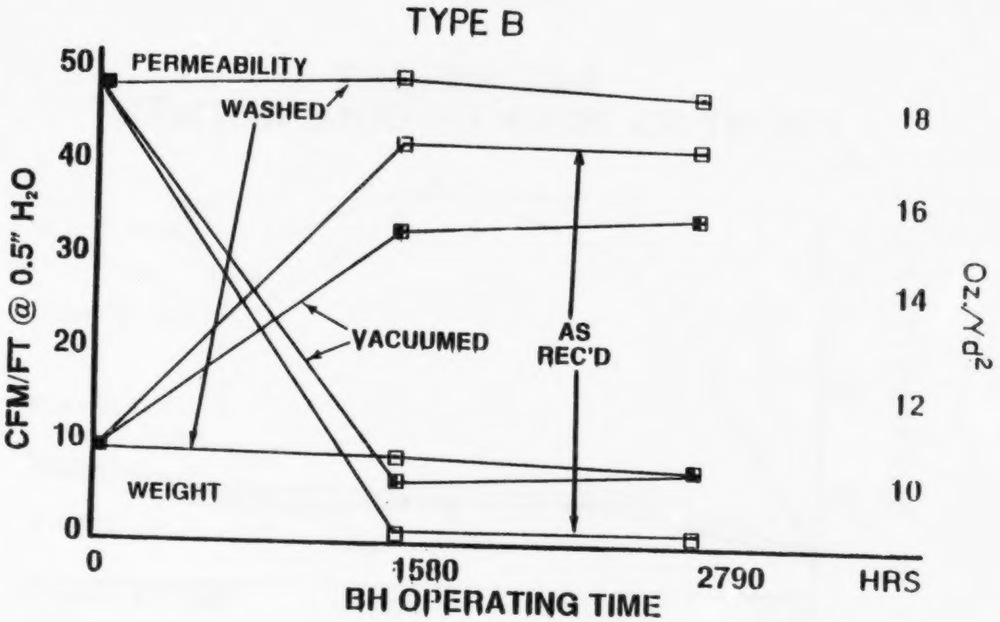

FIGURE 12

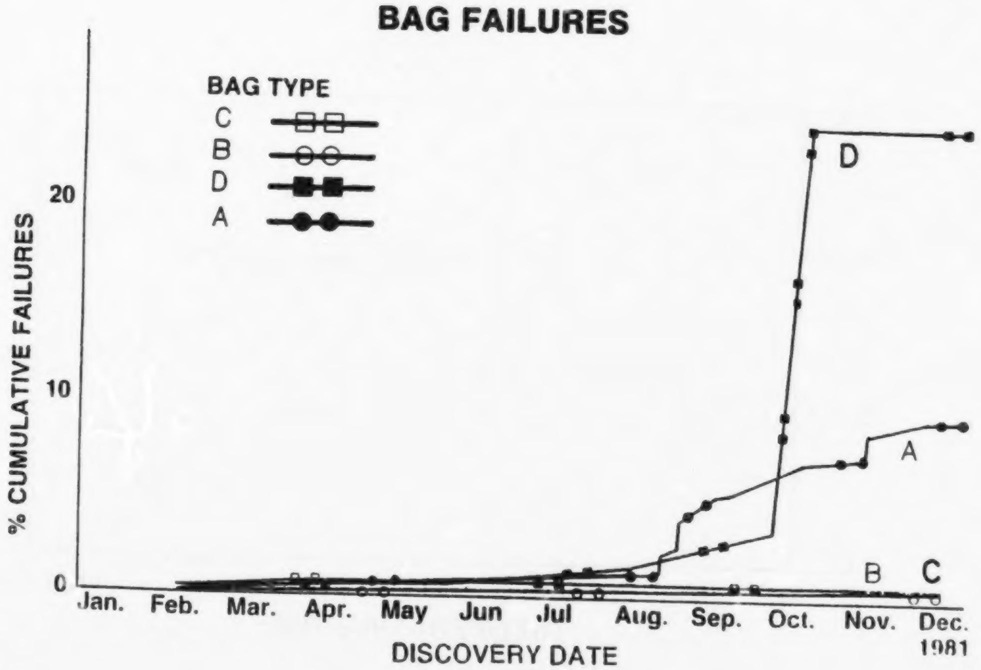

FIGURE 13

TYPICAL BAGHOUSE SYSTEM PRESSURE DROP

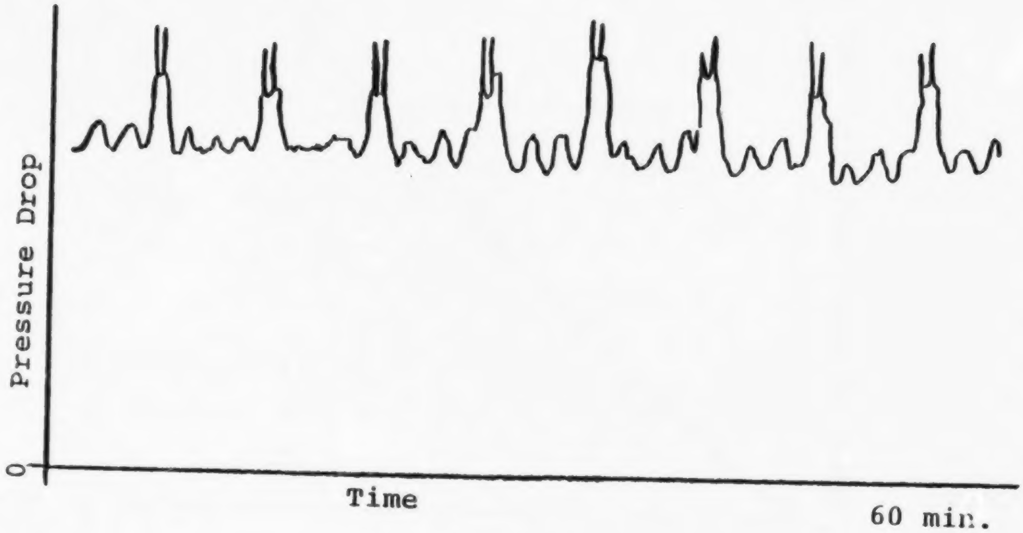

FIGURE 14

AREAL CAKE DENSITY VS. FILTER DRAG

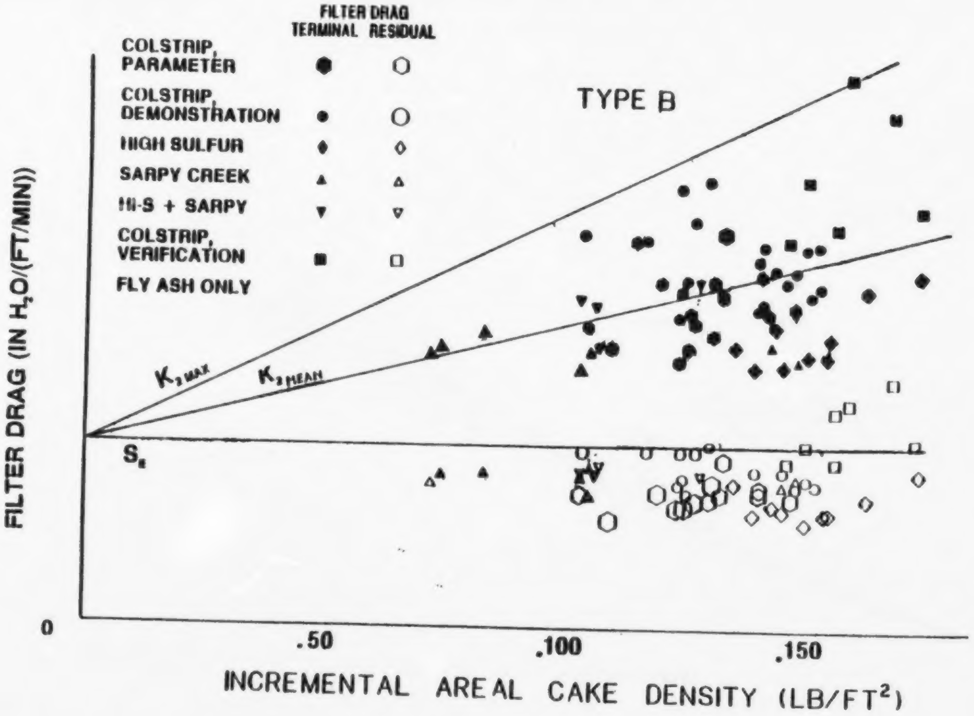

FIGURE 15

COMPARISON OF PRESSURE DROP PREDICTION

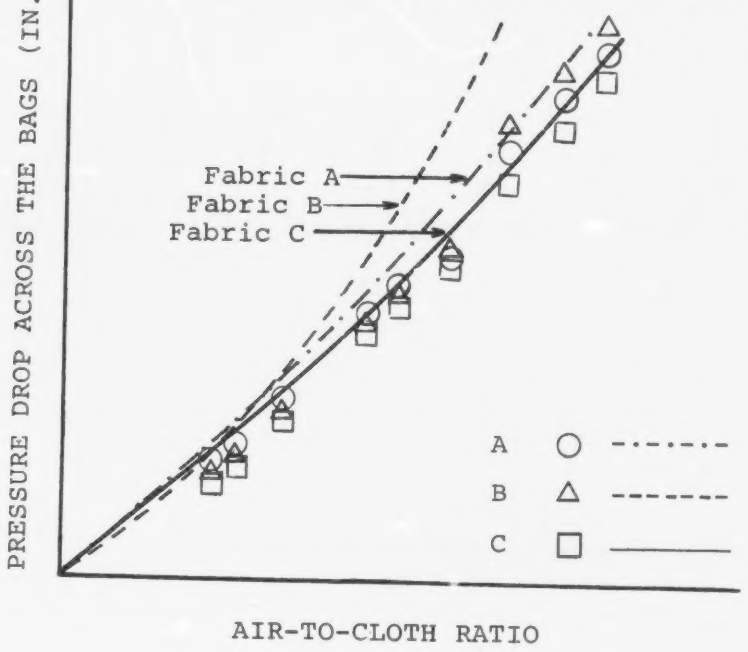

FIGURE 16

ΔP VS. AIR-TO-CLOTH

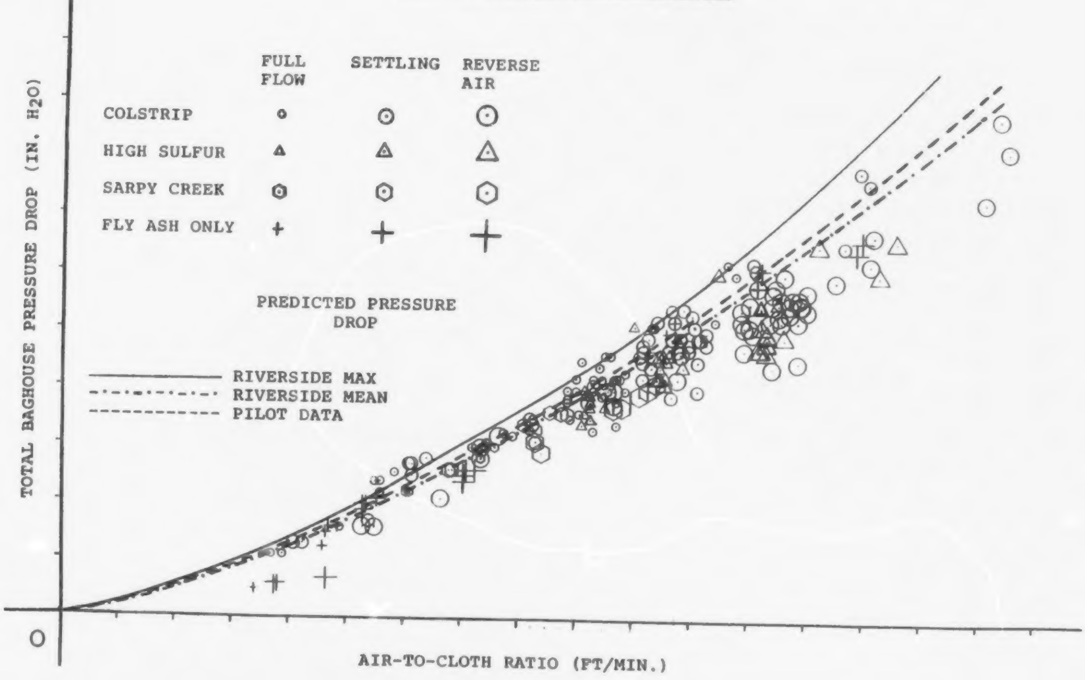

REACTIVITY OF FLY ASHES IN A SPRAY DRYER/FABRIC FILTER FGD PILOT PLANT

by

Wayne T. Davis, Randal E. Pudelek, and Gregory D. Reed

Department of Civil Engineering
The University of Tennessee
Knoxville, Tennessee 37996-2010

ABSTRACT

This paper summarizes the results of a study in which the reactivities of 23 fly ashes were evaluated in a pilot plant spray dryer/fabric filter sulfur dioxide removal system. The primary objective was to determine the ability of each fly ash (including lignite, subbituminous, and bituminous eastern and western ashes) to remove SO_2 when placed in a water-based slurry and atomized by a spinning disk atomizer into a spray dryer located on a slipstream from a stoker-fired boiler.

Data are summarized in both tabular and graphical form including chemical kinetic data as well as SO_2 removal efficiency indicating the enhancement in efficiency resulting from use of fly ash. The SO_2 removal efficiency ranged from 10-50% with only fly ash in the slurry.

INTRODUCTION

In the last five years the use of spray dryers to remove sulfur dioxide from flue gas has moved from pilot plant to full scale applications. The system consisting of a spray dryer and particulate removal device has generally employed a $Ca(OH)_2$ slurry which was atomized in the drying chamber via a nozzle or spinning disk atomizer. It has been observed in these systems that the fly ash may also play an important role in minimizing the reagent requirements, particularly if recycle is employed. The objectives of this study, sponsored by the Department of Energy, were to 1) collect a number of different fly ashes from various coal-fired power plants, 2) quantify the ability of each ash to react with SO_2 in a spray dryer pilot plant, and 3) identify the parameters responsible for the reactivity. To this end, 23 different ashes were studied, the results of which are reported herein.

DESCRIPTION OF THE TEST FACILITY

The spray dryer/fabric filter pilot plant was installed on a Riley spreader-stoker coal-fired boiler at the University of Tennessee steam plant. A slipstream of flue gas with a nominal flow of 1,000 ACFM, taken from the main ductwork, entered the system which consisted of a spray dryer with a spinning disc atomizer followed by a fabric filter collector. The slipstream was pulled through the pilot system by an induced-draft fan. A layout of the system is shown in Figure 1.

The ductwork leading to the spray dryer contained ports for the injection of ambient air and/or SO_2. Other ports labeled one, two and three respectively, enable the monitoring of temperature, static pressure, and SO_2 concentration at the inlet and outlet of the spray dryer find the outlet of the fabric filter collector, respectively.

Once the desired inlet SO_2 concentration and temperature was achieved the flue gas then proceeded to the spray dryer inlet where it encountered the atomization machinery. Atomization was accomplished by a Stork-Bowen high speed AA-6 Spray Machine and a centrifugal atomizer. The water and fly ash slurry passed from the pumping system through the spray machine housing into the atomizer. Rotating at a high speed (17000-18000 RPM), the disc atomized and distributed the slurry as a uniform, fine mist into the hot flue gas entering the drying chamber.

Flue gas exiting the boiler entered the drying chamber through a set of vanes concentric with the spray machine. These vanes imparted an angular downward swirling motion to the air. The rotation of the swirling air was opposite to that of the feed leaving the atomizer thus insuring intimate mixing of the hot air and the fine particulate mist. The drying chamber was a 7 foot diameter vessel with a standard conical bottom which contained a rotary valve for the removal of the spray dryer product.

The particulate-laden gas stream upon leaving the spray dryer entered the fabric filter collector. This collector removed both the suspended fly ash-SO_2 product and any other type boiler ash contained in the flue gas stream. The bag house consisted of one filtration compartment containing four 32 ft. x 12 inch fiberglass bags (14.5 oz./sq. yd.). A low energy shaker mechanism was used to clean the bags. It was operated manually at the completion of or prior to a test.

The control room contained 1) a panel for the control of atomizer rpm and 2) other devices for the monitoring of the system flow rate and the slurry feed rate. Also, monitored in the control room were the following:

1. SO_2 concentration (3 ports) Lear-Siegler SM800
2. Temperature (thermocouples)
    a. Inlet/outlet spray dryer
    b. Inlet bag house
    c. Ambient temperature
    d. Slurry feed temperature

3. Slurry feed rate
4. Concentration of additive (i.e. fly ash percent)
5. Static pressure inlet/outlet of spray dryer/bag house

When the desired range of SO_2 concentration cannot be achieved, a manually controlled supplemental SO_2 injection system is used. This system was located about 80 feet upstream of the spray dryer in the inlet duct to allow for sufficient mixing. Inlet temperature control was maintained by a manually operated ambient air dilution damper located upstream of the SO_2 injection port.

Monitoring of SO_2 was accomplished by extracting samples through heated trace lines into the control room where the flue gas sample was drawn through the sampling cell of a Lear-Siegler SM800. The concentration of SO_2 was measured on a wet basis by this instrument. A dry basis concentration was calculated later after the moisture content was determined.

Slurry preparation in this study consisted of gravimetrically weighing and mixing of a known quantity of a fly ash into a known quantity of water. The detention time was 25-40 minutes prior to conducting each test.

LABORATORY TEST PROCEDURE

The potential SO_2 removal capability of fly ash was investigated using twenty-three fly ashes of different rank, i.e., lignite, subbituminous, and bituminous eastern and western ashes (see Table 1).

Prior to the actual testing of each fly ash, laboratory analyses were performed to quantify both the physical and chemical characteristics of the ash. Table 2 shows the physical and chemical properties measured and the instruments that were used. Chemical analyses conducted for total alkalinity, calcium and sodium content, pH, and total hardness yielded information regarding the behavior of each fly ash in a water-based slurry. These analyses were conducted at a temperature of 140°F(60°C) and a fly ash concentration of 1.45 pounds per gallon of water. These conditions were chosen in order to simulate the condition to be tested at the spray dryer facility.

In addition, laboratory preparation of the fly ashes, according to ASTM procedures (5), followed by analysis with an atomic absorption spectro photometer determined the levels of calcium oxide (CaO), sodium oxide (Na_2O), magnesium oxide (MgO), and potassium oxide (K_2O) as received. Using these data an estimate of total alkaline metal oxides (TAMO) is obtained as follows:

$$\begin{array}{l}\text{Total g-moles Alkaline} \\ \text{Metal Oxides/100g. ash}\end{array} = \frac{\text{g. CaO/100g.}}{\text{56.1 g./g-mole}} + \frac{\text{g. Na}_2\text{O/100g.}}{\text{62.0 g./g-mole}} + \frac{\text{g. MgO/100g.}}{\text{40.3 g./g-mole}} + \frac{\text{g. K}_2\text{O/100g.}}{\text{94.2 g./g-mole}}$$

Table 1. Origin of the Fly Ashes Investigated

Fly Ash I.D.	Power Plant of Origin	Type of Fuel (approximate)	Source
6	Belews Creek Steam Station	bituminous	Low sulfur eastern coal
10	Bowen Steam Plant	bituminous	eastern Kentucky
13*	Clay Boswell Unit 4	subbituminous	Big Sky Mine - Colstrip Montana
14	Nebraska Public Power Station Gerald Gentleman Station	subbituminous	Black Thunder Mine Campbell County, Wyoming
18A	Pacific Power and Light Wyodak Plant	subbituminous	Wyodak Resources - Wyodak Mine
18B	Hunter Steam Plant	bituminous	Wilberg Mine - Emery County, Utah
23B	Cherokee #4	bituminous	Colorado western slope
24	Gallagher Station II Public Service of Indiana	bituminous	Amax Aryshire
27	Texas Utilities Generating Co. Big Brown	lignite	Freestone County
34	New Madrid Power Plant #2	bituminous	Southern Illinois, Seam #6
36	Ohio Edison - Gorge	bituminous	Ohio strip mine
37	Harrington Station: Southwestern Public Service Co.	subbituminous	Black Thunder Mine near Gillette, Wyoming
38B	Laramie River Station	subbituminous	Cordero Mine
38C	Basin Electric Powwer Cooperative - Unit 1	lignite	Consolidated Coal Co. Stanton, North Dakota
41	Milton R. Young Station Center Unit 1	lignite	Bankol-Noonan Mine Center, North Dakota
42	United Power Association Cooperative Power Association	lignite	Falkirk Mine Underwood, North Dakota
43	Black Hills Power and Light Company	subbituminous	Wyodak Mine - Wyoming
44	Otter Tail Power Hoot Lake Station Unit #2	lignite	Knife River Coal Mining Co. Beulah, North Dakota
45*	Minnesota Power and Light Company Clay Boswell Station	subbituminous	Big Sky Mine. Colstrip, Montana
46	Monifer Resources San Antonio Public Service	subbituminous	Cordero Mine, Wyoming
49	University of Tennessee Steam Plant	bituminous	eastern Kentucky
50	Marshall Steam Station	bituminous	Low sulfur eastern coal

*These fly ashes were obtained from the same source, however, their production resulted from different combustion conditions.

Table 2. Fly Ash Physical and Chemical Characteristics

Fly Ash I.D.	MMD[a] (μm)	Geometric[a] Deviation	Particle[b] Density (g/cm³)	Surface Area[c] (m²/g)	pH	Alkalinity mg/l. as $CaCO_3$	Ca, mg/l.	Na, mg/l.	Total Hardness, mg/l. as Ca
6	12.0	2.3	2.7	1.31	5.2	200	472	40	547
10	14.8	2.2	2.1	2.14	6.7	500	265	26	--
13	9.4	1.9	1.5	0.21	11.2	3800	962	48	1094
14	9.5	1.8	2.7	2.09	11.0	3500	132	299	210
18A	15.0	1.9	2.5	0.73	10.6	1200	130	54	160
18B	7.8	1.9	2.3	2.14	11.2	3400	849	88	1000
23B	14.9	2.8	2.2	2.85	11.3	1800	264	51	340
24	12.3	2.2	2.7	2.88	11.4	2900	1151	91	1208
27	9.5	2.5	2.4	0.74	10.3	1700	415	300	547
34	9.2	1.7	2.5	1.23	4.4	0	604	300	717
36	15.3	2.0	2.6	0.22	10.5	1400	245	49	283
37	7.4	2.5	2.7	1.15	11.3	1800	85	200	170
38B	11.5	2.2	2.6	1.66	11.2	1500	123	54	245
38C	15.6	2.6	3.2	0.76	10.8	1600	274	4200	368
41	12.0	1.8	2.7	3.27	10.7	1100	321	8000	396
42	9.4	1.9	2.6	0.29	11.4	3700	887	62	981
43	18.0	2.4	2.5	1.03	10.9	2100	179	75	274
44	11.0	1.9	2.7	2.37	10.9	1300	340	8200	396
45	10.0	2.0	2.5	3.39	10.7	1600	302	58	396
46	8.5	1.8	2.5	1.48	10.9	1600	128	100	170
49	12.9	1.9	2.1	12.52	3.6	0	175	150	--
50	14.0	2.1	2.2	1.47	4.8	0	321	52	358
44M - Fly ash 44 ground in a ball mill ------------					10.9	2100	302	8500	472

[a] Mass mean diameter and geometric standard deviation (Coulter Counter Model TAII)

[b] Helium/air Pyncnometer (Micromeritics Model 1302)

[c] Micromeritics Surface Area Analyzer

This determination was made based on previous studies in which it was shown that TAMO was related to sulfur retention in fly ash (Fiedler, 1). Table 3 contains both the percent of each compound in the ash (wet basis) and the estimate of TAMO. Another term used in some of the correlations was the value of TAMO less the sulfur in the ash:

$$\text{TAMO-S} = \text{TAMO} - \frac{\text{g. S/100g.}}{\text{32.1 g/g-mole}}$$

This term was used to account for reaction that had already occured in the as-received ashes.

FLY ASH TESTING IN THE SPRAY DRYER

Fly ash testing at the spray dryer facility was accomplished by mixing a known mass of fly ash in a known quantity of water with sufficient residence (mixing) time (greater than 30 minutes) to allow any soluble metal oxides to go into solution in the slurry. Figure 2 is a typical example of the dissolution kinetics exhibited by each fly ash. This information was used to deter-

Table 3. Fly Ash Mineral Analysis Summary

Fly Ash I.D.	% S	% CaO	% Na_2O	% MgO	%K_2O	TAMO (moles/100g. Ash)
6	0.43	7.79	10.71	0.97	2.53	0.36
10	0.32	5.44	9.42	0.91	2.36	0.30
13	0.49	13.96	10.96	2.79	1.79	0.52
14	0.73	22.91	10.96	3.49	1.29	0.69
18A	0.70	18.96	10.78	3.79	1.50	0.62
18B	0.45	9.72	10.89	2.14	1.94	0.42
23B	1.87	7.88	10.25	1.18	1.68	0.35
24	1.22	8.66	9.94	1.91	0.76	0.35
27	0.66	14.99	11.19	2.40	1.70	0.53
34	1.04	6.76	11.79	0.97	2.90	0.37
36	0.36	0.98	12.69	0.39	5.56	0.29
37	0.78	24.95	10.98	3.59	1.00	0.72
38B	0.72	21.81	13.48	2.97	1.29	0.70
38C	0.	13.95	35.88	5.58	3.69	1.01
41	4.06	18.01	16.68	3.98	1.52	0.71
42	1.02	18.96	10.97	3.79	1.90	0.63
43	0.66	6.96	10.76	1.00	2.49	0.35
44	0.75	23.80	17.71	4.57	1.14	0.84
44M	0.75	23.80	17.71	4.57	1.14	0.84
45	0.68	11.63	10.66	2.71	1.45	0.46
46	0.75	28.90	14.94	3.98	1.39	0.87
49	2.19	4.02	6.97	0.94	1.94	0.23
50	0.41	5.75	12.47	1.44	2.78	0.37

mine the required duration of mixing and the effect of slurry preparation and temperature. After mixing, the slurry was pumped to a final dilution tank where it awaited final transfer into the spray dryer. Prior to and during the slurry production procedure the following conditions were maintained for all fly ashes tested at the spray dryer/fabric filter facility:

1. Inlet temperature range (300 ± 10°F)
2. Inlet SO_2 concentration (600-800 ppm)
3. Gas volumetric flow rate (1,000 acfm)
4. Slurry preparation temperature (130-140°F)
5. Slurry concentration (1.45 lbs fly ash/gallon H_2O)
6. Approach to saturation in spray dryer (20°F)

The total SO_2 removed by the system (spray dryer plus bag house) was determined from inlet and outlet concentration data obtained from a Lear Siegler SM800 SO_2 analyzer. These data were converted to mass/time and reported in pounds/minute of SO_2 removed as well as g-moles/sec of SO_2. By defining the quantity of SO_2 removed in this manner the existence of any significant correlation with alkaline metal oxide content of the ash could be identified.

Table 4 provides a summary of the actual efficiencies of SO_2 removal across the spray dryer (EFFSD) and the system (EFFSYS) which included the spray dryer plus the baghouse. As can be seen, the system ranged from 0-30% for the fly ashes mixed in the slurry. A ball-milling of fly ash 44 increased the efficiency from 18% up to 46%. It was interesting to note that this improvement was a result of improved efficiency in the baghouse.

Two important checks were conducted periodically on the system during the course of this investigation to minimize the errors involved in actual testing. First, SO_2 balances were conducted at test conditions by measuring concentrations at all three ports without any fly ash injection. A consistent four percent reduction in the level of SO_2 was observed at the system's outlet due to air inleakage. Secondly, water injection (no fly ash), via the spinning disk atomizer, resulted in a two percent SO_2 efficiency. The values in Table 4 and following tables represent values corrected for air leakage and water.

RESULTS OF STATISTICAL ANALYSES

PRELIMINARY ANALYSES

The primary objective of this study was to identify the potential reactivity of various types of ashes and determine their capability for SO_2 removal in the spray dryer/fabric filter system. It was hoped that a high level of correlation could be found between the parameters and the SO_2 removal rates in the system. However, the chemical analyses of the slurries, as shown in Table 2, were measured on the filtrate from the slurries and did not reflect any reactivity which might occur on the surface of the suspended fly ash. Figure 3 shows that the actual number of moles of SO_2 removed per second

Table 4. SO_2 Removal Efficiency by a Fly Ash Slurry

Fly Ash I.D.	EFFSD	EFFSYS
6	0	1
10	12	7
13	7	17
14	35	30
18A	22	21
18B	26	23
23B	4	2
24	7	6
27	3	5
34	6	6
36	2	0
37	27	26
38B	19	26
38C	13	15
41	19	21
42	10	9
43	23	26
44	17	18
45	13	24
46	14	13
49	13	29
50	2	1
44M	17	46

was generally equal to or greater than the calcium plus sodium feed rates into the spray dryer (expressed in moles/sec as Ca).

The ASTM analyses of total alkaline metal oxides (TAMO-S), on the other hand, were a measure of the total values contained in the fly ashes and as such over-predicted the amount available for reaction due to the insolubility of the ashes. This is evident in Figure 4 which shows a graph of SO_2 removed in the system versus TAMO-S. The amount of SO_2 removed was typically only one-tenth of the total amount which could have been theoretically removed assuming a complete reaction with TAMO-S.

A preliminary statistical analysis of sulfur removed versus individual parameters such as TAMO, alkalinity, % calcium, % sodium, % calcium & sodium, hardeness, hardness + sodium, and surface area yielded correlation coefficients, R^2, in the range of .03-0.28. Upon dividing the fly ashes into the three coal ranks (lignite, subbituminous, and bitumminous), the lignite coal yielded values of R^2 of 0.61, 0.61, and 0.85 when linear correlations were conducted of sulfur retained in the system versus slurry sodium, slurry calcium + sodium, and surface area, respectively. Thus, further analyses were concentrated on multiple regressions in which the fly ashes were separated by coal rank. Also in an effort to account for the previous history of the fly ash it was decided to use the parameter total sulfur (TS) removal (sulfur in the ash as received plus sulfur removed in the spray dryer/fabric filter system) rather than just the latter.

PREDICTION OF TOTAL SULFUR RETENTION

As discussed earlier, various sorbents containing one or all of the alkaline metal oxide compounds (CaO, Na_2O, MgO, and K_2O) have demonstrated success in the removal of SO_2. These metals have been suggested as the primary constituents that occur in the formation of sulfate or sulfite end products [Rosenberg, et.al. (2) and Ando, et.al. (3)]. Davis and Fiedler (4) used this information to quantify the ability of fly ash to retain sulfur in the boiler after the coal was burned. Figure 4 shows the curve developed by Davis, et.al. (4) with the fly ashes used in this study plotted in the same manner. The ashes in this investigation exhibited less sulfur retention than found in the previous study presumably due to the lack of lignite data in the previous study.

It was this concept that provided the final basis for the modelling of total sulfur retention. Expressing the amount of SO_2 removed by the spray dryer/fabric filter system as grams of sulfur retained per 100 grams of ash and summing that with the quantity of sulfur already in the fly ash as received (see Table 2), determined the total sulfur retained. Table 5 contains the sulfur retention data for both the fly ash as received and for the fly ash slurry injected into the system.

The total sulfur retention (the sums of the two components) is included in Table 5 and is referred to as TSL, TSSB, and TSB for the lignite, subbituminous, and bituminous data, respectively.

Multiple regression analyses were conducted to determine the correlation and relationship between TS and the three parameters of surface area of fly ash, slurry alkalinity and TAMO. The following equations were found to adequately describe the sulfur retention for the lignite and bituminous fly ashes:

$$TSL = 0.019\ (SAI) + 125.320\ (ALKAL) - 0.507\ (TAMO) - 1.478 \qquad \text{(Eq. 1)}$$

$$TSB = 0.005\ (SAI) + 53.397\ (ALKAL) + 9.758\ (TAMO) - 3.336 \qquad \text{(Eq. 2)}$$

where

TSL = total sulfur retained by lignite ash (g/100g. fly ash)

TSB = total sulfur retained by bituminous ash (g/100g. fly ash)

SAI = surface area injected (m^2/100g. of fly ash)

ALKAL = slurry alkalinity injected (moles/100g. of fly ash)

Table 5. Sulfur Retention by Fly Ash

Fly Ash I.D.	Sulfur Retained by Boiler g./100g. fly ash	Sulfur Retained by SD/BH System g./100g. fly ash	Total Sulfur Retention g./100g. fly ash
Lignite			
27	0.66	0.35	1.01
38C	0.00	1.33	1.33
41	4.06	2.23	6.29
42	1.03	0.88	1.91
44	0.75	1.81	2.56
44M	0.75	4.61	5.36
Subbituminous			
13	0.49	1.44	1.93
14	0.73	3.35	4.08
18A	0.70	2.46	3.16
37	0.78	2.76	3.54
38B	0.72	2.87	3.59
43	0.66	2.89	3.55
45	0.68	2.48	3.16
46	0.75	1.21	1.96
Bituminous			
6	0.43	0.11	0.54
10	0.32	0.53	0.855
18B	0.45	2.95	3.40
23B	1.87	0.15	2.02
24	1.22	1.05	2.27
34	1.04	0.49	1.53
36	0.36	0.00	0.36
49	2.19	3.12	5.31
50	0.41	0.25	0.66

TAMO = total alkaline metal oxides injected (moles/100g. of fly ash)

The correlation coefficients, R^2, for equation 1 and 2 were 0.90 and 0.95 respectively. The R^2 for the subbituminous data was only 0.23, suggesting that further analysis is needed to quantify the relationship.

DISCUSSION

The data and results presented herein support the concept that reactivity is controlled by three factors, none of which is totally independent. For example, the TAMO inherently affe,ts the concentration of calcium and sodium ions which are available to go into solution. Likewise, the alkalinity is a measure not of the cations, but rater the anions (OH^- and $CO_3^=$). Thus, the physical significance of the developed equations is somewhat obscurred. It is certainly reasonable that, as the alkalinity and/or TAMO are increased, the potential for reaction in the spray dryer is enhanced. Likewise, as the surface area is increased, the possibilities of physical adsorption and/or surface reactions are increased. To achieve a higher level of confidence in the above correlations, it is necessary to determine the mechanisms that are controlling the reactivity.

The possible effect of surface area is best illustrated in fly ash 49 which had very low values of alkalinity, and TAMO, the lowest of any of the ashes. Yet it had the third highest sulfur retention (5.31 g/100 gram). This can be attributed to physical adsorption due to the highest observed surface area (12.5 m^2/g).

Fly ash 44 also provides some insight into the mechanisms that are acting to remove SO_2. A light ball milling of this ash resulted in a 17% increase in surface area and a 62% increase in alkalinity. The sulfur retention was increased by 150% due to this action. It is unclear whether the alkalinity or surface area enhanced the removal. It is clear however that the effect is non-linear.

The failure to arrive at a suitable equation for the subbituminous coal ($R^2=0.23$) may be due in part to the narrower range of values of total sulfur retention for the fly ashes studied. The eight values only varied by a factor of 2 whereas the lignite and bituminous data varied by factors of 6 and 10 respectively. The subbituminous data were input into equation 1 and 2 to determine if the measured values fell between the values predicted by the two extreme coal ranks. In all but one case, the data fell within or equal to the values predicted by equations 1 and 2 within the errors of measurement.

CONCLUSIONS

The major conclusions of this effort are summarized below:

1. It was demonstrated that SO_2 efficiencies of up to 30% could be achieved by simply mixing fly ash in water followed by injection into a spray dryer/fabric filter FGD system. The feed rate of 1.45 lbs per gallon is typical of the fly ash collected at a typical loading of 3 grains/CF.

2. Although of a preliminary nature, the data suggest that the surface area, slurry alkalinity and total alkaline metal oxides content affect the removal. Equations were developed through multiple regression analysis to illustrate that these parameters were of value in predicting reactivity.

3. The fly ash preparation technique (ball mill vs. simple mixing) was shown to have a significant effect on reactivity for one lignite fly ash. The removal across the FGD system was improved from 18% to 46% due to ball milling of the fly ash.

This study indicates that it is possible to develop statistical relationships which can be used to determine directions to be taken to enhance SO_2 removal efficiency. The alkaline metal content and surface area of fly ashes has in many cases gone untapped as a source of reactive reagents. Further research is needed to determine the following:

1. The optimum fly ash ratio for SO_2 removal in a spray dryer.
2. Improved extraction methods to extract alkaline metal oxides from fly ash to increase reaction potential of the slurry.
3. Document the advantages of grinding the fly ash in a ball mill and thus, produce corresponding increases in SO_2 removal.

REFERENCES

1. Fiedler, Mark A. Sulfur Retention in Fly Ash. Masters Thesis, University of Tennessee, 1980.
2. Rosenberg, H.S. et al. "The Status of SO_2 Control Systems." Chemical Engineering Progress, 71:5, May, 1975.
3. Ando et al. "Sulfur Dioxide Removal from Waste Gases: A Status Report Japan." Pollution Engineering and Scientific Solutions, Plenum Press, 1973.
4. Davis, W.T., and M.A. Fiedler. "The Retention of Sulfur in Fly Ash from Coal-Fired Boilers," JAPCA, Vol. 32, No. 4, 1982, pp. 395-397.
5. "Gaseous Fuels; Coal and Coke; Atmospheric Analysis." Annual Book of ASTM Standards, Part 26, 1978.

ACKNOWLEDGEMENT

The research conducted in this study was funded under a contract with the Department of Energy located at the Grand Forks Energy Technology Center. The contents do not necessarily reflect the views of DOE, nor does the mention of trade names or commercial products constitute endorsement or recommendation for use.

The work described in this paper was not funded by the U.S. Environmental Protection Agency and therefore the contents do not necessarily reflect the views of the Agency and no official endorsement should be inferred.

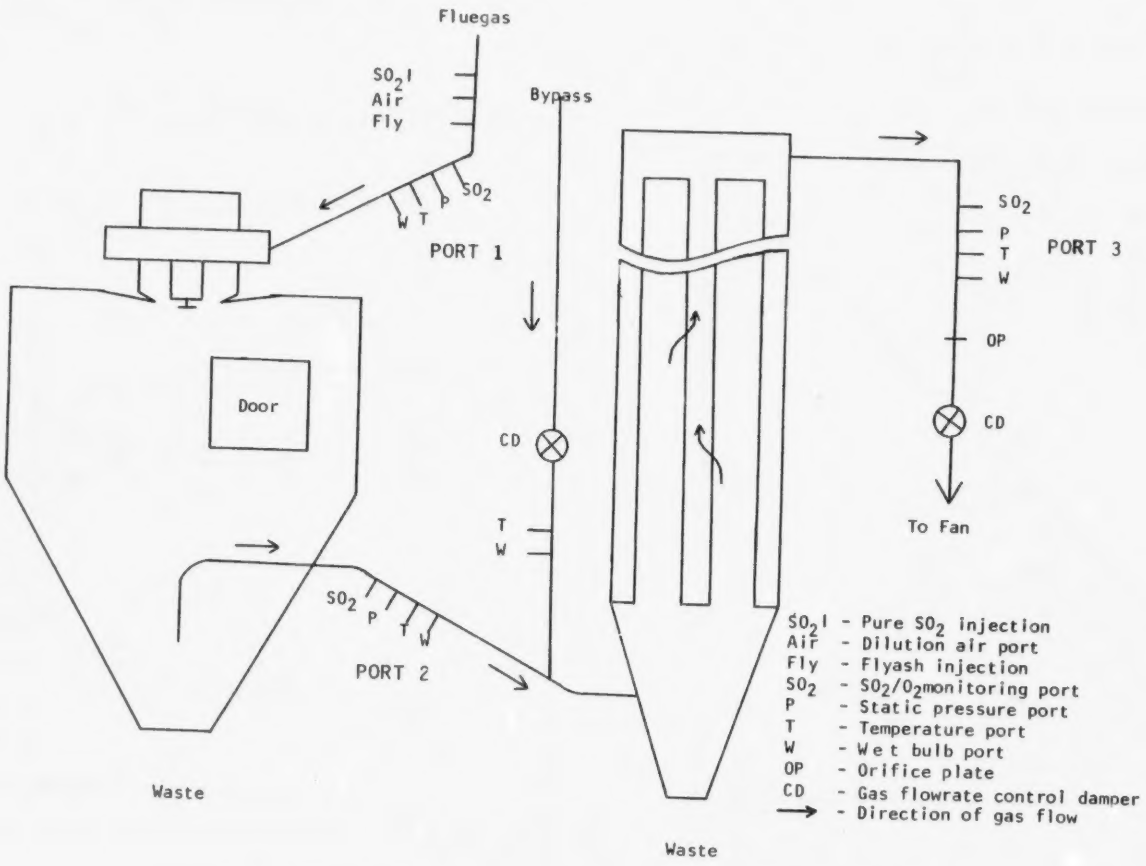
Fluegas
SO_2I
Air
Fly
SO_2
P
T
W
PORT 1
Bypass
Door
CD
T
W
SO_2
P
T
W
PORT 2
SO_2
P
T
W
PORT 3
OP
CD
To Fan
Waste
Waste
SO_2I - Pure SO_2 injection
Air - Dilution air port
Fly - Flyash injection
SO_2 - SO_2/O_2 monitoring port
P - Static pressure port
T - Temperature port
W - Wet bulb port
OP - Orifice plate
CD - Gas flowrate control damper
→ - Direction of gas flow

FIGURE 1: SCHEMATIC OF SPRAY DRYER/FABRIC FILTER SYSTEM.

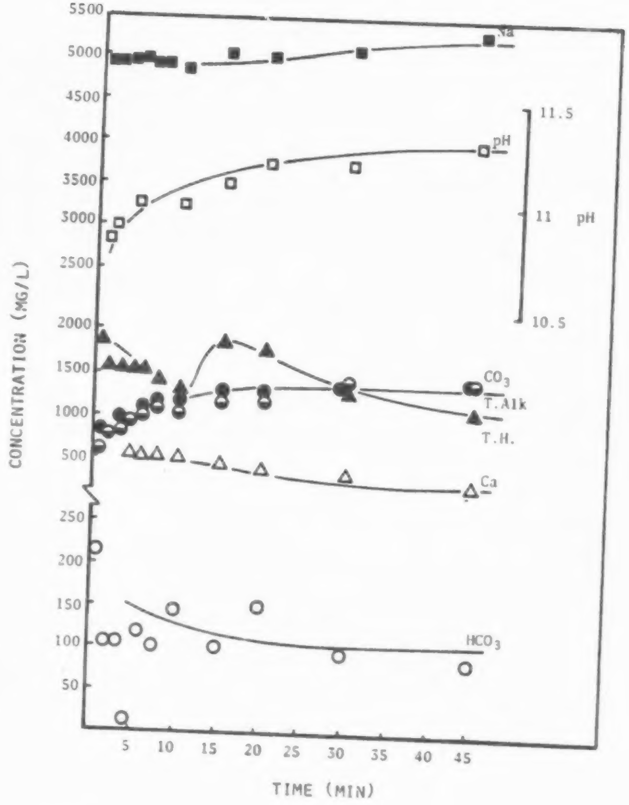

FIGURE 2: DISSOLUTION KINETICS OF HOOT LAKE FLY ASH IN DISTILLED WATER AT 74°C.

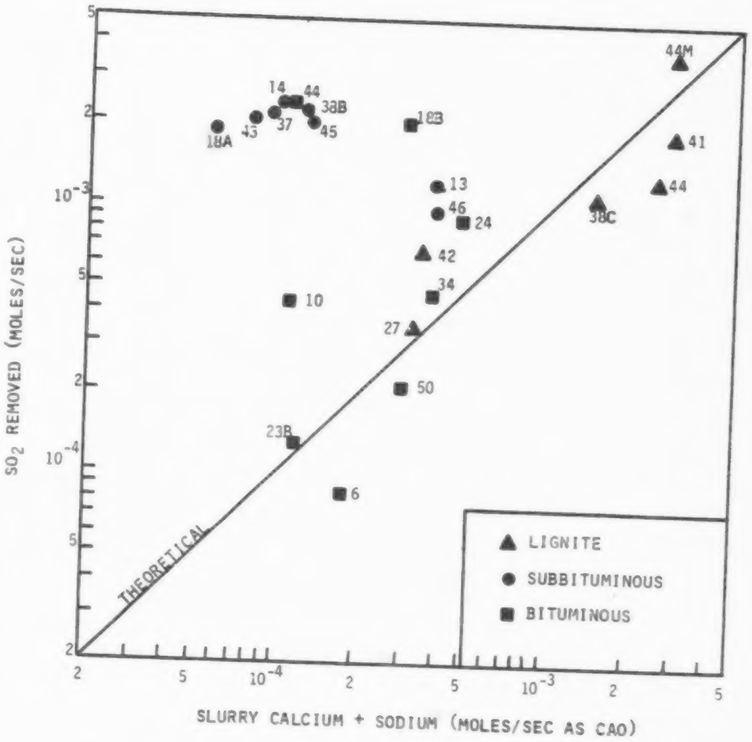

FIGURE 3: SO$_2$ REMOVED VERSUS CALCIUM PLUS SODIUM.

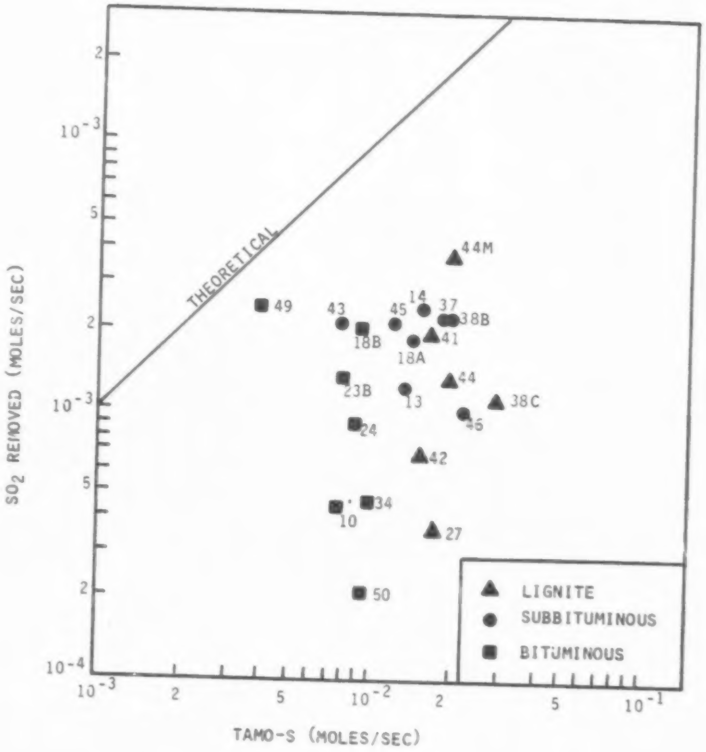

FIGURE 4: SO_2 REMOVED VERSUS TOTAL AVAILABLE METAL OXIDES LESS SULFUR (AS CAO).

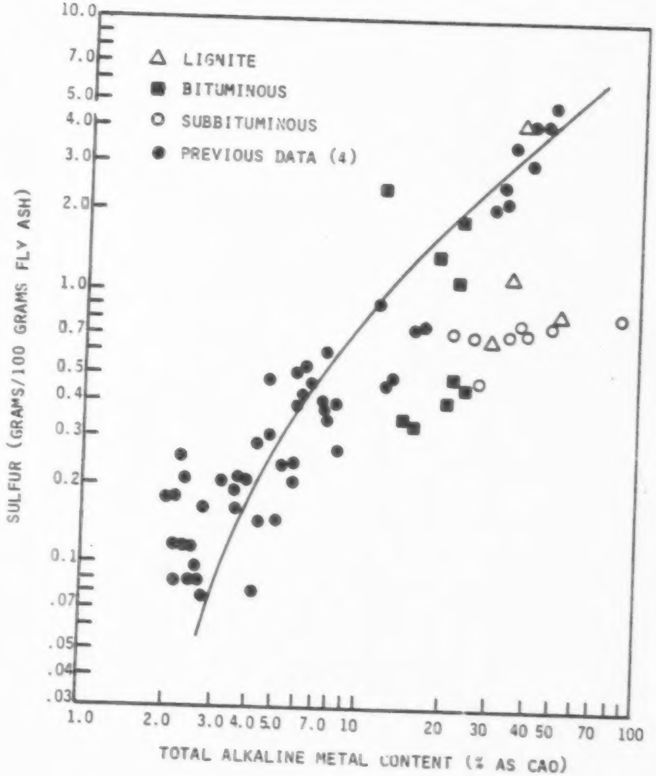

FIGURE 5: SULFUR RETENTION VERSUS TOTAL ALKALINE METAL CONTENT (REPORTED AS CAO).

FABRIC FILTRATION - AS IT WAS, HAS BEEN, IS NOW AND SHALL BE

by: Edward R. Frederick, Technical Director
Air Pollution Control Association
Pittsburgh, PA 15230

ABSTRACT

Since the first baghouse patent issued in 1852, commercial filtration technology has progressed significantly with advances in both collector design and in the performance capability of filter fiber and fabric. With the resulting extended and expanded service of fabric filters, critical issues have evolved concerning electrostatic involvement. Even though the natural charges present on gas entrained particles and on the collecting media interact to play a major role in essentially all filtration operations, more intense interest and study is being devoted to electrical augmentation as a means for optimizing these features and, thereby, all collection parameters. These observations have also stimulated further interest in and the production of new types of electrets, the electrified fibers that retain charges for extended service even under adverse conditions.

Although zinc oxide was first suggested as an absorbant for SO_2 during the last century, more economic reagents now serve with fabric filters to control this emission contaminant commercially by dry and wet/dry scrubbing. Further advances in this technology through the addition of special catalysts/additives and/or with special processing aids, increase SO_2 removal efficiency and also control NO_x effectively.

Normal use temperature filter fabrics are being improved and even better, although more exotic high temperature products are available. Improved processing, finishing and treating practices are in use to offer special value in extending bag life, chemical resistance and cleanability. The major yet unheralded problem of nodule formation, deserves special research consideration in view of the check valve effect that these "dingleberries" have on the filtration process. Corrective measures for this condition and expansion of waste heat/product recovery and utilization will certainly lead to further expansion of fabric filtration technology for SO_2 as well as particulate matter control.

INTRODUCTION

Those of you involved with fabric filtration have had to find the developments during the recent 8 to 10 years very exciting. Technology in this particulate control method has advanced further in this period than during the preceding decades except, perhaps,at the time when synthetic fibers and changes in processing methods were introduced during the 40's and 50's.

The current advancement in the art of fabric filtration, as well as in other control practices, is due in very large measure to the research support and publicity provided by the U. S. Environmental Protection Agency through both in-house and contracted research. Never before were the air pollution control methods so thoroughly and extensively examined and so favorably exploited.

These and independent R & D efforts in particulate control technology have led to very favorable predictions. Market Analysts[1] have noted that "Equipment and media sales in the U. S., totaling $2.7 billion in 1980, were dominated by particle emissions collectors, which accounted for 23 percent of the total market. Electrostatic precipitators and fabric filters comprise the bulk of this category.

This dominance is expected to remain through 1995, when particle emissions collectors will total nearly $3 billion, with fabric filters gaining some market share as the result of advances in fabric technology (especially for high temperature applications) and innovations such as electrostatically charging filter fabrics to increase particulate removal efficiency."

HISTORY

Fabric filtration is as old as the art of textile production; but, industrial particulate collection in baghouses began only during the middle of the last century. Despite this early beginning and more than 130 years of commercial service, fabric filtration remains an art and will not emerge to the sophisticated status of a science until more is known about media, particulates, and their interrelationships.

The commercial baghouse received stimulus early from the nonferrous metals industry for two principal reasons: to recover valuable raw material and to avoid court actions by neighboring farmers. It is especially interesting to note that early in this period (late 19th century) of baghouse development in a lead smelter operation, H. H. Alexander treated woolen bags with titanium chloride to achieve effective acid (sulfuric) resistance. Even before this, Sprague applied zinc oxide as an acid neutralizer in smelter smoke control. This, whether the advocates of dry scrubbing realize it or not, was the beginning of what they now advocate as an important new phase of fabric filtration technology.[2]

Modern baghouse history began with the installation of massive plant-built collectors and continued with the transition to "manufactured" baghouses and the introduction of an array of synthetic fibers. In between these events, a major filtration study--the "1929 Investigation" was undertaken. This is significant as the first extensive field study of filter media, cleaning methods, particulate variables, and other filtration related parameters. According to Armand Labbe[3] who had been responsible for ASARCO'S baghouse operations, this commercial scale evaluation demonstrated the superiority of a fulled, twill weave woolen fabric over a variety of other natural fiber, smooth surfaced, tightly woven materials; the critical importance of the shaking operation, the advantage of a horizontal shake of suitable magnitude, and especially, "that in the collection of two smokes of identical composition and concentration, one could be filtered at 6 times the rate of the other." This difference in performance was ascribed to variations in particle crystallinity and size of the otherwise similar dusts. Other findings revealed, as we now know, that the rate of filtration depended upon the amount and type of dust collected. Also noted was the value of low over high A/C ratios in limiting blinding and for providing often needed reserve capacity. While a primary goal of the investigation was to find the key to high ratio operations, the results demonstrated that such could be realized with substantial initial savings but the end result was increased bag wear with shortened bag life, lower efficiency, and no reserve capacity for unpredictable operational peaks.

During this same historical period, the pressure versus vacuum baghouse contoversy developed. Despite the use of the fan on the dirty side, Labbe favored the pressure type for a number of important reasons.

Subsequently, but much later, studies in our own laboratory demonstrated that not only did different fibers, yarns, and fabrics perform differently but that the more exotic weaves offered real advantages. The common plain weave was found to require tight yarn packing to provide suitable efficiency; whereas, the same yarn woven in twill or sateen configuration leaked less dust even at higher permeability. In the filtration process, particle movement tends to be normal to the fabric surface, passing through visible holes in plain weave fabrics, but, not holes visible only at an angle in a twill or sateen weave medium. At this same time, inherent fiber properties that were not normally considered important were found in most cases to have a far more critical influence on the collection process than fabric construction. For example, the electrostatic character of the media eluded to earlier by several investigators, was found to be influenced by the same property of the collected particulate matter. Electrostatic effects were found to control the filtration process[4]. More will be said about this and similar new developments.

Despite repeated attempts to develop universally acceptable high ratio collectors and the successes realized in some applications, the Labbe guidelines of low A/C ratios and good cleanability have been proven to be indispensible for realizing high efficiency and long bag life. To my knowledge the 30 to 1 ratios achieved with the Hersey or Hersey type reverse air jet collectors are the only commercial devices operating successfully at such levels but only with some dusts and the "right" fabrics. Likewise, and also in a number of less critical applications, many pulse jet high ratio collectors are performing well, generally at less than half this A/C ratio. Here, too, felt type, depth filtration media with suitable qualities, are required for effective performance. The development of, and progressive improvement made in these media have led to expanded use of high ratio collectors whether constructed to employ tubular or pocket type filters.

Conventional shaker and reverse air type collectors continue to serve extensively as the low ratio (up to ∿6 cfm/ft^2 of cloth) collectors. Bag life has been and continues to be a critical operating criteria with 5 years being about the normal expectance. Even the fragile glass bags have reached this level of longevity when optimum conditions prevail but, even much longer periods of use have been reported for organically based fiber systems. The utility industry has adopted baghouse technology to overcome problems associated with fuels and ash by employing mostly low ratio reverse air type systems. By and large the results have been extremely favorable and the development of novel techniques promises to further expand baghouse usage here and elsewhere.

FABRIC DEVELOPMENTS

The key to an effective and efficient filtration operation, assuming the equipment hardware is functioning satisfactorily, is the filter medium. Fiber suppliers, fabric designers, producers, and finishers alike have searched desperately for answers by developing new fibers and processes for fabrics and even for different, better cleaning systems. As a result, the applications of fabric filtration have expanded significantly into regions of higher temperature and conditions of chemical insult never before even considered possible.

FIBERS

During the last 40 years an array of new fibers, semisynthetic and synthetic, have been added to the natural fibers available for fabric filtration. These materials, and especially those of more recent development, provide unique properties and extend performance and operating temperatures up to and even beyond 500°F. Actually, more exotic new products extend the range beyond 1000°F with better chemical resistance.

The fibers commonly available today cover a wide spectrum of properties from those offered by the natural materials like wool and cotton to those given by nylon, polyester, acrylic, polyolefin, aramid, Teflon and glass. They are prepared in a variety of woven, knitted and needled filter media. These filter fabrics offer almost unlimited opportunities for conducting the diverse collection operations needed to recover valuable products, by-products or waste materials and to limit harmful or nuisance type emissions.

Opportunities to vary the base fiber have also brought about a realization among users and suppliers that a given fiber, however desirable otherwise, is not entirely effective in collecting different dusts. This inability to specify desirable fibers unilaterally, especially in certain critical applications, has led to the acceptance of a gray region in our filtration theory. Now, because it is becoming more evident that the electrical relationship between particulate matter and filter media plays a major if not dominant role in the process, an extension to the theory is evolving.

Recognizing the critical influence of the nature of the cake formed on the collecting fabric and the fact that most particulates may be deposited in a porous structure under the influence of favorable electrostatic conditions, new and/or more rational media prescription practices will evolve. In the interim, electrical augmentation or articifical charging of particles and applied electric fields at the fiber surface in pilot scale studies are indicating clearly the interdependence of these conditions. Substantially higher air to cloth ratios, consistently higher efficiencies, better fabric cleanability, less particle penetration and reduced fabric blinding with promises of extended bag life are all evident through electrical augmentation. Couple such developments with the practical experience already gained with fabric filtration in dry scrubbing and in controlling tarry or corrosive emissions, and it becomes apparent that this technology has come a very long way.

By adding neutralizing, absorbing or adsorbing reagents to the filter surface or by including appropriate agents with the reactive emissions, the fabric filter/scrubber process has expanded into critical control operations of aluminum production, coking, galvanizing and flue gas desulfurization. Other opportunities in difficult to control processes and for upgrading those already in use by the ferrous, nonferrous, cement, clay, glass, food products, coal, asphalt, clay, and chemical industries are now more apparent. Even so, this control technology like all of the others, will become even more useful as the by-product and energy reduction product recovery and material utilization processes become more feasible.

ECONOMIC CONSIDERATIONS

An attempt to predict the capital, operating, and maintenance costs of any operation is risky and always subject to correction. One issue about economics, however, seems to be crystal clear even though considerable variation in the predictions occurs here too. I refer to the cost/benefit relationship of particulate control. The analyses carried out by EPA, The National Wildlife Federation, The National Academy of Sciences, and others show without question, that air pollution control, for example, pays off substantially with very significant benefits above costs. The specific advantages, costwise, of one control technology over another are quite difficult to determine without consideration of all specifics. Nevertheless, when a choice is possible, a few, very "broad-brush" guidelines are available from various sources.

An EPA partially funded elaborate 1978 study of the "Capital and Operating Costs of Selected Air Pollution Control Systems"[5] is available. Two years earlier, an extensive review of "The Environmental Control Industry"[6] was prepared for CEQ. An attempt is made in these presentations to compare the various costs as well as some other features of fabric filters with electrostatic precipitators and scrubbers. Quite obviously, it is necessary to acknowledge the questionable reliability of some methods used to equate costs.

In general, and this may be the best way to relate the information concisely, it seems evident that fabric filters:

- are capable of controlling very fine particulate matter at very high efficiency,
- perform at lower cost on a flow throughput basis,
- operate with less energy input than scrubbers but somewhat more than that needed for ESPs,
- show a trend for lower increases in flange-to-flange prices than indicated for the other control methods,
- show less of an advantage in installation, total operating, and maintenance costs than ESPs,
- are less costly to operate than scrubbers.

The filter medium is critically important in its influence on baghouse performance and represents a large part of the capitol, operating, and maintenance costs. In any economic analysis, therefore, a comparison is also necessary.

Substantial variations occur between the price for very light weight filament materials, varying weight woven, spun or combination fabrics, and heavy needled felts. These differences and the fact that the different air to cloth ratios indicate again how difficult and unreliable baghouse cost generalizations can be.

DEVELOPING MATERIALS, PROCESSES AND TECHNIQUES

ELECTRETS

The electrical analog of a magnet, the electret, is a recent commercial development that also serves to verify the value of electrical involvement in the fabric collection process. The Hanson electrostatic filter developed in the 40's for the war effort in England was an outgrowth of Heaveside's work in about 1890, Eguchi's in 1920, and Gemants in 1935. His rosin impregnated wool has since been modified and refined by including acrylic fibers with wool and by using zinc resinate instead of rosin.

Within the last decade an entirely new and different approach has been used. One product is prepared by imposing an electric field on heated polyolefin film after the drawing/orientation stage of the process and then fibrillating the charged film to form durable electrified staple fiber. Fiber systems of this type, usually needled, now offer a high level electrostatic field of long durability even in the presence of moisture and other discharging environments. They have found extensive use as efficient respiratory filters. As far as I know, electrets have not yet been used extensively in commercial filtration service.

DRY AND WET-DRY SCRUBBING

Interest in, and commitment to, powder injection and spray drying for SO_2 and particulate control has increased dramatically in view of the claims for lower costs, dry wastes, lower energy requirements and simplicity as well as the acceptability of needed lower SO_2 removal from low sulfur coals.

Since removal efficiency depends upon many factors such as stoichiometric ratios, temperature and agent reactivity; studies of this technology are continuing at an accelerated pace. For example, considerable effort is being directed toward improvements in removal not only of SO_2 but also of NO_X. More favorable parameters and the use of catalysts[7], promotors[8] and other additives[9] are being investigated for overall increased control.

NO_X and SO_2 Control

In addition to conventional current scrubbing applications of fabric filters for SO_2 control, recent studies[10] have demonstrated the value of electron beam radiation following the spray dryer for removing NO_X and optimizing SO_2 control. The high energy electrons oxidize SO_2 and NO_X to higher oxidation states which react more readily with excess lime from the spray dryer or with alkaline fly ash. The net effect is enhanced SO_2 control plus highly efficient NO_X removal. The practicability and economics of the method are being investigated at several laboratories.

An especially interesting new process offered by the National Bureau of Standards[9] employs ozone and propylene to oxidize SO_2 and NO_X for easier removal of the resulting sulfate and nitrate with included ammonia.

ELECTRICAL AUGMENTATION

Artificial charging, as I prefer to identify the practice of charging particulate matter and/or applying an electric field to the filter medium, has received very considerable attention recently at both the bench and pilot scale level in investigation. The results have been consistently favorable. Lest there be unfavorable results coming from any such study, it must be made clear that the principle benefit of electrical augmentation resides in the porous nature of the deposited material that occurs in the presence of the electric field. Most types of particulate material respond in this way, but I believe that a few do not. Can you imagine the disenchantment that would occur by a report of negative data from studies of electrical augmentation? Recognizing that not all particulate matter are created equal, it seems evident that an attempt should also be made to classify dusts according to their ability to form a porous deposit as well as how they respond to the electrical augmentation process.

Quite possibly, the most serious issue facing the would-be users of electrical augmentation involves the durability of the circuitry. The question is, "how can an electric field be generated and maintained on the collecting surface for very extensive periods of use?" EPA's modification of TRI's charging electrodes has converted the outside fine wire girdle to a more substantial charging cage. These and future developments will certainly hasten the commercial adaptation of electrical augmentation to the filtration operation.

Gaylord Penney[11] has proposed a different approach, one that may offer a simpler practice. By insulating all or half of the bags in a collector, using slightly conductive media ($<10^{10}\Omega/\square$) and by applying charges of opposite polarity to opposing bags, Penney creates a field at the collecting surfaces. He also suggests that it may be advantageous to impose a bipolar charge on the particles entering this augmented collector. But this approach needs further study.

Whatever practice is ultimately devised for providing an electrical field at the filtering surface, it will be apparent that mechanical simplicity and durability will be the keys to its successful commercial utilization. The incentives for adopting electrical augmentation for collecting appropriate particulates are truly significant. The achievable improvements are real and substantial. Energywise, for example, the pressure drop reductions alone can reduce annual fan energy costs by at least a quarter million dollars for very large collectors. Add to this the savings in cleaning energy and bag replacement costs and it will be apparent that electrical effects deserve serious attention.

NATURAL CHARGES AND ELECTRIC FIELDS

A significant portion of the improved filtration performance realized by electrical augmentation or artificial charging is achievable simply by balancing particulate and fabric charges. All industrial processes produce particulate matter with charges, positive and/or negative. Thus, particles entering conventional collectors are charged, sometimes far more extensively than at other times but mostly of mixed polarity. The type of process generating particles greatly influences the magnitude of the charge, with grinding and other energy intensive operations producing particulate matter with extremely high levels of charge.

The electrical field, its polarity and magnitude, that develops on the filter medium by particle contact is determined by the inherent properties of the fibers that make up the fabric, by the construction of the fabric, by the particulate itself, and by operating conditions. It is possible, therefore, under the ideal conditions realized by use of a filter fabric of favorable electrostatic properties relative to those of the particulate being collected and, of course, for a particulate capable of alteration, to deposit a low air flow resistant cake without electrical augmentation. In other words, the natural triboelectrification properties of the medium may be employed to approach the ultimate level of filtration performance now achieved by augmentation.

The opportunities to utilize natural electrostatic effects fully are limited to some extent by the availability of appropriate media and more so by the variability of commercial fabrics. The most serious problem, however, is the limitation that prevails because of our restricted knowledge of the electrical properties of particulates and fabrics. We need to know more about these characteristics separately and how they relate to each other. Here, then, is an area for further study, the results of which could easily lead to more accurate detection and correction of filtration problems and, thereby, even more reliance on this technology by reliable prescription.

In addition to the measurement problems, there are inherent features of particulate and media that need to be dealt with. For example, there tends to be a variation in fiber qualities, even among those of the same or supposedly the same commercial origin. My studies, for instance, showed very significant differences in the electrostatic properties of polyester fibers. Even among those of one type, for example, Dacron fabrics, I've found triboelectric polarities ranging from the very electropositive region characteristic on nylon, to the electronegative levels of the polyolefins. No explanation has been offered for these very significant differences but there is considerable evidence, both from experimental and industrial experience to indicate that they are responsible for otherwise unexplained performance variations.

Other less obscure differences among filter media, regardless of similarity in fiber make-up, are also evident at times and these too influence behavior. Consider what happens when a residual amount of the fiber producer's antistatic finish is allowed to remain on the fabric, even in a trace amount. Lowered electrical resistivity occurs and adverse side effects may be expected. Even though the fast charge bleed off features of this antistatic agent may sometimes be desirable, just as often it tends to be unfavorable since it reduces the available charge below that needed to optimize porous cake formation. Furthermore, these agents are heat sensitive, fugitive quaternary ammonium compounds that degrade to an amine which conveys electropositive properties to the fabric before it too burns off.

These effects and the common problems associated with electrostatic behavior have contributed to the uncertainty and even doubt about the part that electrostatics play in the filtration process. Nevertheless, filter media users, producers, suppliers, and researchers alike are all well aware that electrostatic charges do exist on particulate matter and on the collecting bags. The electrical augmentation studies have now rekindled the issue and seem to make it necessary, to clearly define the role on natural charges.

Since some doubt remains, let's adopt a practice that can be accepted without bias to provide relevant data. I propose that from now on, filter fabric specifications include two additional parameters. These are, the electrical resistivity and triboelectric data. By offering this information and by making a comparative analysis of performance characteristics with other physical properties of the media, it should be possible to determine whether, how, and to what extent the collection process depends upon electrical phenomena. To be more completely effective in such an analysis, electrical and electrostatic data should also be available for the particulate matter being collected.

RESEARCH NEEDS

High Temperature Fabrics

The growth of the fabric filtration market depends upon current and new developments in several other important areas. Better high temperature fabrics with more favorable chemical and mechanical properties tend to be on everybody's wanted list. While I agree that opportunities exist for media to be used in the range of 750° to 1000°F, a continuing demand remains for acid resistant, durable fibers capable of operating in the 300° to 500° range. I fail to see a very large market for exotic, high cost fibers although a moderate demand will certainly remain for those super fibers now being produced.

For many high temperature processes an alternative to high temperature filter media is possible within certain limits, even when dewpoint problems exist. I refer specifically to the prospects for reducing the temperature of emissions through improved heat transfer conversion systems. The more effective use of conventional heat exchangers and more efficient pyroelectrical methods that can make the conversion of heat to other forms of energy more appealing, would make some moderately high temperature filtration processes more viable substitutes for those that are now considered necessary at the higher temperatures.

The need for improvements in the currently available commercial high temperature media will remain. Superior protective and certain special custom finishes for glass fabrics, for example, can be expected to increase performance as well as bag life. Conceiveably too, aramid fabrics might be made more acid resistant than permitted by current treating practices. It must be appreciated, however, that because the filter media market is somewhat limited, certainly as compared to that for apparel fabrics, the incentives, research budgets and overall efforts to effect improvements in media will be limited.

Fabric Variations

Other filter fabric developments deserve mention and appropriate consideration. Seamless filter bags made possible by the tubular knitting technique offer new and different features for a variety of collection operations. Further development in the knitting processes, better fabric stabilizing methods, improved fibers, yarns, weaving, and/or needling and finishing and treating practices will surely provide better media for some better filter service.

In felts and felt-like materials, a major breakthrough can be expected with expanded production of durable and stable scrimless or very low scrim content needled fabrics. I doubt that we fully realize the restrictions imposed by the scrim component of needled fabrics. Felts of appropriate fibers in such new constructions will advance the performance of high ratio collectors substantially. No-scrim Nomex felts are now available. The real value of this change will be soon be apparent.

Filter Cleaning

More effective cleaning of any filter is a continuing goal of everyone involved in this technology. While the introduction of scrimless felts is one approach, other techniques have been applied and will be used for improving cake and plug removal. The prospect for realizing significantly better cleaning is not restricted to fabric changes and treatment. It also applies to the adoption of improved collection procedures, the rigorous application of electrostatic principles, and the use of other cleaning assists like those offered by magnetic and acoustic devices and others.

Nodules (Refer to Figure 1)

For many filtration processes, effective control of nodules would lead to substantially better overall performance. The problem presented by nodules, although not always evident, was most clearly noted by Penney[12] in his description of these so called dingleberries as check valves (note Figure 2) that restrict air transfer and have a serious influence on the cleaning process. The check valves simply swing away from the surface under the influence of reverse air but close the surface voids during the filtration cycle.

Nodule formation, I contend, is in part another electrostatic phenomenon. The initial accumulation of particles at the ends of fibers is easily explained in this way. Conversion of these originally soft deposits to a hard mass seems to occur as a result of a phase or chemical change with a cementing action. Some questions for researchers are, therefore:

1. What mechanisms account for the accumulation of nodules?
2. Is moisture alone critical in the hardening process, and in causing them to adhere tenaciously to fiber(s)?
3. What practices may be followed to avoid, eliminate or negate the influence of these deposits on the filtration process? and
4. What type, if any, treatment may be applied to the fibers/fabric to control nodules without impairing the filtration process?

Waste Recovery/Utilization

Last but not least among the ways for the fabric filtration industry as a whole to improve its usefulness and its image is to promote an energetic program of waste recovery and/or utilization. This applies to the utilization of waste heat as well as to the recovery of waste or seemingly low value by-products. Mountains of fly ash will become another problem unless the contained minerals and included elements are reclaimed or another use can be made of the ash itself. Other, so called waste products are or will be classified as hazardous and will become a serious liability unless they too are reclaimed.

As one example, consider with me the product collected in baghouses on some electric furnaces. With a 20% zinc, 10% lead and trace metal content; reuse of this dust in the furnace was deemed undesirable. As such, it was treated as a waste and disposed of, until recently, by burial. Now in view of the recognized potential hazard of leaching, the burial practice has been forbidden. Would it not be safer and more compatible with the conservation trend to recover the raw materials? If health effects and economics dictate policy, this action appears justified, especially in view of the potential danger of lead and the fact that zinc ore is imported.

In closing, let me show you how different particulate control methods, including fabric filtration, have been useful for pollution control in Pittsburgh. Figure 3 is a photograph of the city taken in 1945. The second was taken in 1956, just eleven years later, from the same location looking toward the downtown area. It will be apparent that Pittsburgh was transformed to a clean city during this period from its well established status as the "Smokey City".

The work described in this paper was not funded by the U. S. Environmental Protection Agency and therefore the contents do not necessarily reflect the views of the Agency and no official endorsement should be inferred.

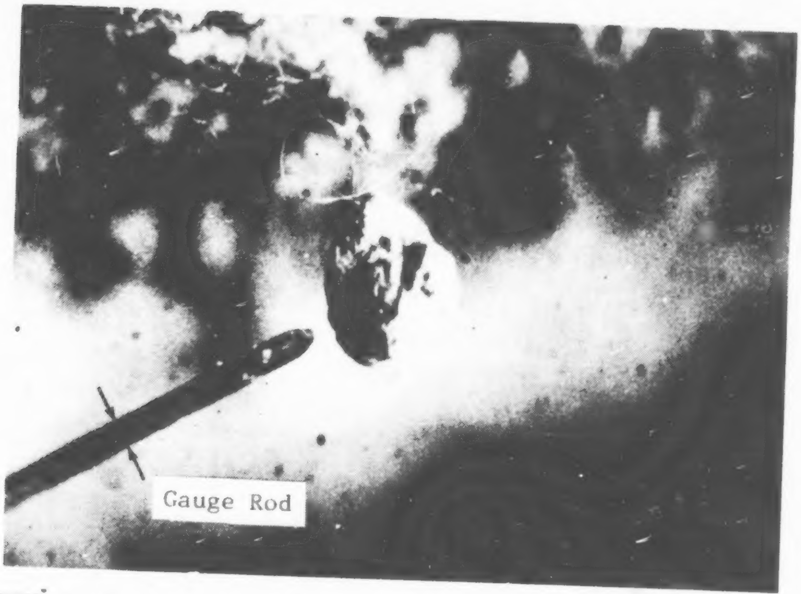

FIGURE 1. Nodule Attached to Fiber

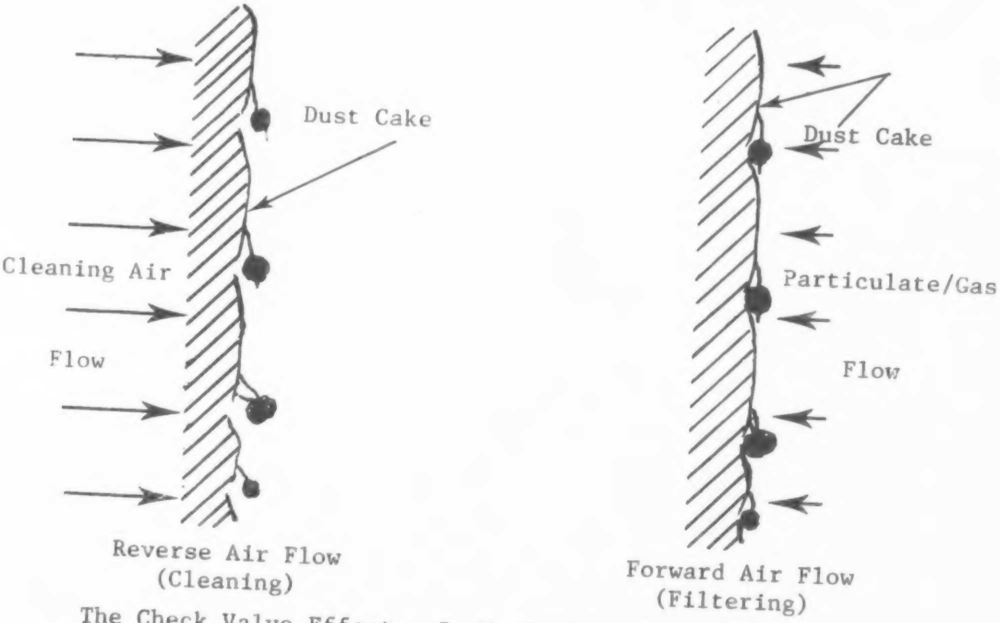
Dust Cake
Cleaning Air
Flow
Reverse Air Flow
(Cleaning)
Dust Cake
Particulate/Gas
Flow
Forward Air Flow
(Filtering)

The Check Valve Effect - G. W. Penney, Electrostatic Effects in Fabric Filtration — EPA—600/7-78-142a September 1978

FIGURE 2. A Model of Nodule Action

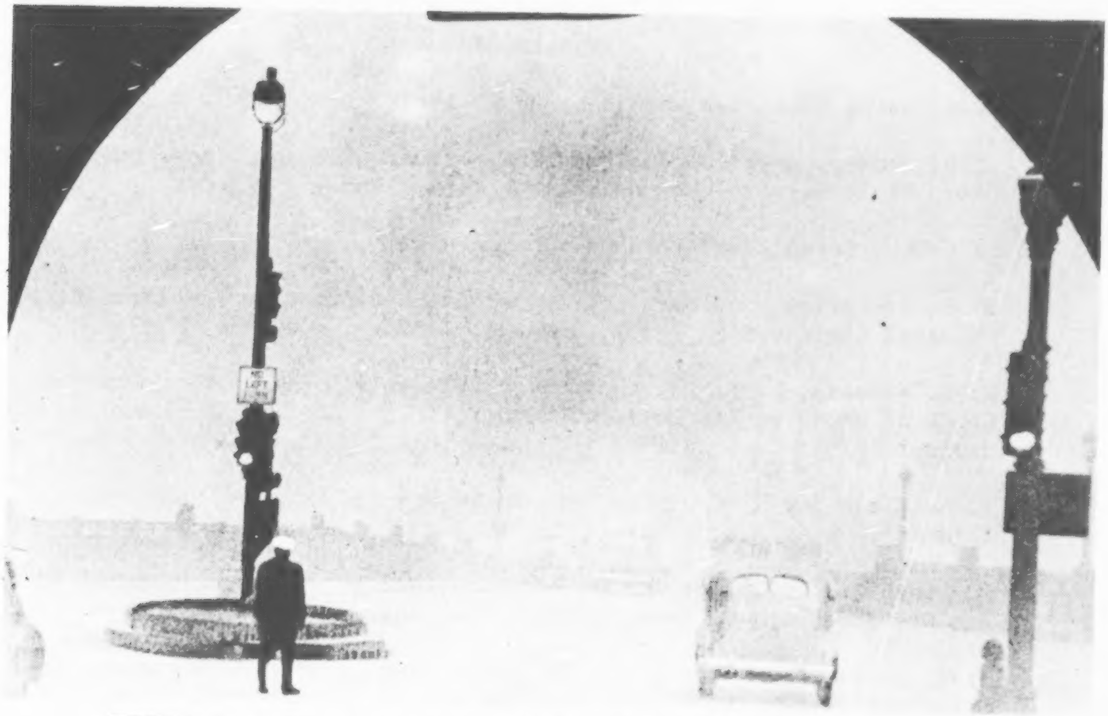

FIGURE 3. View of Downtown Pittsburgh - 1945

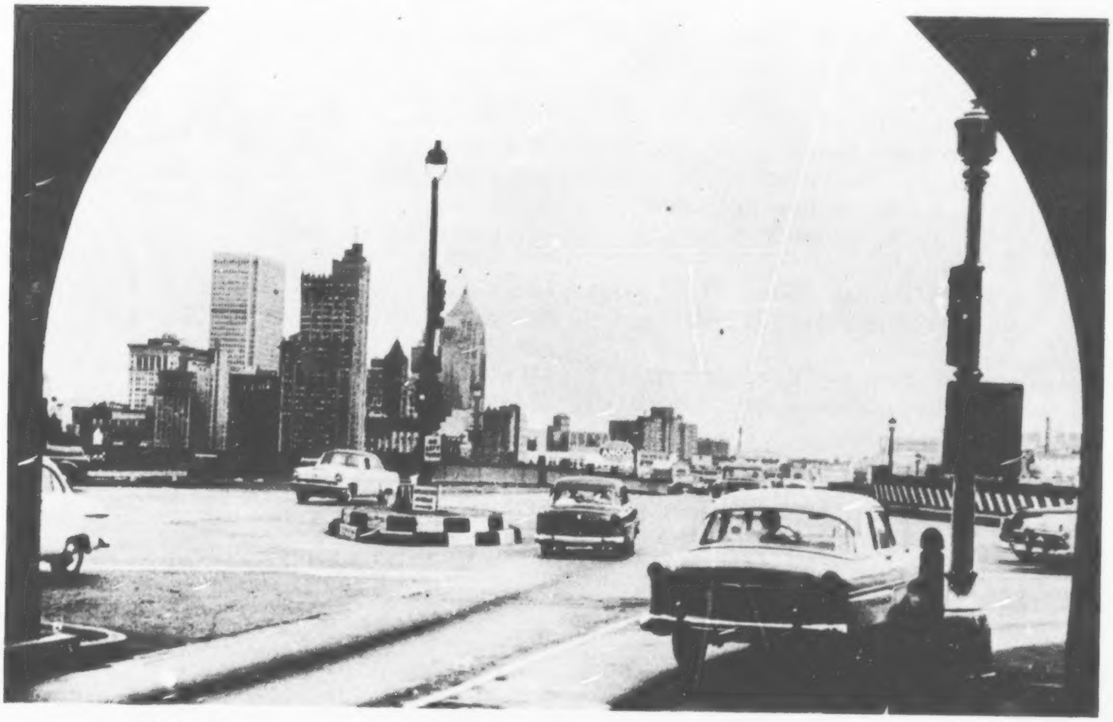

FIGURE 4. View of Downtown Pittsburgh - 1956

Reproduced from best available copy.

REFERENCES

1. Predicasts, Inc. News Release, August 1982.
2. E. S. Godsey, American Smelting and Refining Company, Inc., Salt Lake City, Utal, Personal Communications, July 1980.
3. A. Labbe, Consultant, Personal Communication,
4. E. R. Frederick, How Dust Filter Selection Depends on Electrostatics, Chemical Engineering 68:107, June 26, 1961.
5. R. B. Neveril, J. U. Price and K. L. Engdahl, Capital and Operating Costs of Selected Air Pollution Control Systems, APCA RS-9 Reprint Series. 1979 from J. Air Pollution Control Association 28, 1978.
6. J. A. Klein and K. C. Leung, The Environmental Control Industry, Allanhold Osmun & Co., Montclair, N. J. 1976.
7. M. Linne', J. Klinspor, H. T. Karlsson, and I. Bjerle, Limestone Based Wet-Dry Scrubbing to Form Gypsum, Chem. Eng. Sci., 5, (37), 807, 1982.
8. H. T. Karlsson, J. Klingspor, M. Linne' and I. Bjerle, Activated Dry Scrubbing of SO_2, to be published in the J. Air Pollution Control Assoc.
9. H. T. Karlsson, J. Klingspor and I. Bjerle, Adsorption of Hydrochloric Acid on Solid Slaked Lime for Flue Gas Clean Up, J. Air Pollution Control Assoc. 11, 31, 1981.
10. P. L. Feldman and D. J. Helfritch, Particle Properties and Feasibility of E-Beam Precharging and R. H. Davis, Agenda Overview - E-Beam Workshop on The Combined Removal of SO_2, NO_X and Particulate Matter from Stack Gas by Electron Beam Treatment, Arlington, VA, February 25 and 26, 1982, Sponsored by the U. S. Department of Energy.
11. G. W. Penney, Electrical Augmentation of Fabric Filters, U. S. Patent 3910779 October 7, 1975 and U. S. Patent 3966435, June 29, 1976.
12. G. W. Penney, Electrostatic Effective Fabric Filtration, Volume 1. Fields, Fabrics and Particles, EPA-600/7-78-142A, September, 1978.

AUTHOR INDEX

AUTHOR NAME . . . . . PAGE

ADAIR, L. I-460
ADAMS, R.L. II-35
ANDO, T. II-474
ARMSTRONG, J. III-241
ARSTIKAITIS, A.A. II-194
BALL, C.E. III-370
BANKS, R.R. I-37, I-62
BARRANGER, C.B. I-132
BAYLIS, A.P. II-384
BELTRAN, M.R. II-51
BENSON, S.A. III-97
BERGMAN, F. III-154
BIESE, R.J. I-446
BOSCAK, V. III-66
BRADBURN, K.M. II-499
BRADLEY, L.H. II-369
BRINKMANN, A. III-211
BUCK, V. III-335
BUMP, R.L. II-17
CAPPS, D.D. I-121
CARR, R.C. I-148
CHAMBERS, R. I-226, I-239
CHANG, R. III-271
CHEN, F.L. III-347
CHEN, Y.J. I-506
CHIANG, T. II-184
CHRISTENSEN, E.M. II-243
CHRISTIANSEN, J.V. II-243
CILIBERTI, D.F. III-282, III-318
CLEMENTS, J.S. II-96
COE,JR, E.L. II-416
COLE, W.H. III-1

COOK, D.R. . . . II-349
COWHERD,JR, C. . . . III-183
COY, D.W. . . . III-370
CRYNACK, R.R. . . . II-1
CUSCINO, T. . . . III-154
CUSHING, K.M. . . . I-148
DAHLIN, R.S. . . . I-192
DARBY, K. . . . II-499
DAVIS, R.H. . . . II-96
DAVIS, W.T. . . . I-521
DAVISON, J.W. . . . III-166
DELANEY, S. . . . I-357
DEMIAN, A. . . . III-66
DENNIS, R. . . . I-22, III-81
DIRGO, J.A. . . . III-26, III-81
DISMUKES, E.B. . . . II-444
DONOVAN, R.P. . . . I-77, I-107, I-316, I-327, I-342
DORCHAK, T.P. . . . III-114
DRENKER, S. . . . III-271, III-282
DRIGGERS, G.W. . . . II-194
DUBARD, J.L. . . . II-337
DUFFY, M.J. . . . II-489
DURHAM, M. . . . II-84, III-241
EBREY, J.M. . . . II-349
ENGLEHART, P.J. . . . III-183
ENSOR, D.S. . . . III-347
FAULKNER, M.B. . . . II-204, II-337
FINNEY, W.C. . . . II-96
FORTUNE, O.F. . . . I-482, I-494
FOSTER, J.T. . . . I-37, I-91
FREDERICK, E.R. . . . I-536
FRISCH, N.W. . . . III-114
FURLONG, D.A. . . . I-287, I-342
GARDNER, R.P. . . . I-77, I-107
GAWRELUK, G.R. . . . II-17
GELFAND, P. . . . II-35

GIBBS, J.L. II-430
GILES, W.B. III-41, III-53
GOLAN, L.P. III-226
GOLDBRUNNER, P.R. II-401
GOLIGHTLEY, R.M. I-164
GOOCH, J.P. II-444
GOODWIN, J.L. III-226
GRANT, M.A. III-81
GREEN, G.P. I-192
GREINER, G.P. I-287, I-357
GRONBERG, S. III-141
GRUBB, W.T. I-62, I-91, I-179
HALL, H.J. II-459
HALOW, J.S. II-96
HANSON , P. I-460
HARMON, D. I-226, I-239, III-131
HAWKINS, L.A. II-194
HERCEG, Z. II-489
HOVIS, L.S. I-22, I-77, I-107, I-287, I-316, I-327,
I-342, I-357, III-81, III-347

HOWARD, J.R. I-164
INGRAM, T.J. I-446
ISAHAYA, F. II-154
ITAGAKI, T. II-322
JACOB, R.O. I-446
JENSEN, R.M. I-431
JONES, R. I-303
KASIK, L.A. II-430
KETCHUCK, M. I-482
KINSEY, J. III-154
KOHL, A.L. III-300
KUBY, W. III-271
KUNKA, S. I-239
KUTEMEYER, P.M. III-211
LAMB, G.E.R. I-303
LARSEN, P.S. II-243

LAWLESS, P.A. II-271
LEE, W. I-303
LEITH, D. III-26
LEONARD, G.L. II-230
LEWIS, M. I-179
LIPPERT, T.E. III-280, III-318
LUGAR, T.W. II-184
MARCHANT,JR, G.H. II-444
MASON, D.M. III-256
MASUDA, S. II-139, II-169, II-322, III-386
MATSUMOTO, Y. II-474
MATULEVICIUS, E.S. III-226
MCCAIN, J.D. III-198
MCCOLLOR, D.P. III-97
MCDONALD, J.R. II-204
MCKENNA, J.D. I-210
MCLEAN, K.L. II-489
MENARD, A. I-255
MILLER, M.L. I-482
MILLER, R.L. I-494
MILLER, S.J. III-97
MITCHNER, M. II-230
MOSLEHI, G.B. II-288, II-306
MOSLEY, R.B. II-204
MOYER, R.B. I-460
MUSGROVE, J. I-382
MYCOCK, J.C. I-210
NAKATANI, H. II-169
NG, T.S. II-489
NOVOGORATZ, D. II-349
OGLESBY, S. II-534
O'ROURKE, R. III-318
PEARSON, G. I-121
PETERS, H.J. I-179
PIULLE, W. II-401
PONTIUS, D.H. II-65

PUDELEK, R.E. I-521
PUTTICK, D.G. II-126
QUACH, M.T. I-506
RAMSEY, G.H. I-316, I-327
RANADE, M.A. III-347
REED, G.D. I-521
REHMAT, A. III-256
REIDER, J.P. III-183
REISINGER, A.A. I-179
RICHARDS, R.M. I-255
RICHARDSON, J.W. I-210
RINARD, G. II-84, III-241
ROOP, R.N. I-460
ROSS, D.R. I-164
RUGENSTEIN, W.A. II-430
RUGG, D. II-84, III-241
RUSSELL-JONES, A. II-384
SAIBINI, J. I-132
SAMUEL, E.A. I-1, II-218
SANDELL, M.A. II-1
SAWYER, J. III-271
SEARS, D.R. I-192, III-97
SELF, S.A. II-230, II-228, II-306
SHACKLETON, M. III-271
SHISHIKUI, Y. II-139
SMITH, W.B. I-148
SORENSON, P.H. III-362
SPARKS, L.E. II-204, II-271, II-337
SPENCE, N. I-132
SPENCER,III, H.W. I-506
STELMAN, D. III-300
STOCK, D.E. II-261
SUHRE, D. III-335
SUNTER, T.C. I-48
SURATI, H. II-51
TACHIBANA, N. II-474

TASSICKER, O.J. III-271, III-282
THOMPSON, C.S. III-12
THOMSEN, H.P. II-243
TOKUNAGA, O. II-96
TREXLER, E.C. II-96
TRILLING, C.A. III-300
TSAO, K.C. III-256
VANN BUSH, P. II-65
VANOSDELL, D.W. I-287, I-342
WALSH, M.A. I-482
WEBER, E. II-111
WELLAN, W.G. I-420
WEXLER, I.M. II-521
WHITTLESEY, M. I-482
WILCOX, K. III-154
WILLIAMSON, A.D. III-198
YAMAMOTO, T. III-241
YEAGER, K.E. . . . . III-xv